Methods in Molecular Biology 1390

Springer Protocols

Claire E. McCoy *Editor*

Toll-Like Receptors

Practice and Methods

Second Edition

Humana Press

METHODS IN MOLECULAR BIOLOGY

Series Editor
John M.Walker
School of Life and Medical Sciences
University of Hertfordshire
Hatfield, Hertfordshire, AL10 9AB, UK

For further volumes:
http://www.springer.com/series/7651

Toll-Like Receptors

Practice and Methods

Second Edition

Edited by

Claire E. McCoy

School of Biochemistry and Immunology, Trinity Biomedical Sciences Institute, Trinity College Dublin, Dublin, Ireland; Hudson Institute of Medical Research, Monash University Faculty of Medicine, Clayton, VIC, Australia

Humana Press

Editor
Claire E. McCoy
School of Biochemistry and Immunology
Trinity Biomedical Sciences Institute
Trinity College Dublin
Dublin, Ireland

Hudson Institute of Medical Research
Monash University Faculty of Medicine
Clayton, VIC, Australia

ISSN 1064-3745 ISSN 1940-6029 (electronic)
Methods in Molecular Biology
ISBN 978-1-4939-3333-4 ISBN 978-1-4939-3335-8 (eBook)
DOI 10.1007/978-1-4939-3335-8

Library of Congress Control Number: 2015957396

Springer New York Heidelberg Dordrecht London

Printed on acid-free paper

Humana Press is a brand of Springer
Springer Science+Business Media LLC New York is part of Springer Science+Business Media (www.springer.com)

Preface

This book entitled *Toll-Like Receptors: Methods and Protocols* is a second edition that builds on the success of the first book published in 2009. Since the first edition, Toll-Like Receptors (TLRs) have been shown to have additional functions, playing a role in controlling events such as cross-priming of associated pattern recognition receptors, posttranscriptional regulation, interaction with other cellular and biologic systems, as well as driving cancer progression; all of which have been detailed in this new edition.

Composed of 25 practical chapters, this book has been divided into five parts: Part I, "Toll-Like Receptor Detection and Activation," outlines ligands, methods for TLR detection, interaction, and intracellular trafficking, as well as containing a comprehensive overview of the best read-outs for TLR activation. Part II, "Toll-Like Receptor Cross-Priming of Associated Receptors," describes methods and assays to investigate how TLRs cross-prime other pattern recognition receptors including intracellular DNA receptors and inflammasome formation, RIG-I like receptors, C-type lectin receptors, and transmembrane proteins such as UNC93. Part III, "Toll-Like Receptor Posttranscriptional Regulation," highlights the novel area of RNA regulation, detailing how TLRs can induce RNA transcripts and molecules such as microRNAs and long noncoding RNAs to shape the immune response. Part IV, "Toll-Like Receptors and System Control," describes methods to explore TLR detection and activation in other systems such as T and B lymphocytes, the intestinal barrier, metabolism, and circadian rhythm. Part V, "Toll-Like Receptors and Disease," describes models to delineate the role of TLRs in diseases such as dermatitis, arthritis, experimental autoimmune encephalitis, and gastric cancer as well as methods for the amelioration of disease progression.

Each chapter contains a summary, the materials required, step-by-step methods, and useful notes to investigate TLRs in cell culture, biological systems and disease. Entirely practical in nature, this book will add skill to both students and the more advanced molecular biologist who wishes to learn a new technique or move to a different area within their current repertoire of practical knowledge. Moreover, this book expands and reinforces our current knowledge of TLR function, as well as promoting the sharing and enhancement of practical skills often absent from current literature. This book will provide a valuable resource to immunologists and molecular or medical biologists working in a laboratory setting.

Dublin, Ireland — ***Claire E. McCoy***
Clayton, VIC, Australia

Contents

Contributors

Ana M. Avalos • *Department of Microbiology, Boston University School of Medicine, Boston, MA, USA*

Nilesh J. Bokil • *Institute for Molecular Bioscience, The University of Queensland, Brisbane, QLD, Australia; Australian Infectious Diseases Research Centre, The University of Queensland, Brisbane, QLD, Australia*

Clare E. Bryant • *Department of Veterinary Medicine, University of Cambridge, Cambridge, UK*

Susan Carpenter • *Department of Molecular, Cell and Developmental Biology, University of California Santa Cruz, Santa Cruz, CA, USA*

Sinéad C. Corr • *Trinity Biomedical Sciences Institute, School of Biochemistry and Immunology, Trinity College Dublin, Dublin, Ireland*

Anne M. Curtis • *School of Biochemistry and Immunology, Trinity Biomedical Sciences Institute, Trinity College Dublin, Dublin, Ireland*

Jérome Dellacasagrande • *Blood Assay Solutions, Toulouse Cedex, France*

Jennifer K. Dowling • *Hudson Institute of Medical Research, Monash University, Melbourne, VIC, Australia*

Eric J. Downer • *School of Medicine, Discipline of Physiology, Trinity Biomedical Sciences Institute, Trinity College, Dublin, Ireland*

Sarah L. Doyle • *Department of Clinical Medicine, School of Medicine, Trinity College Dublin, Dublin, Ireland; The National Children's Research Centre, Our Lady's Children's Hospital Crumlin, Dublin, Ireland*

Bart Everts • *Department of Parasitology, Leiden University Medical Center, Leiden, The Netherlands*

Caio T. Fagundes • *Laboratório de Interação Microorganismo-Hospedeiro, Departamento de Microbiologia, Universidade Federal de Minas Gerais, Belo Horizonte, Minas Gerais, Brazil; Laboratório de Imunofarmacologia, Departamento de Bioquímica e Imunologia, Universidade Federal de Minas Gerais, Belo Horizonte, Minas Gerais, Brazil*

Francesca Fallarino • *Department of Experimental Medicine, University of Perugia, Perugia, Italy*

Jonathan Ferrand • *Centre for Cancer Research, Hudson Institute of Medical Research, Clayton, VIC, Australia; Department of Molecular and Translational Science, Monash University, Clayton, VIC, Australia*

Stephanie Flaherty • *Department of Microbiology and Immunology, Chicago Medical School, Rosalind Franklin University of Medicine and Science, North Chicago, IL, USA*

Monique Gangloff • *Department of Biochemistry, University of Cambridge, Cambridge, UK*

Michael P. Gantier • *Centre for Cancer Research, Hudson Institute of Medical Research, Clayton, VIC, Australia; Department of Molecular and Translational Science, Monash University, Clayton, VIC, Australia*

Marco Gargaro • *Department of Experimental Medicine, University of Perugia, Perugia, Italy*

Lucien P. Garo • *Ann Romney Center for Neurologic Diseases, Brigham and Women's Hospital, Harvard Medical School, Boston, MA, USA*

Nicholas J. Gay • *Department of Biochemistry, University of Cambridge, Cambridge, UK*
Teunis B.H. Geijtenbeek • *Academic Medical Center, University of Amsterdam, Amsterdam, The Netherlands*
Matthias Goebeler • *Department of Dermatology, University of Würzburg, Würzburg, Germany*
Bruno Gran • *Division of Clinical Neuroscience, Queen's Medical Centre, University of Nottingham School of Medicine, Nottingham, UK*
Alwin J. van der Ham • *Department of Parasitology, Leiden University Medical Center, Leiden, The Netherlands*
Moritz Haneklaus • *School of Biochemistry and Immunology, Trinity Biomedical Sciences Institute, Trinity College Dublin, Dublin, Ireland*
Nina Hertoghs • *Academic Medical Center, University of Amsterdam, Amsterdam, The Netherlands*
Gabor L. Horvath • *Institute of Innate Immunity, University Hospitals, University of Bonn, Bonn, Germany*
Md. Jakir Hossain • *Division of Clinical Neuroscience, Queen's Medical Centre, University of Nottingham School of Medicine, Nottingham, UK*
Yu-San Huoh • *Department of Biological Chemistry and Molecular Pharmacology, Harvard Medical School, Boston, MA, USA; Program in Cellular and Molecular Medicine, Boston Children's Hospital, Boston, MA, USA*
Sun Hur • *Department of Biological Chemistry and Molecular Pharmacology, Harvard Medical School, Boston, MA, USA; Program in Cellular and Molecular Medicine, Boston Children's Hospital, Boston, MA, USA*
Harald Husebye • *Centre of Molecular Inflammation Research, Norwegian University of Science and Technology, Trondheim, Norway; Department of Cancer Research and Molecular Medicine, Norwegian University of Science and Technology, Trondheim, Norway*
Adi Idris • *School of Chemistry and Molecular Biosciences, The University of Queensland, Brisbane, QLD, Australia*
Brendan J. Jenkins • *Centre for Innate Immunity and Infectious Diseases, Hudson Institute of Medical Research, Melbourne, VIC, Australia*
Daniel G.W. Johnston • *Trinity Biomedical Sciences Institute, School of Biochemistry and Immunology, Trinity College Dublin, Dublin, Ireland*
Wondae Kang • *Division of Integrative Biosciences and Biotechnologies, Department of Life Sciences, Pohang University of Science and Technology, Pohang, Republic of Korea*
You-Me Kim • *Division of Integrative Biosciences and Biotechnologies, Department of Life Sciences, Pohang University of Science and Technology, Pohang, Republic of Korea*
Pia Langhoff • *Institute of Innate Immunity, University Hospitals, University of Bonn, Bonn, Germany*
Eicke Latz • *Institute of Innate Immunity, University Hospitals, University of Bonn, Bonn, Germany; University of Massachusetts Medical School, Worcester, MA, USA*
Yu-Ran Lee • *Division of Integrative Biosciences and Biotechnologies, Department of Life Sciences, Pohang University of Science and Technology, Pohang, Republic of Korea*
Victoria G. Lyons • *School of Biochemistry and Immunology, Trinity Biomedical Sciences Institute, Trinity College Dublin, Dublin, Ireland; Hudson Institute of Medical Research, Monash University Faculty of Medicine, Clayton, VIC, Australia*
Ann Marshak-Rothstein • *Department of Medicine, University of Massachusetts Medical School, Worcester, MA, USA*

Stefan F. Martin • *Department of Dermatology, University Medical Center Freiburg, Freiburg, Germany*

Charalampos (Harris) Mavromatis • *Integrative Systems Biology Laboratory, Division of Biological and Environmental Sciences and Engineering, King Abdullah University of Science and Technology, Thuwal, Kingdom of Saudi Arabia; Division of Computer, Electrical and Mathematical Sciences and Engineering, King Abdullah University of Science and Technology, Thuwal, Kingdom of Saudi Arabia; Division of Medical Genetics, Department of Medicine, University of California, San Diego, La Jolla, CA, USA*

Fiona E. McCann • *Kennedy Institute of Rheumatology, Nuffield Department of Orthopaedics, Rheumatology and Musculoskeletal Sciences, University of Oxford, Oxford, UK*

Claire E. McCoy • *School of Biochemistry and Immunology, Trinity Biomedical Sciences Institute, Trinity College Dublin, Dublin, Ireland; Hudson Institute of Medical Research, Monash University Faculty of Medicine, Clayton, VIC, Australia*

Kim S. Midwood • *Kennedy Institute of Rheumatology, Nuffield Department of Orthopaedics, Rheumatology and Musculoskeletal Sciences, University of Oxford, Oxford, UK*

Giada Mondanell • *Department of Experimental Medicine, University of Perugia, Perugia, Italy*

Tom P. Monie • *Department of Biochemistry, University of Cambridge, Cambridge, UK; Medical Research Council Human Nutrition Research, Elsie Widdowson Laboratory, Cambridge, UK*

Krishna L. Moody • *Department of Microbiology, Boston University School of Medicine, Boston, MA, USA*

Gopal Murugaiyan • *Ann Romney Center for Neurologic Diseases, Brigham and Women's Hospital, Harvard Medical School, Boston, MA, USA*

Leonard R. Pelgrom • *Department of Parasitology, Leiden University Medical Center, Leiden, The Netherlands*

Anna M. Piccinini • *Kennedy Institute of Rheumatology, Nuffield Department of Orthopaedics, Rheumatology and Musculoskeletal Sciences, University of Oxford, Oxford, UK*

Egest J. Pone • *Department of Pharmaceutical Sciences, University of California, Irvine, CA, USA*

Timothy Ravasi • *Integrative Systems Biology Laboratory, Division of Biological and Environmental Sciences and Engineering, King Abdullah University of Science and Technology, Thuwal, Kingdom of Saudi Arabia; Division of Computer, Electrical and Mathematical Sciences and Engineering, King Abdullah University of Science and Technology, Thuwal, Kingdom of Saudi Arabia; Division of Medical Genetics, Department of Medicine, University of California, San Diego, La Jolla, CA, USA*

Joseph M. Reynolds • *Department of Microbiology and Immunology, Chicago Medical School, Rosalind Franklin University of Medicine and Science, North Chicago, IL, USA*

Vitaliya Sagulenko • *School of Chemistry and Molecular Biosciences, The University of Queensland, Brisbane, QLD, Australia*

Mark A. Schembri • *Australian Infectious Diseases Research Centre, The University of Queensland, Brisbane, QLD, Australia; School of Chemistry and Molecular Biosciences, The University of Queensland, Brisbane, QLD, Australia*

Marc Schmidt • *Department of Dermatology, University of Würzburg, Würzburg, Germany*
David P. Sester • *School of Chemistry and Molecular Biosciences, The University of Queensland, Brisbane, QLD, Australia*
Joris K. Sprokholt • *Academic Medical Center, University of Amsterdam, Amsterdam, The Netherlands*
Katryn J. Stacey • *School of Chemistry and Molecular Biosciences, The University of Queensland, Brisbane, QLD, Australia*
Matthew J. Sweet • *Institute for Molecular Bioscience, The University of Queensland, Brisbane, QLD, Australia; Australian Infectious Diseases Research Centre, The University of Queensland, Brisbane, QLD, Australia*
Melissa B. Uccellini • *Department of Microbiology, Icahn School of Medicine at Mt. Sinai, New York, NY, USA*
Gregory A. Viglianti • *Department of Microbiology, Boston University School of Medicine, Boston, MA, USA*
Nazarii Vitak • *School of Chemistry and Molecular Biosciences, The University of Queensland, Brisbane, QLD, Australia*
Alison C. West • *Centre for Innate Immunity and Infectious Diseases, Hudson Institute of Medical Research, Melbourne, VIC, Australia*
Lynn Williams • *Kennedy Institute of Rheumatology, Nuffield Department of Orthopaedics, Rheumatology and Musculoskeletal Sciences, University of Oxford, Oxford, UK*
Bin Wu • *Department of Biological Chemistry and Molecular Pharmacology, Harvard Medical School, Boston, MA, USA; Program in Cellular and Molecular Medicine, Boston Children's Hospital, Boston, MA, USA*

Part I

Toll-Like Receptor Detection and Activation

Chapter 1

Toll-Like Receptors: Ligands, Cell-Based Models, and Readouts for Receptor Action

Jennifer K. Dowling and Jérome Dellacasagrande

Abstract

This chapter details Toll-like receptors (TLRs) and the tools available to study their biology in vitro. Key parameters to consider before exploring TLR action such as receptor localization, signaling pathways, nature of ligands and cellular expression are introduced. Cellular models (i.e., host cells and readouts) based on the use of cell lines, primary cells, or whole blood are presented. The use of modified TLRs to circumvent some technical problems is also discussed.

Key words Toll-like receptors, Cell-based assays, Whole blood assays, Reporter gene assays, TLR ligands

1 Toll-Like Receptors

Toll-like receptors (TLRs) represent a family of Pattern Recognition Receptors (PRRs) that play a critical role in early defence against invading pathogens and responses to endogenous danger signals. To date ten human TLRs have been classified (TLR1-TLR10) and 12 in the mouse (TLR1-9, TLR11-13) [1]. From a technical point of view, TLRs are distinguished by ligand specificity, signal transduction, expression patterns, and cellular localization.

TLRs are type I transmembrane receptors and form part of the Toll/interleukin-1 (TIR) superfamily that includes the IL-1 receptors (IL-1Rs) because of the shared homology of their cytoplasmic regions [2]. In contrast, their extracellular regions (ectodomains) are considerably different. TLR ectodomains contain tandem repeats of leucine-rich regions termed leucine-rich repeats (LRRs), while IL-1Rs have three immunoglobulin (Ig)-like domains. The arrangement of LRR side chains confers a unique combinatorial code to each TLR enabling it to bind a specific ligand. In addition detection of ligand is also dependent on the cellular localization of the TLR in question [3, 4]. The distinct cellular location of different TLRs and the unique combinatorial code of their LRRs

Claire E. McCoy (ed.), *Toll-Like Receptors: Practice and Methods*, Methods in Molecular Biology, vol. 1390,
DOI 10.1007/978-1-4939-3335-8_1,

afford them the ability to interact with structurally unrelated ligands of endogenous and exogenous origin.

1.1 TLR Localization

TLRs are localized to the cell surface (plasma membrane) or intracellular compartments [5]. The location of any given TLR is related to the origin of the ligand it recognizes. TLR1, TLR2, TLR4, TLR5, and TLR6 are expressed on the plasma membrane and are largely involved in the detection of bacterial products in the extracellular space. On the other hand, TLR3, TLR7, TLR8, and TLR9 are located within endocytic compartments that present nucleic acids of viral origin to these TLRs [6, 7]. Localization is also important for the discrimination between "self" and "non-self." For example, in contrast to most TLR ligands nucleic acids can be of self and foreign origin. Studies have demonstrated that a chimeric TLR9 consisting of a transmembrane and cytoplasmic domain of other TLRs localizes to the plasma membrane [8]. Here it is able to detect and respond to mammalian DNA yet remain unresponsive to viral nucleic acids, highlighting the importance of TLR location. Endogenous TLR9 is not exposed to mammalian DNA and can only be activated by viral DNA ingested and acidified within endosomes. As a consequence of their localization, activation of intracellular TLRs in in vitro experiments requires the use of cell permeable ligands or ligands complexed with cationic lipids to facilitate their uptake.

1.2 TLR Signaling

Knowledge of the different signaling pathways mobilized by TLRs is essential for the selection of appropriate readouts or reporter genes in cell-based assays (see Part III). TLR signaling is initiated by the binding of a TLR with its respective ligand, be it exogenous or endogenous. Invading microbes are detected by means of recognizing specific "pathogen-associated molecular patterns" or PAMPs. TLRs have also evolved to detect molecules derived from damaged cells referred to as endogenous "danger-associated molecular patterns" or DAMPs. Recognition of PAMPs or DAMPs by TLRs results in the activation of signaling pathways that induce the upregulation of cytokines, chemokines, and co-stimulatory molecules.

The initial step in signal transduction following the binding of ligand is dimerization of two TLR receptor chains. In the case of TLR4 a homodimer is induced by the binding of MD-2 (Myeloid differentiation protein-2) to the lipid A moiety of Lipopolysaccharide (LPS) [9]. To date the crystal structures of several TLR dimers have been elucidated including dimers of TLR3 [10–12], TLR2/1 [13] and TLR4 [14], TLR5 [15], TLR8 [16], and TLR10 [17].

Following dimerization conformational changes in the receptor leads to the association of the two cytoplasmic receptor TIR domains [4, 18]. It is believed the overall structure of the TLR ectodomain, transmembrane, and cytoplasmic regions in turn con-

stitutes a molecular switch "turned-on" by ligand binding. Ultimately, the association of TLR cytoplasmic TIR domains produces two symmetrically related binding sites for the recruitment of specific adaptor molecules which also contain TIR domains [19]. The result is a post-receptor signaling complex associating relevant adaptor molecules to active TIR domains of TLR dimers.

Subsequently, signaling cascades are activated via recruitment of such adaptors. These include MyD88, Mal/TIRAP, TRIF/TICAM-1, TRAM/TICAM-2, and SARM [3, 20, 21]. The proximal events of ligand binding and adaptor recruitment to the active TIR domains of TLRs can result in the activation of two major signaling cascades, namely the MyD88-dependant and MyD88-independent pathways [22] (*see* Fig. 1).

The MyD88-dependent pathway results in nuclear translocation of Nuclear Factor-kappaB (NF-κB) and induction of pro-inflammatory cytokines, while the MyD88-independent pathway mediates induction of Type I interferons and interferon-inducible genes via Interferon Response Factors (e.g., IRF3/7) [21]. All TLRs with the exception of TLR3 are known to recruit MyD88 and activate the MyD88-dependent pathway activating mitogen activated protein kinases (MAPKs) and NF-κB [6]. In addition to

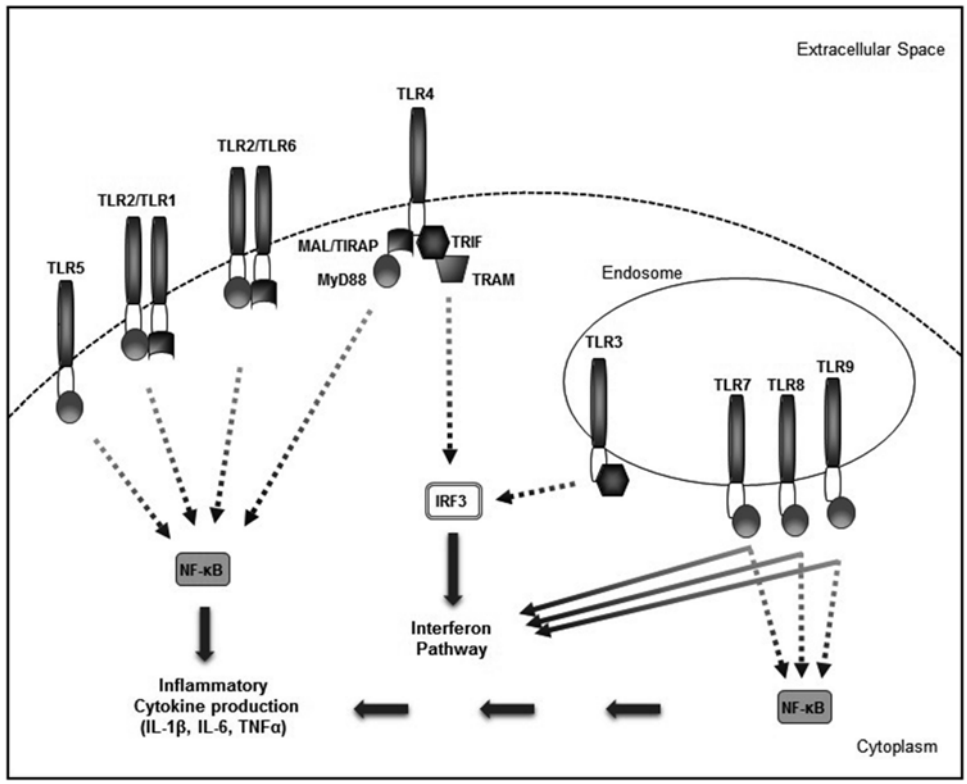

Fig. 1 TLR localization and activation of MyD88-dependant and -independent pathways

MyD88, TLR2 and TLR4 require Mal/TIRAP to activate the MyD88-dependant pathway [23]. TLR3 typically activates IRFs and expression of IFNs from its endocytic compartments via TRIF [24]. Signaling via TLR4 is unique in that it activates both the MyD88-dependant pathway via MyD88 and Mal/TIRAP to activate NF-κB and the MyD88-independent pathway via TRAM and TRIF to activate IRF3. It remains unclear as to whether an activated TLR4 dimer can stimulate Mal and TRAM directed pathways simultaneously or whether the engagement of each adaptor is mutually exclusive [19]. Of particular interest is the fact that TLR4 signaling via TRIF and TRAM also induces a late phase of NF-κB activation [25]. A role for TRAM in the induction of Type I IFN via TLR2 endosomal signaling has also recently been described [26]. TLR7, TLR8, and TLR9 act through MyD88 to induce pro-inflammatory cytokine secretion and the IFNs. A recent study has defined a role for TRIF in TLR9-induced IFNs in response to high doses of CpG [27]. Other than MyD88, the signaling proteins employed by TLR7-8 to activate IFNs remain unidentified.

2 Ligands

Knowledge about how TLRs recognize pathogenic ligands is critical to understand how these receptors are activated and important for designing therapeutic compounds that can target this family of receptors for inflammatory diseases. TLRs are activated by microorganisms such as bacteria, viruses, or fungi and by endogenous ligands. Most of these ligands are by nature complex and undefined. From a technical point of view, defined, specific ligands are needed. This section will focus on commercially available ligands purified for the purpose of TLR study and on the most recent TLR ligands described in the literature. Suppliers offering a large range of TLR-related products are Enzo Life Sciences, Hycult Biotech, Bio-Techne (formally Imgenex, Novus Biologicals), and InvivoGen; and most of the TLR ligands discussed in this chapter are commercially available from them (*see* Table 1). Different formats are proposed including 96-well plates precoated with TLR ligands (InvivoGen), and labeled ligands for staining purposes (e.g., flow cytometry). In addition, several pharmaceutical companies have developed new synthetic TLR ligands and TLR inhibitors (mainly for TLR7/8/9) [28].

The potency of TLR ligands relies on their ability to induce homo- or heterodimerization and/or conformational change of receptor chains [29]. Direct binding of several TLRs to their known ligands has been experimentally demonstrated for TLR9 [30], TLR1/2 [13], TLR4 [14] and TLR3 [10–12], TLR5 [15], TLR8 [16], and TLR13 [31].

Table 1
Prototypic TLR ligands and working concentration

	Ligand	Working concentration
TLR1/2	Pam_3CSK_4	1–100 ng/ml
TLR3	Poly I:C Poly A:U	10–50 μg/ml 300 ng to 100 μg/ml
TLR4	Purified *E. coli* LPS Monophosphoryl Lipid A	10–100 ng/ml 10 ng to 10 μg/ml
TLR5	*S. typhimurium*Flagellin	1 μg/ml
TLR6/2	Pam_2CSK_4 FSL-1 Zymosan	1–100 ng/ml 1–100 ng/ml 1–10 μg/ml
TLR7	Gardiquimod Loxoribine	1–10 μg/ml 0.2–1 mM
TLR8	CL075 (3M-002)	0.1 μg/ml
TLR9	ODN 2006 (human) ODN 1826 (mouse)	10 μg/ml (5 μM)
TLR11 (mouse only)	*T. gondii* Profilin	1–10 ng/ml
TLR13	ORN Sa19	0.02–2 μg/ml

2.1 TLR1

TLR1 forms functional heterodimers with TLR2. TLR1/2 heterodimers are receptors for triacyl lipopeptides found in bacteria and mycobacteria [32]. An artificial model suggests that signaling through TLR1 homodimers would trigger a weak signal characterized by the activation of the TNF promoter [33]. The ligand of choice for TLR1/2 is the synthetic molecule Pam_3CSK_4 and it is active when used at 10 ng/ml.

2.2 TLR2

It is difficult to demonstrate ligand specificity for TLR2 as it forms heterodimers with TLR1, TLR6, and possibly TLR10 to recognize a variety of microorganisms [34]. Zymosan from yeast cell wall, lipoteichoic acid [35], lipoarabinomannan from bacteria and mycobacteria [36], and lipoproteins from mycoplasma or gram-negative bacteria [32] can all activate TLR2 in the absence of TLR1 or TLR6. In vitro, in the absence of TLR1 and TLR6, TLR2 can be activated with High-mobility group box (HMGB) 1 [37], heat-killed *Listeria monocytogenes* [38], Pam_3CSK_4 [32], or *Staphylococcus aureus* peptidoglycan [39]. With regard to

peptidoglycan, it has been shown that this ligand is recognized by the cytosolic receptor NOD1 [40].

2.3 TLR3

TLR3 is an intracellular TLR localized in endosomes; it binds dsRNA of viral origin. In addition, two synthetic TLR3 ligands mimicking dsRNA, polyriboinosinic-polyribocytidylic acid (polyI:C) and polyadenylic-polyuridylic acid (polyA:U), have been described [41]. Both low molecular weight (LMW; 0.2–1 kb) and high molecular weight (HMW; 1.5–1 kb) Poly I:C fragments can activate TLR3. However, low molecular weight fragments are less potent than the large fragments. Polyinosinic acid (polyI) has been shown to activate TLR3 in mouse B cells, macrophages, and bone marrow derived dendritic cells [42].

TLR3 ligands are active when added to the medium at 10–50 μg/ml. Complexation with a lipid-based transfection reagent results in a lower effective concentration but such a delivery system might also activate cytoplasmic receptors such as MDA-5 independently of TLR3 [43].

Direct addition of both HMW- and LMW-poly I:C to the cultures of primary macrophages and a human neuroblastoma cell line (CHP212) activated TLR3 [44]. However, the transfection of poly I:C was necessary to induce TLR3 activation in other cell types studied. The activation efficiency of TLR3 by poly I:C is influenced by various factors, including size of the ligands, delivery methods, and cell types.

2.4 TLR4

TLR4 was the first TLR identified in mammals. It is one of the most studied TLRs [45]. First considered as the receptor for lipopolysaccharide (LPS) from Gram-negative bacteria, it has been later shown that TLR4 requires MD2, LPS binding protein (LBP), and CD14 as co-receptors to function. LPS consists of a polysaccharide moiety and the active component lipid A. Lipid A is composed of a glucosamine disaccharide linked to fatty acids [46]. The potency to activate TLR4 depends on the number of fatty acids. Lipid A from pathogenic bacteria (e.g., *E. coli*, *Salmonella* species) contains six fatty acids whereas lipid A containing 4 or 5 fatty acids is found in less pathogenic bacteria (mutated *E. coli*, *Rhodobacter sphaeroides*, *P. gingivalis*). The latter LPS are considered as antagonists because they can inhibit the activation of TLR4 induced by hexaacylated LPS [47]. Complete competitive inhibition of LPS activity is possible using a 100-fold excess of the antagonistic LPS from *Rhodobacter sphaeroides* (available from InvivoGen).

Agonistic LPS are divided in two categories based on the morphology of bacteria colonies: smooth or rough (S-LPS or R-LPS, respectively). S-LPS contains O-polysaccharide chains which are absent from R-LPS. Wild-type Gram-negative bacteria synthesize S-LPS which needs CD14 to signal through TLR4. Signaling by S-LPS through TLR4/CD14 activates both arms of the TLR4

pathway (i.e., MyD88-dependent and MyD88-independent; *see* Fig. 1). R-LPS can signal in the absence of CD14 but it does not activate the MyD88-independent pathway [48]. This property might be useful for in vitro experiments in the absence of TLR4 co-receptors but such activation of TLR4 is incomplete. Interestingly, it has been demonstrated that monophospholipid A, a candidate vaccine adjuvant, stimulates only the TRIF/TRAM arm of the TLR4 signaling [49]. This ligand is a promising tool to study the MyD88-independent response induced by TLR4 activation.

Basic purification protocols lead to LPS containing associated lipoproteins and thereby activation of TLR2 and TLR4. Phenol re-extraction of LPS is needed to retain only a TLR4 activity [50]. Purified LPS from different bacterial strains are commercially available and are active at 10 ng/ml.

Surprisingly, murine (but not human) TLR4 recognizes the antitumoral agent taxol [51]. Proteins of viral origin (e.g., respiratory syncytial virus, mouse mammary tumor virus) can also activate TLR4 [34]. Recently, heme has been shown to activate TLR4 in a CD14-dependent and MD2-independent manner [52].

TLR4 also recognizes endogenous ligands [53]; these include hyaluronate, fibrinogen, and HMGB1. These substances are generally released after tissue injury and might trigger a danger signal through TLR4 [54]. Activation of TLR4 by heat shock proteins is controversial as some authors have shown that this could be due to endotoxin contamination [55, 56].

2.5 TLR5

TLR5 recognizes monomeric flagellin, a constituent protein of bacterial flagella [57, 58]. Purified flagellin from *Salmonella typhimurium* or *Bacillus subtilis* is commercially available (InvivoGen, Bio-Techne). InvivoGen also proposes a recombinant *S. typhimurium* flagellin produced in mammalian cells that is devoid of TLR2/4 activity of bacterial origin. Flagellins are active at 0.1–1 μg/ml.

2.6 TLR6

TLR6 associates with TLR2 to recognize diacyl lipopeptides such as MALP-2 and FSL-1 [59]. Pam_2CSK_4 is a synthetic ligand for TLR2/6; it activates TLR6-expressing cells when used at 1–10 ng/ml. The level of activation is increased by the presence of CD14 and CD36 [60]. Along with the standard bacterial cell wall components available commercially, whole preparation of heat-killed bacteria (Gram-negative and Gram-positive) is available for TLR2/6 activation (InvivoGen). None of the available TLR ligands seem to activate TLR6 in the absence of TLR2. Nevertheless, artificial activation of a TLR6-specific signaling cascade showed that signaling through TLR6 homodimers is theoretically possible [34].

2.7 TLR7

TLR7 is expressed in endosomes; it is a receptor for ssRNA from viruses, especially U or GU-rich oligoribonucleotides such as RNA40 from the U5 region of HIV-1 RNA [61–63]. Activation

of murine TLR7 but not human TLR7 can be achieved using complexed ssRNAs. Imidazoquinolines, which are synthetic compounds with antiviral activities, including R848 (or resiquimod) and its water soluble derivative CL097 (InvivoGen), imiquimod and gardiquimod (specific for TLR7 when used at less than 1 μg/ml) have also been identified as TLR7 ligands [64]. In addition, TLR7 is specifically activated by nucleoside analogs, e.g., 1 mM loxoribine, a guanosine analog [65], and the adenine analogs CL264 and CL307 from InvivoGen [66]. Notably, while looking for siRNA directed against human TLR9, Hornung et al. have discovered that siRNA can specifically activate TLR7 [67]. This activity was attributed to a nine-base motif within a 19 *mer* sequence. Immune complexes (ICX) formed of RNA-specific antibodies and self-RNA can activate TLR7; this participates in the development of autoimmune diseases [53]. As a result, small nuclear ribonucleoproteins purified from ICX can be used as TLR7 ligands [68].

2.8 TLR8

TLR8 shares high sequence homology with TLR7 and can recognize most of the TLR7 ligands [62]. As mentioned above, ssRNAs activate human TLR8. Technically, it is possible to discriminate between TLR7 and TLR8 activity by using different concentrations of nucleotide analogs. 3M-002 from 3M Pharmaceuticals (sold as CL075 by InvivoGen) can specifically activate human TLR8 when used at 0.1 μg/ml (0.4 μM) whereas higher concentrations of this ligand are required to activate TLR7. Initially, TLR8 was considered to be active only in human and not in mouse, but a combination of 10 μM 3M-002 and 3M-003 with 1–3 μM polyT oligodeoxyribonucleotide (ODN) can activate mouse TLR8 [69].

2.9 TLR9

TLR9 is an intracellular TLR involved in the recognition of DNA from bacterial and viral origin but also self-DNA in ICX [8]. Non-self-DNA is detected by the presence of unmethylated CpG motifs. Extensive research has been done to characterize immunostimulatory CpG DNA motifs [70]. Two main classes have been described. Class A CpG is active on plasmacytoid dendritic cells (pDC). These reagents contain polyG motifs and a palindromic sequence on a mixed phosphodiester/phosphorothioate backbone and can multimerize to form large structures. Class B CpG contains one or more CpG and no polyG motifs on a phosphorothioate backbone and they activate B cells. Class C CpG shares class A and class B characteristics and properties. Despite the endosomal location of TLR9, CpG ODNs are usually added to the culture medium to activate $TLR9^{+}$ cells. The mechanism of activation by CpG has thus been challenging to understand. Tian et al. showed that class A CpG interacts with HMGB1 and the resulting complex is efficiently internalized by a mechanism involving the receptor for advanced glycation end products (RAGE) [71]. This RAGE-dependent mechanism is thought to facilitate the delivery of class A CpG to TLR9.

In vitro, the optimal concentration for immunostimulatory CpG ODN is 1 μM. Higher concentrations are usually less effective. It should be noted that some CpG ODNs show species specificities (human vs. mouse). The specificity of the activation by CpG ODN can be confirmed by the use of control CpG ODN which contains the same sequence as immunostimulatory CpG ODN but in which CpG dinucleotides have been replaced by GpC dinucleotides. Purified endotoxin-free *E. coli* DNA at 50 μg/ml can also be used as a TLR9 ligand. Natural CpG sequences from Gram-negative bacteria termed repetitive extragenic palindromics (REPs) have been isolated and shown to induce innate responses via TLR9 [72]. Immune complexes present in serum from SLE patients activate TLR9 by a mechanism involving the cell surface receptor FcγR (CD32) [73]. In vitro, patients' serum can activate TLR9-expressing cells.

Besides immunostimulatory ODNs acting through TLR9, inhibitory ODNs have been identified. The latter bind TLR9 but fail to induce the switch to an active conformation of TLR9. Inhibitory ODNs block signaling by competing with immunostimulatory ODNs for the binding site on TLR9 [74]. Two types of inhibitory ODNs have been identified: repeated TTAGGG motifs found in telomeres or ODN containing either unmethylated GC or methylated CG [75].

Hemozoin from *Plasmodium falciparum*, which was initially identified as a TLR9 ligand, seems to actually help bringing parasite DNA in close proximity with TLR9 to induce a response [76].

2.10 TLR10

TLR10 is expressed on B cells; it is closely related to TLR1 and TLR6 (48 and 46 % amino acid sequence identity, respectively) and may interact with TLR2 [77]. The ligand for TLR10 is still unknown. By use of homology modeling recent studies have shown the binding orientation of a human TLR10—TLR2 heterodimer to be similar with that of TLR2/1 and TLR2/6. Moreover, the study revealed that Pam_3CSK_4 might be the ligand for a human TLR10/2 complex and $PamCysPamSK_4$ might activate a human TLR10/1 hetero- and TLR10 homodimer [78]. Using chimeric CD4TLR10 (*see* Fig. 2 and Subheading 5), Hasan et al. showed that promoters activated by signaling through TLR10 include CXCL5, IL-4, NF-κB and to a lesser extent IL-2, TNF, and AP-1 [33]. Most recently, Oosting et al. demonstrate that TLR10 acts as an inhibitory receptor, with suppressive effects. The use of specific antibodies to block TLR10 significantly upregulated TLR2-mediated cytokine production [79].

2.11 TLR11 and TLR12

It is worth pointing out that while the mouse genome encodes 13 TLRs, the human genome lacks functional TLR11, TLR12, and TLR13. TLR11 is an endosomal TLR only functional in mice. It was first described as a receptor for uropathogenic bacteria [80] and studies have shown that it is activated by a protein resembling

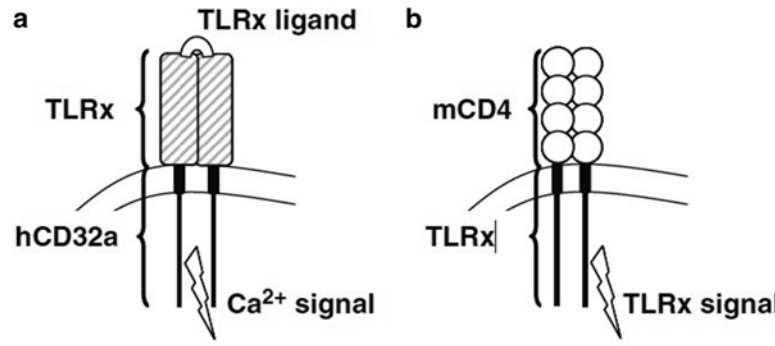

Fig. 2 Example of engineered TLRs (**a**, **b**)

Toxoplasma gondii profilin [81]. TLR12 is expressed in mice and rats [82]. TLR12 has been shown to form heterodimers with TLR11 for sensing and responding to *Toxoplasma gondii* profilin [83]. The expression and distribution of TLRs 11–13 in normal and parasite infected mouse brains has been demonstrated suggesting a role for them in central nervous system (CNS) infections [84].

2.12 TLR13

TLR13 is an endosomal murine receptor; the exact role and ligand for which remains unclear. However, several groups have identified the bacterial 23S ribosomal RNA (rRNA) sequence as a ligand for TLR13. Specifically, the conserved 23S ribosomal sequence "CGGAAAGACC," has been shown to induce cytokine production in a TLR13-, MyD88-, and UNC93B-dependent manner. (UNC93B is an accessory protein involved in the trafficking of intracellular TLRs including, TLR3/7/9). The conserved 23S rRNA sequence is the binding site of the macrolide-lincosamide-streptogramin (MLS) antibiotics, and 23S rRNA from bacteria resistant to these antibiotics is not recognized by TLR13. ORN Sa19 is a 19 *mer Staphylococcus aureus* rRNA derived oligoribonucleotide stabilized by a phosphorothioate modification available commercially and found to be highly stimulatory in murine TLR13-expressing cells (InvivoGen).

3 Host Cells

When it comes to choosing a relevant host cell to study TLR biology in vitro, several options are possible. Firstly, cell lines lacking TLR expression can be transfected with one or two TLRs with or without accessory molecules. The second option is to select cell lines naturally expressing TLR(s). Primary cells are another option as they might be more physiologically relevant (i.e., presence of normal expression level of TLRs and presence of crosstalk between

signaling pathways) but they are technically more difficult to handle than cell lines.

3.1 Cell Lines Lacking TLR Expression

Cells devoid of endogenous active TLR are a valuable tool to study individual TLRs. The most commonly used cell lines are of epithelial origin; they express all the signaling components needed downstream of TLR activation. Stable or transient transfection of one or two TLRs with or without accessory molecules renders them responsive to the corresponding ligand(s). This has been demonstrated in the following cell lines: HEK293 [85, 86], HeLa [87], COS7 [88], or CHO [89]. It should be noted that HEK293 cells, unlike the variant HEK293T, might have endogenous TLR3 and TLR5 activity [90].

Cells lacking endogenous TLR activity have been used to study TLR signaling, interactions between TLRs [91], requirement for accessory molecules [60], intracellular trafficking [85], or localization. The transfection efficiency in these epithelial cells is very high and the experiments described above can be easily done in transiently transfected cells. Alternatively, stable cell lines expressing TLR, accessory molecules, and even a reporter gene can be generated.

HEK293 cells stably expressing functional human or mouse TLR stably transfected or not with a reporter gene are commercially available from InvivoGen (HEK Blue™) and Bio-Techne (SEAPorter™ and LUCPorter™). The one concern about the use of cells overexpressing a TLR is that overexpression could result in mislocalization, i.e., an intracellular TLR might be found on the cell surface when overexpressed [92]. For that reason, cell lines expressing normal levels of TLRs are often the preferred model.

3.2 TLR Expressing Cell Lines

Cell lines expressing TLRs endogenously may also be used to study TLR function. However, they may require transfection of accessory molecules or co-receptors to increase the responsiveness of the cell. It is important to profile cell lines for TLR and accessory molecules expression before using them in an assay. This can be done by RT-PCR and confirmed by flow cytometry or western blot.

The following cell lines have been used in numerous TLR studies: RAW264.7 (mouse macrophage), THP-1 (human acute monocytic leukemia), and U937 (human promonocytic leukemia) and all belong to the monocyte/macrophage lineage. U373 are epithelial human glioblastoma astrocytoma cells and A549 are human alveolar basal epithelial cells. Cell lines having characteristics similar to human pDC have been described: PMDC05 [93], GEN2.2 [94], and CAL-1 [95]. These cell lines could be a good alternative to the use of primary pDC which are present in very low numbers among circulating blood cells. CD14 expression is needed to render U373 cells responsive to LPS [96] or to increase the responsiveness of THP-1 cells to several TLR2/4/5 ligands [97]. Differentiation induced by phorbol myristate acetate (PMA) or

Table 2
TLR responsiveness of selected cell lines (no TLR10 ligand has been identified yet; TLR11 is only functional in mouse cells)

	TLR1/2	TLR2	TLR3	TLR4	TLR5	TLR6/2	TLR7	TLR8	TLR9	TLR10
RAW264.7	+	+	+	+	+/−	+	+	+	+	
THP-1	+	+	−	+	+/−	+	−	+	+	+
U373-CD14	−	−	+	+	−	−	−	−	+/−	
GEN2.2	?	?	?	?	?	+	+	−	+	
A549	+	+	+	+/−	+	+	−	−	+	

See text for references. Symbol ? means "not known"

LPS also increases expression of TLRs and hence responsiveness of THP-1 cells to TLR ligands [98–100]. LPS responsiveness of A549 cells through TLR4 is controversial [101]. Table 2 shows the TLR profile of some of these cell lines. In addition, human myeloma cell lines have been shown to express a variety of TLR genes [102].

There are several TLR expressing cells stably transfected with a reporter gene available on the market which can be used to measure TLR activity: THP1-Blue™, THP1-Lucia™ (human monocytes), Ramos-Blue™ (B lymphocytes), Jurkat-Dual™ (T lymphocytes, TLR3$^+$), Raw-Blue™, Raw-Lucia™ (mouse macrophages) from InvivoGen (San Diego, CA), CellSensor™ (Life Technologies) derived from THP1 or RAW264.7 cells, and SEAPorter™ and LUCPorter™ RAW264.7 from Bio-Techne.

3.3 Isolated Primary Cells

Ideally, cell line studies should be complemented by studies in primary cells. The main problem with the use of primary cells is to choose the right cell type as there are discrepancies in the literature regarding the expression and functionality of TLRs.

It was initially thought that TLRs are restricted to cells of the immune system. However, TLRs have been found in other cell types such as epithelial cells (TLR2, 3, 4, 5, 9) [103], fibroblasts, and even cells from the nervous system [104]. Hornung et al. [105] and Applequist et al. [106] have measured the expression of TLR1-10 mRNA in different types of human or murine immune cells, but the presence of mRNA for a given TLR does not mean that this TLR is active. For example, eosinophils express TLR1, TLR4, TLR7, TLR8, TLR9, and TLR10 mRNA and only respond to stimulation with a TLR7 agonist [107]. Also worth noting is that while naive human CD4+ T cells express significant levels of intracellular TLR2 and TLR4 protein, cell surface expression of TLR2 and TLR4 is found only in activated CD4+ T cells [108]. Expression of TLRs in T cells remains controversial. Hemont et al. have inves-

Table 3
TLRs in human immune cells

	TLR1/2	TLR2	TLR3	TLR4	TLR5	TLR6/2	TLR7	TLR8	TLR9	TLR10
B cells [77, 142]	+	+	–	–	–	+	+	–	+	+
CD4⁺ T cells [143]	+	+	+	+	+	+	+[a]	+[a]	+[a]	–
CD8⁺ T cells [144]	–	+	+	+	–	+[a]	+	+	+[a]	–
Monocytes [145]	+	+	–	+	+	+	–	+	–	–
NK cells [146]	–	–	+	–	–	–	+	–	+	–
pDC [77, 147]	–	–	–	–	–	–	+	–	+	+

[a]Transcript only, i.e., TLR functionality not demonstrated

tigated TLR responsiveness of human mDC subsets using a whole blood assay followed by flow cytometry analysis [109]. Table 3 summarizes the panel of functional TLRs expressed by human immune cells. Expression levels are altered by pro-inflammatory signals or type I IFN treatment [99, 110]. In practice, the most commonly used primary cells are non-sorted peripheral blood mononuclear cells (PBMCs), monocytes, or B cells. Other cell types which are very valuable for the study of TLR biology (e.g., pDC) are more difficult to obtain in sufficient quantity.

Interestingly, mouse cells display a TLR profile similar to the corresponding human cells. One important difference is the LPS responsiveness of murine but not human naïve B cells through TLR4 [111]. Among primary cells, murine embryonic fibroblasts (MEF) isolated from mouse embryos are a very good model to study TLRs as they express all known TLRs [112]. Ex vivo, MEFs can be grown for over ten passages, after which their proliferation rate then declines.

3.4 Whole Blood

Whole blood assays emerged as a powerful way to investigate innate immune responses mediated by TLRs [113, 114]. They allow evaluation of TLR responsiveness in the absence of exogenous additives such as animal serum and antibiotics. In this type of assay, anticoagulated whole blood is incubated 3–48 h in the presence of TLR ligand(s) to activate different populations of blood cells resulting in the release of chemokines, cytokines, and interferons in the supernatant (i.e., plasma). From a practical point of view, several parameters have to be controlled to ensure the robustness of this type of assay: freshness of the blood, choice of anticoagulant, dilution of blood, time of sampling [115, 116], and medical treatment as immunosuppressive treatment will result in decreased ex vivo responses. It has been shown that a few hours after sampling the responsiveness of the blood is reduced possibly

due to the short half-life of some blood cell populations such as neutrophils [114]. Nevertheless, it is still possible to induce a TLR-mediated response in whole blood stored at room temperature for up to 48 h [114]. For whole blood assays, the preferred anticoagulant is heparin over EDTA which might interfere with TLR function. Frozen whole blood (stored at −80 °C) has been proposed as an alternative to the use of fresh blood [117]. Upon thawing, red blood cells are lyzed and hemoglobin is released in the supernatant which can interfere with some detection techniques. According to a supplier of frozen whole blood (e.g., sold as part of the pyrogen detection kit PyroDetect, Merck Millipore), storage at temperatures above −80 °C quickly reduces the responsiveness of frozen blood which limits its use in most of the labs.

Whole blood assays performed in 96- or 384-well plates allows the testing of many different stimuli with a small volume of blood as starting material. Blood from several donors/patients or even from newborns [118–121] can be processed in parallel. Of note, this type of assay is transposable to animal blood which allows the assessment of cross-species TLR responses [122–126].

Whole blood assays reflect donor to donor variability. Hence, in blood from normal donors, the stimulation by TLR ligands often results in secretion of cytokines over a wide range of concentrations. Great efforts are needed to normalize these assays. This process is ongoing in order to be able to use whole blood assays as a diagnostic test to identify immune disorders [127].

The use of cell lines or isolated primary cells remains a technique of choice when high throughput is required. In combination with this technique, whole blood assays bring additional information about the bioactivity of TLRs, their ligands and compounds interacting with them. As a consequence, whole blood assays have also been used in preclinical studies to characterize TLR modulators whether they are small molecules or biologics.

4 Readouts

As mentioned previously, signaling through the different TLRs involves mainly two families of transcription factors: NF-κB via a MyD88-dependent pathway (all TLRs except TLR3) and the IRFs via a MyD88-independent TRIF-dependent pathway (TLR3) or a MyD88-dependent pathway (TLR7/8/9). NF-κB and IRFs induce the expression of different sets of cytokines, chemokines, and interferons [128].

In order to determine TLR activity in each of the cell models outlined in Subheading 3, the following readouts can be used: measurement of cytokines, chemokines, and/or interferons secretion by simplex or multiplex immunoassays (ELISA, AlphaLISA, HTRF®, immunoPCR, Luminex); detection of activation markers

by western blot, RT-PCR, or flow cytometry; phosphorylation of signaling proteins; and nuclear translocation of transcription factors and/or reporter gene assays.

4.1 Protein Secretion

The simplest method to assay for the presence of functional TLR is to measure the production of pro-inflammatory cytokines and/or chemokines after TLR stimulation using specific ligands. ELISA is a widely used technique and validated kits to detect most of the biomarkers are available from several suppliers. ELISA results can be sufficient to distinguish between two signaling pathways, e.g., TRIF vs. MyD88 after TLR4 activation. TRIF activation will result in the production of G-CSF, CXCL10, CCL2, and CCL5 while MyD88 activation induces the secretion of IFNβ, IL-1β, IL-6, and CCL3 [20].

Multiple cytokines and chemokines can be detected simultaneously in a single small volume sample using multiplex techniques. Cytometric Bead Array (CBA; BD Biosciences) is based on the use of beads coated with an antibody recognizing a specific analyte. This system requires the use of a flow cytometer. xMAP technology (Luminex®) also uses beads available from Affymetrix eBioscience (ProcartaPlex™), Bio-Rad (Bio-Plex®), Merck Millipore (Milliplex®), and Bio-Techne but in a 96-well plate format. A compatible microplate reader is needed to process the samples. The multi-array technology by Meso Scale Discovery (MSD) uses electroluminescence detection. Wells of dedicated microplates (96 or 384 well) are coated with specific antibodies directed against cytokines, chemokines, or signaling proteins allowing the detection of up to ten different targets. Secondary antibodies are labeled with the SULFO-TAGTM reagent which emits light upon electrochemical stimulation. Specific readers (SECTOR) are required to process MSD microplates.

Immuno-PCR is a combination of ELISA and PCR [129]. Antibodies specific for the target(s) of interest are conjugated with a short DNA sequence. After the antibodies recognize their target, the DNA tag is amplified by real-time PCR. Compared to ELISA, immuno-PCR is more sensitive (down to fg/ml). Multiplexing and conjugation of DNA tags remain challenging and limit the generalization of this technique. Specialized suppliers are Innova Biosciences, Chimera Biotec, and Olink Bioscience.

Biomarker quantification by HTRF® (CisBio Bioassays) is based on time-resolved fluorescence resonance energy transfer (FRET). Two antibodies specific for the target are labeled with two different fluorophores: an acceptor and a donor. When the two antibodies are in close proximity, i.e., when they recognize their target, the excitation of the donor by a laser will result in energy transfer to the donor which then emits fluorescence. Unlike ELISA which requires several incubation/wash steps, HTRF® is a homogenous technique. HTRF® measurement is typically done in small

volume 384-well plates with only 10 µl sample. The detection range is wider with HTRF® compared to ELISA. There are much less HTRF® than ELISA kits available on the market and HTRF® requires the use of a microplate reader capable of time-resolved FRET measurement.

Finally, in a polymorphic population of cells such as whole blood, intracellular staining of cytokines by flow cytometry combined with cell surface staining allows the identification of cell types responsible for each cytokine produced in response to TLR stimulation [118].

4.2 Phosphorylation

The phosphorylation of signaling components, such as the MAPK p38 or the NF-κB subunit p65, occurs usually within minutes after TLR stimulation. There are several techniques to monitor protein phosphorylation, all of them rely on the availability of phospho-specific antibodies. Flow cytometry is performed on permeabilized cells whereas western blots and immunoassays (e.g., TransAM® from Active Motif and CASE™ from SABiosciences™, HTRF and AlphaScreen® (Perkin Elmer)) are performed using cell lysates. AlphaScreen® is interesting as it is designed to be used in high-throughput screening. This technique is a bead-based luminescent assay used to measure interactions between molecules. In the case of protein phosphorylation, two sets of beads containing different dyes are needed: one set of beads is coated with an antibody against the nonphosphorylated form of the target protein and another set of beads is coated with an antibody against the phosphorylated form of the protein. Beads are mixed with cell lysates and upon excitation light is emitted if both sets of beads are in close proximity, i.e., when the phosphorylated protein is present in the lysates. HTRF allows quantification of protein phosphorylation without the need for beads as antibodies are directly coupled with FRET-compatible fluorophores.

4.3 Translocation of Transcription Factors

Another way to monitor TLR activation is to look at the change in localization of transcription factors (TF) activated after ligand binding, e.g., NF-κB, IRFs. This can be assayed using high content screening (HCS) or high content analysis (HCA) assays. The TF is detected using immunochemistry techniques before and after stimulation and the intensity of the signal in the nucleus vs. cytoplasm is measured. Alternatively, cells can be transfected to express a fluorescent fusion protein with the TF (e.g., GFP-TF) and the change in localization can be observed in live cells [130]. HCS/HCA techniques require using adherent cells having a low nucleus/cytoplasm ratio. Finally, preparation of subcellular fractions using specific lysis buffers followed by protein detection by western blot is another method of choice.

4.4 Reporter Genes

Reporter gene assays are also used to monitor TLR activity. The most widely used promoter is derived from the ELAM-1 gene promoter modified to contain additional NF-κB motifs [131]. An artificial promoter containing five NF-κB binding sites is another option [132]. The reporter gene itself can code for a secreted protein (e.g., human placental alkaline phosphatase (SEAP) [133] or secreted luciferase [134]) or an intracytoplasmic protein like firefly luciferase [135]. Cells can be transiently or stably transfected with the reporter gene construct and a construct coding for a TLR. TLR activation induces NF-κB-dependent production of the reporter gene. SEAP is secreted in the supernatants of cells and can be detected using colorimetric (e.g., Quantiblue™ from InvivoGen) or chemiluminescent (Phosphalight™ from Applied Biosystems) techniques. With a secreted reporter protein, it is possible to measure TLR activation over the time simply by sampling the supernatants. It should be noted that serum (human or animal) often used in culture media contains heat labile alkaline phosphatase activity. Heating of samples at 65 °C for 10 min is sufficient to inactivate endogenous alkaline phosphatase activity prior to the measurement of SEAP activity which is not altered by heating.

Secreted luciferase systems are available from Clontech (Ready-To-Glow™), New England Biolabs (*Gaussia* Luciferase), and InvivoGen. Unlike techniques based on the detection of a secreted protein, "classical" luciferase measurement does not allow to do time course experiments as it requires lysing the cells. Luciferase detection products are available from several suppliers. In reporter gene assays, IRF-dependent and NF-κB-independent promoters are needed to cover the full range of signaling pathways activated by the TLRs. IRF-specific reporter gene assays can be designed based on specific binding sites described for certain cytokines, chemokines, or interferon promoters [33, 136, 137].

5 Engineered TLRs

The study of TLR biology is sometimes rendered difficult by the lack of a known ligand (e.g., for TLR10) or the accessibility of the receptor to its ligand(s) (e.g., TLR3/7/8/9). To overcome these technical problems, two techniques based on the use of engineered TLRs have been described.

In the first technique the extracellular part of a TLR is fused with the transmembrane (TM) and intracellular (IC) parts of hCD32a [41] (*see* Fig. 2a). The resulting chimeric protein can be expressed in HEK293 cells where it localizes on the cell surface. The engagement of this TLR by its ligand(s) results in a Ca^{2+} response/influx mediated by CD32a. The two main advantages of this technique are (1) intracellular TLRs become accessible to their

ligands added exogenously in the culture medium thereby facilitating the identification of new ligands and (2) one single readout (Ca^{2+}) can be used to monitor the activity of any TLR. Ca^{2+} influx is a very fast response that has been widely used as a readout in other domains (e.g., 7-TM receptors) and a lot of screening tools are available [138].

Using this technique, De Bouteiller et al. [41] have demonstrated the need for an acidic pH (~5.7) for TLR3 activity and the minimal requirements for TLR3 ligands (see TLR3 above). Nevertheless, when these chimeras are used to study intracellular TLRs, one should keep in mind that, in normal cells, a ligand identified with this technique will need access to the TLR. In addition, the amount of ligand needed to induce Ca^{2+} mobilization was about 50 times less than the amount needed to induce cytokine secretion by TLR3-expressing cells.

The second technique involves another fusion protein using the extracellular part of mouse CD4 fused with the TM and IC part of a TLR (see Fig. 2b) [39, 45]. These chimeric proteins (CD4TLRx) are expressed on the cell surface when transfected in HEK293T cells. The association of extracellular CD4 domains triggers the signaling cascade corresponding to the TM + IC of the TLR. Hence, the ligand for this TLR can remain unknown to study the signaling. This technique can also be used to select the best readout for a given TLR. For example, besides repeated κB binding sites which are the most used promoter for reporter gene assays, the promoters for the chemokines IL-8 and CXCL5 were shown to be strongly activated by several TLRs. Focusing on TLR10, which has no identified ligand yet, Hasan et al. [33] show that CD4TLR10 specifically activated IL-4, CXCL5, and NF-κB promoters after 48 h stimulation. This could be the basis to design an assay to identify TLR10 ligands. These results stress the importance of looking at more than one readout (usually NF-κB) when one studies TLR activity.

A last example of modified TLRs is the dominant negative (DN) forms. These mutants can be obtained by inserting a point mutation in the TIR domain preventing the binding of adaptor proteins or by deleting the intracellular TIR domain. Such mutated TLRs can bind their ligands but they cannot trigger the signaling cascade. Hence, overexpression of one mutated TLR specifically inhibits the activity of the endogenous TLR by competition [36, 39]. This technique can be used to show the involvement of each individual TLR in cells expressing several TLRs.

With new ligands discovered regularly, novel accessory molecules identified, and the potential for more TLRs to be discovered, there is a need for robust cell-based assays to monitor TLR activity. To keep up to date with latest developments, a rich database of bioassays is maintained by NCBI and hundreds of them are related to TLRs [139]. While “empty shells” such as HEK293 transformed

to express one TLR are still a very convenient tool, the future will probably see the rise of HCS and HTS assays in primary cells as the preferred techniques. Finally, the normalization of TLR assays using whole blood could be the basis for new diagnosis tools.

TLRs have the ability to harness great immunostimulatory signals and are therefore tightly regulated and activated. Incorrect and/or overactivation of these pathways can lead to autoimmune disease [140] and fatal sepsis [141]. Many questions remain surrounding the exact interaction of TLRs and their ligands, the complexities of which remain under constant investigation. TLR signaling and the responses they control continue to challenge thinking regarding the pathogenesis and treatment of cancers, immune and infectious diseases (*see* Part V, Chapters 21–25).

References

1. Takeda K, Akira S (2005) Toll-like receptors in innate immunity. Int Immunol 17:1–14
2. Gay NJ, Keith FJ (1991) Drosophila Toll and IL-1 receptor. Nature 351:355–356
3. Brikos C, O'Neill LA (2008) Signalling of Toll-like receptors. Handb Exp Pharmacol 183:21–50
4. Gay NJ, Gangloff M, Weber AN (2006) Toll-like receptors as molecular switches. Nat Rev Immunol 6:693–698
5. Kawai T, Akira S (2006) TLR signaling. Cell Death Differ 13:816–825
6. Boehme KW, Compton T (2004) Innate sensing of viruses by toll-like receptors. J Virol 78:7867–7873
7. Akira S, Takeda K (2004) Toll-like receptor signalling. Nat Rev Immunol 4:499–511
8. Barton GM, Kagan JC, Medzhitov R (2006) Intracellular localization of Toll-like receptor 9 prevents recognition of self DNA but facilitates access to viral DNA. Nat Immunol 7:49–56
9. Saitoh S, Akashi S, Yamada T, Tanimura N, Kobayashi M, Konno K, Matsumoto F, Fukase K, Kusumoto S, Nagai Y, Kusumoto Y, Kosugi A, Miyake K (2004) Lipid A antagonist, lipid IVa, is distinct from lipid A in interaction with Toll-like receptor 4 (TLR4)-MD-2 and ligand-induced TLR4 oligomerization. Int Immunol 16:961–969
10. Botos I, Liu L, Wang Y, Segal DM, Davies DR (2009) The toll-like receptor 3:dsRNA signaling complex. Biochim Biophys Acta 1789:667–674
11. Wang Y, Liu L, Davies DR, Segal DM (2010) Dimerization of Toll-like receptor 3 (TLR3) is required for ligand binding. J Biol Chem 285:36836–36841
12. Liu L, Botos I, Wang Y, Leonard JN, Shiloach J, Segal DM, Davies DR (2008) Structural basis of toll-like receptor 3 signaling with double-stranded RNA. Science 320:379–381
13. Jin MS, Kim SE, Heo JY, Lee ME, Kim HM, Paik SG, Lee H, Lee JO (2007) Crystal structure of the TLR1-TLR2 heterodimer induced by binding of a tri-acylated lipopeptide. Cell 130:1071–1082
14. Kim HM, Park BS, Kim JI, Kim SE, Lee J, Oh SC, Enkhbayar P, Matsushima N, Lee H, Yoo OJ, Lee JO (2007) Crystal structure of the TLR4-MD-2 complex with bound endotoxin antagonist Eritoran. Cell 130:906–917
15. Yoon SI, Kurnasov O, Natarajan V, Hong M, Gudkov AV, Osterman AL, Wilson IA (2012) Structural basis of TLR5-flagellin recognition and signaling. Science 335:859–864
16. Tanji H, Ohto U, Shibata T, Miyake K, Shimizu T (2013) Structural reorganization of the Toll-like receptor 8 dimer induced by agonistic ligands. Science 339:1426–1429
17. Nyman T, Stenmark P, Flodin S, Johansson I, Hammarstrom M, Nordlund P (2008) The crystal structure of the human toll-like receptor 10 cytoplasmic domain reveals a putative signaling dimer. J Biol Chem 283:11861–11865
18. Gangloff M, Weber AN, Gay NJ (2005) Conserved mechanisms of signal transduction by Toll and Toll-like receptors. J Endotoxin Res 11:294–298
19. Nunez Miguel R, Wong J, Westoll JF, Brooks HJ, O'Neill LA, Gay NJ, Bryant CE, Monie TP (2007) A dimer of the Toll-like receptor 4 cytoplasmic domain provides a specific scaffold for the recruitment of signalling adaptor proteins. PLoS One 2, e788

20. Akira S, Yamamoto M, Takeda K (2003) Role of adapters in Toll-like receptor signalling. Biochem Soc Trans 31:637–642
21. Lu YC, Yeh WC, Ohashi PS (2008) LPS/TLR4 signal transduction pathway. Cytokine 42:145–151
22. Kaisho T, Akira S (2006) Toll-like receptor function and signaling. J Allergy Clin Immunol 117:979–987, quiz 988
23. Yamamoto M, Sato S, Hemmi H, Sanjo H, Uematsu S, Kaisho T, Hoshino K, Takeuchi O, Kobayashi M, Fujita T, Takeda K, Akira S (2002) Essential role for TIRAP in activation of the signalling cascade shared by TLR2 and TLR4. Nature 420:324–329
24. Takeda K, Akira S (2004) TLR signaling pathways. Semin Immunol 16:3–9
25. Kawai T, Adachi O, Ogawa T, Takeda K, Akira S (1999) Unresponsiveness of MyD88-deficient mice to endotoxin. Immunity 11:115–122
26. Stack J, Doyle SL, Connolly DJ, Reinert LS, O'Keeffe KM, McLoughlin RM, Paludan SR, Bowie AG (2014) TRAM is required for TLR2 endosomal signaling to type I IFN induction. J Immunol 193(12):6090–6102
27. Volpi C, Fallarino F, Pallotta MT, Bianchi R, Vacca C, Belladonna ML, Orabona C, De Luca A, Boon L, Romani L, Grohmann U, Puccetti P (2013) High doses of CpG oligodeoxynucleotides stimulate a tolerogenic TLR9-TRIF pathway. Nat Commun 4:1852
28. Hennessy EJ, Parker AE, O'Neill LA (2010) Targeting Toll-like receptors: emerging therapeutics? Nat Rev Drug Discov 9:293–307
29. Gay NJ, Gangloff M (2007) Structure and function of Toll receptors and their ligands. Annu Rev Biochem 76:141–165
30. Rutz M, Metzger J, Gellert T, Luppa P, Lipford GB, Wagner H, Bauer S (2004) Toll-like receptor 9 binds single-stranded CpG-DNA in a sequence- and pH-dependent manner. Eur J Immunol 34:2541–2550
31. Oldenburg M, Kruger A, Ferstl R, Kaufmann A, Nees G, Sigmund A, Bathke B, Lauterbach H, Suter M, Dreher S, Koedel U, Akira S, Kawai T, Buer J, Wagner H, Bauer S, Hochrein H, Kirschning CJ (2012) TLR13 recognizes bacterial 23S rRNA devoid of erythromycin resistance-forming modification. Science 337:1111–1115
32. Takeuchi O, Sato S, Horiuchi T, Hoshino K, Takeda K, Dong Z, Modlin RL, Akira S (2002) Cutting edge: role of Toll-like receptor 1 in mediating immune response to microbial lipoproteins. J Immunol 169:10–14
33. Hasan UA, Dollet S, Vlach J (2004) Differential induction of gene promoter constructs by constitutively active human TLRs. Biochem Biophys Res Commun 321:124–131
34. Akira S, Uematsu S, Takeuchi O (2006) Pathogen recognition and innate immunity. Cell 124:783–801
35. Schwandner R, Dziarski R, Wesche H, Rothe M, Kirschning CJ (1999) Peptidoglycan- and lipoteichoic acid-induced cell activation is mediated by toll-like receptor 2. J Biol Chem 274:17406–17409
36. Sandor F, Latz E, Re F, Mandell L, Repik G, Golenbock DT, Espevik T, Kurt-Jones EA, Finberg RW (2003) Importance of extra- and intracellular domains of TLR1 and TLR2 in NFkappa B signaling. J Cell Biol 162:1099–1110
37. Park JS, Gamboni-Robertson F, He Q, Svetkauskaite D, Kim JY, Strassheim D, Sohn JW, Yamada S, Maruyama I, Banerjee A, Ishizaka A, Abraham E (2006) High mobility group box 1 protein interacts with multiple Toll-like receptors. Am J Physiol Cell Physiol 290:C917–C924
38. Flo TH, Halaas O, Lien E, Ryan L, Teti G, Golenbock DT, Sundan A, Espevik T (2000) Human toll-like receptor 2 mediates monocyte activation by Listeria monocytogenes but not by group B streptococci or lipopolysaccharide. J Immunol 164(4):2064–2069
39. Ozinsky A, Underhill DM, Fontenot JD, Hajjar AM, Smith KD, Wilson CB, Schroeder L, Aderem A (2000) The repertoire for pattern recognition of pathogens by the innate immune system is defined by cooperation between toll-like receptors. Proc Natl Acad Sci U S A 97:13766–13771
40. Girardin SE, Boneca IG, Carneiro LA, Antignac A, Jehanno M, Viala J, Tedin K, Taha MK, Labigne A, Zahringer U, Coyle AJ, DiStefano PS, Bertin J, Sansonetti PJ, Philpott DJ (2003) Nod1 detects a unique muropeptide from gram-negative bacterial peptidoglycan. Science 300:1584–1587
41. de Bouteiller O, Merck E, Hasan UA, Hubac S, Benguigui B, Trinchieri G, Bates EE, Caux C (2005) Recognition of double-stranded RNA by human toll-like receptor 3 and downstream receptor signaling requires multimerization and an acidic pH. J Biol Chem 280(46):38133–38145
42. Marshall-Clarke S, Downes JE, Haga IR, Bowie AG, Borrow P, Pennock JE, Grencis RK, Rothwell P (2007) Polyinosinic acid is a ligand for toll-like receptor 3. J Biol Chem 282(34):24759–24766

43. Kato H, Takeuchi O, Sato S, Yoneyama M, Yamamoto M, Matsui K, Uematsu S, Jung A, Kawai T, Ishii KJ, Yamaguchi O, Otsu K, Tsujimura T, Koh CS, Reis e Sousa C, Matsuura Y, Fujita C, Akira S (2006) Differential roles of MDA5 and RIG-I helicases in the recognition of RNA viruses. Nature 441:101–105
44. Zhou Y, Guo M, Wang X, Li J, Wang Y, Ye L, Dai M, Zhou L, Persidsky Y, Ho W (2013) TLR3 activation efficiency by high or low molecular mass poly I:C. Innate Immun 19:184–192
45. Medzhitov R, Preston-Hurlburt P, Janeway CA Jr (1997) A human homologue of the Drosophila Toll protein signals activation of adaptive immunity. Nature 388:394–397
46. Caroff M, Karibian D (2003) Structure of bacterial lipopolysaccharides. Carbohydr Res 338:2431–2447
47. Coats SR, Reife RA, Bainbridge BW, Pham TT, Darveau RP (2003) Porphyromonas gingivalis lipopolysaccharide antagonizes Escherichia coli lipopolysaccharide at toll-like receptor 4 in human endothelial cells. Infect Immun 71:6799–6807
48. Huber M, Kalis C, Keck S, Jiang ZF, Georgel P, Du X, Shamel L, Sovath S, Mudd S, Beutler B, Galanos C, Freudenberg MA (2006) R-form LPS, the master key to the activation of TLR4/MD-2-positive cells. Eur J Immunol 36:701–711
49. Mata-Haro V, Cekic C, Martin M, Chilton PM, Casella CR, Mitchell TC (2007) The vaccine adjuvant monophosphoryl lipid A as a TRIF-biased agonist of TLR4. Science 316:1628–1632
50. Hirschfeld M, Ma Y, Weis JH, Vogel SN, Weis JJ (2000) Cutting edge: repurification of lipopolysaccharide eliminates signaling through both human and murine toll-like receptor 2. J Immunol 165:618–622
51. Kawasaki K, Akashi S, Shimazu R, Yoshida T, Miyake K, Nishijima M (2001) Involvement of TLR4/MD-2 complex in species-specific lipopolysaccharide-mimetic signal transduction by Taxol. J Endotoxin Res 7:232–236
52. Figueiredo RT, Fernandez PL, Mourao-Sa DS, Porto BN, Dutra FF, Alves LS, Oliveira MF, Oliveira PL, Graca-Souza AV, Bozza MT (2007) Characterization of heme as activator of toll-like receptor 4. J Biol Chem 282:20221–20229
53. Marshak-Rothstein A (2006) Toll-like receptors in systemic autoimmune disease. Nat Rev Immunol 6:823–835
54. Matzinger P (2002) The danger model: a renewed sense of self. Science 296:301–305
55. Gao B, Tsan MF (2003) Recombinant human heat shock protein 60 does not induce the release of tumor necrosis factor alpha from murine macrophages. J Biol Chem 278:22523–22529
56. Ohashi K, Burkart V, Flohe S, Kolb H (2000) Cutting edge: heat shock protein 60 is a putative endogenous ligand of the toll-like receptor-4 complex. J Immunol 164:558–561
57. Smith KD, Andersen-Nissen E, Hayashi F, Strobe K, Bergman MA, Barrett SL, Cookson BT, Aderem A (2003) Toll-like receptor 5 recognizes a conserved site on flagellin required for protofilament formation and bacterial motility. Nat Immunol 4:1247–1253
58. Hayashi F, Smith KD, Ozinsky A, Hawn TR, Yi EC, Goodlett DR, Eng JK, Akira S, Underhill DM, Aderem A (2001) The innate immune response to bacterial flagellin is mediated by Toll-like receptor 5. Nature 410:1099–1103
59. Okusawa T, Fujita M, Nakamura J, Into T, Yasuda M, Yoshimura A, Hara Y, Hasebe A, Golenbock DT, Morita M, Kuroki Y, Ogawa T, Shibata K (2004) Relationship between structures and biological activities of mycoplasmal diacylated lipopeptides and their recognition by toll-like receptors 2 and 6. Infect Immun 72:1657–1665
60. Triantafilou M, Gamper FG, Haston RM, Mouratis MA, Morath S, Hartung T, Triantafilou K (2006) Membrane sorting of toll-like receptor (TLR) -2/6 and TLR2/1 heterodimers at the cell surface determines heterotypic associations with CD36 and intracellular targeting. J Biol Chem 281:31002–31011
61. Diebold SS, Kaisho T, Hemmi H, Akira S, Reis e Sousa C (2004) Innate antiviral responses by means of TLR7-mediated recognition of single-stranded RNA. Science 303:1529–1531
62. Heil F, Hemmi H, Hochrein H, Ampenberger F, Kirschning C, Akira S, Lipford G, Wagner H, Bauer S (2004) Species-specific recognition of single-stranded RNA via toll-like receptor 7 and 8. Science 303:1526–1529
63. Lund JM, Alexopoulou L, Sato A, Karow M, Adams NC, Gale NW, Iwasaki A, Flavell RA (2004) Recognition of single-stranded RNA viruses by Toll-like receptor 7. Proc Natl Acad Sci U S A 101
64. Hemmi H, Kaisho T, Takeuchi O, Sato S, Sanjo H, Hoshino K, Horiuchi T, Tomizawa H, Takeda K, Akira S (2002) Small anti-viral compounds activate immune cells via the TLR7 MyD88-dependent signaling pathway. Nat Immunol 3:196–200

65. Heil F, Ahmad-Nejad P, Hemmi H, Hochrein H, Ampenberger F, Gellert T, Dietrich H, Lipford G, Takeda K, Akira S, Wagner H, Bauer S (2003) The Toll-like receptor 7 (TLR7)-specific stimulus loxoribine uncovers a strong relationship within the TLR7, 8 and 9 subfamily. Eur J Immunol 33:2987–2997
66. Kobold S, Wiedemann G, Rothenfusser S, Endres S (2014) Modes of action of TLR7 agonists in cancer therapy. Immunotherapy 6:1085–1095
67. Hornung V, Guenthner-Biller M, Bourquin C, Ablasser A, Schlee M, Uematsu S, Noronha A, Manoharan M, Akira S, de Fougerolles A, Endres S, Hartmann G (2005) Sequence-specific potent induction of IFN-alpha by short interfering RNA in plasmacytoid dendritic cells through TLR7. Nat Med 11:263–270
68. Savarese E, Chae OW, Trowitzsch S, Weber G, Kastner B, Akira S, Wagner H, Schmid RM, Bauer S, Krug A (2006) U1 small nuclear ribonucleoprotein immune complexes induce type I interferon in plasmacytoid dendritic cells through TLR7. Blood 107:3229–3234
69. Gorden KK, Qiu XX, Binsfeld CC, Vasilakos JP, Alkan SS (2006) Cutting edge: activation of murine TLR8 by a combination of imidazoquinoline immune response modifiers and polyT oligodeoxynucleotides. J Immunol 177:6584–6587
70. Krieg AM (2006) Therapeutic potential of Toll-like receptor 9 activation. Nat Rev Drug Discov 5:471–484
71. Tian J, Avalos AM, Mao SY, Chen B, Senthil K, Wu H, Parroche P, Drabic S, Golenbock D, Sirois C, Hua J, An LL, Audoly L, La Rosa G et al (2007) Toll-like receptor 9-dependent activation by DNA-containing immune complexes is mediated by HMGB1 and RAGE. Nat Immunol 8(5):487–496
72. Magnusson M, Tobes R, Sancho J, Pareja E (2007) Cutting edge: natural DNA repetitive extragenic sequences from gram-negative pathogens strongly stimulate TLR9. J Immunol 179:31–35
73. Boule MW, Broughton C, Mackay F, Akira S, Marshak-Rothstein A, Rifkin IR (2004) Toll-like receptor 9-dependent and -independent dendritic cell activation by chromatin-immunoglobulin G complexes. J Exp Med 199:1631–1640
74. Latz E, Verma A, Visintin A, Gong M, Sirois CM, Klein DC, Monks BG, McKnight CJ, Lamphier MS, Duprex WP, Espevik T, Golenbock DT (2007) Ligand-induced conformational changes allosterically activate Toll-like receptor 9. Nat Immunol 8:772–779
75. Lenert P (2005) Inhibitory oligodeoxynucleotides – therapeutic promise for systemic autoimmune diseases? Clin Exp Immunol 140:1–10
76. Kalantari P, DeOliveira RB, Chan J, Corbett Y, Rathinam V, Stutz A, Latz E, Gazzinelli RT, Golenbock DT, Fitzgerald KA (2014) Dual engagement of the NLRP3 and AIM2 inflammasomes by plasmodium-derived hemozoin and DNA during malaria. Cell Rep 6:196–210
77. Hasan U, Chaffois C, Gaillard C, Saulnier V, Merck E, Tancredi S, Guiet C, Briere F, Vlach J, Lebecque S, Trinchieri G, Bates EE (2005) Human TLR10 is a functional receptor, expressed by B cells and plasmacytoid dendritic cells, which activates gene transcription through {MyD} 88. J Immunol 174:2942–2950
78. Govindaraj RG, Manavalan B, Lee G, Choi S (2010) Molecular modeling-based evaluation of hTLR10 and identification of potential ligands in Toll-like receptor signaling. PLoS One 5, e12713
79. Oosting M, Cheng SC, Bolscher JM, Vestering-Stenger R, Plantinga TS, Verschueren IC, Arts P, Garritsen A, van Eenennaam H, Sturm P, Kullberg BJ, Hoischen A, Adema GJ, van der Meer JW, Netea MG, Joosten LA (2014) Human TLR10 is an anti-inflammatory pattern-recognition receptor. Proc Natl Acad Sci U S A 111:E4478–E4484
80. Zhang D, Zhang G, Hayden MS, Greenblatt MB, Bussey C, Flavell RA, Ghosh S (2004) A toll-like receptor that prevents infection by uropathogenic bacteria. Science 303:1522–1526
81. Yarovinsky F, Zhang D, Andersen JF, Bannenberg GL, Serhan CN, Hayden MS, Hieny S, Sutterwala FS, Flavell RA, Ghosh S, Sher A (2005) TLR11 activation of dendritic cells by a protozoan profilin-like protein. Science 308:1626–1629
82. Roach JC, Glusman G, Rowen L, Kaur A, Purcell MK, Smith KD, Hood LE, Aderem A (2005) The evolution of vertebrate Toll-like receptors. Proc Natl Acad Sci U S A 102:9577–9582
83. Andrade WA, Souza Mdo C, Ramos-Martinez E, Nagpal K, Dutra MS, Melo MB, Bartholomeu DC, Ghosh S, Golenbock DT, Gazzinelli RT (2013) Combined action of nucleic acid-sensing Toll-like receptors and TLR11/TLR12 heterodimers imparts resistance to Toxoplasma gondii in mice. Cell Host Microbe 13:42–53

84. Mishra BB, Gundra UM, Teale JM (2008) Expression and distribution of Toll-like receptors 11–13 in the brain during murine neurocysticercosis. J Neuroinflammation 5:53
85. Latz E, Visintin A, Lien E, Fitzgerald KA, Monks BG, Kurt-Jones EA, Golenbock DT, Espevik T (2002) Lipopolysaccharide rapidly traffics to and from the Golgi apparatus with the toll-like receptor 4-MD-2-CD14 complex in a process that is distinct from the initiation of signal transduction. J Biol Chem 277:47834–47843
86. Yang RB, Mark MR, Gray A, Huang A, Xie MH, Zhang M, Goddard A, Wood WI, Gurney AL, Godowski PJ (1998) Toll-like receptor-2 mediates lipopolysaccharide-induced cellular signalling. Nature 395:284–288
87. Pridmore AC, Wyllie DH, Abdillahi F, Steeghs L, van der Ley P, Dower SK, Read RC (2001) A lipopolysaccharide-deficient mutant of Neisseria meningitidis elicits attenuated cytokine release by human macrophages and signals via toll-like receptor (TLR) 2 but not via TLR4/MD2. J Infect Dis 183:89–96
88. Matsuguchi T, Takagi K, Musikacharoen T, Yoshikai Y (1999) Gene expressions of lipopolysaccharide receptors, toll-like receptors 2 and 4, are differently regulated in mouse T lymphocytes. Blood 95(56):1378–1385
89. Yoshimura A, Lien E, Ingalls RR, Tuomanen E, Dziarski R, Golenbock D (1999) Cutting edge: recognition of Gram-positive bacterial cell wall components by the innate immune system occurs via Toll-like receptor 2. J Immunol 163:1–5
90. Hasan UA, Trinchieri G, Vlach J (2005) Toll-like receptor signaling stimulates cell cycle entry and progression in fibroblasts. J Biol Chem 280:20620–20627
91. Wang J, Shao Y, Bennett TA, Shankar RA, Wightman PD, Reddy LG (2006) The functional effects of physical interactions among Toll-like receptors 7, 8, and 9. J Biol Chem 281:37427–37434
92. Takeshita F, Leifer CA, Gursel I, Ishii KJ, Takeshita S, Gursel M, Klinman DM (2001) Cutting edge: role of Toll-like receptor 9 in CpG DNA-induced activation of human cells. J Immunol 167:3555–3558
93. Watanabe N, Narita M, Yamahira A, Nakamura T, Tochiki N, Saitoh A, Kaji M, Hashimoto S, Furukawa T, Toba K, Fuse I, Aizawa Y, Takahashi M (2010) Transformation of dendritic cells from plasmacytoid to myeloid in a leukemic plasmacytoid dendritic cell line (PMDC05). Leuk Res 34:1517–1524
94. Chaperot L, Blum A, Manches O, Lui G, Angel J, Molens JP, Plumas J (2006) Virus or TLR agonists induce TRAIL-mediated cytotoxic activity of plasmacytoid dendritic cells. J Immunol 176:248–255
95. Maeda T, Murata K, Fukushima T, Sugahara K, Tsuruda K, Anami M, Onimaru Y, Tsukasaki K, Tomonaga M, Moriuchi R, Hasegawa H, Yamada Y, Kamihira S (2005) A novel plasmacytoid dendritic cell line, CAL-1 established from a patient with blastic natural killer, cell lymphoma. Int J Hematol 81:148–154
96. Tapping RI, Orr SL, Lawson EM, Soldau K, Tobias PS (1999) Membrane-anchored forms of lipopolysaccharide (LPS)-binding protein do not mediate cellular responses to LPS independently of CD14. J Immunol 162:5483–5487
97. InvivoGen (2006) InvivoGen Insight Newsletter: TLR7 and TLR8. http://www.InvivoGen.com/docs/Insight200609.pdf
98. Park EK, Jung HS, Yang HI, Yoo MC, Kim C, Kim KS (2007) Optimized THP-1 differentiation is required for the detection of responses to weak stimuli. Inflamm Res 56:45–50
99. Zarember KA, Godowski PJ (2002) Tissue expression of human Toll-like receptors and differential regulation of Toll-like receptor mRNAs in leukocytes in response to microbes, their products, and cytokines. J Immunol 168:554–561
100. Chanput W, Mes JJ, Wichers HJ (2014) THP-1 cell line: an in vitro cell model for immune modulation approach. Int Immunopharmacol 23:37–45
101. Hippenstiel S, Opitz B, Schmeck B, Suttorp N (2006) Lung epithelium as a sentinel and effector system in pneumonia—molecular mechanisms of pathogen recognition and signal transduction. Respir Res 7:97
102. Jego G, Bataille R, Geffroy-Luseau A, Descamps G, Pellat-Deceunynck C (2006) Pathogen-associated molecular patterns are growth and survival factors for human myeloma cells through Toll-like receptors. Leukemia 20:1130–1137
103. Sha Q, Truong-Tran AQ, Plitt JR, Beck LA, Schleimer RP (2004) Activation of airway epithelial cells by toll-like receptor agonists. Am J Respir Cell Mol Biol 31:358–364
104. Ma Y, Li J, Chiu I, Wang Y, Sloane JA, Lu J, Kosaras B, Sidman RL, Volpe JJ, Vartanian T (2006) Toll-like receptor 8 functions as a negative regulator of neurite outgrowth and inducer of neuronal apoptosis. J Cell Biol 175:209–215
105. Hornung V, Rothenfusser S, Britsch S, Krug A, Jahrsdorfer B, Giese T, Endres S, Hartmann G (2002) Quantitative expression of toll-like receptor 1–10 mRNA in cellular subsets of

human peripheral blood mononuclear cells and sensitivity to CpG oligodeoxynucleotides. J Immunol 168:4531–4537

106. Applequist SE, Wallin RP, Ljunggren HG (2002) Variable expression of Toll-like receptor in murine innate and adaptive immune cell lines. Int Immunol 14:1065–1074
107. Nagase H, Okugawa S, Ota Y, Yamaguchi M, Tomizawa H, Matsushima K, Ohta K, Yamamoto K, Hirai K (2003) Expression and function of Toll-like receptors in eosinophils: activation by Toll-like receptor 7 ligand. J Immunol 171:3977–3982
108. Komai-Koma M, Jones L, Ogg GS, Xu D, Liew FY (2004) TLR2 is expressed on activated T cells as a costimulatory receptor. Proc Natl Acad Sci U S A 101:3029–3034
109. Hemont C, Neel A, Heslan M, Braudeau C, Josien R (2013) Human blood mDC subsets exhibit distinct TLR repertoire and responsiveness. J Leukoc Biol 93:599–609
110. Siren J, Pirhonen J, Julkunen I, Matikainen S (2005) IFN-alpha regulates TLR-dependent gene expression of IFN-alpha, IFN-beta, IL-28, and IL-29. J Immunol 174:1932
111. Hoshino K, Takeuchi O, Kawai T, Sanjo H, Ogawa T, Takeda Y, Takeda K, Akira S (1999) Cutting edge: Toll-like receptor 4 (TLR4) -deficient mice are hyporesponsive to lipopolysaccharide: evidence for TLR4 as the Lps gene product. J Immunol 162:6686–6687
112. Kurt-Jones EA, Sandor F, Ortiz Y, Bowen GN, Counter SL, Wang TC, Finberg RW (2004) Use of murine embryonic fibroblasts to define Toll-like receptor activation and specificity. J Endotoxin Res 10:419–424
113. Thurm CW, Halsey JF (2005) Measurement of cytokine production using whole blood. Curr Protoc Immunol Unit 7:18B
114. Blimkie D, Fortuno ES III, Yan H, Cho P, Ho K, Turvey SE, Marchant A, Goriely S, Kollmann TR (2011) Variables to be controlled in the assessment of blood innate immune responses to Toll-like receptor stimulation. J Immunol Methods 366:89–99
115. Hermann C, von Aulock S, Dehus O, Keller M, Okigami H, Gantner F, Wendel A, Hartung T (2006) Endogenous cortisol determines the circadian rhythm of lipopolysaccharide—but not lipoteichoic acid—inducible cytokine release. Eur J Immunol 36:371–379
116. Petrovsky N, Harrison LC (1995) Cytokine-based human whole blood assay for the detection of antigen-reactive T cells. J Immunol Methods 186:37–46
117. Schindler S, Asmus S, von Aulock S, Wendel A, Hartung T, Fennrich S (2004) Cryopreservation of human whole blood for pyrogenicity testing. J Immunol Methods 294:89–100
118. Smolen KK, Cai B, Gelinas L, Fortuno ES III, Larsen M, Speert DP, Chamekh M, Cooper PJ, Esser M, Marchant A, Kollmann TR (2014) Single-cell analysis of innate cytokine responses to pattern recognition receptor stimulation in children across four continents. J Immunol 193:3003–3012
119. Burl S, Townend J, Njie-Jobe J, Cox M, Adetifa UJ, Touray E, Philbin VJ, Mancuso C, Kampmann B, Whittle H, Jaye A, Flanagan KL, Levy O (2011) Age-dependent maturation of Toll-like receptor-mediated cytokine responses in Gambian infants. PLoS One 6, e18185
120. Levy O, Zarember KA, Roy RM, Cywes C, Godowski PJ, Wessels MR (2004) Selective impairment of TLR-mediated innate immunity in human newborns: neonatal blood plasma reduces monocyte TNF-alpha induction by bacterial lipopeptides, lipopolysaccharide, and imiquimod, but preserves the response to R-848. J Immunol 173:4627–4634
121. Labuda LA, de Jong SE, Meurs L, Amoah AS, Mbow M, Ateba-Ngoa U, van der Ham AJ, Knulst AC, Yazdanbakhsh M, Adegnika AA (2014) Differences in innate cytokine responses between European and African children. PLoS One 9, e95241
122. Deitschel SJ, Kerl ME, Chang CH, DeClue AE (2010) Age-associated changes to pathogen-associated molecular pattern-induced inflammatory mediator production in dogs. J Vet Emerg Crit Care (San Antonio) 20:494–502
123. Figueiredo MD, Moore JN, Vandenplas ML, Sun WC, Murray TF (2008) Effects of the second-generation synthetic lipid A analogue E5564 on responses to endotoxin in [corrected] equine whole blood and monocytes. Am J Vet Res 69:796–803
124. Karper JC, Ewing MM, de Vries MR, de Jager SC, Peters EA, de Boer HC, van Zonneveld AJ, Kuiper J, Huizinga EG, Brondijk TH, Jukema JW, Quax PH (2013) TLR accessory molecule RP105 (CD180) is involved in post-interventional vascular remodeling and soluble RP105 modulates neointima formation. PLoS One 8, e67923
125. Chen YW, Smith ML, Sheets MP, Ballaron SJ, Trevillyan JM, Fey TA, Gauvin DM, Kolano R, Pong MS, Hsieh GC, Bauch J, Marsh K, Carter G, Luly J, Djuric S, Mollison KW (1999) Ex vivo assessment of immunosuppression in undiluted whole blood from pigs dosed with tacrolimus (FK506). Clin Immunol 90:133–140
126. Dietsch GN, Dipalma CR, Eyre RJ, Pham TQ, Poole KM, Pefaur NB, Welch WD,

Trueblood E, Kerns WD, Kanaly ST (2006) Characterization of the inflammatory response to a highly selective PDE4 inhibitor in the rat and the identification of biomarkers that correlate with toxicity. Toxicol Pathol 34:39–51

127. Duffy D, Rouilly V, Libri V, Hasan M, Beitz B, David M, Urrutia A, Bisiaux A, Labrie ST, Dubois A, Boneca IG, Delval C, Thomas S, Rogge L, Schmolz M, Quintana-Murci L, Albert ML, Milieu Interieur Consortium (2014) Functional analysis via standardized whole-blood stimulation systems defines the boundaries of a healthy immune response to complex stimuli. Immunity 40:436–450
128. O'Neill LA, Bowie AG (2007) The family of five: TIR-domain-containing adaptors in Toll-like receptor signalling. Nat Rev Immunol 7:353–364
129. Hansen MC, Nederby L, Henriksen MO, Hansen M, Nyvold CG (2014) Sensitive ligand-based protein quantification using immuno-PCR: a critical review of single-probe and proximity ligation assays. Biotechniques 56:217–228
130. Pranada AL, Metz S, Herrmann A, Heinrich PC, Muller-Newen G (2004) Real time analysis of STAT3 nucleocytoplasmic shuttling. J Biol Chem 279:15114–15123
131. Schindler U, Baichwal VR (1994) Three NF-kappa B binding sites in the human E-selectin gene required for maximal tumor necrosis factor alpha-induced expression. Mol Cell Biol 14:5820–5831
132. Johnson CM, Tapping RI (2007) Microbial products stimulate human Toll-like receptor 2 expression through histone modification surrounding a proximal NF-kappaB-binding site. J Biol Chem 282:31197–31205
133. Berger J, Hauber J, Hauber R, Geiger R, Cullen BR (1988) Secreted placental alkaline phosphatase: a powerful new quantitative indicator of gene expression in eukaryotic cells. Gene 66:1–10
134. Markova SV, Golz S, Frank LA, Kalthof B, Vysotski ES (2004) Cloning and expression of cDNA for a luciferase from the marine copepod Metridia longa. A novel secreted bioluminescent reporter enzyme. J Biol Chem 279:3212–3217
135. Zhou S, Cerny AM, Bowen G, Chan M, Knipe DM, Kurt-Jones EA, Finberg RW (2010) Discovery of a novel TLR2 signaling inhibitor with anti-viral activity. Antiviral Res 87:295–306
136. Ehrhardt C, Kardinal C, Wurzer WJ, Wolff T, von Eichel-Streiber C, Pleschka S, Planz O, Ludwig S (2004) Rac1 and PAK1 are upstream of IKK-epsilon and TBK-1 in the viral activation of interferon regulatory factor-3. FEBS Lett 567:230–238
137. Civas A, Genin P, Morin P, Lin R, Hiscott J (2006) Promoter organization of the interferon-A genes differentially affects virus-induced expression and responsiveness to TBK1 and IKKepsilon. J Biol Chem 281:4856–4866
138. Monteith GR, Bird GS (2005) Techniques: high-throughput measurement of intracellular Ca(2+)—back to basics. Trends Pharmacol Sci 26:218–223
139. National Center for Biotechnology Information (NCBI) (2015) http://www.ncbi.nlm.nih.gov/pcassay/?term=tlr
140. Reindl M, Lutterotti A, Ingram J, Schanda K, Gassner C, Deisenhammer F, Berger T, Lorenz E (2003) Mutations in the gene for toll-like receptor 4 and multiple sclerosis. Tissue Antigens 61:85–88
141. Karima R, Matsumoto S, Higashi H, Matsushima K (1999) The molecular pathogenesis of endotoxic shock and organ failure. Mol Med Today 5:123–132
142. Mansson A, Adner M, Hockerfelt U, Cardell LO (2006) A distinct Toll-like receptor repertoire in human tonsillar B cells, directly activated by PamCSK R-837 and CpG-2006 stimulation. Immunology 118:539–548
143. Caron G, Duluc D, Fremaux I, Jeannin P, David C, Gascan H, Delneste Y (2005) Direct stimulation of human T cells via TLR5 and TLR7/8: flagellin and R-848 up-regulate proliferation and IFN-gamma production by memory CD4+ T cells. J Immunol 175:1551–1557
144. Tabiasco J, Devevre E, Rufer N, Salaun B, Cerottini JC, Speiser D, Romero P (2006) Human effector CD8+ T lymphocytes express TLR3 as a functional coreceptor. J Immunol 177:8708–8713
145. Kadowaki N, Ho S, Antonenko S, Malefyt RW, Kastelein RA, Bazan F, Liu YJ (2001) Subsets of human dendritic cell precursors express different toll-like receptors and respond to different microbial antigens. J Exp Med 194:863–869
146. Hart OM, Athie-Morales V, O'Connor GM, Gardiner CM (2005) TLR7/8-mediated activation of human NK cells results in accessory cell-dependent IFN-gamma production. J Immunol 175:1636–1642
147. Ito T, Wang YH, Liu YJ (2005) Plasmacytoid dendritic cell precursors/type I interferon-producing cells sense viral infection by Toll-like receptor (TLR) 7 and TLR9. Springer Semin Immunopathol 26:221–229

Chapter 2

Bioinformatic Analysis of Toll-Like Receptor Sequences and Structures

Tom P. Monie, Nicholas J. Gay, and Monique Gangloff

Abstract

Continual advancements in computing power and sophistication, coupled with rapid increases in protein sequence and structural information, have made bioinformatic tools an invaluable resource for the molecular and structural biologist. With the degree of sequence information continuing to expand at an almost exponential rate, it is essential that scientists today have a basic understanding of how to utilise, manipulate and analyse this information for the benefit of their own experiments. In the context of Toll-Interleukin I Receptor domain containing proteins, we describe here a series of the more common and user-friendly bioinformatic tools available as Internet-based resources. These will enable the identification and alignment of protein sequences; the identification of functional motifs; the characterisation of protein secondary structure; the identification of protein structural folds and distantly homologous proteins; and the validation of the structural geometry of modelled protein structures.

Key words Toll-like receptor, TLR, Toll-Interleukin-1 Receptor Domain (TIR), Bioinformatics, Sequence alignment, Sequence comparison, Homology, Structure validation, FUGUE

1 Introduction

Toll-like receptors (TLRs) are type I transmembrane receptors. They are constituted of a leucine-rich repeat ligand-binding domain, a single membrane spanning helix and a signalling Toll-Interleukin-1 Receptor (TIR) domain [1, 2]. TLRs recognise a diverse range of microbial ligands. Following ligand binding, the TLRs undergo conformational change enabling the initiation of signal transduction [3]. The TIR domains possess a conserved αβ structural organisation essential for signal transduction [4]. Indeed, parologs of individual TLR TIRs show particularly high levels of amino acid conservation.

In this chapter, we describe the use of the classic bioinformatic tools BLAST [5, 6] and ClustalΩ [7], for the identification and alignment of TLR TIR paralogues. We also address the identification of structurally homologous proteins and the annotation of a

Claire E. McCoy (ed.), *Toll-Like Receptors: Practice and Methods*, Methods in Molecular Biology, vol. 1390,
DOI 10.1007/978-1-4939-3335-8_2,

protein's three-dimensional environment through the use of the programs FUGUE [8] and JOY [9]. Moreover, we describe the use of available resources for the identification of functional motifs within proteins and the validation of the stereochemistry of protein structures. These techniques are highlighted with examples from TIR containing proteins.

These tools provide an important set of resources that, when used either individually, or in conjunction with one another, can greatly assist with multiple aspects of the study of TLRs. For example, they enable important functional and structural observations to be made about specific proteins. Additionally, they can aid the design of expression constructs for structural and biochemical studies and assist in the design of rational mutagenesis for functional work.

2 Materials

2.1 TLR Orthologues

1. Human TLR4 amino acid sequence (Accession Number O00206).
2. Multiple TLR4 orthologue sequences (*see* **Note 1**).

2.2 Sequence–Structure Homology

1. Human TLR4 amino acid sequence (Accession Number O00206). Select the region from residue 674 to 839.
2. Key to formatted Joy alignments (*see* Table 1).

2.3 Three-Dimensional Structure Comparison

1. The TLR1, TLR2 and TLR10 TIR crystal structure PDB (Protein Data Bank) codes. These are 1fyv, 1fyw and 2j67 respectively (*see* **Note 2**).

Table 1
Key to formatted Joy alignments

Structural features	Labelling	Residue format
Alpha helix	Red	x
Beta strand	Blue	x
3_{10} helix	Maroon	x
Solvent accessible	Lower case	x
Solvent inaccessible	Upper case	X
Hydrogen bond to main-chain amide	Bold	x
Hydrogen bond to main-chain carbonyl	Underline	x
Disulfide bond	Cedilla	ç
Positive phi torsion angle	Italic	*x*

X: any amino acid; ç: a half-cystine residue

2.4 Structural Validity

1. PDB file for model to be validated.

2.5 Post-translational Modifications

1. Human TRIF-related adaptor molecule, TRAM, also known as TICAM-2, amino acid sequence (Accession number NP_067681).

3 Methods

3.1 TLR Orthologues

Structurally and functionally important regions of homologous proteins often have high levels of amino acid conservation. Alignment and comparison of the amino acid sequence of homologous proteins from different species (i.e. protein orthologues) can be extremely helpful experimentally through the identification of key functional residues and protein domain boundaries. Here, we describe how to identify and align orthologues of TLR4.

3.1.1 BLAST Search

1. BLAST (Basic Local Alignment Search Tool) identifies regions of local similarity between the query and database sequences.
2. Paste the human TLR4 amino acid sequence into the query window of the NCBI-BLAST2—Protein Database page (http://www.ebi.ac.uk/Tools/sss/ncbiblast/).
3. Check that the program selected is blastp and the database is protein and UniProtKB/Swiss-Prot. Run Blast (*see* **Note 3**).
4. A table of results will be generated showing information about homologous sequences such as: protein description and source, length, identity, score and E value (*see* **Note 4**). From these results, it is possible to select TLR4 orthologues identified and download the sequences in a FASTA format (*see* **Note 5**).

3.1.2 ClustalΩ Multiple Sequence Alignment

1. Copy the FASTA formatted orthologues downloaded from the BLAST search (Subheading 3.1.1) into the input query field on the EMBL-EBI ClustalΩ server web-page (www.ebi.ac.uk/Tools/msa/clustalo/).
2. The default parameters can normally be retained. Run ClustalΩ (*see* **Note 3**).
3. A series of alignment and similarity results will be generated. These include pairwise scores for each sequence aligned, phylogram and cladogram trees, and a multiple sequence alignment (Fig. 1).
4. The multiple sequence alignment is especially useful for identifying regions of high and/or low conservation, domain boundaries and potential substitutions for mutagenic studies.

```
                          10        20        30        40        50
                   ....|....|....|....|....|....|....|....|....|....|
Felis_catus        YDAFVIYSSQDEDWVRNELVKNLEEGVPPFQLCLHYRDFIPGVAIAANII
Equus_caballus     YDAFVIYSSQDEDWVRNELVKNLEEGVPPFQLCLHYRDFIPGVAIAANII
Bos_taurus         YDAFVIYSSQDEDWVRNELVKNLEEGVPPFQLCLHYRDFIPGVAIAANII
Homo_Sapiens       YDAFVIYSSQDEDWVRNELVKNLEEGVPPFQLCLHYRDFIPGVAIAANII
Sus_scrofa         YDAFVIYSSQDEDWVRNELVKNLEEGVPPFHLCLHYRDFIPGVAIAANII
Mus_musculus       YDAFVIYSSQNEDWVRNELVKNLEEGVPRFHLCLHYRDFIPGVAIAANII
Clustal Consensus  **********:***************** *:*******************
                            60        70        80        90       100
                   ....|....|....|....|....|....|....|....|....|....|
Felis_catus        QEGFHKSRKVIVVVSQHFIQSRWCIFEYGIAQTWQFLSSRAGIIFIVLQK
Equus_caballus     QEGFHKSRKVIVVVSQHFIQSRWCIFEYEIAQTWQFLSSRAGIIFIVLHK
Bos_taurus         QEGFHKSRKVIVVVSQHFIQSRWCIFEYEIAQTWQFLSSRAGIIFIVLQK
Homo_Sapiens       HEGFHKSRKVIVVVSQHFIQSRWCIFEYEIAQTWQFLSSRAGIIFIVLQK
Sus_scrofa         QEGFHKSRKVIVVVSQHFIQSRWCIFEYEIAQTWQFLRSHAGIIFIVLQK
Mus_musculus       QEGFHKSRKVIVVVSRHFIQSRWCIFEYEIAQTWQFLSSRSGIIFIVLEK
Clustal Consensus  :**************:************ ******** *:::*******.*
                           110       120       130       140       150
                   ....|....|....|....|....|....|....|....|....|....|
Felis_catus        LEKSLLRQQVELYRLLNRNTYLEWEDSVLGRHIFWRRLRKALLDGKPRCP
Equus_caballus     LEKSLLRQQVELYRLLNRNTYLEWEDSVLGRHIFWRRLRKALLDGKPWSP
Bos_taurus         LEKSLLRQQVELYRLLSRNTYLEWEDSVLGRHVFWRRLRKALLAGKPQSP
Homo_Sapiens       VEKTLLRQQVELYRLLSRNTYLEWEDSVLGRHIFWRRLRKALLDGKSWNP
Sus_scrofa         LEKSLLRQQVELYRLLSRNTYLEWEDSVLGRHIFWRRLKKALLDGKPWSP
Mus_musculus       VEKSLLRQQVELYRLLSRNTYLEWEDNPLGRHIFWRRLKNALLDGKASNP
Clustal Consensus  :**:************.*********. ****:*****::*** **.  *
                           160
                   ....|....|....|....
Felis_catus        EGMADAEGS----------
Equus_caballus     AGTADAAESRQHDAETST-
Bos_taurus         EGTADAETNPQ-EATTST-
Homo_Sapiens       EGTVGTGCNWQEATSI---
Sus_scrofa         EGTEDSESNQHDTTAFT--
Mus_musculus       EQTAEEE---QETATWT--
Clustal Consensus
```

Fig. 1 Example ClustalΩ multiple sequence alignment. The TIR signalling domains of six of the TLR4 orthologues (host species as labelled in *figure panel*) identified by a BLAST search (Subheading 3.1.1) were submitted for ClustalΩ multiple sequence alignment (Subheading 3.1.2). The Clustal consensus sequence identifies fully conserved residues (*), strongly similar substitutions (:), weakly similar substitutions (.), and a lack of consensus (). The consensus sequence highlights the high degree of conservation in the TLR4 TIR, in contrast the very C-terminus of the protein shows significant variation

3.2 Sequence–Structure Homology

Sequence and structural information can be simultaneously used to improve the homology recognition power and the accuracy of sequence alignments (*see* **Note 6**). Identifying structural homology between a protein sequence of unknown three-dimensional structure and one with known structure provides useful information for understanding protein function. It also provides another

layer of information and reflects the high evolutionary pressure for structurally and functionally important residues in a given protein family. In other words, such alignments help identify divergently evolved (homologous) proteins with structural and functional relationships. Furthermore, it allows prediction of the three-dimensional structure through comparative modelling, a technique which is beyond the scope of this chapter (*see* **Note 7**). Here, we demonstrate how to use the program FUGUE to identify structural homologues for the TLR4 TIR domain. Unlike the TIR domains of TLR1, 2 and 10, the structure of the TLR4 TIR domain has not yet been solved experimentally.

Annotation of protein sequence alignments with three-dimensional structural features is a useful tool for identifying key structural and functional residues. This can be achieved with a program such as Joy, which provides a modified version of the one-letter amino-acid code in order to convey structural information (*see* Table 1).

3.2.1 Sequence–Structure Homology with Fugue

1. Open the Fugue web-page (http://tardis.nibio.go.jp/fugue/prfsearch.html) and enter your e-mail address and the amino acid sequence of the human TLR4 TIR domain (residues 673–839).
2. Keep the default parameters and click on search. The output is sent via e-mail and results can be accessed at http://tardis.nibio.go.jp/result/fugue/1146/fugue.html.
3. The Fugue result for human TLR4 TIR domain reveals that the HOMSTRAD [10] profile hs1fyxa (*see* **Notes 8** and **9**) has the highest *Z*-score. With over 99 % confidence, the suggested homology is certain (Fig. 2a).
4. The HOMSTRAD family called TIR (*see* **Note 9**), which was built on the crystal structures of human TLR1 and TLR2 TIR domains, is the second best hit. The low *Z*-score of other hits makes them less reliable.
5. Focus only on the two alignments with the highest *Z*-scores by clicking on 'alignment' in the results.

3.2.2 Sequence–Structure Alignment with Joy

1. The alignments mentioned in **step 5**, Subheading 3.2.1 (Fig. 2b) are represented using the Joy annotation described in Table 1. In addition to providing a secondary structure prediction for the query sequence they can also be used to highlight differences and/or problem areas within the sequence-structure alignments. These could be, for example: insertions or deletions in regions of helical structure; proline residues in regions of predicted helix; the presence, or substitution, of charged residues (e.g. lysine, arginine) for hydrophobic (e.g. phenylalanine, leucine, isoleucine, tyrosine) ones, and vice versa.

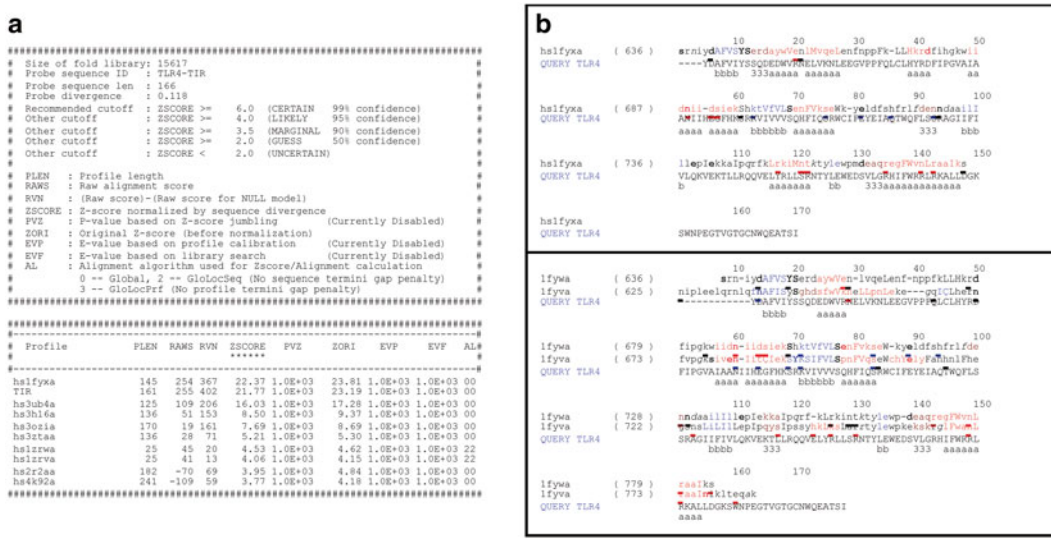

Fig. 2 Example analysis of a TLR4-TIR domain homology search using Fugue. Extract of the output for Fugue sent via e-mail (**a**) and the sequence–structure alignments of the two top hits based on the Joy annotation (**b**)

2. Analysis of the structural alignments reveals that the core of the TIR domain is well conserved between TLR1 (1fyv), TLR2 (1fyw) and TLR4 (Query). There are however apparent differences. For instance, an extra histidine residue at position 724 in human TLR4 interrupts an alpha-helix and is likely to cause some structural distortion. In addition, compared to the structural templates, there are extra residues at the C-terminus of the TLR4 sequence. These are not part of the TIR domain but constitute a tail of unpredictable structure.

3.3 Three-Dimensional Structure Comparison

It can be very helpful to evaluate the degree of three-dimensional structural similarity between either two or more experimentally determined or computer-modelled structures. This can help provide an estimation of structural similarity and/or model/structure reliability. The following method uses the Secondary Structure Matching (SSM) program PDBeFold, available at http://www.ebi.ac.uk/msd-srv/ssm/, to determine the similarity between experimentally determined TLR TIR domains.

3.3.1 Pairwise Structural Comparison

1. Choose the pairwise 3D alignment submission option and select 'PDB entry' for both the query and target sequences.
2. Insert the PDB codes for TLR1 (1fyv) and TLR2 (1fyw) TIR domains in the query and target fields respectively.
3. Retain the default parameters and submit query (*see* **Note 10**).
4. An output table detailing the 3D structural similarity will be generated. In general, the higher the number of aligned residues and the lower the rmsd (Root mean square deviation of

Cα atoms) the greater the degree of structural similarity (*see* **Note 11**). The values for the TLR1 and TLR2 structural comparison suggest a high degree of structural similarity.

3.3.2 Multiple Structural Comparison

1. Choose the multiple 3D alignment submission option and select 'PDB entry' as the source.
2. Input the TLR1 TIR PDB code (1fyv) and press the 'Actualize' button, followed by the new entry button. Repeat for TLR2 (1fyw).
3. Input the TLR10 (2j67) TIR structure files and press 'Find Chains'; delete B, Y and Z from the text box then press 'Actualize'. This removes unnecessary information as the TLR10 structure was a dimer. Submit query.
4. The results page will contain information relating to the similarities of the 3D superposition of the structure. This will include rmsd and Q scores, alignment of secondary structure elements and a structural alignment of input files. The aligned files can be viewed individually, as a superposition, or downloaded.

3.4 Structural Validity

There are many computer packages that will produce structural models with little more user input than an amino acid sequence. However, the models produced may contain regions of either poor, or disallowed, stereochemistry. It is always advisable to validate the geometry of any models generated. Two good ways to do this: use the programs Verify3D and Rampage. Verify3D assesses the sequence position and structural environment of the model and compares them to databases of known high-quality structures. Rampage provides a Ramachandran plot analysis to assess the stereochemical environment of the backbone torsion angles in the modelled structure.

1. Upload, and submit for analysis, the co-ordinate PDB file of the modelled structure to the servers for Verify3D (http://services.mbi.ucla.edu/Verify_3D/) and RAMPAGE (http://mordred.bioc.cam.ac.uk/~rapper/rampage.php).
2. Sample results for a TLR4 TIR homodimer model are in Fig. 3.
3. Verify3D scores each residue on a scale of −1 to +1 and a score of >0.2 suggests that the residue is in a structurally favourable environment. Regions with scores below this suggest that those parts of the model must be viewed as less reliable. The region of output shown in Fig. 3 indicates that the TLR4 model submitted has all Verify3D scores over 0.2 and therefore possesses high-quality stereochemistry, with the individual residues being found in structurally favoured environments.

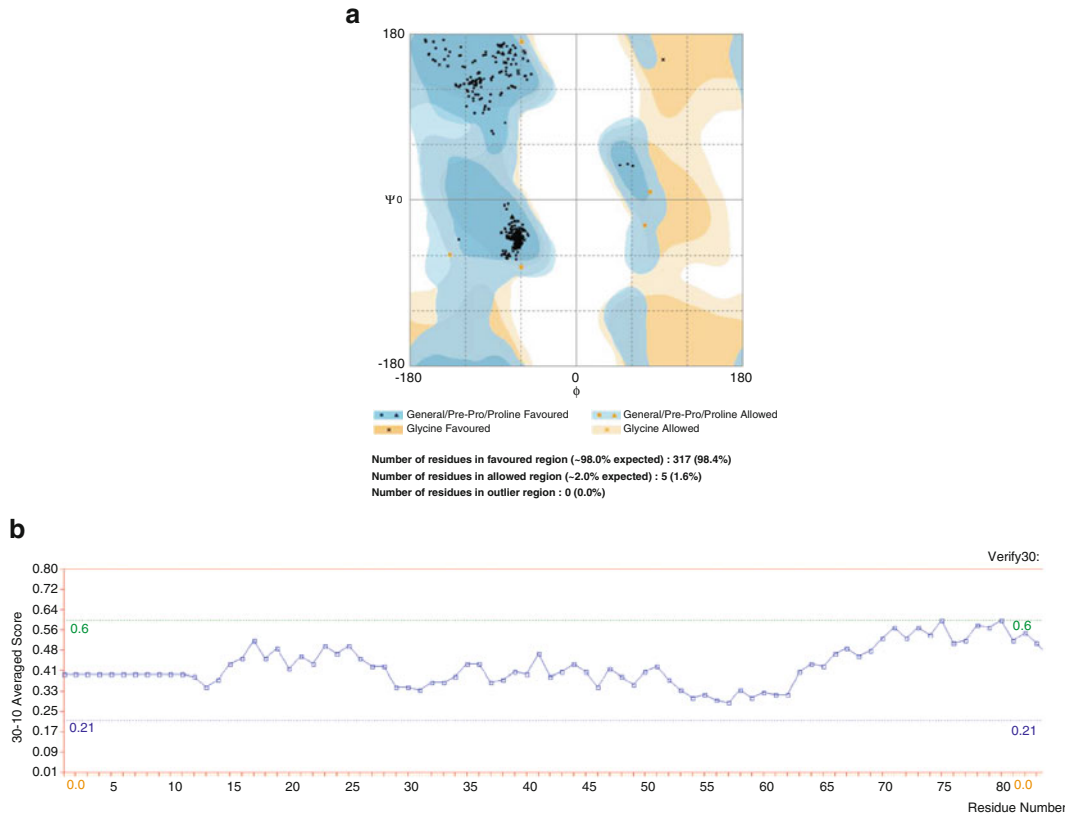

Fig. 3 Example analysis of a modelled TLR4 homodimer using RAMPAGE (**a**) and Verify3D (**b**)

4. RAMPAGE produces a clear graphical output of the Ramachandran plot that identifies the proportion of residues in favoured, allowed and disallowed regions. This provides a clear indication of the stereochemical quality of the model. For the TLR4 model submitted (Fig. 3) over 98 % of the residues have torsion angles in the favoured regions, less than 2 % in allowed regions, and there are no outliers. This helps confirm the high-quality stereochemistry of the model.

3.5 Post-translational Modifications

Assessing the presence of post-translational modifications in the Toll receptor pathway proteins is critical for understanding the biology of Toll signalling. Many tools exist for this purpose (*see* **Note 12**) and here we use one to identify a protein myristoylation site on the TIR containing adaptor protein TRAM. Myristoylation anchors the adaptor protein to the plasma membrane, where it fulfils its biological role in transferring the signal of activated Toll receptors. The linkage occurs on a consensus sequence consisting of Gly-X-X-X-Ser/Thr-Lys/Arg, where X stands for any amino acid. The 14 carbon fatty acid, myristic acid, is covalently attached

by amide linkage to the N-terminal glycine of a protein by an N-terminal myristoyltransferase.

1. Copy the FASTA formatted TRAM protein sequence into the query field on the NMT server web-page (http://mendel.imp.ac.at/myristate/SUPLpredictor.htm).
2. Keep the default parameter of 'Eukaryota' as it fits the taxonomy of the sequence.
3. Run the prediction.
4. A reliable myristoylation site is predicted at residue G2 within the sequence GIGKSKINSCPLSLSWG, with an overall score of 0.85 and a probability of false-positive prediction of 1.98×10^{-3}.
5. A logical progression would be to confirm the presence and biological relevance of this modification. Indeed site-directed mutagenesis of the predicted myristylation residue (Gly2Ala) and confocal microscopy experiments have determined that wild-type TRAM is myristylated and localises to the plasma membrane. In contrast, a G2A mutant TRAM has a cytoplasmic distribution and is unresponsive to lipopolysaccharide stimulation [11].

4 Notes

1. These can be obtained from a BLAST search, *see* Subheading 3.1.1.
2. The full PDB files can be downloaded from the Protein Data Bank (http://www.rcsb.org/pdb/home/home.do).
3. The default search parameters should be fine for these applications. If the user wants further information regarding parameter attributes and variation it is recommended that they read the related program documentation available through the EMBL-EBI web-site (http://www.ebi.ac.uk). The UniProtKB/Swiss-Prot database is the smaller portion of the UniProt database and contains fully annotated sequence information. Using this stops multiple redundant hits being identified. If it was unknown whether orthologues existed then use of the UniProtKB/TrEMBL or UniProt Clusters databases would be more appropriate.
4. The score takes into account the number of gaps and substitutions in the alignment. The greater this number, the better the quality of the alignment. The E value is a measure of the likelihood of the alignment occurring by chance. The smaller this number the less likely the alignment is a result of chance.

5. The first line of a FASTA formatted protein sequence starts with a > followed by descriptive text about the sequence. The second, and subsequent, lines contain the protein sequence in single letter code with no spaces or numbering.
6. A good overview of structural homology modelling can be found in the following reference [12].
7. To find out about the homology modelling approach, go to the Swiss-model (http://swissmodel.expasy.org) and the Modeller (http://www.salilab.org/modeller) web-pages.
8. HOMSTRAD (HOMologous STRucture Alignment Database) is a curated database of structure-based alignments for homologous protein families. Its web-site can be found at http://tardis.nibio.go.jp/homstrad/.
9. FUGUE results are given as a list of potentially matching HOMSTRAD profiles. The code hs1fyxa corresponds to the crystal structure of the TLR2 mutant P681H. 1fyxa relates to the PDB identifier (1fyx; chain A) in the HOMSTRAD 'hs' database. The code TIR refers to the HOMSTRAD family containing the TLR1 and TLR2 crystal structures (PDB 1fyv and 1fyw). Clicking of the listed HOMSTRAD profile in the FUGUE results will open the HOMSTRAD entry and show details of its composition.
10. If using a different query sequence and the whole PDB archive as the target then it may be necessary to lower the percentage similarity cut-off for the lowest acceptable target match in order to get any positive hits.
11. Full details of the interpretation of results and scores can be found at http://www.ebi.ac.uk/msd/EMBO/ssm-tutorial/ssm_tutorial.html. The higher the Z and Q scores the better.
12. A list of programs for the prediction of post-translation modifications can be found on the Expasy tools web-site at http://www.expasy.org/tools.

References

1. Akira S, Takeda K (2004) Toll-like receptor signalling. Nat Rev Immunol 4:499–511
2. Gay NJ, Gangloff M (2007) Structure and function of toll receptors and their ligands. Annu Rev Biochem 76:141–65
3. Gay NJ, Gangloff M, Weber AN (2006) Toll-like receptors as molecular switches. Nat Rev Immunol 6:693–8
4. Xu Y, Tao X, Shen B, Horng T, Medzhitov R, Manley JL, Tong L (2000) Structural basis for signal transduction by the Toll/interleukin-1 receptor domains. Nature 408:111–5
5. Altschul SF, Gish W, Miller W, Myers EW, Lipman DJ (1990) Basic local alignment search tool. J Mol Biol 215:403–10
6. Altschul SF, Madden TL, Schaffer AA, Zhang J, Zhang Z, Miller W, Lipman DJ (1997) Gapped BLAST and PSI-BLAST: a new generation of protein database search programs. Nucleic Acids Res 25:3389–402
7. Chenna R, Sugawara H, Koike T, Lopez R, Gibson TJ, Higgins DG, Thompson JD (2003) Multiple sequence alignment with the Clustal series of programs. Nucleic Acids Res 31:3497–500

8. Shi J, Blundell TL, Mizuguchi K (2001) FUGUE: sequence-structure homology recognition using environment-specific substitution tables and structure-dependent gap penalties. J Mol Biol 310:243–57
9. Mizuguchi K, Deane CM, Blundell TL, Johnson MS, Overington JP (1998) JOY: protein sequence-structure representation and analysis. Bioinformatics 14:617–23
10. Mizuguchi K, Deane CM, Blundell TL, Overington JP (1998) HOMSTRAD: a database of protein structure alignments for homologous families. Protein Sci 7:2469–71
11. Rowe DC, McGettrick AF, Latz E, Monks BG, Gay NJ, Yamamoto M, Akira S, O'Neill LA, Fitzgerald KA, Golenbock DT (2006) The myristoylation of TRIF-related adaptor molecule is essential for Toll-like receptor 4 signal transduction. Proc Natl Acad Sci U S A 103:6299–304
12. Nunez Miguel R, Shi J, Mizuguchi K (2001) Protein fold recognition and comparative modeling using HOMSTRAD, JOY, and FUGUE. In: Tsigelny IF (ed) Protein structure prediction: bioinformatic approach. International University Line, La Jolla, CA

Chapter 3

Toll-Like Receptor Interactions Measured by Microscopic and Flow Cytometric FRET

Gabor L. Horvath, Pia Langhoff, and Eicke Latz

Abstract

Protein–protein interactions regulate biological networks. The most proximal events that initiate signal transduction frequently are receptor dimerization or conformational changes in receptor complexes. Toll-like receptors (TLRs) are transmembrane receptors that are activated by a number of exogenous and endogenous ligands. Most TLRs can respond to multiple ligands and the different TLRs recognize structurally diverse molecules ranging from proteins, sugars, lipids, and nucleic acids. TLRs can be expressed on the plasma membrane or in endosomal compartments and ligand recognition thus proceeds in different microenvironments. Not surprisingly, distinctive mechanisms of TLR receptor activation have evolved. A detailed understanding of the mechanisms of TLR activation is important for the development of novel synthetic TLR activators or pharmacological inhibitors of TLRs. Confocal laser scanning microscopy combined with GFP technology allows the direct visualization of TLR expression in living cells. Fluorescence resonance energy transfer (FRET) measurements between two differentially tagged proteins permit the study of TLR interaction, and distances between receptors in the range of molecular interactions can be measured and visualized. Additionally, FRET measurements combined with confocal microscopy provide detailed information about molecular interactions in different subcellular localizations. These techniques permit the dynamic visualization of early signaling events in living cells and can be utilized in pharmacological or genetic screens.

Key words Confocal microscopy, Laser scanning microscopy (LSM), Fluorescence resonance energy transfer (FRET), Fluorescence lifetime imaging microscopy (FLIM), Flow cytometry, Toll-like receptor (TLR)

1 Introduction

Investigations of protein–protein interactions are important for the understanding of higher organization levels of molecular complexes, their structure–function relationships, and the regulation of signal transduction processes. Many techniques are available to measure and quantify protein–protein interactions in vitro, for example, circular dichroism, isothermal titration calorimetry, surface plasmon resonance, nuclear magnetic resonance spectroscopy, or gel retardation assays. However, some techniques require large

Claire E. McCoy (ed.), *Toll-Like Receptors: Practice and Methods*, Methods in Molecular Biology, vol. 1390,
DOI 10.1007/978-1-4939-3335-8_3,

amount of proteins and protein interactions are assessed outside the more complex context of a living cell. Biophysical approaches combined with light microscopy permit the study of protein–protein interactions in a non-destructive manner in living cells. The lateral resolution of light microscopy is a function of the numerical aperture (NA) of the objective lens and is influenced by the index of refraction of the medium and the wavelength of light. Regular light microscopy and confocal laser scanning microscopy therefore have a practical lateral resolution limit of about 200 nm. Most molecular interactions occur in the range of a few nanometers, and thus, receptor–receptor interactions or conformational changes within receptor complexes cannot be directly visualized by light microscopy due to the limitations given by the resolution of light. However, if light microscopy is combined with techniques such as fluorescence resonance energy transfer (FRET) or bimolecular fluorescence complementation, molecular interactions can be studied dynamically in living cells. Furthermore, if combined with confocal imaging, information about the subcellular localization of protein interactions or conformational changes can be obtained.

We will discuss the different methods of microscopic detection of FRET based on sensitized emission intensity, photobleaching, and fluorescence lifetime measurements. Furthermore, we will describe how to measure sensitized emission-based FRET on a flow cytometer with fluorescently labeled antibodies (Fig. 1).

1.1 Theory of FRET

FRET is a process by which a fluorescent donor molecule in an excited electronic state transfers its energy to a neighboring acceptor molecule via a non-radiative dipole–dipole interaction [1, 2]. The term "fluorescence resonance energy transfer" can be misleading, because the energy is not actually transferred by fluorescence. The acceptor fluorophore molecule can be a dark quencher or another fluorescent molecule (in this article, we only explore the latter). The prerequisites for this process are that (1) there is a substantial overlap between the emission spectrum of the donor and the excitation spectrum of the acceptor fluorophore (gray area in Fig. 2a), (2) the spatial separation of the two molecules is between 1 and 10 nm, and (3) the dipole moments of the molecules are correctly aligned.

The most immediate effect of FRET is a decrease in fluorescence lifetime of the donor fluorophore, as the FRET process competes for the available excited donor states with fluorescent and thermal relaxation. This results in the decrease of donor fluorescent quantum efficiency and fluorescent intensity, and the simultaneous increase of acceptor fluorescent intensity (as excited at the donor excitation wavelength). These two phenomena are referred to as "donor quenching" and "sensitized emission" (arrows in Fig. 2a).

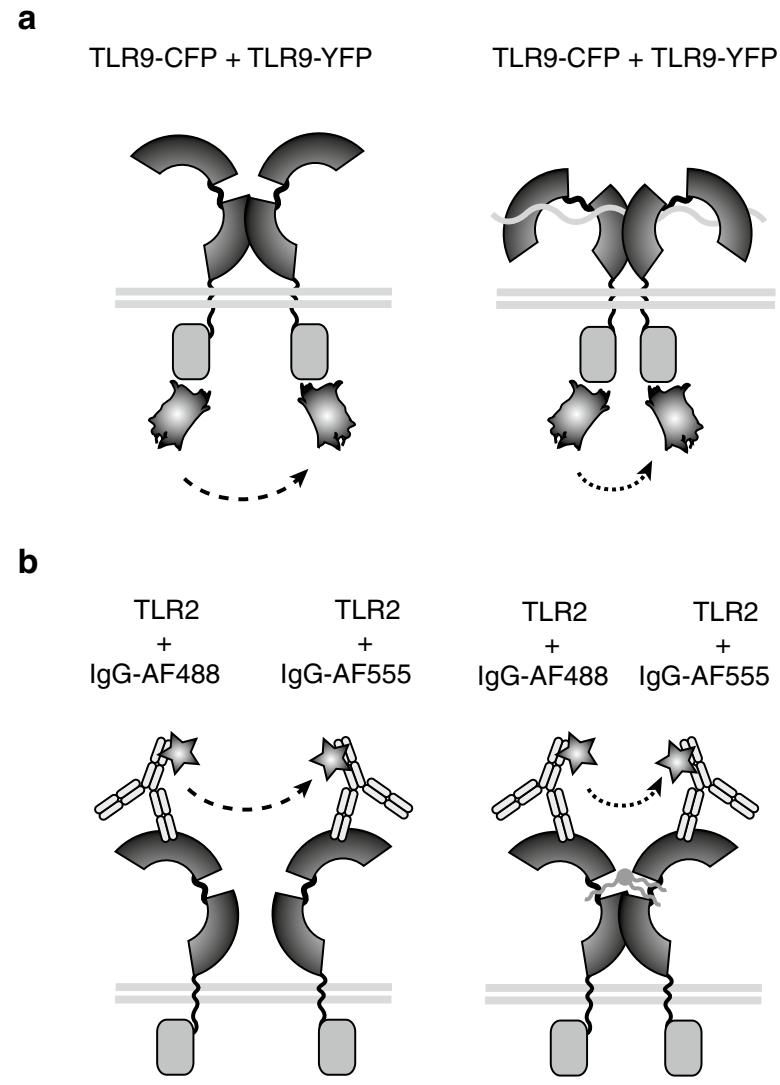

Fig. 1 Model of TLR association and ligand-induced changes in TLR9 conformation reported by CFP-YFP FRET (**a**) or in TLR2 association reported by fluorescently labeled antibodies (**b**)

The extent of the FRET process can be quantified by FRET efficiency (E), which is a direct measure of the fraction of photon energy absorbed by the donor that is transferred to an acceptor. Transfer efficiency can be calculated by using the rate constants of donor relaxation processes:

$$E = \frac{k_T}{(k_T + k_F + k_0)}, \quad (1)$$

where k_T is the transfer rate constant, k_F is the fluorescent rate constant, and k_0 is the sum of any other relaxation rate constants of

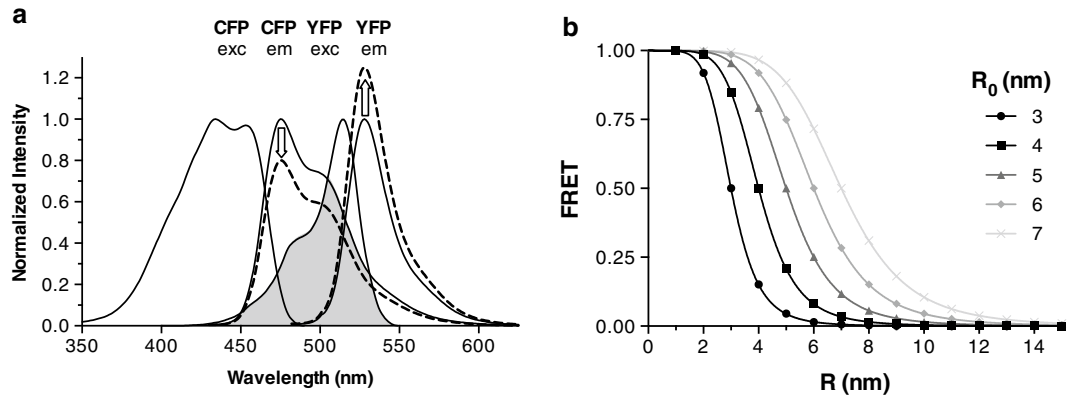

Fig. 2 Excitation and emission spectra of CFP and YFP fluorescent proteins (**a**). *Shaded area* indicates the overlap integral. The *down* and *up arrows* represent donor quenching and sensitized emission, respectively. Distance dependence of energy transfer efficiency with varying critical Förster distances (R_0) (**b**). Note that the relationship is almost linear between 20 and 80 % transfer efficiency

donor fluorophore. Since the transfer rate can also be expressed as a function of the separation of the two fluorophores (*see* **Note 1**), one can yield an equation where the transfer efficiency is determined by the distance (R) between the donor and acceptor fluorescent dyes:

$$E = \frac{R_0^6}{R_0^6 + R^6} = \frac{1}{1 + \left(\frac{R}{R_0}\right)^6}, \qquad (2)$$

where R_0 is the so-called Förster critical distance corresponding to 50 % transfer efficiency for a given donor–acceptor pair (for CFP–YFP, this is 4.9 nm) (*see* **Note 2**). Accordingly, the biggest advantage of any FRET method is the strong dependence of transfer efficiency on the distance between the two fluorescent dyes (Fig. 2b). The FRET efficiency depends on the donor-to-acceptor separation distance with an inverse 6th power law. Subtle changes in distances between FRET fluorophores at the level of molecular interaction or binding are reflected by changes in FRET efficiencies.

1.2 Experimental Approaches for Measuring FRET

The measurement of fluorescence intensity is one of the easiest and most available ways to characterize protein interactions via the FRET process, and it is adapted to fluorescent plate readers, spectrofluorometers, flow cytometers, wide-field microscopes, and confocal laser scanning microscopes.

1.2.1 Acceptor Photobleaching

One measurable characteristic of energy transfer is the decrease in donor fluorescence intensity (i.e. donor quenching). Thus, the analysis of donor quenching can be used to calculate the transfer efficiency E. Equation 3 indicates that only two fluorescent intensities

are required. The fluorescence intensity of the donor is compared in the presence (I_D^{DA}) or absence (I_D^{D}) of an acceptor:

$$E = 1 - \frac{I_D^{DA}}{I_D^{D}}. \quad (3)$$

One possible way to measure fluorescence de-quenching is to bleach the acceptor fluorophore by applying intense laser light at the wavelength of acceptor absorbance to photo-physically destroy the acceptor fluorophore. FRET efficiency is calculated using Eq. 3 by comparing the donor fluorescence before and after acceptor bleaching. This technique is referred to "donor de-quenching after acceptor photobleaching."

1.2.2 Sensitized Emission FRET

Another popular method to study FRET in living samples is to quantify the sensitized emission of the acceptor fluorophore by excitation of the donor fluorophore (termed "sensitized emission FRET"). In this approach, the fluorescence intensity of the acceptor as excited at the donor wavelength in the presence (I_A^{DA}) or absence (I_A^{A}) of a donor is compared. The transfer efficiency is

$$E = \frac{\varepsilon_A c_A}{\varepsilon_D c_D} \cdot \left(\frac{I_A^{DA}}{I_A^{A}} - 1 \right), \quad (4)$$

where ε_D and ε_A are the extinction coefficients of the donor and acceptor fluorophores as excited at the donor wavelength, and c_D and c_A are the concentrations of the donor and acceptor fluorophores. The excitation coefficients and concentrations are practically scaling the calculated transfer efficiency values to an absolute scale, which is only dependent on the Förster critical distance. The advantage of this calculation is that the sensitized emission intensity is compared to very low fluorescence intensity, as the acceptor usually cannot be efficiently excited at the donor excitation wavelength. However, considerable spectral bleed-through from the donor can represent a major technical hurdle. Thus, the sensitized emission intensity should be corrected for both donor bleed-through and acceptor cross-excitation. For this reason, sensitized emission FRET measurements always require the presence of appropriate controls (donor and acceptor fluorophore alone).

1.2.3 Sensitized Emission FRET in Flow Cytometry

The ratiometric image-based sensitized emission FRET method can be adapted to data sets measured on a flow cytometer. The same benefits and restrictions apply to this measurement technique as practically the same lasers and emission filters are used in both the imaging and flow cytometry method. A great advantage here is that while on a microscope usually only a few cells are measured, on a flow cytometer fluorescent intensities of tens of thousands of cells are acquired that allows for robust statistics on a large population and even for distinguishing populations based on different FRET efficiencies [3].

1.2.4 Donor Photobleaching

Another approach to measure FRET efficiency is the photo-physical destruction of the donor fluorophore, which will efficiently decrease the possibility of energy transfer. The complete photo-destruction of the donor molecule would not lead to a feasible method, because it would not leave any measurable fluorescence intensity that can be compared to the initial intensity. Instead, the donor fluorophore is destroyed sequentially by strong excitation light with concomitant imaging of the decreasing fluorescence emission. The photobleaching decay rate of the donor fluorophore is calculated by fitting a double-exponential function to the series of intensities on a pixel-by-pixel basis. The transfer efficiency is obtained by comparing the average photobleaching time constants of a sample with donor only (τ'_{D}) to a sample with both donor and acceptor present (τ'_{DA}):

$$E = 1 - \frac{\tau'_{\mathrm{D}}}{\tau'_{\mathrm{DA}}}, \tag{5}$$

where $\tau'_{\mathrm{DA}} > \tau'_{\mathrm{D}}$, because energy transfer introduced an additional pathway for relaxation beside fluorescence emission and non-radiative photo-destruction [4]. A disadvantage of donor photobleaching is that it requires two separate measurements to calculate transfer efficiency that can result in statistical artifacts. Additionally, the data analysis requires sophisticated software that is not readily available [5], and long acquisition times (usually 5–15 min, depending on the photostability of donor dye) do not allow for live cell imaging.

On the other hand, if the acceptor molecule is sufficiently photo-labile, its photo-destruction would result in the recovery of donor intensity, thus a simple donor quenching calculation will yield transfer efficiency in the same sample:

$$E = 1 - \frac{I_{\mathrm{Dpre}}}{I_{\mathrm{Dpost}}}, \tag{6}$$

where I_{Dpre} and I_{Dpost} are the donor intensities in pre- and post-bleaching conditions. Since donor photobleaching is not frequently used for FRET efficiency analysis, we do not describe this method further in Subheading 3.

1.2.5 FRET Analysis by Fluorescence Lifetime Imaging (FLIM)

Each of the methods to detect FRET described above is based on measuring fluorescence intensities and changes thereof as a consequence of FRET. These methods make use of the fact that fluorophores display characteristic emission spectra that can be used to separate different fluorophores and that FRET leads to intensity changes in both donor and acceptor fluorophores. Another physical process that can be measured with excited fluorophores is the lifetime of fluorescence decay. Each fluorophore exhibits a unique fluorescence lifetime that can be used to separate fluorophores or

to probe for the existence of FRET. The fluorescence lifetime (τ) is the average time during which a fluorescent molecule remains in an excited state before returning to the ground state. Fluorescence lifetime imaging (FLIM) combines the measurement of fluorescence lifetimes with microscopic imaging techniques, such as confocal imaging or other imaging modalities. In confocal-based FLIM for example, fluorescence lifetime decay characteristics of a fluorescent sample are acquired at each position of a confocal scan, i.e. at each pixel of the image. The data can be represented as images, where fluorescence lifetime data are color-coded, and the amount of signal (i.e. the fluorescence intensity) is coded by contrast intensity.

The fluorescence lifetime of a fluorophore is independent of probe concentration, excitation intensity, and photobleaching. In addition, the fluorescence lifetimes are not only different for distinct fluorophores, but the fluorescence lifetime also depends on the molecular environment of the fluorophore molecules. Since the lifetime does not depend on the concentration of the fluorophore, fluorescence lifetime measurements can directly probe changes of, for example, ion concentrations or oxygen saturation. During the process of FRET, donor fluorophores that transfer energy to acceptor fluorophores show decreased fluorescence lifetimes. This phenomenon can be exploited for sensitive and accurate FRET measurements.

A major advantage of FLIM-based FRET measurements is that only the donor fluorescence decay needs to be measured as the donor lifetime changes upon energy transfer. Thus, spectral bleed-through correction for acceptor fluorescence is not required. By measuring the donor lifetime in the presence and the absence of acceptor one can accurately assess the FRET efficiency

$$E = 1 - \frac{\tau_{DA}}{\tau_D}, \tag{7}$$

where r_{DA} is the donor lifetime in the presence of acceptor (energy transfer situation) and r_D is the donor lifetime in the absence of acceptor.

Even though acquiring an acceptor image is not required, it can be really beneficial to see whether the measured FRET efficiency corresponds to areas where acceptor molecules are present. To account and correct for the absence of acceptor molecules, pulsed interleaved excitation (PIE) was developed [6–8]. In PIE-FRET applications, two pulsed laser sources are selected to excite both the donor and acceptor molecules. The laser pulses are delayed to each other in the tens of nanoseconds range (to allow for proper fluorescence relaxation) to generate a pulse sequence, where the pulses are interleaved. When the two fluorophores are within FRET range, the acceptor fluorescence will show up in the first time window in the acceptor channel, which is followed by the

fluorescence of the donor in the second time window in the donor channel that is accompanied by acceptor fluorescence due to FRET. When the separation between the two fluorophores is too large, only direct excitation will produce observable fluorescence. However, when the acceptor molecule is not present or non-fluorescent, there will be no fluorescence in the first-time window. The PIE-FRET method allows correcting for proper stoichiometry in FRET calculations and eliminates zero-peak signals on the FRET efficiency histogram originating from donor-only molecules.

FLIM can be implemented in wide-field, confocal, and multi-photon excitation microscopes. Point scanning methods are advantageous as subcellular resolution can be obtained, and the lifetime measurements do not reflect average lifetimes of entire excited volumes. Instrumental methods for measuring fluorescence lifetimes can broadly be divided into two categories: frequency domain and time domain [9, 10]. Either method can be used in one-photon or two-photon FRET-FLIM microscopy. In the frequency domain mode, the fluorescence lifetimes can be determined by a phase-modulated method. The intensity of a laser continuous wave source can be modulated at high frequency, resulting in modulation of the fluorescence. Since the fluorophore in the excited state has a specific lifetime, the fluorescence will be delayed with respect to the excitation signal. Thus, the lifetime can be determined from the phase shift.

Here, we describe the measurement of fluorescence lifetimes using the time domain method of data acquisition. Fluorescence lifetimes can be determined in the time domain by using a pulsed laser source. Time-correlated single photon counting (TCSPC) is typically employed in time domain FLIM measurements. In TCSPC, the laser pulses excite a population of fluorophores and the timing of single-photon emissions is recorded yielding a probability distribution for the emission of single photons. The time-resolved fluorescence decays exponentially and thus, during lifetime analysis, fluorescence decay curves recorded by TCSPC are fitted to (multiple) exponential decays. The time response of the instrument components is taken into account by an iterative deconvolution technique.

2 Materials

2.1 Instrumentation

In principle, FRET can be analyzed with any instrument that is able to read fluorescence. For example, it is possible to perform FRET measurements with epi-fluorescence microscopes, confocal laser scanning microscopes, spectrofluorometers, flow cytometers, fluorescence plate readers, fluorescence gel documentation systems, or instruments capable of analyzing fluorescence lifetimes. A requirement for intensity-based FRET analysis is a sufficiently

sensitive fluorescence acquisition that allows reliable measurements of donor, sensitized emission, and acceptor fluorescence. Complete fluorescence separation of donor from acceptor or donor from sensitized emission is not a requirement as the FRET efficiency can be obtained by using appropriate mathematical algorithms (described above). The analysis of FRET by confocal microscopy is particularly useful for living biological samples, as the spatial resolution of a confocal microscope allows relating the FRET signal to subcellular structures and to fluorescent ligands. A flow cytometry-based FRET analysis does not permit subcellular FRET resolution, but has the advantage that entire cell populations can be analyzed for the existence of or change in FRET [11, 12]. A combination of confocal FRET analysis with flow cytometric FRET analysis would be an ideal scenario for comprehensive analysis of receptor interactions.

There are many commercial confocal microscope systems available which allow the analysis of FRET. We will describe the analysis of FRET as performed on a Leica AOBS confocal microscope. The Leica SP5 AOBS confocal microscopes have an optical configuration that does not make use of any filters or dichroic mirrors. As a result of this completely filter-free optical set-up, these instruments have less light loss in the optical path than conventional confocal microscopes. In addition, the acousto-optical devices and the spectral detection system allow for a flexible set-up of optical paths. (1) Multi-parameter analysis requires the selection of several laser lines. To select the laser lines or to attenuate intensity for balanced illumination of different fluorophore densities, acousto-optical tunable filters (AOTF) are used. (2) The fluorescence emission from the specimen is separated by an acousto-optical beam splitter (AOBS), which replaces the conventionally used dichroic mirrors. (3) The spectral detector uses a prism to break up the light. The appropriate wavelength range is selected by a series of spectrophotometer modules. These modules carry reflective mirrors at the edges of the spectrophotometer slits that reflect the wavelengths above and below the captured fluorescence range to other detectors having similar setups. Up to five detectors are implemented in the Leica spectral detection confocal microscopes. The spectral detector replaces the arrays of secondary beam splitters and barrier filters found in conventional confocal microscopes. The non-linear optical elements (AOTF, AOBS) and the spectral detection system allow for precise wavelength selection in any range at very high light transmission. The complete freedom of selection of laser lines (due to the AOBS) and range of emission capture (due to the spectral detection) is very beneficial for the set-up of optimal conditions for FRET experiments.

For FLIM measurements in the time-domain on a confocal microscope, a pulsed laser source and drive (PDL-828 “Sepia II”, Picoquant, Berlin, Germany) and a fast detector (LSM_SPAD)

along with a time-correlated single photon counting (TCSPC) module (PicoHarp 300) are necessary. The pulsed excitation can be obtained with a multi-photon laser or a pulsed single-photon laser. For the Leica SP2 AOBS confocal system, a time-domain lifetime attachment system (D-FLIM) can be obtained. The Leica SP5 confocal microscopes can be equipped with up to two internal FLIM detectors and two external high-sensitivity, single-photon avalanche diode (SPAD) detectors, and with external pulsed laser sources. It is advisable to use the external SPAD detectors because of the higher sensitivity; however, the external light path does not use the internal AOBS system, but rather relies on conventional filters and dichroic mirrors that need to be matched to the proper fluorophore pair. The implementation of TCSCP capability in a laser scanning confocal microscope allows the measurement and analysis of fluorescence lifetimes at each pixel of the confocal scan.

For flow cytometric FRET measurements, any flow cytometers would work that have two laser lines corresponding to the excitation of the donor and acceptor fluorophores, and three detectors with two detecting signals from the donor excitation laser and one from the acceptor laser. We have successfully performed FRET measurements on BD FACSCalibur, FACSDiVa, FACSArray, FACSCanto, LSRII, Aria and LSRFortessa, Beckman Coulter MoFlo, and Miltenyi MACSQuant VYB.

2.2 Data Processing

The image acquisition for FRET measurements can be performed with the Leica Application Suite Advanced Fluorescence (LAS AF) software. The software provides an easy-to-use interface for different methods of FRET analysis (e.g. acceptor photobleaching FRET or sensitized emission FRET). For lifetime measurements, data analysis can be performed using SymPhoTime64 from PicoQuant on the SMD acquisition and analysis computer provided with the Leica SP5 system.

The use of the LAS AF software for FRET analysis is not required, as there are many image analysis software packages that can analyze images for the existence of FRET. An excellent freeware program for image analysis is ImageJ that was developed at the NIH (http://rsb.info.nih.gov/ij/index.html), or the Fiji, precompiled ImageJ distribution package [13]. ImageJ operates with various data formats, can perform a multitude of image manipulations, and it is programmable via a macro interface or using Java. Of note is the RiFRET ImageJ plugin that can perform intensity-based ratiometric FRET analysis on multiple images [14].

There are multiple commercial software packages available for analyzing flow cytometry data; unfortunately, these can only calculate simple ratios, and do not have complex mathematical expression of measured parameters implemented. In order to be able to define any mathematical equations between the measured fluorescent intensities, we use a custom-written software, ReFLEX [12].

Table 1
Photo-physical parameters of frequently used fluorescent proteins and fluorophores[a]

Fluorophore names	Extinction coefficient ε (1/M cm)	Fluorescent quantum yield	Excitation maximum (nm)	Emission maximum (nm)	Laser lines (nm)
ECFP	33,900	0.40	435	475	405, 458
EGFP	55,000	0.60	489	508	458, 488
EYFP	84,000	0.61	514	527	488, 514
mRFP	44,000	0.25	584	607	543, 561
FITC	81,000	0.85	495	520	488
Alexa 488	71,000	0.94	495	519	488
R-PE	1,960,000	0.84	498, 565	575	488, 514, 543
Cy3	150,000	0.15	552	570	532, 543
Alexa 546	104,000	0.96	556	573	532, 543
Cy5	250,000	0.28	643	667	633
Alexa 647	239,000	ND	650	665	633
APC	240,000	0.68	650	660	633

[a]All of these values were obtained from the collective fluorophore database available at George McNamara's web-site: http://home.earthlink.net/~pubspectra/

2.3 Fluorophores

The most commonly used fluorophores applicable for FRET analysis are listed in Table 1. Some widely used FRET dye-pairs according to this table are: CFP–YFP, YFP (GFP)–mCherry, R-PE–APC, Alexa 488–Alexa 555, Alexa 546–Alexa 647, and Cy3–Cy5. The fluorescence protein pairs CFP–YFP or GFP–mRFP are mostly used for live cell imaging of FRET.

2.4 Reagents

1. DNA transfection reagents: FuGENE 6 (Promega) or GeneJuice (EMD Millipore) for transient transfection of cells.
2. Slides to use for live cell imaging: CELLView, 35-mm dish (Greiner Bio-One) or μ-Slide, 8-well (Ibidi).
3. Antibodies: anti-TLR2 antibodies (TL2.1; eBioscience) were directly conjugated by Alexa dyes following the protocol provided by the manufacturer (Life Technologies GmbH).
4. Ficoll density gradient (GE Healthcare GmbH).
5. Red cell lysis buffer (Miltenyi Biotec GmbH).
6. RPMI 1640 medium (Life Technologies GmbH).
7. Fetal Bovine Serum (FBS) (Life Technologies GmbH).
8. CD14 microbeads (Miltenyi Biotec GmbH).

3 Methods

3.1 Constructs and Cell Lines

Fluorescent proteins can be fused to either terminus of the protein and the functionality of the fusion partner should be tested empirically. TLRs are type 1 transmembrane receptors with an N-terminal leader sequence. In our experience, C-terminal fusions of fluorescent proteins with TLRs did not disrupt signaling of the published TLR-FP fusions [15–27]. It is advantageous to deliver TLR-FP fusion proteins via viral vectors, such as lentiviruses or retroviruses, as this method permits dosage of gene integration and thus limits effects of gene overexpression. The most reliable and reproducible FRET measurements can be performed in stably transfected or transduced cells. Transient transfection can act as a cell stressor, which could negatively influence the FRET analysis. For FRET measurements, single color controls (donor and acceptor fluorophores) are necessary for sensitized emission FRET analysis. It is advantageous to generate single color control cells of the fusions used for the FRET experiments, as this would ensure that expression levels of controls are similar to that of the double color sample.

1. Human peripheral blood mononuclear cells (PBMCs) were purified from whole blood over Ficoll density gradient according to manufacturer's description.
2. Erythrocytes were lysed in red cell lysis buffer and cells were resuspended in RPMI medium supplemented with 10 % FBS.
3. Human $CD14^+$ monocytes were isolated from PBMCs using CD14 microbeads. These cells are used to describe methods in Subheading 3.2.2.

3.2 Data Acquisition and Analysis

3.2.1 Sensitized Emission FRET

Sensitized emission FRET is a non-destructive method of FRET analysis and is most frequently used for live cell experiments. Any sensitized emission FRET experiment requires at least three samples: a sample containing donor only, a sample containing acceptor only, and a sample containing both fluorophores. The samples containing single fluorophores are used for calculating spectral overlap and cross-excitation from different laser lights at different detectors. In addition, single color controls are generally useful to determine whether the FRET calculation was accurate and did not lead to false-positive FRET assignments. In addition to these required fluorescent samples, it is also advantageous to prepare a positive FRET control, such as a fusion between donor and acceptor fluorescent proteins. The Leica confocal software contains a FRET SE acquisition and analysis wizard. The user follows several steps that are briefly outlined below.

1. The experimental conditions are set for the acquisition of the donor, FRET (sensitized emission), and acceptor channels. These three images are required for the calculation of the

correction factors. Two scans will be performed in a line-by-line fashion. The first scan should be set-up with a laser exciting the donor (e.g. 405 or 458 nm for CFP) and two detectors activated for the emission acquisition of donor fluorescence and FRET fluorescence. Adjust the PMT gains so that pixels are not saturated. For the second scan, a laser that excites the acceptor fluorophore is selected (e.g. 514 nm for YFP) and the emission of the acceptor is captured with the same detector that was used in the first scan for the FRET fluorescence. The PMT settings for this channel should not be changed at all. Instead, adjust the image brightness by changing the laser power until the image setting is satisfactory (*see* **Note 3**). Define the zoom level (around three times with a 63× objective for best digital resolution) and number of averages (usually four or eight for single images, and two for time-series to avoid substantial photobleaching) for best imaging conditions and proceed to the next step.

2. The actual images are acquired. The software is set-up for the acquisition of three samples: FRET, donor, and acceptor (A, B, and C in the FRET algorithm). It is recommended to have single positive cells for donor and acceptor fluorophores in the same or independent dishes (*see* **Note 4**).
3. The calibration is performed. Ensure that you have the appropriate image set active and draw a region of interest (ROI) around a representative cell that expresses either donor or acceptor fluorophore alone. If the background between the samples differs or the background fluorescence is above zero, perform a background correction by selecting ROIs in regions of the sample that are not covered by cells. After the ROIs have been correctly assigned to acceptor and donor fluorescence and the background has been sampled, press the button "Next" to obtain the correction factors. The calculated calibration factors will be applied to the current FRET sequence and to all subsequent images that are acquired with unchanged settings. It is possible to save the correction factors and reuse them. However, the precondition for reusing saved settings is that the measurements are performed with exactly the same imaging conditions.
4. The theoretical background of FRET analysis is given in Subheading 1.2. There are many different ways to calculate FRET efficiency using sensitized emission FRET. The equations differ mostly in the use of correction factors. The Leica LAS AF software for the SP5 and SP8 generation instruments gives the user the choice to select from several methods for the FRET efficiency calculation (*see* **Note 5**).
5. The FRET output is provided as an image in which the FRET efficiencies found at each pixel of the image are false-colored

using a look-up table that codes changes in FRET efficiency as changes in color. It is also possible to analyze particular regions of interest in the image for the amount of FRET efficiency.

3.2.2 Sensitized Emission FRET in Flow Cytometry

The measurement of FRET efficiency based on the sensitized emission of the acceptor fluorophore on a flow cytometer is fairly similar to how that is performed on a microscope. The FRET experiment would require four samples in this case: an unlabeled or non-transfected background sample, a sample containing donor only, a sample containing acceptor only, and a sample containing both fluorophores. The unlabeled sample is used to set up the background autofluorescence of the cells (which is usually not observable on a microscope), the samples containing single fluorophores are used for calculating spectral overspill and cross-excitation from different laser excitations at the different detectors. When the proteins of interest were labeled with antibodies, the proper isotype- and FMO-control samples are also required, but only to identify possible problems with non-specific antibody binding. Using fluorescence compensation is not recommended (especially the hardware-based ones on the older instruments), as the mathematical algorithms to calculate FRET efficiency rely on raw fluorescence intensities and the spectral correction factors in the algorithm act similar to a compensation matrix. In addition to these required fluorescent samples, it is also advantageous to prepare a positive FRET control, such as a fusion between donor and acceptor fluorescent proteins or antibody labeling of some proteins that are known to dimerize (e.g. EGFR upon EGF stimulation).

Since most modern flow cytometers use temporal and spatial separation of the excitation laser lines, the basic default acquisition setup is already equivalent to the sequential scan mode of a confocal microscope. Again, two detectors have to be activated from the donor excitation laser path and one from the acceptor; and the forward (FSC) and side (SSC) scatter signals are used to identify encountered events as cells. If the flow cytometer acquisition software allows for bi-exponential or hyper-log display, that needs to be activated for the fluorescence signal detectors or displays in order to avoid the "picket fencing" visual effect of low signals in normal logarithmic histogram displays.

To set up the acquisition conditions, only the background sample needs to be measured; however, it is advisable to check whether the samples with the highest signal still fit into the dynamic range of the detectors. The PMT voltages of the three fluorescent signals need to be adjusted in a way that the log-Gaussian distribution histogram of the fluorescent signal for the background sample falls between 0 and 100, with median fluorescence of around 30–50 (between 0.1 and 1, with around 0.3 median signal for the MACSQuant VYB instrument). Afterward, the voltage settings should not be changed, and all the samples must be acquired with

the same settings. If there is a drift in the fluorescent signals or the instrument has to be primed or restarted, the samples have to be acquired again with the new instrument setting.

Unfortunately, there is not any flow cytometer acquisition software that can currently perform the mathematical calculations required for FRET analysis on the run, so the FRET efficiency histograms cannot be displayed during the measurement, but has to be calculated afterward in separate dedicated software (*see* **Note 6**).

Identifying the double-positive population during analysis is fairly straightforward and it is outlined in Fig. 3. In this example, we used freshly isolated PBMCs to measure ligand-induced homodimerization of TLR2. The monocyte population was identified with CD14-FITC labeling in a separate sample, so that that wouldn't interfere with our FRET fluorophores. The CD14-FITC back-gated population was further gated to exclude doublets. On the single labeled samples, the donor and FRET channel dot-plot was used to determine spectral correction factors for the donor (S_1 and S_3), and the acceptor and FRET channel dot-plot for acceptor cross-excitation (S_2). For FRET samples, three gates were set on the correlation dot-plots of the three fluorescence intensities to identify positively stained cells, and the population from the intersection of these three gates was used to calculate FRET efficiencies. The cell-by-cell FRET values can be displayed on a histogram or on dot-plots, and the efficiencies can be exported for further analysis.

3.2.3 Acceptor Photobleaching FRET

As outlined in Subheading 1.2.1, FRET acceptor photobleaching involves measuring the donor de-quenching due to the loss of acceptor fluorescence after acceptor photobleaching. In the acceptor photobleaching method, the change in intensity of the donor fluorophore needs to be monitored as it becomes "de-quenched" by the ablation of the acceptor, thus only two channels are detected:

- D = donor, for assessing transfer efficiency.
- A = acceptor, for performing photobleaching and determining the efficiency of photobleaching.

The actual transfer efficiency is calculated from comparing the donor intensity before (D_{pre}) and after (D_{post}) photobleaching:

$$\mathrm{FRET}_{\mathrm{eff}} = \frac{D_{\mathrm{post}} - D_{\mathrm{pre}}}{D_{\mathrm{post}}}, \text{for all } D_{\mathrm{post}} > D_{\mathrm{pre}}. \quad (8)$$

In theory, all FRET fluorophore pairs can be used for this method. However, in practice it is better to choose an acceptor fluorophore that is easily photobleached to minimize bleaching times and phototoxic effects of intense laser illumination. Examples of these pairs are Cy3–Cy5, CFP–YFP, and fluorescein–rhodamine (*see* **Note 7**).

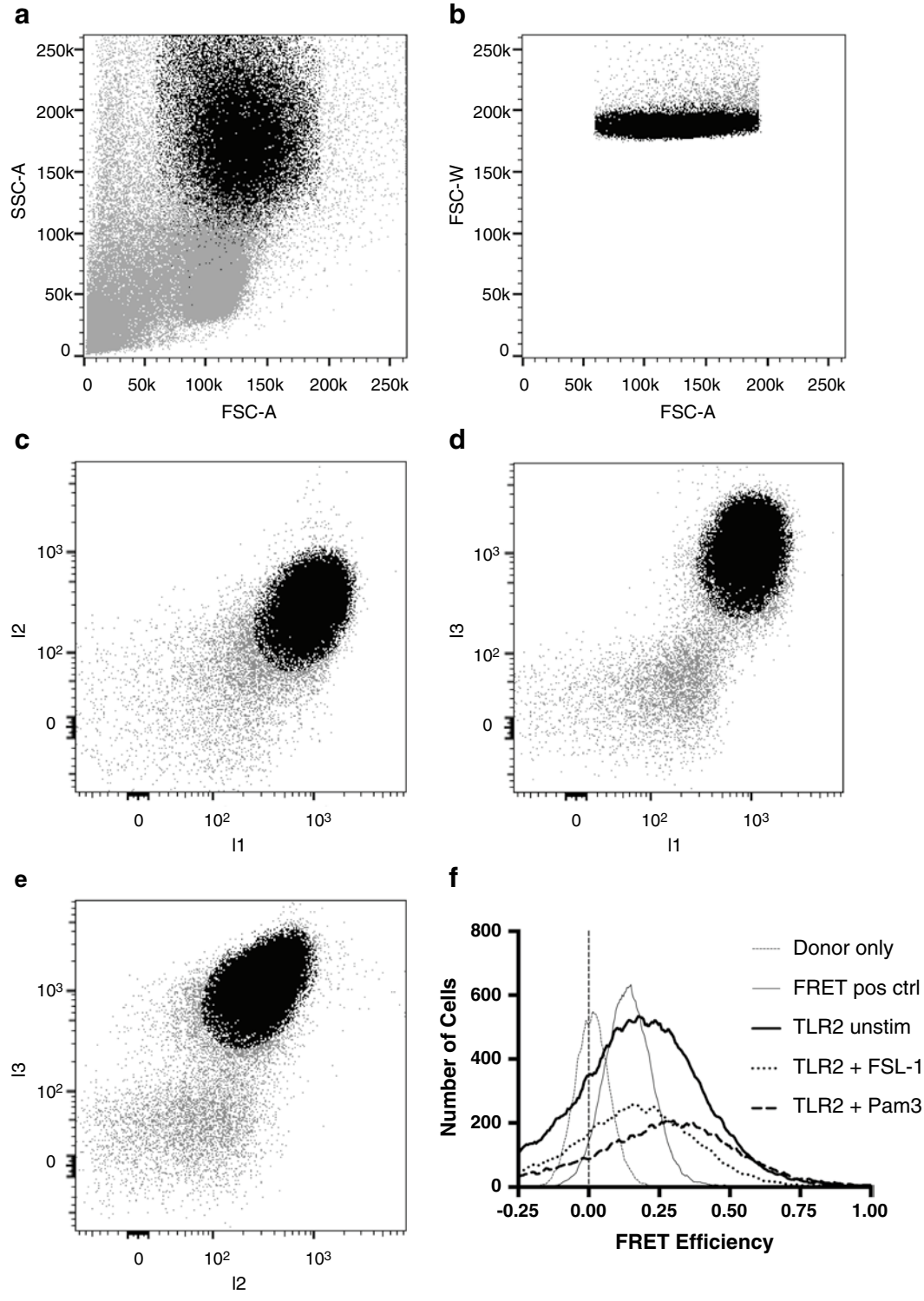

Fig. 3 Gating strategy for flow cytometric FRET evaluation of ligand-induced TLR2 homo-dimers. Gated populations are showed in *black layered* over the *grey* parental populations: monocyte population (**a**), single cells (**b**), positively labeled cells (**c–e**), and FRET efficiency histograms (**f**)

The Leica confocal microscope software has a built-in wizard (FRET AB) that guides the user through an acceptor photobleaching experiment. In the first (setup) step, the experimental conditions are defined. Beam path and PMT settings are defined for the donor and the acceptor fluorophore. PMT and laser power should be adjusted so that the PMT is not saturated. In the second (bleaching) step, a region of interest is selected for the acceptor photobleaching procedure. Here, the laser illuminating the acceptor fluorophore should be adjusted to 100 % power level to ensure efficient photobleaching. In the bleach configuration window, one can chose to bleach a certain number of scans or one can utilize a "regulator" which ascertains that the bleaching is performed up to a set intensity of the acceptor fluorescence. Once the experiment is started, the instrument executes the following steps: (1) acquisition of the pre-bleach images, (2) photobleaching of the selected region of interest, and (3) acquisition of the post-bleach images. In the third (evaluation) step, the software calculates the FRET efficiency according to Eq. 8 and displays a false-colored FRET image and statistical information with FRET efficiency for the defined region.

3.2.4 FLIM-FRET

There are many different microscopy systems available that can analyze fluorescence lifetimes of samples. We only describe the general principle of image acquisition and analysis. The acquisition of FLIM data for FRET analysis is very simple. The first step is to utilize regular intensity-based imaging to find the sample region of interest for the fluorescence lifetime analysis. This area is then scanned by a pulsed laser light source. For CFP–YFP FRET experiments, a pulsed diode laser emitting at 405 nm can be used at a frequency of 20 MHz. The pulsed laser illuminates the sample over a number of image frames until enough photons have been acquired for the analysis of lifetimes. The acquisition time depends on the amount of fluorescence in the sample and on the required analysis method (see below). The photons detected by the FLIM detector are processed in the TCSPC module, which is controlled by the SymPhoTime64 software. The data recorded by the FLIM system are multi-dimensional. The Time-Tagged Time-Resolved (TTTR) data file structure contains all the photon arrival times relative to the laser pulse (TCSPC time in picoseconds) and also relative to the beginning of the experiment (Time Tag up from nanoseconds), and all of these are embedded in the time-frame of a line- or frame-scan in area scan measurements and re-assigned to the proper pixel coordinates. In the output, there are two-dimensional arrays of pixel (i.e. in XY direction) and each pixel contains the information of fluorescence lifetime, which is the counted photon numbers in a series of time channels. The SymPhoTime64 software is able to display the data in various display modes. The number of photons per pixel is typically displayed as shades of grey in an inten-

sity image, which allows an overview on photon counts over the entire image.

The next step of FLIM analysis is the decay data analysis, which is also performed by the SymPhoTime64 software. To obtain fluorescence lifetime decay curves, the photon decay information at each recorded pixel must be fitted with an appropriate mathematical model. Since the measurement system is not infinitely fast, the fitting algorithms have to take the so-called "instrument response function" into account. The instrument response function is a pulse shape that is recorded for an infinitely short fluorescence lifetime. The fitting procedure convolutes the model decay function with the instrument response function and relates the results with the photon numbers in the subsequent time channels in each individual pixel. The algorithm varies the model parameters until the best fit between the convoluted model function and the measured data is obtained. This procedure is termed iterative deconvolution. During the analysis procedure, the user has influence on a variety of parameters including the selection of an appropriate fitting model. Typical models used for lifetime analysis are single exponential or a sum of exponential terms. The selection depends on the sample and one can be guided by the goodness of fit of a particular model that was used.

Biological samples often contain fluorescence components of several fluorescent dyes. For example, when CFP–YFP pair is used, one would expect at least two components: fluorescent decay time of CFP and of YFP, and if FRET exists, another decay time of CFP engaged in energy transfer is observed. The decay curves are then multi-exponential. If more exponential terms are necessary for the curve-fitting procedure, calculation times will become longer and more photon counts are necessary in each pixel in order to achieve an accurate curve fitting. It is advisable to restrict the amount of dyes that are sampled by TCSCP by use of barrier filters that can be placed in front of the FLIM detector (or in the SP5 model by use of the spectral detection system). For example, one could sample CFP-derived photons only by collecting light up to a wavelength of 495 nm. This would ensure that the recorded fluorescence lifetimes are not contaminated with fluorescence decay data of YFP. Thus, a double exponential decay model can be applied to analyze the lifetime components of unquenched CFP and the CFP molecule that is engaged in energy transfer. The fitting procedure delivers lifetimes and amplitude coefficients for the individual exponential components. For example, a double exponential decay function is described by

$$N(t) = a_1 \cdot \mathrm{e}^{-t/\tau_1} + a_2 \cdot \mathrm{e}^{-t/\tau_2}, (a_1 + a_2 = 1). \tag{9}$$

If this model is used for CFP–YFP FRET under conditions where YFP lifetimes are not recorded, the CFP lifetimes, τ_1 and τ_2, and

the amplitudes, a_1 and a_2, are obtained. A slow lifetime component (CFP, non-FRET) can be separated from a fast lifetime component (CFP, FRET). These data can then be utilized to calculate FRET efficiencies at each pixel of the image. Lifetimes can be reported in a variety of ways. For example, mean lifetimes can be reported as distribution plots of lifetimes observed in the images and the color-coded lifetime images represent the number of photons per pixel as brightness and the fluorescence lifetime as color.

The SymPhoTime64 software also provides multiple, easy-to-use scripts to facilitate analysis of specific area or point scan lifetime measurements (FRET, PIE-FRET, fluorescence correlation spectroscopy, time trace or burst analysis, anisotropy; for more details, see: http://www.tcspc.com). Of note of these are the two FLIM-FRET scripts for calculating pixel-by-pixel FRET efficiencies; one for donors with single exponential decay kinetic (e.g. mTurquoise, YFP and TagRFP) and the other for donors with more complicated decay kinetic (CFP, mCerulean, GFP and in general, most of the fluorescent proteins). Both analysis scripts rely on a priori knowledge of the donor lifetime, usually determined empirically from a separate image or from an area of the image that only contains donor signals. With a single exponential donor decay curve, it is possible to determine not only the FRET efficiency for every pixel, but also the percentage of molecules that undergo FRET, which in the end can be used for binding studies as well. The presence of multiple donor decay processes, however, only allows for determining amplitude-weighted average lifetimes and average FRET efficiencies.

4 Notes

1. According to Förster's theory [1], the rate constant of the FRET interaction can be described by the equation

$$k_T = (k_F + k_0) \cdot \left(\frac{R_0}{R}\right)^6, \tag{10}$$

which combined with Eq. 1 gives the distance dependence of transfer efficiency (Eq. 2). The Förster critical distance, R_0 (in nanometer) is calculated from the photo-physical parameters of the interacting fluorophores

$$R_0 = 978 \cdot (Q_D \cdot \kappa^2 \cdot n^{-4} \cdot J_{DA})^{1/6}, \tag{11}$$

where Q_D is the fluorescence quantum efficiency of the donor, n is index of refraction of the conveying medium (assumed

to be 1.4 for cells in aqueous media), κ^2 is the orientation factor (which has a value between 0 and 4, and is assumed to be 2/3 for dynamic averaging [28]), and J_{DA} is the overlap integral. The overlap integral (in the unit of M^{-1} cm^3) can be determined from the emission spectrum of the donor and the excitation spectrum of the acceptor dye normalized to unity:

$$J_{DA} = \frac{\int_{\infty}^{0} F_D(\lambda) \cdot \varepsilon_A(\lambda) \cdot \lambda^4 \, d\lambda}{\int_{\infty}^{0} F_D(\lambda) \, d\lambda}. \quad (12)$$

2. Seeing Eq. 2, it is very tempting to calculate the distance of two proteins from transfer efficiencies, however, extra care should be taken as how to interpret those values.
   If the protein-labeling scheme involves antibodies, one has to note that the size of a Fab fragment has a size of about 5.0 nm and the fluorophores can be unevenly distributed along the protein. If fluorescent proteins were used as protein tags, then the closest separation of two fluorescent proteins is approximately 5.0 nm, as the fluorophore is situated inside the protein. This implies that using the fluorescent protein FRET pair, the FRET transfer efficiency has a practical limit of around 50 % transfer efficiency, but it can also be higher when the orientation of the dipoles of the two fluorescent proteins are close to parallel and free rotation is constrained. Another factor that should be considered is the way the FRET experiment and the transfer efficiency evaluation were carried out. It is possible to obtain transfer efficiency values as an average for a population of cells based on the mean fluorescence intensities of the population or the mean of transfer efficiencies of individual cells, or the mean for a single cell, or the mean of several hundreds of proteins located in one pixel. All of these procedures result in mean transfer efficiencies, however the averaging is fundamentally different, and accordingly the average molecular distances should have different interpretations.
3. Depending on the expression level of the protein, it may be required to open the pinhole to above one airy unit in order to keep the detector gain at levels around 600–800 V, which is required for appropriate image quality.
   For CFP–YFP FRET, the following settings could be used:
   Scan 1: CFP excitation 405 nm (if available) or alternatively 458 nm; CFP emission: 463–509 nm; FRET emission: 519–580 nm. Scan 2: YFP excitation 514 nm. The images are acquired in a line-by-line fashion and it is important to keep the emission acquisition settings for acceptor exactly the same as for the FRET channel. In addition, it is vital to keep the

PMT settings of the acceptor emission exactly the same as for the FRET channel (set in scan 1). In practice, only three things in the set-up for the second scan need change: Firstly, reduce the laser light of the donor laser to 0 %. Secondly, deactivate the CFP channel, leaving the YFP channel (that is the FRET channel in scan 1) at 518–580 nm. Thirdly, adjust the laser power of the 514 nm acceptor laser so that the acceptor cell emission is within the dynamic range of the PMT (no saturation of pixels) and do NOT change the PMT setting of the acceptor channel at all. It is vital to keep all measurements under identical conditions as the calculation of bleed-through and cross-excitation is based on these settings. If your controls do not match the actual imaging conditions, i.e. one of the controls is brighter than the FRET sample and saturates the channel under the conditions where the FRET sample is optimally illuminated; one should try to use cells that express lower amounts of protein (comparable to the FRET sample) for the calibration. One should not readjust the settings of the PMT between control and sample. All measurements performed under differing conditions are invalid and should be discarded!

4. It is not mandatory to have three independent culture dishes with the different samples and to acquire three images. In fact, it is beneficial to have all three cell populations in the same culture dish. It is then possible to only acquire one image having all populations in one field. In the following step, regions of interests are defined for donor and acceptor fluorescence and this can be done from one image containing donor and acceptor single positive cells or from independent images (which can then be background corrected).
5. The Leica SP2 generation LCS software utilizes the following equations for the FRET efficiency calculation. As outlined above, three channels have to be acquired for the FRET calculation:
   - A = donor emission by excitation of the donor
   - B = FRET emission by excitation of the donor
   - C = acceptor emission by excitation of the acceptor

   As mentioned earlier, in a sample containing both fluorophores these channels do not represent pure donor or acceptor signals, but also contain some spectral spillovers from the other dyes, and thus have to be corrected for bleed-through and cross-excitation. These correction factors are obtained from samples containing single fluorophore:
   - $a = A/C$ (acceptor-only sample)
   - $b = B/A$ (donor-only sample)
   - $c = B/C$ (acceptor-only sample).

The transfer efficiency is calculated as follows on a pixel-by-pixel basis:

$$\mathrm{FRET} = B - b \cdot A - (c - a \cdot b) \cdot C, \tag{13}$$

$$\mathrm{FRET}_{\mathrm{eff}} = \mathrm{FRET} / C. \tag{14}$$

The Leica SP5 and SP8 instrument software allows the user to choose from two more methods for FRET efficiency calculation. One method gives the option to correct for further cross-talk; however, in most cases, those effects are miniscule and can be neglected. The third method is a simple ratiometric calculation that can be used for samples with a fixed stoichiometry of donor and acceptor (e.g. FRET sensors).

6. The ReFlex software uses similar equations for the FRET efficiency calculation as the Leica software. A notable difference here is that the FRET efficiency is weighted to the donor signal instead of the acceptor signal.
   For the FRET calculation, three channels have to be acquired:
   - I_1 = donor emission by excitation of the donor
   - I_2 = FRET emission by excitation of the donor
   - I_3 = acceptor emission by excitation of the acceptor

   In a sample containing both fluorophores these channels do not represent pure donor or acceptor signals, but can also contain significant contribution from the other dyes that has to be corrected for. The correction factors are calculated from samples labeled with only one of the fluorophores:
   - $S_1 = I_2/I_1$ (donor-only sample)
   - $S_2 = I_2/I_3$ (acceptor-only sample)
   - $S_3 = I_3/I_1$ (donor-only sample).

   The transfer efficiency is calculated for each cell with the following formulas:

$$A = \frac{1}{\alpha}\left[\frac{I_2 - I_1 \cdot (S_1 - S_2 \cdot S_3) - I_3 \cdot S_2}{I_1}\right], \tag{15}$$

$$E = \frac{A}{1 + A}. \tag{16}$$

The α-factor in Eq. 15 is a scaling factor that allows for absolute FRET efficiency calculations. It can be considered a conversion rate between the measured donor and acceptor intensities, and it is dependent on and empirically calculated from the detection efficiencies of the instrument and the photo-physical properties of the fluorophores [11]. In most cases, relative FRET measurements are sufficient to decide whether a stimulus induces or changes receptor interactions, and the value of 0.5–2.0 can be used for the α-factor; however,

adequate distance estimations require absolute FRET efficiencies. On the other hand, FRET-based distance calculations are more reliable in single molecule and/or fluorescence lifetime measurements.

There are also variations to this set of equations that mostly differ in whether they account for additional cross-talk factors, or use an additional channel for cell-by-cell correction of autofluorescence signal to obtain smaller variations on low-signal samples [3]. However, since any equations can be defined in the software, it is easy to apply new intensity-based FRET methodologies [29, 30].

7. If fluorescent proteins are used for FRET analysis by the acceptor photobleaching method, one should remember that accurate measurements of FRET could only be obtained from fixed cells. In living cells, proteins diffuse through the cells with a diffusion constant that depends on the subcellular compartment in which the protein is situated. The time between the acceptor photobleaching and the acquisition of the post-bleach image allows diffusion of unquenched acceptor fluorophores into the region that is already bleached. It is possible to bleach an entire living cell and compare the donor fluorescence before and after photobleaching; however, depending on cell size and fluorophore expression levels, photobleaching can take longer than the bleaching of smaller regions of interest.

References

1. Förster T (1948) Zwischenmolekulare Energiewanderung und Fluoreszenz. Ann Phys 437:55–75
2. Stryer L (1978) Fluorescence energy transfer as a spectroscopic ruler. Annu Rev Biochem 47:819–846
3. Sebestyén Z, Nagy P, Horvath G et al (2002) Long wavelength fluorophores and cell-by-cell correction for autofluorescence significantly improves the accuracy of flow cytometric energy transfer measurements on a dual-laser benchtop flow cytometer. Cytometry 48:124–135
4. Jovin TM, Arndt-Jovin DJ (1989) Luminescence digital imaging microscopy. Annu Rev Biophys Biophys Chem 18:271–308
5. Szentesi G, Vereb G, Horvath G et al (2005) Computer program for analyzing donor photobleaching FRET image series. Cytometry A 67:119–128
6. Müller BK, Zaychikov E, Bräuchle C, Lamb DC (2005) Pulsed interleaved excitation. Biophys J 89:3508–3522
7. Rüttinger S, Macdonald R, Krämer B et al (2006) Accurate single-pair Förster resonant energy transfer through combination of pulsed interleaved excitation, time correlated single-photon counting, and fluorescence correlation spectroscopy. J Biomed Opt 11:024012–024012–9
8. Hendrix J, Lamb DC (2013) Pulsed interleaved excitation: principles and applications. Methods Enzymol 518:205–243
9. Gratton E, Limkeman M, Lakowicz JR et al (1984) Resolution of mixtures of fluorophores using variable-frequency phase and modulation data. Biophys J 46:479–486
10. Suhling K, Siegel J, Phillips D et al (2002) Imaging the environment of green fluorescent protein. Biophys J 83:3589–3595
11. Horvath G, Petrás M, Szentesi G et al (2005) Selecting the right fluorophores and flow cytometer for fluorescence resonance energy transfer measurements. Cytometry A 65:148–157
12. Szentesi G, Horvath G, Bori I et al (2004) Computer program for determining fluorescence resonance energy transfer efficiency from flow

cytometric data on a cell-by-cell basis. Comput Methods Programs Biomed 75:201–211

13. Schindelin J, Arganda-Carreras I, Frise E et al (2012) Fiji: an open-source platform for biological-image analysis. Nat Methods 9:676–682
14. Roszik J, Lisboa D, Szöllosi J, Vereb G (2009) Evaluation of intensity-based ratiometric FRET in image cytometry--approaches and a software solution. Cytometry A 75:761–767
15. Latz E, Visintin A, Lien E et al (2003) The LPS receptor generates inflammatory signals from the cell surface. J Endotoxin Res 9:375–380
16. Espevik T, Latz E, Lien E et al (2003) Cell distributions and functions of Toll-like receptor 4 studied by fluorescent gene constructs. Scand J Infect Dis 35:660–664
17. Fitzgerald KA, Rowe DC, Barnes BJ et al (2003) LPS-TLR4 signaling to IRF-3/7 and NF-kappaB involves the toll adapters TRAM and TRIF. J Exp Med 198:1043–1055
18. Flo TH, Ryan L, Latz E et al (2002) Involvement of toll-like receptor (TLR) 2 and TLR4 in cell activation by mannuronic acid polymers. J Biol Chem 277:35489–35495
19. Parroche P, Lauw FN, Goutagny N et al (2007) Malaria hemozoin is immunologically inert but radically enhances innate responses by presenting malaria DNA to Toll-like receptor 9. Proc Natl Acad Sci U S A 104:1919–1924
20. Rowe DC, McGettrick AF, Latz E et al (2006) The myristoylation of TRIF-related adaptor molecule is essential for Toll-like receptor 4 signal transduction. Proc Natl Acad Sci U S A 103:6299–6304
21. Fitzgerald KA, McWhirter SM, Faia KL et al (2003) IKKepsilon and TBK1 are essential components of the IRF3 signaling pathway. Nat Immunol 4:491–496
22. Husebye H, Halaas O, Stenmark H et al (2006) Endocytic pathways regulate Toll-like receptor 4 signaling and link innate and adaptive immunity. EMBO J 25:683–692
23. Latz E, Franko J, Golenbock DT, Schreiber JR (2004) Haemophilus influenzae type b-outer membrane protein complex glycoconjugate vaccine induces cytokine production by engaging human toll-like receptor 2 (TLR2) and requires the presence of TLR2 for optimal immunogenicity. J Immunol 172:2431–2438
24. Latz E, Verma A, Visintin A et al (2007) Ligand-induced conformational changes allosterically activate Toll-like receptor 9. Nat Immunol 8:772–779
25. Latz E, Visintin A, Espevik T, Golenbock DT (2004) Mechanisms of TLR9 activation. J Endotoxin Res 10:406–412
26. van der Kleij D, Latz E, Brouwers JFHM et al (2002) A novel host-parasite lipid cross-talk. Schistosomal lyso-phosphatidylserine activates toll-like receptor 2 and affects immune polarization. J Biol Chem 277:48122–48129
27. Visintin A, Halmen KA, Latz E et al (2005) Pharmacological inhibition of endotoxin responses is achieved by targeting the TLR4 coreceptor, MD-2. J Immunol 175: 6465–6472
28. van der Meer BW (2002) Kappa-squared: from nuisance to new sense. J Biotechnol 82:181–196
29. Fábián A, Horvath G, Vámosi G et al (2013) TripleFRET measurements in flow cytometry. Cytometry A. doi:10.1002/cyto.a.22267
30. Szabó A, Horvath G, Szöllosi J, Nagy P (2008) Quantitative characterization of the large-scale association of ErbB1 and ErbB2 by flow cytometric homo-FRET measurements. Biophys J 95:2086–2096

Chapter 4

Using Confocal Microscopy to Investigate Intracellular Trafficking of Toll-Like Receptors

Harald Husebye and Sarah L. Doyle

Abstract

Toll-like receptors (TLR) survey the extracellular space, cytoplasm, and endosomal compartments for signs of infection or tissue injury. Over the past decade, it has become evident that TLR activation and signal transduction can be regulated by subcellular compartmentalization of both the receptors and their downstream signaling components. Immunofluorescence and/or overexpression of fluorescently "tagged"' proteins teamed with confocal microscopy presents a powerful technique for studying the spatial organization of TLRs, their signaling mediators, and the dynamic processes they activate. This chapter details the common methods for determining the subcellular location of TLRs in both live and fixed cells.

Key words Immunofluorescence, Immunocytochemistry, Confocal microscopy, TLR trafficking, Subcellular localization, GFP, Fluorophore

1 Introduction

Understanding how TLR signaling networks are integrated into the cellular infrastructure is key to appreciating the nuances of when and how TLRs respond to their various ligands. A good example of this concept explains why the TRAM-TRIF signaling pathway induced by TLR4 activation [1] occurs with delayed kinetics when compared to the Mal-MyD88-dependent signaling pathway. In response to LPS, TLR4 activates these two signaling pathways. Detailed localization studies have established that MyD88-dependent signaling to NFκB is disrupted by receptor endocytosis [2] and that Mal localizes to the plasma membrane through interaction with phosphatidylinositol-4,5-bisphosphate (PIP2) [3].

In contrast, TLR4 endocytosis was required to induce TRAM-TRIF-dependent interferon (IFN) expression [4]. Together these studies support a mechanism whereby TLR4 at the plasma membrane activates the MyD88-dependent pathway and subsequently upon receptor endocytosis TLR4 signals through TRIF. The

Claire E. McCoy (ed.), *Toll-Like Receptors: Practice and Methods*, Methods in Molecular Biology, vol. 1390,
DOI 10.1007/978-1-4939-3335-8_4,

necessity for receptor endocytosis for the TRIF signal explains the delayed kinetics of activation of this pathway. Consequently, it was found that the reason TLR4 is compartmentalized in an endosome for TRIF-induced IFN induction is to position the receptor complex adjacent to TRAF3 [5]. TRAF3 appears to be restricted in its mobility and is only found intracellularly [4]. The detailed mapping of the dynamic cellular processes involved in TLR responses has come about mainly due to cell biological studies and has relied heavily on fluorescent microscopy.

Immunofluorescence is a specific example of immunocytochemistry that makes use of fluorophores to visualize the location of a specific protein of interest in cells. Antibodies are important tools for demonstrating both the presence and the subcellular localization of an antigen. A primary antibody, that binds your protein of interest, is directly conjugated to a fluorophore or bound by a secondary antibody conjugated to a fluorophore, this allows for visualization of the protein by fluorescent microscopy. Immunofluorescence also allows researchers to determine which subcellular compartments express the protein through co-localization studies.

Sample preparation of cells for immunofluorescence involves a sequence of steps starting with fixing the cells to the slide. Fixation of cells stops cellular metabolism, immobilizing the antigens, maintaining protein structure and retaining authentic cellular and subcellular architecture and location. For intracellular staining, antibodies need to traverse across the membrane, which is impermeable to most antibodies, for this reason the cell membranes must be permeabilized. Permeabilization, usually with detergent, allows for both antibodies and dyes to cross cell membranes while preserving cellular structure. The non-specific binding of antibodies to proteins other than their target antigen causes high background signals. Protein blocking minimizes background fluorescence from non-specific binding of antibodies, maximizing signal-to-background ratios and improving sensitivity. This step is especially important when looking for low-expressing antigens where signals will be dimmer, or when using samples with high autofluorescence. Once fixed, permeabilized and blocked cells are bathed in a quenching buffer to reduce autofluorescence caused by the aldehyde fixatives reacting with amines and proteins.

At this stage the cells are ready for incubation with your primary antibodies of choice. This step is followed by washes, a further incubation with the fluorescently tagged secondary antibodies and further wash steps. Stained cells are then coated in mounting solution and covered with a glass coverslip, ready for imaging.

When planning your experimental set up, it is advisable to plate enough wells to run the appropriate negative controls alongside your experimental wells. Negative controls establish background fluorescence and non-specific staining of the primary

antibodies. Ideally, the controls for non-specific staining should be isotype-matched immunoglobulin fractions obtained from the same animal strain used for generating the primary antibody.

Immunofluorescence is a powerful technique, however, its use for intracellular localization studies is largely limited to fixed (i.e. dead) cells, as antibodies cannot cross the cell membrane of living cells. Overexpression of recombinant fluorescently tagged proteins offers an alternative approach to the study of intracellular trafficking of TLRs. This involves the introduction of a plasmid coding for your protein of interest genetically modified with an N- or C-terminal fluorescent protein, such as green fluorescent protein (GFP). Once transfected or transduced with the fluorescently tagged protein, localization studies can be performed on live or fixed cells and analyzed by confocal microscopy. Another advantage is that this methodology allows an easy way of studying mutant version of the protein of interest. Together, these methods are valuable tools for the determination of subcellular compartmentalization and trafficking of TLR signaling components in individual cells.

2 Materials

2.1 Cell Culture

2.1.1 HEK293 and iBMDM

1. Human embryonic kidney (HEK) 293 cells.
2. HEK293 TLR4^{Cherry} cells [6].
3. HEK293 TLR4^{YFP} cells [7].
4. HEK293 TLR2^{YFP} [7].
5. Immortalized Bone Marrow-Derived Macrophages (iBMDMs).
6. Peripheral Blood Mononuclear Cells (PBMCs).
7. Dulbecco's Modified Eagle's Medium (DMEM) supplemented with 10 % FCS and 2 mM glutamine with 50 μg/ml gentamycin.
8. Phenol-red-free DMEM (*see* **Note 1**) supplemented with 10 % FCS and 2 mM glutamine with 50 μg/ml gentamycin.
9. Trypsin-EDTA solution: 0.5 g/ml Trypsin, 0.2 g/ml EDTA.
10. 0.5 mg/ml G418.
11. T75 cell culture flasks.
12. 35 mm MatTek Glass Bottom Dishes.
13. Chamber slides.
14. Bright light microscope.
15. Coverslips.

2.1.2 Isolation of Human PBMCs

1. Lymphoprep (Axis-Shield).
2. Human A+ serum, pooled from four donors (The Blood Bank, St Olavs Hospital, Trondheim, Norway).
3. RPMI-1640 medium (Sigma).
4. L-Glutamine (Sigma).
5. Dulbecco's phosphate buffered saline (Sigma).
6. Hanks' Balanced Salt solution (Sigma).
7. ZAP-OGLOBIN II Lytic Reagent.
8. Sterile 50 ml Polypropylene tubes.
9. T75 cell culture flasks.
10. 35 mm MatTek Glass Bottom Dishes.

2.2 Transient Transfection

1. Expression plasmids (*see* Subheading 2.2.1).
2. Sterile water.
3. Opti-MEM.
4. GeneJuice™ transfection reagent.
5. Lipofectamine transfection reagent.
6. Lipofectamine® RNAiMAX reagent.
7. Sterile 1.5 ml eppendorfs.

2.2.1 Expression Vectors

1. TLR1-YFP [8].
2. TLR2-GFP [9].
3. TLR3-CFP (*see* **Note 2**).
4. TLR4-mcherry [6].
5. TLR4-YFP [7].
6. TLR5-CFP (*see* **Note 2**).
7. TLR6-YFP (*see* **Note 2**).
8. TLR7-YFP (*see* **Note 2**).
9. TLR8-YFP (*see* **Note 2**).
10. TLR9-YFP (*see* **Note 2**).
11. TLR10-YFP (*see* **Note 2**).
12. MyD88-CFP [7].
13. Mal-CFP [7].
14. TRAM-GFP [10].
15. TRAM-CFP [10].
16. TAG-GFP [11].
17. TMED7-GFP [12].
18. TMED7-CFP [12].

19. TRIF-CFP (*see* **Note 2**).
20. Rab5-CFP [13].
21. Rab7-YFP [14].
22. Rab11-CFP [6].
23. $EEA1_{C\text{-}t}$-CFP [15].
24. $EEA1_{C\text{-}t}$ -GFP [15].
25. LAMP1-GFP [16].
26. ER-CFP (Clontech).
27. Golgi-CFP (Clontech).
28. Unc93b-GFP [17].

2.3 Live Cell Imaging

1. Confocal microscope with a heating stage.
2. 1 M HEPES (*see* **Note 3**).

2.3.1 TLR Ligands

1. TLR1/2: 20 nM Pam3Cys (Invivogen).
2. TLR2/6: 20 nM Malp2 (Alexis Corporation).
3. TLR3: 5–25 μg/ml Poly(I:C) (Invivogen).
4. TLR4: 10–100 ng/ml ultrapure LPS 0111:B4 (Invivogen).
5. 1 μg/ml Fluorescent LPS Alexa fluor conjugates (Life Technologies).
6. TLR5: 10 ng to 10 μg/ml flagellin (Invivogen).
7. TLR7/8: 1–5 μg/ml R848/Clo75 (Invivogen).
8. TLR9: 1–2.5 μM CpG ODN (Invivogen).

2.4 Fixed Cell Imaging

1. Paraformaldehyde (PFA) (*see* **Note 4**).
2. 1 M $MgCl_2$: 4.67 g in 50 ml H_2O.
3. 1 M K-PIPES: 18.93 g in 50 ml H_2O, pH 6.8.
4. 0.17 M EGTA: 3.23 g in 50 ml H_2O (Use a few drops of NaOH to dissolve).
5. 500 mM NH_4Cl: 1.337 g in 50 ml H_2O.
6. 1× Phosphate Buffered Saline (PBS).
7. 10 % Saponin, stored at 4 °C (*see* **Note 5**).
8. PEM (General tubulin buffer): 80 mM K-Pipes, pH 6.8, 5 mM EGTA, 1 mM $MgCl_2$, 0.05 % Saponin.
9. Block and Antibody buffer: 10 % FCS, 1 % BSA, 0.05 % Saponin in PBS.
10. Glycerol.
11. Mowiol® 4-88 (Sigma).
12. 0.2 M Tris–HCl buffer, pH 8.5.

13. 0.1 % aqueous solution of *p*-Phenylenediamine (PPD)
14. Primary antibodies of interest (*see* **Note 6**).
15. Secondary antibodies conjugated to a fluorescent dye such as Alexa Fluor.
16. Hoechst 33342 Fluorescent Stain (Thermo Scientific, Pierce).
17. Antibodies for negative controls (*see* **Note 7**).
18. Confocal microscope.

3 Methods

3.1 Cell Culture

3.1.1 HEK293 and iBMDM

1. HEK293 cells and iBMDMs are cultured in DMEM and maintained at 37 °C in a humidified atmosphere of 5 % CO_2. Cells are seeded at 1×10^5 cells/ml (15 ml per T75 flask) and subcultured two to three times a week when cells reach 50–80 % confluency.
2. Cells are removed from the surface of the flask by incubation with 5 ml of Trypsin-EDTA (0.05 mg/ml) for 1–3 min. Complete medium (10 ml) is then added to the cells, the contents of the cells are then transferred to a 30 ml tube and centrifuged at $110 \times g$ for 5 min.
3. The supernatant is discarded and the cells are resuspended in 1 ml of complete medium and counted using a hemocytometer and a bright light microscope.
4. Cells can be transfected with appropriate DNA plasmids (*see* Subheading 3.2) and set up for fixed cell imaging (*see* Subheading 3.4) or prepared for live cell imaging (*see* Subheading 3.3).

3.1.2 Human PBMCs

1. Add 100 ml PBS to a 75 cm^2 flask and incubate at 37 °C.
2. Incubate 50 ml of Lymphoprep solution at 37 °C.
3. Wash the tube of the infusion bag with 70 % ethanol and cut using a sterile scalpel.
4. Transfer the blood from the infusion bag (~25 ml) to the PBS and mix carefully.
5. Transfer 35 ml of the PBS/blood solution to four separate 50 ml tubes.
6. Add 12.5 ml of Lymphoprep to each of the four 50 ml by carefully applying from the bottom of the tube.
7. Spin at $690 \times g$ for 25 min at 20 °C. Avoid using the centrifugal brakes for fast retardation.

8. Remove the PBMCs (creamy white layer close to the center of the tube) carefully by the use of a pipette.
9. Split the PBMCs into two 50 ml tubes.
10. Spin at 840 × *g* for 10 min at 20 °C. Brakes for fast retardation can now be used in all the following steps.
11. Carefully remove the supernatant by decanting. Always keep an eye on the pellet.
12. Resuspend the pellet in 20 ml Hanks solution and spin at 250 × *g* for 8 min 20 °C. Repeat this step two times.
13. Resuspend the pellet in 20 ml Hanks and remove 20 μl for counting and spin the rest of the cells at 190 × *g* for 8 min at 20 °C.
14. Resuspend the cells in 10 ml isoton solution supplemented with two drops of ZAP-OGLOBIN II Lytic Reagent to lyse red blood cells.
15. Resuspend the cells in 5 ml RPMI medium without serum.
16. Generate a stock solution of 4×10^6 cells/ml in medium containing 5 % A+ serum.
17. Plate 8×10^6 cells (2 ml) in 35 mm MatTech dishes and incubate for 1 h in the CO_2 incubator for adherence of cells.
18. Remove the non-adherent cells by three successive washes in Hanks solution. Allow a 2 min rest between each wash.
19. Add RPMI growth medium supplemented with 10–30 % A+ serum. DO NOT USE ANTIBIOTICS if the cells are to be treated with siRNA.
20. Cells can be set up for fixed cell imaging (*see* Subheading 3.4) or first transfected with siRNA (*see* Subheading 3.2.3).

3.2 Transient Transfection

3.2.1 HEK293 Cells

1. HEK293 cells are seeded at 2.5×10^5 cells per well in 35 mm MatTek Glass Bottom Dishes in 2 ml of complete antibiotic-free medium and grown overnight.
2. GeneJuice is used to transfect HEK293 cells where the ratio of GeneJuice to DNA is 3 μl:1 μg. Cells are transfected with a total of 1 μg DNA per transfection. Ensure that the total DNA concentration still equates to 1 μg DNA even if multiple plasmids are co-transfected. We have most commonly used DNA generated from expression vectors listed in Subheading 2.2.1. Mix the appropriate amount of GeneJuice (3 μl per transfection × 1.2) with serum-free Opti-MEM (100 μl per transfection × 1.2) and incubate at RT for 5 min (*see* **Note 8**).
3. Add the appropriate amounts of DNA (1 μg per transfection × 1.1) to separate eppendorfs.

4. Add 110 µl (i.e. 100 µl × 1.1) of the GeneJuice/Opti-MEM mix to the DNA, invert tube five times and incubate for 15 min at RT.
5. Remove 100 µl of medium from the cell culture dish, discard and replace with 100 µl of GeneJuice/Opti-MEM/DNA mix to each dish.
6. Cells can now be assessed for live cell imaging (*see* Subheading 3.3).

3.2.2 iBMDMs

1. Cells are seeded at 2.5×10^5 cells per well in 35 mm MatTek Glass Bottom Dishes in 2 ml of complete antibiotic-free medium and grown overnight.
2. The ratio of Lipofectamine to DNA is 3 µl:1 µg per transfection.
3. The appropriate amount of Lipofectamine (3 µl per transfection × 1.1) is mixed with serum-free Opti-MEM (250 µl per transfection × 1.1) and incubated at RT for 5 min.
4. In a separate eppendorf add serum-free Opti-MEM (250 µl per transfection × 1.1) to appropriate amount of DNA (1 µg per transfection × 1.1) and incubate for 5 min at RT.
5. Mix 260 µl of each mixture together and incubate for a further 15 min at RT.
6. Remove 500 µl of medium from the cell culture dish, discard and replace with 500 µl of DNA/Opti-MEM/Lipofectamine mixture.
7. Cells can now be assessed for live cell imaging (*see* Subheading 3.3).

3.2.3 PBMCs

1. Isolate the PBMCs as described in Subheading 3.1.2 and incubate the PBMCs in 30 % A+ for 7 days to differentiate them into macrophages. On day 7 transfect the cells to your protein of interest using the following steps.
2. Add 10 µl of siRNA from stock solution (10 µM) and 490 µl Opti-MEM into eppendorf tube A and mix by pipetting.
3. Add 10 µl of RNAiMAX and 490 µl Opti-MEM into eppendorf tube B and mix by gently pipetting.
4. Incubate for 5 min at RT.
5. Transfer the content of tube B into tube A and mix by gentle pipetting.
6. Incubate for 15–20 min at RT.
7. Mix by gentle pipetting before transferring 485 µl of the transfection solution into two separate 35 mm MatTech dishes. The protocol can be scaled up to treat ten dishes at the time.

8. Incubate for 2–3 days before changing the medium (RPMI growth medium supplemented with 30 % A+ serum). If knock down is not sufficient, repeat the treatment with siRNA.
9. Incubate for 1 day before stimulating cells with the appropriate TLR ligand.
10. Cells can now be assessed by fixed cell imaging (*see* Subheading 3.4).

3.3 Live Cell Imaging

1. 24 h after transfection of cells remove the medium in the cell culture dishes and replace with complete clear DMEM (2 ml per dish).
2. Place dishes back in the 37°C incubator overnight to rest.
3. Add 50 μl of 1 M HEPES to dishes if not using a microscope equipped with a CO_2 chamber.
4. Add 1 μg/ml of Hoechst nuclear stain.
5. Remove 1 ml of medium from dishes, leaving 1 ml remaining.
6. Working in the dark, place dish on 37°C heating stage and capture images with a 60× oil objective (*see* **Notes 9** and **10**).
7. Stimulate cells with the appropriate concentration of TLR ligand as listed in Subheading 2.3.1 and continue to capture images.

3.4 Fixed Cell Imaging

3.4.1 Preparation of 4 % PFA

1. Weigh out 4 g PFA (*see* **Note 11**) in a fume hood and dissolve in 50 ml H_2O. Dissolving the powder will require warming the solution on a heating block and the addition of one or two drops of 1 M NaOH. Do not boil the solution.
2. When the solution is clear cool to RT and add 10 ml of 10× PBS.
3. Analyze the pH and make to pH 7.4.
4. Make the solution up to a final volume of 100 ml. This can be aliquoted and frozen.

3.4.2 Preparation of Mounting Solution

1. Weigh out 6 g glycerol in a 50 ml plastic tube, add 2.4 g of Mowiol and stir thoroughly using a stirring bar.
2. Add 6 ml H_2O and leave stirring for 2 h at RT.
3. Continue stirring and add 12 ml of 0.2 M Tris–HCl buffer, pH 8.5, and incubate at approximately 53 °C until the Mowiol dissolves.
4. Clarify by centrifugation at 4000–5000 × *g* for 20 min and aliquot into 1.5 ml tubes. Stored frozen it should last for up to 12 months and is stable at RT for 1 month.

5. Add 1 part of PPD aqueous solution (antifade agent) to 9 parts Mowiol solution to each aliquot immediately before first use (*see* **Note 9**).
6. Add 1 μg/ml of Hoechst nuclear stain to mounting solution before first use.

3.4.3 Fixation, Permeabilizing, and Intracellular Staining

1. Cells (as listed in Subheading 2.1) are seeded at 1.25×10^5 cells/ml of complete medium on chamber slides and grown overnight.
2. Stimulate cells with TLR ligand (*see* Subheading 2.3.1) for required time.
3. Stop the reaction by addition of the same volume of 4 % PFA as there is medium in the well so that there is a final concentration of 2 % PFA. Incubate at RT for 15 min.
4. Remove PFA/medium and wash cells gently by dropping PBS down the sides of the wells with a (Pasteur) pipette three times for 1 min each time (*see* **Note 10**).
5. Block cells at RT for 10 min with blocking buffer.
6. Remove blocking buffer and permeabilize the cells with PEM/Saponin on ice for 15 min.
7. Remove PEM/Saponin and quench-free aldehyde groups with 50 mM NH_4Cl/Saponin for 5 min at RT.
8. Remove Quenching buffer and incubate with blocking buffer for 10 min at RT.
9. Add 80 μl of primary antibody (2–5 μg/ml of polyclonal antibody or 10 μg/ml of monoclonal antibody in antibody buffer) for 60 min at RT (*see* **Note 12**).
10. Wash cells gently in PBS/Saponin three times for 1 min each time.
11. Wash cells in blocking buffer once.
12. Remove all buffers.
13. Add 80 μl of the secondary antibody (1 μg/ml) for 15–30 min at RT.
14. Wash cells gently in PBS/Saponin.
15. Remove well dividers carefully.
16. Add a drop of mounting solution to each fixed area (approximately 15–20 μl total for a 22×22 coverslip or 40–50 μl total for 22×50 mm coverslip).
17. Gently place coverslip onto slide.
18. Leave cover-slipped slides in the dark overnight to harden, coverslips do not require sealing by nail-varnish.
19. Slides can be stored at –20°C or are ready for imaging by confocal microscopy (*see* **Notes 9**, **10**, and **13**).

4 Notes

1. Using clear media can optimize image clarity and signal-to-noise ratio throughout the imaging period. We tend to use clear DMEM, but there are alternatives on the market that are designed specifically for live cell imaging such as "Live Cell Imaging Solution," an optically clear physiological solution that helps keep cells healthy for up to 4 h and FluoroBrite™ DMEM (Life Technologies), an optically clear solution for long-term imaging and subsequent cell culture, which can be used alternatively.
2. Fluorescently tagged TLR expression vectors are available from Addgene.
3. Live-cell imaging of dynamic processes requires active observation over time which can be challenging, it is essential that the cells be healthy and maintained as closely as possible to physiological temperature, pH, oxygen tension, and other conditions. Use of HEPES in the media acts as a CO_2 buffer in the absence of a fully incubated heating stage mounted to the microscope.
4. There are many ways to fix cell samples, each method has its own strengths and unique characteristics. Fixation methods fall generally into two classes: organic solvents and cross-linking reagents. We use PFA, which is a cross-linking reagent. PFA forms intermolecular bridges, normally through free amino groups, creating a network of linked antigens. Cross-linkers preserve cell structure better than organic solvents, but may reduce the antigenicity of some cell components, they also require the addition of a permeabilization step, to allow access of the antibody to the specimen.
5. We use 0.05 % Saponin to permeabilize cells, however alternative detergents can be used such as Triton X-100 or Tween-20 can be used.
6. Fixation may denature protein antigens, and for this reason, antibodies prepared against denatured proteins may be more useful for cell staining. For detecting Rab5, Rab7, Rab11, LAMP1 and LC3, we tend to use antibodies sourced from Santa Cruz.
7. Ideally the controls for non-specific staining should be isotype-matched immunoglobulin fractions obtained from the same animal strain used for generating the primary antibody. For fluorescent analysis of cells with Fc receptors, the use of isotype-matched negative controls is mandatory.
8. Volumes are multiplied by 1.2 or by 1.1 to encompass pipetting error.

9. Loss of fluorescence through irreversible photobleaching processes can lead to a significant reduction in sensitivity. This problem is particularly relevant to live cell imaging when excitation light can be of long duration, or when target molecules are of low abundance so excitation light is of high intensity. While anti-fade reagents minimize photobleaching we recommend that you keep laser power as low as possible and if capturing images using a number of different channels, use only one laser channel to scan for cells of interest imaging to avoid photobleaching as much as possible. Photobleaching occurs due to the decomposition of fluorophores by reactive oxygen species (ROS), if photobleaching is a significant problem ROS inhibitors can extend the life of the fluorophores.
10. Do not let the cells dry at any stage. Especially during washing, handle each dish individually, since leaving a washed dish without medium for even a few seconds can cause drying in the center of the dish.
11. As an alternative to preparing your own PFA, 16 % methanol-free PFA can be purchased from Alfa Aesar GmbH & Co instead.
12. Optimum times for incubating cells with primary antibody can vary, you may find that incubating the cells overnight at 4 °C produces better results. If you are observing high background signal or weak fluorescence, lower the concentration of primary antibody, if this does not work you may need to try an antibody from an alternative manufacturer. If further optimization is required BackDrop® Background Suppressor ReadyProbes™ Reagent (Life technologies), are a set of reagents designed to suppress background fluorescence in live-cell imaging samples.
13. In general when undertaking imaging by confocal microscopy you would be advised to work in the dark and work quickly to minimize photobleaching thereby achieving the best possible images. You will find that some fluorescently tagged plasmids and secondary antibody-conjugated fluorophores are much more sensitive to photobleaching than others.

References

1. Oshiumi H, Sasai M, Shida K, Fujita T, Matsumoto M, Seya T (2003) TIR-containing adapter molecule (TICAM)-2, a bridging adapter recruiting to toll-like receptor 4 TICAM-1 that induces interferon-beta. J Biol Chem 278:49751–49762
2. Husebye H, Halaas O, Stenmark H, Tunheim G, Sandanger O, Bogen B, Brech A, Latz E, Espevik T (2006) Endocytic pathways regulate Toll-like receptor 4 signaling and link innate and adaptive immunity. EMBO J 25: 683–692
3. Kagan JC, Medzhitov R (2006) Phosphoinositide-mediated adaptor recruitment controls Toll-like receptor signaling. Cell 125:943–955

4. Kagan JC, Su T, Horng T, Chow A, Akira S, Medzhitov R (2008) TRAM couples endocytosis of Toll-like receptor 4 to the induction of interferon-beta. Nat Immunol 9:361–368
5. Tanimura N, Saitoh S, Matsumoto F, Akashi-Takamura S, Miyake K (2008) Roles for LPS-dependent interaction and relocation of TLR4 and TRAM in TRIF-signaling. Biochem Biophys Res Commun 368:94–99
6. Husebye H, Aune MH, Stenvik J, Samstad E, Skjeldal F, Halaas O, Nilsen NJ, Stenmark H, Latz E, Lien E, Mollnes TE, Bakke O, Espevik T (2010) The Rab11a GTPase controls Toll-like receptor 4-induced activation of interferon regulatory factor-3 on phagosomes. Immunity 33:583–596
7. Latz E, Visintin A, Lien E, Fitzgerald KA, Monks BG, Kurt-Jones EA, Golenbock DT, Espevik T (2002) Lipopolysaccharide rapidly traffics to and from the Golgi apparatus with the toll-like receptor 4-MD-2-CD14 complex in a process that is distinct from the initiation of signal transduction. J Biol Chem 277:47834–47843
8. Sandor F, Latz E, Re F, Mandell L, Repik G, Golenbock DT, Espevik T, Kurt-Jones EA, Finberg RW (2003) Importance of extra- and intracellular domains of TLR1 and TLR2 in NFkappa B signaling. J Cell Biol 162:1099–1110
9. Manukyan M, Triantafilou K, Triantafilou M, Mackie A, Nilsen N, Espevik T, Wiesmuller KH, Ulmer AJ, Heine H (2005) Binding of lipopeptide to CD14 induces physical proximity of CD14, TLR2 and TLR1. Eur J Immunol 35:911–921
10. Fitzgerald KA, Rowe DC, Barnes BJ, Caffrey DR, Visintin A, Latz E, Monks B, Pitha PM, Golenbock DT (2003) LPS-TLR4 signaling to IRF-3/7 and NF-kappaB involves the toll adapters TRAM and TRIF. J Exp Med 198:1043–1055
11. Palsson-McDermott EM, Doyle SL, McGettrick AF, Hardy M, Husebye H, Banahan K, Gong M, Golenbock D, Espevik T, O'Neill LA (2009) TAG, a splice variant of the adaptor TRAM, negatively regulates the adaptor MyD88-independent TLR4 pathway. Nat Immunol 10:579–586
12. Doyle SL, Husebye H, Connolly DJ, Espevik T, O'Neill LA, McGettrick AF (2012) The GOLD domain-containing protein TMED7 inhibits TLR4 signalling from the endosome upon LPS stimulation. Nat Commun 3:707
13. Galperin E, Sorkin A (2003) Visualization of Rab5 activity in living cells by FRET microscopy and influence of plasma-membrane-targeted Rab5 on clathrin-dependent endocytosis. J Cell Sci 116:4799–4810
14. Henry RM, Hoppe AD, Joshi N, Swanson JA (2004) The uniformity of phagosome maturation in macrophages. J Cell Biol 164:185–194
15. Simonsen A, Lippe R, Christoforidis S, Gaullier JM, Brech A, Callaghan J, Toh BH, Murphy C, Zerial M, Stenmark H (1998) EEA1 links PI(3)K function to Rab5 regulation of endosome fusion. Nature 394:494–498
16. Minin AA, Kulik AV, Gyoeva FK, Li Y, Goshima G, Gelfand VI (2006) Regulation of mitochondria distribution by RhoA and formins. J Cell Sci 119:659–670
17. Tabeta K, Hoebe K, Janssen EM, Du X, Georgel P, Crozat K, Mudd S, Mann N, Sovath S, Goode J, Shamel L, Herskovits AA, Portnoy DA, Cooke M, Tarantino LM, Wiltshire T, Steinberg BE, Grinstein S, Beutler B (2006) The Unc93b1 mutation 3d disrupts exogenous antigen presentation and signaling via Toll-like receptors 3, 7 and 9. Nat Immunol 7:156–164

Chapter 5

Assessing the Inhibitory Activity of Oligonucleotides on TLR7 Sensing

Jonathan Ferrand and Michael P. Gantier

Abstract

Aberrant sensing of self-nucleic acids by Toll-like receptor (TLR) 7, 8, or 9 is associated with several autoimmune disorders, including systemic lupus erythematosus (SLE), rheumatoid arthritis, psoriasis, or systemic sclerosis. In recent years, several classes of synthetic oligonucleotides have been shown to antagonize sensing of immunostimulatory nucleic acids by TLR7/8/9, indicating that these molecules could have therapeutic applications in such autoimmune diseases. Conversely, synthetic oligonucleotides used in therapeutic technologies such as antisense and microRNA inhibitors also have the potential to inhibit TLR7/8/9 sensing, rendering patients more susceptible to viral/bacterial infections. This chapter describes a protocol to define the inhibitory activity of synthetic oligonucleotides on TLR7.

Key words Innate immunity, Oligonucleotides, Toll-like receptors, TLR7, TLR8

1 Introduction

The discovery of Toll-like receptors (TLRs) and their crucial role in the activation of the innate response against pathogen infections in 1997–1998 [1, 2] have revolutionized the field of immunology, leading to the award of the 2011 Nobel Prize in Medicine for this finding. TLRs are specialized in the detection of pathogen-associated molecular patterns (PAMPs), which are normally not expressed by the host. Nonetheless, TLRs specialized in the detection of nucleic acids, such as TLR3, 7, 8, and 9, have the potential capacity to detect both self- and non-self-nucleic acids. To prevent detection of self-DNA/RNA and safeguard the homeostasis of the host, expression of TLR3/7/8/9 is limited to a few cell types and furthermore is restricted to the endosomal compartment.

TLR7 and 8 are specialized in the detection of viral single-stranded RNAs and bacterial RNA [3]. They are predominantly expressed in immune cells, with a prevalence in plasmacytoid dendritic cells (pDCs) and B cells for human TLR7, and monocytes

Claire E. McCoy (ed.), *Toll-Like Receptors: Practice and Methods*, Methods in Molecular Biology, vol. 1390,
DOI 10.1007/978-1-4939-3335-8_5,

for human TLR8 [4]. Their restriction to the endosomal compartment limits their contact with phagocytosed RNAs from infected apoptotic cells, bacteria, or viral particles. Delivery of extracellular RNA to endosomal TLRs can be facilitated by host cargos, such as LL37 or HMGB1/2 [5, 6].

Critically, the specificity of TLR7/8 sensing of non-self-RNA relies on modifications generally absent in foreign RNAs. As such, human ribosomal RNA contains 25 times more 2′-O-methylated bases (2′OMe) and 10 times more pseudo-uridines than bacterial ribosomal RNA [7]. Incorporation of 2′OMe residues directly suppresses TLR7/8 signaling [8–11], presumably by increasing the affinity of the RNA molecules to the TLRs but without allowing structural changes in TLR7/8 required for signaling [12]. As such, one molecule of 2′OMe-modified RNAs can inhibit more than 80 molecules of immunostimulatory RNA [13]. Conversely, posttranscriptional modification of viral RNA, such as conversion of adenosine residues into inosine residues by host deaminases, can facilitate recognition of viral RNA by TLR7/8 [14].

Despite these multiple safeguards to prevent recognition of self-RNA, sensing of host RNAs by TLR7/8 may occur through enhanced expression of TLR7/8 or favored uptake of self-RNAs, to contribute to the development of autoimmune diseases such as systemic lupus erythematosus (SLE), rheumatoid arthritis, psoriasis, or systemic sclerosis (reviewed in [3, 15]). Indeed, TLR7 and 8 being the only TLRs expressed on the X chromosome, it is remarkable to note that SLE incidence is directly correlated with a chromosome X dosage effect in both humans [16, 17] and mice models [18, 19]. Furthermore, overexpressed antimicrobial peptide LL37 can form a complex with self-RNA and activate TLR7/8-driven autoinflammatory responses in psoriasis [5]. In addition, the use of TLR7 agonists exacerbates psoriasis in patients [20] and induces SLE and psoriasis-like symptoms in mice [21, 22], confirming the direct contribution of TLR7/8 engagement in these autoimmune disorders.

Collectively, these data suggest that strategies aimed at antagonizing TLR7/8 could have therapeutic potential against several autoimmune disorders. In favor of this concept, the antimalarial drug hydroxychloroquine is therapeutically used against rheumatic diseases, including rheumatoid arthritis and SLE, through its potential action on endosomal maturation and interaction with nucleic acids, which inhibit TLR7/8 signaling [23, 24]. In addition, recent reports suggest that specific TLR7/8/9 antagonists based on modified synthetic oligonucleotides could have therapeutic potential in the treatment of SLE and psoriasis [25–27]. Such immunosuppressive oligonucleotides can benefit from base modifications, specific motifs, and backbone chemistry [11, 28–31]. In line with this, we have recently discovered that different types of steric antisense oligonucleotides designed to target specific microRNAs could act as specific TLR7/8 inhibitors [13]. Critically, we

demonstrated that 2′OMe-modified oligonucleotides inhibited TLR7/8 with different potencies, independent of TLR9, in a motif-dependent manner [13]. These findings pave the way for the rational design of novel specific TLR7/8 inhibitors, to treat auto-inflammatory disorders. In addition, these studies underline the important immune regulation of synthetic oligonucleotides used in other technologies such as antisense or microRNA inhibitors, potentially inducing long-term immunosuppressive effects in patients. In this chapter, we describe a protocol that allows for the screening of oligonucleotides that antagonize TLR7 signaling.

2 Materials

2.1 Cell Culture

1. L929 cells (ATCC reference CCL-1).
2. Dulbecco's Modified Eagle's Medium (DMEM; Life Technologies) supplemented with 10 % sterile fetal bovine serum (FBS; ICPBio Ltd, New Zealand) and 1× antibiotic/antimycotic (Life Technologies); referred to as complete DMEM.
3. Roswell Park Memorial Institute medium (RPMI) 1640 plus l-glutamine medium (Life Technologies) complemented with 1× antibiotic/antimycotic and 10 % FBS; referred to as complete RPMI.
4. Dulbecco's Phosphate-Buffered Saline (DPBS; Life Technologies).
5. TrypLE™ Express Stable Trypsin (Life Technologies).
6. Tissue culture plastic ware: sterile tissue culture treated microtest™ 96-well plates; 100 mm sterile tissue culture treated dishes; T175 and T75 sterile tissue culture treated flasks (BD Falcon).
7. Corning® 500 ml bottle-top vacuum filter system (Sigma-Aldrich).
8. 0.22 μm polyethersulfone filters (Sigma-Aldrich).
9. Cell scrapers 24 cm (TPP).
10. Sterile carbon steel surgical scalpel blades (No. 10) (Swann-Morton Ltd).
11. 27G ½ PrecisionGlides needles (BD).
12. 10 ml plastipak syringes (BD).

2.2 BMDM Transfection and Stimulation

1. Stimulant of TLR7/8, R848: stock solution at 1 mg/ml in endotoxin-free sterile H_2O (Invivogen).
2. *N*-[1-(2,3-Dioleoyloxy)propyl]-*N*,*N*,*N*-trimethylammonium methylsulfate (DOTAP) (Roche).
3. Nuclease-free TE Buffer, pH 7.0 and 8.0, for RNA and DNA oligonucleotides, respectively (Life Technologies).

4. Oligonucleotides are synthesized as single-stranded molecules by Integrated DNA Technologies (IDT), with standard desalting purification. The oligonucleotides are resuspended into filter-sterilized TE buffer to a concentration of 40 μM.
5. Control RNA sequences used:
   (a) B-406AS-1: 5′UAAUUGGCGUCUGGCCUUCUU 3′ (nonmodified RNA);
   (b) RD: 5′UAACACGCGACAGGCCAACUU 3′ (nonmodified RNA);
   (c) NC1: 5′GzCGUAUUAUAGCCGAUUAACGzA 3′ (all bases are 2′OMe RNA and "z" denotes ZEN groups (IDT) [13, 32]).

2.3 TNF-α ELISA

1. TNF-α OptEIA ELISA set (BD Biosciences).
2. TNF-α coating buffer: 0.084 mg $NaHCO_3$, 0.036 mg Na_2CO_3 in 10 ml of double-distilled H_2O (ddH_2O), freshly made up.
3. 10× PBS: NaCl 8 % (w/v), KCl 0.2 % (w/v), Na_2HPO_4 1.22 % (w/v), KH_2PO_4 0.2 % (w/v) in ddH_2O, pH 7.4.
4. PBS-tween (PBST): 1× PBS diluted in H_2O complemented with 0.05 % tween 20.
5. Pharmingen Assay Diluent (BD Biosciences).
6. F96 maxisorp plates (Nunc).
7. Tetramethyl benzidine substrate (TMB, Sigma-Aldrich).
8. Sulfuric acid 2 N.
9. Plate reader with 450 nm absorbance filter.

3 Methods

This section details a method to measure the inhibitory activity of oligonucleotides on immunostimulatory RNA sensing by TLR7, in the biologically relevant context of primary macrophages. Although more appropriate than the use of HEK293-TLR7 cells for its reliance on macrophages, which naturally express TLR7, the use of primary bone marrow-derived macrophages (BMDMs) has several limitations. It necessitates access to a mouse facility and appropriate local ethics clearance, relies on a 7-day differentiation of the macrophages, and is limited by the maximum amount of cells that can be purified and differentiated from one mouse. As such, this protocol may not be suitable for the screening of more than ~60 to 70 different oligonucleotides at a time, given the variability of responsiveness of BMDMs from mouse to mouse, making it very difficult to combine data from larger sets of oligonucleotides tested in different BMDMs.

3.1 Cell Culture

3.1.1 L929 cell-Conditioned Medium

The differentiation of bone marrow into macrophages is carried out in L929 cell-conditioned medium, as a source of M-CSF. This medium is prepared in 250 ml batches as follows.

1. Culture L929 cells from a frozen vial in complete RPMI at 37 °C in 5 % CO_2 until the cells reach ~95 % confluency in a 100 mm tissue culture dish. Collect the cells, rinse with DPBS with 1.5 ml TrypLE™ Express, and passage them into 3× 100 mm dishes in complete RPMI and expand to ~95 % confluency.
2. Collect the cells from two of the 100 mm dishes and pool them together to inoculate 5× T175 flasks, with 50 ml of complete RPMI per flask. Freeze down the cells from the third dish for stock. This is day 0. Incubate the cells for 5 days at 37 °C in 5 % CO_2 (*see* **Note 1**).
3. On day 5, collect the conditioned medium from each flask into 50 ml sterile tubes and centrifuge at 300 × *g* for 2 min to pellet any potential floating cells. Pool the 5× 50 ml conditioned medium into a Corning® 500 ml bottle-top vacuum filter system and filter sterilize it. Aliquot by 12 ml (in 15 ml tubes), and freeze at −80 °C or use to make BMDMs. The medium can be kept for 2 weeks at 4 °C without any noticeable impact on activity.

3.1.2 BMDM Harvest

1. Collect the two femurs from a humanely killed mouse (4–12 weeks old) and clean them to remove most of the connective tissue (*see* **Note 2**).
2. In a sterile tissue culture cabinet, rinse one femur for 10 s in 80 % (v/v) EtOH, and then in DPBS for 30 s.
3. Cut the two ends of the femur using a sterile scalpel blade while holding the middle of the bone with sterile tweezers (*see* **Note 3**).
4. Flush/collect the bone marrow in a new 15 ml sterile tube using 5 ml of complete DMEM in a 10 ml syringe with a 27G ½ needle, by inserting the needle inside the end of the bone (*see* **Note 4**).
5. Repeat this process with the second femur and pool the 10 ml of bone marrow.
6. Spin down the bone marrow at 300 × *g* for 5 min.
7. Discard the supernatant and vigorously resuspend the bone marrow using a 1 ml pipette with 800 µl of complete DMEM, to minimize cell aggregates.
8. Transfer the cells into 24 ml of complete DMEM in a 50 ml sterile tube. Add 6 ml of L929 cell-conditioned medium to obtain 30 ml and mix the cells by pipetting up and down several times with a 10 ml pipette.

9. Transfer the cells into two tissue culture treated T75 flasks (15 ml per flask) and incubate at 37 °C in 5 % CO_2. This is day 0.
10. On day 3, collect the culture medium into a 50 ml sterile tube, and replenish the medium with 10 ml fresh complete DMEM and 3 ml L929 cell-conditioned medium, per flask. Spin down the culture medium to collect floating cells and resuspend them in 2 ml complete DMEM per flask (i.e., use 4 ml if the culture medium is pooled from two flasks). Add 2 ml of these cells to each flask, giving a final volume of 15 ml (*see* **Note 5**). Further incubate the cells until day 6.
11. In the afternoon of day 6, discard the medium and add 3 ml of complete DMEM to one flask (*see* **Note 6**). Collect the cells with a sterile cell scraper and transfer into a 15 ml sterile tube. Rinse the flask a second time with 2 ml of complete DMEM and renew scraping to maximize the amount of cells collected.
12. Count the cells with a hemacytometer and plate 80,000 macrophages per well of a 96-well plate in 150 µl of complete DMEM supplemented with 20 % L929 cell-conditioned medium. Incubate the cells overnight until day 7, when the cells are stimulated with the TLR7 agonists/inhibitors (*see* **Note 7**).

3.2 BMDM Transfection and Stimulation

This protocol relies on the use of a single-stranded immunostimulatory RNA (ssRNA), referred to as B-406AS-1, which specifically activates TLR7 in mouse BMMs [13, 14, 33]. Importantly, B-406AS-1 is synthesized with unmodified RNA bases, thereby mimicking biologically relevant immunostimulatory RNAs. Given that chemical agonists of TLR7, such as R848 and imiquimod, engage several distinct residues of TLR7 compared to ssRNA with functional downstream consequences [34], it is preferable to use a natural TLR7 ligand (in the form of an ssRNA) to screen for TLR7 antagonists. Importantly, our optimization studies demonstrated that consecutive transfection of the indicated doses of (1) the inhibitory oligonucleotide tested, followed by (2) transfection of the immunostimulatory ssRNA, resulted in optimal reproducibility. The RD RNA sequence can be used as a noninhibitory oligonucleotide (to control for the effect of the first transfection), while the NC1 RNA sequence can be used as a positive inhibitory oligonucleotide, dampening by >50 % the production of TLR7-driven TNF-α.

3.2.1 Transfection of TLR7 Inhibitory Oligonucleotides

Please note that the volumes provided below allow for the use of biological triplicate samples for each condition tested, which is highly recommended.

1. Dilute the oligonucleotides 1/10 to 4 µM in TE buffer under sterile conditions.

2. In a new 0.5 ml tube, mix 6 µl of 4 µM oligonucleotide (such as NC1 or RD) with 32 µl of pure DMEM (without antibiotics or serum). In a separate tube, mix 1.05 µl of DOTAP with 37 µl of pure DMEM and incubate at room temperature (RT) for 2–5 min.
3. Add the DOTAP mix to the oligonucleotide mix with gentle tapping and incubate for 10 min at RT (*see* **Note 8**).
4. In the meantime, rinse the cells with 150 µl of complete DMEM.
5. Add 25 µl of the oligonucleotide/DOTAP mix per well, giving three wells with 175 µl for each condition. Incubate at 37 °C in 5 % CO_2 for 30–45 min maximum, and proceed to the transfection of the immunostimulatory ssRNA (Subheading 3.2.2).

3.2.2 Transfection of Immunostimulatory ssRNA

1. Mix 2.68 µl of 40 µM B-406AS-1 with 36 µl of pure DMEM, per condition, i.e., three wells (a mastermix should be used to increase robustness).
2. Mix 4.75 µl of DOTAP with 33 µl of pure DMEM per condition and incubate for 2–5 min at RT.
3. Add the DOTAP mix to the oligonucleotide mix with gentle tapping and incubate for 10 min at RT.
4. Add 25 µl of B-406AS-1/DOTAP mix per well, giving three wells with 200 µl for each condition (with 40 nM of inhibitory oligonucleotide and 180 nM of immunostimulatory ssRNA). Incubate at 37 °C in 5 % CO_2 overnight (16–18 h) and collect supernatants for analysis of TNF-α production (*see* **Note 9**).

3.3 TNF-α Production Analysis by ELISA

A TNF-α ELISA is performed to assess the inhibitory activity of the oligonucleotides on TLR7 sensing.

1. The day before the assay (or a few days before), coat a maxisorp 96-well plate with 80 µl of capture antibody diluted 1:500 in coating buffer, and leave sealed with tape at 4 °C. The morning of the assay, rinse the plate three times with PBST and block for 1 h at RT with 100 µL Assay Diluent per well, with rocking.
2. Following blocking, wash the plate three times with PBST. Prepare the TNF-α standard curve following the Analysis Certificate leaflet from the kit, to give a concentration range from 1000 to 15.6 pg/ml (seven points). Add 50–75 µl of neat supernatant or standard to each well of the ELISA plate, and incubate for 2 h at RT, with rocking.
3. Wash the plate three times with PBST and prepare the working detector antibody. Dilute both detection antibody and streptavidin-horseradish peroxidase (SAv-HRP) to 1:500 in Assay Diluent. Incubate for 10 min before adding 80 µl per well, and further incubate for 1 h at RT. Following five to

seven PBST washes, perform the enzymatic assay. Add 80 µl of pre-warmed TMB (at 25–37 °C) per well and incubate at RT in the dark until a blue color develops. Stop the reaction with 40 µl sulfuric acid. Read the absorbance in a plate reader within 30 min at 450 nm.

4. To determine the inhibitory effect of the oligonucleotides tested, divide each concentration measured by the average concentration for the condition RD + B-406AS-1.

4 Notes

1. The L929 cells should reach 100 % confluency on day 3 and will then stop growing. The medium will probably get slightly yellow by day 5, but this should have no impact on the health of the cells. Very little cell debris should be present in the medium on day 5.
2. The femurs can be kept in DPBS on ice for less than 24 h. For this however, it is essential to maintain the integrity of the bones, and as such, great care should be taken during collection. Broken bones should be used immediately. Noteworthy, the ability to keep the bones for up to 24 h makes it possible to use overnight shipping to collaborating laboratories.
3. This can be carried out in a lid of a 60 mm sterile dish. Fine movements of the blade with limited pressure on the bone works better than static heavy pressure, as it avoids crushing the bone.
4. Flush the bone from both ends to maximize collection. At the end of this process, the bone should appear mostly white.
5. By day 3, a good proportion of cells should be sticking to the bottom of the flask. The collection of cells in suspension is used here to maximize the amount of cells obtained, but is facultative.
6. On day 6, the cells should be 70–90 % confluent, and the medium probably slightly yellow.
7. It should be noted that by day 7, >90–95 % of the cells will be differentiated into macrophages. Nonetheless, this procedure does not exclude fibroblasts that rapidly adhere between day 0 and 1. Purity of the differentiated cells can be assessed by flow cytometry using expression of CD11c+ and F4/80. The average yield of BMDMs for one mouse should be $>1 \times 10^7$ cells.
8. A mastermix of DOTAP/pure DMEM can be made to increase robustness between the conditions.
9. Appropriate positive and negative controls should also be used. RD + B-406AS-1 condition should be used as a negative control

and reference to calculate inhibitory activity by the oligonucleotide tested. R848 added directly to the medium to a final concentration of 1–2 μg/ml can also be used as a positive control. NC1 + B-406AS-1 condition (or any other inhibitory sequences reported in [13], such as miR-122 AMO "2′OMe 5 in ZEN, 3′ZEN"; Fig. 1) can be used as a positive control for inhibition of TLR7 sensing. Mock and Medium controls, with DOTAP only and no-treatment, respectively, should also be used to define baseline cytokine production by the cells (Fig. 1).

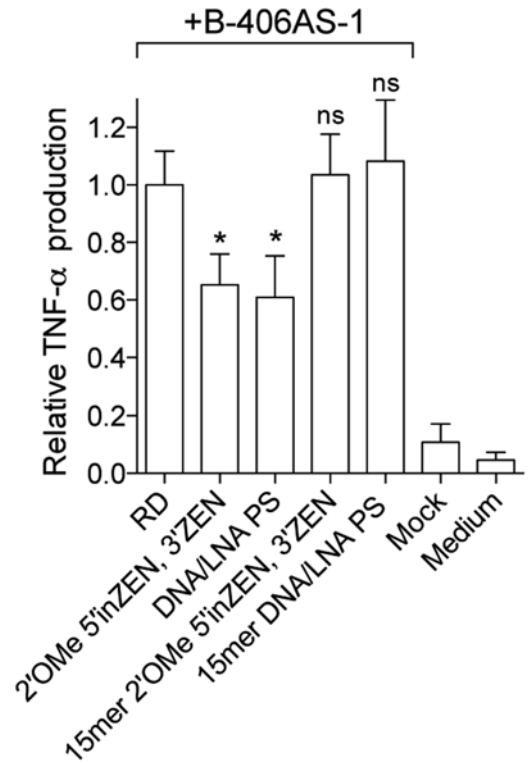

Fig. 1 Inhibition of TLR7 sensing by miR-122 synthetic inhibitors in mouse macrophages. Primary mouse macrophages were treated as presented in Subheading 3.2 with 40 nM of the indicated synthetic oligonucleotides targeting miR-122 (as published in [32]), and 180 nM of B-406AS-1 complexed with DOTAP, for 16–18 h. Each treatment was carried out in biological triplicate and the data are from four independent experiments. Two-tailed unpaired *t*-tests comparing to RD+B406AS-1 condition and standard error of the mean are shown (ns: not significant; $*p<0.05$). The data are shown relative to the condition RD + B406AS-1, and suggest that short versions ("15mer") of the oligonucleotides targeting miR-122 have no inhibitory activity on TLR7 sensing, and are therefore preferable to limit immunosuppression in patients. Mock condition refers to DOTAP control (without any RNA), and Medium condition to nonstimulated cells (to determine basal cytokine production)

Acknowledgments

The authors thank Frances Cribbin for her help with the redaction of this chapter and Soroush Sarvestani for performing the experiments shown in Fig. 1. The authors are supported by funding from the Australian NHMRC (1022144, 1062683 and 1081167 to MPG); the Australian Research Council (140100594 Future Fellowship to MPG); and the Victorian Government's Operational Infrastructure Support Program.

References

1. Medzhitov R, Preston-Hurlburt P, Janeway CA Jr (1997) A human homologue of the Drosophila Toll protein signals activation of adaptive immunity. Nature 388(6640):394–397. doi:10.1038/41131
2. Poltorak A, He X, Smirnova I, Liu MY, Van Huffel C, Du X, Birdwell D, Alejos E, Silva M, Galanos C, Freudenberg M, Ricciardi-Castagnoli P, Layton B, Beutler B (1998) Defective LPS signaling in C3H/HeJ and C57BL/10ScCr mice: mutations in Tlr4 gene. Science 282(5396):2085–2088
3. Sarvestani ST, Williams BR, Gantier MP (2012) Human Toll-like receptor 8 can be cool too: implications for foreign RNA sensing. J Interferon Cytokine Res 32(8):350–361. doi:10.1089/jir.2012.0014
4. Hornung V, Rothenfusser S, Britsch S, Krug A, Jahrsdorfer B, Giese T, Endres S, Hartmann G (2002) Quantitative expression of toll-like receptor 1-10 mRNA in cellular subsets of human peripheral blood mononuclear cells and sensitivity to CpG oligodeoxynucleotides. J Immunol 168(9):4531–4537
5. Ganguly D, Chamilos G, Lande R, Gregorio J, Meller S, Facchinetti V, Homey B, Barrat FJ, Zal T, Gilliet M (2009) Self-RNA-antimicrobial peptide complexes activate human dendritic cells through TLR7 and TLR8. J Exp Med 206(9):1983–1994. doi:10.1084/jem.20090480
6. Yanai H, Ban T, Wang Z, Choi MK, Kawamura T, Negishi H, Nakasato M, Lu Y, Hangai S, Koshiba R, Savitsky D, Ronfani L, Akira S, Bianchi ME, Honda K, Tamura T, Kodama T, Taniguchi T (2009) HMGB proteins function as universal sentinels for nucleic-acid-mediated innate immune responses. Nature 462(7269):99–103. doi:10.1038/nature08512
7. Bokar JA, Rottman FM (1998) Biosynthesis and functions of modified nucleosides in eukaryotic mRNA. In: Modification and editing of RNA. American Society of Microbiology, Washington, DC. doi:10.1128/9781555818296.ch10
8. Kariko K, Buckstein M, Ni H, Weissman D (2005) Suppression of RNA recognition by Toll-like receptors: the impact of nucleoside modification and the evolutionary origin of RNA. Immunity 23(2):165–175. doi:10.1016/j.immuni.2005.06.008
9. Cekaite L, Furset G, Hovig E, Sioud M (2007) Gene expression analysis in blood cells in response to unmodified and 2'-modified siRNAs reveals TLR-dependent and independent effects. J Mol Biol 365(1):90–108. doi:10.1016/j.jmb.2006.09.034
10. Sioud M, Furset G, Cekaite L (2007) Suppression of immunostimulatory siRNA-driven innate immune activation by 2'-modified RNAs. Biochem Biophys Res Commun 361(1):122–126. doi:10.1016/j.bbrc.2007.06.177
11. Robbins M, Judge A, Liang L, McClintock K, Yaworski E, MacLachlan I (2007) 2'-O-methyl-modified RNAs act as TLR7 antagonists. Mol Ther 15(9):1663–1669. doi:10.1038/sj.mt.6300240
12. Hamm S, Latz E, Hangel D, Muller T, Yu P, Golenbock D, Sparwasser T, Wagner H, Bauer S (2010) Alternating 2'-O-ribose methylation is a universal approach for generating non-stimulatory siRNA by acting as TLR7 antagonist. Immunobiology 215(7):559–569. doi:10.1016/j.imbio.2009.09.003
13. Sarvestani ST, Stunden HJ, Behlke MA, Forster SC, McCoy CE, Tate MD, Ferrand J, Lennox KA, Latz E, Williams BR, Gantier MP (2015) Sequence-dependent off-target inhibition of TLR7/8 sensing by synthetic microRNA inhibitors. Nucleic Acids Res 112(5):1177–1188. doi:10.1093/nar/gku1343

14. Sarvestani ST, Tate MD, Moffat JM, Jacobi AM, Behlke MA, Miller AR, Beckham SA, McCoy CE, Chen W, Mintern JD, O'Keeffe M, John M, Williams BR, Gantier MP (2014) Inosine-mediated modulation of RNA sensing by Toll-like receptor 7 (TLR7) and TLR8. J Virol 88(2):799–810. doi:10.1128/JVI.01571-13
15. Santegoets KC, van Bon L, van den Berg WB, Wenink MH, Radstake TR (2011) Toll-like receptors in rheumatic diseases: are we paying a high price for our defense against bugs? FEBS Lett 585(23):3660–3666. doi:10.1016/j.febslet.2011.04.028
16. Voskuhl R (2011) Sex differences in autoimmune diseases. Biol Sex Differ 2(1):1. doi:10.1186/2042-6410-2-1
17. Shen N, Fu Q, Deng Y, Qian X, Zhao J, Kaufman KM, Wu YL, Yu CY, Tang Y, Chen JY, Yang W, Wong M, Kawasaki A, Tsuchiya N, Sumida T, Kawaguchi Y, Howe HS, Mok MY, Bang SY, Liu FL, Chang DM, Takasaki Y, Hashimoto H, Harley JB, Guthridge JM, Grossman JM, Cantor RM, Song YW, Bae SC, Chen S, Hahn BH, Lau YL, Tsao BP (2010) Sex-specific association of X-linked Toll-like receptor 7 (TLR7) with male systemic lupus erythematosus. Proc Natl Acad Sci U S A 107(36):15838–15843. doi:10.1073/pnas.1001337107
18. Santiago-Raber ML, Kikuchi S, Borel P, Uematsu S, Akira S, Kotzin BL, Izui S (2008) Evidence for genes in addition to Tlr7 in the Yaa translocation linked with acceleration of systemic lupus erythematosus. J Immunol 181(2):1556–1562
19. Hwang SH, Lee H, Yamamoto M, Jones LA, Dayalan J, Hopkins R, Zhou XJ, Yarovinsky F, Connolly JE, Curotto de Lafaille MA, Wakeland EK, Fairhurst AM (2012) B cell TLR7 expression drives anti-RNA autoantibody production and exacerbates disease in systemic lupus erythematosus-prone mice. J Immunol 189(12):5786–5796. doi:10.4049/jimmunol.1202195
20. Gilliet M, Conrad C, Geiges M, Cozzio A, Thurlimann W, Burg G, Nestle FO, Dummer R (2004) Psoriasis triggered by toll-like receptor 7 agonist imiquimod in the presence of dermal plasmacytoid dendritic cell precursors. Arch Dermatol 140(12):1490–1495. doi:10.1001/archderm.140.12.1490
21. Yokogawa M, Takaishi M, Nakajima K, Kamijima R, Fujimoto C, Kataoka S, Terada Y, Sano S (2014) Epicutaneous application of toll-like receptor 7 agonists leads to systemic autoimmunity in wild-type mice: a new model of systemic Lupus erythematosus. Arthritis Rheumatol 66(3):694–706. doi:10.1002/art.38298
22. van der Fits L, Mourits S, Voerman JS, Kant M, Boon L, Laman JD, Cornelissen F, Mus AM, Florencia E, Prens EP, Lubberts E (2009) Imiquimod-induced psoriasis-like skin inflammation in mice is mediated via the IL-23/IL-17 axis. J Immunol 182(9):5836–5845. doi:10.4049/jimmunol.0802999
23. Lee SJ, Silverman E, Bargman JM (2011) The role of antimalarial agents in the treatment of SLE and lupus nephritis. Nat Rev Nephrol 7(12):718–729. doi:10.1038/nrneph.2011.150
24. Kuznik A, Bencina M, Svajger U, Jeras M, Rozman B, Jerala R (2011) Mechanism of endosomal TLR inhibition by antimalarial drugs and imidazoquinolines. J Immunol 186(8):4794–4804. doi:10.4049/jimmunol.1000702
25. Jiang W, Zhu FG, Bhagat L, Yu D, Tang JX, Kandimalla ER, La Monica N, Agrawal S (2013) A Toll-like receptor 7, 8, and 9 antagonist inhibits Th1 and Th17 responses and inflammasome activation in a model of IL-23-induced psoriasis. J Invest Dermatol 133(7):1777–1784. doi:10.1038/jid.2013.57
26. Zhu FG, Jiang W, Bhagat L, Wang D, Yu D, Tang JX, Kandimalla ER, La Monica N, Agrawal S (2013) A novel antagonist of Toll-like receptors 7, 8 and 9 suppresses lupus disease-associated parameters in NZBW/F1 mice. Autoimmunity 46(7):419–428. doi:10.3109/08916934.2013.798651
27. Sun S, Rao NL, Venable J, Thurmond R, Karlsson L (2007) TLR7/9 antagonists as therapeutics for immune-mediated inflammatory disorders. Inflamm Allergy Drug Targets 6(4):223–235
28. Kandimalla ER, Bhagat L, Wang D, Yu D, Sullivan T, La Monica N, Agrawal S (2013) Design, synthesis and biological evaluation of novel antagonist compounds of Toll-like receptors 7, 8 and 9. Nucleic Acids Res 41(6):3947–3961. doi:10.1093/nar/gkt078
29. Wang D, Bhagat L, Yu D, Zhu FG, Tang JX, Kandimalla ER, Agrawal S (2009) Oligodeoxyribonucleotide-based antagonists for Toll-like receptors 7 and 9. J Med Chem 52(2):551–558. doi:10.1021/jm8014316
30. Barrat FJ, Meeker T, Gregorio J, Chan JH, Uematsu S, Akira S, Chang B, Duramad O, Coffman RL (2005) Nucleic acids of mammalian origin can act as endogenous ligands for Toll-like receptors and may promote systemic lupus erythematosus. J Exp Med 202(8):1131–1139. doi:10.1084/jem.20050914

31. Gorden KK, Qiu X, Battiste JJ, Wightman PP, Vasilakos JP, Alkan SS (2006) Oligodeoxynucleotides differentially modulate activation of TLR7 and TLR8 by imidazoquinolines. J Immunol 177(11):8164–8170
32. Lennox KA, Owczarzy R, Thomas DM, Walder JA, Behlke MA (2013) Improved performance of anti-miRNA oligonucleotides using a novel non-nucleotide modifier. Mol Ther Nucleic Acids 2, e117. doi:10.1038/mtna.2013.46
33. Gantier MP, Tong S, Behlke MA, Irving AT, Lappas M, Nilsson UW, Latz E, McMillan NA, Williams BR (2010) Rational design of immunostimulatory siRNAs. Mol Ther 18(4):785–795. doi:10.1038/mt.2010.4
34. Colak E, Leslie A, Zausmer K, Khatamzas E, Kubarenko AV, Pichulik T, Klimosch SN, Mayer A, Siggs O, Hector A, Fischer R, Klesser B, Rautanen A, Frank M, Hill AV, Manoury B, Beutler B, Hartl D, Simmons A, Weber AN (2014) RNA and imidazoquinolines are sensed by distinct TLR7/8 ectodomain sites resulting in functionally disparate signaling events. J Immunol 192(12):5963–5973. doi:10.4049/jimmunol.1303058

Part II

Toll-Like Receptor Cross-Priming of Associated Receptors

Chapter 6

Methods for Delivering DNA to Intracellular Receptors

Katryn J. Stacey, Adi Idris, Vitaliya Sagulenko, Nazarii Vitak, and David P. Sester

Abstract

Cytosolic DNA can indicate infection and induces type I interferon (IFN) and AIM2 inflammasome responses. Characterization of these responses has required introduction of DNA into the cytosol of macrophages by either chemical transfection or electroporation, each of which has advantages in different applications. We describe here optimized procedures for both electroporation and chemical transfection, including the centrifugation of chemical transfection reagent onto cells, which greatly increases the speed and strength of responses. Appropriate choice of DNA and use of these methods allow study of either the cytosolic DNA responses in isolation or the simultaneous stimulation of cytosolic receptors and the CpG DNA receptor toll-like receptor 9 (TLR9) in the endosomes.

Key words Cytosolic DNA, Macrophage, Transfection, Electroporation, Centrifection, AIM2, cGAS, Inflammasome, Pyroptosis, Interferon

1 Introduction

Detection of foreign DNA in the cytosol occurs in infections with viruses such as vaccinia and MCMV as well as with cytosolic bacteria such as *Francisella* [1, 2]. Two pathways of response have been characterized, leading either to induction of type I interferon (IFN) [3, 4] or release of IL-1β and cell death [5–7]. Although innate immune cell pattern recognition receptors generally recognize microbial molecules as intrinsically foreign structures not present in the host, this is not the case for DNA. Rather, it is the aberrant location that triggers the alarm; both self and foreign DNAs are perceived as a danger to the cell when found in the cytosol. Following binding to cytosolic DNA, cyclic GMP-AMP synthase (cGAS) catalyzes formation of a cyclic dinucleotide second messenger, which subsequently binds to STING and initiates downstream signaling leading to IFN-β production [4]. A second response to DNA is the activation of the absent in melanoma 2 (AIM2) inflammasome [5, 6]. DNA recruits AIM2, which in turn recruits the inflammasome

Claire E. McCoy (ed.), *Toll-Like Receptors: Practice and Methods*, Methods in Molecular Biology, vol. 1390,
DOI 10.1007/978-1-4939-3335-8_6,

adapter molecule ASC (apoptosis-associated speck-like protein containing a CARD), to form a single focus—the "ASC speck." ASC binds caspase-1, inducing its dimerization and activation. Active caspase-1 elicits rapid lytic cell death termed pyroptosis, as well as cleaving proinflammatory cytokines IL-1β and IL-18 to their active forms prior to their release. Both these responses occur only with double-stranded (ds) DNA in a DNA length-dependent manner, and there is no effect of single-stranded DNA. cGAS and AIM2 both predominantly bind to the phosphate backbone of dsDNA [8, 9] and there is therefore little sequence dependence. In contrast, the CpG DNA receptor TLR9 is located in endosomes and recognizes unmethylated CG dinucleotide-containing motifs in either single- or double-stranded bacterial DNA or oligonucleotides [10, 11]. The choice of DNA as well as the method of application of DNA to cells is important to consider when targeting TLR9, cytosolic receptors, or both simultaneously.

The characterization of pathways in response to cytosolic DNA has depended heavily on the introduction of DNA into macrophage cells. Here we describe methods for both electroporation and chemical transfection of macrophages, for studying these responses. Each of these techniques has advantages for different applications. The mechanism through which electroporation permeabilizes cells is incompletely understood [12]. Electroporation seems to deliver macromolecules directly into the cytosol [13] avoiding endocytic pathways and associated nucleases [14]. In addition, electroporation introduces a bolus of DNA at one instant, and so the response of cells is rapid and relatively synchronous. Electroporation in cuvettes is convenient for analyses of early responses requiring nonadherent cells, such as flow-cytometric detection of pyroptosis by probing membrane integrity as described here, or quantification of ASC speck formation [15]. Chemical transfection, on the other hand, is convenient if adherent cells are to be studied, although nonadherent cells can also be chemically transfected. Advantages over electroporation include the ease of transfecting larger numbers of samples, and when conducted on adherent cells, the suitability for subsequent analysis by microscopy. Complexes of transfection reagent with DNA enter the cells through endocytosis and DNA must escape from the endosome into the cytosol. This is by nature a slower process than electroporation, and generally an inferior method for studying rapid DNA-dependent pyroptosis, which requires a certain threshold of cytosolic DNA. However, here we describe an optimized chemical transfection procedure involving centrifugation of transfection complex onto cells [16], which we term centrifection. Centrifection generates a much more synchronous and profound response than conventional chemical transfection, and also reduces the amount of ligand required for assays. Furthermore, we highlight two techniques which can be used to assess cell death mediated by the

AIM2 inflammasome following transfection of DNA—the MTT assay for cell viability, and the monitoring of membrane integrity in real time, by flow cytometry.

In planning experiments on macrophage DNA responses, it is important to consider whether only TLR9, or only cytosolic DNA responses, or both responses simultaneously are to be measured. Macrophage TLR9 responses can be efficiently elicited by non-transfected bacterial DNA as well as CpG-containing oligonucleotides, but not by vertebrate DNA, which has CpG suppression and methylation [11, 17]. Macrophages bind and take up DNA into the endosomal pathway where it is exposed to TLR9. Chemical transfection of DNA certainly enhances exposure of TLR9 to DNA but is not necessary for studying TLR9 responses, and would be undesirable if double-stranded DNA is used and activation of cytosolic pathways is not wanted. However, chemical transfection of bacterial DNA could be used to elicit simultaneous stimulation of TLR9 and cytosolic DNA recognition pathways. On the other hand, electroporation should not enhance TLR9 responses, as the plasma membrane is directly permeabilized to DNA. With electroporation, TLR9 should only be exposed to the amount of DNA that manages to bind and be internalized though the normal route into the endosomal system. This exposure can be minimized by washing DNA away after electroporation, but to avoid TLR9 activation nonstimulatory vertebrate DNA [11] should be used, such as calf thymus DNA used here. The DNA most frequently used in publications for stimulating cytosolic responses is the alternating copolymer, poly(dA-dT).poly(dA-dT). However, this has been shown to be an RNA polymerase III substrate, generating double-stranded RNA which activates RIG-I pathways [18]. This complicates interpretation of results, and it cannot be considered solely as an activator of DNA response pathways. In summary, careful consideration of the source of DNA (vertebrate, bacterial, or CpG oligonucleotides) and routes of exposure to DNA will allow tailoring of the responses required.

2 Materials

2.1 Centrifection

1. Complete RPMI-1640: RPMI-1640 supplemented with 10 % heat inactivated fetal calf serum (HI-FCS), 1× GlutaMAX, 50 U/mL penicillin, 50 μg/mL streptomycin, and 25 mM HEPES (optional, *see* **Note 1**). (All reagents were purchased from Life Technologies).
2. Additive-free RPMI-1640: RPMI-1640 alone with no additions.
3. Calf thymus DNA (Sigma Aldrich), further extracted with phenol and chloroform to remove protein, and with Triton X-114 to remove any traces of LPS [11].

4. Ultrapure LPS from *E. coli* 0111:B4 (LPS-EB Ultrapure; Invivogen).
5. Lipofectamine®2000 (Life Technologies).
6. MTT reagent ((3-(4,5-Dimethylthiazol-2-yl)-2,5-Diphenyltetrazolium Bromide); Life Technologies). Prepare a 5 mg/mL stock in PBS, and filter (0.22 μm) to sterilize and remove any remaining insoluble material. Aliquot immediately and store at −20 °C. Aliquots should be protected from light, and may be frozen and thawed a number of times unless a blue formazan precipitate develops.
7. MTT solubilization solution (Isopropanol/10 % Triton X-100/0.1 N HCl), stored at room temperature.

2.2 Electroporation

1. Complete RPMI-1640 (*see* **Item 1,** Subheading 2.1).
2. Propidium Iodide (PI) (Life Technologies). A 5 mg/mL stock solution is prepared in PBS and stored at 4 °C.
3. Electroporator, BioRad Gene Pulser MXcell™ fitted with a Gene Pulser MXcell™ ShockPod Cuvette Chamber (or any other suitable electroporation system, e.g., BioRad Gene Pulser, Gene Pulser II)
4. Flow cytometer, e.g., BD Accuri C6 cytometer and regular heating block, or other cytometer allowing temperature control of the sample.

3 Methods

Carry out all techniques aseptically and at room temperature unless otherwise stated. Cell culture should be carried out in a Class II biosafety cabinet/microbiological safety cabinet.

3.1 Centrifection

3.1.1 BMM Cell Culture

1. Bone marrow-derived macrophages (BMMs) differentiated for 6–10 days should be collected after routine culture on bacteriological plastic plates [19]. Collect culture medium into a 50 mL tube, wash cell monolayer twice with Ca^{2+}/Mg^{2+}-free PBS combining washes with culture medium, and allow attached cells to sit at room temperature (RT) in a minimal volume of Ca^{2+}/Mg^{2+}-free PBS for 5 min. Gently harvest attached cells using a 10 mL serological pipette or blunt-ended 18G needle and 10 mL syringe. Combine harvested cells, washes, and residual culture medium, mix and determine cell density.
2. Pellet cells by centrifugation at 300×*g* for 5 min, remove supernatant, resuspend cell pellet in 100–200 μL of penicillin/streptomycin-free complete RPMI-1640 supplemented with 10^4 U/mL CSF1 (*see* **Note 2**), and generate a single cell suspension by pipetting up and down at least ten times with a P200 pipette set to 200 μL (*see* **Note 3**). Add additional peni-

cillin/streptomycin-free complete RPMI-1640 supplemented with 10^4 U/mL CSF1 to generate a cell suspension of 750,000 cells/mL.

3. Add 100 μL of penicillin/streptomycin-free complete RPMI-1640 per well to positions A1–A2 of a 96-well plate (to use as blank for MTT analysis).
4. Plate 75,000 BMMs (100 μL) per well in a 96-well plate and incubate overnight at 37 °C in an air/5 % CO_2 humidified environment.
5. Following overnight incubation, if required (*see* **Note 4**), add 75 μL of 47 ng/mL LPS in penicillin/streptomycin-free complete RPMI-1640, tap plate gently to mix, and incubate for 4 h (to prime cells at a final concentration of 20 ng/mL LPS).

3.1.2 Preparation of DNA Complexes

1. Outlined below is a method for the preparation of material that will allow for 40 replicates of both mock and calf thymus (CT) DNA treatments, in 96-well format, delivering 125 ng CT DNA per well (*see* **Note 5**). Complexes are prepared at a ratio of 1 μg DNA: 2 μL Lipofectamine®2000 and can be scaled to make more or less as desired (*see* **Notes 6** and **7**).
2. Prepare two 1.5 mL microfuge tubes containing either 125 μL of additive-free RPMI-1640 for "mock" samples or 125 μL of additive-free RPMI-1640 containing 5 μg of CT DNA for "CT DNA" samples.
3. In a 1.5 mL microfuge tube combine 20 μL Lipofectamine®2000 and 230 μL of additive-free RPMI-1640 and mix thoroughly (avoiding the introduction of bubbles) by pipetting up and down with a P200 pipette set to 200 μL, and then incubate at room temperature for 4 min.
4. Add 125 μL of the Lipofectamine®2000 complex mix from **step 3** to each of the 125 μL "mock" preparation from **step 2** and the 125 μL "CT DNA" preparation from **step 2**. Mix thoroughly (avoiding the introduction of bubbles) by pipetting up and down at least five times with a P200 set to 200 μL and incubate at room temperature for 20 min. Dilute each tube 1:4 by addition of 750 μL of additive-free RPMI-1640 and mix thoroughly (avoiding the introduction of bubbles) by pipetting up and down at least three times with a P1000 set to 750 μL.

3.1.3 Application of DNA Complexes

1. Following 4 h of LPS priming of BMMs, add either 25 μL of "mock-Lipofectamine®2000" or "CT DNA-Lipofectamine®2000" preparation (from **step 4**, Subheading 3.1.2).
2. Gently tap the 96-well plate to facilitate mixing of transfection complexes in wells.

3. To achieve enhanced and synchronized delivery of DNA to cells, a "centrifection" step is recommended, which involves centrifugation of plates at 1000 × *g* for 10 min at room temperature. Return plates to the 37 °C incubator following completion of centrifugation.
4. Incubate cells for 1–6 h (*see* **Note 8**).

3.1.4 MTT Viability Assay and ELISA

1. AIM2 inflammasome-mediated pyroptosis can be assessed by a number of means including MTT assay for cell viability. Release of IL-1β can be assessed by ELISA as well as western blotting (*see* **Note 9**). To allow assessment of IL-1β release by ELISA, and cell viability on the one sample, carefully harvest 120 μL of cell culture medium making sure not to disturb cell monolayers/debris during the process. Cell supernatants can be stored at −80 °C until assayed by ELISA for cytokine levels such as IL-1β (Fig. 1a) (*see* **Note 10**).
2. To the remaining 80 μL of culture medium in wells, add 20 μL of 5 mg/mL MTT reagent and return to the incubator for 1 h (*see* **Note 11**).
3. Remove plate and add 125 μL of MTT solubilization solution, seal plate with parafilm and leave overnight at room temperature in the dark.
4. The following day, either tap the plate to mix wells or use a P200 pipette if required to achieve a homogenous solution and measure reduced MTT on a plate spectrophotometer at 570 nm. The background from wells without cells is subtracted from all samples. This can be done in conjunction with a reference wavelength at 630 nm to eliminate background absorbance contributed by cell debris, fingerprints on plates, scratches etc. [20]. Representative data for cell viability using this protocol is presented in Fig. 1a and the AIM2-dependence is shown in Fig. 1b.

3.2 Electroporation

Outlined below is a protocol specifically for the electroporation of BMMs or inflammasome-competent RAW mASC-EGFP cells with CT DNA for the purpose of analysis of pyroptosis via flow cytometry. Electroporation is a versatile method for the introduction of nucleic acid ligands into macrophages. It can be used for study of various AIM2 responses such as pyroptosis (Fig. 2a, b), apoptosis, ASC oligomerization, ASC speck formation, caspase cleavage, and IL-1β release [15, 21, 22], as well as induction of IFN-β mRNA via the cGAS pathway (Fig. 2c).

3.2.1 Cell Culture

1. Conditions described below enable introduction of DNA into both BMMs and RAW264.7 macrophage-like cell line. RAW264.7 cells respond to DNA with induction of IFN-β,

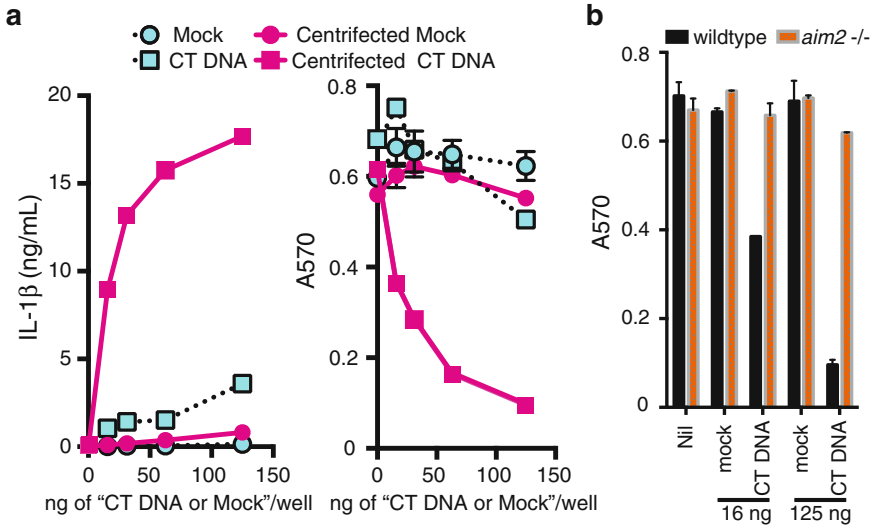

Fig. 1 Centrifection is superior to standard chemical transfection of CT DNA (Subheading 3.1) for eliciting AIM2-dependent pyroptosis and IL-1β production. (**a**) IL-1β levels (*left panel*) (data represent the mean of two technical replicates), and viability of C57BL/6 BMMs measured by MTT reduction (A570—*right panel*) (data represent the mean and range of two technical replicates), exposed for 6 h to varying amounts of CT DNA with transfection reagent (CT DNA). The "mock" controls were treated with transfection reagent alone, at amounts equivalent to those used in the DNA transfections. Plates were treated with or without centrifugation. (**b**) Macrophage cell death after centrifection of CT DNA is dependent on AIM2. Responses of either C57BL/6 BMMs (wildtype) or AIM2-deficient BMMs (*Aim2*−/−) to centrifected DNA of the indicated amount, or transfection reagent alone (Mock). Cell viability was measured by MTT cleavage (A570) after 6 h (data represent the mean and range of two technical replicates)

but have no inflammasome response, due to lack of ASC expression. However, we have generated RAW264.7 cells expressing mouse ASC fused to GFP, and this successfully reconstitutes inflammasome function (*see* Fig. 2a).

2. Harvest cells from routine subculture, count, pellet at 300 × *g* for 5 min (can be conducted as per **step 1,** Subheading 3.1.1). Remove supernatant, resuspend cell pellet in 100–200 μL of complete RPMI-1640, and generate a single cell suspension by pipetting up and down at least ten times with a P200 pipette set to 200 μL (*see* **Note 3**). Add additional complete RPMI-1640 to generate a cell suspension of 2.7×10^6 cells/mL kept at room temperature (*see* **Note 12**).

3.2.2 *Electroporation*

1. Aliquot 380 μL (ca. 1×10^6 cells) of cells in complete RPMI-1640 at room temperature into a BioRad® 0.4 cm electroporation cuvette (*see* **Note 12**). Ensure that the liquid is all in the bottom of the cuvette, and avoid bubbles.
2. Add 10–20 μg of CT DNA in a total volume of 20 μL of PBS, mix thoroughly, pipetting up and down approximately ten times with a P200 pipette set to 200 μL.

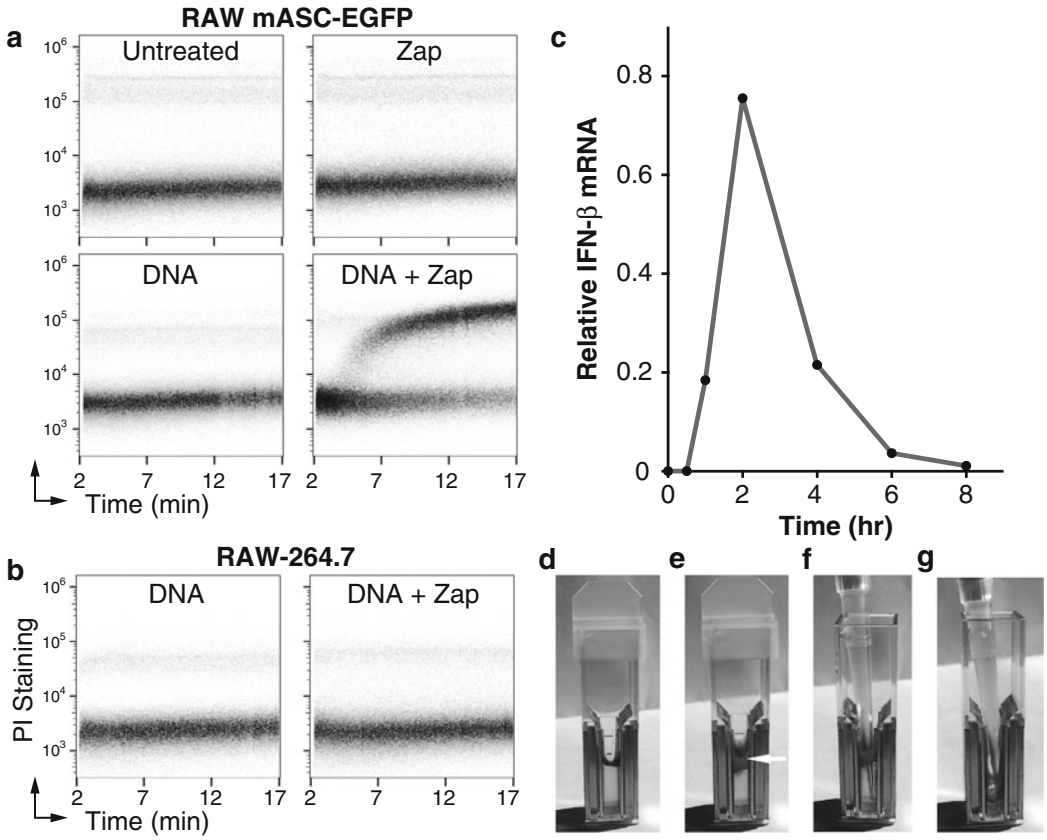

Fig. 2 Methods and analysis of murine macrophages after electroporation with DNA. (**a**) Real-time flow-cytometric analysis of pyroptotic macrophage cell death as described in Subheading 3.2. RAW264.7 cells expressing ASC (RAW mASC-EGFP Clone E5) were analyzed for the indicated time following either no treatment (untreated), electroporation alone (Zap), incubation with 20 μg of CT DNA for 10 min at RT (DNA) or incubation with 20 μg of CT DNA for 10 min at RT followed by electroporation (DNA + Zap). (**b**) The rapid cell death observed with electroporation of DNA into RAW mASC-EGFP cells is inflammasome-dependent as the parental RAW-264.7 cell line, which lacks ASC expression, shows no response. (**c**) A time course of *Ifn-β* mRNA induction following electroporation of *Tlr9–/–* BMMs (C57BL/6 background) with 10 μg of CT DNA. Results were obtained by quantitative real-time PCR and are expressed relative to *Hprt* message levels. (**d–g**) Electroporation and collection of cells as outlined in Subheading 3.2, showing a cell suspension in cuvette prior to electroporation (**d**), following electroporation, noting the floating "gunge" (*arrow*) that forms following electrical discharge (**e**), the positioning of a pipette through the "gunge" (**f**), and collection of cells below the "gunge" (**g**)

3. Incubate at room temperature for 10 min (*see* **Note 13**), and gently flick cuvette contents, without splashing, every 2–3 min to prevent cells settling. The cuvette contents will appear as in Fig. 2d.
4. Electroporate with a BioRad Gene Pulser set to an exponential-decay waveform, 240 V (*see* **Note 14**), 1000 μF (*see* **Note 15**) and infinite resistance. Note the pulse half-life should be 25–35 ms under these conditions (*see* **Note 16**).

3.2.3 Real-Time Flow-Cytometric Analysis

1. Immediately following electroporation a distinctive layer of floating "gunge" will appear (Fig. 2e—see arrow), carefully place a P200 pipette through this material (Fig. 2f), and harvest the lower 300 μL in two 150 μL samplings (Fig. 2g) (*see* **Note 17**).
2. Working quickly, place the first 150 μL aliquot into an empty 1.5 mL microfuge tube, pipette up and down 2–3 times to achieve a single cell suspension, and then transfer to a 1.5 mL microfuge tube containing 950 μL of 37 °C complete RPMI-1640 (*see* **Note 18**) containing 1.5 μg of propidium iodide (PI) (*see* **Note 19**).
3. Repeat **step 2** for the second 150 μL aliquot, transferring it finally to the same 1.5 mL microfuge tube containing the first aliquot and complete RPMI-1640/PI.
4. Place the tube of electroporated cells into a heating block set to 37 °C and position (with support) the heating block under the sample introduction probe (SIP) of a BD Accuri C6 cytometer to allow sample collection (*see* **Note 20**). Collect data with a flow rate of "slow" (14 μL/min), or "custom" (set to 15–25 μL/min), set to "Run Unlimited" for a nominal time (*see* **Notes 21** and **22**).
5. Analyze data using appropriate software (e.g., FlowJo™, C-Flow Plus). Remove debris by SSC-Area v FSC-Area gating, remove doublets by appropriate gating on FSC-Width v FSC-Area. View remaining events in terms of FL3-Area v time.
6. Electroporation cuvettes can be washed and reused (*see* **Note 23**).

4 Notes

1. The addition of 25 mM HEPES is advised for electroporation, to buffer the acidity and alkalinity that results at the anode and cathode of the electroporation cuvette respectively following the electrical discharge.
2. Any commercial source of CSF1 or 20 % L929 cell-conditioned medium may substitute.
3. If larger numbers of cells are being used, and a 200 μL volume does not suffice for resuspending cells, a larger volume (e.g., 5 mL) may be added and a single cell suspension can be generated by passing through a blunt-ended 18G needle at least five times.
4. "Priming" of cells with a toll-like receptor signal like LPS is necessary for effective activation of the NLRP3 inflammasome response, but has only a modest effect on the activation of

caspase-1 and cell death by the AIM2 inflammasome [23]. However, if IL-1β is being measured, priming is necessary to induce pro-IL-1β. The priming time may be reduced to 2 h, when induction of pro-IL-1β is adequate but not maximal.

5. Both the induction of type I IFN and inflammasome responses induced by DNA require double-stranded DNA (dsDNA) and there is no response to single-stranded DNA. Responses are dependent on DNA length; AIM2 responses increase with increasing DNA length from 44 bp and are maximal with DNA greater than 500 bp [6]. Induction of type I IFN was also length-dependent, with optimal responses seen above 90 bp or 245 bp in different cells [18, 24]. Both cGAS and AIM2 bind to the phosphate backbone of DNA in an apparently sequence-independent manner [8, 9]. Consequently any dsDNA of sufficient length will activate these pathways. We routinely use calf thymus DNA (Sigma) [6]. Synthetic polynucleotides have been used as stimuli, and their nomenclature is somewhat confused. The most frequently used ligand is an alternating copolymer poly(dA-dT).poly(dA-dT). This is generally and probably inappropriately written poly(dA:dT) but should not be confused with the hybrid of homopolymers, poly(dA).poly(dT) which has been written poly(dA):(dT) [6]. Poly(dA-dT).poly(dA-dT) is a poor choice of ligand for studying cGAS responses, as it is a template for RNA polymeraseIII and generates dsRNA which induces IFN-β via RIG-I-like receptor pathways [18].
6. We routinely use Lipofectamine2000®, but other transfection reagents may work similarly. The dose of transfection complex should be optimized to minimize effects of the transfection reagent alone. It can be seen in Fig. 1a that the higher concentrations of "centrifected mock" (i.e., transfection reagent alone) caused release of significant amounts of IL-1β. When studying the induction of type I IFN by transfected DNA, we have found occasional induction of IFN-β by Lipofectamine2000® alone, in a batch-dependent manner. Another company's product was superior for that purpose, but its sale is now discontinued. Screening of transfection reagents for induction of IFN-β is recommended.
7. We have found for centrifection that a ratio of 1:2 (μg DNA: μL Lipofectamine®2000) produces a stronger response, in terms of signal to noise, when compared to using a 1:4 ratio.
8. We have observed clear responses to centrifected DNA when assayed as early as 30 min (i.e., cell death as measured by addition of MTT reagent at 30 min followed by a further 1 h incubation). However, sensitivity to lower amounts of DNA may be reduced at shorter time points of incubation. Optimal IL-1β detection may require incubation times of 2 h or more.

9. Here we examine cell medium for the release of IL-1β by ELISA, but for any new procedure more definitive confirmation of inflammasome activation is provided by assessment of IL-1β and caspase-1 cleavage by western blot.
10. Mouse IL-1β IL1F2 DuoSet ELISA kit from R&D Systems (DY401) for assessing levels of IL-1β in culture supernatants, used as per manufacturer's instructions.
11. The MTT assay reagent is reduced to give an insoluble blue formazan product by cellular reductases [25] and is a frequently used measure of cellular viability [20]. The length of incubation with MTT reagent varies depending on plated cell number and metabolic activity of the cells. A 1 h incubation is generally adequate for the 75,000 BMMs plated overnight as described. Some cell lines are significantly more metabolically active and require less time. With experience of this assay, you will be able to judge when to stop the color development to prevent it reaching too high an absorbance after solubilization.
12. The cell number in electroporations can be increased for different applications. We routinely electroporate cells at a concentration of 2×10^7/mL (8×10^6 cells per electroporation) or higher (up to 3×10^7 cells per 400 μL electroporation), when larger numbers are needed for analysis. Cells to be electroporated should be at room temperature and not in warmed medium, to avoid heat stress during the electrical discharge.
13. Electroporation efficiency is improved by prior incubation of cells for up to 10 min with the nucleic acid to allow cell surface binding.
14. The voltage drop across the cell diameter is thought to be the determinant of whether membrane permeabilization will be achieved. Thus small cells would require a higher voltage setting than large cells. We have found for BMMs and RAW264.7 cells that the use of 240 V in a 0.4 cm electroporation cuvette provides effective permeabilization whilst minimizing cell death caused by the electroporation pulse alone. Higher voltages deliver more DNA, but have more pulse-associated toxicity. Note that voltage settings may vary on different instruments; a titration of voltage at a fixed volume and capacitance, in the presence and absence of DNA, will enable optimization to maximize DNA-dependent cell death as an indication of AIM2 response, and minimize the pulse-associated cell death.
15. The capacitance setting determines the total amount of charge that flows through the cuvette. To obtain good transfection of DNA, capacitance must be balanced with the volume in the cuvette. If the volume is reduced, the capacitance should be reduced proportionately, to keep the current density the same.

16. In an exponential decay pulse, an appropriate pulse length $t_{1/2}$ is 25–35 ms. If the pulse length $t_{1/2}$ is above 40, this starts to cause undesirable levels of cell death due to the electrical pulse alone. Increasing the volume or decreasing the capacitance will lower the pulse length.
17. The layer of floating "gunge" consists mainly of cell debris resulting from the electrical discharge. Two 150 μL aliquots are collected with a P200 pipette as a P1000 tip will not reach the bottom of the cuvette. Additionally, a P200 pipette is more efficient at generating a single cell suspension. As an alternative to collecting the lower 300 μL, the entire contents of the cuvette can be collected, added to 10 mL of additive-free RPMI, and centrifuged for 5 min at 350 × *g* to wash out debris and residual DNA. This will normally add another 10 min to the procedure, and hence is not desirable for this real-time death assay. However, this washing step is necessary for removing released cellular proteins from cells lysed directly by the electrical discharge, if analyzing cell-associated and released proteins such as caspase-1 by western blot, or using LDH release as a measure of cell death. Cells need to be maintained at room temperature or less (preferably 4 °C) during the washing step, to prevent the commencement of pyroptosis. Inclusion of the dead cells within the "gunge" resulting from electroporation alone will significantly increase the background % dead cells when analyzed by flow cytometry using DNA-based viability assays (e.g., PI or 7-AAD).
18. Pyroptosis seems to be very temperature sensitive, and is much delayed with medium at room temperature, and prevented at 4 °C. If it is necessary to slow down the initiation of death to allow loading on the flow cytometer, this can be achieved by keeping cells in medium at a lower temperature.
19. This can be easily achieved by addition of 15 μL of 0.1 mg/mL PI solution prepared in PBS, or 150 μL of 0.01 mg/mL PI (in PBS) to 935 μL or 800 μL complete RPMI-1640 respectively.
20. The advantage of the BD Accuri C6 is that the fluidics system utilizes a peristaltic pump, allowing the analysis of samples in a 1.5 mL microfuge tube. Similar analysis can be achieved on other flow-cytometric platforms that allow sample temperature control, by employing appropriate tubes for the given cytometer.
21. It will normally take 2 min from the electroporation of cells to the start of acquiring samples on the cytometer. This may be longer if the cytometer you are using is not in close proximity to where you are conducting electroporations.
22. Data can normally be collected for up to 30 min or longer depending on the flow rate employed. With longer collection

times the sample may have to be gently agitated during acquisition to avoid settling of cells.

23. To wash cuvettes for reuse, place in a container of sterile high quality water immediately after removing cells. As soon as possible after completion of the experiment, wash with multiple changes of high quality water, and then store in 70 % (w/v) ethanol. Before use, tip the ethanol out of cuvettes, and leave to dry in the biosafety cabinet. Bacterial contaminants such as LPS must be excluded from containers and water for washing, and cuvettes must not sit long before washing and sterilizing. Any traces of LPS in the cuvette will lead to induction of IFN-β in cells.

Acknowledgements

This work was supported by National Health and Medical Research Council (NHMRC) grants 1010887 and 1050651. KJS was supported by Australian Research Council (ARC) and NHMRC Fellowships FT0991576 and 1059729. We thank Veit Hornung for the generous provision of bone marrow from *Aim2–/–* mice.

References

1. Rathinam VA, Jiang Z, Waggoner SN, Sharma S, Cole LE, Waggoner L et al (2010) The AIM2 inflammasome is essential for host defense against cytosolic bacteria and DNA viruses. Nat Immunol 11:395–402
2. Dai P, Wang W, Cao H, Avogadri F, Dai L, Drexler I et al (2014) Modified vaccinia virus Ankara triggers type I IFN production in murine conventional dendritic cells via a cGAS/STING-mediated cytosolic DNA-sensing pathway. PLoS Pathog 10:e1003989
3. Ishii KJ, Coban C, Kato H, Takahashi K, Torii Y, Takeshita F et al (2006) A Toll-like receptor-independent antiviral response induced by double-stranded B-form DNA. Nat Immunol 7:40–48
4. Sun L, Wu J, Du F, Chen X, Chen ZJ (2013) Cyclic GMP-AMP synthase is a cytosolic DNA sensor that activates the type I interferon pathway. Science 339:786–791
5. Hornung V, Ablasser A, Charrel-Dennis M, Bauernfeind F, Horvath G, Caffrey DR et al (2009) AIM2 recognizes cytosolic dsDNA and forms a caspase-1-activating inflammasome with ASC. Nature 458:514–518
6. Roberts TL, Idris A, Dunn JA, Kelly GM, Burnton CM, Hodgson S et al (2009) HIN-200 proteins regulate caspase activation in response to foreign cytoplasmic DNA. Science 323:1057–1060
7. Stacey KJ, Ross IL, Hume DA (1993) Electroporation and DNA-dependent cell death in murine macrophages. Immunol Cell Biol 71(Pt 2):75–85
8. Jin T, Perry A, Jiang J, Smith P, Curry JA, Unterholzner L et al (2012) Structures of the HIN domain:DNA complexes reveal ligand binding and activation mechanisms of the AIM2 inflammasome and IFI16 receptor. Immunity 36:561–571
9. Civril F, Deimling T, de Oliveira Mann CC, Ablasser A, Moldt M, Witte G et al (2013) Structural mechanism of cytosolic DNA sensing by cGAS. Nature 498:332–337
10. Hemmi H, Takeuchi O, Kawai T, Kaisho T, Sato S, Sanjo H et al (2000) A Toll-like receptor recognizes bacterial DNA. Nature 408:740–745
11. Stacey KJ, Young GR, Clark F, Sester DP, Roberts TL, Naik S et al (2003) The molecular basis for the lack of immunostimulatory activity of vertebrate DNA. J Immunol 170:3614–3620
12. Escoffre JM, Portet T, Wasungu L, Teissie J, Dean D, Rols MP (2009) What is (still not)

known of the mechanism by which electroporation mediates gene transfer and expression in cells and tissues. Mol Biotechnol 41:286–295

13. Sun C, Cao Z, Wu M, Lu C (2014) Intracellular tracking of single native molecules with electroporation-delivered quantum dots. Anal Chem 86:11403–11409
14. Bamford RA, Zhao ZY, Hotchin NA, Styles IB, Nash GB, Tucker JH et al (2014) Electroporation and microinjection successfully deliver single-stranded and duplex DNA into live cells as detected by FRET measurements. PLoS One 9:e95097
15. Sester DP, Thygesen SJ, Sagulenko V, Vajjhala PR, Cridland JA, Vitak N et al (2014) A novel flow cytometric method to assess inflammasome formation. J Immunol 194(1):455–462
16. Verma RS, Giannola D, Shlomchik W, Emerson SG (1998) Increased efficiency of liposome-mediated transfection by volume reduction and centrifugation. Biotechniques 25:46–49
17. Roberts TL, Dunn JA, Terry TD, Jennings MP, Hume DA, Sweet MJ et al (2005) Differences in macrophage activation by bacterial DNA and CpG-containing oligonucleotides. J Immunol 175:3569–3576
18. Ablasser A, Bauernfeind F, Hartmann G, Latz E, Fitzgerald KA, Hornung V (2009) RIG-I-dependent sensing of poly(dA:dT) through the induction of an RNA polymerase III-transcribed RNA intermediate. Nat Immunol 10:1065–1072
19. Sester DP, Brion K, Trieu A, Goodridge HS, Roberts TL, Dunn J et al (2006) CpG DNA activates survival in murine macrophages through TLR9 and the phosphatidylinositol 3-kinase-Akt pathway. J Immunol 177:4473–4480
20. Mosmann T (1983) Rapid colorimetric assay for cellular growth and survival: application to proliferation and cytotoxicity assays. J Immunol Methods 65:55–63
21. Sagulenko V, Thygesen SJ, Sester DP, Idris A, Cridland JA, Vajjhala PR et al (2013) AIM2 and NLRP3 inflammasomes activate both apoptotic and pyroptotic death pathways via ASC. Cell Death Differ 20:1149–1160
22. Yin Q, Sester DP, Tian Y, Hsiao YS, Lu A, Cridland JA et al (2013) Molecular mechanism for p202-mediated specific inhibition of AIM2 inflammasome activation. Cell Rep 4:327–339
23. Schroder K, Sagulenko V, Zamoshnikova A, Richards AA, Cridland JA, Irvine KM et al (2012) Acute lipopolysaccharide priming boosts inflammasome activation independently of inflammasome sensor induction. Immunobiology 217:1325–1329
24. Abe T, Harashima A, Xia T, Konno H, Konno K, Morales A et al (2013) STING recognition of cytoplasmic DNA instigates cellular defense. Mol Cell 50:5–15
25. Berridge MV, Tan AS (1993) Characterization of the cellular reduction of 3-(4,5-dimethylthiazol-2-yl)-2,5-diphenyltetrazolium bromide (MTT): subcellular localization, substrate dependence, and involvement of mitochondrial electron transport in MTT reduction. Arch Biochem Biophys 303:474–482

Chapter 7

Detection of Interaction Between Toll-Like Receptors and Other Transmembrane Proteins by Co-immunoprecipitation Assay

Yu-Ran Lee, Wondae Kang, and You-Me Kim

Abstract

Toll-like receptors are type I membrane proteins and bind other membrane proteins often via a specific interaction between transmembrane domains. The co-immunoprecipitation assay is a widely used biochemical technique for assessing interactions among proteins in cell lysates or tissue extracts. By isolating a native protein complex with a specific antibody against a protein of interest, followed by western blotting with an antibody for a binding partner, the co-immunoprecipitation assay can be used to confirm a putative interaction between two proteins. The co-immunoprecipitation assay can also be combined with a proteomics approach such as protein mass spectrometry to build an interactome of a target protein. Despite its usefulness and popularity to probe protein interactions within complex biological samples, the co-immunoprecipitation assay of membrane proteins is rather tricky, often resulting in false data. Here, we describe a co-immunoprecipitation method for analyzing interactions between toll-like receptors and other membrane proteins, using the interaction between TLR9 and UNC93B1 as an example. Especially, we describe an optimal cell lysis and sample preparation method to preserve protein interactions mediated by transmembrane domains.

Key words Co-immunoprecipitation, Transmembrane proteins, Toll-like receptors, TLR9, UNC93B1, Digitonin

1 Introduction

Toll-like receptors (TLRs) belong to a major innate immune receptor family and recognize a variety of pathogen-associated molecular patterns as well as endogenous host molecules [1]. TLRs are type I membrane proteins consisting of the N-terminal ligand-binding leucine-rich repeat domain, a single transmembrane domain, and a C-terminal signaling domain [2]. We have shown that several TLRs physically associate with a polytopic membrane protein, UNC93B1, via their transmembrane domain [3]. TLR4, which normally does not bind UNC93B1, becomes associated with UNC93B1 when its transmembrane region is substituted

Claire E. McCoy (ed.), *Toll-Like Receptors: Practice and Methods*, Methods in Molecular Biology, vol. 1390,
DOI 10.1007/978-1-4939-3335-8_7,

with the one from the UNC93B1-interacting TLRs such as TLR3 or TLR9. On the other hand, TLR3 and TLR9 no longer bind UNC93B1 when their transmembrane regions are replaced by that of TLR4. By forming a stable complex with TLRs, UNC93B1 chaperones the receptors from the endoplasmic reticulum to their proper cellular destination, i.e., the plasma membrane or the endosomes, and thereby controls receptor signaling [4–9].

Due to the difficulty of purification and a possible involvement of lipid-embedded regions for binding, an interaction between two membrane proteins are rarely analyzed using highly purified proteins. Instead, a co-immunoprecipitation (co-IP) assay using total cell lysates or a method to visualize the interaction in intact cells, such as a bimolecular fluorescent complementation (BiFC) assay, a fluorescence resonance energy transfer (FRET), or a bioluminescence resonance energy transfer (BRET) assay, is preferred [10–13]. Among these methods, the co-IP assay is most widely used due to several benefits. First, it only requires standard lab equipment whereas the other methods need a complicated fluorescent microscopy setting or a flow cytometer. Second, co-IP can be used to analyze an interaction among endogenous proteins whereas both FRET/BRET and BiFC assays mandate to express each of the two binding partners as a separate fusion protein. Third, co-IP determines a physical interaction among proteins, whereas FRET/BRET and BiFC assays are based on the proximity of two fusion proteins. Lastly, co-IP can be adapted to identify novel protein–protein interactions if combined with a protein identification method such as protein sequencing or mass spectrometry. In contrast, other methods only assess an interaction between two candidate proteins.

Important considerations to achieve successful co-IP experiments include a cell lysis method, a choice of an antibody against the protein of interest, a washing condition to remove nonbinding proteins and more. Among them, the cell lysis condition is especially critical when analyzing an interaction between two membrane proteins. Unlike most of the water soluble proteins, membrane proteins must be solubilized using a detergent, the strength of which will greatly affect the interaction between two membrane proteins. If too strong, it may dissociate the two binding partners, sometimes even denaturing them, and cause a false-negative data. If too weak, it may not sufficiently solubilize membrane lipids and nonbinding neighboring transmembrane proteins remain together as embedded in membrane lipids, leading to a false-positive data.

Digitonin is our choice of detergent for solubilizing TLRs and its transmembrane binding partners [14]. Here, we describe a method to assess the interaction between TLR9 and UNC93B1 proteins by co-IP followed by western blotting. This method can also be applied to monitor interactions between TLRs with other transmembrane proteins.

2 Materials

2.1 Transient Transfection

1. HEK293T cells (ATCC).
2. Dulbecco's Modified Eagle Medium (DMEM; Life Technologies).
3. Fetal bovine serum (FBS; HyClone).
4. Lipofectamine 2000 (Life Technologies).
5. Plasmid DNA: pcDNA3.1-TLR9-myc; pcDNA3.1-UNC93B1 (WT)-HA; pcDNA3.1-UNC93B1 (H412R)-HA.

2.2 Cell Lysis and Co-immunoprecipitation

1. Protease inhibitor cocktail: a mixture of leupeptin, pepstatin A, aprotinin, and phenylmethanesulfonyl fluoride (PMSF) (*see* **Note 1**).
2. Lysis buffer: 50 mM Tris–HCl, pH 8.0, 150 mM NaCl, 5 mM EDTA, 1 % digitonin, and 1× protease inhibitor cocktail (*see* **Notes 2–4**).
3. Bovine serum albumin (BSA) (Roche).
4. BCA protein assay kit (Thermo scientific).
5. Rabbit anti-myc polyclonal antibody (Cell signaling).
6. Protein A-agarose beads (Repligen) (*see* **Note 5**).
7. Washing buffer: 50 mM Tris–HCl, pH 8.0, 150 mM NaCl, 5 mM EDTA, and 0.1 % digitonin (*see* **Note 6**).
8. Sample loading buffer: 50 mM Tris–HCl, pH 6.8, 2 % SDS, 1 % β-mercaptoethanol, 0.02 % bromophenol blue and 10 % glycerol (*see* **Note 7**).

2.3 Sample Preparation and SDS-PAGE

1. Resolving gel buffer: 1.5 M Tris–HCl, pH 8.8 and 0.4 % SDS. Add approximately 300 ml of distilled water in a glass flask. Add 90.86 g of Tris and dissolve with gentle agitation. Adjust the final pH to 8.8 using 5 N HCl (*see* **Note 8**) and add 20 ml of 10 % SDS solution. Add water up to 500 ml and store at room temperature (RT).
2. Stacking gel buffer: 0.5 M Tris–HCl, pH 6.5 and 0.4 % SDS. Weigh 30.29 g Tris to prepare a 500 ml buffer solution as described in **step 1**. Store at RT.
3. 30 % acrylamide/Bis solution (37.5:1) (Bio-Rad). Store at 4 °C (*see* **Notes 9** and **10**).
4. 10 % ammonium persulfate (APS): 10 % APS solution is prepared by dissolving 1 g of APS in 10 ml distilled water (*see* **Note 11**).
5. *N*,*N*,*N*′,*N*′-tetramethyl-ethylenediamine (TEMED) (Bio-Rad). Store at 4 °C.

6. Mini-PROTEAN Tetra Cell electrophoresis apparatus (Bio-Rad). The system includes short plates, spacer plates, gel casting frames, a gel casting stand, combs, an electrode, a buffer dam, a buffer tank, and a lid with power cables.
7. SDS-PAGE running buffer: 25 mM Tris, 192 mM Glycine, and 0.1 % SDS (*see* **Note 12**).
8. PageRuler prestained protein ladder (Thermo scientific).

2.4 Western Blotting

1. Mini Trans-Blot Electrophoretic Transfer Cell system (Bio-Rad). The system includes mini gel holder cassettes, fiber pads, an electrode module, a cooling unit, a buffer tank, and a lid with power cables.
2. Nitrocellulose membrane (GE healthcare).
3. Filter paper (GE healthcare).
4. Transfer buffer: 25 mM Tris, 192 mM glycine, and 20 % methanol (*see* **Note 13**).
5. Tris buffered saline (TBS): 50 mM Tris–HCl, pH 7.4 and 150 mM NaCl (*see* **Note 14**).
6. TBS-T: TBS with 0.1 % Tween-20 (*see* **Note 15**).
7. Blocking solution: 5 % skim milk in TBS-T (*see* **Note 16**).
8. Primary antibodies: mouse anti-myc monoclonal antibody (Cell signaling) and rat anti-HA monoclonal antibody (Roche).
9. Secondary antibodies: goat anti-mouse IgG (H&L) antibody, horseradish peroxidase (HRP)-conjugated (Invitrogen) and goat anti-rat IgG (H&L) antibody, horseradish peroxidase (HRP)-conjugated (Invitrogen).
10. Enhanced chemiluminescence (ECL) solution (Thermo scientific). Store at 4 °C.
11. Antibody stripping buffer: 0.2 M glycine–HCl, pH 2.2, 0.1 % SDS, and 1 % tween-20 (*see* **Note 17**).

3 Methods

The following methods describe the transient expression of TLR9-myc and UNC93B1-HA fusion proteins in HEK293T cells and the subsequent co-immunoprecipitation experiment.

3.1 Transient Transfection

1. Seed 0.8×10^6 HEK293T cells in 2 ml DMEM (10 % FBS) per well in a 6 well plate (*see* **Note 18**). Incubate the cells in a cell culture incubator (37 °C, 5 % CO_2) for 16 h.
2. Before transfection, change the cell culture media with fresh, pre-warmed DMEM (10 % FBS).

3. Aliquot 300 μl of pre-warmed, serum-free DMEM into microtubes and add 9 μl of Lipofectamine 2000 by inserting the pipet tip in the middle of the media and slowly releasing the transfection reagent dropwise (*see* **Notes 19** and **20**). Incubate at RT for 5 min.
4. In new microtubes, mix 2 μg of pcDNA3.1-TLR9-myc with 1 μg of pcDNA3.1-UNC93B1 (WT)-HA or pcDNA3.1-UNC93B1 (H412R)-HA.
5. Transfer the diluted transfection reagent from **step 3** drop by drop into the center of the microtubes containing the DNA mixture. Incubate at RT for 15 min to allow the formation of DNA-containing liposomes.
6. Add the transfection mixture from **step 5** to the cells dropwise. Gently swirl the plate once and culture the cells for 48 h in a cell culture incubator.

3.2 Cell Lysis and Co-immunoprecipitation

1. Harvest the cells and spin them down by centrifugation at 300 × *g* for 5 min. Wash the cells once by resuspending them in 1 ml of cold PBS. After centrifugation, carefully remove the supernatant and add 500 μl of the cold lysis buffer to the cell pellet. Completely resuspend the cell pellet by trituration and incubate at 4 °C for 0.5–1 h with gentle rotation. To remove insoluble cell debris and nuclei, centrifuge the cell lysate at 13,000 × *g* in a microcentrifuge for 10 min and transfer the supernatant to new microtubes. Keep the cell lysates on ice or at 4 °C during the entire procedure of co-immunoprecipitation.
2. To measure the protein concentration of the cell lysate, perform the BCA protein assay (*see* **Note 21**). Prepare the working BCA reagent by mixing the BCA reagent A and the BCA reagent B in the ratio of 50:1 (for example, mix 10 ml of reagent A with 0.2 ml of reagent B) and aliquot 100 μl of the working BCA reagent to each well of a microtiter plate. Transfer 12.5 μl of the cell lysate and BSA standard solution (0–10 μg/ml) into each well (*see* **Note 22**). Incubate at 37 °C for 30 min and measure the absorbance at 562 nm using a microplate reader. Calculate the concentration of the cell lysates using the standard curve prepared with absorbance readings of the BSA standards.
3. Transfer a small portion of the cell lysates (equivalent to 20 μg total protein) into new microtubes and add the lysis buffer to make up to 20 μl. Add 4 μl of 6× sample loading buffer and incubate for 30 min at 37 °C (*see* **Note 23**). The samples are ready for SDS-PAGE and western blotting to check the expression levels of TLR9-myc and UNC93B1-HA in total cell lysates. The samples can be stored at −20 °C.
4. Transfer the remainder of the cell lysates (equivalent to 500 μg total protein) into new microtubes and add the lysis buffer to

make up to 500 μl. Add 2 μl of rabbit anti-myc antibody. Incubate the samples at 4 °C for 3 h or up to overnight with gentle rotation for antibody binding.

5. Aliquot the desired amount of protein-A beads into a microtube using a wide-bore pipet tip and wash the beads with cold PBS to remove the preservatives as follows. Add 1 ml of cold PBS, mix, spin down the beads at 3,000 × *g* in a microcentrifuge for 1 min and remove the supernatant. Repeat three times. When removing the supernatant, be careful not to lose beads. Perform another wash with the lysis buffer. After the final centrifugation and removing the supernatant, add the lysis buffer to make 50 % slurry.
6. Add 40 μl of protein A-agarose bead slurry to each sample using a wide-bore pipet tip. Incubate the samples at 4 °C for 1 h or up to overnight with gentle rotation for binding of the immune complexes to protein A-agarose beads.
7. Spin down the beads at 3,000 × *g* in a microcentrifuge for 1 min and remove the supernatant. If you want to check the efficiency of the immunoprecipitation, save the supernatant at this step for western blotting to assess how much of TLR9-myc is left in the supernatant. Add 1 ml of the cold washing buffer to the beads, incubate at 4 °C for 5 min under gentle rotation, centrifuge, and carefully remove the supernatant. It is okay to leave ~20 μl of the buffer. Repeat three times to remove nonspecific binding. After removing the supernatant at the final washing step, centrifuge the samples again to bring down the buffer sticking to the wall of microtubes. Carefully remove the supernatant as much as possible without losing the beads.
8. Add 20 μl of the 2× sample loading buffer to the beads and incubate for 30 min at 37 °C to elute proteins from the beads (*see* **Note 23**). Centrifuge at 3,000 × *g* in a microcentrifuge for 1 min and the co-immunoprecipitation samples are ready for SDS-PAGE and western blotting. The samples can be stored at –20 °C.

3.3 SDS-PAGE

1. Carefully clean and dry a short plate and a spacer plate. Insert the two plates into the casting frame, keeping the short plate facing the front of the casting frame. Lock the pressure cams to secure the two plates. Make sure that both plates are flush on a level surface. Secure the casting frame into the casting stand by using the spring-loaded lever. For more information, refer to the Mini-PROTEAN Tetra Cell instruction manual.
2. Prepare the 10 % resolving gel solution by mixing 2.5 ml of the resolving gel buffer, 3.33 ml of 30 % acrylamide/Bis solution, and 4.1 ml of distilled water. Add 50 μl of 10 % APS and 5 μl of TEMED and mix by gentle swirling while avoiding

bubble formation. Pour the resolving gel solution (~3.5 ml) into the gel cassette, avoiding bubble formation, and immediately overlay the resolving gel solution with isopropanol or water. Leave the gel to be polymerized for 30 min. Rinse off the isopropanol with distilled water and dry the top of the resolving gel with filter paper.

3. Prepare the stacking gel solution by mixing 750 μl of the stacking gel buffer, 400 μl of 30 % acrylamide/Bis solution, and 1.8 ml of distilled water. Add 30 μl of 10 % APS and 5 μl of TEMED. Pour the stacking gel solution into the gel cassette up to the top of the short plate and carefully insert the comb avoiding bubble formation. Leave the gel to be polymerized for 5 min, carefully pull out the comb, and wash the wells with distilled water. Shake off water from the wells.
4. Take out the gel sandwich from the casting frame, assemble into the electrode assembly module with short plate facing inward, and place in the buffer tank. Fill the inner chamber and the buffer tank with 1× running buffer. Do not fill up the buffer tank so that buffer in the inner chamber and the buffer tank stay unmixed.
5. If using the frozen samples, thaw and incubate for 30 min at 37 °C. Centrifuge the samples at 13,000 × *g* in a microcentrifuge for 1 min and load the prestained protein ladder and the samples into the wells of the gel using sample loading pipette tips. When loading the co-immunoprecipitation samples, avoid loading the beads. Do not leave empty wells and instead load 1× sample loading buffer (*see* **Note 24**). Place the lid and connect power cables to a power supply. Turn on the power and begin electrophoresis at 80 V until the samples are stacked at the border between the stacking gel and the resolving gel. Then, continue at 100 V until bromophenol blue dye reaches the bottom of the gel and the protein ladder is properly separated.
6. After electrophoresis, disassemble the electrode assembly module and take out the gel sandwich. Carefully separate the two glass plates, remove the gel from the glass plate, and soak the gel in 1× transfer buffer for 10 min to remove SDS-PAGE running buffer.

3.4 Western Blotting

1. Cut the nitrocellulose membrane and filter paper a little larger than the size of the gel (*see* **Note 25**). Equilibrate the membrane, filter paper, and fiber pads in the transfer buffer for 5 min.
2. Place the gel holder cassette on a clean surface with the black plate facing downwards. Place a pre-wetted fiber pad on the black plate and place the filter paper on top of the fiber pad. Place the gel on the filter paper avoiding trapping air bubbles

between them (*see* **Note 26**). Place the nitrocellulose membrane on top of the gel. Place a filter paper on the nitrocellulose membrane and finally lay the fiber pad. Close the gel holder cassette and fasten with the white latch, being careful not to move the gel and membrane sandwich.

3. Place the gel holder cassette in the electrode module, with the black plate of the gel holder cassette facing the black side of the electrode module. Put the electrode module, a magnetic stirring bar, and a frozen cooling unit into the buffer tank. Fill the buffer tank with 1× transfer buffer. Place the lid and plug the cables into the power supply. Transfer at 100 V for 1 h on a stirring plate (*see* **Note 27**).
4. After the transfer, take out and disassemble the gel holder cassette. Place the nitrocellulose membrane in TBS.
5. Incubate the membrane in the blocking solution for 1 h at RT on a laboratory rocker.
6. Prepare primary antibody solutions by adding 5 μl of rat anti-HA antibody in 5 ml of the blocking solution.
7. Incubate the membrane in the primary antibody solution for 1 h at RT on a laboratory rocker.
8. Wash the membrane with TBS-T for 10 min on a laboratory rocker. Repeat three times.
9. Prepare a secondary antibody solution by adding 1 μl of HRP-conjugated goat anti-rat IgG antibody in 5 ml of the blocking solution. Incubate the membrane in the secondary antibody solution for 1 h at RT on a laboratory rocker.
10. Wash as in **step 8**.
11. Remove extra buffer on the membrane by picking it up with forceps and gently dabbing the tip of the membrane on a paper towel.
12. Place the membrane on a clean glass plate and evenly add 1 ml of the ECL solution on the membrane. Detect chemiluminescent signals using an ImageQuant LAS 4000.
13. Rinse the membrane with TBS.
14. Remove the antibodies from the membrane by incubating the membrane in the stripping buffer for 30 min at RT on a laboratory rocker.
15. Rinse the membrane with TBS three times.
16. Repeat the **steps 7–12**. This time, use the mouse anti-myc antibody and the HPR-conjugated goat anti-mouse IgG antibody as a primary and a secondary antibody, respectively.
17. An example of data obtained by following the methods described above is shown in Fig. 1.

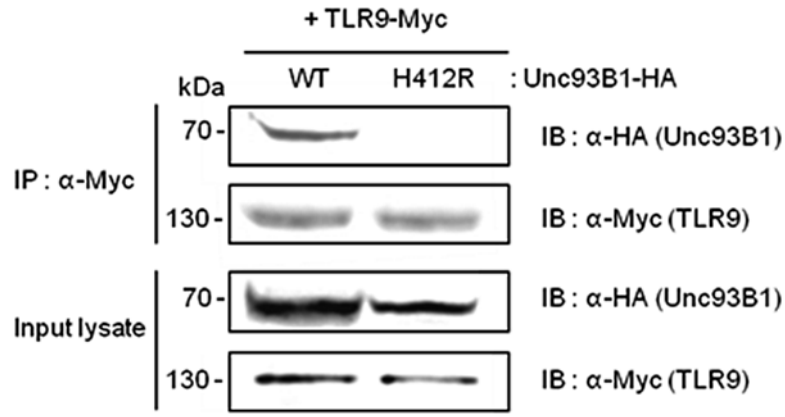

Fig. 1 TLR9-myc interacts with wild-type (WT) UNC93B1, but not with the H412R mutant. HEK293T cells co-expressing TLR9-myc and UNC93B1-HA (WT or H412R) were lysed and TLR9-myc was immunoprecipitated with a rabbit anti-myc antibody. Co-immunoprecipitated UNC93B1-HA was detected by immunoblotting with a rat anti-HA antibody (*top panel*). The blot was reprobed with mouse anti-myc antibody to confirm the equal immunoprecipitation efficiency of TLR9-myc between samples (*second panel*). The *third* and the *bottom panels* show the expression levels UNC93B1-HA and TLR9-myc in the total cell lysates, respectively

4 Notes

1. We usually prepare a 100× protease inhibitor cocktail containing leupeptin, pepstatin A, and aprotinin. First, make a stock solution for each protease inhibitor. Leupeptin stock solution: dissolve 5 mg of leupeptin in 5 ml of distilled water. Pepstatin A stock solution: dissolve 5 mg of pepstatin A in 7.3 ml of ethanol. Aprotinin stock solution: dissolve 5 mg of aprotinin in 5 ml of distilled water. Mix 1 ml of the leupeptin stock solution, 0.1 ml of the pepstatin A stock solution, and 1 ml of aprotinin stock solution with distilled water to make 10 ml of the 100× protease inhibitor cocktail. Make small-volume aliquots of each stock solution and the 100× cocktail and store at −20 °C. PMSF is separately added to the lysis buffer because it is very unstable in water. Prepare a 200× PMSF stock solution by dissolving 0.35 g of PMSF in 10 ml isopropanol and store at −20 °C. If precipitates are formed during storage, warm it up to RT before use.
2. Digitonin is a glycoside purified from a plant *Digitalis purpurea*. It is a mild nonionic detergent ideal for solubilizing transmembrane proteins for probing protein–protein interactions as well as for functional studies. We use 1 % digitonin to solubilize TLRs and other membrane proteins for binding

studies. Other commonly used nonionic detergents such as 1 % Triton X-100 or 1 % NP-40 can be utilized to simply solubilize TLRs, but they do disrupt the interaction between TLRs and UNC93B1, therefore are not suitable for the use in co-IP experiments assessing an interaction mediated by transmembrane regions.

3. To make a 5 % digitonin stock solution, dissolve 1 g of high purity digitonin (Calbiochem) in 20 ml of distilled boiling water and heat at 95 °C until the solution becomes clear (usually for 5–10 min). Cool, make small-volume aliquots, and store at −20 °C. Avoid repeated freezing and thawing. The stock solution is stable up to a week at 4 °C. Sometimes the stock solution becomes cloudy when kept at 4 °C due to presence of impurity in commercially available digitonin preparation. In such a case, centrifuge the stock solution at 18,000 × *g* for 5 min in a microcentrifuge and use the supernatant.
4. To prepare a 10× lysis buffer stock solution (0.5 M Tris–HCl, pH 8.0, 1.5 M NaCl, and 0.05 M EDTA), dissolve 30.38 g Tris, 43.83 g NaCl and 7.31 g EDTA in 400 ml distilled water. Adjust the pH to 8.0 using HCl, and add water up to 500 ml. Store at 4 °C. To prepare the final lysis buffer, mix 500 μl of 10× lysis buffer stock solution, 1 ml of 5 % digitonin stock solution, 50 μl of 100× protease inhibitor cocktail and distilled water to make a 5 ml solution. Just before the use, add 25 μl of 200× PMSF solution and mix well while avoiding bubbles.
5. Protein A strongly binds rabbit IgG antibodies which we use for immunoprecipitation of TLR9-myc. If you use mouse IgG1 or rat IgG antibodies for immunoprecipitation, use protein G-agarose beads instead of protein A-agarose beads.
6. Washing buffer is prepared by using 10× lysis buffer stock solution (*see* **Note 2**) and 5 % digitonin stock solution (*see* **Note 3**). Add 1 ml of 10× lysis buffer stock solution and 200 μl of 5 % digitonin stock solution to 8.8 ml of distilled water to make 10 ml washing buffer.
7. We usually prepare a 6× sample loading buffer stock solution (300 mM Tris–HCl, pH 6.8, 12 % SDS, 6 % β-mercaptoethanol, 0.12 % bromophenol blue and 60 % glycerol) and dilute it to a desired concentration with distilled water before use. To make a 6× sample loading buffer stock solution, dissolve 1.82 g Tris in 10 ml of distilled water, adjust pH to 6.8 using HCl, add 6 g of SDS, 3 ml of β-mercaptoethanol, and add distilled water to make up to 20 ml. Mix gently, while avoiding bubbles, until Tris and SDS are completely dissolved. Add 0.06 g of bromophenol blue and 30 ml of glycerol to make a final 50 ml stock solution. Mix thoroughly by placing it on an inverting rotator overnight. Make small-volume aliquots and

store at −20 °C. When thawing the frozen stock, briefly warm it at 37 °C and make sure that SDS is completely dissolved.

8. The concentrated HCl solution is ~12 N. To avoid a sudden drop of pH, it would be better to use the diluted HCl (1 N) when the pH of the solution is close to the desired pH. For dilution, add a required amount of the concentrated HCl solution into distilled water with an extreme caution because of the strong exothermic reaction. Handling of the concentrated HCl solution should be performed in a chemical hood.
9. Acrylamide monomer is toxic and directly affects the nervous system, so we prefer to purchase the premade 30 % acrylamide/Bis solution. If you make your own acrylamide/Bis solution, make sure to wear protective gear when handling acrylamide powder and avoid skin contact.
10. The pore size and rigidity of the polyacrylamide gel is determined by the concentration of the acrylamide/bis-acrylamide mixture as well as the ratio between acrylamide and bis-acrylamide which cross-links acrylamide polymer. For analyzing TLRs, we generally use 30 % acrylamide/Bis solution with the acrylamide to bis-acrylamide ratio of 37.5:1 to make a final 10 % resolving gel.
11. APS is unstable in a water solution and it is recommended to prepare a fresh APS solution each time.
12. Prepare 10× SDS-PAGE running buffer by dissolving 15.1 g Tris and 72 g glycine in distilled water to make a 450 ml solution. Make sure glycine is completely dissolved. Then, add 50 ml of 10 % SDS to make a final 500 ml stock solution. Store at RT. To make a working buffer solution, dilute 100 ml of the 10× SDS-PAGE running buffer with 900 ml of distilled water.
13. Prepare a 10× transfer buffer stock solution (0.25 M Tris, 1.92 M glycine) by dissolving 30.29 g Tris and 144.13 g glycine in distilled water to make 1 L stock solution. Store at RT or 4 °C. To make a working buffer solution, mix 100 ml of the 10× transfer buffer with 700 ml of distilled water, and then add 200 ml of methanol. Store at 4 °C. We use the cold transfer buffer to minimize heat generation during the transfer procedure. Therefore, it is recommended to prepare the working transfer buffer several hours before the experiment to cool it down, and it is often convenient to keep cold distilled water for dilution of the 10× transfer buffer stock solution.
14. Prepare a 10× TBS stock solution (0.5 M Tris–HCl, pH 7.4 and 1.5 M NaCl). Dissolve 60.57 g Tris and 87.66 g NaCl in 900 ml of distilled water and adjust pH to 7.4 using HCl. Then, add distilled water up to 1 L and store at RT. To make a working solution, mix 100 ml of the 10× TBS stock solution with 900 ml of distilled water.

15. Mix 100 ml of the 10× TBS stock solution (*see* **Note 14**) with 895 ml of distilled water. Then, add 5 ml of 20 % tween-20 dissolved in water to make 1 L TBS-T. Use a stirrer to completely dissolve tween-20 because it is very viscous. Store at RT.
16. Dissolve 2.5 g of skim milk powder in 50 ml of TBS-T. Store at 4 °C. It is easily perishable, so do not store it for more than a couple of days.
17. Dissolve 7.5 g glycine in 400 ml of distilled water and adjust pH to 2.2 using HCl. Add distilled water up to 470 ml, add 5 ml of 10 % SDS and 25 ml of 20 % tween-20. Store at RT.
18. The cell density should be approximately 60 % confluent at the time of the DNA transfection to achieve the best transfection efficiency. If you need to change the time interval between the cell seeding and the transection, adjust the cell seeding density accordingly.
19. Instead of serum-free DMEM, you can also use Opti-MEM (Life technologies). When you add Lipofectamine 2000 into the serum-free media, be careful not to apply the transfection reagent directly to the wall of microtubes because the transfection reagent easily sticks to plastic surface. Due to the same reason, do not mix the transfection reagent with the media by pipetting up and down.
20. In general, the ratio of 3:1 between the volume (μl) of Lipofectamine 2000 and the amount (μg) of plasmid DNA yields a good transfection efficiency. For the best results, optimize the transfection conditions by changing the ratio of the transfection reagent to the plasmid DNA.
21. For quantification of the protein concentration in cell lysates, the BCA protein assay is preferred over the Bradford protein assay because digitonin in the lysis buffer can interfere with the Bradford protein assay.
22. Prepare the BSA stock solution by dissolving 10 mg of BSA in 10 ml of distilled water to make a 1 mg/ml BSA solution. Add 0, 2, 4, 6, 8, or 10 μl of the BSA stock solution and 5 μl of cell lysates to each well of a microtiter plate and add distilled water to make up to 12.5 μl.
23. Do not heat up the samples above 50 °C when working with multi-transmembrane proteins such as UNC93B1. Because transmembrane regions are very hydrophobic, severely denatured multi-transmembrane proteins will aggregate and cannot be separated by SDS-PAGE. Incubating the immunoprecipitates in the sample loading buffer for 30 min at 37 °C is enough to elute binding proteins and antibodies from the protein A-agarose beads. However, in such a condition, most of

the antibody heavy chains remain as dimers whereas the light chains dissociate from the heavy chains.

24. Filling up all the empty wells with 1× sample loading buffer helps make the gel band width of each lane uniform. For the gel loaded with the total cell lysate samples, use 1× sample loading buffer which is prepared by diluting the 6× sample loading buffer with the lysis buffer to ensure that each well is loaded with same amount of digitonin. Digitonin in the sample tends to make the band width wider.
25. When handling the gel and nitrocellulose membrane, always wear gloves to prevent contamination.
26. Air bubbles trapped between a filter paper and the gel and between the gel and the nitrocellulose membrane will interfere with uniform transfer of proteins onto the membrane. If air bubbles are present, use a glass tube or a roller to gently roll out the air bubbles.
27. Circulating the transfer buffer with a stirring bar helps to maintain even buffer temperature and ion distribution in the tank during the transfer.

Acknowledgement

This work was supported by the grant from National Research Foundation of Korea (NRF-2013R1A1A2074573) and BK21 Plus (10Z20130012243).

References

1. Kawai T, Akira S (2010) The role of pattern-recognition receptors in innate immunity: update on Toll-like receptors. Nat Immunol 11:373–384
2. Kang JY, Lee JO (2011) Structural biology of the Toll-like receptor family. Annu Rev Biochem 80:917–941
3. Brinkmann MM, Spooner E, Hoebe K et al (2007) The interaction between the ER membrane protein UNC93B and TLR3, 7, and 9 is crucial for TLR signaling. J Cell Biol 177:265–275
4. Tabeta K, Hoebe K, Janssen EM et al (2006) The Unc93b1 mutation 3d disrupts exogenous antigen presentation and signaling via Toll-like receptors 3, 7 and 9. Nat Immunol 7:156–164
5. Casrouge A, Zhang SY, Eidenschenk C et al (2006) Herpes simplex virus encephalitis in human UNC-93B deficiency. Science 314:308–312
6. Kim YM, Brinkmann MM, Paquet ME (2008) UNC93B1 delivers nucleotide-sensing toll-like receptors to endolysosomes. Nature 452:234–238
7. Kim J, Huh J, Hwang M et al (2013) Acidic amino acid residues in the juxtamembrane region of the nucleotide-sensing TLRs are important for UNC93B1 binding and signaling. J Immunol 190:5287–5295
8. Huh JW, Shibata T, Hwang M et al (2014) UNC93B1 is essential for the plasma membrane localization and signaling of Toll-like receptor 5. Proc Natl Acad Sci U S A 111:7072–7077
9. Lee BL, Moon JE, Shu JH et al (2013) UNC93B1 mediates differential trafficking of endosomal TLRs. Elife 2, e00291

10. Hu CD, Chinenov Y, Kerppola TK (2002) Visualization of interactions among bZIP and Rel family proteins in living cells using bimolecular fluorescence complementation. Mol Cell 9:789–798
11. Pollok BA, Heim R (1999) Using GFP in FRET-based applications. Trends Cell Biol 9:57–60
12. Chan FK (2004) Monitoring molecular interactions in living cells using flow cytometric analysis of fluorescence resonance energy transfer. Methods Mol Biol 261:371–382
13. Issad T, Jockers R (2006) Bioluminescence resonance energy transfer to monitor protein-protein interactions. Methods Mol Biol 332:195–209
14. Regan JW, Barden N, Lefkowitz RJ et al (1982) Affinity chromatography of human platelet alpha 2-adrenergic receptors. Proc Natl Acad Sci U S A 79:7223–7227

Chapter 8

Flow Cytometry-Based Bead-Binding Assay for Measuring Receptor Ligand Specificity

Joris K. Sprokholt, Nina Hertoghs, and Teunis B.H. Geijtenbeek

Abstract

In this chapter we describe a fluorescent bead-binding assay, which is an efficient and feasible method to measure interaction between ligands and receptors on cells. In principle, any ligand can be coated on fluorescent beads either directly or via antibodies. Binding between ligand-coated beads and cells can be measured by flow cytometry, which results in an easily quantifiable readout. Furthermore, it allows measuring of binding by specific cell subsets within a mixed cell population. Overall, this method is a convenient and easily standardized assay for measuring binding.

Key words C-type lectin receptors, CLRs, PRR, Binding, Adhesion assay, Ligand specificity

1 Introduction

Interactions between receptors and their ligands are at the basis of many biological processes. In immunology, elucidating binding between receptors and their ligands is of great interest, but often requires laborious and difficult methods.

In this chapter we describe the fluorescent bead-binding assay, a method to investigate ligand–receptor interactions that is adaptable to a variety of ligands, easily standardized and time efficient. Moreover, this assay allows the measurement of binding of different cell subsets in a mixed cell population. In short, ligand-coated fluorescent beads—otherwise called 'spheres'—are incubated with cells expressing the receptor of interest, and binding of the fluorescent beads can be measured and quantified by flow cytometry [1].

This method was developed to explore binding candidates of C-type lectin receptors (CLRs). CLRs are a specialized subset of receptors that harbor a Calcium (Ca^{2+})-dependent or Ca^{2+}-independent carbohydrate recognition domain. This domain

Author contributed equally with all other contributors.

Claire E. McCoy (ed.), *Toll-Like Receptors: Practice and Methods*, Methods in Molecular Biology, vol. 1390,
DOI 10.1007/978-1-4939-3335-8_8,

contains conserved residue motifs that determine the glycan-specificity of the CLR [2, 3]. CLRs can exist in a soluble form or as transmembrane receptors and fulfill a diverse range of functions. Many transmembrane CLRs have been shown to function as important pattern recognition receptors (PRRs), which can internalize antigens and induce robust immune activation [4, 5]. Since recognition by CLRs leads to ligand binding, the assay described here is particularly suitable for assessing CLR functionality but can also be used to investigate CLR cross talk with TLRs and thereby TLR functionality.

In short, the coating of fluorescent beads with a potential ligand is obtained in two steps: (1) streptavidin is covalently coupled to fluorescent beads and (2) biotin is used to couple ligands to the beads.

These different options enable the use of any type of ligand, such as proteins, carbohydrates, or lipid structures. The beads have a carboxylic group that allows covalent coupling to streptavidin, which facilitates coating of beads with ligands; either directly using biotinylated ligands or indirectly via biotinylated ligand-specific antibodies. The ligand-coated beads are incubated with cells (either purified or a mixture) and binding of beads to cells can be detected by flow cytometry. Combining the fluorescent beads with other antibodies allows the distinction between different cell types and the binding capacity of each subset.

Specificity needs to be assessed by including a block of the proposed interaction, such as a known unlabeled ligand or a blocking antibody for the receptor. The fluorescent bead-binding assay comprises three stages: the coating of streptavidin to fluorescent beads, coupling the ligand of choice to fluorescent beads, and finally performing the binding assay and analyzing binding by flow cytometry.

2 Materials

2.1 Covalent Coupling of Streptavidin to Fluorescent Beads

1. PBS: 50 mM phosphate, 0.9 % NaCl, pH 7.4. Store at room temperature.
2. PBA: 0.5 % BSA, 0.02 % sodium azide in PBS (*see* **Note 1**). Store at 4 °C.
3. MES-buffer: 50 mM 2-(morpholino)ethanesulfonic acid, pH 6.0.
4. 1.1 M Glycine.
5. EDAC: 1.33 mg/ml 1-Ethyl-3-(3-dimethylaminopropyl) carbodiimide in MES-buffer. Prepare fresh (*see* **Note 2**).
6. 5.0 mg/ml Streptavidin in MES-buffer.
7. NaOH: 0.1 M solution.

8. Fluorescent beads: TransFluoSpheres carboxylate-modified microspheres (Life Technologies: 1.0 μm size beads, 488 excitation, 647 emission, provided as 2 % solids in water, supplemented with 2 mM sodium azide).

2.2 Coating Fluorescent Beads with Ligand

1. Streptavidin-coupled fluorescent beads.
2. 1.5 ml microcentrifuge tubes.
3. PBS: 50 mM Phosphate, 0.9 % NaCl, pH 7.4. Store at room temperature.
4. PBA: 0.5 % BSA, 0.02 % sodium azide in PBS (*see* **Note 1**). Store at 4 °C.
5. Purified (biotinylated) recombinant ligand or supernatant containing ligand (*see* **Note 3**).
6. Biotinylated tag-specific or ligand-specific antibody (*see* **Note 4**).

2.3 Fluorescent Bead-Binding Assay

1. Ligand-coated fluorescent beads.
2. 96-well V-bottom plate.
3. TSM: 20 mM Tris–HCl, 150 mM NaCl, 1 mM $CaCl_2$, 2 mM $MgCl_2$. Dissolve in 0.8 L of distilled H_2O, set pH to 7.4 using 11.1 M HCl and add distilled H_2O to a final volume of 1 L (*see* **Note 5**). Store at 4 °C.
4. TSA: 0.5 % BSA in TSM, no sodium azide (*see* **Note 6**). Store at 4 °C.
5. Blocking molecules: carbohydrates, EGTA and/or blocking antibodies (*see* **Note 7**).

3 Methods

3.1 Covalent Coupling of Streptavidin to Fluorescent Beads

In this part of the assay, streptavidin is covalently coupled to the fluorescent beads. The beads are coated with a hydrophilic polymer containing multiple pendent carboxylic acids, which allows covalent binding. EDAC is used to couple carboxyl groups to primary amines, which mediates the binding between streptavidin and the carboxylic acids. EDAC crosslinking is most efficient in acidic conditions (*see* Fig. 1).

1. Thoroughly resuspend (vortex) the fluorescent beads into a homogeneous suspension.
2. Add 50 μl beads to 20 μl streptavidin and vortex.
3. Incubate at room temperature (RT) for 15 min protected from light (*see* **Note 8**).
4. Dissolve a new vial of EDAC in MES-buffer at a final concentration of 1.33 mg/ml (*see* **Note 2**).

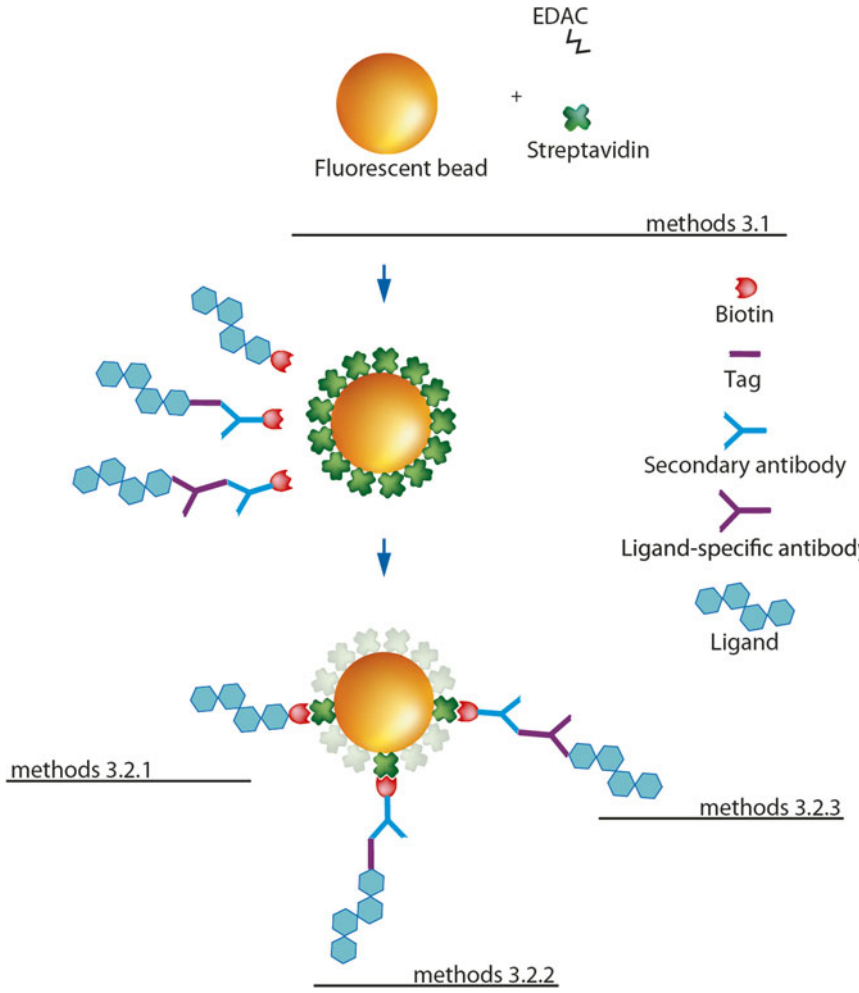

Fig. 1 Schematic representation of different methods to coat spheres with ligands. Streptavidin is coupled to fluorescent beads by covalent binding, mediated by EDAC (Subheading 3.1). Three methods are described to couple ligands to fluorescent beads: (1) coating of biotinylated ligand to streptavidin-coupled beads (Subheading 3.2.1), (2) binding of tag-specific biotinylated antibody to streptavidin-coupled beads followed by recombinant tagged ligand (Subheading 3.2.2), and (3) ligation of biotinylated secondary antibody to streptavidin-coupled beads followed by a ligand-specific antibody and native ligand (Subheading 3.2.3)

5. Add 30 µl of EDAC to the bead solution.
6. Vortex 15 s.
7. Adjust the pH to 6.5 ± 0.2 with diluted NaOH (4.5 µl of 0.1 M NaOH is often enough).
8. Incubate at RT for 2 h on a bench top mixer (e.g., Eppendorff ThermoMixer) and keep the samples protected from light.
9. Add 10 µl of 1.1 M glycine to stop the reaction.
10. Incubate at RT for 30 min, protected from light.

11. Centrifuge at 20,000 × *g* for 2 min in a benchtop microcentrifuge.
12. Wash beads three times with PBS. (Resuspend beads in 500 µl PBS, vortex and centrifuge at 20,000 × *g* for 2 min.)
13. Resuspend pellet in 150 µl PBA.
14. Continue with coating the beads with ligand (*see* Subheading 3.2), or store at 4 °C. Do not freeze. Keep away from light. The beads can be stored for at least a year.

3.2 Coating Fluorescent Beads with Ligand

This section describes how to coat fluorescent beads with ligand, using biotinylated ligand (Subheading 3.2.1), using recombinant tagged protein (Subheading 3.2.2) or using native protein (Subheading 3.2.3) (*see* Fig. 1).

3.2.1 Coating Fluorescent Beads with Biotinylated Ligand

1. Combine 15 µl (±100 × 10^6) of streptavidin-coupled fluorescent beads with 5 µg/ml of biotinylated ligand (*see* **Note 9**) and PBA to a total volume of 300 µl in a 1.5 ml microcentrifuge tube.
2. Incubate at 37 °C for 2 h while rotating or shaking.
3. Centrifuge for 2 min at 20,000 × *g* in a benchtop microcentrifuge at 4 °C.
4. Aspirate supernatant and resuspend fluorescent beads in 100 µl of PBA. After resuspension, add 400 µl of PBA (*see* **Note 10**).
5. Centrifuge for 2 min at 20,000 × *g* in a benchtop microcentrifuge at 4 °C.
6. Aspirate liquid and resuspend fluorescent beads in 100 µl of PBA.
7. Store fluorescent beads at 4 °C protected from light. The stability of coated fluorescent beads depends on the stability of the ligand. Most coated fluorescent beads can be stored for a month up to a year.

3.2.2 Coating Fluorescent Beads with Recombinant Tagged Ligand

1. Combine 15 µl (±100 × 10^6) of streptavidin-coupled fluorescent beads with 10 µg/ml biotinylated tag-specific antibody (*see* **Note 4**) and PBA to a total volume of 300 µl in a 1.5 ml microcentrifuge tube.
2. Incubate at 37 °C for 2 h while rotating or shaking.
3. Centrifuge for 2 min at 20,000 × *g* in a benchtop microcentrifuge at 4 °C.
4. Aspirate supernatant and resuspend fluorescent beads in 100 µl of PBA. After resuspension, add 400 µl of PBA.
5. Centrifuge for 2 min at 20,000 × *g* in a benchtop microcentrifuge at 4 °C.

6. Aspirate supernatant and resuspend fluorescent beads in 100 µl of PBA. Add 0.5–1 µg/ml of recombinant tagged ligand and PBA to a total volume of 300 µl (*see* **Note 3**).
7. Incubate overnight at 4 °C while rotating or shaking.
8. Centrifuge for 2 min at 20,000 × *g* in a benchtop microcentrifuge at 4 °C.
9. Aspirate supernatant and resuspend fluorescent beads in 100 µl of PBA. After resuspension, add 400 µl of PBA.
10. Centrifuge for 2 min at 20,000 × *g* in a benchtop microcentrifuge at 4 °C.
11. Aspirate liquid and resuspend fluorescent beads in 100 µl of PBA.
12. Store fluorescent beads at 4 °C protected from light. The stability of coated fluorescent beads depends on the stability of the ligand and the antibody used. Most coated fluorescent beads can be stored for a month up to a year.

3.2.3 Coating of Fluorescent Beads with Native Ligand

1. Coat fluorescent beads with biotinylated secondary antibody as described in Subheading 3.2.2, **steps 1–5** for tag-specific antibody.
2. Aspirate supernatant and resuspend fluorescent beads in 100 µl of PBA. Add 5 µg/ml of ligand-specific antibody (*see* **Note 11**) and PBA to a total volume of 300 µl.
3. Incubate overnight at 4 °C while rotating or shaking.
4. Centrifuge for 2 min at 20,000 × *g* in a benchtop microcentrifuge at 4 °C.
5. Aspirate supernatant and resuspend fluorescent beads in 100 µl of PBA. After resuspension, add 400 µl of PBA.
6. Centrifuge for 2 min at 20,000 × *g* in a benchtop microcentrifuge at 4 °C.
7. Aspirate supernatant and resuspend fluorescent beads in 100 µl of PBA. Add 0.5–1 µg/ml of recombinant ligand and PBA to a total volume of 300 µl (*see* **Note 3**).
8. Incubate overnight at 4 °C while rotating or shaking.
9. Centrifuge for 2 min at 20,000 × *g* in a benchtop microcentrifuge at 4 °C.
10. Aspirate supernatant and resuspend fluorescent beads in 100 µl of PBA. After resuspension, add 400 µl of PBA.
11. Centrifuge for 2 min at 20,000 × *g* in a benchtop microcentrifuge at 4 °C.
12. Aspirate liquid and resuspend fluorescent beads in 100 µl of PBA.
13. Store fluorescent beads at 4 °C protected from light. The stability of coated fluorescent beads depends on the stability of the ligand and the antibodies used. Most coated fluorescent beads can be stored for a month up to a year.

3.3 Bead-Binding Assay

1. Plate 50,000 cells (*see* **Note 12**) per well of a 96-well V-bottom plate.
2. Centrifuge plate for 3 min at 400 × *g*.
3. Aspirate supernatant or gently invert plate on paper towels.
4. Resuspend cells in 100 μl TSA and centrifuge for 3 min at 400 × *g*.
5. Aspirate supernatant or gently invert plate on paper towels and resuspend cells in 20 μl TSA or TSA containing 2× concentrated blocking agent (*see* **Note 7**).
6. Incubate for 30 min at 37 °C. This step can be skipped if no block is used.
7. Dilute 2 μl of ligand-coated fluorescent beads in 18 μl of TSA for each sample.
8. After 30 min incubation, add 20 μl of diluted fluorescent beads to each well and incubate for 45 min at 37 °C.
9. In case of a heterogeneous cell suspension, a FITC-labeled subset-specific antibody (*see* **Notes 12** and **13**) can be added to the fluorescent bead-cell suspension for the final 15 min of the 45 min incubation step.
10. Centrifuge plate for 3 min at 400 × *g*.
11. Aspirate supernatant or gently invert plate on paper towels.
12. Resuspend cells in 100 μl TSA and centrifuge for 3 min at 400 × *g*.
13. Aspirate supernatant or gently invert plate on paper towels.
14. Resuspend cells in 100 μl TSA and measure adhesion by flow cytometry (*see* **Note 13** and Fig. 2).

4 Notes

1. Sodium azide is added to PBA to inhibit contaminations and increase the shelf life of the streptavidin-coupled beads and ligand-coated beads.
2. It is pivotal to dissolve EDAC freshly before use for successful coupling of streptavidin to fluorescent beads.
3. In addition to coating fluorescent beads using purified ligand, it is also possible to resuspend the beads in supernatant containing the ligand. For example, we have produced several CHO cell lines which stably express ligand-Fc chimeric proteins. The produced ligand-Fc chimeras are secreted in the supernatant which is collected and cleared from debris by centrifuging at 3000 × *g* for 5 min. Aliquots of supernatant are stored at −20 °C and can be used to coat fluorescent beads.
4. The majority of recombinant proteins used in our lab are fused to IgG1 $F(ab')_2$ fragments, although other tags could also be

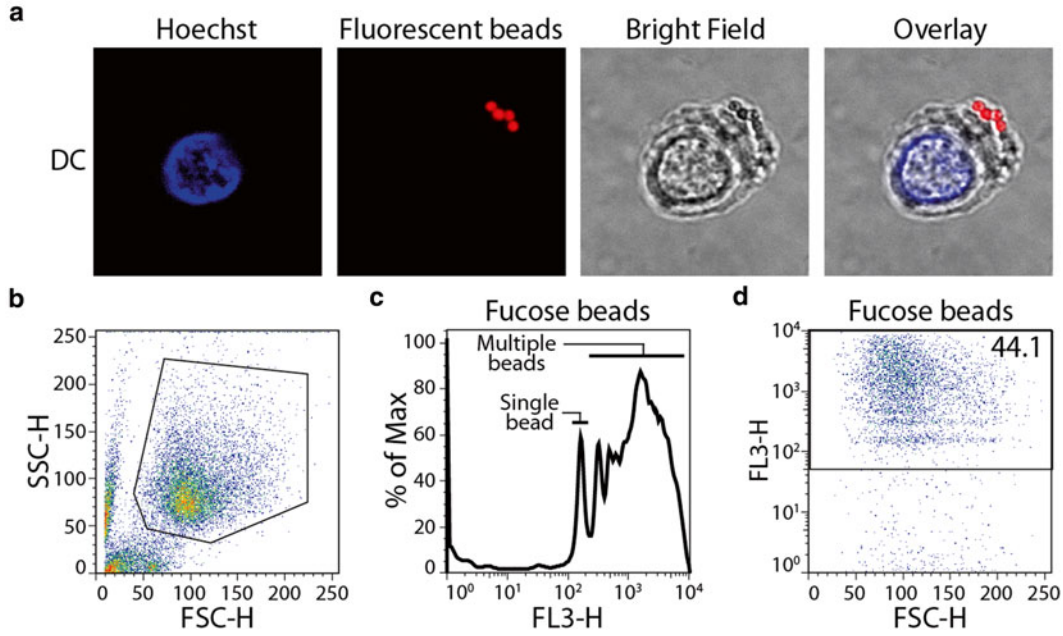

Fig. 2 Interpretation of fluorescent bead-binding assay. Results obtained from a fluorescent bead-binding assay using human dendritic cells and fucose-coated beads. Biotinylated fucose was coupled to fluorescent beads as described in Subheading 3.2.1. (**a**) One cell will typically bind to multiple beads as can be observed by confocal microscopy. (**b**) Unbound beads can be detected along the SSC-H axis of the SSC-H/FSC-H scatterplot and it is important to exclude them from further analysis. (**c**) Multiple peaks are usually observed when the results are presented as a histogram. In this experiment, bead$^-$ cells have a fluorescent intensity below zero and are therefore not visible in the histogram. The first peak in the histogram corresponds to cells which have bound one bead and subsequent peaks correspond to cells which have bound multiple beads. (**d**) The binding-capacity of a receptor or cell is typically expressed as the percentage of bead$^+$ cells

used, such as histidine, GST, or FLAG. We use biotinylated goat-α-human Fc-specific F(ab′)$_2$ (Jackson Immuno Research Laboratories) to couple Fc-proteins to fluorescent beads. If proteins are fused to mouse or rabbit IgG1, we also have good experience with using mouse or rabbit Fc-specific F(ab′)$_2$ antibodies from Jackson Immuno Research Laboratories.

5. We usually make 10× concentrated TSM which can be stored at 4 °C for up to a year. We have tested a wide variety of buffers in combination with the fluorescent bead-binding assay and we have determined that TSM provides us with the best result due to the Ca^{2+} and Mg^{2+} content. In general, most ligand–receptor interactions are optimal in neutral buffers of pH 7.4, but some interactions are stronger in slightly acidic buffers. This has to be determined by the end user.
6. We do not add sodium azide to the TSA as it can affect cell viability.
7. It is important to use blocking agents in the binding assay to determine the specificity of the binding. As our research often

aims to investigate CLR binding, we commonly use mannan (100 μg/ml final concentration), EGTA (10 mM final concentration), or blocking antibodies (20 μg/ml final concentration).

8. We prefer to wrap tubes or plates in aluminum foil to protect fluorescent beads from light. For incubation steps at room temperature, it is also convenient to simply place the plate or tubes in a closed drawer.
9. Lectinity (Moscow, Russia) provides a large range of biotinylated carbohydrates which can be used as ligands to coat fluorescent beads.
10. For complete resuspension, it is important to resuspend fluorescent beads with a 100 μl pipette tip before adding larger volumes.
11. Antibodies might interfere with receptor-ligand binding. It is best to use and test different antibodies for optimal results.
12. A wide variety of cells can be used in the fluorescent bead-binding assay. Cell types commonly used in our lab are dendritic cells, Langerhans cells, T cells and various cell lines, stably expressing different CLR receptors, such as Raji cells, K562 cells, and Jurkat cells. Notably, the binding assay is also suitable to identify ligand-specific cells in a heterogeneous cell suspension by combining the binding assay with cell-specific antibodies (*see* **Note 13**).
13. Fluorescent beads are highly fluorescent and the emission is typically detected in multiple channels, although this depends on the flow cytometer. On the FACSCalibur™ (BD, Franklin Lakes, NJ, USA), the voltage of the FL3 channel should be set at 288 because of limitations in the scale of the fluorescent intensity. On a FACSCanto™ II (BD, Franklin Lakes, NJ, USA), we select Peridinin Chlorophyll (PerCP) as fluorochrome and set the voltage around 300, but final voltage settings should be optimized by each user. The emission spectrum of fluorescent beads overlaps with most fluorochromes, but FITC-coupled antibodies can be used in combination with fluorescent beads to select specific cell types if a heterogeneous cell suspension is used.

References

1. Geijtenbeek TBH, Van Kooyk Y, Van Vliet SJ et al (1999) High frequency of adhesion defects in B-lineage acute lymphoblastic leukemia. Blood 94:754–764
2. Drickamer K (1989) Demonstration of carbohydrate-recognition activity in diverse proteins which share a common primary structure motif. Biochem Soc Trans 17:13–15
3. Zelensky AN, Gready JE (2005) The C-type lectin-like domain superfamily. FEBS J 272:6179–6217
4. Cambi A, Figdor CG (2003) Dual function of C-type lectin-like receptors in the immune system. Curr Opin Cell Biol 15:539–546
5. Geijtenbeek TBH, Gringhuis SI (2009) Signalling through C-type lectin receptors: shaping immune responses. Nat Rev Immunol 9:465–479. doi:10.1038/nri2569

Chapter 9

Measuring Monomer-to-Filament Transition of MAVS as an In Vitro Activity Assay for RIG-I-Like Receptors

Bin Wu, Yu-San Huoh, and Sun Hur

Abstract

During viral infection, the innate immune RIG-I like receptors (RLRs) recognize viral double stranded RNA (dsRNA) and trigger filament assembly of the adaptor protein Mitochondrial Anti-viral Signaling protein (MAVS). The MAVS filament then activates anti-viral signaling events including the up-regulation of type I interferon expression. In recent years, much insight has been gained into how RLRs recognize dsRNA, but the precise mechanism of how activated RLRs stimulate MAVS filament formation remains less understood. In this chapter, we describe an in vitro reconstitution assay that we have previously developed to study the RLR-catalyzed filament assembly of MAVS. We provide technical guidance for purifying the caspase activation recruitment domain (CARD) of MAVS ($MAVS^{CARD}$) as a functional monomer and also preformed filament seed. We also describe the methods to monitor the monomer-to-filament transition of $MAVS^{CARD}$ upon stimulation. This protocol provides a minimalist approach to studying RLR signaling events and can potentially be applied to elucidate signaling mechanisms of other innate immune receptors, such as Toll-like receptors and inflammasomes, that involve higher order assemblies of CARDs or related domains for their downstream signal activation.

Key words RIG-I, MDA5, MAVS, Caspase activation recruitment domain (CARD), Filament formation, IFNα/β signaling pathway, Protein refolding, Filament assembly, Innate immune signaling

1 Introduction

Effective immune defense against microbial infection is dependent upon efficient detection of Pathogen Associated Molecular Pattern (PAMP) by the Pattern Recognition Receptors (PRRs). Retinoic acid-inducible gene 1 (RIG-I) and its paralog, Melanoma Differentiation-Associated protein 5 (MDA5) compose one such family of PRRs. They are broadly expressed, cytoplasmic proteins and are responsible for detection of double-stranded RNA (dsRNA) generated by a wide range of viruses [1–3]. Upon recognition of viral dsRNA, RIG-I/MDA5 activate the type I interferon signaling pathway through the common adaptor molecule, Mitochondrial Anti-viral Signaling protein (MAVS, also known as IPS-1, Cardif, and VISA) [4–7]. Despite the shared downstream pathway, RIG-I

Claire E. McCoy (ed.), *Toll-Like Receptors: Practice and Methods*, Methods in Molecular Biology, vol. 1390,
DOI 10.1007/978-1-4939-3335-8_9,

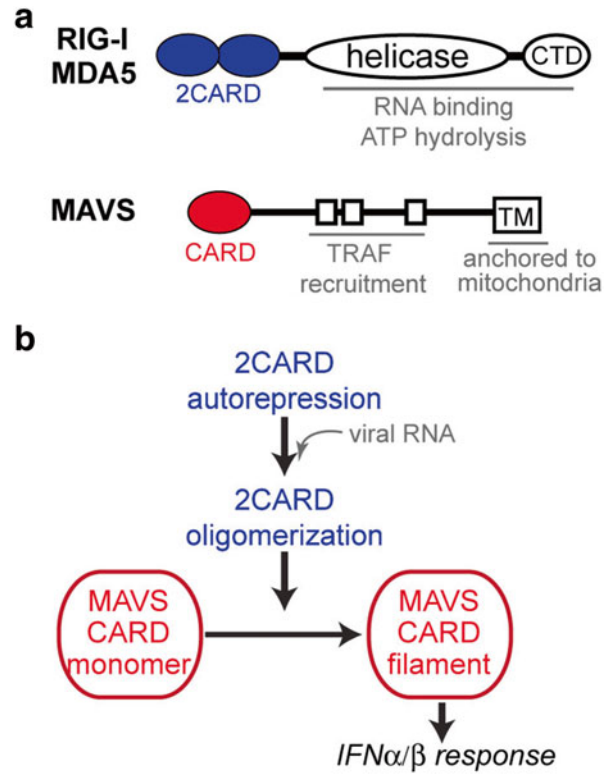

Fig. 1 (**a**) Domain architectures of RIG-I/MDA5 and MAVS. This article focuses on 2CARD of RIG-I/MDA5 and CARD of MAVS. (**b**) Schematic of the signal activation processes of RIG-I/MDA5. Upon viral RNA recognition, 2CARDs of RIG-I/MDA5 are released from auto-repression and undergo homo-oligomerization. The oligomeric 2CARD then nucleates a MAVS CARD filament for activation of the IFNα/β signaling pathway

and MDA5 play nonredundant roles in antiviral immunity by recognizing largely distinct groups of viruses [8–10].

Over the last several years, we and others have investigated the structural and biochemical mechanisms by which these two receptors recognize different types of viral RNAs and activate the IFN signaling pathway [11–14]. RIG-I and MDA5 commonly contain the N-terminal tandem caspase activation recruitment domain (2CARD), the central DExD/H motif helicase domain, and the C-terminal domain (CTD) (Fig. 1a) [15]. 2CARD is responsible for interaction with MAVS and IFN signaling, whereas the helicase domain and CTD together function as an RNA recognition unit (Fig. 1a) [16, 17]. The crystal structure of ligand-free, full-length RIG-I suggested that 2CARD is masked by the protein structure in the absence of RNA, but is released upon dsRNA interaction

(Fig. 1b) [13]. The exposed 2CARD then assembles into a helical oligomer [18], aided by high local concentration of 2CARD within the oligomeric assembly of RIG-I and/or bridged by K63-linked polyubiquitin chains [19, 20]. The assembled oligomer of 2CARD then associates with the CARD domain of MAVS ($MAVS^{CARD}$, Fig. 1b) and nucleates MAVS filament formation (Fig. 1b) by extending the helical trajectory predefined by the 2CARD oligomer [21]. The MAVS filament in turn recruits further downstream signaling molecules, such as TRAF2, 5, and 6, to activate the type I interferon signaling pathway [22].

One of the challenges in the field for some time has been the lack of in vitro biochemical assays to analyze the signaling activities of RIG-I and MDA5. Interactions between RIG-I/MDA5 2CARD and $MAVS^{CARD}$ were often difficult to measure with confidence, possibly indicating the transient nature of their interactions or sufficiency of a few interactions for signal amplification. In our effort to understand the signal activation processes of RIG-I and MDA5, our laboratory has developed an assay (namely MAVS activation assay) that allows one to monitor the transition of $MAVS^{CARD}$ from monomeric to filamentous state in response to RIG-I/MDA5. This assay recapitulates many features of the cellular signaling processes of RIG-I/MDA5, for example the requirement for K63-linked polyubiquitin for isolated 2CARD [19] and alleviation of such requirement in pre-oligomerized full-length RIG-I [18]. Furthermore, this assay enabled detailed mechanistic analysis of the signal activation processes of RIG-I/MDA5 at the level of molecular structure and biochemistry [19, 21]. It should be noted that an analogous cell-free assay has been developed [23]. The advantage of our assay is that our system is reconstituted entirely from purified components (i.e., receptor, ligand, and adaptor), which greatly simplifies data interpretation and allows more detailed investigation of the molecular events.

We here describe our reconstitution of the MAVS activation assay. This assay utilizes a MAVS construct containing just its CARD domain (residues 1–97) fused to a SNAP tag ($MAVS^{CARD}$-SNAP) [24]. The advantage of this fusion construct is that it has superior solubility over the construct having just the CARD domain, and also allows specific fluorescent labeling via the SNAP tag. $MAVS^{CARD}$-SNAP oligomerizes into a filamentous structure with prion-like characteristics similar to those observed with full-length MAVS or $MAVS^{CARD}$ [11, 22]. We provide detailed guidelines on how to purify functional $MAVS^{CARD}$-SNAP in its filamentous and monomeric forms. We also describe how to monitor monomer-to-filament transition of $MAVS^{CARD}$-SNAP using native gel electrophoretic migration shift assay (EMSA).

2 Materials

2.1 Protein Purification

1. pET47b expression vector encoding MAVS CARD (residues 1–97) with an N-terminal His-tag and a C-terminal SNAP-tag ($MAVS^{CARD}$-SNAP) (*see* **Note 1**).
2. LB broth and agar plate containing 30 μg/ml kanamycin.
3. BL21(DE3) competent cells.
4. 0.5 M Isopropyl β-D-1-thiogalactopyranoside (IPTG).
5. 2.8 L fernbach baffled flasks.
6. A temperature-controlled shaking incubator for 2.8 L flasks that can be set to 20–37 °C.
7. A spectrophotometer and cuvette that can measure absorbance at 600 nm.
8. A high-speed centrifuge (e.g., Sorvall refrigerated centrifuge).
9. Lysis buffer: 20 mM Tris, pH 7.5, 250 mM NaCl, 20 mM imidazole, pH 7.5, 0.05 % CHAPS, 10 % glycerol.
10. Emulsiflex (Avestin) for cell lysis.
11. Nickel-nitrilotriacetic acid (Ni-NTA) agarose (Qiagen).
12. Gravity flow column for nickel-affinity protein purification.
13. Ni-NTA wash buffer: 20 mM Tris, pH 7.5, 250 mM NaCl, 40 mM imidazole, pH 7.5, 0.05 % CHAPS, 10 % glycerol.
14. Ni-NTA elution buffer: 20 mM Tris, pH 7.5, 250 mM NaCl, 300 mM imidazole, pH 7.5, 0.05 % CHAPS, 10 % glycerol.
15. HRV 3C protease (GE Healthcare or prepared in-house [25]).
16. Dialysis membrane with a 12,000–14,000 MWCO and clips (Spectrum Labs).
17. 3C protease digestion buffer: 20 mM Tris, pH 7.5, 150 mM NaCl.
18. CARD storage buffer: 20 mM Tris, pH 7.5, 150 mM NaCl, 0.5 mM EDTA.
19. 7 M Guanidinium chloride (GndCl, CalBiochem).

2.2 Preparation of Monomeric MAVS

1. Magnetic stir bar.
2. Stir plate.
3. A temperature-controlled shaking incubator that can be set to 37 °C.
4. Dialysis membrane with a 12,000–14,000 MWCO and clips (Spectrum Labs).
5. $MAVS^{CARD}$-SNAP refolding buffer: 20 mM Tris, pH 7.5, 500 mM NaCl, 0.5 mM EDTA.

6. β-Mercaptoethanol (BME, MP biomedicals).
7. 0.1 μm syringe filter (Millex).
8. 5 ml disposable syringe.

2.3 MAVS Activation Assay

1. Benzylguanosine-conjugated Alexa647 (BG-Alexa-647 surface labeling fluorophore, New England Biolabs).
2. RIG-I truncation variant containing only 2CARD (expression and purification of which is described [19]).
3. Unanchored K63-linked polyubiquitin chains (production of which is described in [19]).
4. CARD storage buffer: 20 mM Tris pH 7.5, 150 mM NaCl, 0.5 mM EDTA.
5. 6× native gel loading dye: 70 % sucrose with 0.0025 % of bromophenol blue and xylene cyanol.
6. SYBR-Gold dye (Life Technologies) for nucleic acid staining.
7. Krypton (Thermo Scientific) for protein staining.
8. 3–12 % Bis-Tris-Tricine native gel (Novex by Life Technologies).
9. Bis-Tris-Tricine running buffer: 50 mM BisTris, 50 mM Tricine.
10. FLA-9000 laser gel image scanner (GE Healthcare) or equivalent machine capable of scanning multiple fluorophore channels (488 nm, 555 nm and 647 nm).

3 Methods

3.1 Protein Purification

MAVS^{CARD}-SNAP purified from *E. coli* is in the form of short filaments, which we refer to as filament seeds. The following protocol describes the purification strategies for MAVS^{CARD}-SNAP filament seeds (*see* Fig. 2).

1. Transform BL21(DE3) cells with pET47b encoding His-tagged MAVS^{CARD}-SNAP and plate transformed cells onto an LB agar + kanamycin plate. Let the cells grow overnight at 37 °C.
2. Pick a colony from the LB agar plate and inoculate 5–20 ml of LB broth + kanamycin. Shake the starter culture at 37 °C overnight.
3. Transfer 5–10 ml of starter culture to 1 L of LB broth + kanamycin in a 2.8 L fernbach flask. Shake at ~200 rpm at 37 °C for a few hours. Monitor cell growth by measuring the OD_{600}.
4. When the OD_{600} of the culture reaches 0.4, lower the incubator temperature to 20 °C. Induce with 0.4 mM IPTG, when the OD_{600} reaches 0.6. Shake the induced culture overnight.

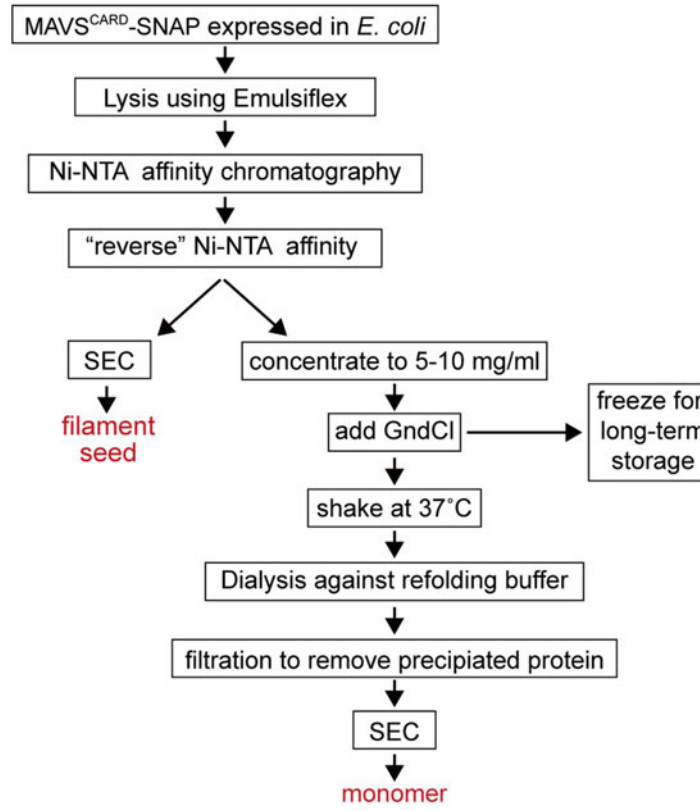

Fig. 2 Schematic of the purification strategies for the MAVS^{CARD}-SNAP filament seed and monomer

5. All subsequent steps are performed at 4–8 °C unless otherwise stated. Harvest the cells by spinning down the culture at 4500 × *g* for 10 min, and resuspend with 25 ml lysis buffer per liter of culture.
6. Cells are lysed using an Emulsiflex (*see* **Note 2**).
7. Once cells are sufficiently lysed, spin the cell lysate at 38,000 × *g* for 30 min.
8. Apply the cleared lysate onto pre-equilibrated Ni-NTA gravity flow column (5–10 ml agarose per liter of culture). To enhance MAVS^{CARD}-SNAP enrichment on Ni-NTA agarose, incubate lysate with the Ni-NTA column for at least 10 min before starting the column flow. Batch Ni-NTA binding can work as well.
9. Wash the Ni-NTA column with 20 column volumes of Ni-NTA wash buffer.
10. First elute MAVS^{CARD}-SNAP with a half column volume of Ni-NTA elution buffer. This fraction will most likely contain

contaminants and should not be pooled with the second Ni-NTA elution.

11. Elute MAVS^{CARD}-SNAP with 2 column volumes of Ni-NTA elution buffer.
12. Cleave off the His-tag using HRV 3C protease (50 μg per 1 mg of MAVS^{CARD}-SNAP) while dialyzing against 3C protease digestion buffer overnight.
13. Remove the His-tag by applying the 3C protease digestion onto pre-equilibrated Ni-NTA beads. MAVS^{CARD}-SNAP will be in the unbound fraction and a subsequent wash using half column volume of the CARD storage buffer. MAVS^{CARD}-SNAP should be of >95 % purity as analyzed by SDS-PAGE.
14. At this point, MAVS^{CARD}-SNAP is a filamentous seed. A few milliliters of MAVS^{CARD}-SNAP seed (~1 mg/ml) can be stored at 4 °C for a month or frozen at −20 °C for longer periods.

3.2 Preparation of Monomeric MAVS

Chemical denaturation of MAVS^{CARD}-SNAP filament seeds with GndCl followed by refolding yields monomeric MAVS^{CARD}-SNAP (*see* **Note 3**).

1. After purification of the MAVS^{CARD}-SNAP filament seed (Subheading 3.1), concentrate it to 5–10 mg/ml (*see* **Note 4**).
2. Denature MAVS^{CARD}-SNAP by adding 6× volumes of 7 M GndCl. Vortex to mix at room temperature.
3. Make 0.5–1.5 ml aliquots of denatured MAVS^{CARD}-SNAP. These aliquots can be snap frozen in liquid nitrogen and stored at −80 °C for 2 months, or can be directly used for preparation of monomeric MAVS^{CARD}-SNAP as in the following steps.
4. Thaw frozen denatured MAVS^{CARD}-SNAP samples by shaking at ~200 rpm for 30 min at 37 °C (*see* **Note 5**).
5. While protein is being thawed, prepare ice-cold refolding buffer (at least 50× volume of the denatured MAVS^{CARD}-SNAP).
6. To the thawed MAVS^{CARD}-SNAP, directly add BME to a final concentration of 100 mM and transfer the MAVS^{CARD}-SNAP + BME mixture into dialysis tubing (*see* **Note 6**).
7. Place the dialysis setup into ice-cold refolding buffer (*see* **Note 7**).
8. Supplement refolding buffer with BME to a final concentration of 20 mM.
9. Dialyze MAVS^{CARD}-SNAP for 45–60 min at 4 °C (*see* **Note 8**). Be sure to have the dialysis setup constantly spinning at ~60 rpm.

10. Recover the refolded MAVS^{CARD}-SNAP. There will be some precipitated protein after dialysis. Spin down the precipitated protein at >12,000 × *g* for 1 min.
11. Syringe filter (0.1 μm) the cleared MAVS^{CARD}-SNAP sample, but be careful not to introduce any air bubbles. Expect to recover ~50 % of the protein after filtration.

3.3 MAVS Activation Assay

Since monomeric MAVS^{CARD}-SNAP will spontaneously oligomerize over the course of several hours, the filament formation assay should be performed as quickly as possible. Each batch of monomeric MAVS^{CARD}-SNAP needs to be tested for proper refolding. In our lab, we use at least two criteria to confirm functionality of monomeric MAVS^{CARD}-SNAP. That is, correctly refolded MAVS^{CARD}-SNAP should (1) efficiently extend the filament seeds (Fig. 3a, b) and (2) form de novo filaments upon addition of RIG-I with K63-linked polyubiquitin chains (Fig. 3c). Below, we describe both strategies.

1. Add BG-Alexa-647 dye (1 μM, final) to monomeric MAVS^{CARD}-SNAP (20 μM or 0.6 mg/ml). Incubate the reaction on ice for 10 min (*see* **Note 9**). Monomeric MAVS^{CARD}-SNAP can be purified by Size Exclusion Chromatography (SEC) to remove free dye. Alternatively, the labeling reaction can be quenched by addition of an excess amount of free benzylguanosine. Labeled MAVS^{CARD}-SNAP will be referred to as MAVS^{CARD}-SNAP*. All reactions with MAVS^{CARD}-SNAP* will be performed using CARD storage buffer (*see* **Note 10**).

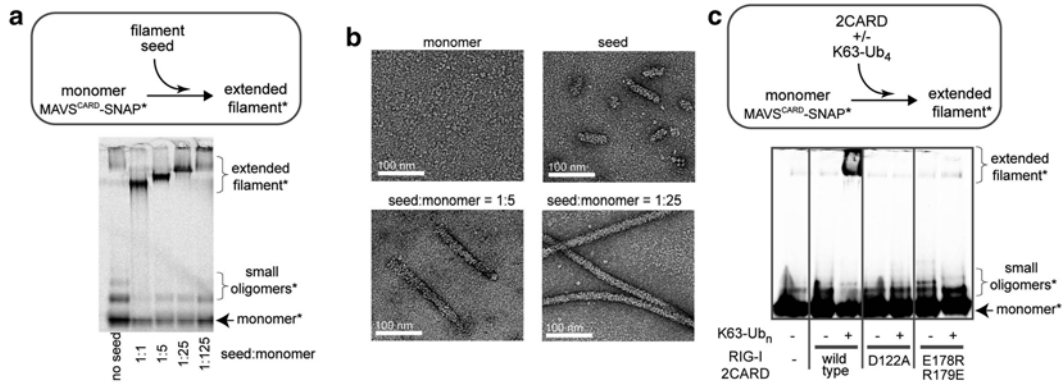

Fig. 3 (**a**) Monomer-to-filament transition of MAVS^{CARD}-SNAP* upon addition of the filament seed. *Asterisk* indicates fluorescent labeling of the SNAP tag. The filament seed is nonfluorescent. (**b**) Representative electron micrographs of filaments extended in (**a**). (**c**) Monomer-to-filament transition of MAVS^{CARD}-SNAP* upon addition of RIG-I 2CARD in the presence or absence of K63-linked polyubiquitin (K63-Ub$_n$). MAVS stimulatory activities of wild-type 2CARD and oligomerization-deficient mutants (D122A and E178R/R179E) were compared. Figure images in (**a**) and (**b**) were adopted from [11], and the image in (**c**) from [19]

2. If $MAVS^{CARD}$-SNAP* was properly refolded, it should not form filaments on its own within ~2 h post-refolding. To test this, incubate 10 μl of 10 μM $MAVS^{CARD}$-SNAP* at 22 °C for 15–30 min.
3. For filament extension, add the $MAVS^{CARD}$-SNAP seed (prepared in Subheading 3.1) to monomeric $MAVS^{CARD}$-SNAP* (10 μM, final) (prepared in Subheading 3.2), and incubate at 22 °C for 15–30 min. We typically use the seed:monomer mass ratio of 25:1, but different ratios can be used to obtain filaments with different lengths (*see* Fig. 3b).
4. For filament induction by RIG-I, add RIG-I 2CARD (10 μM, final) and unanchored K63-linked polyubiquitin chains (80 μg/ml, final) to $MAVS^{CARD}$-SNAP* (10 μM, final) and incubate at 22 °C for 15–30 min.
5. To reactions prepared in **steps 2–4** (10 μl), add 2 μl of 6× native gel loading dye.
6. Immediately load samples into a 3–12 % Bis-Tris-Tricine native gel (*see* **Note 11**). Run the native gel in Bis-Tris-Tricine running buffer at 200 V for 70–80 min at 4 °C or until the dye front runs off the gel.
7. Scan the gel using the Alexa647 fluorescence with a gel scanner FLA-9000. We obtain optimal visualization using the 100 μm resolution and 300–600 V laser sensitivity settings (*see* **Note 12**).

4 Notes

1. The plasmid encoding the CARD domain (residues 1–97) of MAVS (UnitProtKB: Q7Z434.2) fused to the SNAP tag (version 1.0, New England Biolabs) was generated by inserting MAVS CARD between the BamHI and EcoRI restriction sites and SNAP between the EcoRI and XhoI restriction sites in pET47b. The amino acid sequence of the resultant fusion protein, His-tagged $MAVS^{CARD}$-SNAP, is

MAHHHHHHSAALEVLFQGPGYQDPMPFAEDKTYK
YICRNFSNF CNVDVVEILPYLPCLTARDQDRLRATC
TLSGNRDTLWHLFNTLQRRPGWVEYFIAALRGCELVD
LADEVASVYQSYQPEFMDKDCEMKRTTLDSPL
GKLELSGCEQGLHEIKLLGKGTSAADAVEVP
APAAVLGGPEPLMQATAWLNAYFHQPEAIEE
FPVPALHHPVFQQESFTRQVLWKLLKVVKFGE
VISYQQLAALAGNPAATAAVKTALSGNPVPILIP
CHRVVSSSGAVGGYEGGLAVKEWLLAHEGHR
LVNRVWDLQV

2. Other mechanical devices can be used to lyse cells, but avoid using a sonicator as it may increase fragmentation of filament seeds.
3. The refolded monomer displays the same three dimensional structure [21] as the one without refolding [26].
4. We found that the concentration of $MAVS^{CARD}$-SNAP (5–10 mg/ml) at this step is important. At higher concentrations, $MAVS^{CARD}$-SNAP does not refold as well and leads to heavy precipitation.
5. We found that incubating the denatured $MAVS^{CARD}$-SNAP at 37 °C before refolding is critical for obtaining correctly refolded monomeric $MAVS^{CARD}$-SNAP.
6. Since $MAVS^{CARD}$-SNAP has multiple cysteines, it is important to keep high concentrations of BME to maintain a reducing environment during refolding. Add fresh BME to the refolding buffer just before its use. Tris(2-carboxyethyl)phosphine (TCEP) can be used as an alternative reducing agent.
7. It is important to use ice-cold buffer for optimal refolding of $MAVS^{CARD}$-SNAP.
8. If the refolding buffer is not compatible with a downstream assay, you must first refold the protein in the refolding buffer for 30 min and then perform a secondary dialysis using your desired buffer. We have extensively optimized the refolding buffer and do not recommend altering the composition of this buffer.
9. The labeling reaction is not sensitive to buffer conditions and can also be performed at 22 °C.
10. We found that $MAVS^{CARD}$-SNAP* filament formation (in particular seed extension) is not sensitive to salt concentration of the reaction buffer. You may alter these reaction conditions to suit your desired experimental setup.
11. While other native gel buffer systems may be used, we found that the best results were obtained with Bis-Tris-Tricine native gels.
12. While the native gel assay provides a convenient method to examine filament formation of MAVS CARD, it has its limitations. First, it cannot distinguish between the filament of $MAVS^{CARD}$-SNAP and nonfilamentous aggregate. In addition, very long filaments can fail to enter the gel, although disappearance of monomeric $MAVS^{CARD}$-SNAP can be analyzed instead. We recommend using negative stain electron microscopy as a complementary method to verify filament formation.

References

1. Takeuchi O, Akira S (2008) MDA5/RIG-I and virus recognition. Curr Opin Immunol 20(1):17–22. doi:10.1016/j.coi.2008.01.002
2. Yoneyama M, Kikuchi M, Natsukawa T, Shinobu N, Imaizumi T, Miyagishi M, Taira K, Akira S, Fujita T (2004) The RNA helicase RIG-I has an essential function in double-stranded RNA-induced innate antiviral responses. Nat Immunol 5(7):730–737. doi:10.1038/ni1087
3. O'Neill LA, Bowie AG (2010) Sensing and signaling in antiviral innate immunity. Curr Biol 20(7):R328–R333. doi:10.1016/j.cub.2010.01.044
4. Xu LG, Wang YY, Han KJ, Li LY, Zhai Z, Shu HB (2005) VISA is an adapter protein required for virus-triggered IFN-beta signaling. Mol Cell 19(6):727–740. doi:10.1016/j.molcel.2005.08.014
5. Seth RB, Sun L, Ea CK, Chen ZJ (2005) Identification and characterization of MAVS, a mitochondrial antiviral signaling protein that activates NF-kappaB and IRF 3. Cell 122(5):669–682. doi:10.1016/j.cell.2005.08.012
6. Meylan E, Curran J, Hofmann K, Moradpour D, Binder M, Bartenschlager R, Tschopp J (2005) Cardif is an adaptor protein in the RIG-I antiviral pathway and is targeted by hepatitis C virus. Nature 437(7062):1167–1172. doi:10.1038/nature04193
7. Kawai T, Takahashi K, Sato S, Coban C, Kumar H, Kato H, Ishii KJ, Takeuchi O, Akira S (2005) IPS-1, an adaptor triggering RIG-I- and Mda5-mediated type I interferon induction. Nat Immunol 6(10):981–988. doi:10.1038/ni1243
8. Loo YM, Fornek J, Crochet N, Bajwa G, Perwitasari O, Martinez-Sobrido L, Akira S, Gill MA, Garcia-Sastre A, Katze MG, Gale M Jr (2008) Distinct RIG-I and MDA5 signaling by RNA viruses in innate immunity. J Virol 82(1):335–345. doi:10.1128/JVI.01080-07
9. Kato H, Takeuchi O, Sato S, Yoneyama M, Yamamoto M, Matsui K, Uematsu S, Jung A, Kawai T, Ishii KJ, Yamaguchi O, Otsu K, Tsujimura T, Koh CS, Reis e Sousa C, Matsuura Y, Fujita T, Akira S (2006) Differential roles of MDA5 and RIG-I helicases in the recognition of RNA viruses. Nature 441(7089):101–105. doi:10.1038/nature04734
10. Hornung V, Ellegast J, Kim S, Brzozka K, Jung A, Kato H, Poeck H, Akira S, Conzelmann KK, Schlee M, Endres S, Hartmann G (2006) 5′-Triphosphate RNA is the ligand for RIG-I. Science 314(5801):994–997. doi:10.1126/science.1132505
11. Wu B, Peisley A, Richards C, Yao H, Zeng X, Lin C, Chu F, Walz T, Hur S (2013) Structural basis for dsRNA recognition, filament formation, and antiviral signal activation by MDA5. Cell 152(1-2):276–289. doi:10.1016/j.cell.2012.11.048, S0092-8674(12)01436-5 [pii]
12. Luo D, Ding SC, Vela A, Kohlway A, Lindenbach BD, Pyle AM (2011) Structural insights into RNA recognition by RIG-I. Cell 147(2):409–422. doi:10.1016/j.cell.2011.09.023
13. Kowalinski E, Lunardi T, McCarthy AA, Louber J, Brunel J, Grigorov B, Gerlier D, Cusack S (2011) Structural basis for the activation of innate immune pattern-recognition receptor RIG-I by viral RNA. Cell 147(2):423–435. doi:10.1016/j.cell.2011.09.039
14. Jiang F, Ramanathan A, Miller MT, Tang GQ, Gale M Jr, Patel SS, Marcotrigiano J (2011) Structural basis of RNA recognition and activation by innate immune receptor RIG-I. Nature 479(7373):423–427. doi:10.1038/nature10537
15. Yoneyama M, Fujita T (2008) Structural mechanism of RNA recognition by the RIG-I-like receptors. Immunity 29(2):178–181
16. Kato H, Takahasi K, Fujita T (2011) RIG-I-like receptors: cytoplasmic sensors for non-self RNA. Immunol Rev 243:91–98
17. Wilkins C, Gale M Jr (2010) Recognition of viruses by cytoplasmic sensors. Curr Opin Immunol 22:41–47
18. Peisley A, Wu B, Yao H, Walz T, Hur S (2013) RIG-I forms signaling-competent filaments in an ATP-dependent, ubiquitin-independent manner. Mol Cell 51:573–583
19. Peisley A, Wu B, Xu H, Chen ZJ, Hur S (2014) Structural basis for ubiquitin-mediated antiviral signal activation by RIG-I. Nature 509(7498):110–114. doi:10.1038/nature13140
20. Jiang X, Kinch LN, Brautigam CA, Chen X, Du F, Grishin NV, Chen ZJ (2012) Ubiquitin-induced oligomerization of the RNA sensors RIG-I and MDA5 activates antiviral innate immune response. Immunity 36(6):959–973. doi:10.1016/j.immuni.2012.03.022
21. Wu B, Peisley A, Tetrault D, Li Z, Egelman EH, Magor KE, Walz T, Penczek PA, Hur S (2014) Molecular imprinting as a signal-activation mechanism of the viral RNA sensor RIG-I. Mol Cell. doi:10.1016/j.molcel.2014.06.010
22. Hou F, Sun L, Zheng H, Skaug B, Jiang QX, Chen ZJ (2011) MAVS forms functional prion-like aggregates to activate and propagate antiviral

innate immune response. Cell 146(3):448–461. doi:10.1016/j.cell.2011.06.041

23. Zeng W, Sun L, Jiang X, Hou F, Adhikari A, Xu M, Chen ZJ (2010) Reconstitution of the RIG-I pathway reveals a signaling role of unanchored polyubiquitin chains in innate immunity. Cell 141:315–30
24. Keppler A, Gendreizig S, Gronemeyer T, Pick H, Vogel H, Johnsson K (2003) A general method for the covalent labeling of fusion proteins with small molecules in vivo. Nat Biotechnol 21(1):86–89. doi:10.1038/nbt765
25. Alexandrov A, Dutta K, Pascal SM (2001) MBP fusion protein with a viral protease cleavage site: one-step cleavage/purification of insoluble proteins. Biotechniques 30:1194–1198
26. Potter JA, Randall RE, Taylor GL (2008) Crystal structure of human IPS-1/MAVS/VISA/Cardif caspase activation recruitment domain. BMC Struct Biol 8:1–10

Part III

Toll-Like Receptor Post-Transcriptional Regulation

Chapter 10

Co-transcriptomic Analysis by RNA Sequencing to Simultaneously Measure Regulated Gene Expression in Host and Bacterial Pathogen

Timothy Ravasi, Charalampos (Harris) Mavromatis, Nilesh J. Bokil, Mark A. Schembri, and Matthew J. Sweet

Abstract

Intramacrophage pathogens subvert antimicrobial defence pathways using various mechanisms, including the targeting of host TLR-mediated transcriptional responses. Conversely, TLR-inducible host defence mechanisms subject intramacrophage pathogens to stress, thus altering pathogen gene expression programs. Important biological insights can thus be gained through the analysis of gene expression changes in both the host and the pathogen during an infection. Traditionally, research methods have involved the use of qPCR, microarrays and/or RNA sequencing to identify transcriptional changes in either the host or the pathogen. Here we describe the application of RNA sequencing using samples obtained from in vitro infection assays to simultaneously quantify both host and bacterial pathogen gene expression changes, as well as general approaches that can be undertaken to interpret the RNA sequencing data that is generated. These methods can be used to provide insights into host TLR-regulated transcriptional responses to microbial challenge, as well as pathogen subversion mechanisms against such responses.

Key words Host-pathogen, Innate immunity, Intracellular pathogens, Macrophages, RNA sequencing, Toll-like receptors, Transcriptomics, Urinary tract infections, Uropathogenic *E. coli*

1 Introduction

TLR-regulated transcriptional responses enable the host to initiate appropriate defence mechanisms against microbial challenge. Next-generation sequencing technologies have been adopted to study regulated gene expression during infection [1–7]. Such methodologies enable quantification of millions of RNA transcripts in a sample, thus enabling mapping of global differences in gene expression between treatment groups [8, 9]. Since these approaches directly determine absolute transcript levels, they overcome some of the limitations of microarray expression profiling [5, 10]. Most previous infection model studies employing RNA sequencing have characterized either the host or the pathogen response [1, 7, 11, 12].

Claire E. McCoy (ed.), *Toll-Like Receptors: Practice and Methods*, Methods in Molecular Biology, vol. 1390,
DOI 10.1007/978-1-4939-3335-8_10,

Here we detail RNA sequencing and analysis methodology that we have used to characterize the expression profiles of two organisms using the same biological sample (Fig. 1).

The model system that we have employed for host-pathogen co-transcriptomics relates to urinary tract infections (UTI), one of the most common infections in humans. Uropathogenic *Escherichia coli* (UPEC), the main causative agent of UTIs, can invade and replicate within bladder epithelial cells [13], and some UPEC strains can also survive within macrophages [14]. To further understand UPEC-macrophage interactions, we recently performed co-transcriptomics of mouse bone marrow-derived macrophages (BMM) challenged over a 24 h time course with the UPEC genome sequenced reference strains, UTI89 (cystitis strain) and 83972 (asymptomatic bacteriuria strain) [15]. These strains both trigger TLR4-mediated transcriptional responses in the host, but possess contrasting phenotypes for intramacrophage survival. In this chapter, we use our mouse macrophage-UPEC infection studies as a model system to present an approach for performing in vitro infection assays, isolating and sequencing total RNA from cocultures, extracting sequence data for each organism studied, and analyzing the simultaneous changes in expression that occur in the interacting organisms. These methods could be adapted for the study of other host-pathogen systems in which TLRs are engaged, as well as the detailed analysis of organisms that interact in symbiotic relationships.

2 Materials

2.1 BMM Infection Assays

1. Specific pathogen free C57BL/6 male mice at 6–8 weeks age.
2. BMM medium with antibiotic (complete medium): RPMI 1640 containing 10 % heat-inactivated fetal bovine serum, 50 U/mL penicillin, 50 μg/mL streptomycin and 2 mM L-glutamine.
3. Antibiotic-free BMM medium (medium as described in **item 2**, but without penicillin and streptomycin).
4. Gentamicin solution (TC grade).
5. Glycerol stocks of uropathogenic *E. coli* strains UTI89 [16] and 83972 [17].
6. 10 mL syringes.
7. 21G needles.
8. 18G blunt needles.
9. 100 mm square bacteriological petri dishes.
10. Luria Bertani (LB) medium.
11. LB agar plates with no antibiotic selection.
12. Phosphate buffered saline (PBS).

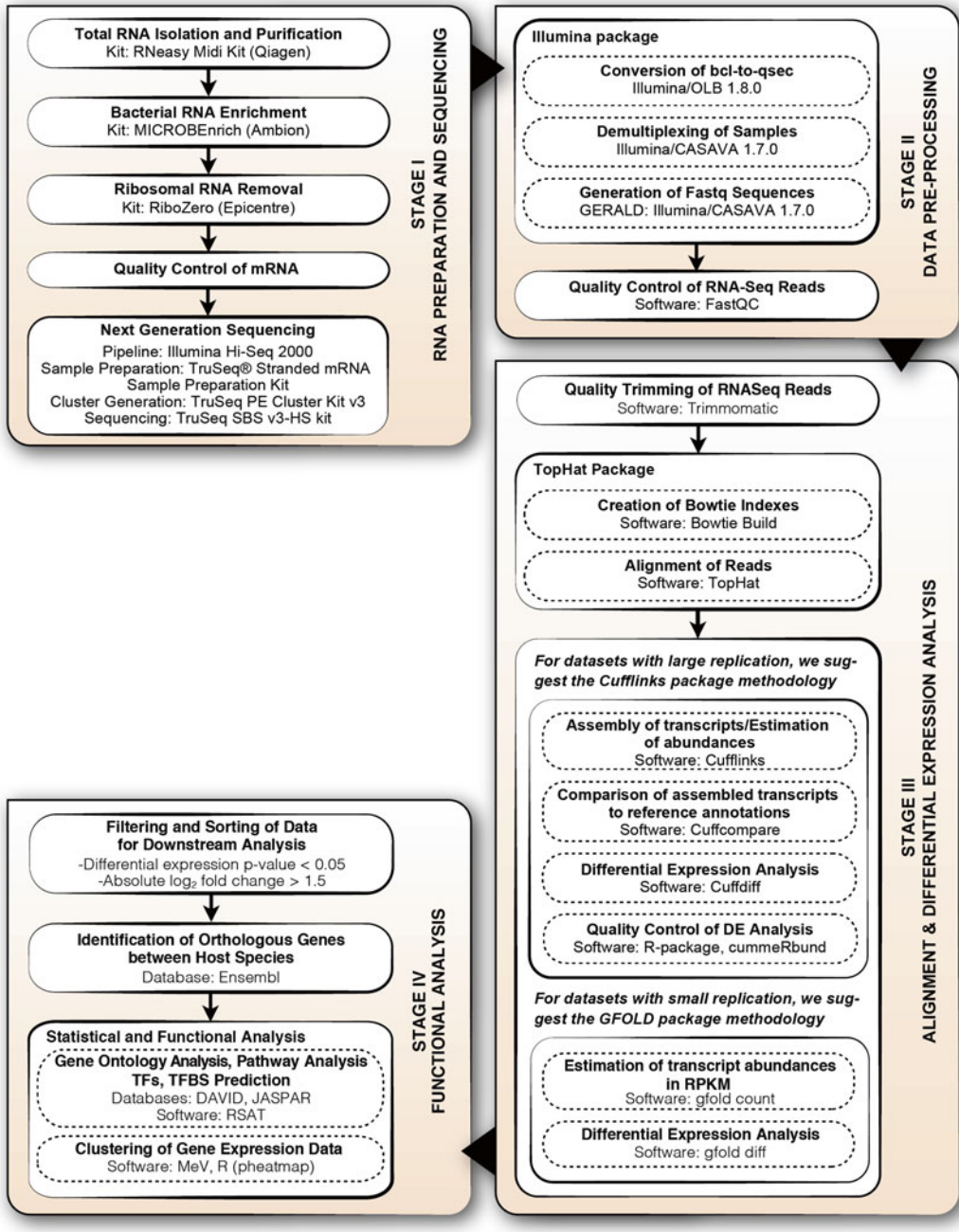

Fig. 1 Bioinformatic analysis pipeline. Summary of the four stages of analysis (RNA preparation and sequencing; data preprocessing; alignment and differential expression analysis; functional analysis), as well as details of the steps involved in each stage

13. Magnesium- and calcium-free sterile PBS (TC grade).
14. 0.01 % (v/v) Triton X-100 made up in PBS.
15. 10 % yeast solution: 10 % (w/v) dry yeast powder made up in PBS.
16. 24 well tissue culture plates.
17. 10 cm tissue culture plates.
18. 50 mL conical centrifuge tubes.

2.2 RNA Preparation, Sequencing, and Analysis

1. Sterile 5 mL and 10 mL plastic serological pipettes.
2. RNase-free 1.5 mL tubes.
3. 5 mL syringes.
4. 25G needles.
5. 16 cm cell scrapers.
6. 50 mL conical centrifuge tubes.
7. RNeasy Maxi kits (Qiagen).
8. 14.3 M β-mercaptoethanol.
9. Absolute ethanol (AR grade).
10. DNase- and RNase-free sterile water.
11. Ambion MICROBEnrich kit (Life Technologies).
12. Ribo-Zero rRNA removal kit (Epicenter).
13. Agilent RNA 6000 Nano Kit (Agilent Technologies).
14. Qubit® RNA BR Assay Kit (Life Technologies).
15. TruSeq® Stranded mRNA Sample Preparation Kit (Illumina).
16. SuperScript II Reverse Transcriptase (Invitrogen).
17. Agencourt AMPure XP 60 mL kit (Beckman Coulter).
18. TruSeq PE Cluster Kit v3 (Illumina).
19. TruSeq SBS v3-HS kit (Illumina).
20. OLB 1.8.0 (Illumina).
21. CASAVA 1.7.0 (Illumina).
22. GERALD (Illumina/CASAVA 1.7.0).
23. FastQC (Babraham Bioinformatics).
24. Trimmomatic (Usadel Lab).
25. Bowtie 2 (John Hopkins University).
26. Tophat 2 (CCB, John Hopkins University).
27. Cufflinks 2 (Cole Trapnell Lab).
28. CummeRbund (CSAIL-MIT, SCRB-Harvard).
29. GFOLD (Tongji University).

30. MCE (Integrative Systems Biology Lab).
31. RSAT (Université libre de Bruxelles).
32. Packages NbClust and pheatmap (CRAN R Project).

3 Methods

Here, we describe an experimental system that includes UPEC only controls, BMM only controls, and BMM and UPEC cocultured at 2, 4, and 24 h (*see* Fig. 2). RNA should be prepared from three or more independent experiments, to ensure that RNA sequencing data generated is biologically robust. When comparing gene expression profiles for different conditions (e.g., different UPEC strains, macrophages from different host species or different sources), it is necessary to determine intracellular bacterial survival in parallel (i.e., using the same preparations of bacteria and macrophages). This is an important quality control measure, and ensures that matched intramacrophage bacterial survival and expression profiling data are generated. We therefore describe methods for determining intracellular survival of UPEC within macrophages, before going on to describe methods to extract RNA, perform RNA sequencing, and analyze the resulting data.

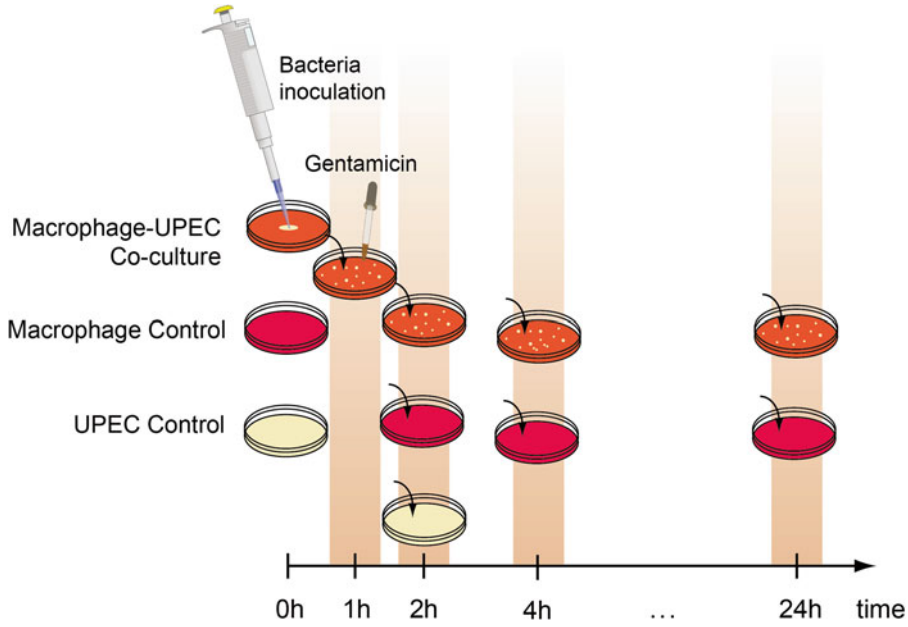

Fig. 2 Experimental design of BMM infection assays, used for quantification of intracellular bacterial loads and RNA generation

3.1 BMM Infection Assay to Determine Intracellular Survival

1. On day 0, sacrifice mice, collect femurs and tibias and place the bones in complete medium.
2. Remove muscle and surrounding tissue from the femoral and tibial bones, then under sterile conditions clean the bones with 70 % ethanol and place in complete medium (*see* **Note 1**).
3. Remove the very tips of the femurs and tibias using surgical scissors, and flush the bone cavity with complete medium and a 21G needle into a 50 mL tube to collect bone marrow (BM) cells (*see* **Note 2**).
4. Wash BM cells twice with complete medium (centrifuge at 500 × *g* for 5 min each time).
5. Divide BM cells into four 100 mm^2 petri dishes with 15 mL complete medium per plate, and culture in the presence of 10,000 U/mL recombinant colony stimulating factor-1 (CSF-1), as described previously [18, 19].
6. On day 5, add fresh complete medium (5 mL), plus fresh CSF-1 to final concentration of 10,000 U/mL (*see* **Note 3**).
7. Also on day 5, streak an antibiotic-free LB agar plate of specific UPEC strain of interest from glycerol stock under aseptic conditions (*see* **Note 4**).
8. On day 6, harvest BMM. To do so, discard the medium from the 100 mm^2 petri dishes, then wash the plates twice with magnesium- and calcium-free sterile PBS, transferring both washes to a 50 mL tube. Add 10 mL magnesium- and calcium-free sterile PBS to the petri dishes and leave for 5 min. Using a 10 mL syringe and 18G blunt needle, wash the BMMs off the plate and collect in the same 50 mL tubes. Spin the cells down at 500 × *g* for 5 min and resuspend in antibiotic-free BMM medium. Plate BMM out in antibiotic-free BMM medium in 24 well tissue culture plates: 2 wells for each treatment and 2 wells for control. Plate a total of 200,000 cells/well in a total volume of 900 μL with 10,000 U/mL CSF-1 (*see* **Note 5**).
9. On day 6, also set up overnight bacterial cultures. UPEC strains are cultured statically in LB broth at 37 °C overnight in conical flasks. Static culture is employed to enrich for the expression of type 1 fimbriae.
10. On day 7, spin down overnight cultures of bacteria at 4000 × *g* for 10 min. Wash two times with magnesium- and calcium-free sterile PBS, then resuspend in 10 mL magnesium- and calcium-free sterile PBS.
11. Assess expression of type 1 fimbriae on the surface of UPEC isolates using the yeast agglutination test [20], prior to performing infection assays. In short, mix a drop of 10 % yeast solution with a bacterial suspension on a glass slide and observe for agglutination. Strains expressing type 1 fimbriae will agglutinate (*see* **Note 6**).

12. Using a spectrophotometer, measure absorbance at 600 nm of the bacterial suspension. Centrifuge the bacterial suspension (4000 × *g* for 10 min), and then resuspend the pellet in a volume of antibiotic-free medium such that the A_{600nm} of the bacterial suspension now equates to 0.7 absorbance units. This is equivalent to 1×10^8 cfu/mL (*see* **Note 7**).
13. Dilute bacteria to the required concentration in antibiotic-free medium such that the volume of bacterial suspension to be added to macrophage cultures is 100 μL/well. For example, for a multiplicity of infection (MOI) of 10; dilute bacterial suspension to 2×10^7 cfu/mL, 100 μL is thus 2×10^6 cfu, which will be used to infect 200,000 BMM (*see* **Note 7**).
14. Plate appropriately diluted bacterial suspension on antibiotic-free LB agar plates and incubate overnight at 37 °C for MOI determination (*see* **Note 7**).
15. Add 100 μL bacterial suspension per well of 24 well plate of BMM, and incubate for 1 h at 37 °C.
16. Aspirate the supernatant from wells, wash twice with 1 mL antibiotic-free medium containing 200 μg/mL gentamicin, add another 1 mL medium containing gentamicin (200 μg/mL) to the wells and incubate at 37 °C for 1 h (*see* **Notes 8** and **9**).
17. Aspirate supernatant from wells, wash wells twice with 1 mL antibiotic-free medium, then add 1 mL antibiotic-free medium containing 20 μg/mL gentamicin to the wells and incubate at 37 °C for the appropriate time (*see* **Notes 8** and **10**).
18. To assess intracellular bacterial loads at designated time points, aspirate medium, wash twice with 1 mL antibiotic-free medium, add 1 mL 0.01 % Triton X-100 in PBS to each well, leave for 5 min at room temperature, then pipette up and down to ensure complete lysis before harvesting lysate into a 1.5 mL eppendorf tube.
19. Vortex the eppendorf tube and plate out 50 μL on LB agar plates at multiple dilutions. Incubate overnight.
20. Count colonies and calculate intracellular bacterial numbers (*see* **Notes 11** and **12**).

3.2 BMM Infection Assay for RNA Preparation

To assess bacterial and mammalian RNA expression profiles by RNA sequencing, infection assays need to be scaled up. Thus, infection assays are carried out essentially as described above, but in a 10 cm round tissue culture plate (Fig. 2).

1. Plate out 7×10^6 BMM in 10 mL antibiotic-free medium 1 day prior to infection.
2. Infect with bacteria and perform washes as described in **steps 13–17**, Subheading 3.1. For an MOI of 10; dilute bacterial suspension to 7×10^8 cfu/mL, 100 μL is thus 7×10^7 cfu, which will be used to infect 7×10^6 BMM.

3. After incubation for designated times (e.g., 2, 4, 24 h), wash cells with ice-cold PBS, then lyse on plates with the appropriate lysis buffer, as per the specific RNA purification protocol.
4. To determine a basal level of bacterial gene expression, culture bacteria statically in 10 mL antibiotic-free BMM medium for 2 h, using the same inoculum that is used to infect the BMM. At the end of 2 h, spin down the bacteria ($4000 \times g$ for 10 min) and lyse with appropriate lysis buffer. Total RNA should also be prepared from uninfected BMM at the same time points as used for coinfections (Fig. 2).
5. Extract RNA using RNeasy Maxi kits. Add 3.5 mL RLT buffer (with added 2-mercaptoethanol) per 10 cm dish, as well as to bacterial pellets from bacteria grown separately.
6. Scrape cell lysates off the plate using a cell scraper for maximum yield. Homogenize lysates by passing them 20 times through a 25G needle and extract total RNA, as per the manufacturer's protocol (including off-column DNase digestion). For enrichment of microbial RNA in coculture samples, use Ambion MICROBEnrich (Life Technologies).
7. rRNA should be removed from all purified RNA samples using kits, such as Ribo-Zero (Epicenter), targeting mammalian, and Gram-negative bacterial rRNAs.
8. Prior to sequencing, all RNA preparations should be quantified and assessed for protein and reagent contamination using Qubit®. RNA samples for analysis must be selected based on a spectroscopic A_{260}/A_{280} nm ratio of 1.8–2.0, and an A_{260}/A_{230} nm ratio of greater than 1.5 (*see* **Note 13**).

3.3 RNA Sequencing, Alignment, Annotation, and Differential Gene Expression Analyses

Next-generation sequencing analyses for $n \geq 3$ biological replicates can be performed on an Illumina Cluster Station and the Illumina HiSeq 2000 System. The first step is to convert the mRNA within the total RNA into a library of template molecules of known strand origin using the reagents provided in the Illumina® TruSeq® Stranded mRNA Sample Preparation Kits. The library generated is suitable for subsequent cluster generation with the TruSeq PE Cluster Kit. The cluster is now ready for sequencing using the TruSeq SBS v3-HS kit that determines the DNA sequence of each cluster on a flow cell using sequencing by synthesis technology on the HiSeq sequencing systems.

1. Use the Solexa Automated Pipeline (OLB, CASAVA, and GERALD) for image analysis, base calling, and quality calibration.
2. Quality control of RNA-Seq reads can be preprocessed by custom java script (FastQC), which checks the raw sequence data from high-throughput sequencing pipelines for any problems.

RNASeq reads can be subjected to quality trimming in order to remove Illumina adapters, low quality leading and trailing bases, bases with low average quality, and reads shorter than 36 bases long. Trimmomatic, a flexible read trimming tool for Illumina NGS data [21], can be used for this purpose.

3. To align reads, bowtie indexes should be created for the host and pathogen reference genomes. To do this, use the bowtie-build algorithm and reference sequences from the GenBank database. To map the raw RNA-Seq reads (fastq files) to the reference genomes, we recommend TopHat. This uses Bowtie as an alignment engine. Reads that Bowtie cannot align on its own are broken up by TopHat into smaller fragments [22]. Both reads of paired-end libraries can be mapped using the standard parameters. All simulations should be performed using a high-memory node cluster system.
4. The approach for transcription annotation is dependent upon the number of replicates per condition. If the number of replicates per condition is large ($n > 10$), after running TopHat, we suggest generating a transcriptome assembly for each condition by providing the resulting alignment files to Cufflinks. Adapter tags, mitochondrial sequences, poly A, poly C, and phiX sequences, and remaining ribosomal sequences will be filtered out within this analysis. Estimated normalized expression levels will be reported in fragments (i.e., reads) per kilobase of exon per million mapped reads (FPKM). These assemblies will be compared with annotation files using the Cuffcompare utility that is included in the Cufflinks package [23, 24]. On the other hand, if the number of replicates per condition is small ($n < 10$), after running TopHat, we suggest providing the resulting mapped short reads in SAM format, along with the gene annotation in GTF format, to GFOLD count to count the number of reads mapped to each gene [25]. Estimated normalized expression levels will be reported in reads per kilobase of exon per million mapped reads (RPKM).
5. The number of replicates also affects the approach to be used for differential gene expression analysis. Where the number of replicates is large, the reads and assemblies can be further imported to Cuffdiff, in order to determine expression levels and test the statistical significance of any changes identified. To compare differentially expressed genes across samples, the Cufflinks package is used to normalize (to FPKM) the number of raw clean tags in each library. A threshold can be set for the minimum number of alignments in a locus needed to test for statistically significant changes in that locus between samples. If no testing is performed, changes in the locus are considered insignificant, and these changes will not contribute to corrections for multiple testing. The Cuffdiff output files can subsequently be imported

to cummeRbund. This plots abundance and differential expression data as expression plots for quality control [24]. Where the number of replicates is small, the reads can be further imported to GFOLD diff, which generalizes the fold change by considering the posterior distribution of log fold change. Consequently, each gene is assigned a reliable fold change (*see* **Note 14**). The GFOLD output files can be further processed for quality control using the R package.

3.4 Ortholog Identification, Dimensionality Reduction, Clustering, and Pathway Analysis

1. Identification of orthologous genes is an essential component of studies comparing multiple host and/or pathogen species. We have used the Ensembl database [26] for this purpose (*see* **Note 15**). All genes that share orthology should be converted to orthologous groups (OG). In the case of one-to-one orthology, an OG will contain a single gene from each species. In the cases of one-to-many and many-to-many orthology relationships, an OG is defined as the set of genes that share this relationship. A new annotation file should be prepared with only orthologous interactions prior to performing a second differential expression analysis, this time comparing species (A vs. B vs. C etc) for each time point. This step is necessary since it eliminates genes present in one species but not the other.
2. Dimensionality reduction enables exploration of the relationships between conditions in RNA sequence data sets. The minimum classification error (MCE) method performs a nonlinear dimension reduction. It does so by embedding high-dimensional data points into a lower-dimensional space through the use of the minimum curvilinear kernel in combination with multidimensional scaling (MDS) [27], or alternatively, the singular value decomposition (SVD) [28]. The nonlinear data distances for MDS or SVD are computed and stored in the minimum curvilinear kernel as the traversal distances over the minimum spanning tree between the data points (sample conditions) in the multidimensional space (the gene space). The minimum spanning tree is constructed from the Pearson correlation-based distances between the samples [27]:

$$\text{Correlation\_based\_distance}(x,y) = 1 \quad \text{Pearson\_Correlation}\left(\text{Sample}_x, \text{Sample}_y\right)$$

As a parameter-free projection algorithm, MCE is especially effective in using only the first dimension of embedding to distinguish classes in small-n (samples: here conditions), large-m (features: here gene expression) datasets [27]. Because $n \ll m$ in the UPEC/macrophage RNA sequence datasets, we adopted the MCE algorithm for unsupervised analysis of the different sample conditions.

3. Genes with similar expression patterns can often have related functions or coexist within a biological pathway. The R package NbClust can be used to perform a cluster analysis of gene expression patterns, in order to identify the optimal number of clusters in the dataset. Selected lists of divergently expressed genes can be further compiled for hypothesis testing and clustering using the Ward's methodology of the R package pheatmap. Significantly enriched gene ontologies (GOs) and pathways can be identified by mapping all divergently expressed genes to terms in the GO and KEGG databases by applying two-sided Fisher's exact and χ^2 tests, respectively [29, 30]. *P*-values should be corrected by calculating the FDR, and only GOs and pathways with an FDR < 0.01 should be chosen.
4. Analysis of promoter sequences of divergently expressed genes can identify likely transcription factors (TFs) and upstream signaling pathways mediating changes in gene expression. Promoter sequences can be retrieved using regulatory sequence analysis tools (RSAT), with subsequent input into the RSAT matrix-scan tool along with host-related matrices for transcription factor binding site (TFBS) prediction [31–33]. The RSAT output should be filtered using an adjusted *P*-value < 0.05 as a cutoff, and lists of the most significant TFBSs and their known corresponding TFs should be compiled. Profiles of the host divergently expressed genes can be clustered, and each cluster can be correlated with the TF profiles using Pearson correlation in R. Finally, the clusters can be further annotated using GO to gain insights into the molecular processes in which each TF is involved.

4 Notes

1. While cleaning femurs and tibias with ethanol do not leave the bones in ethanol for more than 3–5 min, as this can cause the bones to go brittle.
2. While flushing femurs and tibias do not re-aspirate flushed medium using the needle. This can result in cell shearing and decreased yield.
3. Since BMM consume CSF-1, cell density is an important variable if the CSF-1 concentration becomes limiting. We therefore use a high concentration of CSF-1 and replenish the CSF-1 during differentiation to avoid variability between different cell preparations. The actual CSF-1 concentration to be used (in U/mL or ng/mL) will vary, depending on the source.
4. There is no selection, be careful with your technique.
5. Whether to include CSF-1 in BMM cultures post-differentiation is a point of contention. We normally include CSF-1 in cultures

used for our experiments, because this growth factor is constitutively present in vivo. Furthermore, macrophages do proliferate locally in various tissue environments. However, in experiments where cell proliferation may confound data interpretation, CSF-1 should be excluded. In any case, whether this growth factor is included in experimental conditions should be clearly stated, given that it has major effects on the functions of mature macrophages.

6. Optimal type 1 fimbriae expression should result in a rapid time to agglutination (i.e., less than 5 s). If this is not achieved, a second round of static culture, where the inoculum is obtained by removing 100 μL from the air–liquid interface of the first culture, should be performed.
7. As soon as possible after determining cfu/mL, use bacterial suspension for infection assays and plate the inoculum out for MOI determination (to avoid further bacterial growth, which will alter the MOI that is actually used). If this is not possible, place the inoculum at 4 °C or on ice until the plating can be performed. In this case, make sure that the bacterial suspension is returned to room temperature prior to performing infections. Note that each laboratory should independently determine the correlation between A_{600nm} and cfu/mL for determining the MOI.
8. There are several washing steps during infection assays, which can result in detachment of BMM from the tissue culture plastic surface. To avoid this, add the wash solution slowly along the side of the well or plate.
9. There is some literature to suggest that gentamicin can affect intracellular bacteria [34, 35]. If comparing intramacrophage survival and/or responses of different bacterial species or strains, ensure that there are no differences in their sensitivity to gentamicin, as this may confound data interpretation.
10. To confirm that the gentamicin wash has killed all extracellular bacteria, the supernatant from the final wash with antibiotic-free medium can be plated on antibiotic-free LB agar.
11. To calculate intracellular bacterial numbers, plate out at least 2 dilutions per sample, i.e., neat and 1/50 or 1/100, etc. The dilution depends on how high your MOI is, the length of the infection assay and the specific pathogen being investigated. Calculation of MOI and intracellular bacterial numbers:

$$\text{cfu} / \text{mL} = \text{No. of colonies} \times \text{dilution factor} \times 1000 / \text{volume of plated solution.}$$

12. Plate out the supernatant and the lysate from the uninfected samples. This will serve as a control to confirm there was no contamination during the course of the infection assay.

13. Extensive quality control is crucial when undertaking large-scale analyses such as RNA sequencing. Prior to performing RNA sequencing, qPCR analyses should be performed for specific host and pathogen genes for which biological effects are already known.
14. GFOLD overcomes the shortcoming of *p*-value by measuring relative expression changes instead of the significance of whether a gene is differentially expressed [25]. It also overcomes the limitation of using fold change, which suffers from the fact that the fold changes of genes with low-read counts are not as reliable as those of genes with high read counts.
15. There are many freely available resources that can be used to determine orthology relationships. Each method will result in some differences in orthology predictions based on the database used and enrichment score cutoff.

Acknowledgments

This work was supported by grants from the National Health and Medical Research Council (NHMRC) of Australia (APP1005315 and APP1068593). M.J.S. is supported by an Australian Research Council Future Fellowship (FT100100657), as well as an honorary NHMRC Senior Research Fellowship (APP1003470). M.A.S. is supported by an ARC Future Fellowship (FT100100662). T.R. and C.H.M. are supported by The King Abdullah University of Science and Technology.

References

1. Hegedus Z, Zakrzewska A, Agoston VC et al (2009) Deep sequencing of the zebrafish transcriptome response to mycobacterium infection. Mol Immunol 46:2918–2930
2. Huang Q, Dong S, Fang C et al (2012) Deep sequencing-based transcriptome profiling analysis of Oryzias melastigma exposed to PFOS. Aquat Toxicol 120–121:54–58
3. Jager D, Sharma CM, Thomsen J et al (2009) Deep sequencing analysis of the Methanosarcina mazei Go1 transcriptome in response to nitrogen availability. Proc Natl Acad Sci U S A 106: 21878–21882
4. Nie Q, Sandford EE, Zhang X et al (2012) Deep sequencing-based transcriptome analysis of chicken spleen in response to avian pathogenic Escherichia coli (APEC) infection. PLoS One 7, e41645
5. t Hoen PA, Ariyurek Y, Thygesen HH et al (2008) Deep sequencing-based expression analysis shows major advances in robustness, resolution and inter-lab portability over five microarray platforms. Nucleic Acids Res 36:141
6. Wang F, Hu S, Liu W et al (2011) Deep-sequencing analysis of the mouse transcriptome response to infection with Brucella melitensis strains of differing virulence. PLoS One 6, e28485
7. Xiang LX, He D, Dong WR et al (2010) Deep sequencing-based transcriptome profiling analysis of bacteria-challenged Lateolabrax japonicus reveals insight into the immune-relevant genes in marine fish. BMC Genomics 11:472
8. Morozova O, Marra MA (2008) Applications of next-generation sequencing technologies in functional genomics. Genomics 92:255–264
9. Wang Z, Gerstein M, Snyder M (2009) RNA-Seq: a revolutionary tool for transcriptomics. Nat Rev Genet 10:57–63
10. Llorens F, Hummel M, Pastor X et al (2011) Multiple platform assessment of the EGF dependent transcriptome by microarray and

deep tag sequencing analysis. BMC Genomics 12:326

11. Ordas A, Hegedus Z, Henkel CV et al (2011) Deep sequencing of the innate immune transcriptomic response of zebrafish embryos to Salmonella infection. Fish Shellfish Immunol 31:716–724
12. Xiao S, Jia J, Mo D et al (2010) Understanding PRRSV infection in porcine lung based on genome-wide transcriptome response identified by deep sequencing. PLoS One 5, e11377
13. Hannan TJ, Totsika M, Mansfield KJ et al (2012) Host-pathogen checkpoints and population bottlenecks in persistent and intracellular uropathogenic Escherichia coli bladder infection. FEMS Microbiol Rev 36:616–648
14. Bokil NJ, Totsika M, Carey AJ et al (2011) Intramacrophage survival of uropathogenic Escherichia coli: differences between diverse clinical isolates and between mouse and human macrophages. Immunobiology 216:1164–1171
15. Mavromatis CH, Bokil NJ, Totsika M et al (2014) The co-transcriptome of uropathogenic Escherichia coli-infected mouse macrophages reveals new insights into host-pathogen interactions. Cell Microbiol 17(5):730–746. doi:10.1111/cmi.12397
16. Mulvey MA, Schilling JD, Hultgren SJ (2001) Establishment of a persistent Escherichia coli reservoir during the acute phase of a bladder infection. Infect Immun 69:4572–4579
17. Andersson P, Engberg I, Lidin-Janson G et al (1991) Persistence of Escherichia coli bacteriuria is not determined by bacterial adherence. Infect Immun 59:2915–2921
18. Hume DA, Gordon S (1983) Optimal conditions for proliferation of bone marrow-derived mouse macrophages in culture: the roles of CSF-1, serum, Ca2+, and adherence. J Cell Physiol 117:189–194
19. Tushinski RJ, Stanley ER (1983) The regulation of macrophage protein turnover by a colony stimulating factor (CSF-1). J Cell Physiol 116:67–75
20. Schembri MA, Hasman H, Klemm P (2000) Expression and purification of the mannose recognition domain of the FimH adhesin. FEMS Microbiol Lett 188:147–151
21. Bolger AM, Lohse M, Usadel B (2014) Trimmomatic: a flexible trimmer for Illumina sequence data. Bioinformatics 30:2114–2120
22. Kim D, Salzberg SL (2011) TopHat-Fusion: an algorithm for discovery of novel fusion transcripts. Genome Biol 12:R72
23. Roberts A, Trapnell C, Donaghey J et al (2011) Improving RNA-Seq expression estimates by correcting for fragment bias. Genome Biol 12:R22
24. Trapnell C, Roberts A, Goff L et al (2012) Differential gene and transcript expression analysis of RNA-seq experiments with TopHat and Cufflinks. Nat Protoc 7: 562–578
25. Feng J, Meyer CA, Wang Q et al (2012) GFOLD: a generalized fold change for ranking differentially expressed genes from RNA-seq data. Bioinformatics 28:2782–2788
26. Flicek P, Amode MR, Barrell D et al (2014) Ensembl 2014. Nucleic Acids Res 42: D749–D755
27. Cannistraci CV, Ravasi T, Montevecchi FM et al (2010) Nonlinear dimension reduction and clustering by Minimum Curvilinearity unfold neuropathic pain and tissue embryological classes. Bioinformatics 26:i531–i539
28. Cannistraci CV, Alanis-Lobato G, Ravasi T (2013) Minimum curvilinearity to enhance topological prediction of protein interactions by network embedding. Bioinformatics 29: i199–i209
29. da Huang W, Sherman BT, Lempicki RA (2009) Bioinformatics enrichment tools: paths toward the comprehensive functional analysis of large gene lists. Nucleic Acids Res 37:1–13
30. da Huang W, Sherman BT, Lempicki RA (2009) Systematic and integrative analysis of large gene lists using DAVID bioinformatics resources. Nat Protoc 4:44–57
31. Thomas-Chollier M, Defrance M, Medina-Rivera A et al (2011) RSAT 2011: regulatory sequence analysis tools. Nucleic Acids Res 39: W86–W91
32. Thomas-Chollier M, Sand O, Turatsinze JV et al (2008) RSAT: regulatory sequence analysis tools. Nucleic Acids Res 36:W119–W127
33. Turatsinze JV, Thomas-Chollier M, Defrance M et al (2008) Using RSAT to scan genome sequences for transcription factor binding sites and cis-regulatory modules. Nat Protoc 3: 1578–1588
34. Drevets DA, Canono BP, Leenen PJ et al (1994) Gentamicin kills intracellular Listeria monocytogenes. Infect Immun 62:2222–2228
35. Hamrick TS, Diaz AH, Havell EA et al (2003) Influence of extracellular bactericidal agents on bacteria within macrophages. Infect Immun 71:1016–1019

Chapter 11

Simple Methods to Investigate MicroRNA Induction in Response to Toll-Like Receptors

Victoria G. Lyons and Claire E. McCoy

Abstract

In this chapter, we describe simple methods to investigate microRNA (miRNA) induction in response to lipopolysaccharide, the ligand for Toll-Like Receptor-4 activation. In brief, we demonstrate how to investigate global miRNA induction and/or repression in bone marrow-derived macrophages using TaqMan MicroRNA Arrays, followed by methods to measure individual miRNAs and target mRNA expression. Moreover, we explain step-by-step instructions on how to modulate endogenous miRNA expression through the use of miRNA inhibitors and mimics as well as highlight how miRNA modulation can be used to confirm mRNA targeting via Luciferase reporter assay. Moreover, these methods can be applied to whichever cell type and cellular function under investigation.

Key words Toll-like receptors, microRNA, miRNA, miRNA inhibitor, miRNA mimic, Luciferase assay, TaqMan MicroRNA Array, RT-PCR, Bone marrow-derived macrophages, BMDM

1 Introduction

Negative regulation of pathways such as those induced by Toll-Like Receptors is an important mechanism required to control inflammation [1]. Without this, excessive inflammation can result in the numerous inflammatory pathologies prominent in today's population [2]. Moreover, there is now unsurpassed evidence that prolonged inflammation is a key player in the progression of diseases such as type 2 diabetes, atherosclerosis, and cancer [2]. Classic mechanisms of negative regulation have focused on post-translational modifications including phosphorylation, ubiquitination, and degradation of signaling components, induction of transcriptional repressors, and competition by inhibitory molecules. However, more recent discoveries have highlighted the increasing importance of posttranscriptional regulation, such as those undertaken by microRNAs (miRNAs) [3].

Claire E. McCoy (ed.), *Toll-Like Receptors: Practice and Methods*, Methods in Molecular Biology, vol. 1390,
DOI 10.1007/978-1-4939-3335-8_11,

MiRNAs are important regulators of gene expression. Formerly thought to repress translation of target mRNAs, it is more likely that the main effect is to decrease target mRNA levels [4]. miRNAs are 22 nucleotides in length, characterized by a 6–8mer "seed" sequence which binds with partial and/or exact complementarity to the 3′ untranslated region (3′UTR) of target mRNA molecules. There are various reports as to the importance of the seed region over that of the surrounding sequence within an miRNA, but it is likely that both regions play an important role [5].

To date, TLRs have been shown to induce and repress a range of miRNAs (for a detailed review *see* ref. 6). The outcome of TLR-induced miRNAs is to modulate the TLR response by targeting mRNA molecules that play a role in the overall inflammatory response. For example, miR-155 is a pro-inflammatory miRNA potently induced by innate immune cells such as macrophages and dendritic cells, as well as $CD4^+$ T cells. In order to promote an inflammatory response, miR-155 targets the 3′UTR of mRNA molecules such as suppressor of cytokine 1 signaling (SOCS1) and inositol polyphosphate-5-phosphate (SHIP1), two negative regulators of a TLR-driven immune response [6]. Moreover, mice deficient in miR-155 have severe defects in innate and adaptive immune responses and they are protected in models of experimental autoimmune encephalomyelitis (EAE), arthritis, and colitis, again suggesting that miR-155 acts as an essential component of the pro-inflammatory response [7–11].

In general terms, the regulation undertaken by miRNAs should be perceived as that of "fine-tuning," where the induction of miRNAs is a tightly orchestrated, multifaceted lattice required to regulate the mRNA expression within every cell in response to a particular signal to mediate a particular functional response. Although sometimes modest in effect, it is obvious from our studies and those of others that when miRNAs are absent or inhibited, target mRNA molecules are more highly expressed and biological outcomes such as those discovered in miR-155 deficient mice are apparent [4, 7, 8]. It is also clear that specific miRNAs are differentially expressed and induced in different cell types, for example, miR-122 is a liver-specific miRNA whereas TLR-induced miR-155 occurs in cells of the immune system [6, 12]. This specificity makes miRNAs a wonderful tool with which to manipulate and modulate in specific cell types to provide novel approaches for molecular therapeutics, where an outcome of "fine-tuning" is often more beneficial than that of complete mRNA ablation.

Modulation of miRNAs has shown promise as a therapeutic tool in disease. Numerous strategies have been employed to either reduce or over-express miRNAs. miRNA inhibitors, also designated anti-miRNA oligonucleotides (AMOs), are currently the most available tool for miRNA inhibition and have shown to inhibit specific endogenous miRNAs through complementary base-pairing in cell culture, flies, and mice [13]. miRNA mimics

which are small double-stranded RNA molecules can be overexpressed to replace endogenous miRNA levels that may be low or absent. The application of miRNA therapeutics, although in a preclinical stage of development, is rapidly advancing; most compellingly the first study conducted in primates demonstrated that an AMO specifically designed to miR-122 could inhibit viral replication of hepatitis C in the liver [14].

In this chapter, we demonstrate how to investigate miRNA induction in response to the TLR4 ligand, lipopolysaccharide (LPS), in bone marrow-derived macrophages (BMDM). These cells are extremely TLR-responsive and we have found that in primary cells, basal miRNA expression is represented in its most natural state compared to cultured cell lines where miRNAs expression is often dysregulated due to the transforming nature of immortalization. Our first approach aims to characterize the global changes in miRNAs in LPS-stimulated BMDMs which can be assessed using TaqMan microRNA Arrays provided by Applied Biosystems. Changes in miRNA expression can be easily determined by fold induction of a stimulated sample compared to a nontreated sample or as we have previously published by plotting the data according to its relative abundance in the cell. The latter offers the chance to observe induced changes in more abundantly expressed miRNAs, thus adding more weight than those that are more lowly expressed [15, 16].

Once a miRNA of interest has been determined, its expression in different cell types and in response to alternative ligands over various time points can be assessed by individual miRNA assays as described here. Conveniently, we describe a method to extract total RNA so that gene expression of potential mRNA targets for the miRNA in question can be determined using the same sample. This is crucial as induction of a miRNA over-time should decrease its target mRNA expression in a reciprocal manner. Protein analysis of a mRNA target can also be assessed by Western blot, but it should be noted that these effects are often modest and can be masked by enhanced chemiluminescence. An excellent method to confirm miRNA targeting to a specific mRNA is by cloning the 3′UTR of a mRNA gene into vectors such as pMIR-REPORT. These vectors express Luciferase protein under the control of the cloned 3′UTR; thus overexpression of miRNA inhibitors or miRNA mimics will increase or decrease luciferase expression, respectively.

2 Materials

2.1 BMDM Harvest and Stimulation

1. Humanely culled naïve mouse, aged 6–12 weeks.
2. Autoclaved surgical scissors and tweezers.

3. Complete Dulbecco's Modified Eagle Medium (DMEM): 500 ml DMEM supplemented with 10 % Fetal Calf Serum (FCS) and 1 % penicillin/streptomycin.
4. 70 % EtOH
5. Dulbecco's Phosphate-Buffered Saline (DPBS; Life Technologies).
6. TrypLE™ Express Stable Trypsin (Life Technologies).
7. Cell scrapers 24 cm (TPP).
8. Sterile carbon steel surgical scalpel blades (No. 10) (Swann-Morton Ltd).
9. 27G ½ gauge needles.
10. 10 ml syringes.
11. DNA/RNase-free H_2O.
12. L929-conditioned medium [17].
13. LPS from *E. coli*, Serotype 0111:B4 (Alexis). Dilute the 1 mg/ml stock to a working stock concentration of 100 μg/ml in sterile DNA/RNase-free H_2O; use 1:1000 on cultured cells. Store at 4 °C.
14. Tissue culture plates: 10 cm, 6 cm, 24-well and 96-well.

2.2 RNA Extraction

1. Qiagen RNeasy Mini Kit.
2. β-Mercaptoethanol.
3. 1.5 ml DNA/RNase-free microcentrifuge tubes.

2.3 TaqMan MicroRNA Array

1. TaqMan® MicroRNA Reverse Transcription Kit (Applied Biosystems). Stored at –20 °C.
2. Megaplex™ RT Primers (Applied Biosystems) (*see* **Note 1**). Stored at –20 °C.
3. TaqMan® Universal PCR Master Mix, 2×, No Amp Erase UNG (Applied Biosystems). Stored at 4 °C.
4. TaqMan® MicroRNA Array (Applied Biosystems). The Array contains four identical microfluidic cards, enabling detection of 384 miRNAs from four independent samples (*see* **Note 2**). Stored at 4 °C.
5. DNA/RNase-free H_2O.
6. DNA/RNase-free 1.5 ml microcentrifuge tubes.
7. DNA/RNase-free PCR tubes (*see* **Note 3**).
8. 7900HT RT-PCR System with TaqMan Array Block (Applied Biosystems) (*see* **Note 4**).
9. Microfluidic plate sealer (Applied Biosystems) (*see* **Note 4**).
10. Microfluidic plate centrifuge adaptors (Applied Biosystems) (*see* **Note 4**).

2.4 RT-PCR

1. TaqMan® MicroRNA Reverse Transcription Kit (Applied Biosystems). Stored at –20 °C.
2. TaqMan® cDNA Reverse Transcription Kit (Applied Biosystems). Stored at –20 °C.
3. TaqMan MiRNA Assay (Applied Biosystems). Stored at –20 °C. The assay is comprised of two components: 5× primer and 20× FAM-labeled probe per specific miRNA (*see* **Note 5**).
4. Gene expression primers (*see* **Note 6**). Dilute to 2 μM with DNA/RNase-free H_2O.
5. SYBR Green Master Mix (*see* **Note 7**).
6. DNA/RNase-free H_2O.
7. MicroAMP™ Optical 384-well or 96-well reaction plate (Applied Biosystems).
8. MicroAMP™ Optical Adhesive Film (Applied Biosystems).
9. 7900HT RT-PCR System with 384-well or 96-well block (*see* **Note 4**).

2.5 MiRNA Modulation

1. Lipofectamine® 2000 (Life Technologies).
2. Opti-MEM® (Life Technologies).
3. DMEM with 10 % FCS only (minus penicillin/streptomycin).
4. Complete DMEM.
5. DPBS (Life Technologies).
6. TrypLE™ Express Stable Trypsin (Life Technologies).
7. DNA/RNAase-free H_2O.
8. Nuclease-free TE Buffer, pH 8.0 (Life Technologies).
9. RNA Oligonucleotides: miRNA inhibitor, miRNA mimic, and nontargeting control oligos (Integrated DNA Technologies; *see* **Note 8**). Generate working stocks of 4 μM in TE buffer.
10. pMIR-REPORT miRNA Expression Reporter Vector (Ambion) containing the 3′UTR for your miRNA target gene of interest.
11. pRL-*Renilla* plasmid.
12. Dual-Luciferase® Reporter Assay System (Promega).

3 Methods

3.1 BMDM Harvest and Stimulation

1. On day 0, humanely cull a naïve mouse. Collect two femurs using autoclaved surgical scissors and tweezers. Trim off the muscle and place in approximately 10 ml of complete DMEM on ice.

2. In a sterile biological safety cabinet, add 5 ml of 70 % EtOH, DPBS, and complete DMEM into three separate 6 cm tissue culture plates. Holding one femur tightly with the tweezers, briefly rinse the femur first in 70 % EtOH, then DPBS, followed by complete DMEM. The femur should be left in the 6 cm plate containing DMEM while performing the next step.
3. Cut both ends of the femur using a sterile scalpel blade while holding the middle of the bone with sterile tweezers.
4. Fill a 10 ml syringe with 10 ml complete DMEM and attach a 27G ½ needle. Holding the femur with the tweezers, insert the needle into one end of the femur and flush approximately 5 ml of DMEM through the bone, collecting the bone marrow in a 50 ml falcon.
5. Turn the femur bone upside down and insert the needle into the other end of the femur. Continue to flush the bone with the remaining DMEM until the bone marrow has been visibly removed.
6. Repeat **steps 2–5** with the second femur and pool the bone marrow from the two femurs.
7. Vigorously resuspend the bone marrow using a 1 ml pipette and centrifuge at $300 \times g$ for 5 min.
8. Discard the supernatant and resuspend the bone marrow using a 1 ml pipette with 1 ml of complete DMEM.
9. Add 15 ml of complete DMEM and 4 ml of L929 conditioned medium (the final concentration of L929 medium is 20 %). Transfer 10 ml to two 10 cm tissue culture plates and incubate at 37 °C, 5 % CO_2 in a humidified incubator.
10. On day 3, remove the medium and replace with 8 ml complete DMEM and 2 ml L929 conditioned medium.
11. On day 6, check the cells under the microscope to ensure cells look differentiated. The 10 cm plates should be almost ~95 % confluent. If not, they can be left for another day.
12. Remove the medium, wash cells with 5 ml sterile DPBS and remove.
13. Add 1 ml of TrypLE™, place the plates back in the incubator for 5–8 min until cells look partially detached (*see* **Note 9**).
14. Due to the adherent nature of macrophages, use a cell scraper to gently remove any remaining adherent cells from the bottom of the plate before adding 9 ml of complete DMEM. Transfer the cells to a 50 ml tube and centrifuge at $300 \times g$ for 5 min.
15. Resuspend the cell pellet in 5 ml complete DMEM and count cells using a hemacytometer. Generate a stock dilution of 4×10^5/ml with complete DMEM, ensuring that the medium also contains 20 % L929 cell-conditioned medium.

16. Seed 5 ml of BMDM cell suspension on a 6 cm plate for TaqMan MicroRNA analysis (*see* Subheading 3.3); seed 500 µl of BMDM cell suspension on a 24-well plate for miRNA and gene expression analysis (*see* Subheading 3.4) and seed 200 µl on a 96-well plate for miRNA modulation experiments (*see* Subheading 3.5). Place the cells at 37 °C, 5 % CO_2 overnight.
17. On day 7, stimulate the cells with 100 ng/ml LPS for desired length of time (*see* **Note 10**).

3.2 RNA Extraction

This method of RNA extraction from eukaryotic cells is a modified protocol derived from the Qiagen RNeasy Mini Kit. It ensures extraction of total RNA thereby allowing analysis of small RNA molecules such as miRNAs as well as allowing analysis of mRNA expression from the same sample (*see* **Note 11**). All steps should be carried out in the fume hood until β-mercaptoethanol has been completely removed from cell lysates. All reagents are supplied with the Qiagen RNeasy Mini Kit unless otherwise listed in Subheading 2.2.

1. Prepare cell lysis buffer (supplied as RLT buffer) by adding 10 µl of β-mercaptoethanol per 1 ml of RLT buffer in a fume hood.
2. Lyse cells in 600 µl of RLT buffer (containing β-mercaptoethanol) for 10 cm and 6 cm plates or 350 µl for cells plated on 24- or 96-well plates. Gently pipette the buffer over the cells a number of times, whilst gently scraping the cells with the end of the pipette tip. Sometimes a cell scraper is required for larger plates. Transfer lysates to a 1.5 ml micro-centrifuge tube, proceed to **step 3** immediately or store at –80 °C indefinitely.
3. Pipette 100 % EtOH to 1.5× volume of cell lysate (i.e., 525 µl of EtOH if cells are lysed in 350 µl of lysis buffer, or 900 µl EtOH if lysed in 600 µl). Ensure thorough mixing of EtOH by pipetting (do not vortex).
4. Add 650–700 µl of cell lysate to Qiagen column provided (column has a maximum volume limit of 700 µl and is supplied within a collection tube).
5. Centrifuge column at 10,000×*g* for 15 s at room temperature.
6. Discard the eluted liquid in the collection tube. The RNA is contained within the column.
7. If there is remainder lysate from **step 4** that did not fit into the column's maximum volume limit, add it now and repeat **steps 5** and **6**.
8. Add 500 µl of RPE wash buffer to the column.

9. Centrifuge column at 10,000 × *g* for 15 s.
10. Repeat washing **steps 8** and **9** and place the column in a new collection tube.
11. Centrifuge column at 10,000 × *g* for 2 min, to ensure any remaining EtOH will be removed and eluted.
12. Carefully place column into a new microcentrifuge tube.
13. Pipette 30 μl of DNA/RNase-free H_2O to the middle of the column being careful not to touch the membrane.
14. Centrifuge column at 10,000 × *g* for 1 min.
15. The eluate in the microcentrifuge tube contains RNA which should be placed immediately on ice.
16. Nanodrop 1 μl of eluent to determine RNA concentration. Prior to loading sample onto Nanodrop machine, DNA/RNase-free H_2O should be used to clean the sample loading surface area and can also be used as a blank.
17. Once total RNA concentration from samples has been determined, prepare an RNA stock dilution of 100–300 ng/μl for TaqMan MiRNA Array Analysis (*see* Subheading 3.3); 5–10 ng/μl to measure individual miRNA (*see* Subheadings 3.4.1 and 3.4.2), and 5–100 ng/μl to measure gene expression (*see* Subheadings 3.4.3 and 3.4.4). RNA can be stored at −80 °C for 1–2 years before proceeding further.

3.3 TaqMan MicroRNA Array

The TaqMan® MicroRNA Array is an excellent way to efficiently and effectively measure an array of miRNAs in a particular cell type or tissue in response to any stimuli, such as TLR ligands. The array itself is a microfluidic card containing dried TaqMan® primers and probes to enable quantification of up to 384 miRNAs plus controls. The array is sensitive enough to detect miRNAs from a starting total RNA input of 1–1000 ng. However an extra pre-amplification step is required if the starting RNA input is below 350 ng. The following protocol is used for RNA without the pre-amplification step.

In brief, RNA is first synthesized to single-stranded cDNA using the MegaPlex™ RT primers, after which the cDNA is combined with TaqMan® Universal Master Mix and loaded onto the microfluidic cards. The entire procedure including analysis is less than 6 h. It is important before you start, as with any array experimental design, that the cells are responsive to your chosen stimuli. It is also worth removing a small aliquot of RNA (20 ng) to assess any confirmed inducible miRNAs as outlined in Subheadings 3.4.1 and 3.4.2 before proceeding.

3.3.1 Reverse Transcription

1. Thaw on ice the RNA samples prepared at a stock concentration of 100–300 ng/μl from **step 17**, Subheading 3.2.

Table 1
The reagents and volumes required to generate a 4.5 μl RT reaction mix for the reverse transcription stage of the array (*see* Subheading 3.3.1)

Reagent	Volume (μl)
Megaplex RT primers	0.8
dNTP (100 mM)	0.2
RT enzyme	1.5
10× buffer	0.8
$MgCl_2$ (25 mM)	0.9
RNase inhibitor (200 U/μl)	0.1
H_2O (DNA/RNase free)	0.2
Total volume	4.5

These volumes can be multiplied by the number of samples you have (+1 for pipetting error) to create an RT reaction master mix

2. Thaw on ice all the reagents from the TaqMan® MicroRNA Reverse Transcription Kit and the Megaplex™ RT primers. Briefly vortex and microcentrifuge dNTPs, 10× buffer, and Megaplex™ RT primers.
3. Using thawed components and the reverse transcriptase enzyme, generate a 4.5 μl reverse transcription (RT) reaction mix per sample as outlined in Table 1.
4. Pipette 4.5 μl of RT reaction mix into individual PCR tubes.
5. Add 3 μl of RNA (so that the total RNA input is in the range of 350–1000 ng) to the 4.5 μl of RT reaction mix (*see* **Note 12**).
6. Incubate the samples on ice for 5 min.
7. Run the samples on a standard PCR machine with the following program: (16 °C for 2 min, 42 °C for 1 min, 50 °C for 1 s) ×40 cycles, 85 °C for 5 min, 4 °C for ∞.
8. The resultant RT product (cDNA) can be kept at −20 °C for 1 week.

3.3.2 TaqMan MicroRNA Array

1. Remove TaqMan® microfluidic plates from their storage at 4 °C and bring to room temperature on your bench.
2. Thaw samples of RT product from **step 8**, Subheading 3.3.1, on ice. Gently flick the tubes and microcentrifuge briefly to collect the sample at the bottom of the tube.
3. Mix the TaqMan® Universal PCR master mix by gently swirling the bottle.

4. For each sample to be analyzed, combine 450 µl of TaqMan Universal PCR master mix, 6 µl of RT product, and 444 µl of DNA/RNase-free H_2O into a clean 1.5 ml microcentrifuge tube. There is now a total volume of 900 µl.
5. Invert the tube six times and microcentrifuge the tubes briefly.
6. Dispense 100 µl of the reaction mix from **step 5** into each port of one microfluidic plate, of which there are eight ports (*see* **Note 13**). Repeat this process for each sample.
7. Centrifuge the microfluidic plates using special Applied Biosystems centrifuge adaptors at $200 \times g$ for 1 min (*see* **Note 14**).
8. Repeat **step 7**.
9. Seal the plate by using the supplied microfluidic plate sealer (*see* **Note 15**).
10. Ensure the 7900HT system has been set up with the appropriate TaqMan Low Density Array Block (*see* **Note 16**).
11. On the 7900HT System, import the SDS setup file (SDS.txt) located in the CD supplied with the TaqMan® MicroRNA Array.
    (a) Start the SDS v2.2 software.
    (b) In the main menu, select File—New
    (c) In the new document dialog box, select the following from the drop-down menu: Relative Quantification (ΔΔCt) and 384-well TaqMan Low Density Array.
    (d) In the main menu, select File—Import to open the new document.
    (e) In the open dialog box, navigate to the Setup.txt file specific for the array being run and click import.
    (f) Save as an SDS 7900 Template (.sdt) file.
12. Load and run the microfluidic plates using the 384-well TaqMan Low Density Array default thermal-cycling conditions. The run takes approximately 2 h.

3.3.3 *Post-analysis*

1. To review the results, transfer the SDS files from each array into an RQ study (*see* **Note 17**).
2. View the amplification plots, then review the baseline and threshold settings (*see* **Note 18**).
3. To analyze the RQ study, click Analysis—Analyse all. RQ manager automatically calculates the fold changes of individual miRNA targets compared to a reference target (e.g., non-treated/control sample) using the ΔΔCt method. To do this, using the drop-down Endogenous Control Detector, select the same house-keeping gene for each array (typically snoRNA202 or RNAU6) to normalize miRNA targets (ΔCt).

Then using the Calibrator drop-down tab, normalize the arrays to the reference array (ΔΔCt). The results are then represented as fold change which can be exported as a txt.file.

4. The raw CT values can also be exported (File—Export—All wells) and calculated manually on an excel spreadsheet. We have used a method which normalizes the data and plots miRNAs according to their relative abundance in the cell. Any changes in highly abundant miRNAs would thus add weight to their overall contribution to cellular function compared to more lowly abundant miRNAs. Furthermore, plotting data in such a way enabled the quick identification of miRNAs that deviated from any unchanged miRNAs located on the transverse line (*see* Fig. 1). This method has been described previously [15, 16] but in brief is determined using the following filtering:
   (a) miRNAs with Ct values higher than 38 for any of the individual arrays are not analyzed.
   (b) Data is normalized to the snoRNA202 probe present on each array (giving ΔCt values).
   (c) The relative level of each miRNA compared to the most abundant RNA molecule (e.g., RNAU6) (ΔΔCt values) is inferred using $2^{(-\Delta\Delta Ct)}$ and plotted accordingly (*see* Fig. 1).

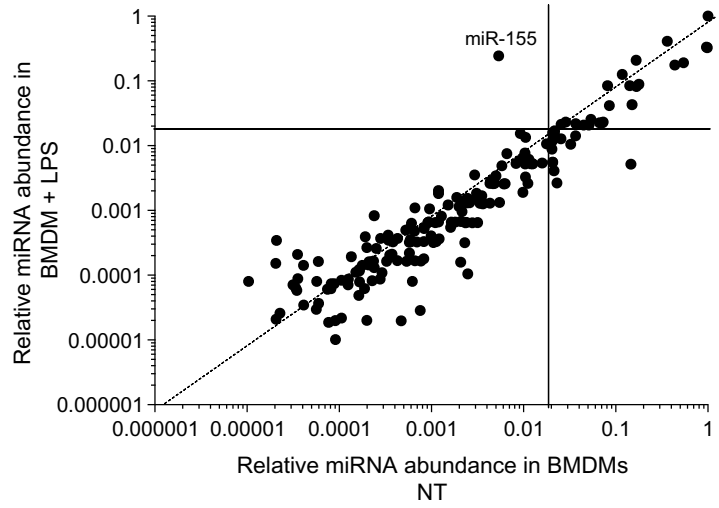

Fig. 1 TaqMan miRNA array performed in BMDMs stimulated with LPS (100 ng/ml). Data was normalized to house-keeping snoRNA202 expression and the relative level of each miRNA was compared to the most abundant miRNA (RNAU6). Data was plotted to demonstrate changes in relative abundance by comparing nontreated (NT) v LPS. Deviation from the transverse line indicates induced/repressed miRNAs. miRNAs located in the upper quadrants signify high abundance. miR-155 falls into both these categories in LPS-stimulated BMDMs

3.4 RT-PCR

Here, we outline protocols to measure individual miRNAs and gene expression from the same sample. These protocols have been modified from the manufacturer's protocols in that the reaction volumes have been reduced and/or altered to increase reagent longevity and save costs. All steps during the RT-PCR protocol should be carried out on ice where possible.

3.4.1 miRNA Reverse Transcription

1. Thaw on ice RNA samples prepared at a stock concentration of 5–10 ng/μl from **step 17**, Subheading 3.2.
2. Thaw on ice all the reagents from the TaqMan® MicroRNA Reverse Transcription Kit and the TaqMan® Primer from the TaqMan® MiRNA Assay Kit. Briefly vortex and microcentrifuge dNTPs, 10× buffer, and TaqMan® MiRNA Primers.
3. In a microcentrifuge tube, prepare an RT reaction master mix as outlined in Table 2 comprising dNTP, 10× buffer, RNase inhibitor, RT enzyme, and desired primers (maximum eight per RT reaction, one of which is a house-keeping miRNA such as snoRNA202 or RNAU6). If there are multiple samples, multiply these volumes by the sample number (+2 for pipetting error) (*see* **Note 19**).
4. Pipette 3 μl of RNA samples into PCR strip tubes (*see* **Note 20**).
5. Add 12 μl of RT reaction master mix to each RNA sample and mix gently with a quick flick.
6. Microcentrifuge samples at a low speed for no longer than 5 s to ensure all liquid is gravitated down to the bottom of the PCR tubes.
7. Run the samples on a PCR machine using the following program: 16 °C for 30 min, 42 °C for 30 min, 85 °C for 5 min, and 15 °C for ∞.
8. Samples may be kept overnight in PCR machine at a holding temperature of 15 °C, stored at 4 °C for 1 week, or stored at −20 °C for up to 1 year before proceeding to Subheading 3.4.2 (*see* **Note 21**).

3.4.2 miRNA RT-PCR

1. Thaw the cDNA samples from **step 8**, Subheading 3.3.1, and keep on ice.
2. Prepare individual master mixes for each miRNA intended to be detected. Each master mix comprises 2× TaqMan Universal Master Mix, 20× probe, and DNA/RNase-free H_2O, made up according to the volumes outlined in Table 3. Each sample must be run in technical duplicates for each miRNA being assessed.
3. Vortex each master mix to ensure all reagents are thoroughly mixed.

Table 2
The reagents and volumes required to generate a 12 μl RT reaction mix for individual miRNA analysis (*see* Subheading 3.4.1)

Reagent	Volume (μl)
dNTP	0.125
10× buffer	1.5
RNase inhibitor	0.18
RT enzyme	1.0
TaqMan primer (5×)	[a]0.375 (per each primer)
H_2O (DNA/RNase free)	[b]Dependent on primer number
Total volume	12

These volumes should be multiplied by the number of samples you have (+2 for pipetting error) to create an RT reaction master mix

[a]The reaction can allow multiple miRNA primers (maximum 8) to be accommodated in the one reaction mix

[b]The volume of H_2O will depend on the amount of primers included in the reaction mix

Table 3
The reagents and volumes required to generate an RT-PCR reaction mix for individual miRNA analysis

Reagent	Volume (μl)
2× TaqMan Universal Master Mix	10.0
H_2O (DNA/RNase free)	8.0
20× probe	0.66

These volumes incorporate enough mix to measure one miRNA in duplicate as well as allowing extra for pipetting error. These volumes should be multiplied by the number of samples in your experiment to generate a master mix

4. Label the layout of your experiment on a 384- or 96-well RT-PCR plate (*see* **Note 22**).
5. Pipette 8.9 μl of each master mix to appropriate wells (e.g., If there are ten samples and two probes, each master mix would be pipetted into 20 wells (technical duplicates) resulting in a total of 40 wells being used (two probes) in the 384- or 96-well plate).
6. Quickly flick the cDNA samples and microcentrifuge briefly to collect the sample at the bottom of the tube.

7. Pipette 1 μl of each cDNA sample into appropriate wells. 2 μl of each cDNA sample should be used per probe due to duplicates (*see* **Note 23**).
8. Seal the RT-PCR plate with an optical adhesive film. Once the film is sufficiently applied (using applicator provided), tear off perforated edges.
9. Centrifuge the RT-PCR plate at 200 × *g* for 1 min. This is to ensure there are no droplets trapped at the edge of any wells (the laser within the RT-PCR machine may not identify these drops causing skewed results).
10. On the 7900HT System, start the SDS v2.2 software. In the main menu, select File—New. In the new document dialog box, select the following from the drop-down menu: Absolute Quantification (ΔΔCt) and 384-well format (or 96-well format depending on the plate used) (*see* **Note 24**).
11. On the right hand side of the screen, open the New Detector tab; name each miRNA being evaluated in your experiment. Make sure the FAM tab is also highlighted.
12. On the left hand side of the screen, highlight the wells that contain your samples and label with the appropriate miRNA detector and sample number.
13. Save as an SDS 7900 Template (.sdt) file.
14. Load and run the RT-PCR plate using the standard default thermal-cycling conditions, changing the reaction volume to 10 μl (*see* **Note 25**). The run takes approximately 1 h 20 min.
15. To retrieve data, go to File and Open saved .sdt file. Click analyse data by pressing the green triangle. Export data as a .txt file to a USB stick.
16. The fold change in miRNA expression is calculated on an excel spreadsheet as follows: data is first normalized to a housekeeping gene (ΔCt), followed by normalization to a reference (control/nontreated) sample (ΔΔCt). Fold induction is then calculated using $2^{-\Delta\Delta Ct}$ method as follows:

$$\mathrm{Ct}_{\mathrm{sample}} - \mathrm{Ct}_{\mathrm{house-keeping\ miRNA}} = \Delta\mathrm{Ct}_{\mathrm{sample}}$$
$$\Delta\mathrm{Ct}_{\mathrm{target\ sample}} - \Delta\mathrm{Ct}_{\mathrm{reference\ sample}} = \Delta\Delta\mathrm{Ct}$$
$$\mathrm{Fold\ Induction} = 2^{-\Delta\Delta\mathrm{Ct}}$$

3.4.3 Gene Expression Reverse Transcription

1. Thaw on ice RNA samples prepared at a stock concentration of 5–100 ng/μl from **step 17**, Subheading 3.2 (*see* **Note 26**).
2. Thaw on ice all the reagents from the TaqMan® cDNA Reverse Transcription Kit. Briefly vortex and microcentrifuge dNTPs, 10× buffer, and random primers.

Table 4
The reagents and volumes required to generate a 12 μl RT reaction mix for gene expression analysis (*see* Subheading 3.4.3)

Reagent	Volume (μl)
dNTP	0.8
10× buffer	2
RNase inhibitor	0.2
RT enzyme	1.0
Random primers	2
H_2O (DNA/RNase free)	6.5
Total volume	12

These volumes should be multiplied by the number of samples you have (+2 for pipetting error) to create an RT reaction master mix

3. Prepare an RT reaction master mix as outlined in Table 4 comprising dNTP, 10× buffer, RNase inhibitor, RT enzyme, and random primers in a microcentrifuge tube. If there are multiple samples, multiply these volumes by the sample number (+2 for pipetting error).
4. Pipette 8 μl of RNA samples into PCR tubes (*see* **Note 20**).
5. Add 12 μl of RT master mix to each RNA sample and mix gently with a quick flick.
6. Microcentrifuge samples at a low speed for no longer than 5 s to ensure all liquid is gravitated down to the bottom of the PCR tubes.
7. Run the samples on a PCR machine using the following program: 25 °C for 10 min, 37 °C for 120 min, 85 °C for 5 min, and 15 °C for ∞.
8. Samples may be kept overnight in PCR machine at a holding temperature of 15 °C, stored at 4 °C for 1 week, or stored at −20 °C for up to 1 year before proceeding to Subheading 3.4.4 (*see* **Note 21**).

3.4.4 Gene Expression RT-PCR

1. Thaw on ice the cDNA samples from **step 8**, Subheading 3.4.3.
2. Prepare individual master mixes for each gene intended to be detected, including a master mix for one house-keeping gene such as GAPDH or 18S. Each master mix comprises 2× SYBR Green Master Mix, forward and reverse primers for your gene of interest, and DNA/RNase-free H_2O, made up according to

Table 5
The reagents and volumes required to generate an RT-PCR reaction mix for gene expression analysis

Reagent	Volume (μl)
2× SYBR Green Master Mix	5
2 μM Forward Primer[a]	0.5
2 μM Reverse Primer[a]	0.5
H_2O (DNA/RNase free)	2

These volumes should be multiplied by the number of samples you have (+2 for pipetting error)

[a]Primer for your gene of interest

the volumes outlined in Table 5. Each sample must be run in technical duplicates for each gene that is being assessed.

3. Vortex each master mix to ensure all reagents are thoroughly mixed.
4. Label the layout of your experiment on a 384- or 96-well RT-PCR plate (*see* **Note 22**).
5. Pipette 8 μl of each master mix to the appropriate wells.
6. Quickly flick the cDNA samples and microcentrifuge briefly to collect the sample at the bottom of the tube.
7. Pipette 2 μl of each cDNA sample into appropriate wells. 4 μl of each cDNA sample should be used per probe due to duplicates (*see* **Notes 23** and **27**).
8. Seal the RT-PCR plate with an optical adhesive film. Once the film is sufficiently applied (using applicator provided), tear off perforated edges.
9. Centrifuge the RT-PCR plate at 200 × *g* for 1 min.
10. On the 7900HT System, start the SDS v2.2 software. In the main menu, select File—New. In the new document dialog box, select the following from the drop-down menu: Absolute Quantification (ΔΔCt) and 384-well format (or 96-well format depending on the plate used) (*see* **Note 25**).
11. On the right hand side of the screen, open the New Detector tab; name each gene being evaluated in your experiment. Make sure the SYBR tab is also highlighted.
12. On the left hand side of the screen, highlight the wells that contain your samples and label with the appropriate gene detector and sample number.
13. Save as an SDS 7900 Template (.sdt) file.

14. Load and run the RT-PCR plate using the standard default thermal-cycling conditions, changing the reaction volume to 10 μl. The run takes approximately 1 h 20 min
15. To retrieve and analyze data, follow **steps 15** and **16**, Subheading 3.4.2.

3.5 MiRNA Modulation

3.5.1 Basic Transfection

1. Generate a stock concentration of 4×10^5 cells/ml in complete DMEM (*see* **Note 28**). Plate 200 μl cells per well in a 96-well flat bottomed plate. This step is best performed in the morning of day 0.
2. Incubate the cells for 6 h at 37 °C, 5 % CO_2 in a humidified tissue culture incubator.
3. Prepare a 4 μM stock solution of miRNA inhibitor and nontargeting control; mimic and nontargeting control in TE buffer (*see* **Note 29**).
4. Pipette 150 μl of Opti-MEM in a microcentrifuge tube and add 1.35 μl of Lipofectamine® 2000 (generate four separate mixes if you are testing inhibitor, mimic, and their corresponding controls). Incubate at room temperature for 5 min.
5. Add 1.5 μl of 4 μM inhibitor, mimic, and control oligos to the individual mixes prepared in **step 4** (the final concentration of oligo is now 40 nM). Incubate at room temperature for up to 20 min.
6. In the meantime, remove the medium from cells in the 96-well plate. Replace with 150 μl fresh DMEM plus 10 % FCS (minus antibiotics).
7. Add 50 μl of Lipofectamine/oligo mix to three wells of the 96-well plate, so that there are three biological triplicates per oligo condition (the final concentration of oligo is now 10 nM).
8. Leave the cells to rest overnight at 37 °C, 5 % CO_2.
9. Stimulate the cells with LPS or other TLR ligands for any desired length of time.
10. Supernatants can be collected and analyzed by ELISA for cytokine expression; and/or the cells can be lysed in 350 μl RLT buffer, RNA extracted and analyzed for miRNA and gene expression as outlined in Subheading 3.4.

3.5.2 Luciferase Assay

The following method investigates the effect of miRNA inhibitors and mimics on their target gene via Luciferase assay. This is a useful method to confirm miRNA targeting to your gene of interest. The 3′UTR of your gene of interest is first cloned into the pMIR-REPORT Vector according to the manufacturer's instructions and transfected according to the following method. Easily transfectable cells are best used for this protocol; we typically use HEK293 or

variants of HEK293 cells. This protocol should be started as early as possible in the morning of day 0.

1. Mix 200 ng of DNA (150 ng pMIR-REPORT plasmid containing the 3′UTR from your gene of interest and 50 ng pRL-Renilla control) in 50 μl Opti-MEM in a microcentrifuge tube. This step is duplicated if you are testing both miRNA inhibitor and mimic.
2. Mix 0.6 μl Lipofectamine® 2000 into 50 μl Opti-MEM and keep at room temperature for 5 min.
3. Combine mixes from **steps 1** and **2**. Leave at room temperature for up to 20 min.
4. In the meantime, split HEK293 cells, count, and resuspend as a 4×10^5/ml stock concentration in DMEM plus 10 % FCS (minus antibiotics).
5. Pipette each mix generated from **step 3** onto one well of a 6-well plate.
6. Add 2 ml of HEK293 cells and place in at 37 °C, 5 % CO_2 for 6 h.
7. After 6 h, cells from each 6 well are replated onto 12 wells of a 96-well plate. To do this, remove the medium from each 6 well, gently wash cells in 1 ml of DPBS and remove. Add 200 μl TrypLE™ and incubate at 37 °C for 5 min until cells are visibly detached. Add 1.8 ml of DMEM plus 10 % FCS (minus antibiotics) and gently resuspend. Plate 150 μl of cells into 12 wells of 96-well plate.
8. Triplicate wells are transfected with a concentration series so that the final concentration of inhibitor and/or mimic transfected into each well is 0, 1, 5, and 10 nM. A total of 10 nM of oligo must always be transfected into each well. Thus to generate 1 nM miRNA inhibitor and/or mimic oligo, 9 nM of corresponding control oligo must be added to make up the difference. Generate dilutions of oligo from 4 μM stocks as outlined in Table 6.
9. Pipette 150 μl of Opti-MEM into four microcentrifuge tubes and add 1.35 μl of Lipofectamine® 2000. Duplicate this step if testing both miRNA inhibitor and mimic. Incubate at room temperature for 5 min.
10. Add 1.5 μl from each oligo dilution mix prepared in **step 8** into Lipofectamine mixes generated in **step 9**. Incubate at room temperature for up to 20 min.
11. Add 50 μl of each Lipofectamine/oligo mix to three wells of pMIR-REPORT transfected cells so that there are three biological replicates per oligo concentration (0, 1, 5, and 10 nM).

Table 6
To generate a dilution series so that the final concentration of inhibitor/mimic oligo is 0, 1, 5, 10 nM; four mixes must be prepared according to the tabled volumes

Mix number	Inhibitor/mimic oligo (4 μM)	Control oligo (4 μM)	Final inhibitor concentration on cells
1.	0 μl	1.5 μl	0 nM
2.	0.15 μl	1.35 μl	1 nM
3.	0.75 μl	0.75 μl	5 nM
4.	1.5 μl	0 μl	10 nM

These volumes are sufficient to transfect triplicate wells

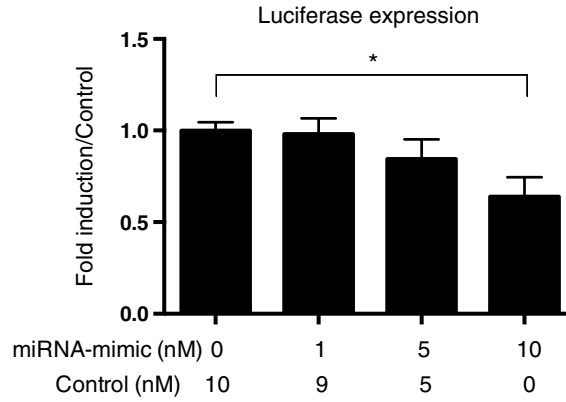

Fig. 2 An example of Luciferase expression in HEK293 cells transfected with various concentrations of miRNA mimic. As the concentration of miRNA mimic increases, Luciferase expression is destabilized. Thus confirming the presence of miRNA binding sites within the cloned 3′UTR of the mRNA in question

12. After 24–36 h, cells are lysed and analyzed for dual Luciferase and Renilla expression according to the manufacturer's instructions.
13. Luciferase expression is normalized to Renilla expression and represented as fold change using control oligo (10 nM) as reference (*see* Fig. 2).

4 Notes

1. There are different Megaplex™ Primer Pools. In general, there are usually two pools of primers per species, Pool A and Pool B, respectively. Pool A comprises miRNAs on the sense strand, whereas Pool B comprises less common miRNAs on the anti-sense strand, often denoted as miRNA*.

2. Be careful that your TaqMan® Array corresponds to the species and Megaplex™ primer pool from **item 2,** Subheading 2.2.
3. It doesn't matter what type or size of PCR tube you use as long it is compatible with your PCR machine.
4. These components are typically available within a gene expression facility.
5. Applied Biosystems uses a technology specific for the detection of 22 nucleotide miRNA molecules. In essence, the primer creates a target specific stem-loop structure by extending the 3′ end of the miRNA during the reverse transcription step. The resultant product is thus longer and more amenable to RT-PCR using the FAM-labeled specific miRNA probe.
6. We have designed primers via the following method:
   (a) Obtain the mRNA sequence for your gene of interest from PubMed.
   (b) Locate the CDS sequence from the mRNA and import in FASTA format into BLAT Search Genome, a program which highlights exon junctions.
   (c) Open Primer3 (v.0.4.0) and insert the CDS sequence in FASTA format.
   (d) Select the top scoring primers ensuring that the product will be approximately 200 bp and crosses an exon junction.
   (e) Using already generated cDNA, test your primers efficiency at final concentrations of 200, 400, and 600 nM in an RT-PCR reaction. Generate a standard curve and calculate the slope of your curve. Using the following calculation: $10\text{^}(-1/\text{slope}) - 1 \times 100$, you can calculate the percentage efficiency of your primers. If they fall between the range of 95 and 110 %, they are good to use.
   (f) It is also essential to perform a dissociation curve at the end of the RT-PCR program. Your primers should generate a single peak, where all samples tested should overlay each other. Multiple peaks indicate the primers are amplifying more than one product and should be discarded.
7. Many companies (e.g., Applied Biosystems, Invitrogen) as well as in-house gene expression facilities supply SYBR Green Master mix. All were found to be functioning with equal capabilities.
8. All synthetic oligos are custom made by Integrated DNA Technologies. The miR-155 inhibitor and nontargeting control are synthesized according to the following sequences and as described in [18]:

   miR-155inhibitor:5′AzCCCCUAUCACGAUUAGCAUUAz,

   Control: 5′ GzCGUAUUAUAGCCGAUUAACGzA;

where "z" denotes ZEN groups, a modification which enhances potency at low nanomolar concentrations [19]. The miR-155 mimic and nontargeting control (an RNA duplex targeting human *lamin A/C*) are generated by annealing sense and antisense strands synthesized according to the following sequences and as described in [20]:

miR-155-Sense: 5′ CCCUAUCACAAUUAGCAUUAAUU,

miR-155-Antisense: 5′ UUAAUGCUAAUUGUGAUAGG GGU;

Control-Sense: 5′CUGGACUUCCAGAAGAACAdTdT;

Control-Antisense: 5′UGUUCUUCUGGAAGUCCAGdTdT.

Annealing is performed by incubating the complementary single-stranded RNAs at 92 °C for 2 min and leaving them for 30 min at room temperature.

9. Differentiated macrophages are notoriously difficult to detach using trypsin reagent alone. Cell scraping is also advised.
10. A 24-h time course such as 0, 4, 8, and 24 h is advised. miRNA induction can be rapid or slow depending on the miRNA and type of TLR ligand chosen. Most miRNAs are fully induced by 24 h.
11. Most RNA extraction kits include wash steps to remove small RNAs. However in our experience, due to the stability of miRNAs, miRNAs are still present in most RNA samples regardless of the type of kit used. Thus it is worth measuring miRNAs in any existing RNA samples you may have stored before buying specific kits for miRNA RNA extraction.
12. We have used both 300 and 800 ng as total RNA input for two separate arrays, both worked sufficiently.
13. Be careful not to expel the remaining liquid from the pipette tip as this will create an air bubble in the ports.
14. Make sure to place the plates so that the ports are facing towards you.
15. Place the plate sealer so that the handle is closest to you. Place the microfluidic card in the appropriate grove, push the handle away from you; remove the card and return the handle to its start position. *IMPORTANT: remember to remove the card before returning the handle.*
16. This step involves specific training on the 7900HT system and is typically performed by the technician within your gene expression service facility.
17. It is recommended that you analyze the study with automatic baseline and manual CT set to 0.2.
18. It is extremely important that the same threshold setting is used across all samples or arrays within a given study.

19. As multiple primers can be added to this master mix (maximum 8), the H_2O volume should be determined once all other reagents have been accounted for, e.g., if there is a master mix prepared for 8 samples (+2 for pipetting error) with 2 primers: (10) 0.125 + (10) 1.5 + (10) 0.18 + (10) 1.0 + [10 (0.375 × 2)] = total volume of all other reagents. Required total master mix volume of 120 μl (12 μl × 10 samples): total volume of reagents – 120 μl = volume of H_2O.
20. We have found using 8× strip tubes to be the most useful PCR tubes for assessing multiple samples and convenient storage.
21. We have experienced significant degradation and destabilization of cDNA if kept longer than 1 year. It is better to repeat **steps 1–7**, Subheading 3.4.1, using stored RNA kept at –80 °C rather than reuse stored cDNA for subsequent RT-PCR analysis.
22. The use of a 384- or 96-well RT-PCR plate depends on the block most frequently used by your gene expression facility and/or the amount of samples you have.
23. We have found that using the same pipette tip between duplicates gives tighter replicates. However, it is necessary to change the pipette tip between samples and when moving onto a new master mix to prevent cross-contamination. It is recommended by the manufacturers that RT-PCR is performed in a final 20 μl volume. However we have found a final volume of 10 μl works just as well, thus saving on overall costs.
24. Relative quantification can also be chosen. If this is the case, the final .sdt file must be opened and analyzed using the RQ manager software. We have found that running an absolute quantification and exporting the raw CT values manually gives you better control of your data.
25. When loading the plate, ensure the alignment is correct by using the corner notch on the plate as a guide.
26. We have standardized our gene expression protocol so that we always use the same amount of total input RNA. The typical total amount of input RNA we use is 640 ng (i.e., 8 μl of 80 ng/μl stock RNA equates to 640 ng in total). However, this can vary and RT-PCR is still successful within the range of 40–800 ng total input RNA. It will depend on various elements such as the starting concentration of original input RNA, RNA purity, cell type, and the primer efficiency.
27. Depending on the concentration of input RNA, cDNA can be further diluted two, five, or tenfold depending on which gene is being amplified. E.g., most house-keeping genes are abundantly expressed and dilution is necessary. As a rule-of-thumb, Ct values should be kept within the 20–30 range for best analysis.

28. Seeding cells at 4×10^5 cells/ml works well for BMDM, Raw264.7 and HEK293.
29. miRNA inhibitors are single-stranded oligos whereas miRNA mimics are double stranded; thus two separate nontargeting control oligos are required for the inhibitor and mimic as described in **Note 8**.

Acknowledgements

The authors would like to acknowledge the Health Research Board (HRB) Ireland together with Marie Curie for funding the project from which the experiments included in this chapter are derived. The authors would also like to acknowledge their current funding from the National Health and Medical Research Council (NHMRC) Australia. The authors would like to thank Charlotte Nejad for her thorough editing of this manuscript.

References

1. Liew FY, Xu D, Brint EK, O'Neill LA (2005) Negative regulation of toll-like receptor-mediated immune responses. Nat Rev Immunol 5:446–458
2. Cook DN, Pisetsky DS, Schwartz DA (2004) Toll-like receptors in the pathogenesis of human disease. Nat Immunol 5:975–979
3. McCoy CE (2012) Alternative regulatory mechanisms of TLR signalling: nucleic acid sensors and antiviral immunity. In: Sambhara S, Fujita T (eds) Nucleic acid sensors and antiviral immunity. Landes Bioscience, Austin, TX, pp 58–65
4. Guo H, Ingolia NT, Weissman JS, Bartel DP (2010) Mammalian microRNAs predominantly act to decrease target mRNA levels. Nature 466:835–840
5. Grimson A, Farh KK, Johnston WK, Garrett-Engele P, Lim LP et al (2007) MicroRNA targeting specificity in mammals: determinants beyond seed pairing. Mol Cell 27:91–105
6. O'Neill LA, Sheedy FJ, McCoy CE (2011) MicroRNAs: the fine-tuners of Toll-like receptor signalling. Nat Rev Immunol 11:163–175
7. Rodriguez A, Vigorito E, Clare S, Warren MV, Couttet P et al (2007) Requirement of bic/microRNA-155 for normal immune function. Science 316:608–611
8. Thai TH, Calado DP, Casola S, Ansel KM, Xiao C et al (2007) Regulation of the germinal center response by microRNA-155. Science 316:604–608
9. O'Connell RM, Kahn D, Gibson WS, Round JL, Scholz RL et al (2010) MicroRNA-155 promotes autoimmune inflammation by enhancing inflammatory T cell development. Immunity 33:607–619
10. Bluml S, Bonelli M, Niederreiter B, Puchner A, Mayr G et al (2011) Essential role of microRNA-155 in the pathogenesis of autoimmune arthritis in mice. Arthritis Rheum 63:1281–1288
11. Oertli M, Engler DB, Kohler E, Koch M, Meyer TF et al (2011) MicroRNA-155 is essential for the T cell-mediated control of Helicobacter pylori infection and for the induction of chronic Gastritis and Colitis. J Immunol 187:3578–3586
12. Sarasin-Filipowicz M, Krol J, Markiewicz I, Heim MH, Filipowicz W (2009) Decreased levels of microRNA miR-122 in individuals with hepatitis C responding poorly to interferon therapy. Nat Med 15:31–33
13. Liu Z, Sall A, Yang D (2008) MicroRNA: an emerging therapeutic target and intervention tool. Int J Mol Sci 9:978–999
14. Lanford RE, Hildebrandt-Eriksen ES, Petri A, Persson R, Lindow M et al (2010) Therapeutic silencing of microRNA-122 in primates with chronic hepatitis C virus infection. Science 327:198–201
15. Fairfax KA, Gantier MP, Mackay F, Williams BR, McCoy CE (2015) IL-10 regulates Aicda expression through miR-155. J Leukoc Biol 97:71–78

16. Gantier MP, Stunden HJ, McCoy CE, Behlke MA, Wang D et al (2012) A miR-19 regulon that controls NF-kappaB signaling. Nucleic Acids Res 40:8048–8058
17. Weischenfelt J, Porse J (2008) Bone marrow-derived macrophages (BMM): isolation and application. Cold Spring Harb Protoc 3:1–6
18. Sarvestani ST, Stunden HJ, Behlke MA, Forster SC, McCoy CE et al (2015) Sequence-dependent off-target inhibition of TLR7/8 sensing by synthetic microRNA inhibitors. Nucleic Acids Res 43:1177–1188
19. Lennox KA, Owczarzy R, Thomas DM, Walder JA, Behlke MA (2013) Improved performance of anti-miRNA oligonucleotides using a novel non-nucleotide modifier. Mol Ther Nucleic Acids 2:e117
20. Gantier MP, McCoy CE, Rusinova I, Saulep D, Wang D et al (2011) Analysis of microRNA turnover in mammalian cells following Dicer1 ablation. Nucleic Acids Res 39:5692–5703

Chapter 12

Determining the Function of Long Noncoding RNA in Innate Immunity

Susan Carpenter

Abstract

The advent of deep sequencing technologies has provided us with an unprecedented view of the human genome. Over 85 % of the genome is actively transcribed, yet we do not know the function of the vast majority of these RNA transcripts. Long noncoding RNAs (lncRNA) represent the largest group of RNA genes transcribed in the cell and currently there is limited experimental data supporting the functions of a very small proportion of these transcripts. lncRNA are expressed in a highly cell type specific manner and our interests involve understanding the role they play in innate immune signaling networks. In this chapter I will outline the approach we took to attempt to uncover the role for lncRNA in innate immune cells. Two of the main techniques required to study lncRNA are RNA-seq and loss of function analysis. This allows us to first identify all lncRNA in a cell type of choice and then try to determine the functional significance of these transcripts. This approach has been successful for us to date in identifying *lincRNA-Cox2* as a highly inflammatory inducible lncRNA that is responsible for activation and repression of distinct immune genes.

Key words Long noncoding RNA (lncRNA), Innate immunity, TLR signaling, Inflammation, RNA sequencing, shRNA

1 Introduction

Deep sequencing has led to a new era in genomics research. Currently there are consortium-wide efforts (Encode, Fantom, 1000 genomes project, epigenetics roadmap, etc.) devoted to trying to understand every regulatory element within the genome. One of the big surprises to emerge from the sequencing of the human genome is that less than 3 % of the genome codes for protein, while over 85 % is actively transcribed [1]. A major outstanding question is whether this widespread transcription has functional roles in fundamental cellular processes. Long noncoding RNAs (lncRNA) represent an exciting class of noncoding RNA that makes up the largest group of RNA produced from the genome [2]. LncRNA are defined as transcripts greater then 200 nucleotide in length lacking protein coding exons.

Claire E. McCoy (ed.), *Toll-Like Receptors: Practice and Methods*, Methods in Molecular Biology, vol. 1390,
DOI 10.1007/978-1-4939-3335-8_12,

The function of the majority of lncRNA remains unknown; hence this class of RNAs greatly requires further investigation.

lncRNA are expressed in a highly cell type specific manner and in general many lncRNA are expressed at lower levels in comparison to protein coding genes [2, 3]. Therefore in order to determine if lncRNA are functional in your cell type of choice it is first necessary to carry out RNA sequencing under the conditions you are interested in investigating. We carried out whole transcriptome analysis of an immortalized murine bone marrow derived macrophage cell line (iBMDM) at basal levels (unstimulated) and following inflammatory stimulation with a TLR1/2 ligand (Pam3CSK4) [4]. This enabled us to determine the differential expression of lncRNA at both resting states and following stimulation. We identified 62 lncRNA that showed a greater than twofold increase in expression following stimulation. We focused on *lincRNA-Cox2*, which was one of the most highly upregulated lncRNA following TLR2 activation. The approach we took to try and determine the functional role for *lincRNA-Cox2* was to knock it down using shRNA in our murine iBMDM cell line, followed by deep sequencing to obtain a global overview of genes that could be regulated by *lincRNA-Cox2*. This has been a successful approach and I believe these two techniques are critical to studying lncRNA in any biological context.

2 Materials

2.1 RNA-Seq

2.1.1 RNA Preparation

1. Bone marrow derived macrophage cell line (iBMDM) (*see* **Note 1**).
2. Dulbecco's Modified Eagle Medium (DMEM) supplemented with 10 % Fetal Bovine Serum (FBS) and antibiotics (PenStrep).
3. 10 cm tissue culture dishes.
4. Trypsin EDTA.
5. Sterile 1× phosphate-buffered saline (PBS).
6. Mercaptoethanol.
7. RNA extraction kit, such as the RNeasy kit (Qiagen).
8. RNase Free DNase kit (Qiagen).
9. iScript Select cDNA synthesis kit (Bio-Rad).

2.1.2 Library Preparation

1. mRNA sample preparation kit (Illumina).
2. RNase free eppendorfs.
3. 1× Tris-acetate EDTA (TAE).
4. 70 % ETOH.
5. 100 % ETOH.

6. 3 M NaOAc, pH 5.2.
7. 6× DNA loading dye (New England Biolabs).
8. Agarose.
9. MinElute PCR purification kit (Qiagen).
10. Qiaquick Gel Extraction kit (Qiagen).
11. SuperScript II Reverse Transcriptase with 100 mM DTT and 5× First Strand Buffer (Invitrogen).
12. Magnetic stand.
13. Heat Block.

2.1.3 Data Analysis

Download the following files and software:

1. SRA toolkit (http://ftp-trace.ncbi.nlm.nih.gov/sra/sdk/2.4.2-1/sratoolkit.2.4.2-ubuntu64.tar.gz).
2. Cufflinks (http://cufflinks.cbcb.umd.edu/downloads/cufflinks-2.2.1.Linux_x86_64.tar.gz).
3. Bowtie (http://sourceforge.net/projects/bowtie-bio/files/bowtie2/2.2.4/bowtie2-2.2.4-linux-x86_64.zip/download).
4. Tophat (http://ccb.jhu.edu/software/tophat/downloads/tophat-2.0.13.Linux_x86_64.tar.gz).
5. Human genome (ftp://igenome:G3nom3s4u@ussd-ftp.illumina.com/Homo_sapiens/UCSC/hg19/Homo_sapiens_UCSC_hg19.tar.gz).
6. Murine genome (ftp://ftp.sanger.ac.uk/pub/gencode/Gencode_mouse/release_M3/gencode.vM3.annotation.gtf.gz).

2.2 Loss of Function Experiments

2.2.1 Cloning shRNA

1. Oligos specific to gene of interest forward and reverse (Integrated DNA Technologies).
2. pLKO.1 vector (Addgene).
3. Restriction enzymes: Age1 and EcoR1.
4. T4 DNA ligase.
5. DH5alpha competent cells.
6. Agarose.
7. LB Broth.
8. Ampicillin.
9. HEK293 cell line.
10. DMEM supplemented with 10 % FBS and antibiotics (PenStrep).
11. Viral packaging plasmids pSpax and pMD2 (Addgene).
12. 0.45 μm Filters.
13. 50 ml Conical Tubes.

2.2.2 Testing shRNA

1. iBMDM.
2. DMEM supplemented with 10 % FBS and antibiotics (PenStrep).
3. 10 cm tissue culture dishes.
4. Puromycin.
5. Polybrene (optional, *see* **Note 2**).
6. Genejuice (transfection reagent, Novagen).

3 Methods

3.1 RNA-Seq

3.1.1 Sample Preparation

1. Seed immortalized Bone Marrow Derived Macrophages (iBMDM) in 10 cm dishes at 1×10^6 cells/condition. Approximately one 10 cm dish will provide you with enough RNA for deep sequencing (*see* **Note 3**). For our experiments, two 10 cm dishes were used for control (unstimulated) and two 10 cm dishes were stimulated with 100 nM Pam3CSK4 for 5 h [4].
2. Extract RNA using RNeasy kit.
3. Freeze 5 μg of RNA and store at −80 °C to await library preparation (*see* Subheading 3.1.2).
4. Use approximately 1 μg of RNA to generate cDNA according to the manufacturer's instructions.
5. Analyze cDNA generated from **step 4** by Real-Time PCR to ensure the cells are behaving as expected prior to deep sequencing (*see* Table 1).

3.1.2 Library Preparation

In brief, 5 μg of total RNA (**step 3**, Subheading 3.1.1) is needed to generate a library according to the Illumina mRNA sample preparation kit (*see* **Note 4**). The Illumina preparation kit comes with all the reagents required (exceptions are listed in Subheading 2.1.2) and

Table 1
RT-PCR primers required to test the induction of *lincRNA-Cox2*, *Ptgs2 Il6*, *Rantes*, *and Tnf-α* following Pam3CSK4 stimulation

Gene name	Forward primer 5′–3′	Reverse primer 5′–3′
LincRNA-Cox2	AAGGAAGCTTGGCGTTGTGA	GAGAGGTGAGGAGTCTTATG
GapDH	CCAATGTGTCCGTCGTGGATC	GTTGAAGTCGCAGGAGACAAC
Ptgs2	GCTGTGGGGCAGGAAGTC	TTGGAATAGTTGCTCATCACC
Il6	AACGATGATGCACTTGCAGA	GAGCATTGGAAATTGGGGTA
Tnf-α	CAGTTCTATGGCCCAGACCCT	CGGACTCCGCAAAGTCTAAG
Rantes	GCCCACGTCAAGGAGTATTTC	ACACACTTGGCGGTTCCTTC

includes an excellent protocol layout that is easy to follow. I will briefly outline each step, adding notes to the areas that need special attention. All steps have also been outlined in Fig. 1.

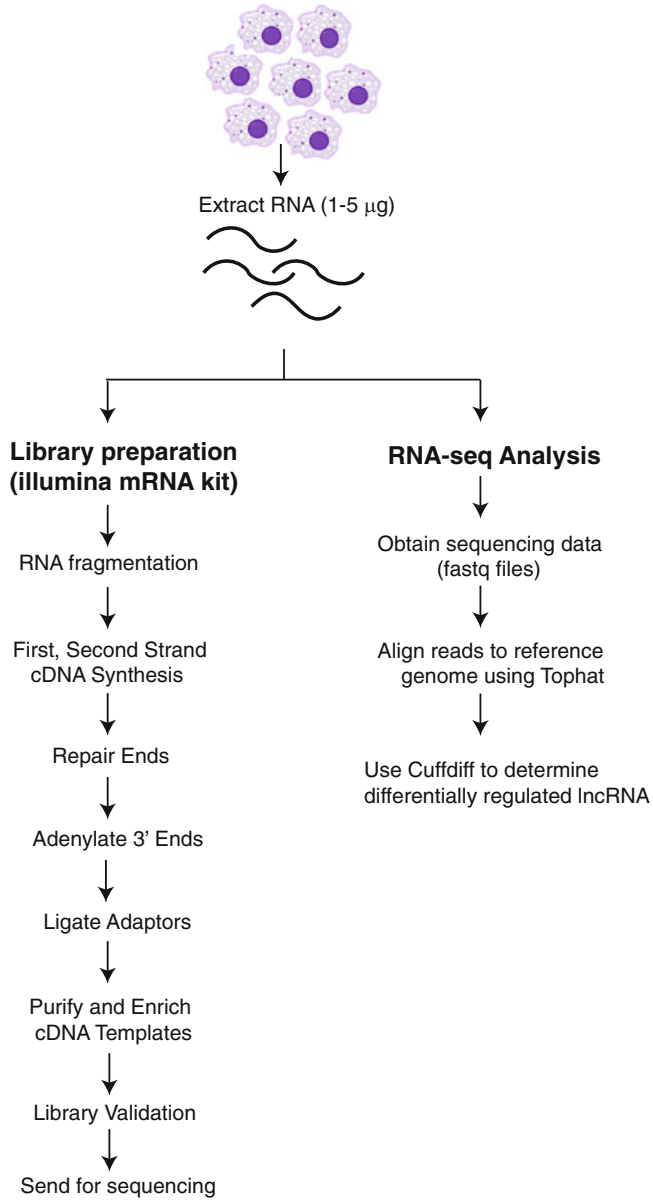

Fig. 1 Workflow to identify differentially regulated lncRNA in Bone Marrow Derived macrophages. RNA is isolated from Bone Marrow Derived Macrophages. The steps for Illumina library preparation are outlined and described in Subheading 3.1.2. In addition the steps required to carry out RNA-seq computational analysis to obtain a list of differentially regulated lncRNA are outlined and described in Subheading 3.1.3

1. Dilute 5 μg total RNA to 50 μl using RNase free water in an RNase free nonstick eppendorf. Place RNA in a heating block at 65 °C for 5 min to disrupt secondary structures and place on ice.
2. Add 15 μl of Oligo dt (magnetic beads) to an RNAse free eppendorf and wash twice with bead buffer. Remove the supernatant each time. After the second wash add 50 μl of bead buffer and 50 μl of RNA from **step 1**.
3. Rotate the tube containing the beads and RNA at room temperature for 5 min. Wash the beads twice with 200 μl of washing buffer and remove the supernatant.
4. Add 50 μl of 10 nM Tris–HCl to the beads and heat at 80 °C in a heating block for 2 min to elute off the polyA RNA from the beads. Immediately place the tube on the magnetic stand and transfer the RNA into a new RNAse free eppendorf containing 50 μl of binding buffer. Do not discard the beads, wash them twice with 200 μl of washing buffer.
5. Place the polyA RNA on a heating block at 65 °C to disrupt the secondary structure. Then place the RNA back into the tube containing the washed beads and rotate at room temperature for 5 min.
6. Place the tube back on the magnetic stand, remove the supernatant, and wash twice with 200 μl of wash buffer, removing the supernatant each time.
7. Add 17 μl of 10 nM Tris–HCl, to the beads and heat at 80 °C in a heating block for 2 min to elute off the RNA from the beads. Immediately place the tube on the magnetic stand and transfer the RNA into a PCR tube. At this point you should have approximately 16 μl of RNA in the PCR tube.
8. *Fragmenting the RNA*. Add 4 μl of 5× fragmentation buffer to the PCR tube containing the 16 μl of RNA from **step 7**. Incubate the tube in a PCR machine at 94 °C for exactly 5 min. Add 2 μl of fragmentation stop solution. Place the tube on ice and then transfer the contents to a new RNAse free nonstick eppendorf.
9. Add 2 μl of 3 M NaOAC, pH 5.2, 2 μl of Glycogen, and 60 μl of 100 % ETOH to the eppendorf from **step 8** and place at −80 °C for 30 min (*see* **Note 5**).
10. Centrifuge the tube at 18,400 rcf in a 4 °C microcentrifuge for 25 min. Carefully remove the ETOH but be careful not to disrupt the RNA pellet (which is colorless and quite difficult to observe).
11. Wash the pellet while trying not to disturb it with 300 μl of 70 % ETOH, centrifuge for 5 min at 18,400 rcf and very carefully remove the ETOH. Allow the pellet to air-dry for 10 min and resuspend in 11.1 μl of RNase Free Water.

12. *Synthesize the first strand of cDNA*. Add 1 μl of random primers to the 11.1 μl of sample from **step 11**. Incubate the sample in the PCR machine at 65 °C for 5 min then place on ice.
13. Set the PCR machine to 25 °C.
14. In a separate PCR tube add the following: 4 μl of 5× First Strand Buffer, 2 μl of 100 nM DTT, 0.4 μl of 25 mM dNTP mix, and 0.5 μl of RNase inhibitor (making a total volume of 6.9 μl). Add the 6.9 μl of the mixture to the PCR tube from **step 12** and mix.
15. Place the PCR tube in the 35 °C PCR machine and leave for 2 min.
16. Add 1 μl of Superscript II to the sample in the PCR tube and place on the following program: 25 °C for 10 min, 42 °C for 50 min, 70 °C for 15 min and hold at 4 °C. Place the tube on ice.
17. *Synthesize the second strand of cDNA*. Add 62.8 μl of ultra pure water to the tube from **step 16**. In addition add 10 μl of GEX Second Strand Buffer and 1.2 μl of 25 mM dNTP mix to the tube. Mix and incubate on ice for 5 min.
18. Add 1 μl RNaseH and 6 μl of DNA Pol 1 to the tube from **step 17**. Mix and incubate at 16 °C in a PCR machine for 2.5 h.
19. Purify the sample using QIAquick PCR purification kit and elute in 50 μl of QIAquick elution buffer.
20. *Perform end repair*. Add the following to a RNAse free nonstick eppendorf: 50 μl of eluted RNA, 27.4 μl of water, 10 μl 10× End Repair Buffer, 1.6 μl of 25 mM dNTP mix, 5 μl T4 DNA polymerase, 1 μl of Klenow DNA polymerase, and 5 μl of T4 PNK. This makes a total volume of 100 μl.
21. Incubate the sample in a heat block at 20 °C for 30 min. Use the QIAquick PCR purification kit to purify the sample and elute in 32 μl of Qiagen EB buffer.
22. *Adenylate 3′ ends*. Prepare the following in an RNAse free nonstick eppendorf: 32 μl of the Eluted RNA from **step 21**, 5 μl of A-Tailing Buffer, 19 μl of 1 mM dATP, and 3 μl of Klenow Exo(3- to 5- exo minus), which brings to a total of 50 μl.
23. Incubate the sample at 37 °C for 30 min and then follow the MinElute PCR purification kit to purify the sample and elute in 23 μl of Qiagen EB buffer.
24. *Ligate the adapters*. Prepare the following in an RNAse free nonstick eppendorf: 23 μl of eluted DNA from **step 23**, 25 μl of 2× Rapid T4 DNA ligase Buffer, 1 μl of PE Adapter oligo Mix, and 1 μl of T4 DNASE Ligase (total volume is 50 μl).

25. Incubate the sample at room temperature for 15 min and follow the MinElute PCR purification kit to purify the sample and elute in 10 μl of Qiagen EB buffer.
26. *Purify the cDNA templates*. Prepare a 2 % agarose gel in 1× TAE buffer. Load 2 μl of 100 bp DNA ladder in the first and third wells. Load the 10 μl of DNA from **step 25** containing 2 μl of 6× DNA loading buffer to the second lane (*see* **Note 6**).
27. Run the gel at 120 V for 60 min (or until the ladder is suitably separated).
28. Excise a band around 250 bp ± 25 bp. Use QIAquick gel extraction kit to purify the sample and elute in 30 μl of Qiagen EB buffer.
29. *Enrich the purified cDNA templates*. Add the following to a PCR tube: 10 μl of 5× Phusion Buffer, 1 μl of PCR Primer PE 1.0, 1 μl PCR Primer OE 2.0, 0.5 μl 25 mM dNTP Mix, 0.5 μl Phusion DNA polymerase, 7 μl of water, and 30 μl of purified ligation mix from **step 28**.
30. *Amplify using the following PCR conditions*: 30 s at 98 °C, 15 cycles of: 10 s at 98 °C, 30 s at 65 °C, and 30 s at 72 °C. 5 min at 72 °C and hold at 4 °C.
31. Use QIAquick PCR purification kit to purify the sample and elute in 30 μl of Qiagen EB buffer.
32. *Library validation*. Run 1 μl of the DNA on an agarose gel to ensure there is a distinct band around 250 bp. Run 1 μl of the sample on an Agilent Technologies Bioanalyzer to check the purity and concentration of your library (*see* **Note 7**).
33. Once samples are sized, quantified, and proofed, they are read on an Illumina High-Seq System as 50*50 single reads for BMDM experiments (*see* **Note 8**) [4].

3.1.3 Data Analysis

An overview of the steps involved in RNA-seq analysis is provided in Fig. 1.

1. RNA-seq 50 bp reads are obtained from the sequencing core as Fastq files (*see* **Note 9**).
2. These reads are aligned to the mouse genome (NCBI137/mm9) using TopHat [5, 6]. Tophat outputs reads as .bam files.
3. Cuffdiff (a component of Cufflinks [7]) can be used to determine differential expression of lncRNA between the aligned reads. For our analysis, annotated lncRNA compiled in Ensembl64 gtf was used as the input annotation file for the program (*see* **Note 10**) [4].
4. Cuffdiff will provide Fragments per kilobase of exon per million mapped reads (FPKM) value for each gene, which will enable the calculation of fold change in gene expression between samples or conditions tested (*see* **Notes 11** and **12**).

5. To visualize the aligned reads upload the .bam files and upload them to IGV (http://www.broadinstitute.org/igv/) (*see* **Note 13**).
6. All raw data from our experiments are available for download from NCBI Gene Expression Omnibus (http://www.ncbi.nlm.nih.gov/geo/) under accession number GSE40978 (*see* **Note 14**).

3.2 Loss of Function Experiments

3.2.1 Cloning shRNA

1. There are a number of very useful programs available for designing shRNA. I used RNAi software developed by Mekentosj (http://nucleobytes.com/index.php/irnai).
2. The general outline for Oligo design is as follows: Forward oligo—5′ CCGG—21 bp sense—CTCGAG—21 bp antisense—TTTTTG 3′; Reverse oligo—5′ AATTCAAAAA—21 bp sense—CTCGAG—21 bp antisense 3′.
3. For RNA interference, three separate shRNA specific to lincRNA-Cox2 were cloned into the plko vector using the oligos detailed in Table 2.
4. There are many options you can use as controls for these experiments. You can clone your own "scrambled version" or there are empty vector (EV) options (*see* **Note 15**).
5. There is an excellent protocol available from Addgene that takes you through each step of the cloning process (http://www.addgene.org/tools/protocols/plko/), which I will describe briefly in the following steps.
6. Resuspend oligos to a concentration of 20 μM. Add 5 μl of Forward, 5 μl of Reverse oligo, 5 μl 10× NEB buffer 2, and 35 μl of sterile water. Incubate for 4 min at 95 °C and allow to cool on the bench for 2 h in order to anneal the oligos.

Table 2
Oligos required for cloning lincRNA-Cox2 into the plko vector

lincRNA-Cox2 shRNA	Forward primer 5′–3′	Reverse primer 5′–3′
shRNA No.1	CCGGAAGAGTAAGATTCTGAA GATCCTCGAGGATCTTCAGAAT CTTACTCTTTTTTTG	AATTCAAAAAAAGAGTAAGATTCTG AAGATCCTCGAGGATCTTCAG AATCTTACTCTT
shRNA No.2	CCGGAAGGAATCCAGCCATCTCT CGCTCGAGCGAGAGATGGCTGG ATTCCTTTTTTTG	AATTCAAAAAAAGGAATCCAGCC ATCTCTCGCTCGAGCGAGAGA TGGCTGGATTCCTT
shRNA No.3	CCGGAACCTAAAGGAGGTTGAC AACCTCGAGGTTGTCAACCTCC TTTAGGTTTTTTTG	AATTCAAAAAAACCTAAAGGAGG TTGACAACCTCGAGGTTGTCAA CCTCCTTTAGGTT

7. Digest Plko vector with Age1 and EcoR1 (to remove the stuffer sequence). Run the DNA on a 1 % DNA gel and cut out the band at 7 kb. Purify using Qiaquick gel extraction kit.
8. In a total reaction mix of 20 μl; ligate 2 μl of the annealed oligos from **step 6**, 20 ng of vector from **step 7** with 1 μl T4 DNA ligase, and 2 μl of ligase buffer overnight at room temperature.
9. Transform 2 μl of the ligation reaction from **step 8** into DH5 alpha cells and grow overnight on ampicillin resistant plates. Mini-prep colonies and send for sequencing to ensure the insert is correct.

3.2.2 *Testing shRNA*

1. Seed HEK293 cells at 1×10^6/ml into 10 cm dishes (containing 10 ml of DMEM).
2. After 24 h, transfect 4 μg of shRNA into HEK293 cells with 3 μg packaging vector pSpax and 1 μg pMD2 using Genejuice according to the manufacturer's instructions. I generally use a ratio of 3 μl Genejuice: 1 μg of DNA.
3. After 48 h, media is removed, centrifuged for 5 min at 290 × *g*, and filter-sterilized using 0.45 μm filter. This media contains un-concentrated virus, which is used to directly transduce immortalized BMDMs using 50 % media to 50 % virus supernatant on your cells. After 48 h positively infected cells are selected using puromycin (3 μg/ml) (*see* **Note 16**).
4. Knockdown of lncRNA can be determined by RT-PCR (Fig. 2).

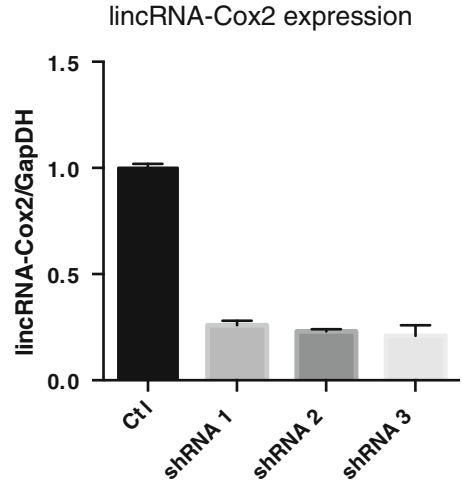

Fig. 2 Knockdown of lincRNA-Cox2 using shRNA. qRT-PCR was carried out on iBMDMs stably expressing lentiviral shRNA specific to lincRNA-Cox2 (shRNA) or a Control shRNA. Expression of *lincRNA-Cox2* was measured and normalized to the house keeping gene, *GapDH*

There are caveats to using shRNA to knockdown lncRNA. shRNA works well at targeting lncRNA that reside or traffic through the cytoplasm. I have encountered difficulties trying to knockdown lncRNA that strictly reside in the nucleus. An alternative approach to using shRNA is to use the newly developed Cas9/Crispr system, which will target the genomic DNA instead of the RNA transcript. I encourage readers to examine the latest publications on Cas9 technology, which is an excellent approach to use for genome editing. Details on vectors and protocols can be obtained at http://www.addgene.org/crispr/zhang/.

4 Notes

1. An immortalized murine bone marrow derived cell line was used for the experiments outlined here. Details can be found in reference [4]. All the techniques described here can be adapted for use in any cell line.
2. Some protocols suggest adding polybrene (1 μg) to your cells to assist in viral entry. I have tried with and without polybrene and I did not observe any difference in uptake of virus by macrophages.
3. As deep sequencing techniques advance the amount of RNA required also changes. At the time I carried out the experiments it was suggested that between 1 and 10 μg of RNA was used. I used two 10 cm dishes and obtained >5 μg of RNA. It is now possible with Illumina kits to use less RNA.
4. It is possible to buy the contents of the Illumina kit separately from different companies (New England Biolabs for example). This approach will be cheaper and you will be able to prepare many more library samples this way. However if you are a complete novice to deep sequencing I could highly recommend using the Illumina kits as they are very easy to follow.
5. At this point (and at **steps 9**, **19**, **21**, **23**, **25**, **28**, and **31**) the protocol can be stopped if necessary and the tube can be stored at −20 °C.
6. Be aware that you require the 100 bp ladder on each side of the sample as you are required to cut out a band that will not be visible under the UV light, you need the ladders as a size guide. Also if you are running multiple libraries, do this on separate gels to avoid contamination.
7. If you are using a core facility to run your sequencing, they often carry out library validation as part of the service.
8. Depending on what you wish to get from your sequencing data, you have the option of carrying out 36 bp or 100 bp reads and these can be single end or paired end. The advantages of

longer reads are that fewer sequences get thrown out during analysis (as it is easier to find unique sequences with longer reads). Another advantage to paired end reading, it can allow you to tell the start and end of your lncRNA sequence which can be very informative. In addition there are kits available from Illumina to do strand-specific sequencing. Since many lncRNA overlap with protein coding genes, strand-specific sequencing can allow you to determine which strand your lncRNA is transcribed from.

9. If you are trying to analyze a data set that has been submitted to GEO, you will need to use the SRA toolkit to convert the SRA files to Fastq files (use command Fastq dump).
10. Ensure you are using the most up to date versions of GTFs for your analysis. You can find them at (http://www.gencodegenes.org/). If you are only interested in looking at differential expression of lncRNA, gencode provides a specific gtf containing murine or human annotated lncRNA.
11. FPKM of 1 generally indicates that there is one copy of the gene in a given cell. This can be a useful cutoff point if you are looking for more abundant transcripts.
12. Make sure to use the most updated versions of all the programs available. The latest version of cufflinks contains a new option cuffquant, when used prior to running cuffdiff provides a file format that allows cuffdiff to complete much faster.
13. Using gencode gtfs for lncRNA only provides information on lncRNA that have already been annotated. Cufflinks can provide also provide data on un-annotated transcripts [7, 8].
14. Gene Expression Omnibus (http://www.ncbi.nlm.nih.gov/geo/) is an excellent source for deep sequencing data. The dataset you are interested in could already be submitted there and you can simply reanalyze the dataset for the genes you are interested in.
15. There are a number of empty vector (EV) options available as controls for shRNA experiments; plko from Open Biosystems (Thermo Fisher Scientific, Waltham, MA) (RHS4080), or GFP ctl shRNA (Thermo Fisher Scientific, Waltham, MA) (# RHS4459).
16. If you obtain concentrated lentivirus, adjust the quantity required to infect your cells of choice accordingly. It is advisable to test the ability of your cells to take up virus before initiating shRNA work. I suggest trying serial dilution of viral supernatant and check for infection by selecting on the marker present on your shRNA vector (in the case outlined here it is puromycin resistance).

References

1. Hangauer MJ, Vaughn IW, McManus MT (2013) Pervasive transcription of the human genome produces thousands of previously unidentified long intergenic noncoding RNAs. PLoS Genet 9, e1003569. doi:10.1371/journal.pgen.1003569
2. Derrien T, Johnson R, Bussotti G et al (2012) The GENCODE v7 catalog of human long noncoding RNAs: analysis of their gene structure, evolution, and expression. Genome Res 22:1775–1789. doi:10.1101/gr.132159.111
3. Cabili MN, Trapnell C, Goff L et al (2011) Integrative annotation of human large intergenic noncoding RNAs reveals global properties and specific subclasses. Genes Dev 25:1915–1927. doi:10.1101/gad.17446611
4. Carpenter S, Aiello D, Atianand MK et al (2013) A long noncoding RNA mediates both activation and repression of immune response genes. Science 341:789–792. doi:10.1126/science.1240925
5. Trapnell C, Pachter L, Salzberg SL (2009) TopHat: discovering splice junctions with RNA-Seq. Bioinformatics 25:1105–1111. doi:10.1093/bioinformatics/btp120
6. Kim D, Pertea G, Trapnell C et al (2013) TopHat2: accurate alignment of transcriptomes in the presence of insertions, deletions and gene fusions. Genome Biol 14:R36. doi:10.1186/gb-2013-14-4-r36
7. Trapnell C, Roberts A, Goff L et al (2012) Differential gene and transcript expression analysis of RNA-seq experiments with TopHat and Cufflinks. Nat Protoc 7:562–578. doi:10.1038/nprot.2012.016
8. Trapnell C, Williams BA, Pertea G et al (2010) Transcript assembly and quantification by RNA-Seq reveals unannotated transcripts and isoform switching during cell differentiation. Nat Biotechnol 28:511–515. doi:10.1038/nbt.1621

Chapter 13

Analysis of Post-transcriptional Gene Regulation of Nod-Like Receptors via the 3′UTR

Moritz Haneklaus

Abstract

Innate immune signaling is the front line of defense against pathogens, leading to an appropriate response of immune cells upon activation of their pattern recognition receptors (PRRs) by microbial products, such as Toll-like receptors (TLRs). Apart from transcriptional control, gene expression in the innate immune system is also highly regulated at the post-transcriptional level. miRNA or RNA-binding protein can bind to the 3′ untranslated region (UTR) of target mRNAs and affect their mRNA stability and translation efficiency, which ultimately affects the amount of protein that is produced. In recent years, a new group of PRRs, the Nod-like receptors (NLR) have been discovered. They often cooperate with TLR signaling to induce potent inflammatory responses. Many NLRs can form inflammasomes, which facilitate the production of the potent pro-inflammatory cytokine IL-1β and other inflammatory mediators. In contrast to TLRs, the importance of post-transcriptional regulators in the context of inflammasomes has not been well defined. This chapter describes a series of experimental approaches to determine the effect of post-transcriptional regulation for a gene of interest using the best-studied NLR, NLRP3, as an example. To start investigating post-transcriptional regulation, 3′UTR luciferase experiments can be performed to test if regulatory sequences in the 3′UTR are functional. An RNA pull-down approach followed by mass spectrometry provides an unbiased assay to identify RNA-binding proteins that target the 3′UTR. Candidate binding proteins can then be further validated by RNA immunoprecipitation (RNA-IP), where the candidate protein is isolated using a specific antibody and bound mRNAs are analyzed by qPCR.

Key words Inflammasomes, Nod-like receptors, Post-transcriptional regulation, 3′untranslated region (3′UTR), RNA-binding proteins, miRNA, RNA immunoprecipitation, RNA aptamers, Luciferase reporter assays

1 Introduction

Increasing evidence suggests that post-transcriptional regulation is an essential part of inflammatory and innate immune signaling [1] and has been particularly well described for Toll-like receptor (TLR) signaling [2, 3]. The hub of post-transcriptional control is the 3′ untranslated region (UTR) of mRNAs, which contains sequence elements that are bound by proteins or non-coding RNAs. The most studied post-transcriptional regulators are

Claire E. McCoy (ed.), *Toll-Like Receptors: Practice and Methods*, Methods in Molecular Biology, vol. 1390,
DOI 10.1007/978-1-4939-3335-8_13,

microRNA (miRNA), a class of small non-coding RNA, which can bind to partly complementary sequences in target 3′UTRs and assemble the RNA-induced silencing complex (RISC), which negatively affects the target mRNA stability and its ability to be translated [4]. Another well-defined class of regulatory motifs are AU-rich elements (ARE), typically containing repeats of the pentamer AUUUA, which can be bound by a range of RNA-binding proteins (RBP). Many ARE-binding proteins, such as TTP and AUF1/hnRNP D negatively affect the stability of bound transcripts by attracting the RNA decay machinery or targeting the mRNA to processing (P) bodies [5]. However, other RBPs, such as HuR/ELAVL1 can increase target mRNA expression by interfering with its degradation or increasing translation efficiency [6]. The ultimate outcome of regulatory factors is also dependent on the cellular context. For example, the effect of at least some miRNAs can vary during the cell cycle, oscillating between repression in proliferating cells and activation of translation upon cell cycle arrest [7].

The inflammasomes are a group of cytoplasmic protein complexes that were recently discovered to play a central role in the immune system by regulating the production of IL-1β and other inflammatory mediators. IL-1β is one of the most potent pro-inflammatory cytokines and it is an important factor in the pathogenesis of a number of inflammatory disorders, including arthritis and Type 2 diabetes [8]. Inflammasomes are formed around pattern recognition receptors (PRR), most prominently the NOD-like receptors NLRP1, NLRP3, IPAF/NLRC4 or the PYHIN protein AIM2 [9]. Apart from the PRR, the inflammasome consists of pro-caspase-1 and in some cases the adaptor ASC as a linker between the two. Once the inflammasome is assembled, it provides a platform for auto-activation of caspase-1, which can in turn cleave pro-IL-1β and pro-IL-18 to produce the active pro-inflammatory cytokines. Other substrates of caspase-1 lead to the initiation of pyroptosis, a pro-inflammatory type of programmed cell death. The best-studied inflammasome is formed by NLRP3, which, after being 'primed' by TLR stimuli [10], can be activated by a large and diverse range of stimuli including crystalline substances, extracellular ATP, and pore-forming toxins [11]. Since NLRP3 is a gatekeeper for the production of the potent pro-inflammatory cytokine IL-1β, both its expression and activation are tightly regulated. However, little is known about the post-transcriptional regulation of NLRP3 or any of the inflammasome components.

In this chapter, I will describe a number of techniques that can help to determine the role of post-transcriptional regulation for the example of an NLR. However, they are equally applicable for non-inflammasome-related genes. The basic techniques that will be covered are luciferase assays, RNA pull-down approaches and RNA immunoprecipitation (RNA-IP).

1.1 Luciferase Assays

A standard assay to assess if a gene is under post-transcriptional control in response to stimulation is to fuse its 3′UTR sequence downstream of a reporter gene that is driven by a constitutive promoter (Fig. 1a). Luciferase reporters are most commonly used, but vectors containing a destabilized GFP are another option. Several companies offer luciferase plasmids specifically designed for assessing post-transcriptional effects, such as the psiCHECK vectors (Promega) or pMIR-REPORT (Ambion).

The rationale of this approach is that transcription from the constitutive promoter, usually of viral origin, and also protein stability of the reporter gene should be unaffected by the desired stimulation, such as TLR ligands. Thus, differences in the amount of luciferase/GFP produced could only be due to a difference of reporter mRNA stability or translation efficiency that are determined by the NLR 3′UTR. However, it is very important to make sure that transcription levels are actually unaffected by the treatment. For example, the PKC activator PMA can transcriptionally activate the herpes simplex virus TK promoter specifically in cells expressing adenoviral E1A proteins, such as the commonly used human cell line HEK293 [12]. The easiest way to assure that no such unspecific effects have to be taken into account is to test if the empty vector that does not contain any 3′UTR is unaffected by stimulation. Especially if plasmids are transiently transfected, a constitutive internal control must be co-expressed in each sample for normalization, either from the same vector or a co-transfected separate plasmid. In the case of luciferase-based reporters, the Firefly and *Renilla* luciferase genes are usually used in combination. In the case of the psiCHECK-2 vector described in this chapter, the *Renilla* gene is the experimental readout fused to the NLR 3′UTR and a Firefly luciferase is expressed from the same plasmid as the internal control. The ratio of *Renilla* to Firefly luciferase activity of each sample is then comparable.

1.2 RNA Pull-down Approaches

To identify post-transcriptional regulators of the NLR 3′UTR, an RNA pull-down approach can be used (Fig. 1b). Different techniques have been developed to this end. For example, biotinylated RNA can be used as bait and isolated in a complex with interacting proteins or RNAs using streptavidin-coated beads [13, 14]. Another possibility is to use RNA aptamer sequences that have been screened to specifically bind to streptavidin [15]. The aptamer sequence can be fused to the NLR 3′UTR and the fusion RNA can be isolated with streptavidin beads. Several optimizations of the S1 aptamer described by Srisawat and Engelke [15] have been developed [16, 17] and the protocol in this chapter is based on the S1 tag combined with a tRNA scaffold to provide structural stability described by Iioka et al. [17]. The protocol is designed for identifying RBPs, however it could equally be adapted to identify interacting miRNAs [18].

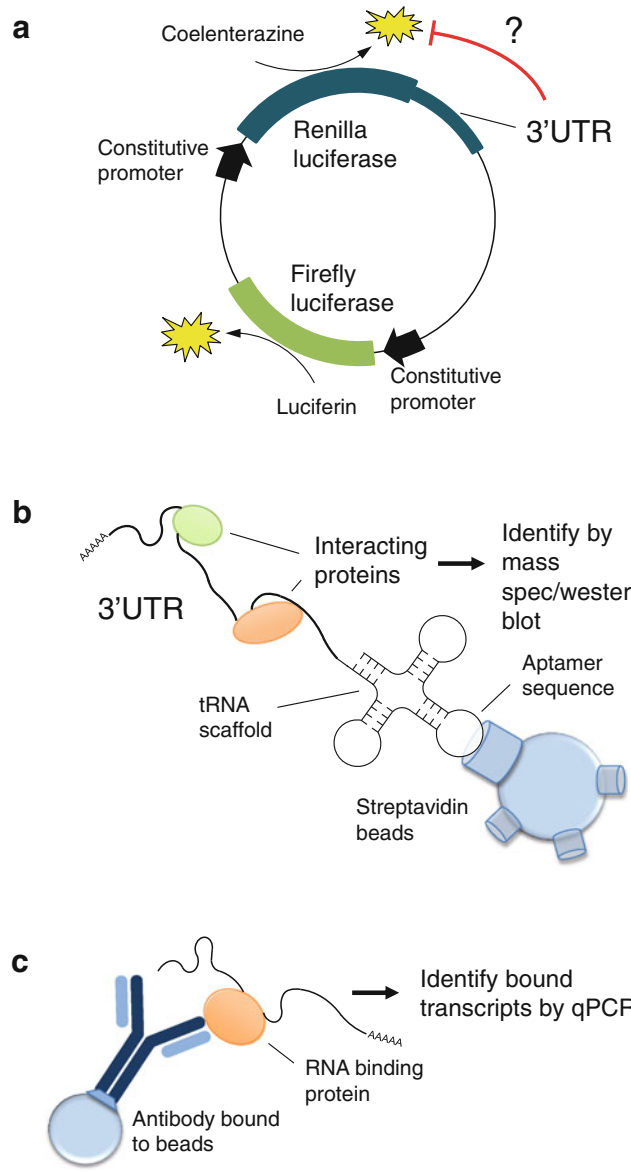

Fig. 1 Overview of methods for analyzing post-transcriptional regulation. (**a**) Luciferase reporter assays can be used to determine the extent of post-transcriptional regulation for a given gene in an artificial system (*see* Subheading 3.2). (**b**) RNA pull-down approaches can be used for unbiased isolation of interacting proteins or miRNA (*see* Subheading 3.3). (**c**) Interaction with RNA binding proteins can be confirmed by RNA immunoprecipitation (*see* Subheading 3.4)

The aptamer vector can be transfected into cells to be transcribed and the RNA then isolated straight from cell lysates. However, Iioka et al. found that it is more efficient to transcribe the constructs in vitro, couple them to streptavidin beads and combine

them as bait with cell lysates. Especially for hard-to-transfect cell types, this is probably the preferable approach.

Due to the high likelihood of unspecific binding, it is necessary to include negative controls in the experiment. These should include the empty vector (only the tag) and a negative control sequence of equal length (e.g., reverse-complement of the NLR 3′UTR or an intronic sequence). Using more than one negative control is highly advisable.

For an unbiased approach, the proteins enriched in the RNA pull-down can be identified by mass spectrometry, which requires scaling up the experiment to provide enough material. To validate mass spec results or to test binding of candidate RBPs, the pulled down proteins can be assessed by Western blot.

1.3 RNA Immunoprecipitation

Finally, a reverse approach to the RNA pull-down, RNA-IP, can be used to test if the candidate RBP binds to the native NLR mRNA (Fig. 1c). This method is based on the enrichment of the candidate protein using a specific antibody followed by the isolation of bound RNAs. As for all immunoprecipitation-based approaches, the success of RNA-IP experiments is dependent on the quality of the antibody that is used. As a negative control, a non-specific antibody such as IgG is used to perform the RNA-IP from the same input material. An important control is to verify the efficient pull-down of the RBP (and lack thereof in the IgG control) by Western blot. While a clear band should be visible in the IP using the RBP-specific antibody, the control lane should be blank.

To test if the target NLR mRNA is interacting with the RBP, the abundance of mRNAs isolated from the IPs can then be assessed by Northern blot or qPCR. The readout is the enrichment of mRNAs in the IP of the RBP compared to the IgG control.

2 Materials

2.1 Cloning

1. Empty plasmids for cloning 3′UTR: psiCHECK-2 empty vector (Promega) for luciferase assays, pcDNA3-tRSA vector (Addgene plasmid 32200, Ian Macara lab [17]) for RNA pull-down assays.
2. KAPA HiFi HotStart ReadyMix PCR kit (or equivalent high fidelity PCR reagents).
3. Oligonucleotides for PCR cloning (Nested PCR setup).
4. Human Genomic DNA (e.g., Promega).
5. Appropriate restriction enzymes and buffers (e.g., from NEB).
6. Calf intestinal phosphatase (CIP) (e.g., from NEB; can be used with NEB restriction enzyme buffer).

7. T4 DNA ligase (Promega).
8. Wizard® SV Gel and PCR Clean-Up System (Promega) or equivalent gel extraction reagents.

2.2 Luciferase Assay

1. THP1 human monocytic leukemia cell line (ECACC).
2. Roswell Park Memorial Institute (RPMI) 1640 Medium, supplemented with GlutaMAX™-I, 10 % fetal calf serum (FCS, endotoxin-tested) and 1 % penicillin/streptomycin (v/v).
3. T75 and T175 tissue culture flasks.
4. Lipofectamine 2000 (Invitrogen).
5. Opti-MEM I (Gibco).
6. Luminometer capable of reading 96-well plates (e.g.,FLUOstar OPTIMA, BMG Labtech).
7. 5× Passive lysis buffer (Promega).
8. Luciferase assay mix: 20 mM tricine, 1.07 mM $(MgCO_3)_4\,Mg(OH)_2{\cdot}5H_2O$, 2.67 mM $MgSO_4$, 0.1 M EDTA, 33.3 mM DTT, 270 mM coenzyme A, 470 mM luciferin, 530 mM ATP; Store in the dark at −20 °C and thaw to room temperature before use (*see* **Note 1**).
9. Coelenterazine (Biotium; 1 mg/ml in 100 % EtOH) stored at −20 °C, diluted 1:1000 in PBS before use (*see* **Note 1**).
10. White opaque 96-well plates.

2.3 RNA Pull-down

1. DEPC-treated RNase-free water (*see* **Note 2**).
2. AmpliScribe™ T7-*Flash*™ in vitro transcription kit (Epicentre) or equivalent.
3. Input: 5 μg tRSA plasmids linearized with XhoI (NEB) and purified with PCR cleanup protocol (Promega Wizard® SV Gel and PCR Clean-Up System); concentration >160 ng/μl.
4. 5 M Ammonium Acetate (Sigma) in RNase-free water.
5. Lysis buffer (prepare in RNase-free water): 1 % NP40 (v/v), 150 mM NaCl, 50 mM Tris–HCl, pH 8.0, 1 mM $MgCl_2$, 10 % glycerol (v/v); add fresh before use: 1 mM dithiothreitol (DTT), 1× Protease inhibitor cocktail I (Fisher Scientific); prepare buffer as 2× and store at 4 °C.
6. RNA binding buffer (prepare in RNase-free water): 50 mM HEPES, pH 7.4, 10 mM $MgCl_2$, 100 mM NaCl.
7. Yeast RNA (Roche), 10 mg/ml in 1× complete lysis buffer.
8. RNasin RNase inhibitor (Promega).
9. Egg-white avidin (Sigma), 2 mg/ml in RNase-free water.
10. Streptavidin, immobilized on Agarose CL-4B beads (Sigma).
11. Coomassie (Bradford) Protein Assay Kit (Pierce).

12. 5× SDS sample buffer: 125 mM Tris–HCl, pH 6.8, 15 % glycerol (v/v), 2 % sodium dodecyl sulfate (SDS) (v/v), 10 mg/ml bromophenol blue; make up to 2× containing 50 mM DTT before use.
13. Qiazol lysis reagent (Qiagen) or equivalent Phenol-based lysis reagent and associated reagents (chloroform & isopropanol).
14. Linear Polyacrylamide (LPA, 5 μg/μl) as carrier, prepared according to Delaney lab protocol (University of Vermont); alternative carrier: yeast tRNA.

2.4 RNA Immunoprecipitation

1. Antibody to RNA-binding protein of interest (must be suitable for immunoprecipitation) and isotype control antibody (e.g., IgG).
2. 36.5 % Formaldehyde (Sigma).
3. Protein A/G PLUS-Agarose beads (Santa Cruz).
4. 2.5 M Glycine, pH 7.0.
5. Sonicator.
6. RIPA lysis buffer (prepare in RNase-free water): 50 mM Tris–HCl, pH 7.5, 1 % Nonidet P-40 (NP-40), 0.5 % sodium deoxycholate, 0.05 % SDS, 1 mM EDTA, 150 mM NaCl; add fresh before use, 1× Protease inhibitor cocktail I (Fisher Scientific) and 20 U/ml RNasin (Promega); prepare buffer as 2× and store at 4 °C.
7. High-stringency RIPA wash buffer: 50 mM Tris–HCl, pH 7.5, 1 % NP-40, 1 % sodium deoxycholate, 0.1 % SDS, 1 mM EDTA, 1 M NaCl, 2 M urea, 1× Protease inhibitor cocktail I (Fisher Scientific); prepare fresh before use.
8. Decrosslink Buffer: 50 mM Tris–HCl, pH 7.0, 5 mM EDTA, 10 mM DTT, 1 % SDS; prepare fresh before use.
9. RNasin RNase inhibitor (Promega).
10. Qiazol lysis reagent (Qiagen) or equivalent Phenol-based lysis reagent and associated reagents (chloroform & isopropanol).
11. Linear Polyacrylamide (LPA, 5 μg/μl) as carrier, prepared according to Delaney lab protocol (University of Vermont); alternative carrier: yeast tRNA.

3 Methods

3.1 Cloning

3.1.1 Nested PCR

1. First, run an outer PCR cycle to enrich for the genomic region covering the 3′UTR (*see* **Note 3**).
2. For the example of NLRP3: assemble a 10 μl PCR reaction with forward primer 5′-TATCTGAAGAGTGCAACCCAGGCT-3′

and reverse primer 5′-ACTCTCAAACCTTTCCCTCC ACGA-3′ using genomic DNA as input (*see* **Note 4**).

3. Run 15 cycles with 60 °C annealing temperature.
4. Next, run a PCR reaction using the PCR product from **step 3** as input with primers spanning from the start to the end of the 3′UTR that contain restriction enzyme sites in their 5′ end.
5. For the example of NLRP3: assemble a 50 μl PCR reaction with Fwd_XhoI and Rev_NotI for cloning into psiCHECK-2 and Fwd_EcoRI and Rev_XhoI for cloning into pcDNA3-tRSA with 0.5 μl outer cycle PCR product as input (*see* Table 1 for primer sequences).
6. Run three cycles with 55 °C and 23–27 cycles with 60 °C annealing temperature.

3.1.2 Isolation and Cloning

1. Separate PCR products on a 1–1.5 % agarose gel, excise specific bands and extract the DNA from the gel.
2. To prepare for cloning, digest both vector and inserts with the appropriate restriction enzymes (e.g., XhoI + NotI for psiCHECK-2 and EcoRI + XhoI for pcDNA3-tRSA) (*see* **Note 5**). Total reaction volume: 30–50 μl with 1 μl of each enzyme and 1× of the appropriate buffer for at least 1 h at 37 °C. For the vector: add 1 μl CIP for at least 30 min to prevent religation of the empty vector.
3. Purify digested inserts using a PCR purification protocol; vectors often have to be gel-purified to remove the excised piece of DNA.
4. Assemble ligation reaction and incubate overnight at 4 °C. Setup for a 5 μl reaction: 0.5 μl 10× ligation buffer, 0.5 μl

Table 1
Example primer sequences for cloning the human NLRP3 3′UTR (restriction sites are in *bold*)

Name	Sequence
Fwd_XhoI	5′-CTGACG**CTCGAG**AGAGTGGAAACGGGG CTGCCAGA-3′
Rev_NotI	5′-CGCATG**GCGGCCGC**GTTTTTTAAAATT AAGAAAAGGA-3′
Fwd_EcoRI	5′-ATCTGACG**GAATTC**AGAGTGGAAACGG GGCTGCCAGA-3′
Rev_XhoI	5′-CGCATG**CTCGAG**GTTTTTTAAAATTAAGAAA AGGA-3′

T4 DNA ligase, 0.5 μl digested vector DNA, 3.5 μl digested insert DNA.

5. Transform ~2 μl of the ligation into 25 μl competent *E. coli* DH5α and streak on LB-Agar plate containing the correct antibiotic for the transformed plasmid (for psiCHECK-2 and pcDNA: Ampicillin); incubate overnight at 37 °C.
6. Pick single colonies and inoculate 2 ml LB media containing selection antibiotic and isolate plasmid DNA using a miniprep kit.
7. Screen clones for positive ligation by restriction digest and agarose gel electrophoresis; check for mutations by sequencing positive clones.
8. Grow up 100 ml of bacterial overnight culture of the sequenced clone and extract plasmid DNA (use endotoxin-free kits for use in immune cells, e.g., Qiagen EndoFree Plasmid Maxi kit).

3.2 Luciferase Assay

1. Prepare plasmids to be transfected (*see* **Note 6**): empty vector control and different 3′UTRs or wild-type and mutated 3′UTR (*see* **Note 3**).
2. Wash 3×10^6 THP1 cells with PBS, resuspend in 3 ml antibiotic-free RPMI.
3. Mix 300 μl OptiMEM with 5.63 μl Lipofectamine 2000.
4. Mix 300 μl OptiMEM with 2.25 μg plasmid DNA.
5. Combine and mix **steps 3** and **4**, incubate for 15 min at room temperature.
6. Add transfection mix to cells (dropwise) and shake.
7. After 4–5 h, change media to 5 ml complete RPMI.
8. The next day or 48 h later, each transfection can be split into up to nine wells of a 24-well plate (adjust volume to 0.5–1 ml per well) before treatment with desired agonists such as TLR stimuli.
9. Lyse each well in 50 μl 1× Passive Lysis Buffer (usually about 48 h after transfection) (*see* **Note 7**).
10. Split each sample into two separate wells of an opaque 96-well plate. 20 μl each: one for *Renilla* and the other for Firefly luciferase activity reading.
11. To measure *Renilla* luciferase activity: Add 40 μl Coelenterazine (1:1000 in PBS).
12. To measure Firefly luciferase activity: Add 40 μl Luciferase assay mix.
13. Read plates in a luminometer (*see* **Note 8**).
14. For each sample, divide Firefly luciferase readings by *Renilla* readings, then average ratios of replicates.

3.3 RNA Pull-down

3.3.1 In Vitro Transcription

1. In vitro transcribe tRSA constructs from linearized plasmid DNA according to the manual (*see* **Note 9**). A 10 µl reaction with 500 ng linearized vector will yield 80–90 µg RNA.
2. Add 40 µl water and 50 µl 5 M NH_4Ac to precipitate the RNA.
3. Incubate on ice for 10 min, then centrifuge for 10 min at max speed at 4 °C.
4. Wash the pellet twice with 70 % EtOH (spin 5 min at 4 °C).
5. Dissolve in appropriate amount of RNase-free water (about 250 µl for 10 µl reactions).
6. Measure RNA concentration and check quality on agarose gel.
7. Store RNA at −80 °C (short-term storage at −20 °C is possible).

3.3.2 Determine Scale of the Experiment

1. For mass spec analysis: couple 50 µg of in vitro transcribed RNA (*see* Subheading 3.3.1) to 100 µl bed volume beads (*see* Subheading 3.3.3) and incubate with 6–8 mg total protein (*see* Subheading 3.3.4).
2. For Western blot analysis: couple 10 µg of in vitro transcribed RNA (*see* Subheading 3.3.1) to 30 µl bed volume beads (*see* Subheading 3.3.3) and add 0.5–1.5 mg total protein (*see* Subheading 3.3.4).

3.3.3 RNA Bead Preparation

1. Heat RNA (for amount *see* Subheading 3.3.2) in 1× RNA binding buffer to 65 °C for 5 min, let it cool down slowly to room temperature (e.g., floating in a beaker with warm water).
2. Wash required volume of streptavidin beads (*see* Subheading 3.3.2) once in Lysis buffer followed by once in RNA annealing buffer.
3. Combine RNA and beads in RNA annealing buffer (1 ml for 100 µl beads) and incubate rotating at 4 °C for 1 h.
4. Wash beads twice with 1× Lysis buffer.

3.3.4 Cell Lysate Preparation

1. Lyse ~2.5×10^7 cells (e.g., THP1) in 1.5 ml 1× complete Lysis buffer (for mass spec, ~1.2×10^8 cells are needed).
2. Incubate on ice for 10 min and vortex repeatedly.
3. Centrifuge for 5 min at 500 × *g* at 4 °C.
4. Quantify protein concentration with Bradford (expect ~1.5–3 mg/ml).
5. Preclear the lysate by adding 10 µg egg white avidin and 0.5 mg yeast RNA per mg of total protein.
6. Incubate rotating at 4 °C for 20 min.
7. Centrifuge 10 min at >14,000 × *g* in a microcentrifuge at 4 °C. Transfer the supernatant to a new tube.

8. Add 10 U/ml RNasin.
9. Optional: adjust protein concentration to 400–500 ng/ml if RNA degradation is an issue (*see* **Note 10**).

3.3.5 RNA Pull-down

1. Add precleared lysates (*see* Subheading 3.3.4; for mass spec: 6–8 mg, for Western blot: 0.5–1.5 mg total protein per tube) to coupled beads (*see* Subheading 3.3.3) and incubate shaking at 4 °C for 1–2 h.
2. Wash 5× with 0.5–1 ml 1× Lysis buffer.
3. To elute protein from beads; add 20–40 µl SDS sample buffer, boil and analyze bound proteins by either mass spectrometry (whole sample or cut out single bands) or SDS-PAGE and Western blot.
4. To elute RNA from beads; lyse in 100–200 µl QIAzol reagent and isolate RNA according to the manufacturer's instructions and resuspend in RNase-free water (*see* **Note 11**).
5. Run RNA on 1–1.5 % agarose gel to check for degradation and compare to in vitro transcribed input RNA (*see* Subheading 3.3.1).

3.4 RNA Immunoprecipitation

3.4.1 Bead Preparation

1. Equilibrate 30 µl protein A/G beads per sample by washing 3× with Lysis buffer.

3.4.2 Cell Lysate Preparation

1. Incubate 0.5–1 × 10^7 cells (e.g., THP1) with 0.2 % formaldehyde in PBS for 10 min on a shaker (*see* **Note 12**).
2. Add glycine to a final concentration of 0.25 M (1/9 volume), mix and incubate for 5 min.
3. Centrifuge the fixed cells at 370 × *g* for 3–5 min and discard supernatant.
4. Lyse cell pellet in 1 ml Lysis buffer per 10^7 cells.
5. Sonicate 3× 20 s (keep on ice for at least 1 min in between rounds of sonication).
6. Centrifuge for 10 min at full speed (>14,000 × *g*) in a microcentrifuge at 4 °C. Transfer the supernatant to a new tube.

3.4.3 Preclear Lysate

1. Preclear the lysates (*see* Subheading 3.4.2) with 10 µl equilibrated protein A/G beads per sample (*see* Subheading 3.4.1) and 0.1 mg/ml yeast RNA. Rotate for 30 min at 4 °C.
2. Centrifuge samples for 5 min at 1300 × *g* at 4 °C. Transfer the supernatant to a new tube.
3. Remove aliquots of supernatant from **step 2** (30–50 µl) to measure lysate input. For example, to measure RNA input lyse the aliquot in 150 µl Qiazol and extract RNA according to the

manufacturer's instructions (*see* **Note 11**); or lyse the aliquot in an appropriate volume of SDS sample buffer to measure protein input.

3.4.4 Immunoprecipitation

1. Add 1–3 µg IP antibody (RBP-specific or control) to the remainder of lysate generated in Subheading 3.4.4, **step 2**. Incubate for 1–1.5 h rotating at 4 °C (*see* **Note 13**).
2. Add 20 µl equilibrated Protein A/G beads per sample (Subheading 3.4.1) and incubate for 2 h at 4 °C.
3. Wash 5× with ice-cold high stringency RIPA buffer (centrifuge for 4 min at 500 × *g* at 4 °C between washes); remove as much of the buffer as possible after the last wash.

3.4.5 Reverse Cross-Links and Extract RNA

1. Add 80 µl Decrosslink Buffer to each sample, incubate at 70 °C for 45 min to reverse cross-links.
2. Add 150 µl Qiazol to beads and extract RNA according to the manufacturer's instructions and resuspend in RNase-free water (*see* **Notes 11** and **14**).
3. To check IP efficiency by Western blot: add SDS sample buffer to beads instead, boil and run on SDS-PAGE.

3.4.6 Readout by qPCR

1. Convert equal volumes of RNA (Subheading 3.4.5, **step 2**) to cDNA using a standard reverse transcription protocol.
2. Measure target gene expression by standard qPCR.
3. Determine the ratio of the mRNA in the IP of the candidate RBP to the non-specific IP (*see* **Note 15**). For strong interactions, relative enrichment can be 50–300×.

4 Notes

1. Instead of individual substrates, Dual luciferase assays (e.g., Promega) can be used to measure Firefly and Renilla luciferase activity.
2. *General note for RNA work*: RNA is relatively unstable and very susceptible to RNase contamination. In order to maximize stability, keep samples and solutions on ice if not stated otherwise. To prevent RNase contamination, wear gloves that are exclusively used for RNA work and clean the working bench with 70 % ethanol. Always use RNase-free tubes and filter tips and be very careful not to touch the outside of tubes or any other potentially contaminated "outside" area such as the bench or your gloves. If in doubt, change the pipet tip. Buffers used for incubations with RNA can also be supplemented with RNase inhibitor cocktails, but if the buffers were prepared and handled RNase-free, this can usually be omitted. If samples are

handled carefully enough, the use of other precautions (e.g., RNaseZAP spray or similar) is not necessary. However, it is good practice to routinely check the RNA quality in different steps of the workflow by running samples on an agarose gel or Bioanalyzer.

3. Different 3′UTRs can be cloned to serve as positive and negative controls (e.g., TNFα, β-actin, GAPDH); use site-directed mutagenesis to mutate potential regulatory sites and test their functionality or make truncations of the 3′UTR to narrow down-regulatory regions.
4. Design primers with dedicated program like the freely available online tools PrimerQuest (http://www.idtdna.com/Primerquest/), Primer3 or Primer-BLAST.
5. Adding three to six extra bases after the restriction site at the 5′ end of cloning primers will increase the efficiency of restriction digests.
6. Any plasmid-compatible transfection reagent can be used for easy-to-transfect cells; for more difficult cells such as THP1, harsher reagents like Lipofectamine 2000 are necessary; to minimize toxicity with Lipofectamine 2000 use antibiotics-free media and change media 4–5 h after transfection.
7. Exact timings need to be optimized for each cell type, luciferase construct and treatment. Usually, robust luciferase expression can be measured between 24 and 72 h post transfection and the signal is strongest around 48 h.
8. For consistency between the readings of different wells, it is advisable to use a plate reader with built-in injectors to dispense the substrates. This ensures equal time between addition of the substrate and luminescence reading.
9. The template for in vitro transcription can either be linearized plasmid DNA or a PCR product from the plasmid DNA that contains the T7 promoter and the tRSA-3′UTR fusion construct.
10. Some RNAs coupled to the beads can be very sensitive to degradation when incubated with cytoplasmic lysate. This can be checked by isolating RNA from beads incubated with lysate or buffer only, running them on an agarose gel and comparing the size of the bands. If degradation is an issue, it can help to dilute the lysate or try other lysis buffers. Beware that diluting the lysate for mass spec preparation (6–8 mg total protein) will increase the volume to about 15 ml, which requires bigger tubes (e.g., 15 ml Falcon tubes).
11. Where small amounts of RNA are expected (e.g., off RNA-coupled beads in Subheading 3.3 or from RNA-IP samples in Subheading 3.4.5), a carrier such as LPA or yeast tRNA can be

added to increase the efficiency of RNA precipitation and the RNA pellet size. After phase-separation, transfer aqueous phase to new tube and add 3 μl LPA or other carrier before adding isopropanol. When using LPA, be careful when removing liquid because the pellet is less sticky.

12. Formaldehyde is toxic and needs to be handled in a fume hood. However, cells can be transferred to an airtight tube for incubation outside the hood.
13. Alternatively, protein A/G beads can be coated with antibody before incubation with cell lysate. In this case, add antibody to equilibrated beads and incubate for at least 2 h at 4 °C. Then wash 3× with lysis buffer and incubate with lysate.
14. Make sure to use equal volumes for resuspension between samples, because no internal control can be used for quantification.
15. Optimally, at least one positive and several negative control genes should be analyzed to determine if the experiment worked and assess the amount of non-specific background binding of the antibodies to RNAs.

References

1. Carpenter S, Ricci EP, Mercier BC et al (2014) Post-transcriptional regulation of gene expression in innate immunity. Nat Rev Immunol 14:361–376
2. O'Neill LA, Golenbock D, Bowie AG (2013) The history of Toll-like receptors—redefining innate immunity. Nat Rev Immunol 13:453–460
3. O'Neill LA, Sheedy FJ, McCoy CE (2011) MicroRNAs: the fine-tuners of Toll-like receptor signalling. Nat Rev Immunol 11:163–175
4. Djuranovic S, Nahvi A, Green R (2011) A parsimonious model for gene regulation by miRNAs. Science 331:550–553
5. Garneau NL, Wilusz J, Wilusz CJ (2007) The highways and byways of mRNA decay. Nat Rev Mol Cell Biol 8:113–126
6. Fan XC, Steitz JA (1998) Overexpression of HuR, a nuclear-cytoplasmic shuttling protein, increases the in vivo stability of ARE-containing mRNAs. EMBO J 17:3448–3460
7. Vasudevan S, Tong Y, Steitz JA (2007) Switching from repression to activation: microRNAs can up-regulate translation. Science 318:1931–1934
8. Dinarello CA, Simon A, van der Meer JW (2012) Treating inflammation by blocking interleukin-1 in a broad spectrum of diseases. Nat Rev Drug Discov 11:633–652
9. Schroder K, Tschopp J (2010) The inflammasomes. Cell 140:821–832
10. Bauernfeind FG, Horvath G, Stutz A et al (2009) Cutting edge: NF-kappaB activating pattern recognition and cytokine receptors license NLRP3 inflammasome activation by regulating NLRP3 expression. J Immunol 183:787–791
11. Horvath GL, Schrum JE, De Nardo CM et al (2011) Intracellular sensing of microbes and danger signals by the inflammasomes. Immunol Rev 243:119–135
12. Shifera AS, Hardin JA (2009) PMA induces expression from the herpes simplex virus thymidine kinase promoter via the activation of JNK and ERK in the presence of adenoviral E1A proteins. Arch Biochem Biophys 490:145–157
13. Mehta A, Driscoll DM (1998) A sequence-specific RNA-binding protein complements apobec-1 to edit apolipoprotein B mRNA. Mol Cell Biol 18:4426–4432
14. Hassan T, Smith SG, Gaughan K et al (2013) Isolation and identification of cell-specific microRNAs targeting a messenger RNA using a biotinylated anti-sense oligonucleotide capture affinity technique. Nucleic Acids Res 41, e71
15. Srisawat C, Engelke DR (2001) Streptavidin aptamers: affinity tags for the study of RNAs and ribonucleoproteins. RNA 7:632–641

16. Leppek K, Stoecklin G (2014) An optimized streptavidin-binding RNA aptamer for purification of ribonucleoprotein complexes identifies novel ARE-binding proteins. Nucleic Acids Res 42, e13
17. Iioka H, Loiselle D, Haystead TA et al (2011) Efficient detection of RNA-protein interactions using tethered RNAs. Nucleic Acids Res 39, e53
18. Liu H, Zhang S, Lin H et al (2012) Identification of microRNA-RNA interactions using tethered RNAs and streptavidin aptamers. Biochem Biophys Res Commun 422:405–410

Part IV

Toll-Like Receptors and System Control

Chapter 14

TLR Function in Murine CD4+ T Lymphocytes and Their Role in Inflammation

Stephanie Flaherty and Joseph M. Reynolds

Abstract

Toll-like receptor (TLR) signaling represents an evolutionary-conserved mechanism allowing for the rapid detection of broad molecular patterns that are common to different groups of pathogens. TLRs are traditionally associated with cells of the innate immune response where ligation of a TLR alone can lead to cellular activation and the initialization of an immune response. Cells of adaptive immunity, namely different classes of T and B lymphocytes, are also known to express a variety of TLRs. Conversely, the functional and signaling outcomes of TLRs are decidedly different in cells of the adaptive immune response. T lymphocytes generally have substantially lower TLR expression compared to innate cells, suggesting that TLRs function in a highly specialized capacity in this cell type. Certain TLRs act in a co-stimulatory capacity on T cells, amplifying activation only in the presence of simultaneous T-cell receptor engagement. However, the full array of TLR signaling events and outcomes in T lymphocytes remains poorly understood. Here, we describe a few methods for investigating the general function of TLRs on T lymphocytes in vitro and in vivo with an emphasis on the study of CD4+ T cells. Most of these procedures can be adapted for the study of TLR signaling on other classes of lymphocytes as well.

Key words Toll-like receptor, T helper cell, T helper differentiation, T-cell receptor, Co-stimulation, T-cell transfer

1 Introduction

The characterization of a *Drosophila* toll protein analog, toll-like receptor 4 (TLR4), in mammalian cells [1] led to a dramatic shift in our understanding of how the innate immune response recognizes and responds to invading pathogens. In the past 20 years, 10 human and 12 mouse TLRs have been identified with each having a unique recognition site for patterns that are shared amongst various classes of pathogens, including gram-positive bacteria, gram-negative bacteria, viruses, and fungi [2]. Although TLRs share many common functions, such as the activation of innate immune cells to produce pro-inflammatory cytokines, differential localization and signaling molecules allow for further pathogen response diversity in addition to receptor specificity. For example, TLRs 1,

Claire E. McCoy (ed.), *Toll-Like Receptors: Practice and Methods*, Methods in Molecular Biology, vol. 1390,
DOI 10.1007/978-1-4939-3335-8_14,

2, 4, 5, and 6 are localized on the external surface of a cell allowing them to detect free pathogen [2]. TLRs 3, 7, 8, and 9, on the other hand, are located on intracellular compartments where they recognize foreign nucleic acids as a result of pathogen internalization [3, 4]. TLR4 can act as both an external and intracellular receptor. Most of the TLRs share a common signaling adaptor molecule, myeloid differentiation factor 88 (MyD88), that functions in the transmission of downstream signals following TLR ligation [5]. Conversely, TLR3 exclusively utilizes the TIR domain-containing adaptor inducing IFNβ (TRIF) adaptor for signal transduction where TLR4 utilizes both MyD88 and TRIF [6, 7]. Most of the studies that have characterized the signaling pathways and functions of the various TLRs, however, have done so exclusively in cells of the innate immune response.

TLRs are expressed on lymphocytes as well, although most lymphocytes probably do not simultaneously express all of the known TLRs at any given time [8]. In B cells, the activation of multiple TLRs is critical for proliferation, expansion, and antibody production [9, 10]. Regulatory T cells (Treg) are also known to utilize multiple TLR signaling pathways to promote proliferation and survival as well as to regulate their suppressive functions [11–13]. Our studies have primarily focused on the role of TLRs in $CD4^+$ T lymphocytes, commonly known as T helper (Th) cells. Previous work demonstrated that TLR4 stimulation of $CD4^+$ T cells in combination with T-cell receptor (TCR) activation could promote proliferation, survival, and suppress IL-4 production [14–16]. Furthermore, TLR2 activation on $CD4^+$ T cells promoted proliferation and IFNγ production from T helper 1 (Th1) cells [17, 18] and IL-17 production from T helper 17 (Th17) cells [19]. In most of these studies, induction of proliferation and the production of lineage-specific cytokines were only observed with simultaneous TCR activation, suggesting that certain TLRs act as co-stimulatory receptors on $CD4^+$ T cells [18]. In vivo, MyD88-deficient $CD4^+$ T cells lose their inflammatory capacity in a murine model of colitis [20]. Moreover, $CD4^+$ T cells lacking TLR2 expression were unable to generate effective Th17 responses and promote inflammation in the experimental autoimmune encephalomyelitis (EAE) model [19]. In humans, TLR2 expression on $CD4^+$ T cells was found to be an important mechanism for the host defense against both tuberculosis and filarial infection [21, 22]. In mice, TLR4 deletion solely on $CD4^+$ T cells was found to exacerbate experimental colitis while also protecting against the development of EAE [15, 23]. Thus, although the expression of TLRs is generally lower on $CD4^+$ T cells, they still can have a dramatic influence on T-cell function.

T helper cells differentiate into various lineages or subsets depending on environmental signals at the time of TCR activation [24]. Within each lineage, functional plasticity is common [25,

26]; however, for the purpose of these methods we will be referring to each Th subset as an independent lineage. TLR expression is variable among different types of T cells [8], so consideration must be taken into expression levels before performing these types of experiments. For example, TLR2 expression has been shown to be constitutively expressed [14], measurable only on activated cells [18], or enriched in Th17 cells [19] compared to other subsets. Here, we describe some methods that have been successfully used in the past to study the effect of TLR activation on $CD4^+$ T-cell function [15, 19]. However, an analysis of TLR expression on the T cells of interest should be performed before starting these types of experiments.

2 Materials

Prepare all solutions using sterile ultrapure deionized water, PBS, or DMSO as described. All reagents should be stored at 4 °C, –20 °C, or –80 °C as indicated prior to use. After lymphoid tissue homogenization, all steps should be performed on ice unless indicated otherwise. Media should be warmed to room temperature before culturing of cells.

2.1 CD4+ T-Cell Isolation and Analysis

1. PBS+: autoclaved PBS with 1 % FBS (Life Technologies).
2. Cell filtration: nylon mesh (~100 μm pore size) autoclaved and cut into square pieces to fit over a 15 ml conical tube. Alternatively, commercially available cell strainer caps that fit onto 15 ml conical tubes can be used.
3. 10× ACK lysis buffer: 0.15 M NH_4Cl, 10 mM $KHCO_3$, and 0.1 mM in H_2O. Filter-sterilize before use. Dilute to a 1× working concentration using autoclaved H_2O and store at 4 °C until immediately before use.
4. Magnetic beads and buffers if performing $CD4^+$ T-cell enrichment prior to sorting. Many companies offer these systems so please follow the individual manufacturer's instruction for preparation.
5. FACS buffer: 1 mM EDTA, pH 8, and 1 % BSA (w/v). Mix into solution (warming may be necessary), sterile filter, and store at 4 °C before use. Add 0.1 % NaN_3 for long-term storage at 4 °C.
6. Complete RPMI media: 500 ml RPMI1640 (Life Technologies), 5 ml of 100× penicillin/streptomycin solution (Life Technologies), 5 ml of 100× L-glutamine (Life Technologies), 10 % FBS, and 500 μl of 55 mM 2-mercaptoethanol (Life Technologies). Store at 4 °C and then warm before use (*see* **Note 1**).

7. Phorbol 12-myristate 13 acetate (10,000×; PMA): 0.1 mg/ml diluted in sterile DMSO. Aliquot and store at −20 °C prior to use. Do not re-freeze aliquots after use.
8. Ionomycin (1000×): 1 mg/ml diluted in DMSO. Aliquot and store at −20 °C prior to use. Do not re-freeze aliquots.
9. ^{3}H-thymidine for proliferation assays: dilute ^{3}H-thymidine (Amersham) to 1 μCi/ml in complete RPMI media. Store in a shielded container at 4 °C.
10. Carboxy-fluorescein diacetate, succinimidyl ester (CFDA or CFSE): dilute stock (Life Technologies) to a 10 mM solution in sterile DMSO. Store at −20 °C until ready for use. Dilute CFDA to a working concentration of 25 μM in sterile PBS (no FBS) to label the cells.
11. TLR agonists, antagonists, and antibodies: multiple companies offer a variety of TLR modulators that can be utilized for these types of experiments. Follow the manufacturer's instructions for reconstitution and storage.
12. Recombinant cytokines and antibodies: many different vendors offer the cytokines and antibodies necessary for the Th differentiation protocols listed here. Follow the manufacturers' instructions for reconstitution and storage (*see* **Note 2**).

3 Methods

Here, we describe methods to investigate the influence of TLR activation on CD4+ T-cell differentiation (Subheading 3.1), T lymphocyte proliferation and survival (Subheading 3.2) and T-cell analysis in vivo (Subheading 3.3).

3.1 CD4+ T-Cell Differentiation

1. For Th differentiation experiments, coat wells of a 48-well or 24-well plate with anti-CD3 (clone 2C11) and anti-CD28 (clone 37.51) in 0.5–1 ml of sterile PBS (*see* **Note 2**). Incubate the plate at 4 °C overnight or at 37 °C for 1 h before isolating T cells. Wash each well 2–3 times with 1 ml of sterile PBS before plating T cells. We typically coat 1 μg/ml 2C11 and 1 μg/ml 37.51 for performing Th1, Th2, and Treg differentiations. For Th17 experiments, we coat each well with 2 μg/ml 2C11 and 1 μg/ml 37.51 as stronger TCR activation seems to promote better Th17 differentiation (*see* **Note 3**).
2. Isolate total lymphocytes from secondary lymphoid organs, including spleen and the easily accessible lymph nodes (inguinal, axillary, brachial, and cervical) from healthy mice. C57BL/6 mice are commonly used for Th1 and Th17 differentiation, while Balb.c mice are typically used for Th2 differentiation. We normally isolate tissues from female mice, 6–12

weeks old, due to their low fat content and high frequency of naïve $CD4^+$ T cells amongst the total lymphocyte population. However, T cells isolated from male mice or older mice are effective for these experiments as well.

3. Place lymphoid tissue in a 60 mm dish or a 6-well plate containing 3 ml of PBS+ and transfer to a tissue-culture hood. Pool the lymph nodes together and homogenize by placing a piece of sterile nylon mesh over the tissue and grinding into solution using the thumb-side end of a 3–10 ml syringe. Alternatively, the tissue may be placed between two autoclaved glass slides and homogenized into suspension. Pass the tissue homogenate through a nylon filter placed on top of a 15 ml conical tube. Repeat for spleen homogenization but keep the suspension in a separate 15 ml conical tube as spleens require erythrocyte lysis.
4. Spin the 15 ml conical tubes at $475 \times g$ for 5 min at 4 °C. Aspirate and resuspend the lymph node cells in 2 ml of PBS+ and store on ice. For the splenocytes, resuspend the cellular pellet in 1 ml of ice-cold ACK lysis buffer per spleen (*see* **Note 4**) and incubate for 2–4 min at room temperature. After the incubation, fill the remainder of the tube with 10 ml of PBS+ and centrifuge at $475 \times g$ for 5 min at 4 °C.
5. Resuspend the splenic pellet in 5 ml of PBS+ and filter again through nylon mesh into a new 15 ml conical tube to remove debris. At this point the lymph node cells can be combined with the splenocytes if pooling cells is desired. Centrifuge at $475 \times g$ for 5 min at 4 °C.
6. Isolate naive $CD4^+$ T cells. If performing $CD4^+$ enrichment by magnetic bead separation followed by naïve T-cell sorting, resuspend the cells in CD4 magnetic beads and separate according to the manufacturer's instructions. After enrichment, wash and then stain the cells with CD4, CD44, CD25, and CD62L in FACS buffer (*see* **Note 5**). Prepare collection tubes containing 1–2 ml of complete media that are compatible with your cell sorter. Sort the naïve cells as a highly purified $CD4^+CD25^-CD44^-CD62L^+$ population. Alternatively, many companies offer kits for the direct isolation of naïve $CD4^+$ T cells from total splenic and lymph node suspensions without the use of a cell sorter. If using one of these kits, be sure to check the purity of the naïve cell population by flow cytometry prior to performing experiments.
7. After naïve cell purification, wash the cells with complete RPMI media and centrifuge at $475 \times g$ for 5 min at 4 °C. Resuspend the cell pellet in complete RPMI, count the cells, and adjust the concentration to 1×10^6 cells/ml for optimal cell growth.

8. Setup T-cell differentiation cultures based on the desired subset(s) to be tested. Our typical cytokine and antibody parameters are listed below but be sure to titrate cytokine and antibody concentrations to optimize conditions before performing large experiments. Th1: 30 U/ml human IL-2 (hIL-2), 15 ng/ml mouse IL-12 (mIL-12), and 5 μg/ml anti-IL-4 (clone 11B11). Th2: 30 U/ml hIL-2, 10 ng/ml mIL-4, 2 μg/ml soluble 37.51, and 5 μg/ml anti-IFNγ (clone XMG1.2) (*see* **Note 6**). Th17: 20 ng/ml mIL-6, 3 ng/ml hTGFβ, 5 μg/ml 11B11, and 5 μg/ml XMG1.2. Inducible Treg (iTreg): 30 U/ml hIL-2, 15 ng/ml hTGFβ, 5 μg/ml 11B11, and 5 μg/ml XMG1.2. Plate cells at 1×10^6 cells per well in a 48- (0.5 ml culture volume) or 24-well (1 ml total culture volume) plate.
9. After adding the preferred differentiation reagents, add specific TLR agonists, antagonists, or blocking antibodies at the desired concentration. Keep in mind that the expression of TLRs on T cells tends to be lower compared to cells of the innate immune response so often times larger amounts (μg/ml range) are necessary to observe an effect. Furthermore, these TLR modulators may be added at the start, during, or at the end of T-cell differentiation depending on the experiment. Finally, always make sure to include control cells without TLR stimuli for each experiment (*see* **Note 7**).
10. Culture the T lymphocytes for 4–5 days while closely observing cellular proliferation daily. Expended media (yellow in color) can be replaced with 25–50 % volume of fresh RPMI, which does not require the addition of fresh cytokines or antibodies. Alternatively, cells can be removed from TCR stimuli after 2 days (*see* **Note 8**). Typically we observe that Th1, Th2, and iTreg cytokine and transcription factor expression is optimal at day 4 where Th17 cells are optimized at day 5.
11. After the preferred incubation period, restimulate cells with PMA, ionomycin, and brefeldin A for 4–6 h at 37 °C with 5 % CO_2. Perform intracellular cytokine staining to determine the frequency of lineage-specific cells and the efficiency of differentiation (*see* **Note 9**). Non-lineage-specific cytokines and transcription factors should also be stained for efficiency controls. Commercially available antibodies for IFNγ (Th1), IL-4 and IL-5 (Th2), IL-17 (Th17), and Foxp3 (iTreg) are readily available.
12. Differentiated cells may also be assayed for cytokine production by ELISA. For protein measurements, supernatants can be directly assessed by ELISA if the TLR modulator does not promote or inhibit cellular proliferation or survival in comparison to untreated controls. If your treatment does result in proliferation of survival changes, pipette the cells out of the dish,

count, normalize the concentration, and replate with fresh RPMI in a well containing 1 μg/ml plate-bound 2C11. Incubate the cells overnight and then collect supernatant for ELISA determinations. Th2 cells should always be washed first and then normalized and replated in this manner for IL-4 ELISA analysis as the original culture conditions required the addition of exogenous IL-4 cytokine.

13. Lineage-specific gene expression may also be analyzed in the differentiated cells by quantitative PCR (qPCR). To perform such assays, remove the cells from the plate, wash, and count. Normalize the cellular concentrations between groups with fresh RPMI media and then replate in a well containing 1 μg/ml plate-bound 2C11 for 2–4 h. Isolate mRNA using your preferred method and then synthesize cDNA using one of the many commercially available kits. Perform expression analysis by qPCR using primers specific for lineage- and non-lineage-specific genes (*see* **Note 10**).

3.2 T Lymphocyte Proliferation and Survival

1. Isolate the desired T-cell compartment by FACS sorting ($CD4^+$, $CD8^+$, γδ, etc.) or set up naïve T-cell culture conditions to obtain Th subsets as described in Subheading 3.1 (*see* **Note 11**).
2. Stimulate T cells with the desired concentrations of 2C11 and 37.51 with or without TLR signaling modulators in complete RPMI media. Previous reports have demonstrated that suboptimal co-stimulation of CD28 will exacerbate the influence of TLR signaling on proliferation [15, 18, 27]. Thus, consider titrating 2C11 and 37.51 concentrations to determine the range where the optimal TLR-dependent proliferative and survival effects will occur.
3. To analyze proliferation by CFSE staining, label the cells according to the manufacturer's protocol. We typically resuspend cells with 25 μM CFDA in 1 ml PBS (no serum) per 1×10^6 cells and incubate for 15 min at 37 °C. Complete RPMI is then added to the remaining tube volume to quench the CSFE for at least 10 min at room temperature. Centrifuge at $475 \times g$ for 5 min at 4 °C and plate the cells according to the experiment. After 2–4 days in culture, analyze the cells by flow cytometry to obtain the degree of CFDA dilution as a measure of T-cell proliferation.
4. To analyze proliferation by ^{3}H-thymidine incorporation, set up desired T-cell and TLR conditions as described in **step 2** and then plate in a format suitable for your cell harvester and beta scintillation counter (e.g., 1×10^5 cells per well in triplicate in a 96-well plate). After 2–4 days in culture, wash cells and then pulse each well with ^{3}H-thymidine in RPMI for 8–12 h at 37

°C and 5 % CO_2. Lyse the cells with water and transfer the ^{3}H-thymidine bound DNA to compatible filters using a cell harvester. Analyze ^{3}H incorporation using a scintillation counter (*see* **Note 12**).

5. To analyze cellular survival, isolate and stimulate your preferred T lymphocyte population with TLR signaling modulators as described in **step 2**. After 2–5 days in culture, perform staining for apoptotic cells using a commercially available annexin V antibody. The staining of DNA through disrupted cellular membranes, typical of necrotic and dead cells, should also be analyzed using a dye such as propidium iodide (PI) or 7-aminoactinomycin D (7-AAD) (*see* **Note 13**).

3.3 T-Cell Analysis In Vivo

1. To determine the effect of a specific TLR signaling pathway in vivo, many experimental tools exist such as gene silencing and conditional knockout systems. However, to study a specific TLR pathway solely on T cells in vivo, simple T-cell transfer experiments into lymphopenic hosts can be performed as previously described [15, 19].
2. Obtain TLR-deficient T lymphocytes. These can be isolated from a variety of full TLR knockout animals commercially available. Alternatively, TLR expression can be silenced in primary WT lymphocytes through methods such as shRNA and lentiviral transduction. Isolate lymphocytes from the spleen and lymph node tissues and homogenize into suspension as described in Subheading 3.1.
3. Purify the total $CD4^+$ T-cell population (or alternative T-cell population to be studied) by magnetic separation as described in Subheading 3.1. If using gene silencing methods, virally transduce the cells according to your preferred method. Verify TLR ablation; wash the cells with complete RPMI media, and then count. If transferring lymphocytes isolated from full TLR-deficient animals separate the total $CD4^+$ T-cell population and then count the number of cells. In both cases, normalize the concentration to $10–20 \times 10^6$ cells/ml in complete RPMI media. Store on ice until immediately ready for transfer into lymphopenic animals (*see* **Note 14**).
4. Wash the T cells 3× with PBS (no serum) to remove contaminating proteins that may activate the host immune system upon transfer. Load 1 ml syringes with 500 μl volume containing $5–10 \times 10^6$ T cells. Attach 26 + ½ gauge needles to the syringes, remove air from the syringe by tapping, and store on ice. Proceed immediately to the T-cell transfer step (*see* **Note 15**).
5. Place lymphocyte-deficient host animals, such as $Rag1^{-/-}$ mice, under a heat lamp for a few minutes to enable easier visualization of lateral tail veins. Place the mouse in an appropriate

restrainer, such as a tail veiner, to allow for free access to the tail. Hold the tail straight and carefully insert the syringe needle containing T cells into the vein. Slowly push the syringe plunger to determine if the needle is properly inserted into the vein. The syringe will be easy to push and fluid flowing into the vein can be visualized if done properly. Once confirmed, slowly eject the remaining contents of the syringe into the vein and place the mouse into a clean cage (*see* **Note 16**).

6. Wait at least 24 h for the transferred cells to establish the T lymphocyte compartment in the host animals. Visually inspect the tail veins to ensure damage did not occur during the transfer process. Initialize an in vivo model system to determine the influence of TLR signaling solely on $CD4^+$ T cells according to national and institutional animal approvals and guidelines (*see* **Note 17**).

4 Notes

1. We routinely use RPMI 1640 for in vitro $CD4^+$ T-cell experiments. However, other media such as DMEM or IMDM may be just as or even more effective depending on your experiment. In all cases, 2-mercaptoethanol is added to the media to reduce oxygen radicals and promote cystine uptake. For sensitive cells such as lymphocytes, 2-ME is required for stronger activation and proliferation.
2. For differentiation cytokines, we purchase the following from Peprotech (stock concentration in sterile DI water): hIL-2 (1×10^6 U/ml), mIL-4 (10 μg/ml), and mIL-12 (10 μg/ml). We purchase the following from R & D Systems (stock concentration in sterile PBS + 0.1 % BSA): mIL-6 (10 μg/ml) and hTGFβ (2 μg/ml). For antibodies, the following are purchased from BioXcell (concentration in sterile PBS): 2C11 (1 μg/ml), 37.51 (1 μg/ml), XMG1.2 (1 μg/ml), and 11B11 (1 μg/ml). Cytokines and antibodies are reconstituted at the stock concentrations upon arrival and stored in aliquots at −80 °C prior to use. Individual laboratories should titrate both the cytokines and the antibodies before performing experiments to determine their optimal Th differentiation conditions.
3. We typically use plate-bound 2C11 and 37.51 to activate $CD4^+$ T cells. However, some laboratories use antigen-presenting cells in combination with 2C11 for T-cell activation [28]. This method, however, may be problematic for this type of experiment as antigen-presenting cells will readily respond to the TLR stimulation. Alternatively, some laboratories prefer to coat with anti-hamster Ig and add soluble 2C11 and 37.51, which are both raised in hamster. Thus, coating with anti-ham-

ster Ig can improve 2C11 and 37.51 cross-linking and lead to enhanced TCR activation.

4. ACK lysis buffer should be stored at 4 °C until immediately before use. Using cold ACK prevents damage to the leukocytes. If purchasing pre-made ACK lysis buffer, follow the manufacturer's instructions regarding volume, cell density, and incubation time.
5. For naive T-cell sorting, we stain with the following concentrations of antibodies from Biolegend: CD62L-FITC (1:100), CD25-PE (1:400), CD4-PerCP (1:1000), and CD44-APC (1:500). Labeling is performed at 4 °C for 30 min in PBS+ followed by washing with PBS+. Cells are then resuspended in 1–2 ml of PBS+ or FACS buffer. Sorting is the preferred method in our laboratory to prevent contamination of undesired populations. The presence of Tregs ($CD25^+$) or fully differentiated effector cells ($CD44^+$, $CD62L^-$) in Th differentiation cultures may drastically influence results, especially considering that various TLR pathways can be highly active in these populations [8].
6. For Th2 differentiations, we add soluble 37.51 antibody in addition to the plate-bound 37.51. For unknown reasons, this additional co-stimulation promotes further Th2 polarization in our laboratory. However, many laboratories find that treating with soluble 37.51 is unnecessary.
7. In addition to including non-TLR-treated controls, it is also beneficial to include T cells that are deficient in the TLR under study. These controls will allow for the determination of TLR modulator specificity.
8. For differentiation, proliferation, and survival experiments, T cells may be removed from the plate-bound 2C11 and 37.51 stimuli after 2 days of culture. Many labs have demonstrated that this method leads to optimal proliferation and a higher yield of differentiated cells at the end of the experiment. To perform such experiments, remove the cells from the well after 2 days of culture and count. Normalize the cells to 1×10^6 cells/ml with fresh RPMI and replate in the appropriate number of wells. In this case, it is unnecessary to add fresh cytokine and antibody. However, for Th1, Th2, and iTreg conditions, 10 U/ml of hIL-2 should be added to the fresh RPMI.
9. Intracellular cytokine or transcription factor staining can be performed with a variety of different commercially available reagents and antibodies. For iTreg cells, Foxp3 staining often requires the use of specialized kits that normally are not com-

patible with other intracellular cytokine staining kits. Be sure to check the manufacturer's instructions prior to staining.

10. qPCR primers for lineage-specific cytokines and transcription factors have been described previously [15, 19]. If performing relative mRNA analysis, be sure to include primers for housekeeping reference genes such as β-actin or GAPDH.
11. In addition to $CD4^+$ T cells, we have also adopted these methods for the study of TLRs on γδ T cells and $CD8^+$ T cells [15, 19].
12. Proliferation assays using ^3H-thymidine incorporation are not as common due to the dangers of handling radioactive materials and the cost of the necessary equipment. If your facility is not equipped for this type of experiment, many commercially available kits exist for assaying cell proliferation, including the use of CFDA as outlined in this protocol.
13. For cell survival, the PI or 7-AAD dyes will not be able to penetrate the membranes of viable cells to stain the DNA. Thus, only necrotic or damaged cells will stain with these dyes. Often times, researchers stain for both annexin V and PI in one reaction and quantitate the frequency of annexin V and PI double-positive cells as an assessment of viability.
14. For T-cell transfer studies, we commonly inject $5–10 \times 10^6$ total $CD4^+$ T cells, which is an effective range for most of our in vivo models. However, it is up to individual laboratories to determine the optimal number of T cells to transfer for their experiments.
15. Some find it useful to keep the tube of $CD4^+$ cells on ice until mice are ready to be individually injected instead of pre-loading syringes. This method may help to minimize the loss of cells if there are difficulties in injecting the tail vein. In this case, bring extra syringes and needles to the housing facility and load them individually as mice are being heated in preparation for lateral tail vein injection.
16. We commonly use tail vein injections for the reconstitution of lymphopenic animals. However, others find it easier to anesthetize the mice and perform retro-orbital i.v. injections to transfer $CD4^+$ T cells. Both methods are effective and the method choice is usually determined by comfort with technique and institutionally approved animal protocols.
17. For $CD4^+$ transfer studies, we have successfully performed these methods for models of influenza, colitis, asthma, EAE, and peptide immunizations. Make sure to check the relevant literature to determine if the desired TLR-T-cell pathway experimental model system will be compatible with these protocols.

Acknowledgement

The authors thank members of the Reynolds lab at RFUMS and the Chen Dong lab at the MD Anderson Cancer Center for developing and optimizing these procedures. This work was supported by a grant to J.M.R. (K22AI104941) from the National Institutes of Health.

References

1. Medzhitov R, Preston-Hurlburt P, Janeway CA Jr (1997) A human homologue of the Drosophila Toll protein signals activation of adaptive immunity. Nature 388:394–397
2. Kawai T, Akira S (2010) The role of pattern-recognition receptors in innate immunity: update on Toll-like receptors. Nat Immunol 11:373–384
3. Blasius AL, Beutler B (2010) Intracellular toll-like receptors. Immunity 32:305–315
4. Kawai T, Akira S (2009) The roles of TLRs, RLRs and NLRs in pathogen recognition. Int Immunol 21:317–337
5. Akira S, Takeda K (2004) Toll-like receptor signalling. Nat Rev Immunol 4:499–511
6. West AP, Koblansky AA, Ghosh S (2006) Recognition and signaling by toll-like receptors. Annu Rev Cell Dev Biol 22:409–437
7. Yamamoto M, Sato S, Hemmi H et al (2003) Role of adaptor TRIF in the MyD88-independent toll-like receptor signaling pathway. Science 301:640–643
8. Reynolds JM, Dong C (2013) Toll-like receptor regulation of effector T lymphocyte function. Trends Immunol 34:511–519
9. Pasare C, Medzhitov R (2005) Control of B-cell responses by Toll-like receptors. Nature 438:364–368
10. Rawlings DJ, Schwartz MA, Jackson SW et al (2012) Integration of B cell responses through Toll-like receptors and antigen receptors. Nat Rev Immunol 12:282–294
11. Conroy H, Marshall NA, Mills KH (2008) TLR ligand suppression or enhancement of Treg cells? A double-edged sword in immunity to tumours. Oncogene 27:168–180
12. Liu G, Zhao Y (2007) Toll-like receptors and immune regulation: their direct and indirect modulation on regulatory CD4+ CD25+ T cells. Immunology 122:149–156
13. Sutmuller RP, Morgan ME, Netea MG et al (2006) Toll-like receptors on regulatory T cells: expanding immune regulation. Trends Immunol 27:387–393
14. Matsuguchi T, Takagi K, Musikacharoen T et al (2000) Gene expressions of lipopolysaccharide receptors, toll-like receptors 2 and 4, are differently regulated in mouse T lymphocytes. Blood 95:1378–1385
15. Reynolds JM, Martinez GJ, Chung Y et al (2012) Toll-like receptor 4 signaling in T cells promotes autoimmune inflammation. Proc Natl Acad Sci U S A 109:13064–13069
16. Watanabe T, Inoue T, Ochi H et al (1999) Lipid A directly inhibits IL-4 production by murine Th2 cells but does not inhibit IFN-gamma production by Th1 cells. Eur J Immunol 29:413–418
17. Imanishi T, Hara H, Suzuki S et al (2007) Cutting edge: TLR2 directly triggers Th1 effector functions. J Immunol 178:6715–6719
18. Komai-Koma M, Jones L, Ogg GS et al (2004) TLR2 is expressed on activated T cells as a costimulatory receptor. Proc Natl Acad Sci U S A 101:3029–3034
19. Reynolds JM, Pappu BP, Peng J et al (2010) Toll-like receptor 2 signaling in CD4(+) T lymphocytes promotes T helper 17 responses and regulates the pathogenesis of autoimmune disease. Immunity 32:692–702
20. Tomita T, Kanai T, Fujii T et al (2008) MyD88-dependent pathway in T cells directly modulates the expansion of colitogenic CD4+ T cells in chronic colitis. J Immunol 180:5291–5299
21. Babu S, Blauvelt CP, Kumaraswami V et al (2006) Cutting edge: diminished T cell TLR expression and function modulates the immune response in human filarial infection. J Immunol 176:3885–3889
22. Chen X, Zhang M, Zhu X et al (2009) Engagement of Toll-like receptor 2 on CD4(+) T cells facilitates local immune responses in patients with tuberculous pleurisy. J Infect Dis 200:399–408
23. Gonzalez-Navajas JM, Fine S, Law J et al (2010) TLR4 signaling in effector CD4+ T cells regulates TCR activation and experimental colitis in mice. J Clin Invest 120:570–581

24. Dong C, Flavell RA (2000) Cell fate decision: T-helper 1 and 2 subsets in immune responses. Arthritis Res 2:179–188
25. O'Shea JJ, Paul WE (2010) Mechanisms underlying lineage commitment and plasticity of helper CD4+ T cells. Science 327:1098–1102
26. Zhou L, Chong MM, Littman DR (2009) Plasticity of CD4+ T cell lineage differentiation. Immunity 30:646–655
27. Mercier BC, Cottalorda A, Coupet CA et al (2009) TLR2 engagement on CD8 T cells enables generation of functional memory cells in response to a suboptimal TCR signal. J Immunol 182:1860–1867
28. Veldhoen M, Hocking RJ, Atkins CJ et al (2006) TGFbeta in the context of an inflammatory cytokine milieu supports de novo differentiation of IL-17-producing T cells. Immunity 24:179–189

Chapter 15

Analysis by Flow Cytometry of B-Cell Activation and Antibody Responses Induced by Toll-Like Receptors

Egest J. Pone

Abstract

Toll-like receptors (TLRs) are expressed in B lymphocytes and contribute to B-cell activation, antibody responses, and their maturation. TLR stimulation of mouse B cells induces class switch DNA recombination (CSR) to isotypes specified by cytokines, and also induces formation of IgM^+ as well as class-switched plasma cells. B-cell receptor (BCR) signaling, while on its own inducing limited B-cell proliferation and no CSR, can enhance CSR driven by TLRs. Particular synergistic or antagonistic interactions among TLR pathways, BCR, and cytokine signaling can have important consequences for B-cell activation, CSR, and plasma cell formation. This chapter outlines protocols for the induction and analysis of B-cell activation and antibody production by TLRs with or without other stimuli.

Key words Antibody, AID, B cells, B-cell receptor (BCR), CpG, Class switch DNA recombination (CSR), Cytokine, Germinal center, Immunoglobulin, Lipopolysaccharides (LPS), T-independent antibody response, Toll-like Receptor (TLR)

1 Introduction

The role of Toll-like receptors (TLRs) in B-cell activation and antibody responses has a long history, predating the identification of the actual receptors. One of the first reports of antibody production in vitro [1] was followed by more detailed studies of microbe-associated molecular patterns (MAMPs), such as lipopolysaccharides (LPS) [2–4] and flagellin [5, 6], in the production of immunoglobulin (Ig) M (19 Svedberg, 19S) and class-switched, mainly IgG (7S) antibodies. LPS was found to induce not only primary, but also memory antibody responses in mice [7, 8]. The mechanisms behinds such phenomena become clearer only after mammalian TLRs were first identified in the late 1990s [9, 10]. Whether nonprotein MAMPs such as LPS could induce genuine antibody responses in a T-independent way remained contentious even after TLRs were discovered [11–14], though the current overall view is

Claire E. McCoy (ed.), *Toll-Like Receptors: Practice and Methods*, Methods in Molecular Biology, vol. 1390,
DOI 10.1007/978-1-4939-3335-8_15,

that TLR signaling in B cells contributes significantly to multiple aspects of their antibody responses [13, 15–18].

B-cell activation, proliferation, and antibody production is now known to require signals from a multitude of receptors with unique functions, including the quintessential B-cell receptor (BCR), tumor necrosis factor receptors (TNFRs), particularly CD40, cytokine receptors, and pattern recognition receptors (PRRS), particularly TLRs [17, 19–21]. Although dendritic cells (DCs) sense MAMPs to activate T and B lymphocytes, signals from both innate and adaptive immune receptors can be triggered directly in B cells [20, 21]. Human and mouse B cells express most TLRs and respond to their ligands, which is in agreement with their capability to phagocytose and extract antigen [22–25]. TLR activation of B cells leads to their proliferation and production of IgM antibodies to contain pathogens, particularly for blood-borne infections, during the early stages of infection [26], and also leads to upregulation of MHC-II and co-stimulatory CD40, CD80/CD86 receptors, thereby priming B cells for interactions with activated cognate Th cells [27, 28]. Thus, TLR stimulation of B cells during the germinal center (GC) reaction may enhance antibody maturation [29].

Maturation of the antibody response includes class switch DNA recombination (CSR), which substitutes constant heavy chain regions to change Ig biological effector functions, and somatic hypermutation (SHM), which introduces mutations in variable regions to alter affinity for antigen. As the contribution of TLRs in antibody responses has been more extensively characterized for CSR than SHM, this chapter addresses the role of TLR signaling in B-cell activation and CSR, though the B-cell-intrinsic role of TLRs in SHM is likely also highly important. CSR is central to the maturation of antibody responses and is induced in both T cell-dependent (T-dependent) and T-independent ways, in both cases requiring expression of activation induced cytidine deaminase (AID) and germline, or sterile, transcription of the immunoglobulin (Ig) constant heavy chain (C_H) gene loci participating in recombination [17]. Cytokines, such as IL-4, IFNγ, and TGFβ do not directly induce sustained B-cell activation or AID induction, but rather enhance CSR to particular isotypes through their induction of germline transcription [17, 19]. AID catalyzes the deamination of deoxycytosines (dC) to deoxyuracils (dU), which are then are removed by base excision repair (BER) and mismatch-repair (MMR) pathways [30], eventually resulting in double strand DNA breaks in the two recombining S regions. Ligation of these DNA breaks mainly by nonhomologous end joining (NHEJ) then completes CSR [19, 31]. Whether there are any mechanistic differences in these CSR steps by various T-dependent or T-independent stimuli is largely unknown. The TLR4 ligand LPS induces both

AID and germline transcription associated with CSR to IgG2b and IgG3, in effect inducing CSR to these two isotypes independent of any other known stimuli. Other stimuli, such as cytokines and BCR crosslinking reagents, may enhance TLR-induced CSR [32].

During the changing phases of the immune response in vivo, TLR signals likely play a particularly informative role as direct reporters of microbe burden and instruct the immune system on how best to respond to the threat. Presumably, in vivo, different TLR ligands in various states of aggregation are sensed by phagocytes, including B cells, on the plasma membrane and in phagocytic compartments (including TLR endosomes). For the dectin receptor, zymosan was shown to be more potent at higher aggregation states compared to the soluble forms [33]. Antibody responses to whole microorganisms have also been intensely investigated, and arguably most closely reflect the natural immune response to infection [34]. Integrating TLR and BCR signals typically increases B-cell activation and CSR, but pairwise or more combinations of TLRs does not necessarily result in increased CSR. This interesting phenomenon of TLR signaling paralysis has been reported in the literature but remains poorly understood. For example, prolonged stimulation with TLR7 agonists diminished B-cell responses, but BCR signaling could reverse this homologous TLR-induced tolerization [35]. B cells stimulated with combinations of TLR agonists exhibited synergistic or antagonistic responses [36, 37]. CpG was reported to suppress CD40-induced CSR to IgG1 and IgE, but enhanced CSR to IgG2a isotype [38]. Telomeric DNA or DNA from apoptotic cells suppressed B-cell activation [39, 40], whereas repetitive vaccination of mice with high doses of CpG suppressed germinal centers and antibody responses [41]. Thus, the sequence and timing of activation of particular TLRs can either heighten or reduce the B-cell responsiveness to additional stimulation by homologous or heterologous TLRs or other receptors.

TLR research has benefited by the availability of high quality, purified, or synthetic TLR ligands and associated reagents from a number of commercial sources. Nevertheless, certain features of TLRs and their ligands necessitate optimization of protocols for specific experiments, and several important points are detailed in Subheading 4. For example, since some TLRs require accessory factors for delivery of their ligands, such as LPS-binding protein (LBP), which facilitates the binding of LPS to TLR4, or granulin and HMGB1, which bind CpG to influence TLR9 responses [42], the particular lot or batch of fetal bovine serum (FBS) containing these accessory factors is critical for optimal B-cell activation, proliferation, and CSR. The use of CFSE to track CSR across each division is essential to evaluate the influence of TLRs in different culture conditions. For example, the cytokines IFNγ and TGFβ are

required to direct TLR-driven CSR to IgG2a and IgG2b isotypes, respectively; however, at the concentrations required to induce CSR (on the order of ng/ml) these cytokines exert their well-known anti-proliferative effects. Plotting CFSE in the *x*-axis vs. Ig in the *y*-axis gives a more objective measure of CSR compared to 'bulk' CSR measured by other flow cytometry configurations or by PCR or ELISA.

Other considerations apply to the unique features of particular TLR ligands or agonists. For example, in the author's experience, the TLR3 ligand poly I: poly C does not induce strong B-cell activation and CSR regardless of conditions, but other modified ligands (e.g., poly I: poly C12U, also known as Rintatolimod or Ampligen) may be tested to possibly elicit stronger TLR3 signaling. Monomeric flagellin may not cross-link TLR5 as efficiently as polymerized flagellin or flagellar segments. The TLR9 ligand CpG oligodeoxynucleotide (ODN) containing certain unmethylated CG sequences stimulates B cells most strongly when it is from a particular class of sequences known as class B/K [43, 44]; also, murine and human cells also sense different CG sequence motifs and may not always be interchangeable [43, 45]. Furthermore, CpG modified with a phosphorothioated backbone resists nucleases and thus has a longer half-life [44], whereas GpC ODN or methylated CpG ODN can be used as controls. In some studies, anti-TLR antibodies can also be used to trigger TLR signaling. Since some TLR ligands may engage more than their cognate receptor depending on conditions, wherever possible TLR or TLR adaptor knockout mice may be used. This chapter describes flow cytometry procedures of analyzing the contribution of TLRs in murine B-cell activation, proliferation, and class-switched antibody production in vitro (*see* **Notes 1–3**). An earlier article in the same series also contains useful information [46].

2 Materials

2.1 Isolation of Murine B Cells

1. C57BL/6 J mice maintained in pathogen-free vivaria are typically used at 8–12 weeks of age unless otherwise required (*see* **Note 4**).
2. Surgical tools, such as forceps and scissors, for mouse dissection.
3. 70 % Ethanol.
4. Naïve B-cell purification kit (STEMCELL Technologies, Inc. or Miltenyi Biotec).
5. Cell strainers, 70 μm (BD Biosciences).
6. Red blood cell (RBC) lysis solution (ACK lysing buffer, Lonza).

7. Fetal bovine serum (FBS). Individual lots or batches must first be tested as described in the Introduction (also, *see* **Note 5**).
8. RPMI-1640 (*see* **Note 6**), supplemented with 10 % FBS, antibiotics and 50 μM β–mercaptoethanol (BME) (*see* **Note 7**). Antibiotics include, e.g., penicillin and streptomycin with or without the anti-fungal amphotericin B.
9. PBS buffer for B-cell purification.
10. General cell culture materials: 1.5 ml, 15 ml and 50 ml sterile tubes.

2.2 B-Cell Labeling and Stimulation

1. A fluorescent dye to label B cells to track their cell divisions, e.g., carboxyfluorescein succinimidyl ester (CFSE; Life Technologies).
2. TLR ligands include: LPS from *E. coli* (e.g., serotype 055:B5, Sigma-Aldrich) used at 0.1–10 μg/ml; Pam_3CSK_4 (Invivogen) used at 0.1–1 μg/ml; R848 (Invivogen) used at 0.01–0.1 μg/ml; CpG ODN 1826, abbreviated to "CpG", sequence 5′-TCCATGACGTTCCTGACGTT-3′ with a phosphorothioate backbone, typically ordered on a 1 μmol scale, desalted (the sequence of the control "GpC" ODN 1745 is 5′-TCCATGAGCTTCCTGAGTCT-3′) used at 0.1–1 μM. Resuspend stock solutions (e.g., 100×–1000×) of TLR ligands in molecular biology grade and endotoxin-free water, store in small (~50–200 μl) aliquots frozen at −80 °C and avoid multiple freeze-thaw cycles.
3. Commonly used cytokines (R&D Systems, TONBO Biosciences) include: recombinant murine IL-4 (IL-4) used at 0.5–5 ng/ml for CSR to IgG1 and IgE; recombinant murine IFNγ used at 5–50 ng/ml for CSR to IgG2a/IgG2c; recombinant murine TGFβ used at 0.5–5 ng/ml for CSR to IgG2b and IgA; recombinant murine IL-5 used at 0.5–5 ng/ml for enhancing the production of plasma cells.
4. Other reagents that synergize with TLRs to enhance CSR and/or plasma cell formation, or that can serve as comparisons: dextran-conjugated rat anti-mouse IgD ("anti-IgD-dextran", which is δ chain specific, clone 11–26, Fina Biosolutions, LLC); soluble goat $F(ab')_2$ anti-mouse IgM (μ chain specific, Southern Biotech); anti mouse-CD40 mAb (clone 1C10, eBioscience) or purified membranes containing glycosylated, trimeric CD40 ligand from baculovirus-infected insect cells [47] (*see* **Note 8**).
5. Common cell culture materials: 24 well plates, PBS buffer to make appropriate reagent stocks, pipets, hemocytometer, and trypan blue to count cells.

2.3 Flow Cytometry Acquisition and Analysis

1. Flow cytometer with at least 4 channels (e.g., BD FACSCalibur™), with 7 channels preferred (e.g., BD™ LSR II) and manufacturer's data acquisition and analysis software.
2. Additional flow cytometry analysis software (e.g., FlowJo, Tree Star, Inc.).
3. Flow cytometry staining buffer: PBS with 1 % BSA.
4. Appropriate flow cytometry tubes or plates
5. A fluorescent viability dye, such as 7-aminoactinomycin D (7AAD).
6. Antibodies to detect key B-cell markers: CD45R/B220 to mark B cells and reveal their developmental/differentiation stage(s); CD38 to mark germinal center B cells in vivo and germinal center-like B cells in vitro (where CD38 is downregulated); CD138 (syndecan-1) to mark plasmablasts and plasma cells; and IgM and other antibody isotypes relevant to the experiment. Other common markers used for various activation stages of murine B cells, such as CD19, PNA or GL7, can be used depending on experiment (*see* **Note 9**). A 7-color staining configuration for the BD™ LSR II cytometer is:
   (a) CFSE
   (b) PE—anti-B200
   (c) 7AAD
   (d) PerCP-Cy5.5—anti-IgM (or IgD)
   (e) PE-Cy7—anti-CD38
   (f) APC—anti-IgG1 (or other IgG isotypes, IgE, IgA)
   (g) APC-Cy7—anti-CD138

3 Methods

3.1 Isolation of Murine B Cells

1. Sacrifice mouse by CO_2 asphyxiation followed by cervical dislocation. Spray mouse with 70 % ethanol to disinfect and minimize hair contamination.
2. Remove spleen and/or lymph nodes of interest (*see* **Note 10**) and place in RPMI or PBS in a 1.5 ml tube and proceed to the next step as soon as practicable; several mice can be processed in vivarium and then transported to laboratory for B-cell purification by a single researcher, though working in teams can minimize delays. For a description of murine lymph nodes and their anatomical location refer to [48].
3. Prepare single cell suspensions of splenocytes or lymph node cells by crushing spleen or nodes with a sterile object, such as

a 15 ml tube or syringe plunger, through the 70 μm cell strainer placed on top of a 50 ml tube. Flush cells from strainer repeatedly with a total of ~10–15 ml RPMI or PBS. Note that the spleen can be dissociated rather quickly, but lymph nodes tend to clog the filter and require more time. Avoid crushing dark spots in the spleen, occasionally found near either tip of spleen. If filter breaks during crushing, re-filter all cell suspension through a new strainer.

4. Centrifuge at 500 × *g* for 5 min to collect all cells.
5. Remove supernatant carefully without disturbing the last few hundred microliters close to the pellet. Spleen pellets are consistently smaller than lymph node pellets, which are less defined and overlaid by adipose material. Nevertheless, this loose material is typically lost in the next purification steps.
6. Lyse RBCs by resuspending each splenocyte or lymph nodes cell pellet in 5 ml ACK lysing buffer for 5 min, followed by quenching with 20 ml RPMI or PBS.
7. Centrifuge as in **step 4** above; pellets should have no visible RBC layer and instead should appear in off-white color.
8. Resuspend in ~ 1 ml PBS or in medium recommended by the manufacturer of the B-cell purification kit. Determine cell concentration by making several dilutions in trypan blue and counting using a hemocytometer. Adjust cell concentration to that recommended by the manufacturer of the B-cell purification kit, frequently ~10^7 cells/ml. Save an aliquot of this whole cell preparation to determine the purity of the B-cell isolation in subsequent steps.
9. Purify B cells by exactly following instructions on the B-cell purification kit. Purification based on negative selection (e.g., depleting cells that express CD43, CD4, or Ter-119) is preferred to that based on positive selection of B cells, as the former method ensures receptors on B cells are not engaged. For specialized applications, certain B-cell subpopulations can be isolated by fluorescence activated cell sorting (FACS).
10. Determine the purity of the B-cell prep by flow cytometry as suggested in Subheading 2.3.6 above. Alternatively, the cell preparation can be stained and fixed with 1 % formaldehyde and analyzed by flow cytometry together with the stimulated cultures several days later.

3.2 B-Cell Labeling and Stimulation

1. Label purified B cells with CFSE as follows (*see* **Note 11**). Briefly, prepare a cell suspension of ~ 10 million B cells in PBS and equilibrate at 37 °C in a water bath (there should be no BSA or FBS in this suspension as they quench CFSE; to change

buffers if necessary, spin cells at 500 × *g* for 5 min and resuspend in PBS). Then add a final concentration of 2.5 μM CFSE (e.g., from a 2.5 mM, 1000× stock), quickly flicker the tube several times to ensure uniform distribution of the dye, and incubate for 2.5 min at 37 °C. Quench with 5–10 volumes of complete RPMI containing 10 % FBS (e.g., to quench 15 million CFSE-labeled B cells in a 1.5 ml tube, add these cells to a 15 ml tube containing 13.5 ml complete RPMI). Centrifuge at 500 × *g* for 5 min to collect the cells, resuspend pellet in 1.5 ml complete RPMI and centrifuge again to pellet the cells (this step removes any remaining CFSE that is otherwise toxic to the cells).

2. Resuspend the purified, CFSE-labeled or unlabeled B cells (*see* **Note 12**) at 50×10^5/ml in complete RPMI (10 % FBS, antibiotics and 50 μM BME as in **item 7**, Subheading 2.1) and use this B-cell suspension in the subsequent stimulation assays.

Assay 1. The purpose of this assay is to determine how concentrations of LPS and IL-4 induce CSR to IgG1 and IgG3. In a 24 well plate, titrate LPS along plate columns at six different concentrations (at 0, 0.1, 0.3, 1.0, 3.0, and 10.0 μg/ml) and IL-4 along plate rows at 4 different concentrations (at 0, 0.2, 1.0, and 5.0 ng/ml), as illustrated in Table 1. Approximately 5–15 % of the cells will undergo CSR to IgG3 at 10.0 μg/ml LPS without IL-4, and 20–40 % of the cells will undergo CSR to IgG1 at 10.0 μg/ml LPS with 5 ng/ml IL-4.

Assay 2. The purpose of this assay is to determine how concentrations of the TLR9 ligand CpG ODN 1826 and BCR crosslinking in the presence of IL-4 induce CSR to IgG1.

In a 24 well plate, include IL-4 at 2 ng/ml in all wells. Then titrate CpG (at 0, 0.03, 0.1, 0.3, 1.0, and 3.0 μM) and anti-IgD-dextran (at 0, 1, 10, and 100 ng/ml) or soluble anti-mouse IgM (at 0, 10, 100, and 1000 ng/ml, *see* **Note 13**), as shown in Table 2. Typically, about 20–40 % of the cells will undergo CSR to IgG1 at 0.3 μM CpG and 100 ng/ml anti-IgD-dextran (and 2 ng/ml IL-4).

Table 1
Titration of LPS and IL-4 for induction of CSR to IgG1 and IgG3

	LPS (μg/ml):					
IL-4 (ng/ml):	**0**	**0.1**	**0.3**	**1.0**	**3.0**	**10.0**
0						
0.2						
1.0						
5.0						

Table 2
Titration of CpG and anti-IgD-dextran ("α-IgD") for CSR to IgG1 in the presence of IL-4

	CpG (μM):					
α-IgD (ng/ml):	**0**	**0.03**	**0.1**	**0.3**	**1.0**	**3.0**
0						
1						
10						
100						

Assay 3. The purpose of this assay is to determine how concentrations of several TLR ligands in the presence of BCR crosslinking (where indicated) and cytokines induce CSR to specific isotypes. Add the following TLR ligands (and BCR crosslinking antibodies where indicated): in all six wells of the first row, add 100 ng/ml Pam_3CSK_4 plus 100 ng/ml anti-IgD dextran; in all six wells of the second row, add 10 μg/ml LPS; in all six wells of the third row, add 30 ng/ml R848 plus 100 ng/ml anti-IgD dextran; in all six wells of the third row, add 0.3 μM CpG plus 100 ng/ml anti-IgD dextran. Next, add the following cytokines down each column as follows: in all four wells of the first column, add no cytokines (this column will be analyzed for CSR to IgG3); in all four wells of the second column, add 2 ng/ml IL-4 (this column will be analyzed for CSR to IgG1); in all four wells of the third column, add 2 ng/ml IL-4 (this column will be analyzed for CSR to IgE by an intracellular staining protocol, also *see* **Note 4**); in all four wells of the third column, add 25 ng/ml IFNγ (this column will be analyzed for CSR to IgG2a/IgG2c); in all four wells of the fifth column, add 2 ng/ml TGFβ (this column will be analyzed for CSR to IgG2b); in all four wells of the sixth column, add 2 ng/ml TGFβ (this column will be analyzed for CSR to IgA). This assay is illustrated in Table 3. CSR efficiencies will vary from ~ 5 % CSR to IgE, 5–15 % CSR to IgG2a, IgG2b, IgG3, and IgA and 20–40 % CSR to IgG1. To obtain even higher levels of CSR to IgG1, the best condition typically includes intermediate concentrations of LPS, 100 ng/ml anti-IgD-dexran, and 5 ng/ml IL-4.

In summary, variations of these basic assays can be designed to investigate how two or more TLRs and other receptors influence B-cell activation, proliferation, CSR, and plasma cell formation.

3.3 Flow Cytometry Acquisition and Analysis

1. After 4 days of culture (*see* **Note 14**), analyze the cells by flow cytometry as follows.
2. Resuspend cells and transfer to 1.5 ml tubes.

Table 3
Induction of CSR to specific isotypes by TLR ligands, BCR crosslinking, and cytokines

Isotype analyzed:	IgG3	IgG1	IgE	IgG2c	IgG2b	IgA
Cytokine:	None	IL-4 (2 ng/ml)	IL-4 (2 ng/ml)	IFNγ (25 ng/ml)	TGFβ (2 ng/ml)	TGFβ (2 ng/ml)
Pam_3CSK_4 (30 ng/ml)[a]:						
LPS (10 μg/ml):						
R848 (30 ng/ml)[a]:						
CpG (0.3 μM)[a]:						

[a]Note: in each of the six wells of these rows also add 100 ng/ml anti-IgD-dextran

3. Centrifuge at 500 × *g* for 5 min to collect the cells and remove the supernatant by vacuuming and leaving behind ~20 μl of supernatant so as not to disturb the pellet; although this volume of liquid left behind generally does not interfere with analysis, if necessary it can be removed manually using a fine pipet. The supernatant can also be stored for analysis by ELISA (*see* **Note 1**).
4. Stain cells in 50 μl of mastermix containing fluorescent antibodies (*see* **Note 15**) and cell viability dye (such as 7-AAD) in PBS (*see* **Note 16**) for 15 min at room temperature.
5. Wash by adding 10–20 volumes (~1.4 ml) of PBS and centrifuge at 500 × *g* for 5 min.
6. Resuspend in ~ 300–500 μl PBS and transfer to flow cytometry tubes.
7. Collect flow cytometry data following manufacturer's instructions and core facility guidelines. Use unstained cells to set appropriate voltages and singly stained compensation controls. Collect at least 10,000 live events, which can mean collecting even more total events.
8. Process data by first performing compensation using software such as FlowJo.
9. Gate live cells in the forward scatter (cell size) vs. side scatter (cell surface granularity) plot. Figure 1a shows representative gating strategies in this and subsequent steps.
10. Gate single cells using a diagonal pulse area vs. height gate [49].
11. Exclude dead cells using the 7-AAD$^-$ gate [50].
12. Determine cell division gating either manually (if individual divisions are clearly visible) or by deconvolution of individual divisions using the "proliferation platform" of FlowJo.

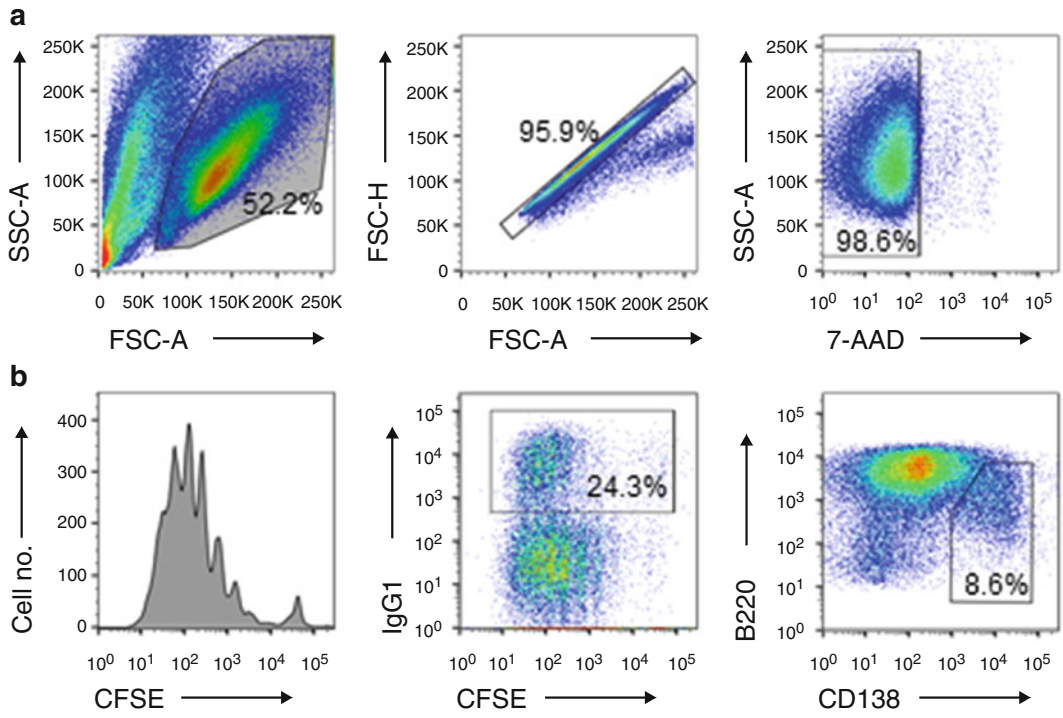

Fig. 1 Analysis of B-cell proliferation, class switching, and plasma cell formation in response to stimulation with LPS and IL-4. (**a**) Gating strategy for single, live cells involves gating the appropriate forward scattering vs. side scattering (*left panel*), then gating for single cells by selecting the diagonal in a pulse area vs. pulse height plot (*middle panel*), and finally gating for live cells that are able to expel 7-AAD and thus are 7AAD$^-$ (*right panel*). (**b**) CFSE-labeled B cells purified from the combined lymph nodes of a C57BL/6 J mouse were stimulated with LPS and IL-4, and B-cell proliferation (*left panel*), CSR to IgG1 (*middle panel*) and B220^{lo} CD138^{hi} plasma cell formation (*right panel*) were measured by flow cytometry 4 days later as described in the main text

13. Plot CFSE (*x*-axis) vs. surface Ig or other markers (*y*-axis). Figure 1b illustrates typical examples of plots. For more examples, see reference [32] and supplementary figures therein.
14. For plasma cells, plot CD138 in *x*-axis vs. B220 in *y*-axis.
15. Analyze other pairwise plots according to relevance to the particular experiment and by applying appropriate gates (*see* **Note 17**).
16. Typical results should include about 5–10 cell divisions after 3–4 day stimulation. Plasma cell formation (defined as B220^{lo} CD138$^+$) should be readily visible by day 2, and class-switched B cells by day 3. Although most of the plasma cells are IgM$^+$ until days 3–4, by day 5 a significant fraction of the plasma cells can be class-switched (*see* **Note 18**). When analyzing all B cells, class-switching to IgG1 is most efficient, reaching ~ 20–40 % by day 4 under most optimal stimulations with TLRs and other stimuli.

4 Notes

1. Other methods of analyzing B-cell activation and CSR include, e.g., immunoblotting, PCR, and ELISA [32]. Immunoblotting can be used to analyze the activation of TLR and other signaling pathways. Immunoblotting was also traditionally used to analyze the various chains and isotypes of antibodies (and remains in use for selected clinical tests of antibodies) but has been largely superseded by the above methods. PCR, whether semiquantitative or real-time quantitative, provides important information on Ig germline transcripts, circle transcripts, post-recombination transcripts, and mature transcripts, that reflect various stages of CSR and antibody production [17]. For example, the levels of Ig circle transcripts indicate active or ongoing CSR and therefore can distinguish between CSR occurring across a large fraction of B cells as opposed to amplification of only a few class-switched B cells [51], which is information that cannot be attained by flow cytometry or ELISA. Likewise, assays such as ELISA and ELISPOT provide complementary information on the levels of antibodies secreted by plasma cells [52]. Newer technologies, particularly next generation and single cell sequencing, are increasing the nature and amount of information on antibody biology [53].
2. The influence of TLRs on B-cell activation and antibody responses has also been studied in vivo in wt and genetically modified mice [15, 16, 54]. B cells and plasma cells can be purified from lymphoid organs and blood and analyzed by flow cytometry similar to their in vitro analysis in this chapter. For more experimental details see references [55, 56].
3. Human B cells also express and respond to TLR stimulation by making class-switched antibodies [57, 58], though there are two main differences compared to murine B cells. First, human B cells express low levels of TLR4 and therefore are not as sensitive to LPS stimulation. Second, CSR to IgG1, IgG2, IgG3, and IgG4 in human B cells does not appear to depend as strongly on specific cytokines (e.g., IL-4, IFNγ, TGFβ) the way murine IgG1, IgG2a/IgG2c, IgG2b, and IgG3 depend. IL-21 greatly enhances CSR to IgG induced by CD40 and IL-4 [59], though whether this applies to TLR-induced CSR has not been investigated. Of course, additional cytokine combinations and other signals may enhance CSR to specific isotypes both human and murine B cells.
4. B cells from different mouse strains can have subtle differences in CSR to certain isotypes, as shown in reference [60]. Also, IgG2a may be sufficiently different in C57BL/6 mice compared to other strains to be classified as the separate isotype IgG2c [61], and therefore may require higher concentrations of anti-IgG2a

antibodies for their detection in flow cytometry and ELISA experiments. IgE binds the high affinity FCεRI on B cells, and therefore requires special processing to detect it unambiguously [62]. Similar methods may be used if there are concerns about binding of other isotypes to Fc receptors on B cells.

5. It is highly recommended that B-cell researchers test samples of 5–10 different FBS lots/batches from different vendors, and reserve 1–2 lots that give optimal results [63]. The particular FBS company or catalog number is not important. FBS can be heat-inactivated (e.g., 30 min at 56 °C) to inactivate bovine complement that may otherwise lyse antibody-opsonized murine lymphocytes, though the method of FBS heat-inactivation, if any, is best determined by individual laboratories. Although lymphocytes can be grown in serum-free media under some conditions [64], the requirement for extracellular accessory molecules for TLRs (such as LBP or granulin) complicates the use of serum-free media in B-cell TLR studies.
6. The source of the commercial RPMI-1640 medium is not important since it is a chemically defined medium and essentially the same. Some researchers supplement media with additional glutamine or pyruvate; in the author's experience, this is not necessary. For specific studies, the concentration of particular nutrients (e.g., glucose) can be controlled by using appropriate medium formulations. If the use of particular antibiotic or anti-mycotic agents interfere with some assays, other agents, e.g., gentamycin, can be tested.
7. The role of reducing agents such as BME and dithiothreitol (DTT) is critical for optimal murine B-cell activation and CSR. This issue was investigated in the 1970s and 1980s [65–67] as well as more recently [68]. The requirement for reducing agents in medium is less important for human compared to murine B cells. In the author's experience, DTT (titrated at submillimolar levels) can substitute for BME in inducing comparable B-cell activation and CSR. These mild reducing agents may enhance the intracellular concentrations of cysteine or maintain normal intracellular redox potential via the glutathione system, but nevertheless the actual mechanisms remain mysterious. It is intriguing that lymphocytes contain abundant redox-labile surface receptors [69], and chemokines and certain cytokines (such as TGFβ) are sensitive to redox conditions [70].
8. Although it is recommended that reagents be matched to the B-cell species under study, some reagents work well in other species depending on degree of molecular homology; e.g., human TGFβ and CD40L can be used to stimulate both human and mouse B cells.

9. The particular staining scheme depends on the purposes(s) of the experiment and flow cytometer available. If only a 4-color cytometer is available, the 7-color scheme can be broken down into several 4-color schemes, which increases the amount of work while decreasing the quality of information obtained. If antibodies are not available directly conjugated to certain fluorophores, indirect streptavidin : biotin staining can be used, with these two components preferably titrated to determine optimal concentration ranges.
10. Murine spleens contain mostly IgM^{lo} IgD^{hi} B2 follicular B cells, but also a distinct IgM^{hi} IgD^{lo} marginal zone (MZ) B-cell population. If experiments on MZ B cells are needed, they can be obtained by cell sorting; conversely, essentially pure B2 follicular B cells can be obtained by purifying B cells from lymph nodes which do not contain MZ B cells. In the author's experience, B cell from both spleen and lymph nodes readily respond to TLR stimulation.
11. Variables in the CFSE staining protocol, particularly dye and cell concentration, buffer and temperature, are critical for optimal assays. Using high concentrations of CFSE on the one hand strongly labels the naïve (zero division) population and allows for up to ~10 discernible individual divisions, but on the other hand is toxic to the cells and the response may therefore be due to amplification of resistant cells rather than the original population. Using low concentrations of CFSE is not toxic to the cells and thus results are representative of the bulk of the original population (similar to the unlabeled population), but only a few divisions can be seen before merging with the autofluorescent (or unlabeled) population [71]. In the author's experience, 1–5 μM CFSE staining 10 million B cells for 1–5 min at 37 °C represent the low and high range of staining; 2.5 μM CFSE for 2.5 min followed by 2 washes is a good compromise.
12. When culturing purified B cells that are not labeled with CFSE, although the purification kit's B-cell elution buffer typically contain 2 mM EDTA (which chelates Ca^{2+}, a cation that is essential for cell activation and proliferation), diluting this cell suspension at least tenfold into culture medium allows for essentially normal levels of Ca^{2+} in RPMI. Alternatively, for measurement of Ca^{2+} influx in response to BCR or MHCII crosslinking, or for other sensitive assays, cells can be centrifuged and then resuspended in the appropriate solution or medium.
13. BCR signaling can be induced by crosslinking the BCR either with polymeric antigen, which would require use of BCR-transgenic mouse strains specific for the antigen, or more commonly with antibodies that bind to conserved regions of

IgM or IgD on naïve B cells. Follicular B2 cells express high levels of IgD and low levels IgM, so using antibodies that crosslink IgD is more efficient. Also, antibodies that are either immobilized on the assay plate, or are conjugated on polymeric scaffolds such as acrylamide, agarose beads, or dextran can trigger BCR signaling at lower doses than soluble antibodies due to avidity effects [72]. In the author's experience, anti-IgD antibodies conjugated to dextran (Fina Biosolutions, LLC) enhance TLR-driven CSR at concentrations on the order of 1–100 ng/ml, whereas unconjugated, soluble $F(ab')_2$ anti-mouse IgD or $F(ab')_2$ anti-mouse IgM require 10–100 fold more antibodies to give comparable CSR. Although reagents such as goat $F(ab')_2$ anti-mouse IgM are typically used at ~ 10 μg/ml to trigger Ca^{2+} influx, these are proximal BCR signaling events that occur within minutes, whereas for more distant events that require days to occur, such as the CSR assays described here, lower concentrations of BCR crosslinking reagents can be used; in fact, very high concentrations of BCR crosslinking reagents may result in signal paralysis and even activation-induced cell death (AICD). Since the particular combination of reagents, TLR ligands, and assay conditions vary, it is best to titrate each critical component.

14. For strongly stimulated, scaled-up B-cell cultures (typically used to yield sufficient material for biochemical studies not covered in this chapter), medium can be changed when acidified (indicated by intense yellow color that typically develops 2–3 days after stimulation). Medium can simply be aspirated by placing a 200 μl pipet at the tip of the aspirating 2 ml pipet and gently aspirating from top to bottom of the well, touching the side of the well (although B cells grow in suspension, the clumps are heavy and fall to the bottom during this gentle aspiration). For large, dense B-cell cultures or for more complete medium change, cells can be resuspended, centrifuged at $500 \times g$ for 5 min in a swinging-bucket centrifuge and resuspended in fresh medium; this step also removes debris from dead cells. Since material released from apoptotic/necrotic cells may include damage-associated molecular patterns (DAMPs) that can dampen the immune response [73, 74], resuspended cells can be centrifuged on a ficoll layer to remove dead cells and debris [6]. Regardless of the medium change method, activated B cells maintain some activation and division 'momentum' upon stimulus withdrawal [75], but typically require continuous stimuli in the medium to maintain robust proliferation [76].
15. Antibodies should be titrated to make sure populations are resolved yet the 'negative' population should show no to moderate staining [77, 78]. Typically, titrated antibodies can

be combined in a mastermix to stain reasonably well 0.1–10 million cells in 50–100 μl staining solution, though obviously less concentrated cell solutions may show a more pronounced shift, and conversely, dense cultures may show less resolved populations. Isotype control antibodies labeled with the same fluorophores as the staining antibodies should be used in initial or pilot experiments to validate antibody specificity.

16. Flow cytometry staining buffers can be tested by users for optimal results, with the two most common buffers being PBS and HBSS. These are frequently supplemented with reagents to block nonspecific interactions, such as 1 % BSA or 1 % FBS. A high background staining can frequently be reduced by blocking Fc receptors (several of which are expressed on B cells) with normal mouse serum prior to staining with antibodies. It is recommended that these buffers be made in 1 L batches and aliquoted in 50 ml tubes stored at 4 °C to minimize bacterial contamination; if necessary, a bacteriostatic agent, such as 0.05 % NaN_3, can be added. Staining intracellular targets may require additional considerations, and several commercial kits are available (e.g., from BD Biosciences or TONBO Biosciences).
17. Although gating of the population of interest should ideally be identical in all samples, it is more important that gates are correctly applied to not arbitrarily cut off populations. The use of MFI is inappropriate when two or more distinct populations exist, but may be appropriate when only shoulder shifts are observed, or to measure the 'average cell division' in the case of CFSE studies. For more details on flow cytometry analysis see reference [79].
18. LPS appears to be the most effective TLR ligand for in vitro induction of $B220^{lo}$ $CD138^{+}$ plasma cells. However, IL-5 can enhance plasma cell induction by other TLR ligands [80], whereas IL-6 is thought to prolong the survival of these plasma cells [81]. Although BCR signaling enhances TLR-induced CSR, it also seems to delay plasma cell formation [82, 83], perhaps allowing for completion of CSR to be followed by differentiation of newly switched B cells to short- or long-lived plasma cells.

References

1. Carrel A, Ingebrigtsen R (1912) The production of antibodies by tissues living outside of the organism. J Exp Med 15:287–291
2. Stevens KM, McKenna JM (1958) Studies on antibody synthesis initiated *in vitro*. J Exp Med 107:537–559
3. Moller G (1965) 19S antibody production against soluble lipopolysaccharide antigens by individual lymphoid cells *in vitro*. Nature 207:1166–1168
4. Moller G, Wigzell H (1965) Antibody synthesis at the cellular level. Antibody-induced

suppression of 19s and 7s antibody response. J Exp Med 121:969–989
5. Nossal GJ, Szenberg A, Ada GL, Austin CM (1964) Single cell studies on 19S antibody production. J Exp Med 119:485–502
6. Pike BL, Alderson MR, Nossal GJ (1987) T-independent activation of single B cells: an orderly analysis of overlapping stages in the activation pathway. Immunol Rev 99:119–152
7. Rudbach JA (1971) Molecular immunogenicity of bacterial lipopolysaccharide antigens: establishing a quantitative system. J Immunol 106:993–1001
8. Von Eschen KB, Rudbach JA (1974) Immunological responses of mice to native protoplasmic polysaccharide and lipopolysaccharide: functional separation of the two signals required to stimulate a secondary antibody response. J Exp Med 140:1604–1614
9. Medzhitov R, Preston-Hurlburt P, Janeway CA Jr (1997) A human homologue of the Drosophila Toll protein signals activation of adaptive immunity. Nature 388:394–397
10. Poltorak A, He X, Smirnova I, Liu MY, Van Huffel C, Du X, Birdwell D, Alejos E, Silva M, Galanos C, Freudenberg M, Ricciardi-Castagnoli P, Layton B, Beutler B (1998) Defective LPS signaling in C3H/HeJ and C57BL/10ScCr mice: mutations in Tlr4 gene. Science 282:2085–2088
11. Coutinho A, Moller G (1975) Thymus-independent B-cell induction and paralysis. Adv Immunol 21:113–236
12. Coutinho A, Poltorack A (2003) Innate immunity: from lymphocyte mitogens to Toll-like receptors and back. Curr Opin Immunol 15:599–602
13. Pasare C, Medzhitov R (2005) Control of B-cell responses by Toll-like receptors. Nature 438:364–368
14. Gavin AL, Hoebe K, Duong B, Ota T, Martin C, Beutler B, Nemazee D (2006) Adjuvant-enhanced antibody responses in the absence of toll-like receptor signaling. Science 314:1936–1938
15. Kasturi SP, Skountzou I, Albrecht RA, Koutsonanos D, Hua T, Nakaya HI, Ravindran R, Stewart S, Alam M, Kwissa M, Villinger F, Murthy N, Steel J, Jacob J, Hogan RJ, Garcia-Sastre A, Compans R, Pulendran B (2011) Programming the magnitude and persistence of antibody responses with innate immunity. Nature 470:543–547
16. Hou B, Saudan P, Ott G, Wheeler ML, Ji M, Kuzmich L, Lee LM, Coffman RL, Bachmann MF, DeFranco AL (2011) Selective utilization of Toll-like receptor and MyD88 signaling in B cells for enhancement of the antiviral germinal center response. Immunity 34:375–384
17. Xu Z, Zan H, Pone EJ, Mai T, Casali P (2012) Immunoglobulin class-switch DNA recombination: induction, targeting and beyond. Nat Rev Immunol 12:517–531
18. Koh YT, Scatizzi JC, Gahan JD, Lawson BR, Baccala R, Pollard KM, Beutler BA, Theofilopoulos AN, Kono DH (2013) Role of nucleic acid-sensing TLRs in diverse autoantibody specificities and anti-nuclear antibody-producing B cells. J Immunol 190: 4982–4990
19. Stavnezer J, Guikema JE, Schrader CE (2008) Mechanism and regulation of class switch recombination. Annu Rev Immunol 26: 261–292
20. Pone EJ, Zan H, Zhang J, Al-Qahtani A, Xu Z, Casali P (2010) Toll-like receptors and B-cell receptors synergize to induce immunoglobulin class-switch DNA recombination: relevance to microbial antibody responses. Crit Rev Immunol 30:1–29
21. Rawlings DJ, Schwartz MA, Jackson SW, Meyer-Bahlburg A (2012) Integration of B cell responses through Toll-like receptors and antigen receptors. Nat Rev Immunol 12:282–294
22. Gururajan M, Jacob J, Pulendran B (2007) Toll-like receptor expression and responsiveness of distinct murine splenic and mucosal B-cell subsets. PLoS One 2, e863
23. Jendholm J, Morgelin M, Perez Vidakovics ML, Carlsson M, Leffler H, Cardell LO, Riesbeck K (2009) Superantigen- and TLR-dependent activation of tonsillar B cells after receptor-mediated endocytosis. J Immunol 182:4713–4720
24. Souwer Y, Griekspoor A, Jorritsma T, de Wit J, Janssen H, Neefjes J, van Ham SM (2009) B cell receptor-mediated internalization of salmonella: a novel pathway for autonomous B cell activation and antibody production. J Immunol 182:7473–7481
25. Bekeredjian-Ding I, Jego G (2009) Toll-like receptors—sentries in the B-cell response. Immunology 128:311–323
26. Casali P, Schettino EW (1996) Structure and function of natural antibodies. Curr Top Microbiol Immunol 210:167–179
27. Meyer-Bahlburg A, Rawlings DJ (2008) B cell autonomous TLR signaling and autoimmunity. Autoimmun Rev 7:313–316
28. Palm NW, Medzhitov R (2009) Pattern recognition receptors and control of adaptive immunity. Immunol Rev 227:221–233
29. Hwang IY, Park C, Harrison K, Kehrl JH (2009) TLR4 signaling augments B lymphocyte migration and overcomes the restriction that limits access to germinal center dark zones. J Exp Med 206:2641–2657

30. Wu X, Tsai CY, Patam MB, Zan H, Chen JP, Lipkin SM, Casali P (2006) A role for the MutL mismatch repair Mlh3 protein in immunoglobulin class switch DNA recombination and somatic hypermutation. J Immunol 176:5426–5437
31. Zan H, Zhang J, Al-Qahtani A, Pone EJ, White CA, Lee D, Yel L, Mai T, Casali P (2011) Endonuclease G plays a role in immunoglobulin class switch DNA recombination by introducing double-strand breaks in switch regions. Mol Immunol 48:610–622
32. Pone EJ, Zhang J, Mai T, White CA, Li G, Sakakura JK, Patel PJ, Al-Qahtani A, Zan H, Xu Z, Casali P (2012) BCR-signalling synergizes with TLR-signalling for induction of AID and immunoglobulin class-switching through the non-canonical NF-κB pathway. Nat Commun 3:767
33. Goodridge HS, Reyes CN, Becker CA, Katsumoto TR, Ma J, Wolf AJ, Bose N, Chan AS, Magee AS, Danielson ME, Weiss A, Vasilakos JP, Underhill DM (2011) Activation of the innate immune receptor Dectin-1 upon formation of a 'phagocytic synapse'. Nature 472:471–475
34. Snapper CM (2012) Mechanisms underlying *in vivo* polysaccharide-specific immunoglobulin responses to intact extracellular bacteria. Ann N Y Acad Sci 1253:92–101
35. Poovassery JS, Vanden Bush TJ, Bishop GA (2009) Antigen receptor signals rescue B cells from TLR tolerance. J Immunol 183:2974–2983
36. Barr TA, Brown S, Ryan G, Zhao J, Gray D (2007) TLR-mediated stimulation of APC: Distinct cytokine responses of B cells and dendritic cells. Eur J Immunol 37:3040–3053
37. Ghosh TK, Mickelson DJ, Solberg JC, Lipson KE, Inglefield JR, Alkan SS (2007) TLR-TLR cross talk in human PBMC resulting in synergistic and antagonistic regulation of type-1 and 2 interferons, IL-12 and TNF-alpha. Int Immunopharmacol 7:1111–1121
38. Liu N, Ohnishi N, Ni L, Akira S, Bacon KB (2003) CpG directly induces T-bet expression and inhibits IgG1 and IgE switching in B cells. Nat Immunol 4:687–693
39. Gursel I, Gursel M, Yamada H, Ishii KJ, Takeshita F, Klinman DM (2003) Repetitive elements in mammalian telomeres suppress bacterial DNA-induced immune activation. J Immunol 171:1393–1400
40. Miles K, Heaney J, Sibinska Z, Salter D, Savill J, Gray D, Gray M (2012) A tolerogenic role for Toll-like receptor 9 is revealed by B-cell interaction with DNA complexes expressed on apoptotic cells. Proc Natl Acad Sci U S A 109:887–892
41. Heikenwalder M, Polymenidou M, Junt T, Sigurdson C, Wagner H, Akira S, Zinkernagel R, Aguzzi A (2004) Lymphoid follicle destruction and immunosuppression after repeated CpG oligodeoxynucleotide administration. Nat Med 10:187–192
42. Lee CC, Avalos AM, Ploegh HL (2012) Accessory molecules for Toll-like receptors and their function. Nat Rev Immunol 12:168–179
43. Vollmer J, Weeratna R, Payette P, Jurk M, Schetter C, Laucht M, Wader T, Tluk S, Liu M, Davis HL, Krieg AM (2004) Characterization of three CpG oligodeoxynucleotide classes with distinct immunostimulatory activities. Eur J Immunol 34:251–262
44. Krieg AM (2006) Therapeutic potential of Toll-like receptor 9 activation. Nat Rev Drug Discov 5:471–484
45. Bauer S, Kirschning CJ, Hacker H, Redecke V, Hausmann S, Akira S, Wagner H, Lipford GB (2001) Human TLR9 confers responsiveness to bacterial DNA via species-specific CpG motif recognition. Proc Natl Acad Sci U S A 98:9237–9242
46. Kracker S, Radbruch A (2004) Immunoglobulin class switching: *in vitro* induction and analysis. Methods Mol Biol 271:149–159
47. Jumper MD, Nishioka Y, Davis LS, Lipsky PE, Meek K (1995) Regulation of human B cell function by recombinant CD40 ligand and other TNF-related ligands. J Immunol 155:2369–2378
48. Van den Broeck W, Derore A, Simoens P (2006) Anatomy and nomenclature of murine lymph nodes: Descriptive study and nomenclatory standardization in BALB/cAnNCrl mice. J Immunol Methods 312:12–19
49. Wersto RP, Chrest FJ, Leary JF, Morris C, Stetler-Stevenson MA, Gabrielson E (2001) Doublet discrimination in DNA cell-cycle analysis. Cytometry 46:296–306
50. Lecoeur H, de Oliveira-Pinto LM, Gougeon ML (2002) Multiparametric flow cytometric analysis of biochemical and functional events associated with apoptosis and oncosis using the 7-aminoactinomycin D assay. J Immunol Methods 265:81–96
51. Kinoshita K, Harigai M, Fagarasan S, Muramatsu M, Honjo T (2001) A hallmark of active class switch recombination: transcripts directed by I promoters on looped-out circular DNAs. Proc Natl Acad Sci U S A 98:12620–12623
52. Czerkinsky CC, Nilsson LA, Nygren H, Ouchterlony O, Tarkowski A (1983) A solid-phase enzyme-linked immunospot (ELISPOT) assay for enumeration of specific antibody-secreting cells. J Immunol Methods 65:109–121

53. Georgiou G, Ippolito GC, Beausang J, Busse CE, Wardemann H, Quake SR (2014) The promise and challenge of high-throughput sequencing of the antibody repertoire. Nat Biotechnol 32:158–168
54. Teichmann LL, Schenten D, Medzhitov R, Kashgarian M, Shlomchik MJ (2013) Signals via the adaptor MyD88 in B cells and DCs make distinct and synergistic contributions to immune activation and tissue damage in lupus. Immunity 38:528–540
55. McHeyzer-Williams LJ, McHeyzer-Williams MG (2004) Analysis of antigen-specific B-cell memory directly *ex vivo*. Methods Mol Biol 271:173–188
56. Moody MA, Haynes BF (2008) Antigen-specific B cell detection reagents: use and quality control. Cytometry A 73:1086–1092
57. Bernasconi NL, Onai N, Lanzavecchia A (2003) A role for Toll-like receptors in acquired immunity: up-regulation of TLR9 by BCR triggering in naive B cells and constitutive expression in memory B cells. Blood 101:4500–4504
58. He B, Qiao X, Cerutti A (2004) CpG DNA induces IgG class switch DNA recombination by activating human B cells through an innate pathway that requires TLR9 and cooperates with IL-10. J Immunol 173:4479–4491
59. Avery DT, Bryant VL, Ma CS, de Waal Malefyt R, Tangye SG (2008) IL-21-induced isotype switching to IgG and IgA by human naive B cells is differentially regulated by IL-4. J Immunol 181:1767–1779
60. Kaminski DA, Stavnezer J (2007) Antibody class switching differs among SJL, C57BL/6 and 129 mice. Int Immunol 19:545–556
61. Martin RM, Brady JL, Lew AM (1998) The need for IgG2c specific antiserum when isotyping antibodies from C57BL/6 and NOD mice. J Immunol Methods 212:187–192
62. Wesemann DR, Magee JM, Boboila C, Calado DP, Gallagher MP, Portuguese AJ, Manis JP, Zhou X, Recher M, Rajewsky K, Notarangelo LD, Alt FW (2011) Immature B cells preferentially switch to IgE with increased direct Smu to Sepsilon recombination. J Exp Med 208:2733–2746
63. Mond JJ, Brunswick M (2001) *In vitro* antibody production. Curr Protoc Mol Biol Chapter 11, Unit 11.13
64. Iscove NN, Melchers F (1978) Complete replacement of serum by albumin, transferrin, and soybean lipid in cultures of lipopolysaccharide-reactive B lymphocytes. J Exp Med 147:923–933
65. Fanger MW, Hart DA, Wells JV, Nisonoff A (1970) Enhancement by reducing agents of the transformation of human and rabbit peripheral lymphocytes. J Immunol 105:1043–1045
66. Bevan MJ, Epstein R, Cohn M (1974) The effect of 2-mercaptoethanol on murine mixed lymphocyte cultures. J Exp Med 139:1025–1030
67. Ohmori H, Yamamoto I (1983) Mechanism of augmentation of the antibody response *in vitro* by 2-mercaptoethanol in murine lymphocytes. III. Serum-bound and oxidized 2-mercaptoethanol are available for the augmentation. Cell Immunol 79:186–196
68. Guikema JE, Schrader CE, Brodsky MH, Linehan EK, Richards A, El Falaky N, Li DH, Sluss HK, Szomolanyi-Tsuda E, Stavnezer J (2010) p53 represses class switch recombination to IgG2a through its antioxidant function. J Immunol 184:6177–6187
69. Metcalfe C, Cresswell P, Ciaccia L, Thomas B, Barclay AN (2011) Labile disulfide bonds are common at the leucocyte cell surface. Open Biol 1:110010
70. Barcellos-Hoff MH (2005) How tissues respond to damage at the cellular level: orchestration by transforming growth factor-β (TGF-β). BJR Suppl 27:123–127
71. Quah BJ, Warren HS, Parish CR (2007) Monitoring lymphocyte proliferation *in vitro* and *in vivo* with the intracellular fluorescent dye carboxyfluorescein diacetate succinimidyl ester. Nat Protoc 2:2049–2056
72. Snapper CM, Mond JJ (1996) A model for induction of T cell-independent humoral immunity in response to polysaccharide antigens. J Immunol 157:2229–2233
73. Lim SY, Raftery MJ, Geczy CL (2011) Oxidative modifications of DAMPs suppress inflammation: the case for S100A8 and S100A9. Antioxid Redox Signal 15:2235–2248
74. van Eden W, Spiering R, Broere F, van der Zee R (2012) A case of mistaken identity: HSPs are no DAMPs but DAMPERs. Cell Stress Chaperones 17:281–292
75. Rush JS, Hodgkin PD (2001) B cells activated via CD40 and IL-4 undergo a division burst but require continued stimulation to maintain division, survival and differentiation. Eur J Immunol 31:1150–1159
76. Donahue AC, Fruman DA (2003) Proliferation and survival of activated B cells requires sustained antigen receptor engagement and phosphoinositide 3-kinase activation. J Immunol 170:5851–5860
77. Holmes K, Lantz LM, Fowlkes BJ, Schmid I, Giorgi JV (2001) Preparation of cells and reagents for flow cytometry. Curr Protoc Immunol Chapter 5, Unit 5.3

78. Stewart CC, Stewart SJ (2001) Titering antibodies. Curr Protoc Cytom Chapter 4, Unit 4.1
79. Hawkins ED, Hommel M, Turner ML, Battye FL, Markham JF, Hodgkin PD (2007) Measuring lymphocyte proliferation, survival and differentiation using CFSE time-series data. Nat Protoc 2:2057–2067
80. Emslie D, D'Costa K, Hasbold J, Metcalf D, Takatsu K, Hodgkin PO, Corcoran LM (2008) Oct2 enhances antibody-secreting cell differentiation through regulation of IL-5 receptor alpha chain expression on activated B cells. J Exp Med 205:409–421
81. Cassese G, Arce S, Hauser AE, Lehnert K, Moewes B, Mostarac M, Muehlinghaus G, Szyska M, Radbruch A, Manz RA (2003) Plasma cell survival is mediated by synergistic effects of cytokines and adhesion-dependent signals. J Immunol 171:1684–1690
82. Modigliani Y, Demengeot J, Vasconcellos R, Andersson J, Coutinho A, Grandien A (1997) Differential sensitivity of B lymphocyte populations to IgM receptor ligation is determined by local factors. Int Immunol 9:755–762
83. Rui L, Healy JI, Blasioli J, Goodnow CC (2006) ERK signaling is a molecular switch integrating opposing inputs from B cell receptor and T cell cytokines to control TLR4-driven plasma cell differentiation. J Immunol 177:5337–5346

Chapter 16

Toll-Like Receptor-Dependent Immune Complex Activation of B Cells and Dendritic Cells

Krishna L. Moody, Melissa B. Uccellini, Ana M. Avalos, Ann Marshak-Rothstein, and Gregory A. Viglianti

Abstract

High titers of autoantibodies reactive with DNA/RNA molecular complexes are characteristic of autoimmune disorders such as systemic lupus erythematosus (SLE). In vitro and in vivo studies have implicated the endosomal Toll-like receptor 9 (TLR9) and Toll-like receptor 7 (TLR7) in the activation of the corresponding autoantibody producing B cells. Importantly, TLR9/TLR7-deficiency results in the inability of autoreactive B cells to proliferate in response to DNA/RNA-associated autoantigens in vitro, and in marked changes in the autoantibody repertoire of autoimmune-prone mice. Uptake of DNA/RNA-associated autoantigen immune complexes (ICs) also leads to activation of dendritic cells (DCs) through TLR9 and TLR7.

The initial studies from our lab involved ICs formed by a mixture of autoantibodies and cell debris released from dying cells in culture. To better understand the nature of the mammalian ligands that can effectively activate TLR7 and TLR9, we have developed a methodology for preparing ICs containing defined DNA fragments that recapitulate the immunostimulatory activity of the previous "black box" ICs. As the endosomal TLR7 and TLR9 function optimally from intracellular acidic compartments, we developed a facile methodology to monitor the trafficking of defined DNA ICs by flow cytometry and confocal microscopy. These reagents reveal an important role for nucleic acid sequence, even when the ligand is mammalian DNA and will help illuminate the role of IC trafficking in the response.

Key words AM14 transgenic BCR, Rheumatoid factor B cell, Immune complex, Autoantibodies, B cells, IFNα, Flt3L-DCs, TLR7, TLR9, Endogenous ligands, Biotinylated DNA

1 Introduction

Autoimmune diseases such as SLE are characterized by the presence of autoantibodies directed against endogenous DNA and RNA ligands. Immune system activation and IC deposition in vital organs leads to tissue destruction, with concomitant release of self-DNA and RNA that results in sustained tissue damage and

Author contributed equally with all other contributors.

Claire E. McCoy (ed.), *Toll-Like Receptors: Practice and Methods*, Methods in Molecular Biology, vol. 1390,
DOI 10.1007/978-1-4939-3335-8_16, © Springer Science+Business Media New York 2016

inflammation [1]. TLR9 and TLR7 are innate immune receptors located in endosomal compartments, originally shown to be responsible for immune responses to viral hypomethylated CpG DNA and ssRNA, respectively [2–5]. While their role in response to infection is firmly established, studies performed in vivo and in vitro have also shown that aberrant expression of TLR9 and TLR7 has a profound effect on the autoimmune phenotypes found in diverse mouse models of systemic autoimmune disease [6, 7]. These observations have led to the hypothesis that under the appropriate conditions, the prevalence of certain RNA and DNA autoantigens could lead to activation of an immune response through engagement of TLR9 and/or TLR7. In this case, autoantigens would serve as autoadjuvants to the immune system [8].

Use of the AM14 rheumatoid factor (RF) B-cell receptor (BCR) transgenic model has been instrumental in demonstrating that activation of autoreactive B cells by endogenous DNA is BCR and TLR9-dependent. AM14 transgenic B cells recognize IgG2a of the a or j allotype with low affinity, and therefore serve as prototypic autoreactive RF B cells. In vitro, AM14 B cells provide an excellent system to test the immunostimulatory capacity of specific autoantigens by simply adding, as ligands, ICs consisting of autoantigen-specific IgG2a and the candidate autoantigen. Using this system, we have shown that ICs containing mammalian chromatin activate AM14 B cells in a TLR9-dependent manner [9, 10]. However, at the time, these results were somewhat surprising given that mammalian DNA is generally considered a poor ligand for TLR9. In order to better define the mammalian DNA ligand, we have produced defined ICs incorporating dsDNA fragments of known sequence composition. To avoid the high background stimulation associated with DNA-reactive antibodies, which invariably bind to cell debris, we have developed a simple method for labeling DNA fragments with biotin, or the hapten trinitrophenol (TNP). These DNA fragments can then be delivered to the AM14 BCR with antibodies specific for biotin or TNP. To demonstrate that the dsDNA fragments have been appropriately modified, the derivatized fragments can be mixed with the anti-biotin or anti-TNP antibodies, and formation of ICs can be assessed by a modified electrophoresis mobility shift assay. This technique allows us to directly compare the immunostimulatory capacity of various sequences. This kind of analysis has shown that ICs containing CpG-rich dsDNA fragments can activate AM14 B cells, while fragments lacking CpG motifs cannot [11]. We have also demonstrated that IgG2a antibodies specific for RNA-associated autoantigens stimulate AM14 B cells in a TLR7-dependent manner [12].

The adjuvant activity of defined DNA ICs, or RNA-containing ICs can also be tested on cells that express an activating Fcγ receptor. In this case, the Fcγ receptor binds the IC and delivers the ligand to an intracellular compartment containing the TLR.

Activation of both conventional DC (cDCs) and plasmacytoid (pDCs) can be assessed by measuring cytokine production [13–15]. The contribution of pDCs, a lymphoid DC subset responsible for interferon-α (IFN-α) production, is of particular interest since this cytokine is present at high levels in many patients with SLE. In addition, elevated amounts of IFN-α induce global changes in gene expression designated the "IFN-α signature" [16]. Interestingly, B-cell responses to RNA-associated IC are significantly enhanced by IFN-α, suggesting that crosstalk between these two cell types appears to be important in disease progression [17, 18].

2 Materials

2.1 Antibody Preparation

1. IgG depleted medium: growth medium passed over a protein G column (*see* **Note 1**).
2. Disposable polypropylene columns (Pierce).
3. Protein G Sepharose™4 Fast Flow (GE Healthcare).
4. Phosphate buffered saline (PBS; Life Technologies): 1 mM KH_2PO_4, 155 mM NaCl, 3 mM Na_2HPO_4.
5. Spectrophotometer.
6. Nanodrop (ThermoFisher Scientific).
7. Elution buffer: 0.1 M glycine-HCl, pH 2.7.
8. Neutralization buffer: 1 M Tris–HCl, pH 9.
9. pH paper (ThermoFisher Scientific).
10. Storage buffer: 0.02 % (w/v) Sodium Azide in PBS.
11. Centricon® Centrifugal Filter, 10,000 molecular weight cut off (EMD Millipore).
12. 1D4 (anti-biotin) [11].
13. Hy1.2 (anti-TNP).
14. 1E11.1 (anti-streptavidin).
15. Y2 (anti-Sm) [12].
16. PA4 [19].
17. PL2-3 [9].

2.2 DNA Fragment Preparation

1. Dam-/dcm-competent *E. coli* (e.g., GM2163).
2. Carbenicillin (1000×; American Bioanalytical) is dissolved in dH_2O at 50 mg/mL and stored in aliquots at –20 °C for up to 1 year.
3. Luria-Bertani (LB) carbenicillin medium: 1 % (w/v) tryptone, 0.5 % (w/v) NaCl, 0.5 % (w/v) yeast extract are dissolved in water. pH to 7.4 with NaOH and autoclave. Store at 4 °C and add carbenicillin to 50 μg/mL just before use.

4. Luria-Bertani (LB) carbenicillin plates: LB carbenicillin medium is made with 1.2 % (w/v) agar, autoclaved, and cooled to 50 °C prior to addition of carbenicillin to 50 μg/mL. Pour plates and store at 4 °C for up to 2 months.
5. EndoFree® Plasmid Maxi Kit (Qiagen).
6. EndoFree® TE buffer (Qiagen): 10 mM Tris–HCl, 1 mM EDTA, pH 8.0.
7. TAE running buffer (50×): 2 M Tris base, 2 M acetate, 50 mM EDTA, pH 8.0.
8. Agarose gel: 1 % (w/v) SeaKem® GTG® agarose (Cambrex) is dissolved in 1× TAE buffer containing 0.5 μg/mL ethidium bromide (Sigma).
9. EcoRI buffer (10×; New England BioLabs). Store at −20 °C.
10. Bovine serum albumin (BSA, 10×; New England BioLabs). Store at −20 °C.
11. EcoRI and BamHI (New England BioLabs). Store in enzyme block at −20 °C.
12. Distilled water DNase, RNase free (dH_2O; Life Technologies).
13. DNA Clean & Concentrator-25™ kit (Zymoresearch).
14. Loading dye (6×): 0.2 % Orange G, 50 % (v/v) glycerol in dH_2O.
15. Zymoclean Gel DNA Recovery Kit™ (Zymoresearch).
16. Plasmid templates: pLITMUS29-C11, pUC19-CGNEG and pLITMUS29-CG50
17. CGneg primers: H931 (5′-AACTGGATCCCCTGGCCT TTTAGAGACATCAGAAGG-3′) H1560 (5′-GGCAGAATT CGGGATAGGTGGATTATGTGTCATCCATCC-3′).
18. 5′ Biotinylated C11 primers: 3558-EcoRI (5′-ACGG AATTCGGCCGCCTGCAGGTCGACCATAA-3′) and 3559-EcoRI (5′-ACGGAATTCAACGCGTTGGGAGCTCTCC CATAA-3′).
19. GoTaq® Flexi Buffer (5×; Promega Madison).
20. GoTaq® Flexi DNA Polymerase (Promega).
21. Deoxyribonucleotide triphosphates (dNTPs; Roche) are dissolved in dH_2O at 2.5 mM and aliquots are stored at −20 °C. Avoid multiple freeze-thaws.
22. 1 mM biotin-16-deoxyuridine triphosphate (biotin-16-dUTP; Roche). Store at −20 °C, loses activity after 1 year.
23. Klenow Fragment (3′→5′ exo-) (New England BioLabs). Store in enzyme block at −20 °C.
24. PBS (*see* Subheading 2.1, **Item 4**).
25. 5-(3-aminoallyl)-2′-deoxy-uridine 5′-triphosphate, trisodium salt (Aminoallyl dUTP; Molecular Probes). Store at −20 °C.

26. Sodium bicarbonate buffer: sodium bicarbonate (Sigma) is dissolved in dH_2O at 25 mg/mL and aliquots are stored at −20 °C for up to 1 year.
27. TNP-e-Aminocaproyl-OSu (reactive TNP; Biosearch Technologies) is dissolved in dimethylformamide at 20 mg/mL and stored in aliquots at −20 °C for up to 1 year.

2.3 RNA Particle Preparation

1. RNP/Sm antigen (Arotec Diagnostics Limited, New Zealand).
2. RPMI 1640 (Life Technologies).
3. Amicon Ultra-4 filter units (centricon) 10,000 molecular weight cutoff (Millipore).

2.4 Preparation of Immune Complexes

1. RPMI medium: RPMI 1640 is supplemented with 10 % (v/v) fetal bovine serum (Hyclone); Penicillin/Streptomycin/Glutamine solution—100 U/mL penicillin G sodium, 100 μg/mL streptomycin sulfate, 0.29 mg/mLl-glutamine (Life Technologies); 10 mM HEPES, pH 7.5, 22 mM β-mercaptoethanol (Sigma). Filter-sterilize and keep at 4 °C for up to 1 month.
2. Serum-free RPMI: RPMI, without addition of fetal bovine serum.
3. DNA fragments, RNP/Sm particles, antibodies (*see* **Note 2**).
4. DMEM (Life Technologies).
5. Unconjugated streptavidin (Bioworld).
6. FITC, Oregon Green 488 and/or AF647 conjugated Streptavidin (Life technologies).

2.5 B-Cell Proliferation Assay

1. Cell culture plasticware: 60 × 15 mm Petri dishes, 5 mL syringes, 96-well flat bottom plates, 15 mL conical tubes (ThermoFisher).
2. 25 Gauge needles (ThermoFisher).
3. Frosted slides (ThermoFisher).
4. Cotton-plugged and unplugged Pasteur pipettes (ThermoFisher).
5. Brandel Harvester (Brandel).
6. 90 × 120 mm glass fiber filter, printed filtermat A (PerkinElmer).
7. Filtermat Sample bag (PerkinElmer).
8. Betaplate scintillation cocktail (PerkinElmer).
9. Microbeta Trilux counter (PerkinElmer).
10. Hanks balanced salt solution (HBSS; Life Technologies): HBSS medium is supplemented with 10 mM sodium phosphate (3.2 mM Na_2HPO_4, 7.2 mM $NaH_2PO_4.2H_2O$), pH

7.2, and 5 % (v/v) fetal bovine serum. Filter-sterilize and keep at 4 °C.

11. IMag buffer: PBS (*see* Subheading 2.1, **Item 4**) is supplemented with 0.5 % (w/v) bovine serum albumin fraction V (Roche), and 2 mM EDTA. Store at 4 °C.
12. Anti-Mouse CD45R/B220 magnetic particles, (BD Biosciences).
13. IMagnet (BD Biosciences).
14. RPMI medium (*see* Subheading 2.4, **Item 1**).
15. Mouse interferon alpha-A (PBL).
16. ^{3}H-thymidine medium: RPMI medium is supplemented with 25 μCi/mL [methyl-^{3}H] thymidine (Amersham). Store at 4 °C.

2.6 pH Determination of Immune Complex Location

1. 96-Well flat bottom plates (Thermofisher Scientific).
2. RPMI medium (*see* Subheading 2.4, **Item 1**).
3. 0.9 % NaCl (w/v).
4. 10 mM Phosphate-Citrate buffers, pH 7.7 and pH 4, containing 150 mM NaCl and 4 mM KCl.
5. Monensin (Sigma).
6. Nigericin (Sigma).
7. FACS Buffer: PBS containing 3 % bovine sera.

2.7 Confocal Microscopy Determination of Immune Complex Location

1. 12 mm round coverslips (#1.5; Warner Instruments).
2. 0.1 % Poly-l-Lysine (Sigma).
3. 2% Gelatin type B (Sigma).
4. Blocking buffer: 5 % Goat sera, 0.2 % NaN_3 in PBS.
5. Fixation buffer: 4 % Paraformaldehyde in PBS.
6. Permeabilization buffer: blocking buffer with 0.2 % Saponin.
7. Fluorophore conjugated 1D4B (anti-LAMP1; DSHB).

2.8 Dendritic Cell Cytokine Assay

1. Cell culture plasticware: 60 × 15 mm Petri Dishes, 20 mL syringes, 15 mL conical tubes, 70 μm cell strainer (ThermoFisher).
2. 25 Gauge needle (ThermoFisher).
3. PBS (*see* Subheading 2.1, **Item 4**).
4. RBC lysis buffer (Sigma).
5. RPMI 1640 (Invitrogen).
6. RPMI medium (*see* Subheading 2.4, **Item 1**).
7. FL B16 cells: Fms-like tyrosine kinase ligand (Flt3L)-transfected B16 melanoma cell line.

8. Flat Bottom MaxiSorp ELISA plates (ThermoFisher).
9. Mouse interferon alpha A standard (PBL).
10. Rat monoclonal antibody against mouse interferon alpha, 2 mg/mL (PBL).
11. ELISA wash buffer: 0.05 % (v/v) Tween-20 (Sigma) in PBS.
12. ELISA blocking buffer: 1 % (w/v) bovine serum albumin fraction V (Roche) in PBS.
13. Rabbit polyclonal antibody against mouse interferon alpha, 0.94 mg/mL (PBL).
14. $F(ab')_2$ donkey anti-rabbit IgG (H+L)-horseradish peroxidase, 0.8 mg/mL (Jackson Immunoresearch).
15. 3,3′,5,5′ Tetramethyl benzidine (TMB) Liquid Substrate (Sigma).
16. ELISA stop solution: 1 M H_3PO_4.
17. Spectrophotometer.

3 Methods

3.1 Antibody Preparation

AM14 RF B cells bind to $IgG2a^{a/j}$, therefore $IgG2a^{a/j}$ antibodies of the correct specificity can be used to deliver ligands to TLR9 and TLR7. By an analogous mechanism DCs can take up antibodies through Fcγ receptors and deliver ligands to TLR9 and TLR7. Monoclonal antibodies of interest are obtained from hybridomas [9, 11, 12] and the antibody is purified from culture supernatants using protein G Sepharose.

1. Grow hybridoma of interest to high density in appropriate IgG depleted medium and harvest 500 mL of supernatant.
2. Prepare protein G column by pipetting enough of the Protein G slurry into the column for about 1 mL of packed Sepharose. Rinse column with 20 mL of PBS (*see* **Note 3**).
3. Apply hybridoma supernatant to column and save flow-through fraction.
4. Wash column with 30 mL of PBS. Read A_{280} of wash on spectrophotometer and continue rinsing with PBS until reading is below 0.01 absorbance units.
5. Elute column with 10 mL of elution buffer. Collect 900 μL fractions (approximately 10), into 100 μL of neutralization buffer (*see* **Note 4**).
6. Read A_{280} of fractions and pool the most concentrated 3–4 fractions. Apply antibody to Centricon and exchange against PBS with at least 3 changes of PBS according to the manufacturers instructions.

7. Read A_{280} of the antibody to determine concentration (A_{280} of a 1 mg/mL solution of IgG is approximately 1.5 absorbance units). Antibody should also be tested for endotoxin contamination (*see* **Note 5**). Aliquots of antibody are stored at –80 °C. Use a fresh aliquot for each assay, and avoid freeze-thawing.
8. Rinse column with PBS and check that the column has returned to pH 7.6 using pH paper. Store column in storage buffer with both ends capped.

3.2 DNA Fragment Preparation

AM14 RF B cells can be activated by ICs composed of anti-nucleosome or anti-DNA antibodies in association with cell debris present in the culture supernatant. This activation was found to be DNase-sensitive and TLR9-dependent, supporting a model in which the B-cell receptor binds to ICs containing chromatin/DNA and delivers them to an intracellular compartment where they are able to engage TLR9 [9, 10]. DCs can also take up ICs through Fcγ receptors and deliver ligands to TLR9 [13, 14]. We have used the antibodies PL2-3 (anti-nucleosome) [20], and PA4 (anti-DNA) [21] in order to assess the role of TLR9 in autoreactive B-cell and DC activation. In addition, we have used the defined DNA fragments CGneg (629 bp, no CpG), C11 (570 bp, 42 CpG) and CG50 (607 bp, 50 optimal CpG) [22, 23, 11] in order to assess the role of CpG motifs in the activation of TLR9.

3.2.1 DNA Preparation from Plasmid

1. CGneg, C11, and CG50 are cloned into the EcoRI and BamHI restriction sites of pUC19, LITMUS 29, and LITMUS 29, respectively.
2. Plasmids are transformed into dam/dcm-deficient *E. coli* (*see* **Note 6**) and streaked onto LB carbenicillin plates.
3. Single colonies are used to inoculate a 3 mL starter culture of LB carbenicillin, and 50 µL of the starter culture is used to inoculate 100 mL of LB carbenicillin (*see* **Note 7**).
4. Plasmid DNA is prepared using the using the EndoFree Plasmid Maxi Kit according to the manufacturer's instructions and resuspended in 500 µL of TE buffer. DNA concentration is determined by running a 1 µL sample on a 1 % agarose gel and comparing to a known concentration of DNA ladder. Alternatively, DNA concentration can be determined by reading A_{260} (A_{260} of a 50 µg/mL solution is 1 absorbance unit).
5. DNA fragments are prepared by digesting plasmid DNA with EcoRI and BamHI to separate the CGneg and CG50 fragments from the plasmid backbone. Incubate for 16 h at 37 °C: 200 µg of plasmid DNA, 30 µL of EcoRI buffer, 30 µL BSA, 400 U EcoRI, 400 U BamHI, and dH_2O to 300 µL (*see* **Note 8**).

6. Run a small 100 ng sample on a 1 % agarose gel to check for complete digestion, indicated by the presence of only 2 bands on the gel.
7. Isolate the remainder of the CGneg and CG50 fragments by adding 60 μL loading dye to the restriction digest from **Step 5** and mix.
8. Pour a 1 % agarose gel with a comb large enough to hold 360 μL (*see* **Note 9**).
9. Load the DNA sample and run at 120 V until the two bands are separated by at least 3 cm (*see* **Note 10**) and excise the CGneg or CG50 band with a new razor blade, removing any excess agarose.
10. Use Zymoclean Gel DNA Recovery Kit™ according to the manufacturer's instructions to extract DNA from agarose (*see* **Note 11**). The maximum theoretical yield is 40 μg; actual yields are usually 70–80 % of this.

3.2.2 DNA Preparation by PCR

1. DNA sequences of interest may also be prepared by PCR. As an example, to prepare CGneg by PCR, primers that incorporate EcoRI and BamHI restriction sites are used. Make PCR master mix by combining to a final concentration: 1× GoTaq Flexi buffer, 1.5 mM $MgCl_2$, 0.8 μM H931 and H1560 primers, 250 μM dNTP mix, 2.5 ng CGneg fragment, and 0.5 U Promega GoTaq to a total volume of 100 μL with dH_2O. Amplify using cycling conditions: 94 °C for 5 min, 35 cycles of 95 °C for 30 s, 65 °C for 40 s, and 72 °C for 45 s, followed by 72 °C for 5 min. Estimate DNA concentration by running a 5 μL sample on a 1 % agarose gel and comparing to a known concentration of DNA ladder.
2. Run DNA through DNA Clean & Concentrator-25™ kit according to the manufacturer's instructions and elute in TE buffer (*see* **Note 12**).
3. Digest DNA with EcoRI and BamHI as in **Step 5**, Subheading 3.2.1.

3.2.3 End-Labeling with Biotin

1. In order to deliver DNA to TLR9, we have used ICs composed of an anti-biotin antibody and biotinylated DNA fragments. Biotinylated DNA is made by filling in 5′ overhangs left by digestion with EcoRI and BamHI, with biotin-16-dUTP using the Klenow Fragment of DNA polymerase I. DNA is prepared and digested with EcoRI and BamHI (*see* Subheading 3.2.1, **Step 5**), and an agarose gel is run to confirm that digestion is complete.
2. DNA is end-labeled by adding dATP, dCTP, dGTP, and biotin-16-dUTP to the digestion reaction to a final concentration of 25 μM each in the presence of 0.25 U/μg of Klenow

Fragment of DNA polymerase I (3′→5′ exo-), and incubating for 30 min at 37 °C (*see* **Notes 13** and **14**).

3. DNA prepared from plasmid is then gel purified, or DNA prepared by PCR is run through DNA Clean & Concentrator-25™ kit (*see* Subheading 3.2.2, **Step 2**).

3.2.4 End Labeling by PCR

1. To permit the formation of brightly fluorescent ICs, we have used ICs composed of an anti-streptavidin antibody, fluorescent streptavidin, and DNA fragments biotinylated at both ends.
2. To form DNA fragments biotinylated at both ends, biotinylated oligonucleotides are used for PCR. As an example, to prepare C11 biotinylated at both ends by PCR, make the PCR master mix by combining 1× GoTaq Flexi buffer, 1.5 mM $MgCl_2$, 0.8 μM Bio-3558 and Bio-3559 primers, 250 μM dNTP mix, 2.5 ng C11 fragment, and 0.5 U Promega GoTaq to a total volume of 100 μL with dH_2O. Amplify using cycling conditions: 94 °C for 2 min, 35 cycles of 95 °C for 30 s, 60 °C for 30 s, and 72 °C for 45 s, followed by 72 °C for 5 min. Determine DNA concentration by Nanodrop.
3. Run DNA through DNA Clean & Concentrator-25™ kit according to the manufacturer's instructions and elute in TE buffer (*see* **Note 12**).

3.2.5 Internal Labeling with Biotin

1. DNA can alternatively be labeled internally with biotin by PCR. CGneg PCR is performed as in Subheading 3.2.2, **Step 1**, except that biotin-16-dUTP is substituted for a portion of the dTTP.
2. dATP, dCTP, and dGTP are added to a final concentration of 62.5 μM each. To label 10 % of the dTTP residues, biotin-16-dUTP is added to a final concentration of 6.3 μM and dTTP is added to a final concentration of 56.3 μM. PCR is performed as in Subheading 3.2.2, **step 1**.
3. Free biotin and primers are removed by running DNA through the DNA Clean & Concentrator-25™ kit.

3.2.6 Gel Shift Assay

1. A DNA gel shift is used in order to confirm that DNA is labeled with biotin. 50 ng of biotin-labeled DNA is combined with 2 μg of antibody 1D4 (anti-biotin) or irrelevant control antibody Hy1.2 (anti-TNP) [24] in 10 μL PBS. No incubation is necessary.
2. Separate sample on an agarose gel. 2 μL of loading dye is added and samples are loaded on a 1 % agarose gel. Biotin labeling is confirmed by complete shift of the free DNA band (*see* **Note 15**). An example of the results is shown in Fig. 1.

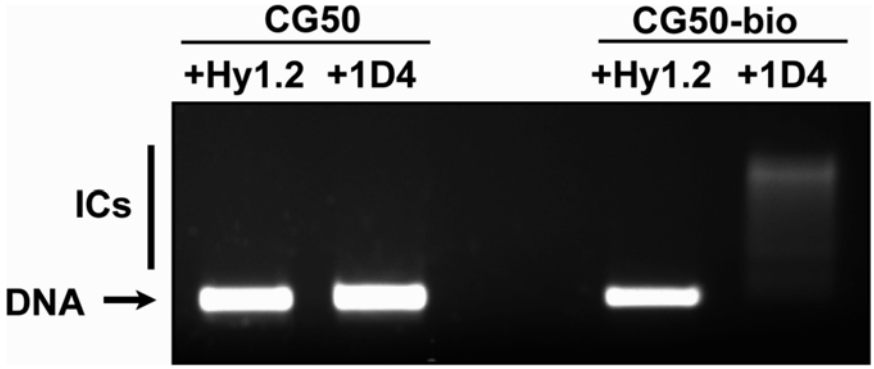

Fig. 1 Gel shift to confirm biotin labeling of DNA. 50 ng of DNA was mixed with 2 μg of antibody and run on a 1 % agarose gel. *Left 2 lanes* contain unmodified DNA combined with irrelevant control anti-TNP antibody (Hy1.2) or anti-biotin antibody (1D4). *Right 2 lanes* contain biotin labeled DNA combined with irrelevant control anti-TNP antibody (Hy1.2) or anti-biotin antibody (1D4). Biotin labeling is indicated by depletion of free DNA and presence of shifted DNA

3.3 RNA Particle Preparation

AM14 RF B cells can be activated by ICs composed of anti-RNA antibodies in association with cell debris present in the culture supernatant. Additionally, AM14 B cells are activated by sn/RNP particles in complex with anti-Sm/RNP antibodies. This activation was found to be RNase-sensitive and TLR7-dependent, supporting a model in which the B-cell receptor binds to ICs containing RNA/RNPs and delivers them to an intracellular compartment where they are able to engage TLR7 [12]. DCs can also take up ICs through Fcγ receptors and deliver ligands to TLR7 [13, 14]. We have used the antibodies BWR4 (anti-RNA) [25], and Y2 (anti-SmD) [26] in combination with snRNP particles in order to assess the role of TLR7 in autoreactive B-cell activation. AM14 B-cell stimulation by BWR4 depends on interaction with RNA present in cell debris in the culture, and hence addition of BWR4 alone induces activation. Conversely, sm/RNP particles are not present in high enough concentrations in cell debris in the culture, and hence addition of sm/RNP particles to Y2 is necessary in order to observe stimulation.

1. RNP/Sm particles are supplied in glycerol, which must be removed by filtration prior to use in tissue culture. Wash centricon 2× with 4 mL of RPMI 1640 by centrifuging 20 min at 1455 × *g* at 4 °C. Discard flow through.
2. Combine 25 μg of RNP/Sm antigen with 4 mL RPMI 1640, add to centricon, and spin at 1455 × *g* at 4 °C for 20 min. Discard flow through.
3. Wash centricon 2× with 4 mL RPMI 1640.

4. After the last centrifugation, use a Pipetman to measure the remaining volume of sm/RNP particles in the top of the centricon. Complete final volume to 1.25 mL by adding RPMI 1640. This will yield a stock solution of 20 μg/mL. Store in 100 μL aliquots at −80 °C for up to 1 month.

3.4 Preparation of Immune Complexes

3.4.1 DNA Immune Complexes without Streptavidin

1. DNA ICs are formed by combining DNA fragments generated in Subheading 3.2.2 antibody, and RPMI.
2. Calculate volumes for preparation of 4× stocks of DNA and antibody in duplicates per stimulation condition (*see* **Note 16**).
3. Mix antibody and DNA and incubate complexes for 1–2 h at 37 °C. If using biotin-labeled DNA, no incubation is necessary.

3.4.2 Streptavidin DNA Immune Complexes

1. Calculate volumes for preparation of 4× stocks of DNA fragment biotinylated at both ends, streptavidin and anti-streptavidin antibody in duplicates per stimulation condition
2. Streptavidin DNA ICs are formed by first combining streptavidin and DNA fragment biotinylated at both ends in biotin free medium and incubating on ice for 10 min (*see* **Note 17**).
3. Mix antibody with streptavidin-DNA complexes in RPMI (*see* **Note 18**).

3.4.3 RNA Immune Complexes

1. RNA-containing ICs are formed by combining anti-RNA antibody BWR4 and RPMI.
2. RNP/Sm IC are formed by combining RNP/Sm antigen and anti-SmD antibody Y2 in serum-free RPMI and incubating complexes for 1–2 h at 37 °C (*see* **Note 19**).

3.5 B-Cell Proliferation Assay

AM14 B-cell activation by ICs is measured by incorporation of ^{3}H-thymidine into DNA of dividing cells. B cells are hence stimulated for 24 h after which they are pulsed with ^{3}H-thymidine, harvested, and incorporated radioactivity is measured in a scintillation counter.

3.5.1 B-Cell Preparation

1. Pipette 10 mL HBSS into one 15-mL conical tube per spleen.
2. Sacrifice mouse, harvest spleen using aseptic technique and transfer to tube containing HBSS.
3. Inside the hood, pour contents of tube into a Petri dish. Trim any excess fat from the tissue and perfuse spleen with 5 mL of HBSS using a 5 mL syringe and a 25 gauge needle.
4. Unwrap frosted slides and wet with HBSS from the cell suspension. Crush spleen gently between the frosted side of the slides, making sure the spleen and the slides are wet with media, until only white matrix is left on the slide.

5. Rinse the slides with 1–2 mL of cell suspension using a Pasteur pipette. Discard slides and matrix.
6. Transfer the cell suspension to a new 15 mL conical tube using a Pasteur pipette.
7. Rinse the Petri dish with 3 mL of fresh HBSS and add to cell suspension. Pipette up and down to break up cell clumps. Leave on ice for 5 min. Remove supernatant from cell suspension leaving debris at the bottom of the tube, and transfer to a new 15 mL conical tube.
8. Centrifuge tubes at 300 × *g* at 4 °C for 5 min.
9. Aspirate supernatant using a Pasteur pipette attached to a vacuum flask.
10. Flick the tube to resuspend the cells, add 10 mL of IMag buffer and pipette up and down (*see* **Note 20**). Count cells.
11. Centrifuge tubes at 300 × *g* at 4 °C for 5 min.
12. Aspirate supernatant using a Pasteur pipette attached to a vacuum flask. Flick to resuspend cells.
13. Add anti-Mouse CD45R/B220 Magnetic Particles, and proceed to B-cell purification following the manufacturer's specifications.
14. After the final wash, resuspend cells in 3 mL RPMI and count.

3.5.2 B-Cell Stimulation

1. Plate 100 μL of purified B cells at a density of 4×10^6 cells/mL in a flat bottom, 96-well plate. Seed cells in duplicate per stimulation condition (*see* **Note 21**).
2. If testing the effect of inhibitors, pre-incubate cells with inhibitor for 1–2 h at 37 °C before addition of ICs. If testing RNA IC, pre-incubate cells with IFNα for 1–2 h at 37 °C before addition of ICs (*see* **Note 22**).
3. Add ICs and controls for B-cell stimulation, complete volume to 200 μL with RPMI if necessary.
4. Incubate plates for 24 h in 37 °C incubator, 5 % CO_2.
5. Pulse plates by adding 50 μL of ^{3}H-thymidine medium per well and incubating for 6 h in 37 °C incubator, 5 % CO_2.
6. Harvest cells using one filtermat per plate and rinsing 10× with water and once with methanol. Dry filtermat for at least 2 h at RT (*see* **Note 23**).
7. Insert filtermat into sample bag, add 4 mL of scintillation cocktail and completely wet filtermat. Remove excess scintillation cocktail and seal bag.
8. Count filtermat in Microbeta Trilux counter. An example of the results is shown in Fig. 2.
9. An example result of streptavidin DNA ICs in Fig. 3.

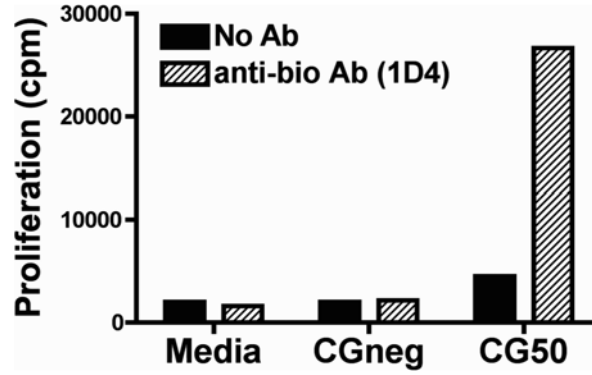

Fig. 2 AM14 B-cell proliferation to ICs containing anti-biotin antibody and biotin-labeled DNA. AM14 B cells were purified with B220 magnetic beads and stimulated with ICs composed of 5 μg/mL anti-biotin antibody (1D4) and 100 ng/mL biotin-labeled CGneg or CG50 fragments. Proliferation was measured by incorporation of ^{3}H-thymidine

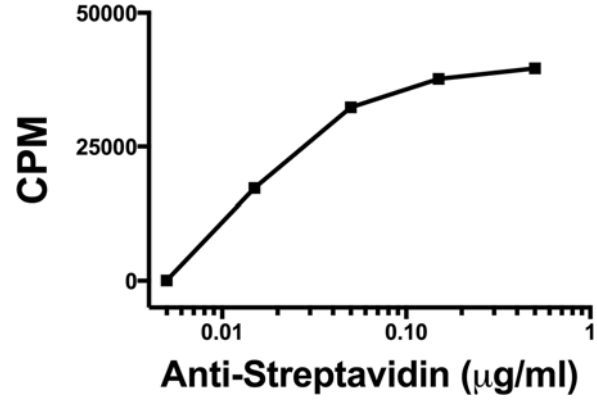

Fig. 3 AM14 B-cell proliferation to ICs containing anti-streptavidin antibody, streptavidin and biotin labeled DNA. AM14 B cells were purified with B220 magnetic beads and stimulated with a titration of an IC composed of 0.5 μg/mL anti-streptavidin, 0.05 μg/mL streptavidin AF647, 0.36 μg/mL streptavidin FITC and 500 ng/mL C11 fragment biotin labeled at both ends for 24 h. Proliferation was measured by the incorporation of ^{3}H-thymidine

3.6 pH Determination of Immune Complex Location

Following internalization, endocytosed cargo can have a variety of fates from degradation to recycling depending on the environment within the intracellular compartment. Very broadly, the functions of intracellular compartments and their receptors therein can be regulated by pH. This is especially the case for endosomal TLRs because their proteolytic activation requires an acidic milieu. The determination of pH by flow cytometry is performed by ratiometric measurement between two fluorophores (1) a fluorophore (e.g., FITC or Oregon Green 488) whose fluorescence decreases

with decreasing pH and (2) a fluorophore (e.g., Alexa Fluor 647) whose fluorescence is insensitive to pH changes [27]. The AF647 serves an internal control for total IC while the fluorescence of FITC is dependent on the pH of the compartment where the IC resides and serves as the sensor. Briefly, a dual fluorescent pH sensing IC is formed by first mixing streptavidin-FITC and streptavidin-AF647, then adding DNA fragments biotinylated at both ends and lastly an antibody specific for streptavidin. Using flow cytometry, the ratio of the FITC/AF647 mean fluorescence intensity (MFI) gives a relative indication of the pH where the IC resides within a stimulated cell. To assign a pH value to an unknown FITC/AF647 MFI, a standard curve is constructed by equilibrating the pH of the ICs within the cell to the extracellular environment of a known pH. This is accomplished by incubating IC treated cells in buffers between pH 8 and pH 4 containing ionophores. The pH buffers containing ionophore treated cells will have an FITC/AF647 MFI that corresponds to the pH of the buffer. In short, as the pH decreases, the FITC/AF647 MFI will decrease because the FITC fluorescence (numerator) is quenched while the AF647 fluorescence (denominator) remains constant. A pH value can be assigned to experimental samples via a standard curve generated by graphing pH versus FITC/AF647 MFI. As AF647 is relatively brighter than FITC, it is necessary to use more FITC streptavidin than AF647 conjugated streptavidin to generate an effective curve.

1. Calculate volumes for preparation of 4× stocks of DNA fragment biotinylated at both end streptavidin-FITC and streptavidin-AF647 and antibody in duplicates per stimulation condition and standard curve (*see* **Note 24**).
2. pH sensing streptavidin DNA ICs are formed by first combining fluorophore conjugated streptavidins and DNA fragment biotinylated at both ends in biotin free medium and incubating on ice for 10 min (*see* **Note 25**).
3. Mix antibody with streptavidin-DNA complexes in RPMI.
4. Incubate plates for 24 h in 37 °C incubator, 5 % CO_2
5. To construct the pH curve, wash the cells 2× with physiological saline and resuspend the experimental samples in FACS buffer.
6. Next, resuspend the cells used to construct the standard curve in pH buffer solutions between pH 7.7 and pH 4 containing 4 μM monensin and 20 μM nigericin and incubate at RT for 5 min.
7. Acquire the samples by flow cytometry in the pH buffers.
8. A sample standard curve generated from B cells stimulated with the dual fluorescent ICs between pH 7.7 and pH 4 is presented in Fig. 4.

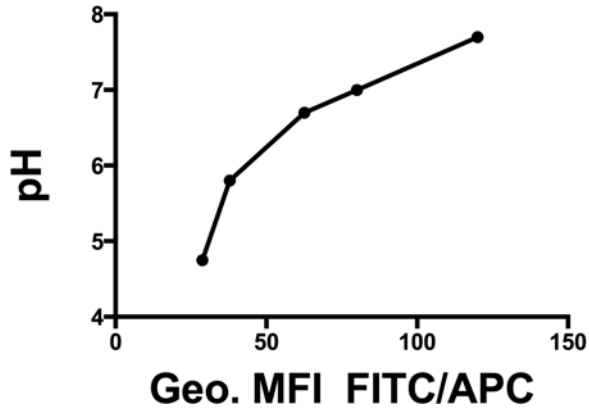

Fig. 4 pH curve generated from B cells stimulated with pH sensing ICs composed of anti-streptavidin antibody, streptavidin-FITC/AF647, and biotin-labeled DNA. AM14 B cells were purified with B220 magnetic beads and stimulated with ICs composed of 0.5 μg/mL anti-streptavidin, 0.05 μg/mL streptavidin AF647, 0.36 μg/mL streptavidin FITC, and 500 ng/mL of DNA fragments biotinylated at both ends for 24 h. The ratio of geometric mean fluorescent intensity (Geo. MFI) of FITC to AF647 was plotted against pH to generate the standard curve

3.7 Confocal Microscopy Determination of Immune Complex Location

Although pH measurements offer a rapid and physiologically relevant means to interrogate the intracellular trafficking of ICs, confocal microscopy and immunofluorescence allow for more precise information about colocalization between the IC and compartment specific markers (e.g., LAMP-1) or relevant endosomal receptors (e.g., TLR9-gfp). Multi color fluorescent microscopy experiments are often times constrained by a limited palette of detecting antibody conjugates and/or fluorescent protein fusions to endosomal markers and endosomal receptors. Incorporation of fluorescent streptavidin into the IC adds an element of flexibility because streptavidin is commercially available conjugated to nearly any fluorophore conjugate.

3.7.1 Preparation of Cover Slips

1. Place coverslips in a 24 well tissue culture plate (*see* **Note 26**).
2. Next, add 200 μL of 0.1 % poly-l lysine to each cover slip and incubate at RT for 10 min.
3. Aspirate the poly-l-lysine and add 200 μL of prewarmed 2 % type B gelatin solution and incubate at 37 °C for 10 min.
4. Finally, aspirate the gelatin solution and dry the cover slips by removing the lid from the tissue culture plate and placing it at the back of the tissue culture hood overnight.

3.7.2 Confocal Microscopy of Immune Complex Treated B Cells

1. Plate the B cells at $4–8 \times 10^5$ cells per well and allow them to settle down onto the coverslips.
2. Next, add the streptavidin-AF647 fluorescent IC and incubate plate for 24 h in 37 °C incubator, 5 % CO_2.
3. After 24 h, transfer the coverslips to a 24 well plate containing 500 μL of fixation buffer.
4. Fix the cells for 10–15 min at RT and then gently add 250 μL of PBS containing 125 mM glycine to quench excess PFA.
5. Aspirate the quenched PFA solution.
6. Add blocking buffer and incubate the cells for 1 h to O/N at 4 °C.
7. Aspirate the blocking buffer and then gently add 250 μL of 1D4B-Dy550 diluted 1:100 to 1:500 in permeabilization buffer.
8. Incubate for 2 h at RT with gentle shaking or rocking in the dark.
9. Aspirate the fluid and then gently add 500 μL of permeabilization buffer and then gently shake or rock the plate for 5 min at RT in the dark.
10. Repeat **step 8** twice and then add 500 μL of PBS containing 0.2 % sodium azide.
11. To mount the coverslips, place 10–20 μL of ProLong Gold Antifade mounting medium on the center of a glass slide and place the coverslip on top of the mount cell side DOWN.
12. Gently seat the coverslip on the slide by pressing down gently on the coverslips with the eraser side of a pencil or inverted P100 tip.
13. Allow the mount to cure overnight and then seal the edges of the cover slips with CLEAR nail polish.
14. The slides can be imaged by conventional epifluorescence microscopy or confocal microscopy.
15. A sample image generated using the protocol above is included in Fig. 5.

3.8 Dendritic Cell Cytokine Assay

Activation of DCs by ICs is measured by cytokine production. Hematopoietic cells extracted from mouse bone marrow are stimulated with Flt3L, which induces differentiation of stem cells into pDC and cDCs. The resulting population, designated "FLt3L-DCs", consists of a mix of pDC and cDC. IFNα is secreted exclusively by pDCs, and is used as indicator of pDC activation by ICs. IL-6 is secreted by both pDCs and cDC, but predominately by cDCs, and can be used as an indicator of cDC activation by ICs.

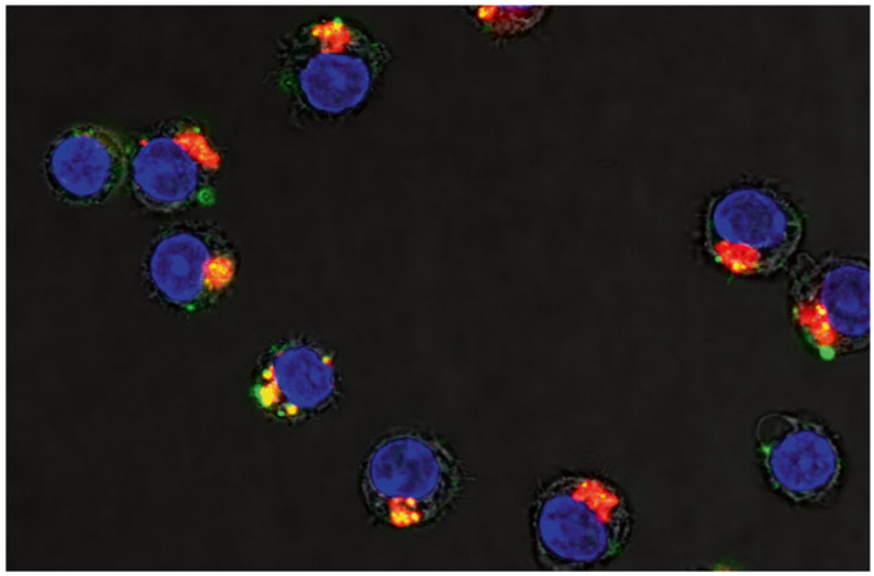

Fig. 5 Immunofluorescence of AM14 B cells stimulated with ICs composed of anti-streptavidin, streptavidin-AF488, and DNA fragments biotinylated at both ends. AM14 B cells were purified with B220 beads and stimulated with ICs composed of 0.5 μg/mL anti-streptavidin, 0.4 μg/mL streptavidin AF488 (*Green*) and 500 ng/mL of DNA fragments biotinylated at both ends for 24 h. The cells were fixed, permeabilized, stained with Dy550-1D4B (*Red*) and DAPI (*Blue*). Images were acquired on a Leica SP8 spectral confocal microscope

3.8.1 DC Preparation

1. Dissect femur and tibia and place in 10 mL of PBS in a 15 mL conical tube. Keep on ice.
2. Transfer to Petri dish and trim off extra tissue.
3. Flush out bone marrow cells inside a 50 mL conical tube by applying 20 mL of RPMI 1640 with a 20 mL syringe and a 25 gauge needle.
4. Spin cells 300 × *g* for 5 min at 4 °C.
5. Aspirate supernatant using a Pasteur pipette attached to a vacuum flask.
6. Flick cells to resuspend, add 500 μL of RBC lysis buffer, and incubate 1 min at room temperature.
7. Immediately add RPMI 1640 to bring to a total volume of 15 mL.
8. Spin cells at 300 × *g* for 5 min at 4 °C, aspirate supernatant using a Pasteur pipette attached to a vacuum flask, and flick cells to resuspend.
9. Add 10 mL RPMI medium, run cells through a 70 μm cell strainer, and rinse strainer with 5 mL RPMI.
10. Spin cells at 300 × *g* for 5 min at 4 °C, aspirate supernatant using a Pasteur pipette attached to a vacuum flask, and flick cells to resuspend.

11. Add 5 mL RPMI medium and count.
12. Seed cells at a 1.5×10^6 cells/mL in RPMI, and add supernatant from FL-B16 cells at a final concentration of 7.5 % (v/v) (*see* **Notes 26 and 27**).
13. Incubate plates for 8 days in 37 °C incubator, 5 % CO_2.

3.8.2 DC Stimulation

1. Count cells and seed at a density of 3×10^6 cells/mL in 100 μL RPMI medium in a flat-bottom, 96-well plate (*see* **Note 28**).
2. Stimulate Flt3L-DC by addition of ICs (2× in 100 μL or 4× in 50 μL, complete to final volume of 200 μL).
3. Incubate plates for 24 h in 37 °C incubator, 5 % CO_2.
4. Harvest supernatants for measurement of cytokines.

3.8.3 Measurement of DC Cytokines by ELISA

1. Coat ELISA plates with 50 μL/well of rat monoclonal anti-mouse IFN-α at 2 μg/mL in PBS. Incubate O/N at 4 °C.
2. Wash 3× with ELISA wash buffer.
3. Add 100 μL of ELISA blocking buffer and incubate for 2 h at room temperature.
4. Wash 3× with ELISA wash buffer.
5. Add 50 μL of supernatant, or mouse alpha-interferon standard, at a range of 5000 pg/mL to 78 pg/mL in ELISA blocking buffer. Incubate O/N at 4 °C.
6. Dilute rabbit polyclonal anti-mouse IFN-α to a final concentration of 0.2 μg/mL in ELISA blocking buffer, add 50 μL/well, and incubate 4 h at room temperature.
7. Wash 3× with ELISA Wash buffer.
8. Dilute peroxidase-conjugated donkey anti-rabbit IgG $F(ab')_2$ fragment, to a final concentration of 80 ng/mL in ELISA blocking buffer, and add 50 μL per well. Incubate 1.5 h at room temperature.
9. Wash 5× with ELISA wash buffer.
10. Develop using 50 μL of TMB detection substrate. Stop reaction by adding 50 μL ELISA stop solution and measure absorbance at 450 nm.

4 Notes

1. Growth medium will vary depending on the hybridoma to be grown. Fetal calf serum contains IgG that is capable of binding to protein G during antibody purification, therefore medium must be depleted of IgG prior to use for growing hybridomas. IgG is removed by running medium over a protein G column as described for antibody purification, except

that IgG is discarded. Alternatively, serum free medium for hybridoma culture is available commercially.

2. All reagents, glassware, and plasticware used for cell culture should be sterile and endotoxin-free.
3. It is important to never let the protein G Sepharose dry out. Column should be capped at both ends with liquid remaining above the Sepharose whenever the column is not in use.
4. Before eluting, check that pH of elution buffer and neutralization buffer mix is around 7.6 using pH paper. The time that the antibody is in elution buffer should be minimized to prevent denaturing of antibody at low pH. If antibody is denatured using this method of elution, alternative elutions at higher pH can be used. See the manufacturer's information regarding alternative elution methods.
5. Antibodies should be tested for endotoxin contamination at 3× the concentration used in cell culture using the Limulus Amoebocyte Lysate Assay (Cambrex) according to the manufacturer's instructions. Endotoxin levels used in assay are below 0.03 EU/mL. Endotoxin can be removed from samples testing positive using a Triton® X-114 extraction [28].
6. Dam/dcm-deficient *E. coli* are used to prevent methylation at adenosine and cytosine residues.
7. LITMUS29 and pUC19 are high-copy plasmids, so do not exceed 100 mL of culture or grow for more than 16 h at 37 °C at 250 rpm in a rotary shaker. Poor lysis and low DNA yield result from using too much bacteria, so we recommend weighing the bacterial pellet and using no more than 300 mg/maxiprep column. Including the LyseBlue reagent provided with the kit helps to monitor complete lysis.
8. This reaction can be scaled up, 2–4 U of each restriction enzyme/μg of DNA should be used, and enzyme should remain less than 10 % of the total reaction volume. DNAse/RNAse free water should be used for all steps of DNA preparation.
9. If you do not have a comb this large, wells can be taped together using thick packing tape, or DNA can be loaded into multiple wells.
10. Running the gel this long is necessary to ensure complete separation of the plasmid backbone from the DNA fragment insert. We have also found that using high quality agarose such as SeaKem® GTG® agarose is critical for high fragment yields.
11. The CGneg and CG50 fragments make up approximately 20 % of the plasmid, so 40 μg of fragment is expected from digesting 200 μg of plasmid. Each column binds a maximum of 25 μg of DNA, so 2 columns should be used. We have also used

Qiagen's Gel Extraction kits and have found that yields are much better with the Zymoclean Gel DNA Recovery Kit™. DNAs are stored at 100–200 ng/μL in TE buffer. EDTA in TE buffer inhibits DNAses, but EDTA can be toxic to cells, so storing DNA at this concentration allows for dilution of the EDTA when adding to cell culture. All DNA preparations are tested for endotoxin using the Limulus Amoebocyte Lysate Assay (Cambrex) according to the manufacturer's instructions, at 3× the concentration to be used in cell culture assays. Endotoxin levels used in assay are below 0.03 EU/mL. Most DNA made by these methods is endotoxin-free, but if DNA is contaminated, running DNA through an additional DNA Clean & Concentrator-25™ kit and/or extracting with Triton-X-114 [28] usually removes endotoxin.

12. Yields are usually about 5 μg/100 μL of PCR reaction, so 4–5 PCR reactions can be sequentially loaded onto 1 column.
13. The Klenow enzyme works most efficiently in the presence of all four dNTPs. Single ends may be labeled by leaving out selected dNTPs. Klenow Fragment has 3′→5′ exonuclease activity in the absence of dNTPs, so (3′→5′ exo-) Klenow Fragment must be used if dNTPs are left out. As with restriction digests, enzyme should remain less than 10 % of the total reaction volume.
14. Alternatively IC composed of antibody Hy1.2 (anti-TNP) and TNP-labeled DNA may be used. TNP-labeled DNA is made by substituting aminoallyl-dUTP for biotin-16-dUTP in the labeling reaction. DNA prepared from plasmid is then gel purified, or DNA prepared by PCR is run through DNA Clean & Concentrator-25™ kit. DNA is eluted in dH_2O (do not use TE buffer, as Tris base contains amines that interfere with labeling). TNP label is added by combining up to 10 μg of DNA in 50 μL of dH_2O, 30 μL of sodium bicarbonate buffer, and 20 μL of reactive TNP, vortexing, and incubating 60 min. at room temperature in the dark. DNA is then run through a DNA Clean & Concentrator-25™ kit to remove excess TNP. Whenever possible we use biotin-labeling, as the DNA preparation involves fewer steps, yields are better, and measuring the extent of labeling is easier.
15. Alternatively, a gel shift can be used to confirm that DNA was labeled with TNP. The affinity of the anti-TNP antibody is lower than the anti-biotin antibody, making TNP-labeling more difficult to measure. Because of this, it is critical that all steps are performed at 4 °C. 100 ng of TNP-labeled DNA is combined with 2 μg of Hy1.2 (anti-TNP) or irrelevant control antibody 1D4 (anti-biotin) in 40 μL of PBS. 8 μL of loading dye is added and samples are incubated O/N at 4 °C. A 2.5 % agarose gel is run at 4 °C with prechilled running buffer until

the dye is about 0.5 in. below the wells (running further will dissociate complex).

16. We have routinely used antibodies at a final concentration of 0.1–1 μg/mL, DNA fragment at 50–500 ng/mL, and streptavidin at 0.1–0.5 μg/mL.
17. We have routinely used anti-streptavidin at a final concentration of 0.1–10 μg/mL, and DNA fragments at a final concentration of 10 ng/mL–1 μg/mL. Antibodies and DNA fragments should be titrated to determine optimal concentrations.
18. Complex formation between streptavidin and biotinylated DNA should be performed in a small volume of biotin-free solution such as DMEM or PBS.
19. We have used BWR4 at a range of 0.5–10 μg/mL, and Y2 at 1–20 μg/mL. RNP/Sm particles are added at a final concentration of 1–2 μg/mL.
20. When working with primary B-cell suspensions, avoid any bubbles and pipette up and down gently.
21. Have all the reagents ready for B-cell stimulation after B-cell preparation and seed cells as soon as possible. B cells die quickly and leaving them on ice while preparing other reagents will decrease your final yield.
22. AM14 B cells stimulated by RNA IC or snRNP IC need to be primed for 1–2 h with 1000 U/mL of IFN-α. Prepare 4× stock solution of IFN-α and add 50 μL per well.
23. It is important to completely dry the filtermats, as remaining water in the filter may quench scintillation fluid with significant reduction of cpms. Drying for at least 2 h or O/N is recommended.
24. For acidic compartment below pH 5, Oregon Green 488 is more sensitive than FITC because it has a lower pKa.
25. We have routinely used anti-streptavidin at a final concentration of 0.1–1 μg/mL, DNA fragment at 50–500 ng/mL and streptavidin-FITC at 0.35 μg/mL and streptavidin-AF647 at 0.05 μg/mL.
26. For live cell imaging, glass bottom dishes can be coated using the same methodology.
27. We have used conditioned medium from FL B16 cells as a source of Flt3L. Alternatively, Flt3L is commercially available through R&D Systems, Minneapolis, MN).
28. Profiling of Flt3L-DCs by flow cytometry is recommended to determine the relative percentage of pDCs ($CD11b^{-}B220^{+}$) and cDCs ($CD11b^{+}B220^{-}$) after culture.

References

1. Chan OT, Madaio MP, Shlomchik MJ (1999) The central and multiple roles of B cells in lupus pathogenesis. Immunol Rev 169:107–121
2. Diebold SS, Kaisho T, Hemmi H, Akira S, Reis e Sousa C (2004) Innate antiviral responses by means of TLR7-mediated recognition of single-stranded RNA. Science 303(5663):1529–1531
3. Hemmi H, Takeuchi O, Kawai T, Kaisho T, Sato S, Sanjo H, Matsumoto M, Hoshino K, Wagner H, Takeda K, Akira S (2000) A Toll-like receptor recognizes bacterial DNA. Nature 408(6813):740–745
4. Heil F, Hemmi H, Hochrein H, Ampenberger F, Kirschning C, Akira S, Lipford G, Wagner H, Bauer S (2004) Species-specific recognition of single-stranded RNA via toll-like receptor 7 and 8. Science 303(5663):1526–1529
5. Lund JM, Alexopoulou L, Sato A, Karow M, Adams NC, Gale NW, Iwasaki A, Flavell RA (2004) Recognition of single-stranded RNA viruses by Toll-like receptor 7. Proc Natl Acad Sci U S A 101(15):5598–5603
6. Christensen SR, Shupe J, Nickerson K, Kashgarian M, Flavell RA, Shlomchik MJ (2006) Toll-like receptor 7 and TLR9 dictate autoantibody specificity and have opposing inflammatory and regulatory roles in a murine model of lupus. Immunity 25(3):417–428
7. Pisitkun P, Deane JA, Difilippantonio MJ, Tarasenko T, Satterthwaite AB, Bolland S (2006) Autoreactive B cell responses to RNA-related antigens due to TLR7 gene duplication. Science 312(5780):1669–1672
8. Marshak-Rothstein A (2006) Toll-like receptors in systemic autoimmune disease. Nat Rev Immunol 6(11):823–835
9. Leadbetter EA, Rifkin IR, Hohlbaum AM, Beaudette BC, Shlomchik MJ, Marshak-Rothstein A (2002) Chromatin-IgG complexes activate B cells by dual engagement of IgM and Toll-like receptors. Nature 416(6881):603–607. doi:10.1038/416603a
10. Marshak-Rothstein A, Busconi L, Lau CM, Tabor AS, Leadbetter EA, Akira S, Krieg AM, Lipford GB, Viglianti GA, Rifkin IR (2004) Comparison of CpG s-ODNs, chromatin immune complexes, and dsDNA fragment immune complexes in the TLR9-dependent activation of rheumatoid factor B cells. J Endotoxin Res 10(4):247–251
11. Uccellini MB, Busconi L, Green NM, Busto P, Christensen SR, Shlomchik MJ, Marshak-Rothstein A, Viglianti GA (2008) Autoreactive B cells discriminate CpG-rich and CpG-poor DNA and this response is modulated by IFN-alpha. J Immunol 181(9):5875–5884
12. Lau CM, Broughton C, Tabor AS, Akira S, Flavell RA, Mamula MJ, Christensen SR, Shlomchik MJ, Viglianti GA, Rifkin IR, Marshak-Rothstein A (2005) RNA-associated autoantigens activate B cells by combined B cell antigen receptor/Toll-like receptor 7 engagement. J Exp Med 202(9):1171–1177. doi:10.1084/jem.20050630
13. Boule MW, Broughton C, Mackay F, Akira S, Marshak-Rothstein A, Rifkin IR (2004) Toll-like receptor 9-dependent and -independent dendritic cell activation by chromatin-immunoglobulin G complexes. J Exp Med 199(12):1631–1640
14. Means TK, Latz E, Hayashi F, Murali MR, Golenbock DT, Luster AD (2005) Human lupus autoantibody-DNA complexes activate DCs through cooperation of CD32 and TLR9. J Clin Invest 115(2):407–417
15. Yasuda K, Richez C, Maciaszek JW, Agrawal N, Akira S, Marshak-Rothstein A, Rifkin IR (2007) Murine dendritic cell type I IFN production induced by human IgG-RNA immune complexes is IFN regulatory factor (IRF)5 and IRF7 dependent and is required for IL-6 production. J Immunol 178(11):6876–6885
16. Baechler EC, Batliwalla FM, Karypis G, Gaffney PM, Ortmann WA, Espe KJ, Shark KB, Grande WJ, Hughes KM, Kapur V, Gregersen PK, Behrens TW (2003) Interferon-inducible gene expression signature in peripheral blood cells of patients with severe lupus. Proc Natl Acad Sci U S A 100(5):2610–2615
17. Green NM, Laws A, Kiefer K, Busconi L, Kim YM, Brinkmann MM, Trail EH, Yasuda K, Christensen SR, Shlomchik MJ, Vogel S, Connor JH, Ploegh H, Eilat D, Rifkin IR, van Seventer JM, Marshak-Rothstein A (2009) Murine B cell response to TLR7 ligands depends on an IFN-beta feedback loop. J Immunol 183(3):1569–1576. doi:10.4049/jimmunol.0803899
18. Green NM, Moody KS, Debatis M, Marshak-Rothstein A (2012) Activation of autoreactive B cells by endogenous TLR7 and TLR3 RNA ligands. J Biol Chem 287(47):39789–39799. doi:10.1074/jbc.M112.383000
19. Uccellini MB, Busto P, Debatis M, Marshak-Rothstein A, Viglianti GA (2012) Selective binding of anti-DNA antibodies to native dsDNA fragments of differing sequence. Immunol Lett 143(1):85–91. doi:10.1016/j.imlet.2012.01.003
20. Monestier M, Novick KE (1996) Specificities and genetic characteristics of nucleosome-reactive antibodies from autoimmune mice. Mol Immunol 33(1):89–99

21. Monestier M, Novick KE, Losman MJ (1994) D-penicillamine- and quinidine-induced antinuclear antibodies in A.SW (H-2s) mice: similarities with autoantibodies in spontaneous and heavy metal-induced autoimmunity. Eur J Immunol 24(3):723–730
22. Viglianti GA, Lau CM, Hanley TM, Miko BA, Shlomchik MJ, Marshak-Rothstein A (2003) Activation of autoreactive B cells by CpG dsDNA. Immunity 19(6):837–847
23. Krieg AM, Wu T, Weeratna R, Efler SM, Love-Homan L, Yang L, Yi AK, Short D, Davis HL (1998) Sequence motifs in adenoviral DNA block immune activation by stimulatory CpG motifs. Proc Natl Acad Sci U S A 95(21):12631–12636
24. Shlomchik MJ, Zharhary D, Saunders T, Camper SA, Weigert MG (1993) A rheumatoid factor transgenic mouse model of autoantibody regulation. Int Immunol 5(10):1329–1341
25. Eilat D, Fischel R (1991) Recurrent utilization of genetic elements in V regions of antinucleic acid antibodies from autoimmune mice. J Immunol 147(1):361–368
26. Bloom DD, Davignon JL, Retter MW, Shlomchik MJ, Pisetsky DS, Cohen PL, Eisenberg RA, Clarke SH (1993) V region gene analysis of anti-Sm hybridomas from MRL/Mp-lpr/lpr mice. J Immunol 150(4):1591–1610
27. Vergne I, Constant P, Laneelle G (1998) Phagosomal pH determination by dual fluorescence flow cytometry. Anal Biochem 255(1):127–132. doi:10.1006/abio.1997.2466
28. Aida Y, Pabst MJ (1990) Removal of endotoxin from protein solutions by phase separation using Triton X-114. J Immunol Methods 132(2):191–195

Chapter 17

Analysis of TLR-Induced Metabolic Changes in Dendritic Cells Using the Seahorse XF^{e}96 Extracellular Flux Analyzer

Leonard R. Pelgrom, Alwin J. van der Ham, and Bart Everts

Abstract

Engagement of Toll-like receptors (TLRs) on dendritic cells (DCs) triggers the expression of a large set of genes involved in DC activation and maturation, which allow them to act efficiently as antigen-presenting cells. Recently, it has become clear that TLR signalling in DCs also results in dramatic metabolic changes that are integral to their changed biology. Here, we describe a detailed protocol on how DC metabolism can be studied after TLR stimulation using the 96-well format Extracellular Flux (XF^{e}96) Analyzer from Seahorse Bioscience, a machine that allows one to simultaneously assess rates of oxidative phosphorylation and glycolysis in real-time, in live cells and in a high-throughput manner.

Key words Toll-like receptors, Dendritic cells, Glycolysis, Oxidative phosphorylation, Respiration, Metabolism, Cellular bioenergetics, Extracellular acidification, Oxygen consumption, Seahorse Bioscience, Extracellular Flux Analyzer

1 Introduction

Signalling via Toll-like receptors (TLRs) on dendritic cells (DCs) drives a program of activation that includes the enhanced capturing and processing of antigens for loading and presentation on major histocompatibility complex (MHC) class I and II, and the increased expression of chemokine receptors, cytokines and co-stimulatory molecules. It is not surprising that this dramatic change in the biology of DCs requires a metabolic adaptation to meet the bioenergetic and anabolic demands of this activation process. We and others have recently found that in murine DCs, triggering of TLRs is accompanied by a metabolic switch characterized by an increase in glycolysis and a complementary decrease in oxidative phosphorylation [1–5]. Specifically, loss of mitochondrial oxidative function was found to be a direct consequence of TLR-induced production of nitric oxide (NO) by inducible nitric oxide synthase (iNOS) that poisons the mitochondrial respiratory chain in an autocrine fashion. This forces the cells to increase glycolytic flux to maintain sufficient

Claire E. McCoy (ed.), *Toll-Like Receptors: Practice and Methods*, Methods in Molecular Biology, vol. 1390,
DOI 10.1007/978-1-4939-3335-8_17,

ATP levels [2, 6]. In addition to this bioenergetic adaption, we have recently observed that TLR engagement also triggers a rapid increase in glycolysis, preceding iNOS expression, that primarily appears to serve an anabolic role allowing DCs to express activation markers and cytokines and therefore, to acquire their full T-cell-priming potential [1].

Some of these observations regarding TLR-driven metabolic changes in DCs have been performed using traditional cellular metabolic assays that typically involve radioactivity, cell destruction and large numbers of cells [7]. Recently, Extracellular Flux (XF) Analyzers from Seahorse Bioscience have been developed that perform highly accurate real-time measurements of cellular metabolism of living cells and tissues by simultaneously quantifying rates of extracellular acidification (ECAR) and oxygen consumption (OCR) as measures of glycolysis and mitochondrial respiration, respectively. This apparatus has allowed us to gain exciting new insights in immune cell metabolism and has been shown to be instrumental in moving the field of DC metabolism forward [8]. This state-of-the-art technology offers a robust and simple high-throughput method for studying substrate utilization, mitochondrial function, and energy expenditure in a 24- or 96-well plate format, without the use of large number of cells, electrodes, dyes, radioactive materials or lysis of cells that is typical of other more laborious metabolic assays. During measurements, the XF assay cartridge is lowered, creating a temporary 7 μL microchamber with limited diffusion. In this small volume of medium, oxygen consumption and lactic acid excretion by the cells will rapidly result in significant changes in oxygen and proton concentration, which is registered by proton and oxygen-quenchable fluorophores that are embedded in the sensor (*see* Fig. 1).

In addition, as the assay is running, compounds can be injected through the four injection ports surrounding the sensor. This allows evaluation of the acute effects that compounds such as TLR ligands, metabolic substrates, activators/inhibitors of signalling pathways and other compounds of interest have on cellular metabolism and energetics. In conclusion, XF Analyzers from Seahorse Bioscience are easy to use and allow for the measurement and manipulation of metabolic pathways in real-time, helping the researcher to elucidate the involvement of metabolic processes in TLR-driven changes in DC biology. We here describe a detailed protocol of how cellular metabolism of DCs can be studied following TLR stimulation, using the 96-well format Extracellular Flux (XF^e96) Analyzer (*see* **Note 1**). We will provide one example of how changes in metabolism can be followed in real-time in response to acute TLR stimulation and one example of how mitochondrial function can be assessed in TLR-activated DCs.

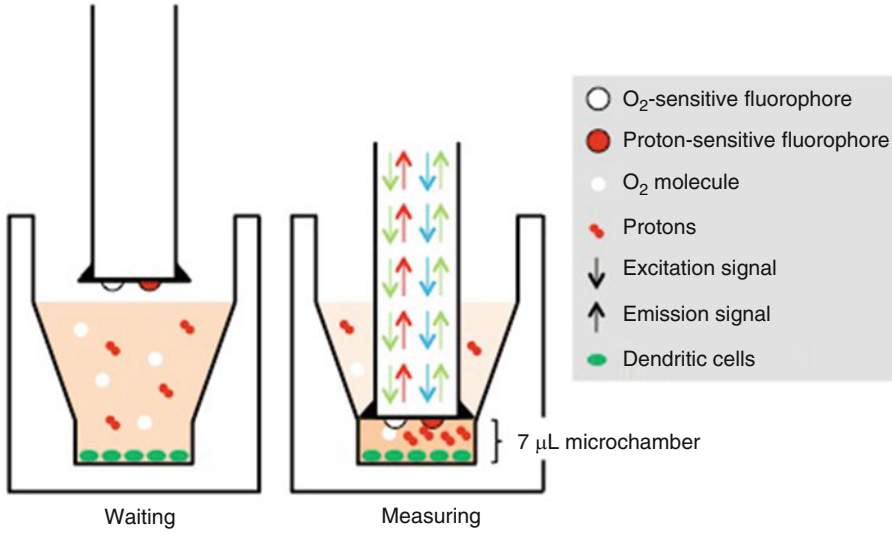

Fig. 1 Schematic representation of the XF Analyzers from Seahorse Bioscience

2 Materials

1. Poly-D-lysine hydrobromide (PDL; Sigma).
2. RPMI-1640 medium powder with L-glutamine, without glucose and sodium bicarbonate (Sigma) (*see* **Note 2**).
3. 37 % HCl solution.
4. 500 mL vacuum filter/storage bottle system, 0.22 μM pore 40 cm^2 PES membrane (Corning).
5. Oligomycin (Cayman Chemical).
6. Carbonyl cyanide 4-(trifluoromethoxy)phenylhydrazone (FCCP; Sigma).
7. Rotenone (Sigma).
8. Antimycin A (Sigma).
9. DMSO.
10. XF^{e}96 FluxPak (Seahorse Bioscience) (*see* **Note 3**).
11. XF Calibrant (Seahorse Bioscience).
12. 10 % D-glucose (Sigma).
13. Fetal calf serum, heat-inactivated at 56 °C for 30 min (HI-FCS; Bodinco).
14. 200 μL Flextop ultra-fine point tips (VWR).
15. XF^{e}96 Extracellular Flux Analyzer (Seahorse Bioscience).

3 Methods

3.1 Preparation of the Reagents

3.1.1 Poly-D-Lysine Hydrobromide

1. Dissolve 5 mg poly-D-lysine hydrobromide (PDL) in 100 mL MilliQ H_2O to reach a concentration of 50 μg/mL.
2. Sterilize by filtration (0.2 μM) and store at 20 °C. Thawed aliquots can be stored at 4 °C.

3.1.2 Assay Media

1. Dissolve 8.4 mg RPMI-1640 medium powder with L-glutamine in 500 mL MilliQ H_2O by gentle swirling.
2. Once the powder is dissolved, add MilliQ H_2O to a total of ~1000 mL.
3. Adjust the pH with 37 % HCl solution to pH 7.4.
4. Sterilize the medium using a filter system.
5. To prepare 0 % FCS/XF media containing 10 mM D-glucose for use in the injection ports (*see* **Note 4**), add 0.91 mL of 10 % D-glucose to 49.09 mL of RPMI-1640 medium with L-glutamine. To prepare 5 % FCS/XF media containing 10 mM D-glucose for the cells (*see* **Notes 5** and **6**), add 0.91 mL of 10 % D-glucose and 2.5 mL of HI-FCS to 46.59 mL of RPMI-1640 medium with L-glutamine.

3.1.3 Oligomycin

1. To prepare a 1 mM stock solution, dissolve 1 mg of oligomycin in 1.26 mL DMSO. This stock needs to be diluted to 1 μM (1000×) for use in an XF assay run (*see* Table 2).
2. Prepare aliquots of 27 μL/vial and store at −20 °C.

3.1.4 FCCP

1. To prepare a 30 mM superstock, dissolve 10 mg of FCCP in 1.3 mL DMSO.
2. Subsequently, dilute 30 mM FCCP 1:10 with DMSO to generate a 3 mM stock solution. This stock needs to be diluted to 3 μM (1000×) for use in an XF assay run (*see* Table 2).
3. Prepare aliquots of 29 μL/vial and store at −20 °C.

3.1.5 Rotenone

1. To prepare a 10 mM superstock, dissolve 10 mg of rotenone in 2.5 mL DMSO.
2. Subsequently, dilute 10 mM rotenone 1:10 with DMSO to generate a 1 mM stock solution. This stock needs to be diluted to 1 μM (1000×) for use in an XF assay run (*see* Table 2).
3. Prepare aliquots of 35 μL/vial and store at −20 °C.

3.1.6 Antimycin A

1. To prepare a 10 mM superstock, dissolve 25 mg of antimycin A in 4.5 mL DMSO.
2. Subsequently, dilute 10 mM antimycin A 1:10 with DMSO to generate a 1 mM stock solution. This stock needs to be diluted to 1 μM 1000× for use in an XF assay run (*see* Table 2).
3. Prepare aliquots of 35 μL/vial and store at −20 °C.

3.2 Preparation of the XF^{e}96 Assay Run

In brief, the general procedure for an XF assay run consists of the following steps:

1. Hydrate the XF assay cartridge.
2. Seed the cells in the cell culture plate.
3. Replace the culture medium with the assay medium.
4. Load the injection ports of the assay cartridge with the drugs/stimuli of interest.
5. Create an assay template using XF Wave.
6. Start the calibration of the sensors in the cartridge.
7. Load the cell culture plate that contains the cells.
8. Optional: recover the cells for future cell count normalization (*see* **Note 7**).

3.2.1 Hydration of the XF Assay Cartridge

1. Place the assay cartridge upside down next to the utility plate.
2. Fill each well of the utility plate with 200 μL of calibration solution and put the cartridge back onto the utility plate, submerging the sensors in the solution.
3. Incubate for 4–24 h at 37 °C in a dry incubator without CO_2.

3.2.2 Seeding and Adherence of DCs

1. If using murine bone marrow-derived dendritic cells (BMDCs) that are cultured with GM-CSF, proceed to **Step 5**. If using any other type of DCs, coat the wells of the XF cell culture 96-well microplate with 25 μL 50 μg/mL PDL (*see* **Note 8**). Gently tap the plate to make sure that the liquid completely covers the bottom of the well.
2. Incubate with PDL for at least 1 h at 37 °C. The type of incubator does not matter at this specific step.
3. Add 175 μL sterile MilliQ H_2O to the wells, resuspend and pipet off as much liquid as possible (*see* **Note 9**).
4. Let the cell culture plate dry in a sterile flow hood for 30–60 min.
5. Culture or isolate your preferred type of DC for use in the XF assay run according to protocols described elsewhere for human monocyte-derived DCs (moDCs) [9], murine BMDCs [10] or DCs isolated from human or murine tissues [1, 11].
6. Seed the number of DCs needed to obtain a confluent monolayer in 50 μL of the same type of culture medium in which the DCs were grown. Different DC types have different sizes and therefore, their seeding density differ (*see* Table 1).
7. Quick-spin the plate to bring all DCs to the bottom of the well.
8. Check under the microscope for a confluent monolayer.
9. Incubate the cells for 1 h at 37 °C, 5 % CO_2, 95 % humidity to allow the cells to adhere.

Table 1
Proposed seeding densities for different DC types to reach a confluent monolayer in a XF cell culture 96-well microplate

Source	Cells/well
Mouse bone marrow-derived, cultured with GM-CSF	70,000
Mouse bone marrow-derived, cultured with Flt3L	150,000
Mouse spleen	150,000
Human skin	200,000
Human blood	200,000
Human monocyte-derived	50,000

10. Check under the microscope for adherence.
11. Proceed to Subheading 3.2.3 to perform a mitochondrial stress test or Subheading 3.2.4 to assess in real-time metabolic changes in response to acute TLR stimulation. Of note, the assays described here are only examples of assays that can be performed using XF Analyzers (*see* **Note 10**).

3.2.3 Mitochondrial Stress Test

The mitochondrial stress test allows one to interrogate the functional properties of the electric transport chain. It consists of the sequential injection of oligomycin (inhibitor of mitochondrial ATP synthase), FCCP (ionophore) and rotenone + antimycin A (inhibitors of complex one and three of the respiratory chain respectively). This allows one to assess baseline respiration (BR), oxygen consumption used for ATP production (ATP) following oligomycin injection, the maximum rate of mitochondrial respiration (MR) following FCCP injection, and non-mitochondrial respiration (NMR) following rotenone/antimycin A injection. The difference in Oxygen Consumption Rate (OCR) between BR and MR is known as the spare respiratory capacity (SRC) and the difference in OCR after oligomycin treatment versus rotenone/antimycin A is the amount of respiration used to compensate for proton leak (PL), which is also known as uncoupling. An example of a mitochondrial stress test performed on LPS-stimulated murine BMDCs is shown in Fig. 2. The concentrations of oligomycin, FCCP and rotenone + antimycin A used in this assay can be found in Table 2.

1. Slowly add 150 μL more culture medium with or without your Toll-like receptor (TLR) ligand(s) of interest.
2. Incubate the TLR-stimulated DCs for 2 up to 48 h at 37 °C, 5 % CO_2 and 95 % humidity.
3. An hour before the XF assay run, prepare 10× working concentrations of oligomycin, FCCP and rotenone + antimycin A

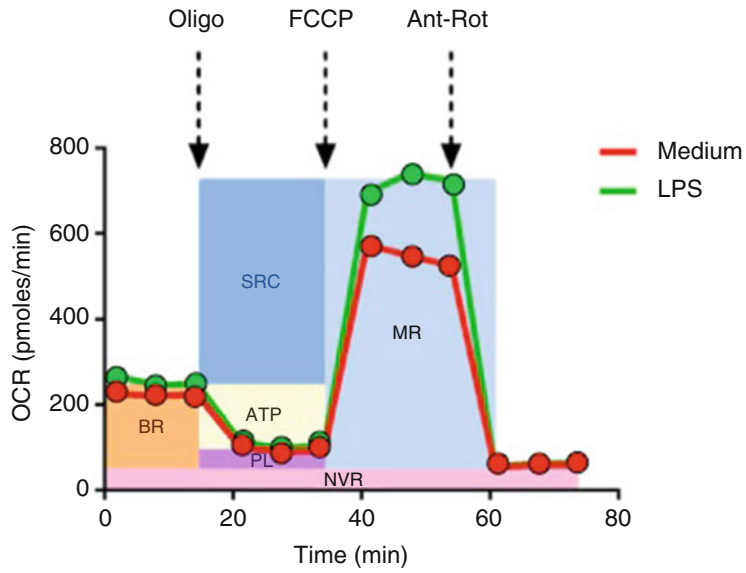

Fig. 2 Murine BMDCs are stimulated with medium or LPS for 2 h and then subjected to the mitochondrial stress test. This graph suggests that short-term LPS stimulation promotes maximal respiration and spare respiratory capacity in these DCs [1]

Table 2
Proposed final concentrations of the mitochondrial stress test compounds

Oligomycin	1 μM
FCCP	3 μM
Rotenone	1 μM
Antimycin A	1 μM

by diluting the drugs 1:100 in 0 % FCS/XF assay medium. For example, dilute 25 μL oligomycin in 2475 μL 0 % FCS/XF assay medium. Do not use 5 % FCS/XF assay medium for injection of compounds (*see* **Note 4**) and dilute rotenone and antimycin A together.

4. Carefully pipette off all the culture medium (*see* **Note 8**).
5. Slowly add 180 μL 5 % FCS/XF assay medium to the cells. Be especially careful with the first 50 μL (*see* **Note 8**). If the cells detach, spin-down the plate again.
6. Incubate the cells for 1 h at 37 °C in a dry incubator without CO_2 in order to remove any CO_2 dissolved in the assay medium (*see* **Note 11**).
7. Add 20 μL oligomycin to port A, 22 μL of FCCP to port B and 25 μL of rotenone + antimycin A to port C (*see* Fig. 3). Use a multichannel, special narrow tips (*see* **Item 14**, Subheading 2) and the provided loading guides to pipet the compounds of

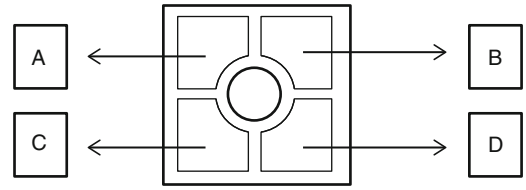

Fig. 3 Schematic drawing of the four injection ports per well

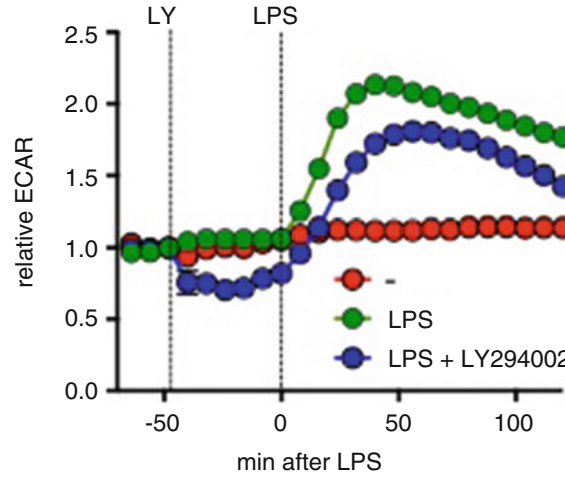

Fig. 4 Murine BMDCs are stimulated with medium or LPS during a XF Assay run and the effects on extracellular acidification rate (ECAR) are assessed in real-time. Moreover, in one condition, an inhibitor of PI3K signalling (LY204002) is injected into the wells prior to LPS stimulation. This suggests that baseline glycolysis rates are partially dependent on PI3K signalling, whereas LPS-induced glycolysis is not [1]

interest into the injection ports of the XF assay cartridge via a single stream (*see* **Note 12**).

8. Fill any empty injection ports of series A, B and C with 20, 22 and 25 μL of 0 % FCS/XF assay medium respectively (*see* **Note 12**).
9. Put the assay cartridge back into a 37 °C incubator without CO_2 until the start of the run (*see* Subheading 3.3).

3.2.4 Tracking Real-Time Metabolic Changes

DCs can also be stimulated with TLR ligands during a run in the XF analyzer. This enables one to follow in real-time the immediate metabolic changes that are induced by TLR engagement. This can easily be combined with pre-incubations of stimulatory/inhibitory compounds to interrogate the involvement of specific signalling pathways in TLR-induced metabolic changes. An example is given in Fig. 4.

1. Slowly add an additional 150 µL culture medium.
2. Allow the cells to fully adhere and rest overnight at 37 °C, 5 % CO_2 and 95 %.
3. The next day, prepare 10× working concentrations of your TLR ligand(s) and stimulatory/inhibitory compound(s) of interest in 0 % FCS/XF assay medium. Do not use 5 % FCS/XF assay medium for injection (*see* **Note 3**).
4. Carefully pipette off all the culture medium (*see* **Note 7**).
5. Slowly add 180 µL 5 % FCS/XF assay medium to the cells. Be especially careful with the first 50 µL (*see* **Note 7**).
6. Incubate the cells for 1 h at 37 °C in a dry incubator without CO_2 in order to remove the CO_2, which was dissolved in the culture medium (*see* **Note 11**).
7. Add 20 µL of your stimulatory/inhibitory compound(s) of interest to port A and 22 µL of your TLR ligand(s) to port B (*see* Fig. 3). Use a multichannel, special narrow tips (*see* **Item 14**, Subheading 2) and the provided loading guides to pipet the compounds of interest into the injection ports via a single stream (*see* **Note 12**).
8. Fill any empty injection ports of series A and B with 20 and 22 µL of 0 % FCS/XF assay medium respectively (*see* **Note 12**).
9. Put the assay cartridge back at 37 °C in a dry incubator without CO_2 until the start of the run (*see* Subheading 3.3).

3.3 Starting a XF Assay Run

A Seahorse XF Analyzer comes with a desktop computer and software (XF Wave) that is used to set up the assay template (i.e. plate layout, number and timing of injection(s), and measurement frequency and duration) and to start or cancel the XF assay run.

1. Select the 'Blank' template and click the 'Design' button.
2. Click on the vertical bar of the 'Group definitions' tab. Define your assay conditions and then, click the 'Generate Groups' button. XF Wave will automatically generate groups based on every possible combination of assay conditions you define.
3. Click on the vertical bar of the 'Plate Map' tab. Determine the groups in the plate layout by first selecting a specific group and then, clicking on or dragging across the corresponding well(s).
4. Click on the 'Instrumental Protocol' tab. Then, click on the 'Injection Button' three times when performing the mitochondrial stress test (*see* Subheading 3.2.3) or two times when performing the real-time tracking of metabolic changes (*see* Subheading 3.2.4). For each new injection, the software will automatically select the next available port, i.e. injection 1 = port A, 2 = B, 3 = C and 4 = D.

5. A measurement typically consist of 3 min of 'mixing' and 3 min of 'measuring', repeated for 3 times (i.e. 3 cycles). Correspondingly, with one basal measurement and 3 measurements after injection, the mitochondrial stress test as described here is 72 min long (*see* Fig. 2), excluding calibration and equilibration. Longer measurement times, for example after stimulation with TLR ligands (*see* Fig. 3), can easily be achieved by increasing the number of cycles (*see* **Notes 10** and **13**). Do not forget to set the 'waiting' time at 0 min and 0 s.
6. Go to the 'Review and Run' tab to find the 'Run' button. Click 'Run'.
7. The machine will first ask to load the XF assay cartridge and the utility plate in which the sensors of the assay cartridge were hydrated (*see* Subheading 3.2.1). It is important to remove the lid from the assay cartridge and orient the cartridge and plate in a way that the blue-marked corner faces you. In this orientation, the barcode on the cartridge should not be visible.
8. Press 'continue'.
9. The sensors in the cartridge will now be calibrated to assure the accuracy of your instrument. Equilibration occurs after calibration and ensures temperature stability before beginning your assay. Together this will take approximately 20–25 min.
10. After the calibration and equilibration, the XF analyzer will eject the utility plate. Replace this plate with the cell culture plate containing the DCs as prepared in Subheading 3.2.3. Again, it is important to remove the lid from the plate and to orient the plate in a way that the blue marked corner faces you.
11. Press 'continue' to start the XF assay run. Data will be displayed in real-time during the measurement.

A full tutorial on how to set up an assay template using the XF Wave software can be found on the website of Seahorse Bioscience: http://www.seahorsebio.com/resources/pdfs/user-guide-xfe-wave.pdf.

3.4 Data Analysis

Data that are obtained include ECAR and OCR as well as the raw pH and O_2 tension values. XF Wave software allows one to visualize all these parameters by creating and exporting various graphs. Moreover, this software allows one to directly export the raw data tables to programs such as Excel or GraphPad Prism, which you can use to make your own graphs. An extensive guide on how to analysis your data using Wave can be found on the website of Seahorse Bioscience: http://www.seahorsebio.com/resources/pdfs/user-guide-xfe-wave.pdf.

4 Notes

1. The same assays can be performed using a 24-well format. The number of cells per well in the XF^{e}24 Extracellular Flux Analyzer needs to be increased by 2.5-fold compared to the 96-well format described here (*see* Table 1). In addition, the volumes of assay media in the wells and the injection ports need to be increased by 2.5-fold.
2. The assay medium should not contain any buffering reagents, because glycolysis is determined by changes in extracellular pH.
3. An XF^{e}96 FluxPak contains equal amounts of XF assay cartridges and XF cell culture 96-well microplates. Each assay cartridge comes with its own 96-well microplate, which is referred to as the XF utility plate and is used to hydrate the cartridge sensors. Moreover, each cartridge comes with its own loading guides. The XF cell culture 96-well microplate is used for loading the cells.
4. Large proteins such as BSA may block the injection port.
5. FCS has some buffering capacity. The more FCS is added to the XF assay medium, the lower your ECAR readings will be.
6. FCCP concentration is dependent on the amount of protein in the XF assay medium. The higher the protein concentration, the more the effect of FCCP is quenched. In our hands, 3 μM FCCP works well with the amount of proteins present in 5 % FCS/assay medium to induce maximum respiration and glycolysis (*see* Table 2).
7. Generally, DCs are fully differentiated, non-dividing cells. However, in the case observed differences in metabolism are suspected to be due to differences in cell density rather than inherent differences in metabolism, one can do a normalization after the XF Assay run. For example, one can normalize the obtained metabolic readouts based on protein quantification methods such as the bicinchoninic acid (BCA) assay. The XF Wave software has a feature to enter such data and automatically perform normalization.
8. During measurement, the XF assay cartridge sensors only measure the bottom 7 μL of the XF cell culture 96-well microplates. Therefore, your cells need to be at the bottom of the well and immobilized. XF cell culture microplates are made of polystyrene and are tissue culture-treated, but in our experience, all DCs, except murine bone marrow-derived DCs cultured with GM-CSF, require an additional plate bound substrate such as PDL for proper adherence. Note that adherence by PDL may cause some activation of DCs.
9. It is preferable to wash with unbuffered solutions.

10. Other regularly performed assays include the beta-oxidation assay and the glycolysis stress test. Reagents for these assays are available through Seahorse Bioscience. Moreover, the flexibility of XF analyzers allows one to easily deviate from standard protocols in order to address specific metabolic questions. For example, the presence of certain nutrients in the medium, the nature of the compounds, the timing of injections and the duration of measurements can be adjusted.
11. CO_2 reacts with H_2O to form $HCO_3^- + H^+$, which acidifies the medium and results in incorrect ECAR readings.
12. XF analyzers use compressed air to inject compounds from the ports into the wells. Moreover, series of injection ports are linked (i.e. all A ports, all B ports, etc.). Therefore, each series of injection ports must contain the same amount of volume for the injections to work.
    (a) The combination of these tips (*see* **Item 14**, Subheading 2) and the loading guides allows on to insert the tip into the injection port at a specific depth. Too high and droplets may stick at the top of the well. Too low and the solution may be pipetted through the injection port.
    (b) Dispense the solution via a single stream. Otherwise, droplets may stick at the end of the tip.
    (c) Do not tap the XF assay cartridge in order to get the solution at the bottom of the injection port. The XF assay cartridge is fragile and tapping may cause leaking of the injection ports.
13. We experienced that reliable ECAR and OCR reads can be obtained up to 6 h into a run. After 6 h, XF assay medium becomes too acidified.

References

1. Everts B, Amiel E, Huang SC et al (2014) TLR-driven early glycolytic reprogramming via the kinases TBK1-IKKvarepsilon supports the anabolic demands of dendritic cell activation. Nat Immunol 5(4):323–332
2. Everts B, Amiel E, van der Windt GJ et al (2012) Commitment to glycolysis sustains survival of NO-producing inflammatory dendritic cells. Blood 120(7):1422–1431
3. Jantsch J, Chakravortty D, Turza N et al (2008) Hypoxia and hypoxia-inducible factor-1 alpha modulate lipopolysaccharide-induced dendritic cell activation and function. J Immunol 180(7):4697–4705
4. Krawczyk CM, Holowka T, Sun J et al (2010) Toll-like receptor-induced changes in glycolytic metabolism regulate dendritic cell activation. Blood 115(23):4742–4749
5. Pantel A, Teixeira A, Haddad E et al (2014) Direct type I IFN but not MDA5/TLR3 activation of dendritic cells is required for maturation and metabolic shift to glycolysis after poly IC stimulation. PLoS Biol 12(1):e1001759
6. Amiel E, Everts B, Fritz D et al (2014) Mechanistic target of rapamycin inhibition extends cellular lifespan in dendritic cells by preserving mitochondrial function. J Immunol 93(6):2821–2830
7. Ferrick DA, Neilson A, Beeson C (2008) Advances in measuring cellular bioenergetics using extracellular flux. Drug Discov Today 13(5-6):268–274

8. Pearce EJ, Everts B (2015) Dendritic cell metabolism. Nat Rev Immunol 15(1):18–29
9. Sallusto F, Lanzavecchia A (1994) Efficient presentation of soluble antigen by cultured human dendritic cells is maintained by granulocyte/macrophage colony-stimulating factor plus interleukin 4 and downregulated by tumor necrosis factor alpha. J Exp Med 179(4): 1109–1118
10. Lutz MB, Kukutsch N, Ogilvie AL et al (1999) An advanced culture method for generating large quantities of highly pure dendritic cells from mouse bone marrow. J Immunol Methods 223(1):77–92
11. Stoitzner P, Romani N, McLellan AD et al (2010) Isolation of skin dendritic cells from mouse and man. Methods Mol Biol 595: 235–248

Chapter 18

Toll-Like Receptor Signalling and the Control of Intestinal Barrier Function

Daniel G.W. Johnston and Sinéad C. Corr

Abstract

Epithelial barrier function and innate immunity are fundamental to the pathogenesis of inflammatory and infectious disease. Along with plasma membranes, epithelial cells are the primary cellular determinant of epithelial barrier function. The mechanism by which polarized epithelia form a permeability barrier is of fundamental importance to the prevention of many infectious and inflammatory diseases. Moreover, epithelial cells express Toll-like receptors (TLRs) which upon recognition of conserved microbial factors such as lipopolysaccharide (LPS) induce epithelial responses including epithelial cell proliferation, secretion of secretory IgA into the lumen and production mucins and antimicrobial peptides, thereby promoting intestinal barrier function. Understanding gut barrier integrity and regulation of permeability is crucial to increase our understanding of the pathogenesis of intestinal disease. A variety of tests have been developed to assess this barrier, including assessing intestinal epithelial cell proliferation or death, intestinal tight junction status and the consequence of intestinal barrier integrity loss such as increased intestinal permeability and susceptibility to bacterial infection. Using a mouse model, this chapter describes some of the methods to assess the functional integrity of this epithelial barrier and the part played by a TLR signalling pathway.

Key words Defence, Permeability, Leakiness, Epithelial, Barrier, Tight junction, Infection, TLR, MAL

1 Introduction

Intestinal epithelial barrier dysfunction and leaky gut are linked to the development of infectious and inflammatory disease [1, 2]. In order to gain access to the host and cause disease, bacterial pathogens must first breach the epithelial barrier, and as such, this is the first line of defence against entry of most human pathogens. Intestinal epithelial cells express pattern recognition receptors (PRRs) including TLRs and NOD-like receptors (NLRs) which have an important role in the regulation of intestinal homeostasis and barrier integrity [3]. These PRRs recognize microbial moieties and promote intestinal homeostasis through induction of cytokines including IL-10, antimicrobial peptides including

Claire E. McCoy (ed.), *Toll-Like Receptors: Practice and Methods*, Methods in Molecular Biology, vol. 1390,
DOI 10.1007/978-1-4939-3335-8_18,

β-defensins, epidermal growth factor receptor (EGFR) ligands including amphiregulin and epiregulin which promote cell proliferation and tissue repair, and anti-apoptotic factors which promote epithelial restitution [3].

TLR signalling also fortifies a crucial component of the epithelial barrier, intercellular tight junctions (TJ) or zonula occludens [4]. TJ are important structures which regulate intestinal barrier permeability or leakiness. TJ join epithelial and endothelial cells, and thereby regulate the permeability of the intestinal epithelium [2] (Fig. 1). They are dynamic structures which are regulated by the crosstalk of many signalling pathways, allowing absorption of nutrients but limiting entry of potentially harmful pathogens, toxins and antigens [3]. TJ are multiprotein complexes composed of the transmembrane proteins occludin and claudin, and the intracellular protein zonula occudens (ZO) [5]. TJ and barrier function are regulated by multiple kinases which phosphorylate TJ proteins to determine their expression and localization and ultimately TJ formation [2, 6]. Disruption of TJ structure and increased permeability as a result of specific mutation or aberrant regulatory signals can be the cause of disease due to uncontrolled entry of bacteria or antigens. Indeed, dysregulation of epithelial barrier function

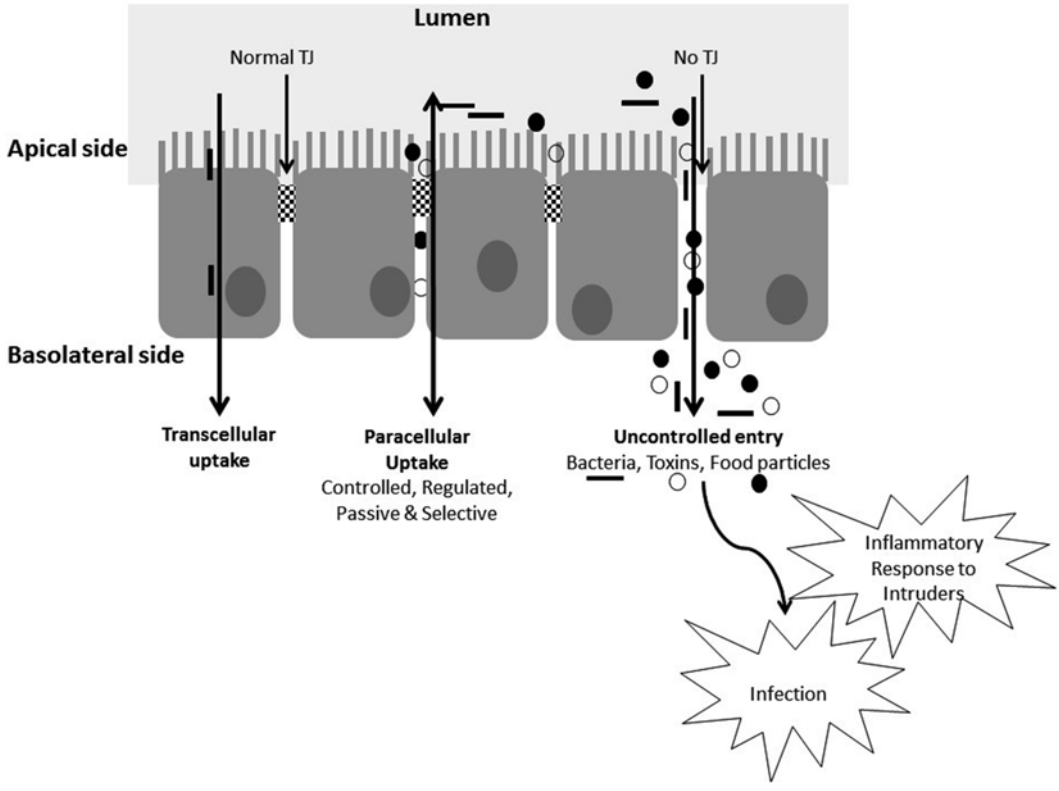

Fig. 1 Epithelial tight junctions regulate the paracellular pathway and contribute to intestinal permeability

including altered TJ formation and "leaky gut" have been associated with the pathogenesis of a variety of infectious, inflammatory and autoimmune diseases including IBD, infectious enterocolitis, rheumatoid arthritis, diabetic retinopathy and asthma [2, 3].

There is accumulating evidence of the role played by TLR signalling pathways in the regulation of intestinal epithelial barrier function. Intestinal barrier function and the role of TLR signalling can be assessed both in vitro using models of intestinal epithelium such as the Caco2 adenocarcinoma cell line or in vivo in mice in which specific components of TLR signalling pathways have been knocked out or silenced [5, 7]. Using these models, $TLR4^{-/-}$ and $MyD88^{-/-}$ mice display reduced expression of the EGF-R ligands and reduced epithelial cell proliferation. MyD88 also induces the antibacterial peptides RegIIIγ and α-defensins thereby promoting defence against infection. TLR2 has been shown to regulate TJ formation and promote barrier integrity, through induction of anti-apoptotic factors which promote epithelial cell survival and regulate ZO-1 localization. Furthermore, the TLR2/TLR4 adaptor MAL plays a critical role in maintaining barrier integrity during infection or assault, by regulating TJ formation via PKC [5].

In mice, intestinal permeability or leakiness can be determined by analysing the mucosal-blood flux of a tracer molecule such as FITC-dextran which is administered orally [5, 8]. Increased mucosa-blood flux in a knockout mouse or across an epithelial monolayer like Caco2 cultured on a transwell system suggests increased leakiness and impaired barrier function. Electrophysical measurements can also be used to assess permeability across intestinal epithelium segments or monolayers of Caco2 [5]. Reduced transepithelial electrical resistance (TEER) suggests impaired barrier function and increased permeability. Measurement of epithelial permeability is essentially a measure of how intact the interepithelial TJ are and passage through the paracellular pathway. TJ formation and structure can be investigated by analysing expression of TJ proteins by Western blot and RT-PCR, while localization can be determined by immunohistochemistry [5, 8, 9]. Expression of antimicrobial factors and EGFR ligands can also be measured in this way. As TJ formation and indeed barrier integrity can also be impaired due to loss of epithelial cells themselves, assays can be used to measure both epithelial cell proliferation and apoptosis [10]. Finally, the functional importance of an intact epithelial barrier can be shown by performing an oral infection model and determining bacterial dissemination from the intestinal epithelium, across the mucosae and to distant organs [5]. Generation of chimeric mice in which a TLR signalling component such as MAL has been knocked out specifically in epithelial cells can be used to confirm the importance of this TLR component in regulation of epithelial barrier integrity [5, 10, 11]. In this model, bone marrow from a TLR knockout donor mouse is reconstituted into a WT

recipient mouse, so that hematopoietic cells in the WT mouse now lack the signalling component being investigated. In this way, you can test the role of the TLR component in epithelial and immune cells. Using the TLR adaptor MAL as an example, this chapter describes some of these assays and their use in assessment of intestinal barrier function, specifically focusing on regulation of intestinal permeability by epithelial TJ.

2 Materials

2.1 Infection Model

1. *S.* Typhimurium UK-1.
2. Luria Bertani (LB) broth (Merck).
3. 37 °C Incubator.
4. Gavage needle.
5. 1 ml syringe.
6. Sterile phosphate buffered saline (PBS) solution.
7. Dissection kit.
8. Stomacher bags (80 m; Seward, UK).
9. Eppendorf tubes containing 900 μl sterile PBS.
10. LB agar (Merck).
11. Mice.

2.2 Intestinal Permeability

1. FITC-dextran, molecular mass 4 kDa (Sigma).
2. Gavage needle.
3. 1 ml syringe.
4. Sterile phosphate buffered saline (PBS) solution.
5. Acid-citrate dextrose.
6. Black 96-well microplate (Nunc).
7. Coloured Eppendorf tubes or similar.

2.3 Electrophysiological Measurements

1. Ussing chambers: 0.6 cm^2 aperture.
2. Superfusate (KBR Ringer's solution): 140 mM Na, 5.2 mM K, 1.2 mM Ca_2, 0.8 mM Mg_2, 120 mM Cl, 25 mM HCO_3, 2.4 mM K_2HPO_4, 0.4 mM KH_2PO_4, 10 mM glucose.
3. Voltage–current clamp (VCC) (Physiological Instruments, San Diego, CA, USA)
4. Intestinal preparation: Mouse distal colon section stripped of seromuscular layer.
5. Amiloride.
6. Secretagogues: carbachol (CCh; 100 μM basolaterally) and forskolin (FSK; 10 μM apically).

2.4 Immunohistochemistry (IHC)

1. Ileum tissue sections obtained from experimental mice: removed, placed in histology cassettes and stored in 4 % paraformaldehyde prior to dehydration.
2. Dehydration kit: Graded ethanol concentrations.
3. Paraffin wax (Eli Lilly) plus moulds (~6 mm).
4. Polysine® Slides (ThermoFisher Scientific).
5. Isocitrate buffer.
6. Blocking buffer: 1 % Fc blockers (Miltenyi Biotec) and 10 % donkey serum (Jackson ImmunoResearch Laboratories).
7. Primary Antibodies: polyclonal rabbit anti-mouse ZO-1, occludin and claudin-3 (Life Technologies). Store at 4 °C.
8. Secondary antibody: Alexa Flour 555 donkey anti-rabbit (Invitrogen).
9. Nuclear stain: 40-6-diamidino-2-phenylindole nucleic acid stain (Invitrogen).
10. DeltaVision PersonalDV Deconvolution microscopy (Applied Precision, Issaquah, WA)
11. Image J software (National Institute of Mental Health, Bethesda, MD).

2.5 RT-PCR

1. RNA isolation: Qiagen RNeasy Mini Kit (Qiagen).
2. NanoDrop spectrophotometer (ThermoFisherScientific).
3. Reverse Transcription reagents (Applied Biosystems): Multiscribe™ reverse transcriptase (RT), RNase inhibitor, dNTP (10 mM solution of 2.5 mM each of dATP, dCTP, dGTP, and dTTP), 10× RT buffer, random primers. Store all reagents at −20 °C.
4. Probes for real-time PCR (Applied Biosystems): various targets, FAM labelled; 18S endogenous control labelled with VIC to allow multiplexing. Store at −20 °C.
5. Endogenous Controls: 18S rRNA (Applied Biosystems). Store at −20 °C.
6. qPCR Mastermix: 2× TaqMan Universal PCR Mastermix (Applied Biosystems). Store at −20 °C.
7. ABI Prism 7700 Sequence Detection system (Applied Biosystems).

2.6 Western Blotting

1. Radioimmunoprecipitation assay buffer (RIPA buffer) for protein extraction: 50 mM Tris, pH 8, 150 mM NaCl, 0.1 % (w/v) SDS, 0.5 % (w/v) sodium deoxycholate and 1 % (v/v) NP-40 dissolved in dH_2O, supplemented with 5 mM EDTA and proteinase inhibitors: aprotinin, phenylmethansulfonyl and leupeptin (1:1000 dilution).

2. Micro-BCA protein quantification kit (Thermo Fisher Scientific).
3. Sample Buffer for protein denaturation: 0.125 M Tris–HCl, pH 6.8, 10 % SDS 0.02 % Bromophenol blue, 10 % glycerol, dH_2O. Add 5 % DTT prior to use as a reducing agent. Store sample buffer and DTT at –20 °C.
4. 12 % resolving gel (10 ml/gel): 3.25 ml H_2O, 4 ml 30 % Protogel, 2.55 ml 1.5 M Tris–HCl, pH 8.8, 100 µl 10 % SDS, 100 µl 10 % APS, 4 µl TEMED.
5. 5 % Stacking gel (6 ml/gel): 4.1 ml H_2O, 1 ml 30 % Protogel, 0.75 ml 1 M Tris–HCl, pH 6.8, 60 µl 10 % SDS, 60 µl 10 % APS, 6 µl TEMED (*see* **Note 1**).
6. Water-saturated Butanol: 50 % Butanol, 50 % dH_2O (*see* **Note 2**).
7. Running Buffer: 0.3 % Tris (w/v), 1.44 % Glycine (w/v), 0.1 % SDS (w/v), dH_2O (*see* **Note 3**).
8. Tris-Buffered Saline (TBS): 0.303 % Tris (w/v), 0.801 % NaCl (w/v), 0.037 % KCl, 0.0103 % $CaCL_2$ (w/v), 0.0072 % NaH_2PO_4 (w/v), dH_2O.
9. Tris-Buffered Saline Tween (TBS-Tween): 0.303 % Tris (w/v), 0.801 % NaCl (w/v), 0.037 % KCl, 0.0103 % $CaCL_2$ (w/v), 0.0072 % NaH_2PO_4 (w/v), dH_2O, 0.05 % Tween.
10. Transfer Buffer 10×: 0.303 % Tris (w/v), 1.5014 % Glycine (w/v), dH_2O. Make up to 1× with 20 % methanol and 70 % water for use in Western blotting.
11. Blocking reagent: 5 % Dried Milk in TBS-Tween (w/v), store at 4 °C for up to 4 days.
12. Primary Antibodies: Phospho-PKC (pan) and phospho-PKC antibodies from sampler kit (Cell Signalling Technologies), PKCz (H-1) (Santa Cruz Biotechnologies), anti-hemagglutinin (Covance, Princeton, NJ). Store at 4 °C.
13. Negative Control Antibodies: IgG control antibody, store at 4 °C.
14. Secondary Antibodies: Anti-rabbit heavy+light chain and anti-mouse heavy+light chain (Jackson ImmunoResearch).
15. Developing reagents: 20× LumoFlur ECL reagents (Cell Signalling Technologies) and acetate film (Fuji Film). Store at 4 °C.

2.7 Quantification of Epithelial Cell Apoptosis

1. Rabbit polyclonal anti-Ki67 antibody (Abcam).
2. 10 % Normal goat serum (DakoCytomation).
3. Mayer's haematoxylin (Sigma-Aldrich).
4. In Situ Cell Death Detection kit (Roche).
5. EnVisionTM Detection System (DakoCytomation, UK).
6. Leica® microscope (Leica® DM 3000 LED) equipped with Leica® DFC495 camera (Leica® Microsystem, Germany).

2.8 Bone Marrow Chimeras

1. Mice: CD45.1$^+$ C57Bl6, CD45.2$^+$*Mal*$^{-/-}$ (or mice lacking TLR component of interest).
2. Radiation Source.
3. Tin foil.
4. 23G needles and 10 ml syringes.
5. Sterile dissection kit.
6. Cell culture media: DMEM with 10 % FCS and penicillin/streptomycin, store at 4 °C.
7. Sterile phosphate buffered saline (PBS) solution.
8. Tuerk solution.
9. 240 V heat lamp and mouse restrainer for i.v. injection.
10. 25 G needles and 1 ml syringes.
11. Flow cytometry markers: CD45.1, CD45.2 (A20, 104; BD Biosciences).

3 Methods

3.1 Infection Model

1. S. Typhimurium culture: Use a sterile pipette tip to take a single culture from an existing plate. Place in 10 ml LB broth in a 15 ml tube and incubate overnight in a 37 °C shaker.
2. The next day, spin down the culture at $3000 \times g$ for 10 min. Resuspend with PBS and centrifuge again before finally resuspending in PBS to give a concentration of 5×10^8 CFU/ml.
3. Using a gavage needle, administer 100 μl (approximately $5 \times 10^{7)}$) of the bacterial suspension per mouse orally. Serially dilute the remainder of the bacterial suspension in sterile PBS from 10^{-1} to 10^{-7} and spread 100 μl with a spot plate technique onto LB plates. Place in a bacterial incubator overnight at 37 °C with % CO_2. Perform bacterial counts and retrospectively enumerate bacteria delivered.
4. Every other day, collect faecal samples from inoculated mice and homogenize in 1 ml sterile PBS. Serially dilute the homogenate from 10^{-1} to 10^{-7} in sterile PBS and spread with an altered spot plate technique: divide each plate into four quadrants and label each quadrant with a dilution (*see* **Note 1**). Add 20 μl to each quadrant and spread by spot plate technique. Place in a bacterial incubator overnight at 37 °C with % CO_2. The next day, perform bacterial counts.
5. At the end of the experiment, cull mice and harvest organs as follows: Remove spleens and livers aseptically, weigh and manually crush in 2 ml of PBS in a stomacher bag by rolling the bag with a 10 ml pipette (*see* **Note 2**). Serially dilute and plate onto LB agar before incubating overnight at 37 °C to enumerate bacterial dissemination into these organs.

6. Additionally, aseptically remove the large intestine and flush with sterile PBS using a 10 cm dish filled with PBS and a 10 ml syringe with a 23G needle. Separate into 1 cm samples for various analyses:
   (a) RNA isolation: place in RNA later and snap freeze at −80 °C.
   (b) Protein Isolation: snap frozen at −80 °C.
   (c) Immunohistochemistry: Place in 4 % paraformaldehyde (PFA) for subsequent dehydration and paraffinization.
   (d) Electrophysiological Measurements: snap freeze at −80 °C.

3.2 Intestinal Permeability

1. Prepare fluorescein isothiocyanate conjugated dextran (FITC-dextran) for gavage, keeping away from light using coloured Eppendorf tubes for aliquots. Make up in sterile PBS at 12 mg per mouse in 100–200 μl per mouse.
2. Administer FITC-dextran to the mice in the various experimental groups by gavage. Mice can be either uninfected or orally infected with a pathogen of choice prior to gavage.
3. Sacrifice the mice 4 h later by CO_2 asphyxiation and perform a terminal bleed. Immediately after the blood is collected in coloured Eppendorf tubes, add acid-citrate dextrose and maintain in the dark throughout the following steps.
4. Centrifuge the samples at 4 °C for 12 min at $1000 \times g$. Remove the serum using a micropipette and add to a black 96-well microplate. In addition, prepare a serial dilution of the fluorescein and add to the 96-well microplate to be used as a standard curve.
5. Assess the concentration of fluorescein in the blood samples by spectrophotofluorometry with an excitation wavelength of 485 nm and an emission wavelength of 535 nm.

3.3 Electrophysiological Measurements

1. Intestinal epithelial layer preparation: after euthanasia, dissect out the distal colon with careful sharp dissection. Then remove the seromuscular layer by scraping that side off a pre-cooled glass slide.
2. Equilibrate the Ussing chamber to ensure there is no electrical bias. Add superfusate solution to both sides of the chamber and allowing it to come to 37 °C and "zeroing" by applying an offset voltage and compensating the resistance. This is achieved using the built-in "fluid resistance compensation" on the VCC.
3. After zeroing is completed the epithelial preparation can be fixed to the pins of the Ussing chamber, which should be filled with fresh superfusate.
4. Transepithlial resistance (TER) is then measured every 5 min for 1 h and the average is taken and used to calculate basal TER and expressed in Ω/cm^2.

5. To examine Cl– secretion, add amiloride (10 μM) to the basolateral side. The secretagogues carbachol (CCh) (100 μM basolaterally) and forskolin (FSK) (10 μM apically) are then used to stimulate Ca^{2+} and cAMP-mediated Cl– secretion, respectively. Normalize results and express as ΔI_{sc} (μA/cm^2).

3.4 Immunohistochemistry (IHC)

1. Paraffin embedding: Take the ileal section from its histology cassette. Pour a small drop of wax into the plastic mould and insert the section vertically so that is resembles a column. Fill the rest of the mould with paraffin and place the labelled base of the original cassette on top. Allow to cool on a cold plate until set (~4 h).
2. Sectioning: Transfer the embedded ileum sections to the cryostat and allow 5 min equilibration time to reach cryostat temperature (–20 °C). Cut 5 μm sections and mount sections on Polysine slides. Allow sections air dry for ~30 min at room temperature.
3. Deparaffinate sections by two washes of xylene, 5 min per wash. Rehydrate the sections via exposure to a decreasing ethanol gradient: Hydrate in 2 changes of 100 % ethanol for 3 min each, 95 % and 80 % ethanol for 1 min each. Rinse in PBS.
4. Antigen retrieval: Heat a water bath containing appropriate staining dishes containing isocitrate buffer to 95 °C. Place the slides in the staining dishes for 30 min. Rinse with PBS twice with 2 min per rinse.
5. Blocking: Incubate slides in 1 % Fc blockers and 10 % donkey serum for 30 min. Wash with PBS (*see* **Note 3**).
6. Incubate with primary antibody solution (polyclonal rabbit anti-mouse ZO-1, occludin, and claudin-3) overnight at 4 °C. Wash with PBS.
7. Incubate in secondary antibody for 1 h at room temperature. Wash with PBS.
8. Counterstain with 40-6-diamidino-2-phenylindole nucleic acid stain to visualize the nuclei.
9. Collect images using a DeltaVision PersonalDV Deconvolution microscopy. Image the 5-mm tissue slices using Z-stack with 0.2 mm per section (25 sections total), using 2_2 binning during image acquisition. Image J software is used to calculate the sum of fluorescence intensity from the stack and MFI from the epithelial regions of the tissue.

3.5 RT-PCR

1. Isolate total RNA from tissue samples according to the RNeasy Mini Kit manufacturer's instructions. Assess the RNA concentration using a NanoDrop spectrophotometer and equalize to desired concentration.

2. Reverse Transcription (RT): Total RNA is reverse transcribed into cDNA with random primers to transcribe all RNA (mRNA, rRNA, tRNA). Prepare RT reaction mix as follows per 20 µl point: 2 µl 10× buffer, 1 µl dNTP, 1 µl Reverse Transcriptase, 2 µl random primers, 0.25 µl RNase inhibitor, 1.75 µl H_2O. Pipette 8 µl of this RT reaction mix into each appropriate labelled PCR reaction tube followed by 12 µl of RNA at 100 ng/ml. Cap the tubes and tap or flick gently to mix. Centrifuge the tubes briefly to force all the solution to the bottom of the tube. Transfer tubes to the thermal cycler and run the RT reaction as follows: 10 min at 25 °C, 30 min at 37 °C, 5 min at 85 °C, hold at 4 °C.
3. TaqMan real-time PCR: Prepare individual reaction mixture for each mRNA target, including appropriate endogenous controls, as follows per 10 µl reaction (each reaction should be performed in duplicate): 5 µl TaqFast, 2.5 µl H_2O, 0.5 µl 20× primer/probe (*see* **Note 4**). Vortex all target reaction mixtures and pipette 8 µl per reaction well of a MicroAmp 96-well reaction plate. Add 2 µl cDNA to the appropriate reaction mix. Cover and seal the reaction plate before centrifuging briefly to mix solution and remove air bubbles. Transfer the reaction plate to the ABI Prism 7700 Sequence Detection system (*see* **Note 5**).
4. Use the endogenous control to normalize the results, according to the comparative threshold cycle (*Ct*) method for relative quantification as described by the manufacturer. Calculate the ΔCT between the target and control values and calculate the relative expression levels with the $\Delta\Delta CT$ method.

3.6 Western Blotting

1. Take colon sections for protein extraction as mentioned in Subheading 3.1, **step 6**. Add 400 µl RIPA buffer and leave on ice for 10 min before homogenizing using either a benchtop rotor-stator homogenizer or the Qiagen TissueLyserII system. Centrifuge the resulting homogenate using a benchtop microcentrifuge at 14,000 rpm for 10 min at 4 °C.
2. Take 50 µl of the supernatant and use the Micro BCA kit to quantify the protein present according to the manufacturer's instructions. It is likely that you will need to dilute your supernatants between 1:25 and 1:100 to get them into the range of the kit standard.
3. Dilute a portion of your supernatants in PBS to allow you load a total of 20 µg protein/well in 25–30 µl. This dilution must take into account a further 1:2 dilution in sample buffer. Once the sample buffer is added, the sample is boiled for 5–10 min. Samples can be stored at −20 °C or used immediately with prepared gels as outlined in **steps 4**–**5**. Remaining supernatant can be stored at −20 °C.

4. Make up 12 % resolving gel and pour between plates sealed with plastic gasket (all thoroughly cleaned with 70 % EthOH beforehand) up to ~1 cm below base of the comb (*see* **Note 6**). Add water-saturated butanol ~1 cm over gel edge to give straight top. Allow set for 20 min.
5. Tilt gel to drain off butanol (*see* **Note 7**). Make up 5 % stacking gel (keeping components on ice throughout) and pour between plates before adding comb to generate wells. Leave to set for 15–20 min.
6. Gently remove comb and rinse wells twice with running buffer (*see* **Note 8**). Remove seal gaskets from plates. Place gels into running tank, avoiding bubbles, with wells facing in towards each other. Add running buffer to cover wire. Load sample with gel-loading tips (25–30 μl/well), empty wells should be loaded with sample buffer.
7. Run at 25 mA/gel, unlimited voltage, for 50–60 min. Ensure gel is not run for too long so that proteins do not run into dye front.
8. Remove plates and free gel by bending plate pairs apart with a spatula. Cut off stacking gel, wells, edges and top right hand corner of the gel with a razor blade or scalpel.
9. Soak gels in transfer buffer three times for 5 min after a brief wash in TBS. Prepare transfer cassettes as follows: fill open container with transfer buffer and lay back of cassettes down into the container. Add soaked sponge, then two soaked filter papers followed by the gel. Cut the filter papers to the shape of the gel, including the missing top right corner. On top of this add a methanol activated PVDF membrane very carefully before adding two more soaked filter papers. Cut the filter papers to fit the gel. Replace in cassette in original orientation, roll over with roller or 50 ml tube to remove bubbles and add the second sponge on top. Close the cassette. Avoid air bubbles throughout.
10. Add cassettes to transfer tank in correct orientation as dictated by the manufacturer. Fill chamber to top with transfer buffer after adding cooling pack to rear (Ice or Polyethylene Glycol Pack). Run transfer for 1.5 h at 200 mA, 2 h at 150 mA or overnight at 30 mA.
11. Wash membrane three times for 5 min in TBS-Tween before blocking in 5 % marvel for a minimum of 1 h (*see* **Note 9**).
12. Wash the membranes three times for 5 min in TBS-Tween. Place the membranes into 50 ml tubes containing 5 ml of antibody solution containing relevant antibodies (1:1000 dilution in 5 % Marvel). Place the tubes on a roller overnight at 4 °C.
13. The next day, wash the membranes three times for 5 min in TBS-Tween before placing them into tubes containing 5 ml of

secondary antibody solution (1:1000 in 5 % Marvel). Place the tubes on the roller for 1 h at room temperature.

14. Wash the membranes in TBS-Tween for a total of 25 min, once for 15 min and twice for 5 min.
15. Prepare ECL solution for developing blots (25 μl of reagent 1, 25 μl of reagent 2 and 450 ml dH_2O per membrane). Cut several acetate sheets on the top right corner to maintain orientation during analysis. Develop the membranes in a darkroom using ECL, acetate film, the ECL processor and a film cassette (*see* **Note 10**).

3.7 Quantification of Epithelial Cell Apoptosis

1. Immunohistochemistry: prepare paraffin-embedded sections as detailed in Subheading 3.4.
2. Deparaffinate sections by two washes of xylene, 5 min per wash. Rehydrate the sections via exposure to a decreasing ethanol gradient: Hydrate in 2 changes of 100 % ethanol for 3 min each, 95 % and 80 % ethanol for 1 min each. Rinse in PBS.
3. Block for non-specific background staining using 10 % normal goat serum. Cover the section and incubate for minimum 1 h.
4. Wash briefly in water before incubating overnight in anti-Ki67 antibody (1:1000). Following this incubation counterstain using Mayer's haematoxylin.
5. Visualize using EnVisionTM Detection System (DakoCytomation, UK).
6. Epithelial cell apoptosis is analysed by TUNEL assay using a commercial kit (In Situ Cell Death Detection kit, Roche) according to the manufacturer. Sections are imaged by a Leica® microscope (Leica® DM 3000 LED) equipped with Leica® DFC495 camera (Leica® Microsystem, Germany).

3.8 Bone Marrow Chimeras

1. Separate the wild-type (WT) and *Mal*$^{-/-}$ recipient mice (or mice lacking TLR component of interest) into the appropriate experimental groups for bone marrow transfer. Irradiate the mice with a sublethal dose of 9 Gy in two doses, 3 h apart. Allow 24 h to elapse before reconstitution with bone marrow suspension.
2. Extract bone marrow from donor mice legs as follows: Warm cell culture media and PBS. Lay out a sheet of tin foil in a biosafety cabinet. Isolate the femur and tibia bones and cut both ends. Flush the bone marrow into a 50 ml tube containing 5 ml DMEM by placing a 10 ml syringe containing cell culture media with 23G needle into the larger orifice and depressing. Pool bone marrow from all donor mice of the same strain and count using Tuerk solution. Resuspend cells in sterile PBS for reconstitution at 5×10^7 cells/ml.

3. Reconstitute the bone marrow of the recipient mice with appropriate donor cells depending on their experimental group (WT > WT, *Mal*$^{-/-}$ > WT, WT > *Mal*$^{-/-}$ and *Mal*$^{-/-}$ > *Mal*$^{-/-}$ [donor > recipient]) by injecting 1×10^7 cells/mouse via the lateral tail veins. Begin by incubating the individual cage beneath a heat lamp for ~5 min. Prepare 1 ml syringes with 200 μl of cell suspension and top with 25G needles. Take each mouse and insert into the restrainer, ensuring the mouse is held securely. Wipe the tail with ethanol to sterilize and help make the veins visible. Insert the needle, bevel up, half way down the tail and inject the cell suspension.
4. After 6 weeks reconstitution can be assessed by flow cytometry of blood for markers CD45.1 vs. CD45.2.
5. Following generation of chimeras, oral infection of mice can be repeated to determine the role of Mal or other TLR components in epithelial cells and thus epithelial barrier integrity.

4 Notes

1. This spot plating technique is used for efficacy and also to reduce amount of agar plates required. Alternatively, perform bacterial enumeration using traditional spread plating technique of 100 μl per agar plate, one dilution per plate.
2. This method of homogenizing organs is used for speed, as you do not need to sterilize a hand-held homogenizer in-between each sample, as one sterile stomacher bag is used per sample.
3. Use a wax pen to encircle the section on the slide. This will keep the block/antibody solutions on the slide for a more consistent incubation.
4. If you wish to multiplex using multiple channels (e.g. FAM and VIC) replace 0.5 μl H_2O with 0.5 μl primer/probe.
5. Plates can be prepared to be run in advance and stored temporarily at 4 °C.
6. Mix H_2O, Protogel, Tris and SDS first and then add APS and TEMED.
7. Add butanol to vessel and add water on top. Shake vigorously until mixture becomes milky. Allow separation and use upper layer, store at room temperature.
8. Final pH should be 8.3 but do not use a pH meter as SDS will damage electrode.
9. This step is very flexible: the membrane can be blocked overnight if necessary.

10. It is best to prepare several acetates ahead of time to ensure you get a clear exposure. Writing the approximate exposure time on the acetate will allow you know what to expect for repeat experiments with the antibodies in use.

References

1. Turner JR (2009) Intestinal mucosal barrier function in health and disease. Nat Rev Immunol 9:799–809
2. Harhaj NS, Antonetti DA (2004) Regulation of tight junctions and loss of barrier function in pathophysiology. Int J Biochem Cell Biol 36:1206–1237
3. Fasano A, Shea-Donohue T (2005) Mechanisms of disease: the role of intestinal barrier function in the pathogenesis of gastrointestinal autoimmune diseases. Nat Clin Pract Gastroenterol Hepatol 2:416–422
4. Balkovetz DF, Katz J (2003) Bacterial invasion by a paracellular route: divide and conquer. Microbes Infect 5:613–619
5. Corr SC, Palsson-McDermott EM, Grishina I et al (2014) *MyD88* adaptor-like (Mal) functions in the epithelial barrier and contributes to intestinal integrity via protein kinase C. Mucosal Immunol 7(1):57–67
6. Gonzalez-Mariscal L, Tapia R, Chamorro D (2008) Crosstalk of tight junction components with signaling pathways. Biochim Biophys Acta 1778:729–756
7. Guo S, Al-Sadi R, Said HM et al (2013) Lipopolysaccharide causes an increase in intestinal tight junction permeability in vitro and in vivo by inducing enterocyte membrane expression and localization of TLR-4 and CD14. Am J Pathol 182(2):375–387
8. Alenghat T, Osborne LC, Saenz SA et al (2013) Histone deacetylase 3 coordinates commensal-bacteria-dependent intestinal homeostasis. Nature 504:153–157
9. Cario E, Gerken G, Podolsky DK (2004) Toll-like receptor 2 enhances ZO-1 associated intestinal epithelial barrier integrity via protein kinase C. Gastroenterology 127(1):224–238
10. Aviello G, Corr SC, Johnston DGW et al (2014) MyD88 adaptor-like (Mal) regulates intestinal homeostasis and colitis-associated colorectal cancer in mice. Am J Physiol 306(9):G769–G778
11. Brandl K, Sun L, Neppl C (2010) MyD88 signaling in nonhematopoietic cells protects mice against induced colitis by regulating specific EGF receptor ligands. Proc Natl Acad Sci 107(46):19967–19972

Chapter 19

Understanding the Role of Cellular Molecular Clocks in Controlling the Innate Immune Response

Anne M. Curtis and Caio T. Fagundes

Abstract

The importance of the 24-h daily cycle, termed circadian, on immune function has been highlighted by a number of recent studies. Immune parameters such as the response to bacterial challenge or immune cell trafficking change with time of day and disruption of circadian rhythms has been linked to inflammatory pathologies. We are beginning to uncover that the key proteins that comprise the molecular clock, most notably BMAL1, CLOCK, and REV-ERBα, also control fundamental aspects of the immune response. Given the ubiquitous nature of the molecular clock in controlling many other types of physiologies such as metabolism and cardiovascular function, a more thorough understanding of the daily rhythm of the immune system may provide important insight into aspects of patient care such as vaccinations and how we manage infectious and inflammatory diseases. In this chapter, we describe a series of experiments to look at circadian expression and function in immune cells. The experiments described herein may provide an initial assessment of the role of the molecular clock on an immune response from any cell type of interest.

Key words Circadian clock, Molecular clock, Synchronization, Serum shock, Zeitgeber time, Clock-controlled genes

1 Introduction

The molecular clock, the timekeeping system within our cells, integrates all aspects of our biology to align with the daily external environment. At the core of this 24-h pacemaker lies the heterodimeric partnership of the basic helix loop helix PER-ARNT-SIM (PAS) domain proteins, BMAL1 (also known as ARNTL) and CLOCK, which bind E-box sites and induce the expression of the repressors period (PER) and cryptochrome (CRY) which in time translocate back into the nucleus and inhibit their own expression (Fig. 1, shaded loop) [1]. As PER and CRY proteins are gradually degraded, the repression on BMAL1 and CLOCK is relieved and the cycle begins again. Over the past decade, this loop has enlarged to encompass another interlocking genetic loop—that of the nuclear receptors, ROR(α,β,γ) and REV-ERBs(α,β). Activated by

Claire E. McCoy (ed.), *Toll-Like Receptors: Practice and Methods*, Methods in Molecular Biology, vol. 1390,
DOI 10.1007/978-1-4939-3335-8_19,

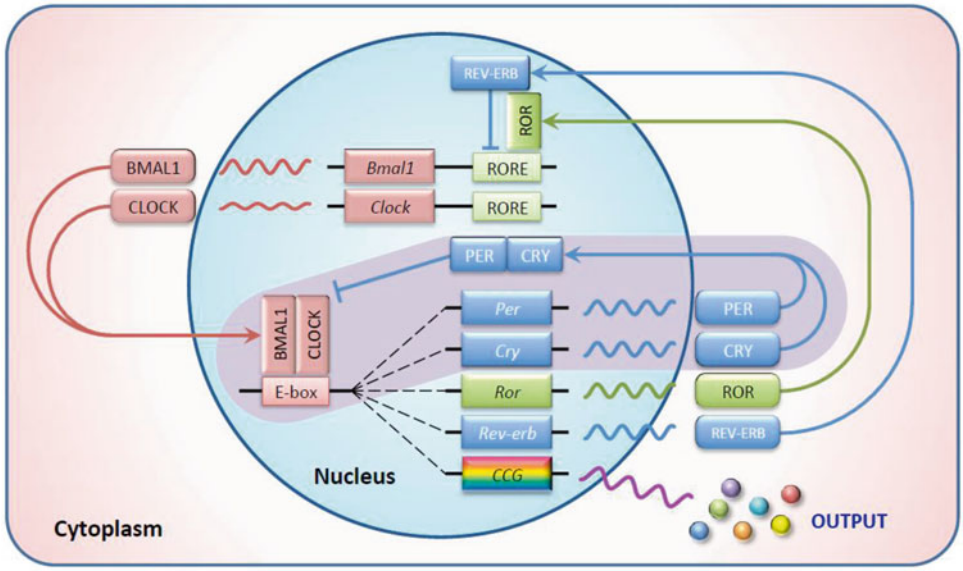

Fig. 1 Feedback loops involved in molecular clock function. The first loop comprises the core clock components BMAL1 and CLOCK that bind to E-box sequences within the genes that encode the repressors PER and CRY. PER and CRY translocate to the nucleus and repress their own expression by inhibiting BMAL:CLOCK complex (*Shaded area* of the figure). A second loop encompass an interlocking genetic loop involving the nuclear receptors ROR(α,β,γ) and REV-ERBs(α,β). Activated by BMAL1:CLOCK, REV-ERBs/RORs translocate to the nucleus and bind receptor-related orphan receptor response elements (ROREs) in the promoters of *Bmal1* and *Clock* to activate or repress respectively their transcription (*Unshaded loop*). Clock factors bind thousands of sites in the genome, and it is this oscillation of binding of clock factors to promoters that causes circadian expression of clock-controlled genes (CCGs)

BMAL1:CLOCK, REV-ERBs/RORs translocate back to the nucleus and bind receptor-related orphan receptor response elements (ROREs) in the promoters of *Bmal1* and *Clock* to activate or repress respectively their transcription (Fig. 1, unshaded).

Collectively, these loops drive waves of gene expression within a 24-h timescale, termed circadian gene expression. Clock factors bind thousands of sites in the genome, and it is this oscillation of binding of clock factors to promoters that causes circadian expression of clock-controlled genes (CCGs) (Fig. 1). This clockwork machinery exists in almost all cells in the body, where the central clock located in the SCN (suprachiasmatic nucleus) of the brain receives light input from the environment and ensures proper alignment of the clocks in peripheral tissues.

A number of studies have highlighted the tight coupling between the molecular clock and immune function [2]. Mice are more susceptible to lipopolysaccharide (LPS) [3] and bacterial challenge [4] ahead of their activity phase. Chronic disruption of external cues to the molecular clock, as imposed by shift work and airline travel, augments the inflammatory response [5] and increases susceptibility to atherosclerosis, obesity, and diabetes[6]. It has

also been concluded that "shift work that involves circadian disruption is probably carcinogenic to humans" [7]. Mouse models of clock ablation have increased severity of rheumatoid arthritis [8], a condition in humans which has a daily rhythm in activity [9]. Ultimately, this indicates that there are multiple nodes of crosstalk between the circadian and immune system.

In this chapter, we will describe two techniques: in vitro (*see* Subheading 3.1) and ex vivo (*see* Subheading 3.2) to assay the status and phase of the molecular clock and also to investigate the effect of the molecular clock on an immune response. For expression to be considered circadian there must be a peak and trough within 24 h, and the time between the peak and trough needs to be 12 h apart. In order to assay circadian function in an in vitro system, cells within the population must be synchronized together so that all cells at any given time are at the identical timepoint within the circadian cycle. Cells cultured in vitro as per normal protocols are "asynchronous." Each cell within the population is at a different timepoint within the circadian cycle, and therefore assaying the status of the clock at any given timepoint within this population is not possible. Synchronization of cells can be performed using transient exposure to either 50 % serum or dexamethasone. In certain situations, the use of dexamethasone as the synchronization agent may not be appropriate as this may confound certain immune responses post synchronization. For ex vivo analysis of circadian gene expression, animals ahead of experimentation must be entrained to the desired light–dark regimens. Zeitgeber time corresponds to the time (hours) after the onset of the environmental cue that entrains the daily or diurnal cycle. Usually, the environmental cue utilized is light. Therefore, in an animal facility with 12 h of light and 12 h of darkness, ZT0 will correspond to the moment when lights go on and ZT12 will refer to the moment lights go off. For analyzing clock gene expression across the whole diurnal cycle, it is recommended to collect cells from mice every 4 h at a minimum, for at least one entire cycle. Circadian time (CT) corresponds to the times when there is free running of the clock, this is without any external environmental cue such as light. In order to assay clock gene expression across multiple CTs, animals must first be housed in complete darkness for at least one cycle (24 h) ahead of sampling and left in complete darkness for the period of time when sampling is being performed. Animals can only be exposed to red light (safelight conditions) during this period, therefore all handling and harvesting of tissues must be performed under safelight conditions.

Enclosed light cabinets can be used to invert or phase shift the light–dark cycle to allow all collections during daytime hours. One full day acclimatization under the new lighting regimen is required for every hour that is changed. For example if the aim is to invert

a cohort of mice by 12 h, the mice must be placed under the new lighting regime (for example lights on at 8 pm and off at 8 am) for at least 12 days prior to experimentation.

2 Materials

2.1 M-CSF Generation

1. 1 Vial of frozen L929 cells.
2. Roswell Park Memorial Institute (RPMI) 1640 Medium supplemented with GlutaMAX™-I, 10 % fetal calf serum (FCS, endotoxin-tested) and 1 % penicillin/streptomycin (v/v).
3. 0.25 % Trypsin EDTA.
4. 10 ml Serological pipettes.
5. T175 culture flasks.
6. Vacuum pump.
7. 0.20 μm membrane filters.

2.2 Harvesting BMDMs

1. Dissection materials such as scissors and forceps.
2. 5 ml Syringes.
3. 23G needles.
4. Red Cell Lysis Buffer.
5. Phosphate-buffered saline (PBS).
6. 70 μm Cell Strainers.
7. Dulbecco's Modified Eagle Medium (DMEM) supplemented with 10 % fetal calf serum (FCS, endotoxin-tested) and 1 % penicillin/streptomycin (v/v).
8. M-CSF-containing medium.
9. 10 cm Petri dishes.
10. 12-Well culture plates.
11. Heat-inactivated Horse Serum.

2.3 BMDM Synchronization and Stimulation

1. Serum-free DMEM: DMEM supplemented with 1 % penicillin/streptomycin (v/v) but without addition of FCS.
2. Heat-inactivated Horse Serum.
3. Dexamethasone: Stocks at 100 μM in Dimethyl sulfoxide, use at a final concentration of 100 nM.
4. 10 μg/ml LPS, use at a final concentration of 100 ng/ml.

2.4 RT-PCR Analysis

1. RNeasy Mini Kit® from Qiagen® for RNA extraction.
2. High capacity cDNA Reverse Transcription Kit from Applied Biosystems® for cDNA synthesis.

3. SYBR® Green Real-Time PCR Master Mix for qPCR reaction.
4. Pairs of primers for the genes of interest.

2.5 Harvesting Primary Leukocytes

1. Dissection material such as scissors and forceps.
2. Mice entrained to a 12 h light/dark cycle.
3. 5 ml syringes.
4. 23G needles.
5. Red Cell Lysis Buffer.
6. PBS.
7. 70 μm cell strainers.
8. DMEM with 10 % fetal calf serum (FCS, endotoxin-tested) and 1 % penicillin/streptomycin (v/v).
9. 12-Well culture plates.
10. CD11c Microbeads for dendritic cell separation (Miltenyi Biotec).
11. MACS Cell Separation Columns (Miltenyi Biotec).
12. AutoMACS Pro Separator (Miltenyi Biotec).
13. 10 μg/ml LPS, use at a final concentration of 100 ng/ml.

3 Methods

3.1 Assessing Circadian Gene Expression in Synchronized BMDMs

The supernatant of L929 cells is used as a source for M-CSF required for differentiating bone marrow cells into macrophages. All the following procedures must be conducted in a sterile environment, using sterile reagents.

3.1.1 M-CSF Generation

1. Thaw–frozen L929 cells and grow them in RPMI complete medium at 37 °C, 5 % CO_2.
2. Subculture the cells until you have five confluent T175s flasks.
3. Count the cells and replate at 0.5×10^6 cells/mL, adding 40 mL of complete RPMI medium into each T175 (i.e. 20 million cells per T175).
4. Culture the cells at 37 °C, 5 % CO_2 for 7 days.
5. Collect supernatant, filter through a 0.20 μm membrane with a vacuum pump, aliquot and store the M-CSF containing medium at −20 °C until use.

3.1.2 Harvesting BMDMs

1. Cull mice by an approved humane method.
2. To obtain the femur and tibia bone, first dissect the peritoneum from the skin, and pull the skin down the spine of the animal toward its ankles.
3. For the femur, isolate the thigh muscle until you reach the hip joint, cut across the femur at this point and above the knee joint. Dissect out the bone with a closed scissors.

4. For the tibia that remains below the knee, isolate the ankle joint and cut above it, remove the calve muscles using the closed scissors and dissect out the bone.
5. Insert a 5 ml syringe filled with DMEM into the larger orifice of the femur and tibia bone. Flush out the bone marrow into a falcon containing 5 ml of DMEM media.
6. Resuspend the bone marrow using a 3 ml Pasteur pipette. Centrifuge at 300 × *g* for 5 min. Decant the supernatant.
7. Add 3 ml of Red Cell Lysis Buffer for 3 min. Carefully pipette up and down twice before leaving for exactly 5 min. Stop the reaction by adding 20 ml of DMEM.
8. Filter the cells through a 70 μm cell strainer placed on top of a fresh 50 mL falcon.
9. Centrifuge cells at 300 × *g* for 5 min. Remove supernatant and suspend cells in 10 ml DMEM.
10. Count the cells by your preferred method and generate a stock concentration of 1×10^6 cells/ml.
11. Seed 10 ml of cells per 10 cm sterile Petri culture dish (*see* **Note 1**) and add a final concentration of 20 % M-CSF containing medium (*see* Subheading 3.1.1).
12. Three days later, add a further 2 ml of M-CSF containing medium per plate.
13. Three days later, remove the medium from the plates and lift cells with cold PBS and scraping.
14. Centrifuge at 300 × *g* for 5 min. Remove supernatant and resuspend cells in 10 ml of DMEM.
15. Count cells by your preferred method and generate a stock concentration of 1×10^6 cells/ml.
16. Seed cells for experimental set-up at a concentration of 1×10^6 cells per well in 12-well tissue culture plates. You will need one plate for asynchronous control cells and one plate for each timepoint of analysis (*see* **Note 2**).
17. Perform synchronization the following day, using serum shock (*see* Subheading 3.1.3) or dexamethasone (*see* Subheading 3.1.4).

3.1.3 Synchronizing BMDMs with Serum Shock

Synchronization of cells can be performed using transient exposure to high serum concentrations, what is generally called a serum shock. Briefly, cells are incubated with medium containing 50 % serum for 2 h, this is sufficient to synchronize clock gene expression for several hours in a variety of mammalian cells [10]. An example of the experimental design for synchronizing BMDMs through serum shock is shown in Fig. 2a (*see* **Note 2**). The goal of this experimental set up is to demonstrate if any gene of interest is

expressed in a circadian pattern and whether such pattern involves the cell intrinsic molecular clock.

1. Collect one plate of cells cultured in DMEM as your asynchronous control cells.
2. Remove medium from the other plates and add serum-free DMEM (*see* **Note 3**) to wells designated to asynchronous cells or DMEM containing 50 % (v/v) Heat-inactivated Horse Serum to wells designated as synchronized cells (Fig. 2a).
3. Incubate plates for 2 h at a 37 °C, 5 % CO_2 incubator. The moment when the medium containing 50 % horse serum is added is considered Time 0 (T0).
4. After 2 h, remove media from the wells designated as synchronized cells and add serum-free DMEM (*see* **Note 4**). Return plates to incubator.
5. Collect cells from the other plates at the previously defined timepoints (*see* **Notes 2** and **5**) by removing the medium from the well and lysing the cells with Lysis Buffer for RNA extraction according to the manufacturer`s instructions. These cells can then be assessed for oscillating gene expression after synchronization (*see* Subheading 3.1.6).
6. After discrete timepoints after T0 (for example, 24 or 36 h later, Fig. 2c), cells can be treated as desired (e.g. LPS) and changes in cytokine production upon TLR activation may be evaluated (*see* Subheading 3.1.5. and Subheading 3.1.6).

3.1.4 Synchronizing BMDMs with Dexamethasone

Synchronization of cells can be performed using transient exposure to Dexamethasone. Briefly, cells are incubated with 100 nM of this synthetic corticosteroid for 2 h, this is sufficient to synchronize clock gene expression for several hours in a variety of mammalian cells [11]. An example of the experimental design for synchronizing BMDMs through Dexamethasone exposure is shown in Fig. 2b (*see* **Note 2**). The goal of this experimental set up is also to demonstrate if any gene of interest is expressed in a circadian pattern and whether such pattern involves the cell intrinsic molecular clock.

1. Collect one plate of cells cultured in DMEM as your asynchronous control cells.
2. Remove medium from the other plates and add complete DMEM (*see* **Note 6**) to wells designated as asynchronous cells or complete DMEM containing Dexamethasone (Dex) at final concentration of 100 nM to wells designated as synchronized cells (Fig. 2b).
3. Incubate plates for 2 h at a 37 °C, 5 % CO_2 incubator. The moment when the medium containing Dex is added is considered Time 0 (T0).

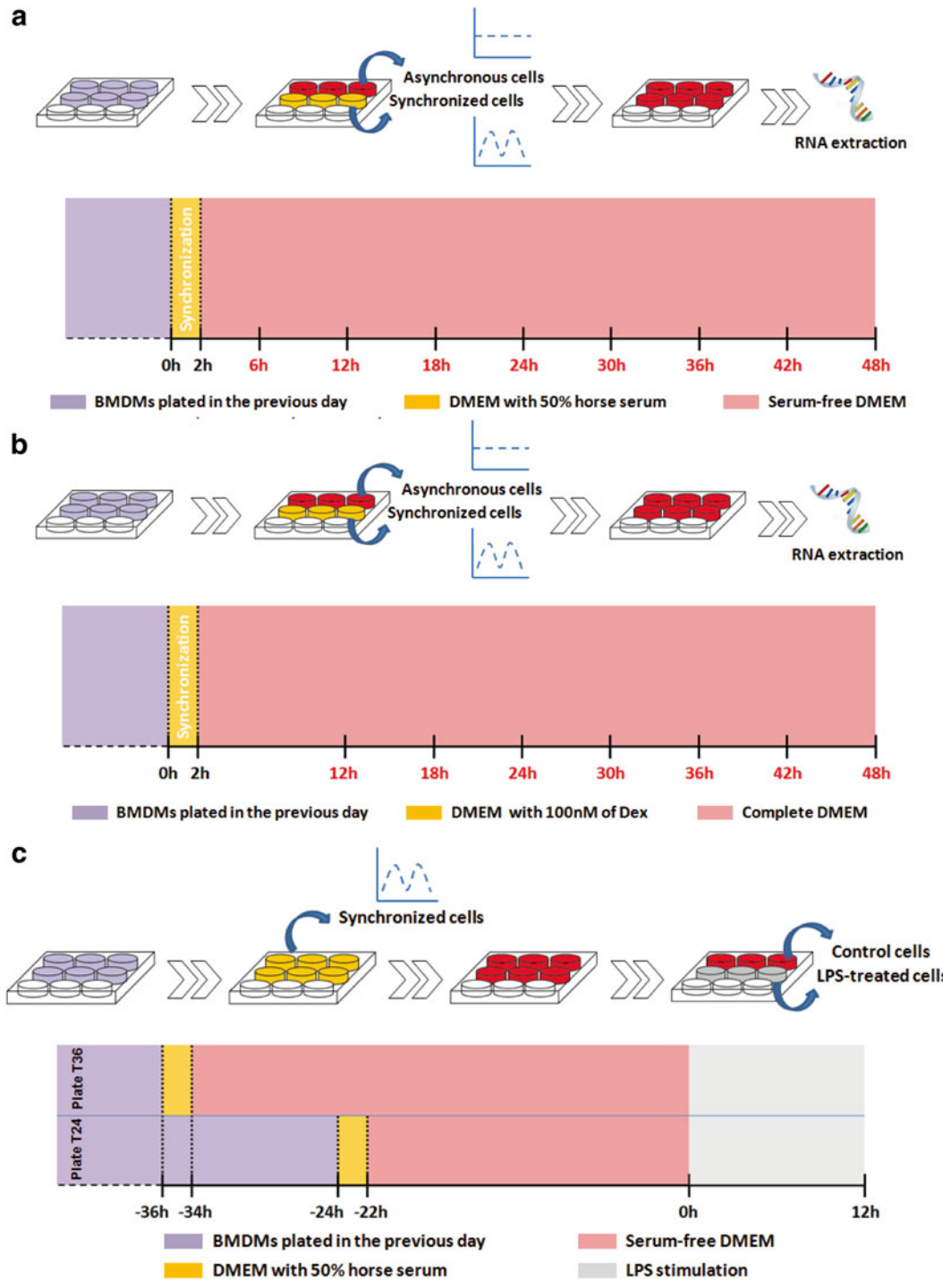

Fig. 2 Experimental setups for evaluating clock gene expression and cytokine response after BMDM synchronization in vitro. (**a**) BMDM synchronization by serum shock (Subheading 3.1.3) involves replacing complete DMEM media (*purple*) on the day after cells were plated by serum-free DMEM (*red*) in a group of wells designated as asynchronous cells or by DMEM containing 50 % (v/v) horse serum (*yellow*). The moment when 50 %

4. After 2 h, remove media from the wells designated as synchronized cells and wash wells with 1 ml of PBS and then add complete DMEM medium (*see* **Note 6**). Return plates to incubator.
5. Start collecting cells 12 h after T0 (*see* **Note 7**). Collect cells from the other plates at the previously defined timepoints (*see* **Note 2**) by removing the medium from the well and lysing the cells with Lysis Buffer for RNA extraction according to the manufacturer's instructions. These cells can then be assessed for oscillating gene expression upon synchronization (*see* Subheading 3.1.6).
6. After discrete timepoints post T0 (for example, 24 or 36 h later), cells can be treated as desired (e.g. LPS) and changes in cytokine production upon TLR activation may be evaluated (*see* Subheading 3.1.5. and Subheading 3.1.6).

3.1.5 Stimulation of Synchronized BMDMs with TLR agonists

Synchronization of BMDMs after serum shock or Dex treatment leads to expression of clock genes in a circadian-like pattern. To assess whether cells in different moments of a circadian cycle respond differently to TLR activation, cells may be stimulated with TLR agonists at different times post synchronization. In the following example, serum-shocked BMDMs were stimulated with LPS 36 or 24 h post exposure to the synchronizing agent (Fig. 2c).

Fig. 2 (continued) serum DMEM is added is considered time 0. After 2 h of incubation (synchronization period), medium in wells designated as synchronized cells is replaced by serum-free DMEM and cells are kept in this medium until the time of collection. One plate containing asynchronous and synchronized cells must be prepared per timepoint of collection. In this example, cells were collected every 6 h (in *red*). In addition, one plate must be collected before synchronization and designated as control cells. At the defined timepoints of collection, medium is removed and cells are lyzed for RNA extraction. (**b**) BMDM synchronization by Dexamethasone (Dex) (Subheading 3.1.2) involves replacing complete DMEM media (*purple*) on the day after cells were plated in fresh complete DMEM (*red*) in a group of wells designated as asynchronous cells or by complete DMEM containing 100 nM of Dex (*yellow*). The moment when DMEM supplemented with Dex is added is considered time 0. After 2 h of incubation (synchronization period), medium in wells designated as synchronized cells is replaced by complete DMEM and cells are kept in this medium until the time of collection. One plate containing asynchronous and synchronized cells must be prepared per timepoint of collection. In this example, the first plate was collected 12 h after Dex addition (*see* **Note 7**) and each plate was collected every 6 h (in *red*). In addition, one plate must be collected before synchronization and designated as control cells. At the defined timepoints of collection, medium is removed and cells are lyzed for RNA extraction. (**c**) In order to assess changes in response to LPS by cells in different moments of the circadian cycle, BMDMs were serum-shocked as described above (Subheading 3.1.3) 36 or 24 h before stimulation with LPS at a final concentration of 100 ng/ml (Subheading 3.1.5). Prepare one plate for synchronization 36 h before LPS addition (T36) and another one for synchronization 24 h before LPS addition (T24). Each plate must contain synchronized cells for both LPS-treated and non-treated groups. Plates must be prepared in a way that they will be treated with LPS at the same moment. The moment when LPS is added is considered time 0. After 12 h of incubation, supernatant is collected for ELISAs assay

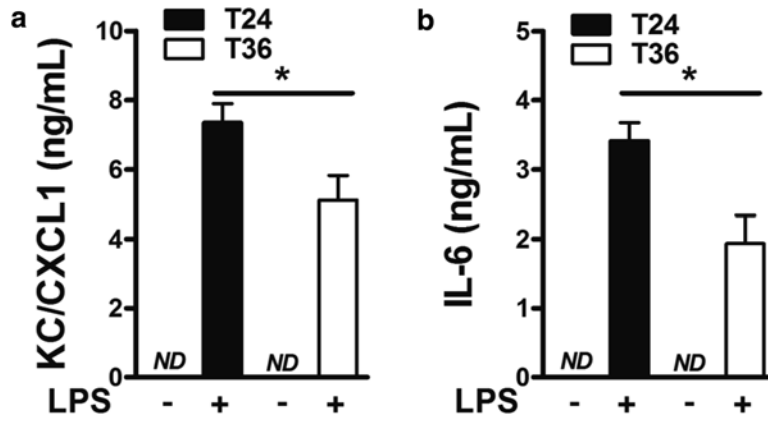

Fig. 3 Synchronization of BMDMs by serum shock leads to circadian-like cytokine production upon LPS stimulation. (**a**, **b**) BMDMs were submitted to serum shock as described (Subheading 3.1.3) 36 h (T36) or 24 h (T24) before stimulation with LPS (100 ng/mL). 12 h later, supernatants were collected for measuring CXCL1 (**a**) and IL-6 (**b**) by ELISA. Results represented are the mean ± SEM of cytokine concentration in ng/mL of three wells per condition

These timepoints were chosen based in the differences in expression of BMAL1 by the synchronized cells (*see* Subheading 3.1.6. and Fig. 4).

1. Make sure that there are enough synchronized cells in each plate for LPS-treated and non-treated groups (*see* **Note 8**).
2. Add 10 μl of the stock LPS solution (at 10 μg/ml) to the designated wells of both plates (the one submitted to serum shock 24 h before and to the one submitted to serum shock 36 h before) in order to obtain a final concentration of 100 ng/ml of LPS (Fig. 2c).
3. Collect supernatants after incubation with LPS for the established time (12 h in the example) and perform ELISAs according to the manufacturer's instructions to test for inflammatory cytokines such as CXCL1 and IL-6 (Fig. 3).

3.1.6 RT-PCR Analysis

BMDMs synchronization by serum shock or dexamethasone leads to circadian-like oscillation in expression of some clock-controlled genes. Analysis of such oscillation involves simply assessing gene expression at 6 h intervals (*see* **Note 4**) after the synchronizing stimulus (*see* **step 5**, Subheadings 3.1.3 and 3.1.4). For analyzing gene expression in this case follow the steps below:

1. Follow manufacturer's protocol for RNA extraction.
2. Convert equal quantities of RNA to cDNA using a standard reverse transcription protocol.
3. Measure target gene expression by standard qPCR.

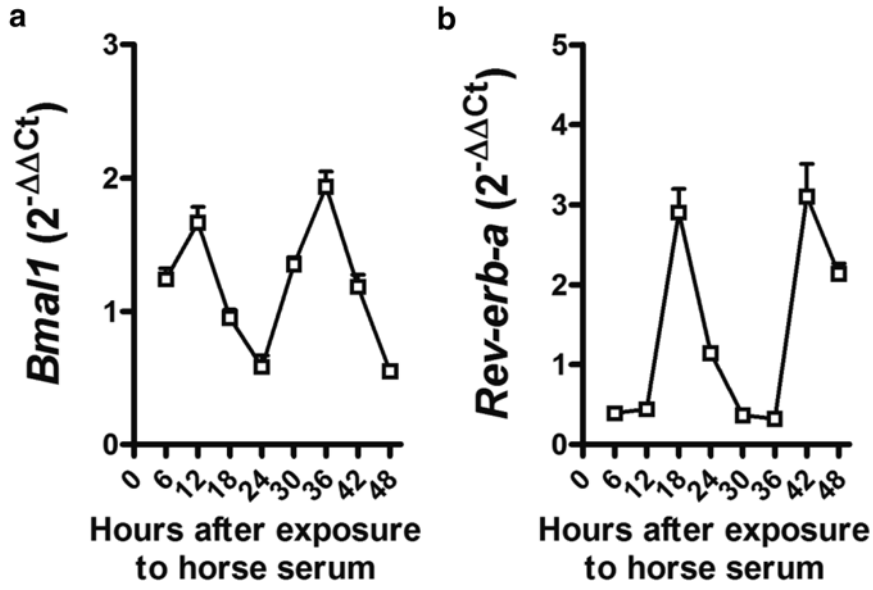

Fig. 4 Synchronization of BMDMs by serum shock leads to circadian-like expression of clock genes. (**a**, **b**) BMDMs were submitted to serum shock as described (Subheading 3.1.3) and every 6 h, cells were collected for assessing *Bmal1* (**a**) and *Rev-erb-a* (**b**) expression. Results represented are the mean ± SEM of relative gene expression in three wells per timepoint

4. For analyzing circadian-like oscillation in expression of a gene of interest (Fig. 4a, b), the ΔΔCt method of analysis may be used. For this, first calculate the ΔCt over a constitutive non-variable gene (such as *Rpl4* or *Tbp*) and then calculate the ΔΔCt over the average of the ΔCts of all the timepoints collected of the synchronized cells.

3.2 Assessing Circadian Gene Expression in Primary Leukocytes

3.2.1 Harvesting Peritoneal Cells

1. Cull mice by an approved humane method at ZT0 and every 4 h until the next ZT0.
2. Adherent peritoneal cells are obtained by peritoneal lavage.
3. Dissect apart the peritoneum from the skin and inject 5 mL of serum-free DMEM.
4. Massage for 30 s and retrieve the injected volume with a sterile Pasteur pipette and store in a Falcon tube in ice.
5. After cell collection, centrifuge cells at 300 × *g* for 5 min at 4 °C. Decant supernatant and suspend cells in serum-free DMEM.
6. Count cells and dilute the suspension with serum-free DMEM to obtain a concentration of 1×10^6 cells/ml.
7. Plate 1 ml of the cells suspension per well of a 12-well dish.
8. Incubate at 37 °C 5 % CO_2 for 30 min to allow cells to attach to the plate.

9. Remove the media from the wells, wash out non-adherent cells by pipetting up and down 1 ml of sterile PBS.
10. For simply analyzing circadian gene expression (Fig. 5a), lyse cells for RNA extraction as recommended by the manufacturer at this point (*see* Subheading 3.2.4).
11. In the case of assessing response to TLR activation, add 1 ml of complete DMEM and proceed to stimulation with the desired TLR agonist (*see* Subheading 3.2.3).

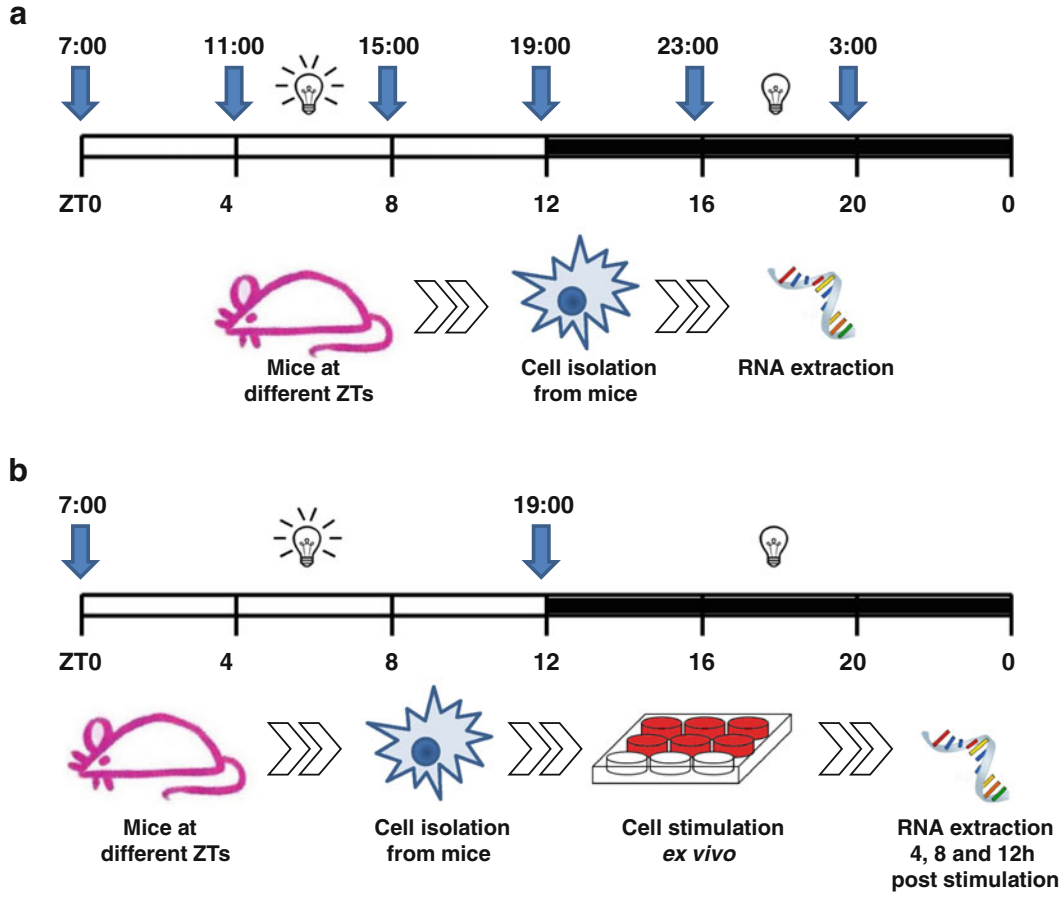

Fig. 5 Experimental setups for ex vivo evaluation of clock gene expression and cytokine response in primary leukocytes extracted from mice at different Zeitgeber times (ZT). (**a**) Mice entrained to a 12 h light/dark cycle (ZT0 corresponds to the moment when lights go on—7:00; and ZT12 refers to the moment lights go off—19:00). For analyzing clock gene expression across the whole diurnal cycle, it is recommended to collect cells from mice every 4 h, for at least one entire cycle (*blue arrows*). After cell isolation (Subheading 3.2.1) from the group of mice at each ZT, they are immediately lyzed for RNA extraction. (**b**) For analysis of cell response to TLR activation at different ZTs (Subheading 3.2.2), cells are isolated from groups of mice entrained to the same 12 h light/dark cycle described in (**a**) at ZT0 and ZT12 (*blue arrows*) and put in culture in the presence or not of a TLR agonist. 4, 8 or 12 h after cell stimulation, they are lyzed for RNA extraction

3.2.2 Harvesting CD11c Cells

1. Dissect spleen and store in RPMI 1640 medium on ice.
2. For obtaining single cells suspensions, homogenize each organ in 1 ml of RPMI 1640 and filter the cell suspension through a 70 μm nylon cell strainer.
3. Centrifuge the cells at 300 × *g* for 5 min at 4 °C.
4. For red cell lysis, discard supernatant and suspend cells in 3 mL of Red Cell Lysis Buffer and carefully pipette up and down twice.
5. Incubate for 5 min at room temperature. Stop reaction by adding 20 mL of RPMI 1640.
6. Filter the cell suspension through a 70 μm nylon cell strainer.
7. Centrifuge the cells at 300 × *g* for 5 min at 4 °C.
8. Decant supernatant, suspend cells in 3 mL of PBS for labeling with microbeads and subsequent cells separation.
9. In order to obtain macrophage and dendritic cells, label cells with CD11c mouse microbeads according to the manufacturer's instructions.
10. Magnetic cell separation may be achieved by using MACS Cell Separation Columns and the autoMACS Pro Separator.
11. For simply analyzing circadian gene expression (Fig. 5a), lyse cells for RNA extraction as recommended by the manufacturer at this point (*see* Subheading 3.2.4).
12. In the case of assessing response to TLR activation, add 1 ml of complete RPMI 1640 and proceed to stimulation with the desired TLR agonist (*see* Subheading 3.2.3).

3.2.3 Leukocyte Stimulation

After obtaining the adherent peritoneal cells or purified cell suspensions from Spleen at each ZT, cells can be treated as desired (e.g. LPS) and changes in gene expression upon TLR activation may be evaluated. Experiments analyzing responses to TLR agonists may involve stimulating cells obtained from mice in two different ZTs, such as ZT0 and ZT12 (Fig. 5b) or in several different ZTs.

1. Add LPS to obtain a 100 ng/ml final concentration at the well to cells extracted at ZT0 or at ZT12.
2. Lyse cells for RNA extraction in the adequate buffer 4, 8, and 12 h after LPS treatment.

3.2.4 RT-PCR Analysis

Analysis of circadian gene expression in leukocytes ex vivo involves simply assessing gene expression at each ZT timepoint collected (Fig. 5a). Also, after discrete timepoints post-stimulation of cells obtained in two different ZTs (for example, ZT0 or ZT12), changes in gene expression upon TLR activation may be evaluated (Fig. 5b). For analyzing gene expression in both cases:

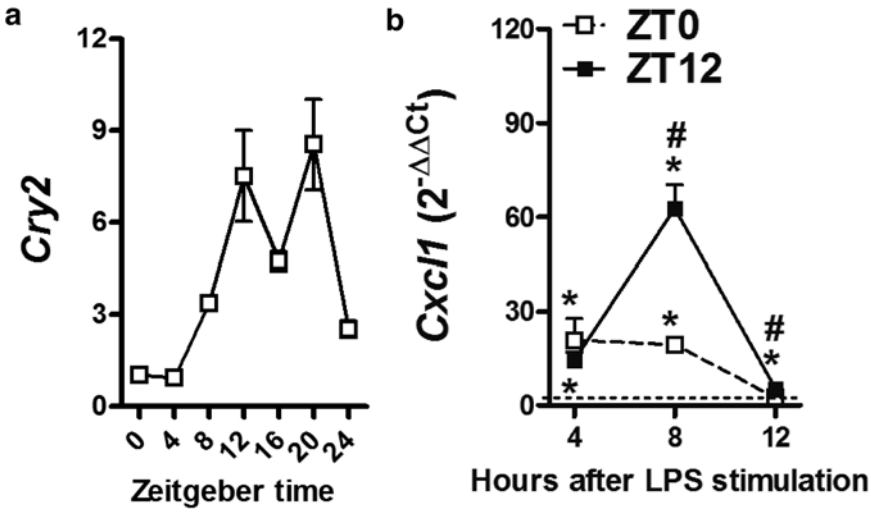

Fig. 6 Analysis of clock gene expression and of response to LPS stimulation in peritoneal cells obtained from mice at different Zeitgeber times. (**a**) Adherent peritoneal cells were collected from mice kept in a 12 h light/dark cycle every 4 h and assayed for *Cry2* expression. Results represented are the mean ± SEM of relative expression of cells obtained from 4 animals per timepoint. (**b**) Adherent peritoneal cells were collected from mice kept in a 12 h light/dark cycle at ZT0 or at ZT12. Cells were stimulated ex vivo with 100 ng/mL of LPS. 4, 8 and 12 h later, cells were lyzed for analysis of expression of *Cxcl1* by qPCR. Results represented are the mean ± SEM of relative gene expression in cells extracted from 4 animals per condition

1. Follow manufacturer's protocol for RNA extraction.
2. Convert equal quantities of RNA to cDNA using a standard reverse transcription protocol;
3. Measure target gene expression by standard qPCR.
4. For analyzing circadian gene expression of a gene of interest (Fig. 6a), the ΔΔCt method of analysis may be used. For this, first calculate the ΔCt over a constitutive non-variable gene (such as *Rpl4* or *Tbp*) and then calculate the ΔΔCt over the average of the ΔCts of ZT0 group.
5. For analyzing changes in gene expression upon TLR activation at different ZTs (Fig. 6b), using the ΔΔCt method, calculate the ΔCt over a constitutive non-variable gene (such as *Rpl4* or *Tbp*) and then calculate the ΔΔCt over the average of the ΔCts of the non-stimulated cells of the respective ZT (e.g. LPS-treated ZT0 cells over Medium-treated ZT0 cells and LPS-treated ZT12 cells over Medium-treated ZT12 cells).

4 Notes

1. Polystyrene Petri dishes for mammalian cell cultures are used as they provide a greater yield of BMDMs for the following steps of the procedure.

2. Expression of clock-controlled genes oscillate in different kinetics and therefore the length of the intervals chosen for analysis of expression of a given gene will impact whether one might detect or not circadian like expression. Assaying gene expression in intervals of 12 h may not be adequate to detect the peaks and troughs of an oscillating gene. Therefore, experimental designs for synchronization usually involve analyzing gene expression every 4 or 6 h. In addition, for expression to be considered circadian there must be a peak and trough within 24 h, and the time between the peak and trough needs to be 12 h apart. Therefore, experimental design should include evaluating gene expression for at least 24 h, ideally 48 h, to make sure the pattern of oscillation is stable along two entire circadian cycles. Experimental setup must include one plate with asynchronous and synchronous cells per analyzed timepoint (Fig. 2a, b, as examples).
3. As the synchronizing agent of this experimental approach is present in serum, to avoid confounding factors, asynchronous cells are kept in serum-free DMEM for the entire experimental period. Cells submitted to serum shock are kept in serum-free DMEM after the 2 h of exposure to 50 % serum DMEM. BMDMs are usually viable for 48 h in DMEM supplemented only with antibiotics.
4. There is no need to wash with PBS or plain DMEM after removing the 50 % serum DMEM from shocked cells. Simply remove media and add serum-free DMEM with antibiotics (the same medium that asynchronous cells are kept during the whole experimental period).
5. The goal of this experimental set up is to demonstrate if any gene of interest is expressed in a circadian pattern. Each plate will contain wells with asynchronous cells and wells with synchronized cells. After gene expression assessment, genes that present a peak and trough 12 h apart in the synchronized cells, but not in the asynchronous cells, are considered to be expressed in a circadian-like fashion.
6. As the synchronizing agent of this experimental approach is Dexamethasone, asynchronous cells may be kept in DMEM containing 10 % FBS for the entire experimental period. Cells exposed to Dexamethasone are kept in 10 % FBS DMEM after the 2 h of treatment.
7. Dexamethasone interferes with the expression of some clock genes directly through activation of the Glucocorticoid receptor (GR) and this modulation does not follow a circadian pattern [12]. Therefore, to avoid interference of this direct GR-mediated effect, assessment of gene expression after syn-

chronization by this method is conducted using a later timepoint, usually beginning 12 h after exposure to Dexamethasone.

8. The goal of this experiment is to assess whether cells in different moments of the circadian cycle respond differently to TLR activation. Therefore, there is no need to keep asynchronous cells in this experimental setup. In fact, for this purpose, experiment design must contain wells with cells in two different moments of circadian cycle that will be treated or not with TLR agonists in the same plate. In the example in Figs. 2c and 3, cells shocked 36 or 24 h before were treated or not with LPS and 12 h later, supernatants were collected to measure cytokine production by ELISA (Fig. 4). Alternatively, cells could be lyzed for RNA extraction and analysis of gene expression in a similar way to that of primary cells obtained from mice at different Zeitgeber times (*see* Subheadings 3.2.1, 3.2.2, and 3.2.3).

References

1. Partch CL, Green CB, Takahashi JS (2014) Molecular architecture of the mammalian circadian clock. Trends Cell Biol 24:90–99
2. Curtis AM, Bellet MM, Sassone-Corsi P et al (2014) Circadian clock proteins and immunity. Immunity 40:178–186
3. Curtis AM, Fagundes CT, Yang G et al (2015) Circadian control of innate immunity in macrophages by miR-155 targeting Bmal1. Proc Natl Acad Sci U S A 112:7231–7236
4. Nguyen KD, Fentress SJ, Qiu Y et al (2013) Circadian gene Bmal1 regulates diurnal oscillations of Ly6C(hi) inflammatory monocytes. Science 341:1483–1488
5. Castanon-Cervantes O, Wu M, Ehlen JC et al (2010) Dysregulation of inflammatory responses by chronic circadian disruption. J Immunol 185:5796–5805
6. Antunes LC, Levandovski R, Dantas G et al (2010) Obesity and shift work: chronobiological aspects. Nutr Res Rev 23:155–168
7. Straif K, Baan R, Grosse Y et al (2007) Carcinogenicity of shift-work, painting, and fire-fighting. Lancet Oncol 8:1065–1066
8. Hashiramoto A, Yamane T, Tsumiyama K et al (2010) Mammalian clock gene Cryptochrome regulates arthritis via proinflammatory cytokine TNF-alpha. J Immunol 184:1560–1565
9. Haus E, Sackett-Lundeen L, Smolensky MH (2012) Rheumatoid arthritis: circadian rhythms in disease activity, signs and symptoms, and rationale for chronotherapy with corticosteroids and other medications. Bull NYU Hosp Jt Dis 70:3–10
10. Balsalobre A, Damiola F, Schibler U (1998) A serum shock induces circadian gene expression in mammalian tissue culture cells. Cell 93:929–937
11. Balsalobre A, Brown SA, Marcacci L et al (2000) Resetting of circadian time in peripheral tissues by glucocorticoid signaling. Science 289:2344–2347
12. Reddy TE, Gertz J, Crawford GE et al (2012) The hypersensitive glucocorticoid response specifically regulates period 1 and expression of circadian genes. Mol Cell Biol 32:3756–3767

Part V

Toll-Like Receptors and Disease

Chapter 20

Methods to Investigate the Role of Toll-Like Receptors in Allergic Contact Dermatitis

Marc Schmidt, Matthias Goebeler, and Stefan F. Martin

Abstract

Allergic contact disease is a common inflammatory skin disease resulting from hyperresponsiveness to harmless nonprotein substances such as metals, fragrances, or rubber. Recent research has highlighted a prominent role of Toll-like receptors, particularly TLR4 in contact allergen-induced innate immune activation that crucially contributes to the pathogenesis of this disease.

Here we describe several methods to investigate the role of Toll-like receptors in contact allergen-induced pro-inflammatory responses. These include expansion of disease-relevant human primary cells including endothelial cells and keratinocytes and their manipulation of TLR signaling by transfection, retroviral infection and RNA interference, basic methods to induce contact hypersensitivity in mice, and protocols for adoptive transfer of hapten-stimulated dendritic cells and T cells from TLR-deficient mice to wild-type mice and vice versa wild-type mice to TLR-deficient mice in order to explore cell-specific roles of TLRs in contact hypersensitivity responses.

Key words Allergic contact dermatitis, Contact hypersensitivity, TLR4, Hapten, Metal allergen

1 Introduction

Allergic contact dermatitis (ACD) is one of the most prevalent skin disorders. It is triggered by epicutaneous contact with low molecular weight (<500 Da) chemicals (haptens) that act as allergens [1, 2]. More than 4000 defined substances are known that are capable of inducing ACD [3]. Prominent examples are nickel (a frequent component of fashion jewelry and many consumer products) or fragrances. For studying the mechanisms of contact allergy, animal models have been extremely useful, especially investigating contact hypersensitivity (CHS), the mouse equivalent of ACD. Development of ACD (and CHS) requires a sensitization phase during which haptens are processed and presented by antigen-presenting dendritic cells (DCs) to prime for an adaptive T lymphocyte-mediated immune response; this phase is clinically inapparent. Upon reexposure to the same hapten, the so-called elicitation phase is initiated,

Claire E. McCoy (ed.), *Toll-Like Receptors: Practice and Methods*, Methods in Molecular Biology, vol. 1390,
DOI 10.1007/978-1-4939-3335-8_20,

in which hapten-specific T lymphocytes locally proliferate in the skin [4] and orchestrate a clinically visible inflammation in dermis and epidermis. Belonging to the delayed-type (type IV) hypersensitivity diseases, the clinical signs of hypersensitivity typically emerge late after exposure, i.e., ~72 h after hapten contact in sensitized humans or after ~24–48 h in sensitized mice, respectively. They manifest as characteristic erythematous, scaling and itchy skin lesions, clinically known as eczema (dermatitis). Pathophysiologically, these result from cytotoxicity and inflammation triggered by a complex interplay of locally activated skin-resident cells including keratinocytes, endothelial cells (EC) and DCs as well as locally proliferating and infiltrating leukocytes [5, 2]. The latter most importantly comprise cells of the adaptive immune system such as hapten-specific cytotoxic T (Tc) cells and different T helper (Th) populations but also include innate immune cells such as neutrophils and macrophages that aggravate the inflammatory response.

While ACD and CHS have long been considered to be entirely dependent on the adaptive immune system it has recently become clear that generation of adequate innate immune signals is a prerequisite for initiation of both the sensitization and elicitation phase [1]. These can either be delivered by direct stimulation of innate immune receptors by the hapten itself, or result from indirect activation of membrane-bound or cytosolic pattern recognition receptors (PRR) by damage-associated molecular patterns (DAMPs) that are released in response to metabolization or hapten reactivity against endogenous cell components, respectively [1, 6]. An important consequence of hapten-induced innate immune activation is the stimulation and mobilization of hapten-loaded DCs to the skin-draining lymph node where they encounter and educate naïve T cells to respond to a given hapten [5]. Additionally, hapten-induced innate immune activation results in release of pro-inflammatory cytokines such as IL-1 by keratinocytes and licences local ECs to express various cell surface receptors and chemokines that support recruitment of leukocytes from the blood into the skin [1]. Thus, innate immune activation of skin resident cell populations is crucial for development of ACD.

Recently, evidence has accumulated that Toll-like receptors (TLR) play a key role in hapten-dependent innate immune activation and CHS induction. The first hint came from the observation that TLR2/4 double-deficient mice were protected from CHS induction by the model hapten 2,4,6-trinitro-1-chlorobenzene (TNCB), suggesting a critical role of those two PRRs in TNCB-induced CHS [7]. The indispensable requirement of TLR2 and TLR4 likely relies on TNCB-induced oxidation and enzymatic degradation of the extracellular matrix component hyaluronic acid triggering release of low-molecular hyaluronan [7, 8], which acts as DAMP for TLR2 and TLR4 [9–11] and induces the necessary innate immune activation for efficient T-cell priming.

In contrast to indirect innate immune activation via DAMPs, the metal allergens nickel, cobalt, and recently also palladium were shown to trigger innate immune activation via direct stimulation of TLR4 signaling [12–14]. In case of nickel and cobalt this requires the presence of two non-conserved histidine residues, H456 and H458, at the dimerization interface of human TLR4 [12, 13]. Metal binding to those residues supports cross-linking of two TLR4 receptor dimers as demonstrated by co-immunoprecipitation experiments with differently tagged TLR4 receptors exogenously expressed in TLR4-deficient HEK293 cells [13]. Notably, mouse TLR4 lacks equivalents of the above-mentioned metal-responsive histidines H456 and H458. As a result, wild-type mice are insensitive to nickel-induced TLR4 activation and fail to induce a significant innate immune signal and CHS upon nickel treatment [12]. However, the missing innate immune signal in mice can be restored by transgenic expression of human TLR4 [12], co-treatment with the natural TLR4 agonist lipopolysaccharide (LPS) [15], or co-incubation with other adjuvants [16] allowing CHS induction by nickel. This provides evidence that (a) innate immune activation is crucial for nickel-induced CHS but can be replaced by alternative TLR4/PRR activation and (b) that reconstitution with human TLR4 is sufficient to restore responsiveness to nickel in mice [17].

TLR-deficient cells sustaining intact TLR-dependent intracellular signaling circuits provide valuable tools to analyze direct stimulatory effects of haptens on TLR-mediated pro-inflammatory gene expression, as they are amenable for reconstitution experiments. A well-established human cell line suitable for reconstitution experiments with TLRs and other innate immune receptors is the human embryonic kidney cell line HEK293. This cell line has the advantage that it is deficient for most TLRs including TLR2 and TLR4 [18], is easy to cultivate and manipulate, and expresses enormous amounts of exogenously expressed proteins, which facilitates, e.g., co-immunoprecipitation experiments. Another extremely useful primary epidermal cell for contact allergy research are normal human foreskin epithelial keratinocytes (NHEK), which express a variety of endogenous TLR receptors as well as the TLR4 co-receptor MD2 but are deficient for TLR4 under undifferentiated, differentiated, and inflammatory conditions [13], respectively. Albeit more challenging with respect to culture conditions and manipulation, these cells can be transiently transfected to rates up to 50 % with appropriate reagents and are thus likewise well suited for reconstitution experiments with TLR4 [13]. Moreover, manipulated NHEKs can be used for in vitro 3D skin reconstitution models, which can be transplanted onto mice for further analysis.

Other useful primary cells for contact allergy research include endothelial cells. Vessel endothelium is among the first to respond

to hapten challenge in vivo and is highly responsive to proinflammatory activation by various stimuli including LPS, TNF, and IL-1β [12, 17]. Since microvascular dermal endothelial cells are difficult to isolate human umbilical vein endothelial cells (HUVEC) are frequently used as substitutes. HUVEC endogenously express TLR4 along with MD2 as well as intracellular TLR3, but show no functional expression of other surface TLRs [19] making them an ideal model to test hapten-induced TLR4 activation. Similarly to NHEKs they are commercially available from various suppliers but unlike those are relatively easy to cultivate and can well be manipulated via small-interfering RNA (RNAi) as well as by retroviral gene transduction in order to interfere with TLR4 signaling [12].

As mentioned above, wild-type mice and mouse cells are poor models to study metal-induced CHS and innate immune activation due to the failure of mouse TLR4 to respond to metal haptens [12, 13]. However, this deficit turned out to be extremely handy to dissect the exact molecular requirements for metal-induced TLR4 activation since ex vivo isolated primary cells from wild-type mice could be used as reconstitution system to test the responsiveness of human TLR4 mutants to nickel-induced proinflammatory activation [12]. Moreover, the availability of human TLR4-transgenic *Tlr4*$^{-/-}$ mice opens the unique opportunity to analyze the relative contributions of distinct lymphocyte or DC populations to metal-induced CHS in adoptive transfer experiments in which purified cell populations from human TLR4-transgenic *Tlr4*$^{-/-}$ donor mice are transferred to wild-type or TLR4-deficient receptor mice.

The methods described below are categorized into two parts addressing different aspects of hapten-induced TLR activation: The first one deals with methods to analyze direct TLR activation and dimerization by haptens in human primary cells and HEK293 cells. In the second part we elaborate on methods of CHS-induction by haptens and provide methods for the in vitro generation of DCs and isolation of T cells for adoptive transfer. The latter is particularly designed to test the role of distinct cell populations isolated from hapten-sensitized donor mice with genetic alteration in TLR signaling components for the induction of CHS responses in nonresponsive wild-type or TLR-deficient recipient mice.

2 Materials

2.1 Cell Culture

1. NHEK and HUVEC cells from single donors (Promocell) (*see* **Note 1**).
2. Wild-type HEK293 and HEK293 stably expressing human MD2 and CD14 (HEK293-MD2/CD14) (Invivogen).
3. ϕNX ampho virus producer cells [20] (The National Gene Vector Biorepository).

4. FLYRD18 human fibrosarcoma virus producer cells [21] (Sigma).
5. Culture medium for HEK293 cells, ϕNX ampho, and FLYRD18: Dulbecco's modified Eagle's Medium (DMEM) GlutaMAX I™ with high glucose (Life Technologies) supplemented with 10 % fetal calf serum (FCS; GE Healthcare) (*see* **Note 2**).
6. HUVEC culture medium: mix 1 part endothelial growth medium (EGM™; Lonza) as specified under (a) and 2 parts of medium 199 Earle's Salts GlutaMAX I™ (Life Technologies) as detailed under (b).
   (a) EGM: Endothelial basal medium (500 ml) is supplemented with EGM SingleQuot Supplements and Growth Factors (Lonza) as follows: 10 ml FBS, 0.5 ml of human epidermal growth factor, 0.5 ml hydrocortisone, 0.5 ml gentamycin/amphotericin B, and 2 ml of bovine brain extract with heparin.
   (b) M199 medium with Earle's Salts GlutaMAX™ supplemented with 10 % FCS, 30 μg/ml gentamycin, 15 pg/ml amphotericin B, and 0.8 IU/ml heparin.
7. NHEK culture medium: A 1:1 mix of serum-free keratinocyte growth medium (KSFM) containing 50 μg/ml bovine pituitary extract (BPE) and 5 ng/ml hEGF (Life Technologies) and calcium-free Eagle's Minimum Essential Medium (EMEM; Lonza) without supplementation. The final calcium chloride concentration of the mixture medium is 0.05 mM, which impedes spontaneous differentiation and keeps cells in optimal proliferative condition [22].
8. Chelex 100 Resin (analytical grade, 100–200 mesh; Bio-Rad), for removal of calcium from FCS in order to avoid calcium-induced differentiation of NHEK keratinocytes upon subculture.
9. Phosphate buffered saline (PBS).
10. Trypsin/EDTA (0.05 %/0.02 % in sterile PBS).
11. 0.05 % EDTA pH 8.0 (sterile filtered).
12. DMSO.
13. FCS or Chelex-treated FCS (in case of NHEK) for passaging and freezing of cells.
14. Antibiotics for selection: hygromycin (50 μg/ml) for re-selection of stable HEK293-MD2/CD14; hygromycin (300 μg/ml) and diphtheria toxin (1 μg/ml) for co-selection of retroviral *gag/pol* and *env* genes stably expressed by ϕNX ampho cells; Blasticidin S (4 μg/ml) and Zeozin (Phleomycin, 10 μg/ml) for re-selection of viral packaging genes of FLYRD18; puromycin (2 μg/ml) for selection of stable viral producers

containing retroviral expression constructs for dominant-negative signaling components or small hairpin RNA (shRNA).

15. Metal salt stock solutions for stimulation:
    (a) 150 mM Nickel Chloride ($NiCl_2 \cdot 6H_2O$, ACS grade; Merck Millipore), in aqua ad injectabilia (pyrogen-free water), sterile filtered and used at a final concentration of 1.5 mM.
    (b) 150 mM Cobalt chloride ($CoCl_2 \cdot 6H_2O$, premium quality; Sigma), in aqua ad injectabilia (pyrogen-free water), sterile filtered and used at final concentration of 1.5 mM.
16. LPS as positive control for TLR4 stimulation:
    (a) Smooth LPS *E. coli* Serotype O55-B5 (TLR*grade*; Enzo), used at 1 μg/ml.
    (b) Rough LPS: LPS *E. coli* Serotype R515 or LPS *Salmonella minnesota* R595 (TLR*grade*; Enzo), used at 1 μg/ml.
17. Polymyxin B-sulfate (PMB; Sigma) used at 50 μg/ml to control for endotoxin contamination of metal solutions.

2.2 Transfection

1. Oligofectamine™ and OptiMEM medium (Life Technologies) for transfer of small interfering RNA (siRNA) into HUVEC.
2. Scrambled siRNA and validated siRNA directed against TLR signaling compounds commercially available (Qiagen or Life Technologies).
3. Retroviral vectors pBABE puro [23] and pRetro Super (pRS) [24] with and without gene insert for generation of stable ϕNX ampho and FLYRD18 retroviral producer cell lines producing amphotropic retroviruses for expression of dominant-negative signaling components or shRNA directed against TLR signaling-relevant genes in primary HUVEC.
4. Polybrene (5 mg/ml in aqua destillata; Sigma).
5. 0.8 μm syringe filter (Sartorius) for filtration of virus supernatant.
6. Puromycin (10 mg/ml in aqua destillata; AppliChem). Use at 2 μg/ml for selection of positive integration of retroviral constructs.
7. FuGENE HD® (Roche) and Lipofectamin® 2000 (Life Technologies) transfection reagents.

2.3 Co-immunoprecipitation

1. HA-tagged human TLR4 (pDisplay-HA-TLR4 [25]), FLAG-tagged TLR4 (pCMV-FLAG-TLR4) (Tularik Inc.), and mutagenized variants thereof [12, 13].
2. E1A Lysis Buffer (ELB): 150 mM Sodium chloride, 50 mM HEPES, pH 7.5, 5 mM EDTA, 0.1 % NP-40 in dd H_2O. Before use, freshly add 20 mM β-Glycerophosphate (as protein threonine phosphatase inhibitor), 0.5 mM sodium-ortho-vanadate

(as protein tyrosine phosphatase inhibitor) [26], and 1× Complete® protease inhibitor (Roche) to obtain ELB^{+++}.

3. Mouse α-FLAG® (M2; Sigma) and Mouse α-HA (12CA5; Abgent) antibodies for immunoprecipitation used at 0.5 or 1 μg/ml, respectively.
4. Protein G Agarose (Roche).
5. 2× SDS-sample buffer: 125 mM Tris–HCl, pH 6.8, 4 % Sodium dodecyl sulfate (SDS), 20 % Glycerol, 5 % β-Mercaptoethanol, 0.005 % Bromophenol blue in dd H_2O.
6. Rat α-HA (high affinity) (3F10; Roche) and Rabbit α-FLAG antibody (Rockland) used for Western blotting at 50 ng/ml or 0.5 μg/ml, respectively.
7. Secondary horseradish peroxidase- (POD-)coupled antibodies: α-rat-POD (1:2000; Santa Cruz), α-rabbit-POD, and α-mouse POD (1:2000; GE Healthcare).
8. Enhanced chemiluminescence (ECL) detection buffer. Freshly prepared 1:1 mixture of:
   (a) Solution A: 0.1 M Tris–HCl, pH 8.5, freshly supplemented with 2.5 mM Luminol and 0.4 mM p-coumaric acid.
   (b) Solution B: 0.1 M Tris–HCl, pH 8.5, freshly supplemented with 0.18 % H_2O_2.
9. Antibodies for Western blots: mouse α-(human) IL-8 (G265-8) (1 μg/ml; BD Pharmingen), mouse α-alpha-Tubulin used as loading control (B-5-1-2) (1:10,000; Sigma).
10. ELISAs: BD OptEIA human IL-8 ELISA Set and OptEIA human MCP1 (CCL2) ELISA Set (BD Pharmingen).
11. FACS antibodies: mouse α-(human) IL-8 (G265-8) (1:100; BD Pharmingen), Mouse α-(human) ICAM1 (84H10) (1:100; Beckman-Coulter), mouse anti-human E-selectin (1.2B6) (1:100; Merck Millipore), and mouse α-(human) VCAM1 (1.G11B1) (1:100; AbD Serotec).

2.4 CHS Responses

1. Inbred mice: wild-type mice (C57BL/6, C57BL/10, or other), mutant mice (e.g., TLR-deficient) on the same genetic background, 6–8 weeks of age from an SPF facility.
2. Electric shaver to remove hair from abdominal skin.
3. Contact allergens: TNCB (Sigma), dissolve in acetone prior to use; 2,4,6-trinitrobenzene sulfonic acid (TNBS; Sigma), prepare 3 mM stock in PBS and adjust pH to 7.4, store aliquots at −20 °C; $NiCl_2$ ($NiCl_2 \cdot 6H_2O$; ACS grade; Merck Millipore) prepare 1, 5, and 10 mM stock solutions in 0.9 % NaCl, store at 4 °C.

4. Irritant: croton oil (Sigma).
5. LPS *E. coli* Serotype O55-B5 (TLR*grade*; Enzo), prepare 1 μg/ml stock solution.
6. 20, 200, and 1000 μl pipettes and pipette tips.
7. Thickness gauge, e.g., from Käfer Messuhrenfabrik GmbH, Villingen-Schwenningen, Germany.
8. 1 ml syringes with 0.3 mm × 12 mm needles for intracutaneous dendritic cell injections or 0.45 × 12 mm for i.v. injections.
9. RPMI medium: RPMI-1640 supplemented with 10 % heat-inactivated fetal calf serum (FCS), 2 mM l-glutamine, 25 mM HEPES buffer, 50 μg/ml penicillin-streptomycin (all from Life Technologies), and 10 μM 2-mercaptoethanol (2-ME) (Sigma).
10. PBS.
11. Acetone.

3 Methods

3.1 Cell Culture

All cell culture works are carried out under sterile conditions (under laminar air flow, using sterile solutions and media, sterile consumables). All primary cells and cell lines are grown at 37 °C, 5 % CO_2 and high humidity and should regularly be tested for negativity of mycoplasm infection.

Primary human NHEK and HUVEC cells from single donors can either be isolated freshly from donor material or purchased from a commercial supplier (e.g., Promocell) as frozen cell aliquots (passage 1 or 2 for HUVEC or NHEK, respectively) for expansion (*see* **Note 1**).

Below we provide a protocol for expansion of primary human NHEK keratinocytes or endothelial cells.

1. Thaw frozen aliquots of NHEK or HUVEC (containing ~5×10^5) cells as quickly as possible at 37 °C in a water bath (requires about 90 s) and add about 1 ml of the appropriate pre-warmed medium (*see* Subheading 2.1) to gently resuspend cells.
2. Transfer immediately to one T175 flask (NHEK) or three T75 flasks (HUVEC) containing at least the tenfold volume of pre-warmed medium (*see* **Note 3**).
3. At 70–80 % density (this takes about 5 days) wash cells twice with pre-warmed PBS.
4. Pre-incubate for 12 min in 0.05 % sterile EDTA, pH 8.0, followed by a short trypsin/EDTA (0.05 %/0.02 % in sterile PBS) treatment (NHEK) or trypsinize directly (HUVEC) to detach cells from the dish (*see* **step 5**).

5. Add trypsin/EDTA carefully to the culture vessel and swirl gently to cover the cells.
6. Remove Trypsin/EDTA solution immediately and incubate cells briefly at 37 °C (for no longer than 3 min!).
7. Neutralize trypsin by addition of 5 ml of 10% FCS (HUVEC) or 10 % Chelex-treated FCS (NHEK) (*see* **Note 4**).
8. Rinse cells gently off the culture vessel, and transfer to 15 ml tubes for centrifugation at 250 × *g* (~1100 rpm in a common table centrifuge) to obtain cell pellets.
9. After resuspension in fresh medium seed cells onto 18 T175 culture flasks (HUVEC) or count and seed at a density of ~3000 cells/cm^2 onto new culture vessels (NHEK).
10. Culture cells with media replacement every second day until they reach 70–80 % confluency (after about 4–6 days).
11. Detach cells as described above, pool and count cells prior to distribution into 50 ml tubes and centrifugation at 250 × *g*.
12. Gently resuspend in an appropriate amount of ice-cold freezing medium containing 10 % FCS (for NHEK: 10 % Chelex-treated FCS), 10 % DMSO, and 80 % of the respective growth medium and distribute cells to precooled cryowells at portions of 5×10^5, 1×10^6, 2×10^6, and 4×10^6 cells.
13. Put cryowells into styroracks and place at −80 °C for freezing.
14. After 2–3 days transfer the frozen cell aliquots to liquid nitrogen for long-term storage (*see* **Note 5**). For experiments or manipulation an appropriate amount of cells (*see* Subheading 3.2 below) is thawed and either used directly (HUVEC) or passaged once prior to use (NHEK).

3.2 Transfection

Below we describe three transfection methods to manipulate human primary cells for analysis of TLR-dependent signaling: (a) knockdown of essential signal transducers of TLR signaling by siRNA transfection (*see* Subheading 3.2.1), (b) retroviral expression of dominant-negative signaling mediators or shRNA constructs (*see* Subheading 3.2.2), or (c) TLR4 reconstitution experiments by transient transfection (*see* Subheading 3.2.3).

3.2.1 siRNA Transfection

1. Seed expanded HUVEC (passage 3) onto 6-well dishes at a density of 1.2×10^5 cells/well.
2. On day 2, check cell morphology and density by phase contrast microscopy. If cells have reached the desired cell density of ~70–80 % proceed with **step 3**, otherwise grow cells for one more day. Discard altogether if cultures show increased cell death or do not reach the above specified density by Day 3.

3. Dilute 10 µl of a 20 µM siRNA oligo solution (*see* **Note 6**) directed against a TLR4-relevant signaling component such as MD2 and in parallel a scrambled siRNA (as negative control) with each 90 µl prewarmed OptiMEM (without supplements and FCS) and for each siRNA 10 µl Oligofectamine™ with 90 µl OptiMEM (*see* **Note 7**) in separate polypropylene tubes.
4. Incubate the solutions for 10 min at room temperature.
5. Add the RNAi-containing solutions to the respective tubes containing the Oligofectamine™ dilution and mix gently by tapping.
6. Incubate another 30 min and then add 800 µl OptiMEM (without supplements) to obtain 1 ml solution for each transfection.
7. Wash cells twice with prewarmed OptiMEM medium and then add the Oligofectamine™/RNAi mixture directly to the cells (final concentration of the RNAi oligo is 200 pmol/ml).
8. Incubate for 4 h at 37 °C, then replace by fresh culture medium.
9. After about 2–3 days (*see* **Note 8**) stimulate cells with a hapten such as 1.5 mM $NiCl_2$ or $CoCl_2$ for 5 h to test the direct effect of a hapten on proinflammatory gene expression at RNA level by quantitative real-time PCR or for 8–16 h if protein-based readouts such as ELISA, Western blot, or FACS are used [12, 13]. Typical readout genes expressed by HUVEC are the chemokines CXCL8 (IL-8) and CCL2 (MCP-1) and the surface receptors E-selectin, ICAM or VCAM-1 as indicators of IKK2/NFκB-dependent gene expression [27] and CCL5 (RANTES) and CXCL10 (IP-10) as genes regulated by TLR4 via the TRAM/TRIF pathway [28, 29].

3.2.2 Retroviral Infection

HUVEC are rather difficult to transfect by conventional methods but can well be manipulated by retroviral gene expression, which usually yields transfection rates of >90 % (*see* **Note 9**). In order to produce the appropriate retrovirus required, we employ a stable amphotropic ϕNX cell line (for overexpression of dominant-negative signaling components) or stable high-titre producing FLYRD18 cell lines (for shRNA constructs) (*see* **Note 10**) established by standard methods as described elsewhere [30]. The following protocol describes the procedure using an established ϕNX producer cell line for dominant-negative IRAK1 (IRAK1 dn) or an FLYRD18 cell line for shRNA-expressing IRAK1.

1. On day 1, seed amphotropic ϕNX producer cells with stable integration of a retroviral expression vector (e.g., pBABE puro [23]) for a gene of interest (e.g., IRAK1 dn) or FLYRD18 producer cells stably expressing a specific shRNA construct (e.g., pRS-IRAK1) along with matched producer lines for the

respective empty retroviruses at densities of ~3.5×10^4 cells/cm^2 (ϕNX ampho) or $1 \times 10^4/cm^2$ (FLYRD18) into DMEM containing 10 % FCS and a selection antibiotic for the integrated retroviral backbone (e.g., puromycin at a concentration of 2 μg/ml). Choose appropriate culture vessel sizes corresponding to the amount of HUVEC cells to be infected (e.g., for infection of each 10 cm dish of HUVEC seed one 10 cm dish containing 2×10^6 ϕNX ampho or 6×10^5 FLYRD18 cells).

2. On day 2, replace medium of producer cultures by fresh medium lacking antibiotics (*see* **Note 11**).
3. Thaw appropriate amounts of HUVEC from a frozen aliquot (*see* **Note 3**) and seed them at densities of 4300–5200 cells/cm^2 into HUVEC-Mix (for an experiment with three stimulation conditions as shown in Fig. 1 typically seed one 10 cm dish with $2.5–3 \times 10^5$ cells per infection). Seed one additional dish to control for efficiency of the employed selection antibiotic used at later steps for enrichment of infected HUVEC (optional).
4. On day 3, replace medium of producer cell lines by an appropriate volume of HUVEC-Mix (e.g., add 6 ml to a 10 cm dish) for the first virus production. Change medium from HUVEC cultures to remove traces of DMSO and sustain HUVEC under optimal growth conditions.
5. In the morning of day 4, pipet virus supernatants from the different producer cell lines into separate 50 ml tubes (for infection of multiple dishes pool supernatants containing identical viruses to ensure equal infection efficiency) and immediately add fresh HUVEC-Mix to the producer cells for production of the second virus harvest (see below).
6. Filtrate the virus supernatant through a sterile 0.8 μm syringe filter (*see* **Note 12**) into a new 50 ml tube and add Polybrene at a final concentration of 5 μg/ml to facilitate infection.
7. Invert several times to mix, aspirate medium from the endothelial cells and immediately add the virus solution.
8. Incubate at 37 °C (in a CO_2 incubator) for 6 h and repeat **steps 5**–**7** for the second infection in the evening. Keep second virus supernatant on the cells overnight and add HUVEC-Mix to the producer cells for a third harvest (*see* **Note 13**).
9. On day 5, perform a third infection as described in **step 8**. Discard producer cells and incubate HUVEC at 37 °C for 6 h before replacing the virus supernatant with fresh HUVEC-Mix (8 ml per 10 cm dish).
10. On day 7–8, start with the selection procedure for positive infection using an appropriate antibiotic (e.g., add 2 μg/ml puromycin to the cells for 16–18 h) (*see* **Note 14**).

11. On day 8–9, reseed the infected HUVEC cells at a density of 6000 to maximally 15,500 cells/cm^2 according to the requirements of your experiment. For instance, in order to test the impact of shRNA expression on hapten-induced expression of pro-inflammatory genes on RNA level seed approximately 1×10^5 cells/well on 6-well dishes and stimulate cells the following day for 5 h with a hapten (e.g., 1.5 mM $NiCl_2$) along with a positive control for TLR activation (e.g., 1 μg/ml LPS from *Salmonella minnesota* for TLR4 activation in HUVEC) and a diluent control [13] (*see* **Note 15**). For protein-based readouts such as Western blot or FACS for IL-8 [12] seed cells into 10 cm dishes (e.g., 5×10^5) and stimulate for 8–16 h the following day. An exemplary knockdown experiment in HUVEC using retrovirally expressed shRNA for IRAK1 and nickel-induced IL-8 expression as readout is shown in Fig. 1.

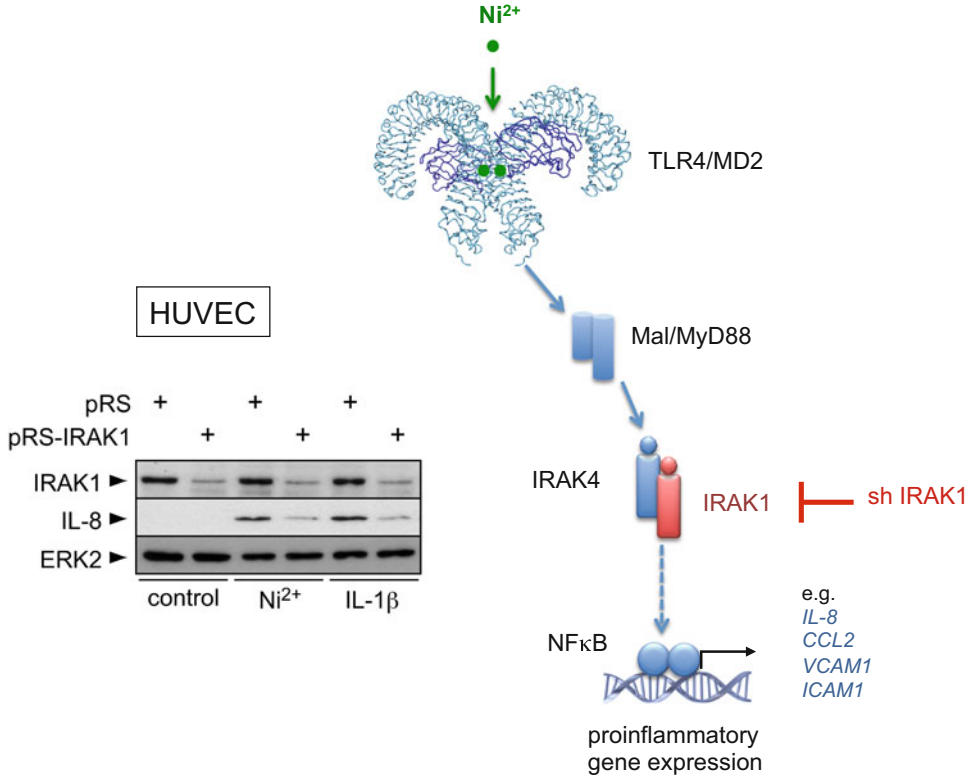

Fig. 1 Retrovirus-mediated knockdown of IRAK1 demonstrates decreased nickel responsiveness in HUVEC cells. HUVEC were retrovirally infected with either an empty retrovirus (pRS) or an shRNA construct for IRAK1 (pRS-IRAK1) and 96 h post infection stimulated for 8 h with the TLR4-activating metal allergen nickel (Ni^{2+}) or IL-1 (as positive control), respectively. Western blot analysis demonstrates a reduction of nickel-induced IL-8 production in IRAK1-depleted cells. The schematic shows the central position of IRAK1 downstream of TLR4 signaling and illustrates the proposed mechanism of nickel-induced TLR4 activation by triggering TLR4/MD2 heterodimers [12, 13]

3.2.3 TLR4 Reconstitution

We provide a procedure to test hapten responsiveness upon reconstitution of TLR4 or a point-mutated TLR4 variant into NHEK cells, which lack detectable TLR4 expression but express endogenous MD2 [13].

1. Recover NHEK cells from frozen stocks (*see* **Note 3**) and plate at a density of ~1.7×10^4/cm^2 (e.g., 1×10^6 cells onto a 10 cm dish).
2. Passage cells once prior to seeding at a density of 1×10^5 cells per well into 6-well culture dishes for transfection.
3. After 1–2 days (cells should be 70–80 % dense) transiently transfect cells with each 2 μg total DNA and 12 μl of FuGENE® HD reagent (Roche) as follows:
4. Replace medium by fresh growth medium lacking antibiotics.
5. Prepare two polypropylene tubes per transfection and stimulation condition (for instance to test the responsiveness of a TLR4 point mutant in comparison to wild-type TLR4 and empty vector, prepare six tubes per stimulation condition).
6. To the first tube add 2 μg of the DNA solution to be transfected (*see* **Note 16**); to the second one add 12 μl FuGENE® HD to 88 μl calcium-free EMEM (without supplements) (*see* **Note 7**).
7. Incubate for 5 min and then add the FuGENE® HD solution dropwise to the DNA under gentle shaking.
8. Incubate for another 15 min at room temperature.
9. Add transfection mixture dropwise to the cells and swirl to mix.
10. Change medium 6 h post-transfection and grow in culture medium for at least 40 h prior to stimulation with hapten and appropriate controls such as LPS for 5 or 8–16 h in order to analyze TLR-dependent gene expression (e.g., of IL-8 as readout for TLR4-dependent NFκB activation) at RNA or protein level, respectively (*see* **Note 17**).

3.3 Co-immunoprecipitation

Hapten-induced dimerization of TLRs can be investigated by transfection of differently tagged TLR constructs into HEK293 cells and subsequent analysis of basal or hapten-induced interaction of the two co-expressed TLR molecules by co-immunoprecipitation (Fig. 2). The following protocol describes how to analyze TLR4 dimerization in response to nickel or cobalt stimulation in the presence or absence of its co-receptor MD2 using HEK293 cells or HEK 293-MD2/CD14 cells, respectively [13] but can easily adapted to address different questions.

1. Seed HEK293 and HEK293 hMD2 cells into antibiotic-free culture medium at a density of 5×10^6 cells per 10 cm culture dish, 1 day prior to transfection.
2. Transfect at least one dish each with 24 μg empty vector, a combination of empty vector and each one of the tagged TLR4 constructs (12 μg each, 24 μg DNA in total), or a 1:1 mixture of FLAG-tagged TLR4 and HA-tagged TLR4 and for each combination 60 μl of Lipofectamine® 2000 (Life Technologies) according to manufacturer's suggestions (*see* **Note 18**).
3. The following day split transfected cells 1:3 for stimulation with a hapten such as nickel, LPS, or diluent control.
4. After 30 min of stimulation, harvest cells by washing twice with ice-cold PBS and lyse directly on the dish by adding 500 μl supplemented ELB (*see* **Note 19**).
5. Calculate protein concentration and per sample distribute a volume equivalent to 1.5 mg total protein into separate 1.5 ml microcentrifuge tubes for immunoprecipitation.
6. To each tube add 500 μl of supplemented ELB containing 1 μg of mouse α-FLAG antibody (if necessary adjust total volumes with supplemented ELB).
7. Tumble over night at 4 °C using an end-over-end rotary shaker.
8. Add 25 μl of protein G agarose beads and precipitate immune-complexes by centrifugation at 14,000 rpm using a bench top microcentrifuge.
9. Wash three times at 4 °C by addition of 1 ml high salt ELB buffer containing 500 mM sodium chloride and subsequent centrifugation at 14,000 rpm.
10. Resuspend beads by the addition of 25 μl 2× SDS buffer.
11. Boil at 95 °C for 5 min and centrifuge briefly to pellet beads.
12. Subject 10 μl of the supernatant to SDS-PAGE.
13. Perform Western blotting using a rat-α-HA high affinity primary antibody (50 ng/ml) and a POD-coupled α-rat secondary antibody to detect co-precipitated HA-TLR4 (indicating TLR4 dimerization) by ECL.
14. Control for equal precipitation of FLAG-tagged TLR4 by reprobing membranes with 0.5 μg/ml rabbit α-flag antibody.

3.4 CHS Responses

Here, we describe the measurement of ear swelling as a readout for the CHS model. It is, however, necessary to analyze immune responses to contact allergens or irritants in detail with respect to TLR-dependent differences. This is done by using skin, lymph nodes, spleen, blood, etc. to study innate and adaptive cellular

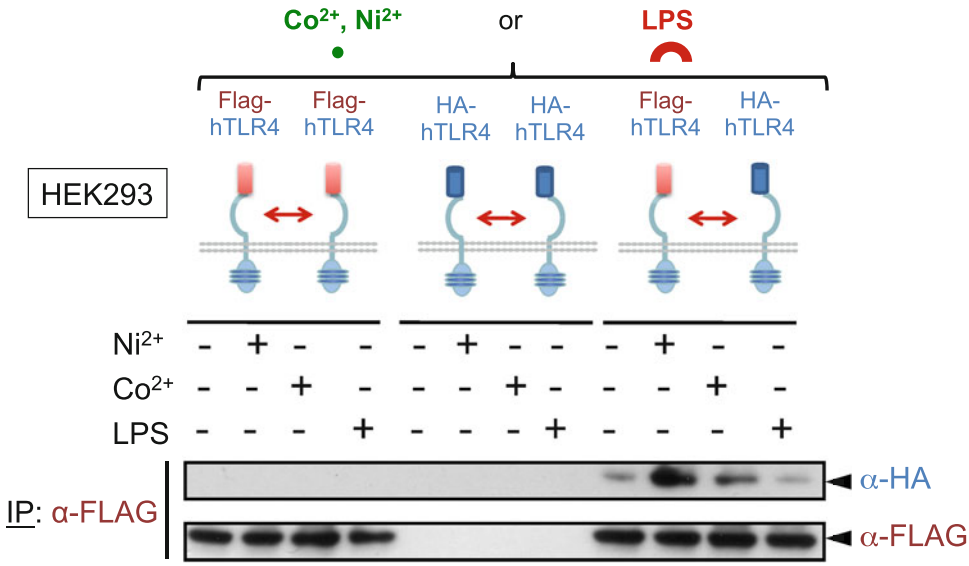

Fig. 2 Co-immunoprecipitation demonstrates hapten-induced TLR4 dimerization. HEK293 cells were transiently transfected with empty vector (not shown), a combination of empty vector plus FLAG-tagged human TLR4 (*left*), empty vector plus HA-tagged human TLR4 (*middle*), or a combination of both (*right*), respectively. After 48 h cells were stimulated for 30 min with nickel (Ni^{2+}), cobalt (Co^{2+}), LPS or diluent and subjected to immunoprecipitation with a FLAG-antibody. Co-immunoprecipitated HA-TLR4/FLAG-TLR4 dimers were then detected by immunoblot using an HA-specific antibody. An immunoblot for FLAG-tagged TLR4 using a FLAG-tag-specific antiserum is shown as control for equal precipitation of FLAG-TLR4. Equal transfection of the tagged TLR construct was confirmed by Western blotting of total lysate with Tag-specific antibodies (not shown). Data demonstrate that, unlike LPS, which requires MD2 to stimulate TLR4 dimerization above basal levels [13], the metal allergens nickel and cobalt are capable of inducing TLR4 dimerization independently of MD2. Modified from [13]

immune responses and the production of mediators such as cytokines and chemokines using a great variety of common techniques such as ELISA, flow cytometry, or qRT-PCR. These protocols apply to general research in immunology and the field of ACD/CHS, and their description is beyond the scope of this chapter.

3.4.1 *Conventional CHS*

The mouse CHS model is suitable to study the general role of TLRs for the disease. According to standard protocols [31], different contact allergens can be used for sensitization and challenge of wild-type mice or mice lacking single or multiple TLRs or components of the TLR signaling pathways (e.g., the adaptor proteins MyD88 or TRIF). In addition, irritants such as croton oil can be used to study the role of TLRs in irritant contact dermatitis, which is T cell-independent. The so-called mouse ear swelling test (MEST) represents the most common readout for studying CHS. Below we provide a standard protocol that can easily be modified for different haptens. Ideally, experimental groups of five mice should be used (*see* **Note 20**).

1. Sensitize mice by "painting" (slow pipetting and distribution with the pipet tip) 100 µl of a hapten solution (e.g., 3 % TNCB in acetone) on the shaved abdominal skin with a pipette.
2. On Day 5 measure basal ear thickness and elicitate the CHS response by painting 20 µl of a lower concentration of the same hapten (e.g., TNCB 1 % in acetone) on the dorsal side of both ears.
3. Determine the increase in ear thickness over time by measuring with an engineer's micrometer. Measurements are typically performed at 24 and 48 h. In addition, the increase in ear thickness can be measured 6 h after sensitization. The early ear swelling response is dependent on histamine released by mast cells [32].

In the case of metal ions such as nickel and cobalt, solutions of metal salts (10 mM $NiCl_2$ or $CoCl_2$ in 0.9 % NaCl solution) are injected into the abdominal skin for sensitization (2× 50 µl as described in Subheading 3.4.2 for DCs) and into the ear skin for elicitation (20 µl per ear) as described for human TLR4 transgenic mice [12]. LPS must be added for the sensitization of wild-type mice due to the lack of binding sites for the metal ions in the murine TLR4. Suitable concentrations of nickel and LPS must be determined experimentally and different combinations and protocols have been tested [15, 33]. As a standard protocol, mice are sensitized by intraperitoneal injection of 250 µl of a 1:1 (v/v) mixture of 1 mM $NiCl_2$ and 1 µg/ml LPS stock solutions. Elicitation of CHS is then done 10 days later by injection of 20 µl of a 5 mM $NiCl_2$ solution into the ear pinnas. Ear swelling peaks at 48 h. The use of ultrapure metal salts is recommended to avoid immunogenic contaminants [33].

3.4.2 Sensitization by DC Injection

The advantage of DC injection for sensitization lies in the possibility to address the role of TLRs specifically in DCs. Bone marrow-derived DCs are generated in vitro according to standard protocols [31].

1. One half of the DCs harvested at the end of the culture is left unmodified, the other half is hapten-modified in vitro by resuspension of the pellet after centrifugation in 1 ml of 3 mM TNBS (the water-soluble form of TNCB) in PBS and incubation for 7 min in a water bath in the dark.
2. Fill up the tube with RPMI medium containing 10 % FCS to prevent further reaction and toxicity.
3. Wash the TNBS-modified DCs twice in medium to remove residual TNBS and then once in PBS.
4. Resuspend and adjust cell concentration to 3×10^6/ml in PBS for injection.

5. On Day 0, inject 3×10^5 unmodified or TNBS-modified DCs from wild-type or TLR-deficient mice into the skin at two sites (100 μl per mouse: inject 2× 50 μl of the respective cell suspensions) left and right of the median of the shaved abdomen for sensitization. Formation of a subcutaneous bubble indicates the correct injection.
6. Perform elicitation as usual on Day 5 with 1 % TNCB applied on the dorsal side of the ears (*see* **Notes 20–22**). Pretreatment of DCs with e.g., TLR ligands can be done prior to the injection. In our studies this allowed us to demonstrate that triggering of TLR9 with CpG-oligodeoxynucleotides (CpG-ODN) as synthetic TLR9 ligands in vitro restored the absent sensitizing potential of DCs lacking TLR4 and IL-12Rβ2 [7].

3.4.3 Adoptive T-Cell Transfer

The transfer of lymph node cells or purified T cells can address the role of TLRs for the T-cell response both in the sensitization and the elicitation phase of CHS. The former requires the transfer of T cells from wild-type or TLR-deficient mice into wild-type recipients. This experiment provides information about the dependency of T-cell priming on the TLR of interest. The latter requires the transfer of T cells from wild-type mice into wild-type or TLR-deficient recipients. This experiment is designed to investigate the role of TLRs for the recruitment and activation of the transferred wild-type T cells. Challenge of the recipient mice is performed as usual following i.v. injection of the T cells.

1. Sensitize donor mice by painting of not only the shaved abdominal skin with 100 μl 3 % TNCB but also the dorsum of both ears with 20 μl 1 % TNCB to obtain enough cells from the local skin draining lymph nodes.
2. Sacrifice the mice 5 days later.
3. Dissect the superficial inguinal and auricular lymph nodes, pool and prepare a single-cell suspension.
4. Inject 2×10^7 lymph node cells in 200 μl PBS i.v. into the tail vein of recipient mice.
5. Directly after the injection, challenge the recipient mice on the dorsum of both ears with 20 μl 1 % TNCB.
6. Measure the increase in ear thickness as described above at 24 and 48 h. As controls, lymph node cells from solvent-treated or untreated donor mice can be used.

4 Notes

1. Each batch should be individually tested for basal and induced pro-inflammatory activation by analysing expression of appropriate activation markers (e.g., FACS staining for the endothelial

surface receptors VCAM1, E-selectin and ICAM1 in case of HUVEC). For experiments we routinely use expanded frozen aliquots stored in liquid nitrogen from passage 3 or 4, respectively (*see* Subheading 3.1). Primary cells can also be freshly prepared from donors using appropriate protocols but this is a quite cumbersome and time-consuming procedure. In our experience, the expanded cultures of NHEK and HUVEC from commercial suppliers are comparable to those of homemade cells, but expansion of commercially produced cell preparations is more convenient and economic (particularly for small labs that do not routinely use those cells on a daily basis) and has the advantage that cells have routinely been tested for HBV, HCV, and HIV infection by the supplier. Moreover, suppliers usually keep greater cell batches with different growth characteristics (e.g., doubling time, seeding efficiency) in stock that can be tested for proliferation and pro-inflammatory responsiveness before larger amounts of cell aliquots are ordered.

2. Each batch of FCS should be tested for the absence of endotoxin contaminants. We routinely monitor this by confirming lack of pro-inflammatory VCAM1 and E-selectin expression 16 h after switching HUVEC cultures from medium containing a tested FCS batch to one supplemented with a new FCS batch.
3. Do not centrifuge prior to seeding as this reduces viability. For NHEK, medium should be removed as quickly as possible as they are sensitive to DMSO (e.g., thaw in the morning and replace by fresh medium upon adherence in the evening). HUVEC withstand DMSO quite well but it is recommended to replace medium the day after seeding in order to increase viability. Never warm up more medium than required and always keep supplemented media at 4 °C. Do not use any of the supplemented media for longer than 4 weeks.
4. As FCS contains a substantial amount of calcium, which triggers differentiation of keratinocytes at levels as low as 0.1 mM [22], for NHEK culture we treat all our FCS with Chelex resin to remove calcium. We use the "batch method" suggested by the supplier, filter sterilize after incubation, and store the Chelex-treated FCS aliquoted at −20 °C until use.
5. Do not keep primary cells at −80 °C for longer periods of time as this may result in enhanced cytotoxicity at re-thawing.
6. In our experience pools of up to three (functional) siRNAs against one target work significantly more efficient than single oligos. This approach also reduces the risk of off-target effects. In the case where multiple oligos are used, reduce the amount of the individual oligos accordingly to keep the total siRNA

amount constant (e.g., if a pool of two oligos is used, add 5 μl of oligo 1 and 5 μl of oligo 2).

7. Oligofectamine™/FuGENE® transfection reagents should not come into contact with plastic in order to retain optimal efficiency. Thus, directly pipet transfection reagents into the media (without touching the wall) and not vice versa. Mix gently by tapping against the tube (do not pipet up and down).
8. Required times for efficient knockdowns should be optimized for different gene products using appropriate readouts. Usually knockdown is best between 48 and 72 h after siRNA transfection, so the total time of the experiment should preferentially not exceed 72 h. If longer times are required use retroviral approaches to stably express small-hairpin RNA (shRNA) in the cells (*see* Subheading 3.2.2).
9. This procedure uses amphotropic retroviruses, which can infect human (dividing) cells. Make sure that adequate lab facilities and legal permissions are in place.
10. FLYRD18 cells produce extremely high virus titres and in our experience provide superior infections with pRetro Super (pRS) backbone-based shRNA vectors.
11. This step is necessary to remove traces of the selection antibiotic and dead cells from the culture as well as keeping producer cells in the log phase of proliferation. You may add 5 μg/ml Polybrene at this stage to facilitate self-infection of the employed producer cell line to boost infection efficiency (optional).
12. This step is meant to remove potential contaminations of the supernatant with detached virus producer cells. Do not use pore sizes smaller than 0.45 μm as this significantly reduces infection rates for unknown reasons.
13. This step is optional for infection with regular expression constructs but in our experience enhances knockdown levels when using shRNA-containing retroviruses.
14. Selection is not mandatory for ectopic expression of signaling components since infection rates are usually >90 % but still enhances expression levels and functionality when dominant-negative constructs or shRNAs are expressed. For infection with shRNA constructs, we recommend waiting one extra day before selection. Alternatively, select shRNA-infected HUVEC at 1 μg/ml puromycin for 40 h prior to reseeding cells for experiments. Do not keep antibiotic on cells for longer than suggested as this might interfere with responsiveness to stimuli. If strong signs of cell death are observed you may give cells an extra day for recovery prior to reseeding.
15. To exclude contamination of hapten solutions with endotoxin it is mandatory for initial experiments to include additional

controls in which 50 μg/ml Polymyxin B-sulfate is added prior to hapten- and LPS-stimulation [12].

16. For co-transfections of two (e.g., TLR4 and MD2) or more plasmids reduce the amount of each construct (e.g., 1 μg each for two constructs) to maintain a total amount of 2 μg.
17. Depending on your requirements and readout you may consider positive selection of your transfected cells prior to stimulation. This can be done by co-transfection of limiting amounts of an additional plasmid containing a resistance marker for a fast working antibiotic such as puromycin that is suitable for overnight selection. For enrichment of selected cells we usually add 0.25–0.5 μg of pBABE puro vector, and select puromycin-resistant cells two days after transfection by 16 h treatment with 2 μg/ml puromycin. Make sure to reduce the amount of the construct of interest (e.g., TLR4) accordingly to maintain a total amount of 2 μg.
18. The classical calcium phosphate-based transfection is an option, but in our experience Lipofectamin-based reagents are superior for co-transfection experiments.
19. Adding β-glycerophosphate and sodium orthovanadate to the lysis buffer is essential when examining the phosphorylation status of intracellular signaling proteins. However, this may not be necessary for analysis of TLR dimerization.
20. In order to assess antigen specificity of the MEST, only one ear can be painted with the contact allergen used for sensitization. The second ear can be painted with solvent or with a different contact allergen. In that case the group sizes must be doubled.
21. Different kinetics may be observed if TNCB is used at different concentrations or in a different mouse strain or if other contact allergens are used.
22. The standard CHS protocol works with plateau concentrations of contact allergen. In order to avoid compensation of subtle effects on CHS due to mutations in TLR etc. it is recommended to titrate the sensitizing and/or elicitation dose of the contact allergen. Similarly, when DC injection is used for sensitization, titration of the DC number used for sensitization may be worthwhile.

References

1. Martin SF, Esser PR, Weber FC, Jakob T, Freudenberg MA, Schmidt M, Goebeler M (2011) Mechanisms of chemical-induced innate immunity in allergic contact dermatitis. Allergy 66:1152–1163
2. Honda T, Egawa G, Grabbe S, Kabashima K (2013) Update of immune events in the murine contact hypersensitivity model: toward the understanding of allergic contact dermatitis. J Invest Dermatol 133:303–315

3. De Groot A (2009) Patch testing. In: Test concentrations and vehicles for 4350 allergens, 3rd edn edn. ACDEGrootpublishing, Wapserveen
4. Natsuaki Y, Egawa G, Nakamizo S, Ono S, Hanakawa S, Okada T, Kusuba N, Otsuka A, Kitoh A, Honda T, Nakajima S, Tsuchiya S, Sugimoto Y, Ishii KJ, Tsutsui H, Yagita H, Iwakura Y, Kubo M, Ng LG, Hashimoto T, Fuentes J, Guttman-Yassky E, Miyachi Y, Kabashima K (2014) Perivascular leukocyte clusters are essential for efficient activation of effector T cells in the skin. Nat Immunol 15:1064–1069
5. Kaplan DH, Igyarto BZ, Gaspari AA (2012) Early immune events in the induction of allergic contact dermatitis. Nat Rev Immunol 12:114–124
6. McFadden JP, Puangpet P, Basketter DA, Dearman RJ, Kimber I (2013) Why does allergic contact dermatitis exist? Br J Dermatol 168:692–699
7. Martin SF, Dudda JC, Bachtanian E, Lembo A, Liller S, Dürr C, Heimesaat MM, Bereswill S, Fejer G, Vassileva R, Jakob T, Freudenberg N, Termeer CC, Johner C, Galanos C, Freudenberg MA (2008) Toll-like receptor and IL-12 signaling control susceptibility to contact hypersensitivity. J Exp Med 205:2151–2162
8. Esser PR, Wölfle U, Dürr C, von Loewenich FD, Schempp CM, Freudenberg MA, Jakob T, Martin SF (2012) Contact sensitizers induce skin inflammation via ROS production and hyaluronic acid degradation. PLoS One 7, e41340
9. Termeer C, Benedix F, Sleeman J, Fieber C, Voith U, Ahrens T, Miyake K, Freudenberg M, Galanos C, Simon JC (2002) Oligosaccharides of Hyaluronan activate dendritic cells via toll-like receptor 4. J Exp Med 195:99–111
10. Jiang D, Liang J, Fan J, Yu S, Chen S, Luo Y, Prestwich GD, Mascarenhas MM, Garg HG, Quinn DA, Homer RJ, Goldstein DR, Bucala R, Lee PJ, Medzhitov R, Noble PW (2005) Regulation of lung injury and repair by Toll-like receptors and hyaluronan. Nat Med 11:1173–1179
11. Scheibner KA, Lutz MA, Boodoo S, Fenton MJ, Powell JD, Horton MR (2006) Hyaluronan fragments act as an endogenous danger signal by engaging TLR2. J Immunol 177:1272–1281
12. Schmidt M, Raghavan B, Müller V, Vogl T, Fejer G, Tchaptchet S, Keck S, Kalis C, Nielsen PJ, Galanos C, Roth J, Skerra A, Martin SF, Freudenberg MA, Goebeler M (2010) Crucial role for human Toll-like receptor 4 in the development of contact allergy to nickel. Nat Immunol 11:814–819
13. Raghavan B, Martin SF, Esser PR, Goebeler M, Schmidt M (2012) Metal allergens nickel and cobalt facilitate TLR4 homodimerization independently of MD2. EMBO Rep 13: 1109–1115
14. Rachmawati D, Bontkes HJ, Verstege MI, Muris J, von Blomberg BM, Scheper RJ, van Hoogstraten IM (2013) Transition metal sensing by Toll-like receptor-4: next to nickel, cobalt and palladium are potent human dendritic cell stimulators. Contact Dermatitis 68:331–338
15. Sato N, Kinbara M, Kuroishi T, Kimura K, Iwakura Y, Ohtsu H, Sugawara S, Endo Y (2007) Lipopolysaccharide promotes and augments metal allergies in mice, dependent on innate immunity and histidine decarboxylase. Clin Exp Allergy 37:743–751
16. Artik S, von Vultee C, Gleichmann E, Schwarz T, Griem P (1999) Nickel allergy in mice: enhanced sensitization capacity of nickel at higher oxidation states. J Immunol 163: 1143–1152
17. Schmidt M, Goebeler M (2011) Nickel allergies: paying the Toll for innate immunity. J Mol Med (Berl) 89:961–970
18. Latz E, Visintin A, Lien E, Fitzgerald KA, Monks BG, Kurt-Jones EA, Golenbock DT, Espevik T (2002) Lipopolysaccharide rapidly traffics to and from the Golgi apparatus with the toll-like receptor 4-MD-2-CD14 complex in a process that is distinct from the initiation of signal transduction. J Biol Chem 277: 47834–47843
19. Müller V, Viemann D, Schmidt M, Endres N, Ludwig S, Leverkus M, Roth J, Goebeler M (2007) Candida albicans triggers activation of distinct signaling pathways to establish a proinflammatory gene expression program in primary human endothelial cells. J Immunol 179:8435–8445
20. Swift S, Lorens J, Achacoso P, Nolan GP (2001) Rapid production of retroviruses for efficient gene delivery to mammalian cells using 293T cell-based systems. Curr Protoc Immunol Unit 10:17
21. Cosset FL, Takeuchi Y, Battini JL, Weiss RA, Collins MK (1995) High-titer packaging cells producing recombinant retroviruses resistant to human serum. J Virol 69:7430–7436
22. Schmidt M, Goebeler M, Posern G, Feller SM, Seitz CS, Bröcker EB, Rapp UR, Ludwig S (2000) Ras-independent activation of the Raf/MEK/ERK pathway upon calcium-induced

differentiation of keratinocytes. J Biol Chem 275:41011–41017
23. Morgenstern JP, Land H (1990) Advanced mammalian gene transfer: high titre retroviral vectors with multiple drug selection markers and a complementary helper-free packaging cell line. Nucleic Acids Res 18:3587–3596
24. Brummelkamp TR, Bernards R, Agami R (2002) Stable suppression of tumorigenicity by virus-mediated RNA interference. Cancer Cell 2:243–247
25. Hajjar AM, Ernst RK, Tsai JH, Wilson CB, Miller SI (2002) Human Toll-like receptor 4 recognizes host-specific LPS modifications. Nat Immunol 3:354–359
26. Brautigan DL, Shriner CL (1988) Methods to distinguish various types of protein phosphatase activity. Methods Enzymol 159:339–346
27. Viemann D, Schmidt M, Tenbrock K, Schmid S, Müller V, Klimmek K, Ludwig S, Roth J, Goebeler M (2007) The contact allergen nickel triggers a unique inflammatory and proangiogenic gene expression pattern via activation of NF-kappaB and hypoxia-inducible factor-1alpha. J Immunol 178:3198–3207
28. Yamamoto M, Sato S, Hemmi H, Hoshino K, Kaisho T, Sanjo H, Takeuchi O, Sugiyama M, Okabe M, Takeda K, Akira S (2003) Role of adaptor TRIF in the MyD88-independent toll-like receptor signaling pathway. Science 301: 640–643
29. Yamamoto M, Sato S, Hemmi H, Uematsu S, Hoshino K, Kaisho T, Takeuchi O, Takeda K, Akira S (2003) TRAM is specifically involved in the Toll-like receptor 4-mediated MyD88-independent signaling pathway. Nat Immunol 4:1144–1150
30. Cepko C (2001) Preparation of a specific retrovirus producer cell line. Curr Protoc Mol Biol 9:10
31. Martin SF (2013) Induction of contact hypersensitivity in the mouse model. Methods Mol Biol 961:325–335
32. Dudeck A, Dudeck J, Scholten J, Petzold A, Surianarayanan S, Köhler A, Peschke K, Vöhringer D, Waskow C, Krieg T, Müller W, Waisman A, Hartmann K, Gunzer M, Roers A (2011) Mast cells are key promoters of contact allergy that mediate the adjuvant effects of haptens. Immunity 34:973–984
33. Kinbara M, Sato N, Kuroishi T, Takano-Yamamoto T, Sugawara S, Endo Y (2011) Allergy-inducing nickel concentration is lowered by lipopolysaccharide at both the sensitization and elicitation steps in a murine model. Br J Dermatol 164:356–362

Chapter 21

Allergens and Activation of the Toll-Like Receptor Response

Tom P. Monie and Clare E. Bryant

Abstract

Pattern recognition receptors (PRRs) provide a crucial function in the detection of exogenous and endogenous danger signals. The Toll-like receptors (TLRs) were the first family of PRRs to be discovered and have been extensively studied since. Whilst TLRs remain the best characterized family of PRRs there is still much to be learnt about their mode of activation and the mechanisms of signal transduction they employ. Much of our understanding of these processes has been gathered through the use of cell based signaling assays utilizing specific gene-reporters or cytokine secretion based readouts. More recently it has become apparent that the repertoire of ligands recognized by these receptors may be wider than originally assumed and that their activation may be sensitized, or at least modulated by the presence of common household allergens such as the cat dander protein Fel d 1, or the house dust mite allergen Der p 2. In this chapter we provide an overview of the cell culture and stimulation processes required to study TLR signaling in HEK293 based assays and in bone marrow-derived macrophages.

Key words TLR, Allergy, Fel d 1, Luciferase assay, Bone marrow-derived macrophage, Innate immunity, Signal transduction, NFκB, HEK293

1 Introduction

Knowledge of how TLRs are activated and how they propagate signaling is crucial for understanding the innate immune system, for the development of novel therapeutics against inflammatory diseases, and for the creation of new vaccine adjuvants [1]. The ability to manipulate and mutate the receptors, and their adaptor proteins, in order to probe molecular function at the level of individual amino acids has been highly informative and continues to be a mainstay in studies of receptor function. Interpretation of the results from these studies must always be done in full consideration of the caveat that these are overexpression systems making use of transient transfection of mutant receptors into potentially non-physiological cell types. It is therefore important, wherever possible, to validate observations using more physiological cell types

Claire E. McCoy (ed.), *Toll-Like Receptors: Practice and Methods*, Methods in Molecular Biology, vol. 1390,
DOI 10.1007/978-1-4939-3335-8_21,

such as macrophages. This is particularly relevant when looking at ligand-mediated activation as the doses required to activate the two systems are often disparate.

In addition to the classical pathogen-derived TLR ligands it has recently become apparent that allergens also interface with TLRs to modulate their signaling [2]. These may be proteinaceous ligands such as the dust mite allergen Der p 2 [3, 4] or the cat dander protein Fel d 1 [5]; or they may constitute chemical allergens such as the metal nickel [6, 7]. The connections of these allergens with disabling conditions such as asthma [8, 9] and contact hypersensitivity has led to an upsurge in research aimed at understanding how they interface with TLRs and how they contribute to the initiation of TLR signaling. In order to understand the connection between allergens and TLR signaling researchers are employing both gene reporter based assays and the stimulation of primary cells such as bone marrow-derived macrophages from mice or primary human antigen presenting cells.

The use of gene reporters is widespread in biology, particularly in studies investigating changes in gene expression, promoter function, signaling pathways, activation or inhibition of receptor signaling, and the effect of transcription factors. Reporter assays have retained their status as a key experimental tool in these systems despite the increased accessibility of array based technology, quantitative reverse transcriptase PCR, and next generation RNA sequencing. This reflects not only the inherent robustness and flexibility of the assays, but also the fact that they don't require complex or highly expensive pieces of equipment. Most reporter assays utilize a dual reporter system in which changes in the expression of two reporter enzymes (such as luciferase or secreted embryonic alkaline phosphatise) are measured. One enzyme is placed under the control of a promoter that will respond to changes in the system of study—this is often nuclear factor kappa B or interferon response factors for TLR signaling pathways. This is the experimental reporter. The other enzyme is placed under the control of a promoter that will be expressed at basal levels in the cell population and serves as an internal control for variation in transfection efficiency and cell death. This is the control promoter. Normalizing the activity measured for the experimental reporter by that measured for the control reporter allows a much more robust and reliable interpretation of the experimental data.

One of the most common dual reporter systems used in cell signaling studies is the Dual-Luciferase Reporter (DLR™) Assay System developed by Promega [10]. This system utilizes two separate luciferases, one from the firefly (*Photinus pyralis*) and the other from the sea pansy *Renilla* (*Renilla reniformis)*. The firefly gene, under the control of a suitable promoter sequence, serves as the experimental reporter and the *Renilla* luciferase, controlled by a constitutively active promoter, acts as the internal control reporter. The activity of both luciferases is measured sequentially, but rap-

idly, as a stabilized signal from the same sample, with the firefly luciferase being measured first. The assay is linear in nature and extremely sensitive with detection thresholds reported to be at the subattomole level [10]. A major advantage of these reporters is the lack of any endogenous signal.

It is often difficult, or time-consuming, to develop reporter systems in primary cells. Consequently, receptor signaling in these systems is often measured through the detection of secreted cytokines such as tumor necrosis factor alpha (TNFα) or suitable members of the interleukin (IL) family. Here we outline the procedure for establishing systems for studying TLR receptor activation by either gene reporter based approaches, or through stimulation of primary cells.

2 Materials

2.1 Plating HEK293 Cells

1. 0.05 % trypsin–EDTA.
2. HEK293 media: DMEM, 10 % fetal calf serum (FCS), 1× penicillin–streptomycin.
3. 1X phosphate buffered saline (PBS): 1 mM potassium phosphate monobasic, 155 mM NaCl, 3 mM sodium phosphate dibasic, pH 7.4.
4. 96-well plate.

2.2 Trypan Blue Staining

1. 70 % Ethanol.
2. Hemocytometer.
3. Trypan Blue.
4. Handheld counter.
5. Light microscope.

2.3 Transfection and Stimulation

1. DNA stocks of required receptor, adaptor and reporter constructs.
2. 150 mM NaCl.
3. 10× TE: 100 mM Tris–HCl, pH 7.5, 10 mM EDTA, pH 8.0.
4. jetPEI® transfection reagent.
5. Ligand stocks for stimulation.
6. 1× PBS (*see* **item 3**, Subheading 2.1).

2.4 Luciferase Quantification

1. 1× Passive Lysis Buffer (Promega).
2. Dual Luciferase Assay Kit (Promega).
3. Luminometer.

2.5 Bone Marrow-Derived Macrophage Culture

1. Basic BMM medium: RPMI 1640, 10 % FCS, 5 % Horse serum, 2 mM L-Glutamine, 0.05 mM 2-Mercaptoethanol, 10 μg/ml gentamycin, 1 mM sodium pyruvate (55 mg in 500 ml RPMI1640—dissolve the powder in 2–3 ml of medium and filter-sterilize).
2. Complete BMM medium: 80 % basic BMM medium, 20 % conditioned medium from L929 cells (LCM).
3. LCM: Culture supernatant from confluent L929 cells (fibroblasts producing M-CSF) grown in RPMI 1640 containing 10 % FCS and 2 mM L-glutamine. Medium is filter sterilized (pre-absorb filter with FCS) and stored at –20 °C in 40 – 50 ml aliquots. L929 cells should be initially seeded at approximately 20 % confluent.
4. 0.02 % EDTA
5. Cell scraper
6. 1× PBS (*see* **item 3**, Subheading 2.1).

2.6 Stimulation of Bone Marrow-Derived Macrophages

1. Appropriate stocks of ligands for stimulation.
2. 96-well plate.
3. ELISA kits: TNFα.

3 Methods

3.1 Plating HEK293 Cells

1. Detach HEK293 cells from the surface of the flask or dish used for routine subculture (*see* **Note 1**) by incubation with pre-warmed 0.05 % trypsin–EDTA for 5 min at 37 °C.
2. Add an equal volume of pre-warmed HEK293 media, gently resuspend cells and transfer to an appropriate tube (*see* **Note 2**).
3. Count the number of viable cells using either an automated cell counter or a hemocytometer with Trypan Blue staining (*see* Subheading 3.2) (*see* **Note 3**).
4. Centrifuge the cells at 1200×*g* for 5 min at room temperature.
5. Gently resuspend cells in 1× PBS (pre-warmed) then centrifuge at 1200×*g* for 5 min at room temperature.
6. Gently resuspend cells in pre-warmed HEK293 media at a density of 1.5×10^5/ml.
7. Seed plates at the densities outlined in Table 1 to ensure an appropriate cell population for stimulation experiments 2 days later (*see* **Note 4**).

3.2 Trypan Blue Staining

1. Clean the hemocytometer with 70 % ethanol, moisten the shoulders slightly, and gently apply the coverslip.
2. Gently agitate the cell suspension (**step 3**, Subheading 3.1) and remove 100 μl into a 1.5 ml microcentrifuge tube.
3. Add 100 μl of Trypan Blue to the cells in the microcentrifuge tube and gently pipette up and down (*see* **Note 5**).
4. Carefully transfer some of the Trypan Blue stained cells to the hemocytometer by allowing it to be drawn into the chamber through capillary action.
5. Place the hemocytometer on a light microscope and focus using the 10× objective.
6. Locate the 16 squares in one corner of the grid lines.
7. Count the number of live cells (not stained by Trypan Blue) positioned either fully within these 16 squares, or on the right-hand or bottom boundary lines.
8. Repeat **step 7** for the other three corner groups of 16 squares (*see* **Note 6**).
9. Take the average number of cells per 16 square grid and multiply by 2 (the Trypan Blue dilution factor). Then multiply this number by 10^4. This will produce the cell number per ml of initial suspension.
10. Clean the hemocytometer with 70 % ethanol.

3.3 Transfection and Stimulation

1. Plate the required number of cells for the experiment to be performed at the seeding densities described in Subheading 3.1 and Table 1.
2. Prepare DNA master mixes as required (*see* **Note 7**). For the study of human TLR4 signaling we use the following quantities of DNA to give a total of 1 μg DNA per ten wells: 865 ng pcDNA3, 10 ng pcDNA3:hTLR4, 5 ng pcDNA3:hCD14, 19 ng pEFIRES, 1 ng pEFIRES:hMD-2, 50 ng pNFκB-luc, and 50 ng phRG-TK (*see* **Note 8**).

Table 1
Volume of media and total number of HEK cells for transient transfection assay

Plate	Volume of media	Number of cells
96-well	200 μl	3×10^4
24-well	1 ml	1.5×10^5
6-well	3 ml	4.5×10^5

3. Add 5 μl of 10× TE to the DNA master mix and make up to a total volume of 50 μl with 150 mM NaCl.
4. Prepare 50 μl solution of jetPEI® transfection reagent by adding 2 μl jetPEI to 48 μl 150 mM NaCl to give 2 μl:1 μg ratio of transfection reagent to DNA (*see* **Note 9**).
5. Add the 50 μl jetPEI® solution to the 50 μl DNA solution (*see* **Note 10**).
6. Vortex briefly to mix and incubate at room temperature for 30 min.
7. Add 900 μl pre-warmed HEK293 medium with antibiotics to the jetPEI®/DNA mix.
8. Add 100 μl of jetPEI®/DNA/medium mix to each well and incubate at 37 °C and 5 % CO_2 for 48 h or until stimulated.
9. After 48 h, stimulate cells for 6–8 h with an appropriate ligand (*see* **Note 11**).
10. Following cell stimulation, carefully remove the media from the wells and gently wash the cells with 100 μl 1× PBS/well.
11. Remove 1× PBS and add 50 μl 1× Passive Lysis Buffer (*see* **Note 12**).
12. Incubate at room temperature for 15 min with gentle rocking.
13. Store the plate at −80 °C freezer until ready for reading of the luminescence (*see* **Note 13**).

3.4 Luciferase Quantification

1. Measurement of receptor activation is achieved by dual detection of Renilla and luciferase activity (*see* **Note 14**).
2. Thaw assay plates at room temperature.
3. Set autoinjectors 1 and 2 on the plate reader to dispense 100 μl of LARII® and Stop & Glo® reagent respectively.
4. Scrape each well of the thawed assay plate then transfer 10 μl of cell lysate to each well of a white polystyrene flat bottom 96-well plate.
5. Read plate on the luminometer using a 1–2s delay and a 5–10s read time.
6. Check the raw luciferase (LARII®) and Renilla readings (Stop & Glo®). Discard low Renilla values as these indicate cell death (<2000 on our plate reader (Fluostar OMEGA; BMG Laboratories)).
7. Divide the luciferase reading (LARII®) by the Renilla reading (Stop & Glo®) to get the relative luciferase value (Fig. 1).

3.5 Bone Marrow-Derived Macrophage Culture

1. Primary BMDM should be grown for 3 days at 37 °C and 5 % CO_2 in a total volume of 10 ml of complete media in Petri dishes.

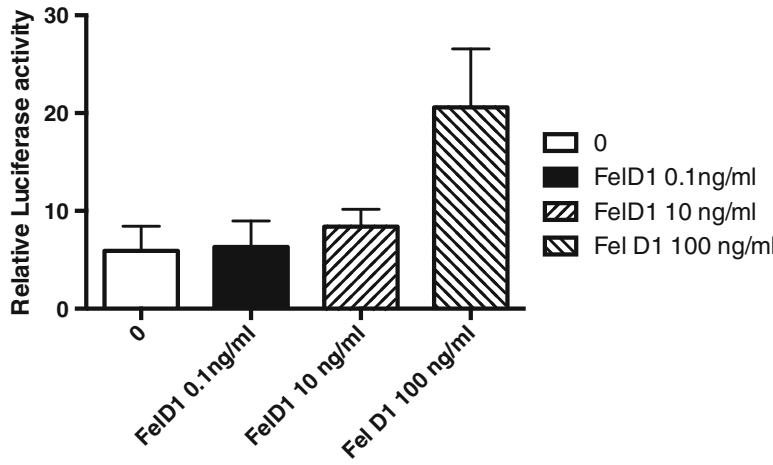

Fig. 1 A graph of the relative luciferase activity of FelD1 after addition to HEK cells transfected with TLR4, MD2, CD14, p-NfkB-Luc, and pHR-Renilla

2. On day 4 add 10 ml of pre-warmed complete medium to each BMDM-containing petri dish and incubate for an additional 2–3 days at 37 °C and 5 % CO_2.
3. On Day 6 or 7 carefully remove all medium and gently wash the cells 2–3 times using 5 ml pre-warmed basic BMM medium (*see* **Note 15**). Remove the media after each wash.
4. Add 10 ml of pre-warmed complete BMM medium.
5. Continue to incubate cells at 37 °C and 5 % CO_2.
6. Change the culture medium every 2–3 days until the BMDMs are confluent (*see* **Note 16**). At this point detach the adherent cells by gentle scraping or with EDTA and split the cells 1:3 into pre-warmed complete BMM medium in fresh culture dishes.
7. If detaching the cells using EDTA the method is as follows:
   (a) Remove medium.
   (b) Add 5 ml of ice-cold 0.02 % EDTA solution.
   (c) When the cells start to detach gently pipette over the surface and collect into a 15-ml tube.
   (d) Centrifuge at 300 × *g* for 5 min with gentle braking.
   (e) Remove supernatant and resuspend the cells in 6 ml of BMM medium supplemented with LCM and gentamycin.
   (f) Add 8 ml of fresh BMM medium supplemented with LCM and gentamycin to each of three new petri dishes.
   (g) Add 2 ml of resuspended BMDMs to each petri dish.
   (h) Incubate at 37 °C and 5 % CO_2.

8. If using the scraping method the method is as follows:
   (a) Remove medium.
   (b) Add 6 ml of fresh complete BMM medium.
   (c) Gently scrape cells off the surface of the petri dish (*see* **Note 17**).
   (d) Place 8 ml of fresh complete BMM medium.
   (e) Add 2 ml of resuspended BMDMs to each petri dish.
   (f) Incubate at 37 °C and 5 % CO_2.

3.6 Stimulation of Bone Marrow-Derived Macrophages

1. Seed each well of 96-well plates with 2×10^5 cells (200 μl of 10^7 cells/ml in antibiotic-free medium) one night before the experiment. Incubate at 37 °C and 5 % CO_2 in complete BMM medium.
2. Add 20 μl of ligand to each well at an appropriate dilution (*see* **Note 18**). Use 20 μl 1× PBS as a negative control ligand.
3. Incubate at 37 °C and 5 % CO_2 for 2 h.
4. Transfer 50 μl of culture supernatant to a fresh 96-well plate and store this at −80 °C for TNFα detection (*see* **Note 19**).
5. Remove rest of the culture medium and add 200 μl of ligand free complete BMM medium.
6. After 4–6 h (7–9 h after addition of stimulant), transfer 50 μl of culture supernatant to a fresh 96-well plate and store this at −80 °C for TNFα detection (*see* **Note 20**).

4 Notes

1. Cell passage number should be similar for experiments that are to be compared with one another. As the passage number of HEK293 cells increases the cells often become less responsive to stimulation. In general aim to use cells with a passage number less than 30.
2. For a T75-flask use 3–5 ml of 0.25 % trypsin–EDTA and resuspend cells using cell culture media to a total volume of approximately 10 ml prior to transfer to a 15 ml Falcon tube.
3. Accurate determination of cell number is crucial for accurate and reproducible cell seeding and experimental reproducibility.
4. If seeding for experimentation 3 days later (i.e., seeding on a Friday, begin experiment on a Monday) then use 1.5×10^4 cells/well (200 μl 7.5×10^4 ml^{-1}) for a 96-well plate.
5. Do not over pipette or vigorously mix the cells as this will lead to cell lysis.

6. If cell viability data is also wanted then additionally count the number of dead cells that are Trypan Blue positive.
7. The following plasmid amounts are for 96-well plates, other sizes of culture vessel will need scaling appropriately.
8. The precise plasmids will depend on the reporter system being used and the signaling pathway being studied. The example here is for dual luciferase reporters of TLR4 signaling. Total DNA concentration is bulked with empty vector plasmids, e.g., pcDNA3 and pEFIRES. To determine whether allergens activate other TLRs we use 10X the DNA concentration of the receptor plasmid because TLR4 shows high levels of basal activity when over expressed.
9. Manufacturers recommend trying two ratios of jetPEI to DNA. Firstly, 2 μl jetPEI®–1 μg DNA and secondly 3.2 μl jetPEI®–1 μg DNA. For a 2 μl–1 μg ratio add 2 μl jetPEI to 48 μl NaCl; and for a 3.2 μl–1 μg ratio add 3.2 μl jetPEI to 46.8 μl NaCl. We have found no difference between the two ratios.
10. The jetPEI® solution must be added to the DNA solution, not the other way round.
11. Stimulating ligands should be prepared in media containing 0.1 % FCS. Whilst the precise composition and concentration of these stimuli will depend on the system being studied examples for the stimulation and/or study of TLR4 signaling include. Whenever assay conditions are changed, including the use of different cells or plasmids, a dose response for the ligands should be performed to ensure use of the optimal concentration. For HEK293 based reporter assays we have previously used the following concentrations of stimulatory ligands [5, 11]: Lipoteichoic acid (TLR2) 10 ng/ml; Lipid A (TLR4) 10-100 ng/ml; Lipid IVa (TLR4) 1 μg/ml; LPS (TLR4) 1–100 ng/ml; Fel d 1 (TLR4) 0.1–100 ng/ml; Flagellin (TLR5) 5–50 ng/ml.
12. Prepare from stock diluted in 1× PBS. The Passive Lysis Buffer is formulated to minimize background auto-luminescence.
13. Ensure that the 96-well plate containing the samples for analysis is suitable for use in luminescence studies. A freeze thaw step enhances the efficiency of cell lysis.
14. We use the Dual Luciferase Assay from Promega. Best results are obtained if the samples are equilibrated to room temperature.
15. This will remove non-adherent cells and transiently attached cells.
16. BMM cultures may not become as full in petri dishes as macrophage cell-lines. Watch the cultures to see if cells start to detach from the plastic.

17. Gently pipette cell suspension up and down a few times to reduce clumping. Do not pipette over-vigorously and avoid any foaming.
18. The concentration of ligand used will vary with experimental setup and nature of stimuli. As examples we have used: lipoteichoic acid (TLR2) 50 ng/ml; PAM3CSK4 (TLR2) 1 ng/ml; LPS (TLR4) 0.05–0.5 ng/ml; Fel d 1 (TLR4) 25–100 μg/ml. If infecting with bacterial suspensions (i.e., *Salmonella*) then 20 μl of the appropriate concentration of bacteria (resuspended in 1× PBS) to provide the desired multiplicity of infection should be added to each well containing macrophages.
19. If other cytokines are to be measured then remove suitable volumes of supernatant for downstream analysis by ELISA or other suitable approach. Detection of TNFα works well as a positive control.
20. Remove additional volumes of supernatant as required for cytokine targets. 200 μl fresh medium can be added and incubation continued for the desired period of analysis.

References

1. Gay NJ, Symmons MF, Gangloff M, Bryant CE (2014) Assembly and localization of Toll-like receptor signalling complexes. Nat Rev Immunol 14:546–558. doi:10.1038/nri3713
2. McFadden JP, Puangpet P, Basketter DA et al (2013) Why does allergic contact dermatitis exist? Br J Dermatol 168:692–699. doi:10.1111/bjd.12145
3. Chiou Y-L, Lin C-Y (2009) Der p2 activates airway smooth muscle cells in a TLR2/MyD88-dependent manner to induce an inflammatory response. J Cell Physiol 220:311–318. doi:10.1002/jcp.21764
4. Trompette A, Divanovic S, Visintin A et al (2009) Allergenicity resulting from functional mimicry of a Toll-like receptor complex protein. Nature 457:585–588. doi:10.1038/nature07548
5. Herre J, Grönlund H, Brooks H et al (2013) Allergens as immunomodulatory proteins: the cat Dander protein Fel d 1 enhances TLR activation by lipid ligands. J Immunol 191:1529–1535. doi:10.4049/jimmunol.1300284
6. Raghavan B, Martin SF, Esser PR et al (2012) Metal allergens nickel and cobalt facilitate TLR4 homodimerization independently of MD2. EMBO Rep 13:1109–1115. doi:10.1038/embor.2012.155
7. Schmidt M, Raghavan B, Müller V et al (2010) Crucial role for human Toll-like receptor 4 in the development of contact allergy to nickel. Nat Immunol 11:814–819. doi:10.1038/ni.1919
8. Hammad H, Chieppa M, Perros F et al (2009) House dust mite allergen induces asthma via Toll-like receptor 4 triggering of airway structural cells. Nat Med 15:410–416. doi:10.1038/nm.1946
9. Perros F, Lambrecht BN, Hammad H (2011) TLR4 signalling in pulmonary stromal cells is critical for inflammation and immunity in the airways. Respir Res 12:125. doi:10.1186/1465-9921-12-125
10. Sherf BA, Navarro SL, Hannah RR, Wood KV (1996) Dual-Luciferase® reporter assay: an advanced co-reporter technology integrating firefly and Renilla luciferase assays. Promega Notes 57:2–22
11. Walsh C, Gangloff M, Monie T et al (2008) Elucidation of the MD-2/TLR4 interface required for signaling by lipid IVa. J Immunol 181:1245–1254

Chapter 22

Investigating the Role of Toll-Like Receptors in Models of Arthritis

Anna M. Piccinini, Lynn Williams, Fiona E. McCann, and Kim S. Midwood

Abstract

Rheumatoid arthritis (RA) is a chronic autoimmune disease characterized by persistent synovial inflammation leading to tissue destruction and progressive loss of joint function. Here we describe two methods that can be used to assess the contribution of toll-like receptors (TLRs), and their potential ligands, to RA pathogenesis. We focus on the antigen-induced model of murine arthritis and human synovial tissue explant models. Both enable detection of TLR, and TLR ligand, expression, as well as investigation of the effect of inhibition of these molecules. Each offers a unique insight into disease; with murine models allowing kinetic analysis in live animals and explant models allowing examination of inflamed human tissue, which together can help us to dissect the role of TLRs in the onset and progression of RA.

Key words Toll-like receptor, Endogenous ligands, DAMPs, Sterile inflammation, Antigen-induced arthritis, Human synovial tissue, Rheumatoid arthritis

1 Introduction

The hallmarks of rheumatoid arthritis (RA) include synovial inflammation and destruction of joint cartilage and bone; mediated by persistent production of pro-inflammatory cytokines and matrix metalloproteinases (MMPs). Compelling evidence supports a role for TLRs in contributing to the aberrant inflammatory response observed in RA. On one hand, ex vivo and in vitro studies using human tissue and cells have shown expression and functionality of specific TLRs in RA joints. On the other hand, many in vivo experimental models of arthritis have demonstrated TLR ligand requirement for disease induction as well as disease amelioration in animals lacking specific TLRs. In particular, immunohistochemical and immunofluorescence analysis of synovial tissue obtained from RA patients at the time of joint replacement, and FACS and real-time PCR analysis of cells isolated from this tissue, revealed expression of TLRs 2–4 and 7–9 compared to normal or osteoarthritic synovium [1–5]. Moreover, ELISA-based measurement of levels of

Claire E. McCoy (ed.), *Toll-Like Receptors: Practice and Methods*, Methods in Molecular Biology, vol. 1390,
DOI 10.1007/978-1-4939-3335-8_22,

cytokines and metalloproteinases produced by these cells in culture showed TLRs 2–4 and 7–9 to be responsive to ligand stimulation [1, 5–7]. Both intact tissue explants from RA synovia, and mixed cell population cocultures isolated from RA tissue synthesize high levels of inflammatory mediators. These models have been used to show that antibody blockade of TLR2 [8] and TLR4 [9], chemical inhibition of endosomal TLRs, specifically TLR8 [5], and adenoviral transfection with dominant-negative forms of TLR adapter proteins MyD88 and Mal/TIRAP [7] can reduce the spontaneous production of cytokines. A range of murine models of arthritis, including collagen-induced arthritis (CIA), antigen-induced arthritis (AIA), IL1-receptor antagonist knockout model, serum transfer model, and microbial TLR ligand (e.g., LPS, bacterial DNA, streptococcal cell wall, and zymosan)-induced arthritis, have been used to examine TLR contribution to disease in vivo; typically using mice with targeted deletions in specific TLRs, for example TLR2, TLR4, TLR3, TLR7, and TLR9 [10–15]. Moreover, inhibitors of TLRs have shown therapeutic benefit in some of these models, for example, TLR4 [15, 16] and TLR7, 8, and 9 [17–19]. Together these data indicate that the activation of a number of TLRs drives persistent inflammation in RA (reviewed in Refs. [20, 21]).

These models have also been used to try to answer the question of which ligands drive TLR activation in disease. In particular, activation of TLRs by endogenous molecules generated upon tissue damage, damage-associated molecular patterns (DAMPs), is of interest in this autoimmune disease. The destructive environment of the RA joint harbors high levels of DAMPs, including intracellular molecules released during necrosis (e.g., HMGB1, nucleic acids) and extracellular matrix (ECM) molecules that are specifically upregulated upon injury (e.g., tenascin-C and biglycan) or degraded following tissue damage (e.g., low molecular weight hyaluronan) [22, 23]. Some of these ligands have been shown to enhance spontaneous cytokine synthesis upon addition to human RA cell populations, as well as being essential for the progression of disease in murine models of RA, as in the case of tenascin-C [24]. For other ligands, their inhibition in vivo during experimental arthritis, as shown for HMGB1, HSP90, or neutrophil elastase [25–27], ameliorates disease. Moreover, a number of these activators were shown to be arthritogenic upon injection into mice, and for many this process was dependent on expression of TLR4 [24, 28–30]. Together these data show that a wide variety of TLR ligands likely contribute to inflammation in the RA joint (reviewed in Ref. [22]).

In this chapter we discuss two different techniques to examine TLR and TLR ligand involvement in RA. One murine model that has emerged as being useful for analysis of TLR driven inflammation

in vivo is antigen induced arthritis (AIA). Originally developed in rabbits by Dumonde et al. [31], the AIA model was established later in the mouse by Brackertz et al. [32], and characterized and optimized by van den Berg et al. [33, 34]. We describe here a modified protocol for AIA induction, and detail evaluation of arthritis by histological analysis, relative quantification of pro-inflammatory cytokine gene expression by real-time PCR and assessment of DAMP expression by western blot analysis. We also describe how to administer TLR ligands to mice joints to assess their arthritogenic potential.

Both AIA and the more widely used collagen-induced arthritis (CIA) mimic disease symptoms seen in human RA, for example infiltration of inflammatory cells in the synovium, synovial hyperplasia, immune complex deposition in the cartilage, and progressive cartilage and bone destruction [32, 33]. However, where CIA manifests as a systemic polyarthritic disease, AIA is a more localized, monoarthritic disease. The induction of arthritis exclusively in the injected joint, does allow comparison of arthritic changes with a normal contralateral joint from the same mouse. Moreover AIA has other advantages including (1) it can be induced in any mouse strain [32], (2) disease induction is not affected by the mouse sex [32]; (3) 100 % disease incidence; (4) onset of disease occurs at a defined time, facilitating kinetic studies; (5) disease severity can be controlled by the dose of intra-articularly injected antigen; (6) episodes of exacerbation and remission occurring in RA patients can be mimicked by controlled rechallenge with antigen. However, both animal models of RA progress significantly more rapidly than the human disease and are characterized mostly by acute inflammatory responses, necessitating complementary approaches to examine some aspects of disease.

Ex vivo models of the human disease that consists of the culture of cells from RA synovial membranes from patients undergoing joint replacement surgery can be helpful in obtaining a picture of late stage human disease. Originally described by Brennan et al. [35], this system led to the discovery that arthritic joints have elevated levels of pro-inflammatory cytokines [36], and provided the rationale for testing TNF-α blockade in RA [37]. Here, we provide a detailed description of the protocol to isolate, phenotype and culture RA membrane cells, which represent a mixed population of all synovial cell types that spontaneously produce high amounts of pro-inflammatory mediators. Furthermore, we describe the protocol for TLR activation, inhibition and expression as well as cytokine level quantification. A major advantage of this model is that the cells continue to release cytokines in short term culture (~up to 3 days), presenting an opportunity to study pathological processes that drive inflammation and allowing the study of disease intervention and efficacy of novel therapeutics. Two prominent

disadvantages are that the nature of this model requires disruption of intact tissue and therefore certain important cell contact dependant processes. Secondly, not all cell populations from the intact synovium are fully represented following dissociation (e.g., neutrophils and endothelial cells). The current protocol may be modified to favor retention of additional subsets.

2 Materials

2.1 Induction of Arthritis

2.1.1 Antigen-Induced Arthritis (AIA)

1. Inbred mice strains of relevant phenotypes, including single TLR and DAMP knockout mice, 10–12 weeks of age, housed under conditions approved by the European Directive 2010/63/EU and the institutional health committee, including regular night-day cycling, 21 °C, individual cage ventilation and free access to autoclaved bedding, food, and water.
2. Methylated bovine serum albumin (mBSA). Store at 4 °C.
3. Freund's complete adjuvant (FCA). Store at 4 °C.
4. Concentrated 10× phosphate buffered saline (PBS; VWR). Store at room temperature.
5. 0.20 μm syringe filters.
6. Hypnorm (VetaPharma Ltd, Leeds, UK). Store at room temperature.
7. Sterile water for injections. Store at room temperature.
8. Syringes (10 and 1 ml).
9. Sterile Microlance needles (27 G × ½ in. and 23 G × 1 in.) for intraperitoneal and subcutaneous injections, respectively.
10. 0.3 ml MicroFine demi insulin syringes.
11. 30 G × 8 mm needles for intra-articular injections.
12. Electric clippers.

2.1.2 TLR-Induced Arthritis

1. Inbred mice strains of relevant phenotypes, 10–12 weeks of age (*see* Subheading 2.1.1., **item 1**).
2. Recombinant DAMP (*see* Table 1) with levels of LPS < 10 pg/ml. Store at −80 °C.
3. Limulus Amebocyte Lysate (LAL) assay QCL-1000™ (Lonza), including lyophilized lysate prepared from the circulating amebocytes of the horseshoe crab *Limulus Polyphemus*, E. coli 0111:B4 endotoxin, chromogenic substrate and LAL reagent water. Store at 4 °C.
4. Concentrated 10× phosphate buffered saline (PBS; VWR). Store at room temperature.

Table 1
DAMPs administered intra-articularly

DAMP	Dose	Effect	Reference
Tenascin-C (FBG domain)	1 μg	Induced TLR4-dependent joint inflammation and tissue erosion	[24]
FNEDA	10 μg	Induced TLR4-dependent transient ankle swelling, cytokine synthesis, and synovial inflammation	[28]
HMGB1	5 μg	Induced synovial inflammation and some pannus formation	[29]
S100A8	5 μg	Induced minor synovial inflammation and upregulated mRNA levels of activating FcγRI and FcγRIV in the synovium	[30]

FBG fibrinogen-like, *FNEDA* fibronectin extra domain A

5. Hypnorm (VetaPharma Ltd, Leeds, UK). Store at room temperature.
6. Sterile water for injections. Store at room temperature.
7. 1 ml syringes.
8. 27 G × ½ in. sterile Microlance needles for intraperitoneal injections.
9. 0.3 ml MicroFine demi insulin syringes.
10. 30 G × 8 mm needles for intra-articular injections.

2.2 Immunohistochemistry

1. Sharp scissors.
2. Fixation solution for freshly isolated knee joints: 10 % (vol/vol) neutral buffered formalin.
3. Decalcification of knee joints: 10 % EDTA (Sigma-Aldrich) in PBS.
4. Paraffin wax processing: graded series of ethanol 70, 95 and 100 %, xylene (certified ACS; Fisher Scientific) and wax (Paraplast X-tra, Sigma-Aldrich). Ethanol and xylene are stored with flammables at room temperature.
5. Superfrost™ Plus Slides (Menzel-Gläser, Braunschweig, Germany).
6. Dewaxing of paraffin sections: xylene and ethanol 100 % (*see* **item 4**).
7. Hematoxylin and eosin (H and E) staining: hematoxylin (Sigma-Aldrich); 0.3 % acid alcohol (combine 997 ml ethanol 70 % with 3 ml of 1 M HCl solution); ammonia water (add 1.6 ml of 1 M NH_4OH to 600 ml of tap water) and eosin (Sigma-Aldrich).
8. Safranin-O staining: hematoxylin; 0.3 % acid alcohol (*see* **item 7**); ammonia water (*see* **item 7**); 0.1 % fast green FCF

(Sigma-Aldrich); 1 % acetic acid; 0.1 % safranin-O (Sigma-Aldrich), and 0.1 % fast green (Fisher Scientific).

9. Dehydration of tissue sections: ethanol 100 % and xylene (*see* **item 4**).
10. DPX mountant (Sigma-Aldrich). Store at room temperature.
11. Coverslips 20 × 40 mm.

2.3 Real-Time PCR

1. Sharp scissors.
2. Liquid nitrogen (use an appropriate, non-sealed, liquid nitrogen container, wear proper safety gear and use liquid nitrogen in a well-ventilated area).
3. BioPulverizer (BioSpec Products, USA; *see* Fig. 1).
4. RLT buffer (Qiagen).
5. QIAshredder (Qiagen).
6. RNeasy Mini kit (Qiagen).
7. AffinityScript™ Multiple Temperature cDNA synthesis kit (Stratagene), includes AffinityScript™ multiple temperature reverse transcriptase, 10× AffinityScript™ RT buffer, RNase block ribonuclease inhibitor (40 U/μl), oligo(dT) primer (0.5 μg/μl), dNTPs (100 mM; 25 mM each dNTP), and RNase-free water.
8. Real-Time PCR system (Applied Biosystems Viia 7™ or Rotor-Gene 6000, Corbett Life Science, now Qiagen).

Fig. 1 Appearance of BioPulverizer (BioSpec Products, USA) used for pulverizing knee joints for Real-Time PCR and western blot analysis

9. TaqMan primers and probes: mouse TNF-α (dye: FAM/TAMRA; Mm99999068_m1; Applied Biosystems); mouse CXCL1 (dye: FAM/TAMRA; Mm00433859_m1; Applied Biosystems); and mouse HPRT1 (dye: FAM/TAMRA; Mm00446968_m1; Applied Biosystems). Store at –20 °C.
10. TaqMan PCR master mix: 2× reaction buffer containing AmpliTaq Gold® DNA polymerase, uracil-DNA glycosylase, dTNPs with dUTP, ROX™ passive reference, and AmpErase® UNG (Applied Biosystems). Store at –20 °C.
11. RNase-free water.
12. 384-well MicroAmp® Optical microplates (Applied Biosystems) or 0.1 ml strip tubes and caps (Qiagen).

2.4 Western Blot Analysis

2.4.1 SDS-PAGE

1. T-PER tissue protein extraction reagent (Thermo Scientific). Store at room temperature.
2. Protease inhibitor cocktail (Sigma-Aldrich). Store at –20 °C.
3. Ultrasonic processor (Vibra-Cell VCX130, Sonics & Materials, USA).
4. Resolving gel buffer: 1.5 M Tris–HCl, pH 8.8.
5. Stacking gel buffer: 1 M Tris–HCl, pH 6.8.
6. Thirty per cent (v/v) acrylamide–bis solution (37.5:1). Acrylamide is a potent neurotoxin and gloves should be worn at all times.
7. *N*,*N*,*N*′,*N*′-tetramethyl-ethylenediamine (TEMED, Sigma-Aldrich).
8. Ammonium persulfate: make a 10 % solution in water and store in aliquots at –20 °C.
9. Water-saturated butanol: mix equal volumes of water and isobutanol in a glass container and shake vigorously. Allow to separate into upper (isobutanol) and lower (water) phases overnight. Use the upper top layer. Store at room temperature.
10. Running buffer (10×): 250 mM Tris, 1.92 M glycine, and 10 % SDS. Confirm pH is 8.3 but do not alter due to the presence of SDS. Store at room temperature.
11. Modified Laemmli buffer (5×): 250 mM Tris–HCl, pH 8, 10 % SDS, 50 % glycerol, 0.005 % bromophenol blue, and 25 % β-mercaptoethanol.
12. Pre-stained molecular weight marker (broad range molecular weight markers, New England Biolabs). Store in aliquots at –20 °C.

2.4.2 Immunoblotting

1. Transfer buffer (10×): 250 mM Tris–HCl, 1.92 M glycine. Before transfer, dilute to 1× with deionized water and add methanol (stored with flammables at room temperature) to 20 %. The buffer may be stored at 4 °C.
2. Nitrocellulose membrane (GE Healthcare).
3. Concentrated 10× phosphate buffered saline (PBS; VWR). Store at room temperature.
4. PBS containing Tween 20 (PBS-T). Dilute a 10× solution of PBS to 1× with deionized water and add Tween 20 to a final concentration of 0.1 % (v/v).
5. Blocking buffer: 5 % (w/v) bovine serum albumin (BSA) in PBS-T.
6. Antibody diluent: 2 % BSA in PBS-T.
7. Primary antibody raised against the protein of interest. For instance, here we use anti-tenascin-C rat monoclonal (MTn-12) antibody (Sigma-Aldrich).
8. Anti-actin goat polyclonal antibody (Santa Cruz Biotechnology).
9. Horseradish peroxidase conjugated anti-rat IgG secondary antibody (Sigma-Aldrich).
10. Horseradish peroxidase conjugated anti-goat IgG secondary antibody (R&D Systems).
11. Enhanced chemiluminescent (ECL) substrate (immediately before use, combine solution 1 and solution 2 [1:1], GE Healthcare). Store at 4 °C.
12. Stripping buffer: Re-Blot Plus Strong 10× solution (Chemicon). Dilute to 1× with deionized water.
13. Fuji Medical X-ray film (FUJIFILM).

2.5 Synovial Tissue Preparation

RA synovial membrane tissue was obtained from patients who fulfilled the American College of Rheumatology criteria for RA [38] and were used with the informed consent of the patients. Ethics approval was obtained from the London Riverside Research Ethics Committee (REC reference nos. 1752 and 07/H0706/81). RA synovial membrane tissue was collected at the time of joint replacement surgery/synovectomy preparation from Elective Orthopaedic Centre, Epsom and St Helier University Hospitals, UK, Royal United Hospital Bath and Royal Free Hospital NHS Trust, London, UK (*see* **Note 1**).

1. Collagenase NB1 Premium Grade and neutral protease (SERVA, AMS Biotechnology Europe Ltd., Abingdon, UK). Store at 4 °C.

2. Liberase TL Research Grade (Roche Diagnostics, Mannheim, Germany). Store at –20 °C.
3. DNase I (Roche Diagnostics, Mannheim, Germany). Store at 4 °C.
4. RPMI 1640 (Gibco, Life Technologies, Paisley, UK) supplemented with 10 % heat-inactivated fetal calf serum (HIFCS) (Labtech, Uckfield, UK) and 1 % penicillin–streptomycin (Lonza, Verviers, Belgium).
5. Double layer Cell Microsieves 200 μm pore (Fisher Scientific, Loughborough, UK), placed over a small beaker, fixed in place with autoclave tape, then autoclaved to sterilize.
6. CaN_2O_6 (Sigma-Aldrich).
7. Red Blood Cell Lysis buffer (Sigma-Aldrich).

2.6 Phenotype Analysis

1. Cell fixation buffer: cytofix (Becton Dickinson, Oxford, UK).
2. Precooled washing buffer: PBS (Gibco, Life Technologies, Paisley, UK) supplemented with 2 % FBS (Labtech, Uckfield, UK) and 0.01 % NaN_3 (Sigma-Aldrich).
3. Antibodies: all Becton Dickinson unless specified; CD14 APC and CD56 PE(ebioscience), NK p46 PE, HLA-DR PE, CD90 FITC, CD15 Cy7, CD20 FITC, CD3 APC, CD4 APC-H7, CD8 PE Cy5, CD25 v450, CD11c V450, CD45 PER-CP, and CD163 APC (BioLegend, London, UK).
4. Viability assay: LIVE/DEAD fixable Aqua dead cell kit (Life Technologies, Paisley, UK).

2.7 Synovial Cell Culture

1. Ligands: TLR2/6 agonist, FSL-1 (10 ng/ml); TLR 3 agonist, Polyinosinic-polycytidylic acid (poly(I:C)) high molecular weight (HMW) (20 ng/ml); TLR5 agonist, flagellin (10 ng/ml); TLR7 agonist, R847/ Imiquimod (1 μg/ml); TLR7/8 agonist, R848 (1 μg/ml) and TLR9 agonist, ssDNA / LyoVec (50 ng/ml) (Invivogen, San Diego, CA, USA). Store at –20 °C.
2. TLR4 agonist: ultrapure LPS derived from *E. coli* (10 ng/ml) (Alexis, Enzo Life Sciences, Exeter, UK). Store at 4 °C.
3. RPMI 1640 (Gibco, Life Technologies, Paisley, UK) supplemented with 10 % heat-inactivated FCS (Labtech, Uckfield, UK) and 1 % penicillin–streptomycin (Lonza, Verviers, Belgium).
4. Costar 96-well tissue culture plate (Corning, NY, USA).
5. AdEasy Adenoviral Vector Systems (Agilent Technologies, Santa Clara, CA, USA).

2.8 Cytokine Analysis

2.8.1 ELISA

1. Costar 96-well EIA/RIA plate and plate sealer (Corning, NY, USA).
2. Antibodies: purified mouse anti-human TNF-α; biotinylated mouse anti-human TNF-α; purified mouse anti-human IL-8 and biotinylated mouse anti-human IL-8 (BD Biosciences, Becton Dickinson, Oxford, UK). Store at 4 °C.
3. Recombinant TNF-α and IL-8 (Peprotech, London, UK). Store at −20 °C.
4. Bovine serum albumin.
5. Tween 20.
6. Stop solution: 0.128 M sulfuric acid.
7. 10× PBS (Sigma-Aldrich).
8. Streptavidin–HRP (R&D Systems, Oxon UK).
9. TMB substrate (KPL Gaithersburg, MD, USA).
10. Multiscan Ascent microplate reader (Thermo Scientific).

2.8.2 Mesoscale Discovery (MSD) Platform

1. MMP 3 plex plate (MMP1, MMP3, MMP9) custom plates as per customer design. All reagents supplied with kit.

3 Methods

3.1 Induction of Arthritis

3.1.1 Antigen-Induced Arthritis (AIA)

1. Preparation of antigen. Transfer 10 ml of FCA in a small, sterile plastic vial. In a separate vial, make a mBSA stock solution by dissolving 20 mg mBSA in 9 ml of sterile water and then add 1 ml of 10× PBS to obtain a 10 ml of a 2 mg/ml mBSA solution. Aspirate this solution with a 10 ml syringe, attach a 23 G × 1 in. needle on the syringe, press the syringe plunger to inject with force the solution in the 10 ml of CFA previously prepared. Emulsify this white oil–water emulsion by repeatedly aspirating and flashing with a 1 ml syringe to homogeneity or until the emulsion is thick enough to remain in the vessel when inverted (*see* **Note 2**).
2. Sedation of mice. Dilute Hypnorm 1:10 (vol:vol) in sterile water for injections. Sedate 10- to 12-week old mice with an intraperitoneal (i.p.) injection of 150–200 μl diluted Hypnorm using a 27 G × ½ in. needle (*see* **Notes 3** and **4**).
3. Immunization of mice (*see* **Note 5**). Gently shave the rumps of the mice with electric clippers to completely remove the fur at the base of the tail. Inject 100 μl in total of the emulsion intradermally at two sites at the base of the tail using a 1 ml syringe with a 23 G × 1 in. needle (*see* **Notes 6** and **7**).
4. Induction of arthritis. Seven days later, mice are sedated (*see* **step 2**) and unilateral arthritis is induced by intra-articular

injection of mBSA in PBS into the right knee joint. Prepare a 40 mg/ml mBSA stock solution using sterile water and dilute it 1:2 (vol:vol) in PBS. Before injection, sterilize the solution using a 0.20 μm syringe filter. Gently shave the right leg of the mice with electric clippers to completely remove the fur around the knee joint.

Inject 200 μg of mBSA in PBS (10 μl total volume) into the intra-articular space of the knee joint (*see* Fig. 2 and **Note 8**). Control mice are injected intra-articularly with 10 μl of PBS, while the contralateral, left joint functions as untreated control.

5. Monitor mice every day after the intra-articular injection. Knee swelling should be evident 24 h after the injection (*see* **Note 9**).

3.1.2 TLR-Induced Arthritis

1. Preparation of DAMP. In order to avoid TLR activation by endotoxin contamination of endogenous TLR ligands, a LAL test should be carried out to quantify endotoxin levels in recombinant DAMPs according to the manufacturer's instructions (LAL assay QCL-1000™). Only preparations with endotoxin levels <1 EU/ml should be injected in the mouse. Dilute DAMP of choice (*see* Table 1) in sterile PBS to the desired concentration (e.g., 0.1 mg/ml FBG).
2. Induction of arthritis. Mice are sedated (*see* Subheading 3.1.1, **step 2**) and unilateral arthritis is induced by intra-articular injection of the DAMP of choice into the right knee joint. Gently shave the right leg of the mice with electric clippers to completely remove the fur around the knee joint. Inject 1–10 μg of DAMP in PBS (10 μl total volume)

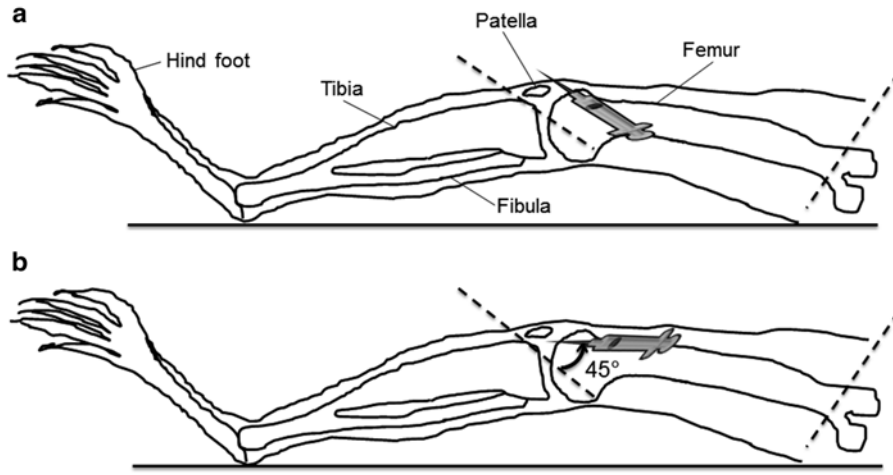

Fig. 2 Intra-articular injection into the cavity of the knee joint. Syringe positioning to locate correct injection site (A) and insert the needle into the cavity of the knee joint (B)

into the intra-articular space of the knee joint (*see* Fig. 2 and **Note 8**). Control mice are injected intra-articularly with 10 μl of PBS, while the contralateral, left joint functions as untreated control. Induction of joint inflammation by the C-terminal fibrinogen-like (FBG) domain of the extracellular matrix glycoprotein tenascin-C (*see* Table 1) is shown in Fig. 3 as an example.

3. Monitor mice every day after the intra-articular injection. Knee swelling should be evident 24 h after the injection (*see* **Note 9**).

3.2 Immunohistochemistry

1. Mouse knee joints are excised 1, 3 or 7 days after intra-articular injection by removing the skin and subcutaneous tissue, cutting longitudinally the muscles that cover the front and side of the femur and the side of the tibia and cutting the femur 1–2 mm above the knee joint and the tibia 1–2 mm below the patella. Carefully remove muscle tissue in excess without damaging the knee joint.
2. Fix the freshly isolated knee joints in 10 % (vol/vol) neutral buffered formalin for 48 h at room temperature.
3. Decalcify the knee joints in 10 % EDTA/PBS for 4 weeks, changing the solution three times per week (*see* **Note 10**).
4. Embed the tissue in paraffin wax using a cycle on an automatic tissue processing machine (e.g., a representative cycle is ethanol 70 % for 90 s at 40 °C, 5× ethanol 100 % for 90 s at 40 °C, 3× xylene 90 s at 40 °C and paraffin for 90 s at 63 °C).
5. Cut coronal tissue sections at a thickness of 4 μm at seven depths throughout the joint, 80 μm apart. Mount sections onto glass microscope slides made to ensure firm electrostatic attraction of paraffin sections (e.g., Superfrost™ Plus Slides).

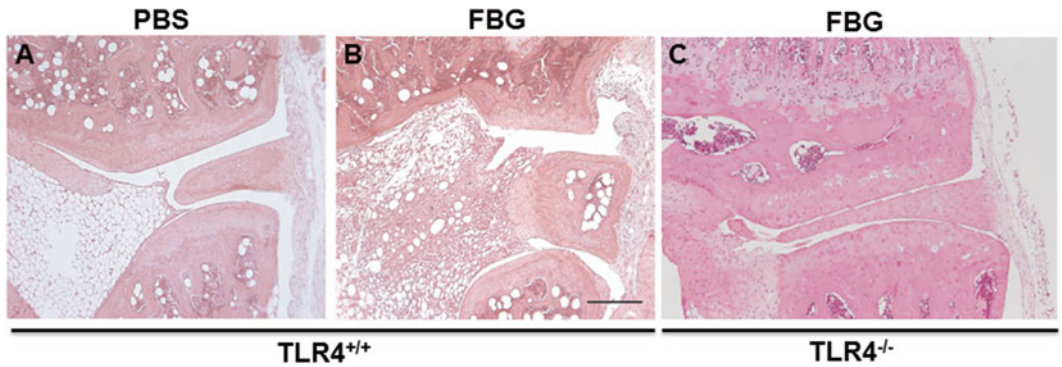

Fig. 3 Sections of the knee joints of wild type (A-B) and TLR4−/− (C) mice 3 days after intra-articular injection of PBS (A) or 1 μg FBG (B-C) stained with H and E. Sections show inflammatory cell infiltration, mild synovitis, and pannus formation exclusively in wild type mice injected with FBG [24]

Let the tissue sections air-dry for 1 h or until dry and place them in an oven at 60 °C overnight. This will help with adherence of the sections to the slides.

6. Dewax sections in xylene (2 × 5 min) and rehydrate through ethanol 100 % (2 × 1 min) followed by 1 min in tap water.
7. H and E staining: place slides in hematoxylin for 6 min and 30 s and rinse under tap water for 2 min; dip slides 2–3 times in 0.3 % acid alcohol for 40 s and rinse under tap water for 2 min; dip slides 8–10 times in ammonia water for 1 min and rinse under tap water for 1 min; finally, place slides in eosin for 1 min and 45 s and rinse under tap water for 3 min. *See* Fig. 4a as an example of the results that can be produced.
8. Safranin-O staining: place slides in hematoxylin for 30 s and rinse under tap water for 2 min; dip slides 2–3 times in 0.3 % acid alcohol for 20 s and rinse under tap water for 2 min; dip slides 8–10 times in ammonia water for 1 min and rinse under tap water for 1 min; place slides in 0.1 % fast green for 6 min followed by 1 % acetic acid for 15 s and rinse under tap water for 2 min; finally, place slides in 0.1 % safranin-O for 5 min and rinse under tap water for 1 min. *See* Fig. 4b as an example of the results that can be obtained.
9. Dehydrate samples by transferring slides to 100 % ethanol (3 × 1 min) and then to xylene (2 × 1 min).
10. Remove slides from xylene and apply DPX mountant and coverslips using an automated coverslipping machine (*see* **Note 11**).
11. Histological analysis of H and E and safranin-O stained sections is performed using a light microscope, a camera and image acquisition software (e.g., BX51 microscope, Olympus; 18.2 Color Mosaic camera, Diagnostic Instruments; Spot

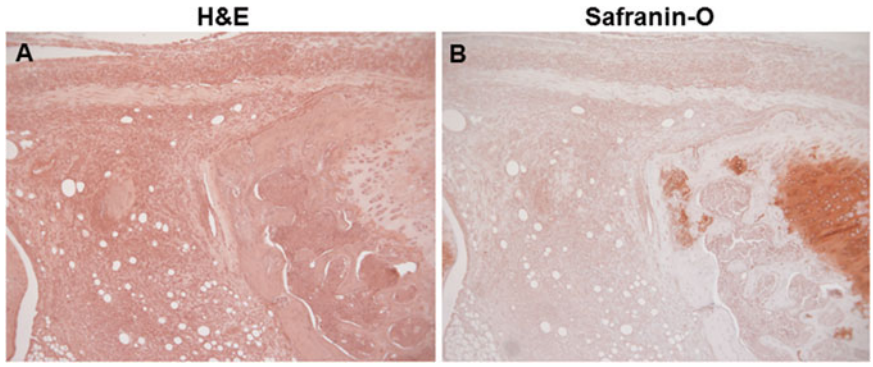

Fig. 4 Sections of the knee joints of 129/sv mice 7 days after intra-articular injection of mBSA stained with H and E (A) and safranin-O (B). Sections show inflammatory cell infiltration in the joint space, synovial hyperplasia, pannus formation, destruction of articular cartilage, and bone erosion [24]

Advanced or DP Manager acquisition software) (*see* **Note 12**). Score histopathological changes using the following parameters as previously described [39]. Grade the influx of inflammatory cells into synovium (infiltrate) and the joint cavity (exudate) with an arbitrary scale from 0 (no inflammation) to 3 (severe inflammation). Determine chondrocyte death as the percentage of cartilage area containing empty lacunae in relation to the total area and cartilage surface erosion as the amount of cartilage lost in relation to the total cartilage area. Assess bone destruction in ten different areas of the total knee joint section and grade it on an arbitrary scale of 0 (no damage) to 3 (complete loss of bone structure). Calculate the mean score for each mouse in an experimental group by averaging the histopathological scores in at least five section depths per joint.

3.3 Real-Time PCR

3.3.1 RNA Preparation

1. Excise mouse knee joints at day 1, 3, or 7 after intra-articular injection (*see* **Note 13**), carefully removing muscle tissue, and immediately freeze them in liquid nitrogen. Maintain tissues at −80 °C until pulverization is carried out using a BioPulverizer (*see* Fig. 1) following manufacturer's instructions.
2. Lyse pulverized tissue by adding 700 μl of RLT buffer (included in the RNeasy mini kit) per sample.
3. Extract and purify total RNA according to manufacturer's instructions (RNeasy Mini kit) including homogenization of tissue lysate with a shredder (QIAshredder Homogenizer) (*see* **Note 14**).
4. Assess total RNA concentration and purity by measuring the sample absorbance at 260 nm and the ratio of absorbance at 260 and 280 nm respectively, using a spectrophotometer.
5. Using the AffinityScript™ Multiple Temperature cDNA synthesis kit, reverse transcribe 500 ng total RNA into cDNA with oligo(dT) primers (*see* **Note 15**) according to manufacturer's instructions.
6. Dilute cDNA 1:3 (vol:vol) in RNase-free water.

3.3.2 Real-Time PCR

1. Prepare TNF-α, CXCL1 and HPRT1 TaqMan reaction mix for each cDNA sample (10 μl per sample per well/tube, in triplicates). For each sample, pipette 1.5 μl of RNase-free water, 5 μl of 2× TaqMan PCR master mix, 0.5 μl of 20× TaqMan primers and probe set and 3 μl of diluted cDNA. Seal microplates and centrifuge the reaction briefly to force the solution to the bottom and to remove any air bubble (*see* **Note 16**). Transfer the microplate to the Applied Biosystems Viia 7™ Real-Time PCR system or to the Rotor-Gene 6000 instrument.

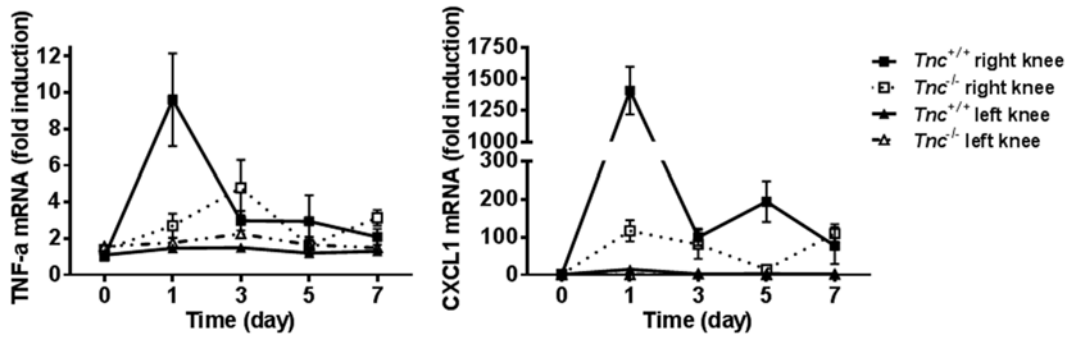

Fig. 5 TNF-α and CXCL1 mRNA induction in the right and contralateral control knee of *Tnc+/+* and *Tnc–/–* mice 1, 3, 5, and 7 days after intra-articular injection of mBSA

2. Analyze relative expression of gene of interest by using the endogenous control HPRT1 to normalize the results, according to the comparative threshold cycle (C_t) method for relative quantification, as indicated by the manufacturer. Calculate the differences in C_t values (ΔC_t) between the sample and the endogenous control. Finally, calculate relative expression levels according to the change-in-threshold ($\Delta\Delta C_t = \Delta C_t$ [injected knee sample] – ΔC_t [untreated knee sample]. An example of results generated is reported in Fig. 5.

3.4 Western Blot Analysis

3.4.1 SDS-PAGE

1. Follow **step 1** in Subheading 3.3.1.
2. Prepare lysis buffer by adding 1 μl of protease inhibitor cocktail to 1 ml of T-PER tissue protein extraction reagent and keep it on ice.
3. Lyse pulverized tissue by resuspending it in ice-cold T-PER tissue protein extraction reagent containing protease inhibitor in a 1.5 ml Eppendorf tube at a final concentration of 100 mg/ml.
4. Sonicate samples on ice using the following program: 80 s total time; pulse ON for 10 s; pulse OFF for 30 s; amplitude 40 %.
5. Centrifuge samples at 10,000 rpm for 5 min at 4 °C using a microcentrifuge and transfer supernatant to a fresh 1.5 ml Eppendorf tube. Keep samples on ice at all times. If not proceeding immediately to immunoblotting, store samples at –80 °C.
6. Determine the protein concentration of each sample using either the Coomassie (Bradford) or bicinchoninic acid (BCA) protein assay and adjust total protein concentration by adding ice-cold T-PER reagent as appropriate to ensure equal protein loading. Add 12.5 μl 5× Laemmli buffer to 50 μl lysate and

boil the samples for 10 min at 95 °C and centrifuge them at maximum speed for 5 min.

7. SDS-PAGE is carried out using the Laemmli method [40] and the following instructions assume the use of the Atto Electrophoresis system.
8. Glass plates are assembled according to manufacturer's instructions.
9. Prepare a 1 mm thick, 5 % gel (*see* **Note 17**) by mixing 1.875 ml of 4× separating buffer, with 1.25 ml acrylamide–bis solution, 4.375 ml water, 25 µl APS, and 5 µl TEMED. Pour the gel between clean glass plates, leaving space for a stacking gel (~1.5 cm). Overlay with water-saturated isobutanol to obtain a smooth surface. Let gel polymerize at room temperature for 30 min.
10. Remove the isobutanol, rinse the top of the gel with deionized water and carefully remove any residual water with Whatman paper.
11. Prepare the stacking gel by mixing 0.625 ml 4× stacking buffer with 0.325 ml acrylamide–bis solution, 1.5 ml water, 12.5 µl APS, and 2.5 µl TEMED. Pour the stacking gel on top of the separating gel, insert a comb and let polymerize at room temperature for 30 min.
12. Remove the comb, rinse the wells with deionized water and fill them with 1× running buffer.
13. Place the gels in the tank filled with 1× running buffer and load samples for analysis of tenascin-C (or other endogenous TLR ligands). Include one well with pre-stained molecular weight marker and one with mouse embryonic fibroblast cell lysates as positive control.
14. Finalize the assembly of the gel unit and connect to the power supply. Run the gel at 100–200 V for 1–1.5 h.

3.4.2 Immunoblotting

1. Transfer the protein samples that have been separated by SDS-PAGE to nitrocellulose membranes using a semi-dry blotting system (Bio-Rad).
2. Soak two sponges, two sheets of Whatman paper and one nitrocellulose membrane per gel in ice-cold 1× transfer buffer.
3. Disconnect the gel unit from the power supply and disassemble it. Remove and discard the stacking gel. Lay sponges, paper, membrane and gel on the surface of the blotting device in the following order to form a sandwich: one sponge, one sheet of Whatman paper, one membrane, one gel, one sheet of Whatman paper, and one sponge.
4. Once the assembly of the blotting device is complete, transfer at 150 mA for 1.5 h.

5. When transfer is complete, incubate the membrane in 5 ml blocking buffer for 1 h at room temperature on a shaker set at 70 rpm
6. Discard blocking buffer and replace it with 1:1000 dilution of the anti-tenascin-C antibody in antibody diluent. Incubate overnight at 4 °C on a shaker set at 70 rpm.
7. Discard the primary antibody and wash the membrane three times for 10 min each with 10 ml PBS-T at room temperature on a shaker set at 70 rpm.
8. Incubate the membrane with a 1:50,000 dilution of the secondary antibody in antibody diluent for 1 h at room temperature on a shaker set at 70 rpm.
9. Discard the secondary antibody and wash the membrane three times for 10 min each with 10 ml PBS-T at room temperature on a shaker set at 70 rpm.
10. Mix 1 ml of each solution of the ECL substrate and add it immediately to the membrane and incubate for 2 min at room temperature on a shaker set at 70 rpm.
11. Drain excess ECL substrate and place the membrane between two transparent plastic leaves in an X-ray film cassette and expose to an X-ray film for 1 min at a start. Increase or decrease exposure time if signal is too weak or too strong, respectively.
12. Strip the membrane by incubating it with stripping buffer for 15 min at room temperature on a shaker set at 70 rpm.
13. Remove the stripping buffer and store it at 4 °C for subsequent use. Block the membrane twice for 5 min with blocking buffer at room temperature on a shaker set at 70 rpm.
14. Discard the blocking buffer and replace it with 1:200 dilution of the anti-actin antibody in antibody diluent. Incubate overnight at 4 °C on a shaker set at 70 rpm.
15. Discard the primary antibody and wash the membrane three times for 10 min each with 10 ml PBS-T at room temperature on a shaker set at 70 rpm.
16. Incubate the membrane with a 1:5000 dilution of the secondary antibody in antibody diluent for 1 h at room temperature on a shaker set at 70 rpm.
17. To detect actin, follow **steps 9–11** as in Subheading 3.4.2. An example of the results obtained is showed in Fig. 6.

3.5 Synovial Tissue Preparation

3.5.1 Enzyme Preparation

1. Adjust Collagenase NB1 to a concentration of 4 mg/ml and neutral protease (NP) to 0.4 μl/ml per gram of tissue weighed (*see* **Notes 18** and **19** and Fig. 7).

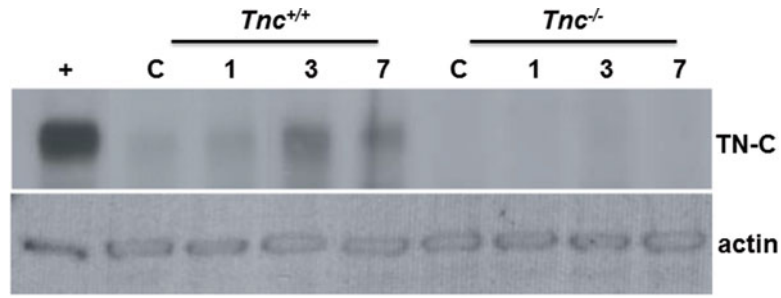

Fig. 6 Tenascin-C protein levels in the joint were assessed 1, 3 and 7 day after intra-articular injection by western blot analysis of equal amounts of total joint lysate with a rat monoclonal antibody to mouse tenascin-C (TN-C). Mouse embryonic fibroblast cell lysate was used as a positive control (+) and non-injected mice as a negative control (c). Blots were re-probed with an antibody to actin to demonstrate equal protein loading in each lane (actin)

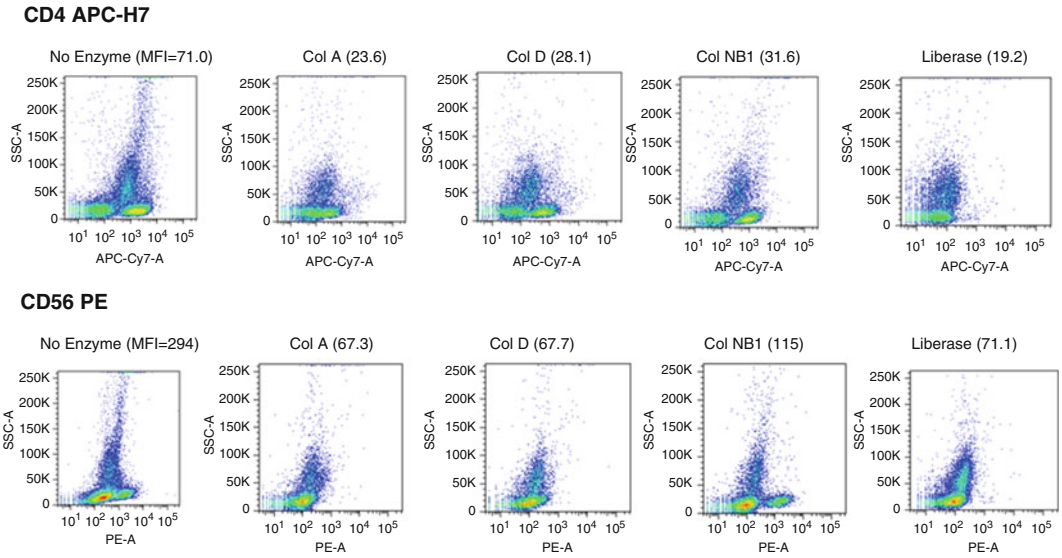

Fig. 7 To test the potential for cleavage of cell surface markers by enzymes commonly used for synovial tissue digestion, PBMCs were treated with a range of collagenases for 90 min and staining intensity for CD4 (*top row* CD4-APC-H7) and CD56 (*lower row* CD56-PE) was compared to that obtained following no enzyme treatment. The mean fluorescence intensity (MFI) for the relevant parameter is shown in brackets next to the name of enzyme used. Col A = collagenase A, Col D = collagenase D, Col NB1 = collagenase NB-1 and Liberase = Liberase TL. Comparative staining shows that Col NB1 spares cleavage of both CD4 and CD56, unlike the other collagenases used

2. Combine solution of either Collagenase NB1 and neutral protease, or Liberase TL (4 mg/ml final) and 2 ml of DNase1 (1 mg/ml) to make a final concentration of 0.2 mg/ml respectively. Add CaN_2O_6 to the collagenase NB1/NP (to give a

final concentration of 2 mM) to the enzyme mixture in a total of 10 ml of RPMI and sterile filter (0.20 μm) the mixture into a sterile 50 ml conical flask. Set aside.

3. Place 50 ml of RPMI media supplemented with 10 % FCS and 1 % Pen/Strep on ice to be used to terminate the reaction after digestion.

3.5.2 Synovial Processing

1. Discard any unnecessary tissue (i.e., fat) using sterile scissors and forceps, then cut the tissue into small pieces (<2 mm) or use McIlwain tissue chopper to get finely chopped synovium; there should be no large clumps. To further increase the surface area for optimal digestion, the tissue pieces are forcibly pressed using the flat end of a 5 ml syringe plunger for 2 min.
2. Using the forceps, scrape the finely chopped synovial tissue from the petri dish into a small conical flask. Wash the petri dish with 2 ml RPMI/enzyme mix using a Gilson pipette, there should be no visible tissue remaining on the plate. Mix tissue/enzyme thoroughly. Add the remaining RPMI/enzyme mix to the flask and transfer the flask to a shaking water bath at 175 strokes per minute or 40rpm for 1–2 h at 37 °C. At the end of first hour, check the tissue. It should appear "gloopy" or "stringy." The pinkish color of RPMI in media should discolor. If the tissue is still visibly clumpy, continue incubating for up to 60 min. It is critical not to go over 2 h, as this will begin to affect viability. Swirl every 20–30 min by hand.
3. Transfer 20 ml of ice-cold medium (RPMI with 10 % FBS) to the flask containing the digested tissue to terminate the digestion.
4. Sieve cells through sterilized beaker covered with Microsieves 200 μm material allowing the digested synovium to pass through. It is important to aggressively force through the tissue clumps using a Corning Cell lifter, again pressing with the rubber end of a plunger from a 2 ml syringe.
5. Wash the flask with a further 10 ml of ice-cold medium and rinse membrane covered beaker. Remove any remaining tissue from the Microsieve membrane and place in 10 ml of medium (RPMI containing 10 % FBS) in a 10 cm^2 tissue culture dish and leave overnight in an incubator; cells still remaining within the tissue will egress overnight from the tissue and adhere to plastic and can be further passaged to yield synovial fibroblasts.
6. Transfer filtered cells from beaker into a 50 ml falcon tube, add medium (RPMI containing 10 % FBS) to make up to 50 ml and spin at $360 \times g$ for 10 min. Resuspend the pellet with 10 ml Red Blood Cell Lysis buffer, incubate for 5 min at room temperature, terminate the reaction by the addition of

40 ml RPMI, and spin for 5 min at 360 × *g*. Resuspend cells in 50 ml RPMI and spin for 5 min again. If the pellet is not clean (has fibers) sieve cells through a 70 μm cell strainer to get single cell suspension and spin at 360 × *g* for 5 min. Cells are now ready for phenotype analysis or cell culture.

3.6 Phenotype Analysis

3.6.1 Antibody Labeling

1. For basic phenotyping place a minimum of 200,000 cells in each of three wells (for Panel A, Panel B, and unstained, *see* Table 2) in a 96-well (U or V bottom) culture plate for antibody labeling (*see* **Note 20**).
2. Add 150 μl per well of cold FACS wash buffer (2 % FCS in PBS containing 0.01 % NaN_3) and spin at 530 × *g* for 2 min to pellet cells.
3. Remove supernatant by a gentle flick to minimize residual buffer.
4. Add Fc Receptor blocking reagent (*see* **Note 21**) diluted 1:5 in a total volume of 10 μl per sample. Incubate at 4 °C for 10 min.
5. Add antibody cocktails (*see* Table 2) in a total volume of 20 μl directly on top of FcR block without washing. Incubate at 4 °C for a further 20 min.
6. Wash 3 times by addition of 150 μl of FACS wash buffer, spin at 530 × *g* and flick off supernatant as in 3.
7. Resuspend after final wash in 150 μl of FACS wash buffer and proceed directly to flow cytometer (e.g., BD Facs Canto II equipped with three lasers: blue (488 nm), red (633 nm), and violet (405 nm) for excitation of all fluorophores specified.

3.6.2 FACS Analysis

Using antibody panels A and B (*see* Table 2), it is possible to identify the main immune cell types within the typical RA synovial tissue. After exclusion of dead cells and debris, first gate on CD45+ and

Table 2
Antibody cocktails for synovial cell FACS analysis

Panel A	Panel B
CD45 PerCP	CD3 APC
CD14 APC	CD25 V450
CD11c V450	CD8 PeCy7
CD15 PeCy7	CD56 PE
HLADR PE	CD4 APC-Cy7
CD90 FITC	Viability dye (Am Cyan)
Viability dye (Am Cyan)	

CD45- populations to facilitate identification of further subsets (*see* Fig. 8 and **Notes 22–25**). CD45+ cells usually make up the bulk (approx. 60 %) but there is a significant degree of heterogeneity in the cellular composition of RA synovial membrane tissue from each RA donor, as demonstrated in Fig. 9, with CD45+ cells ranging between 20 and 80 % of all viable cells recovered. The remaining

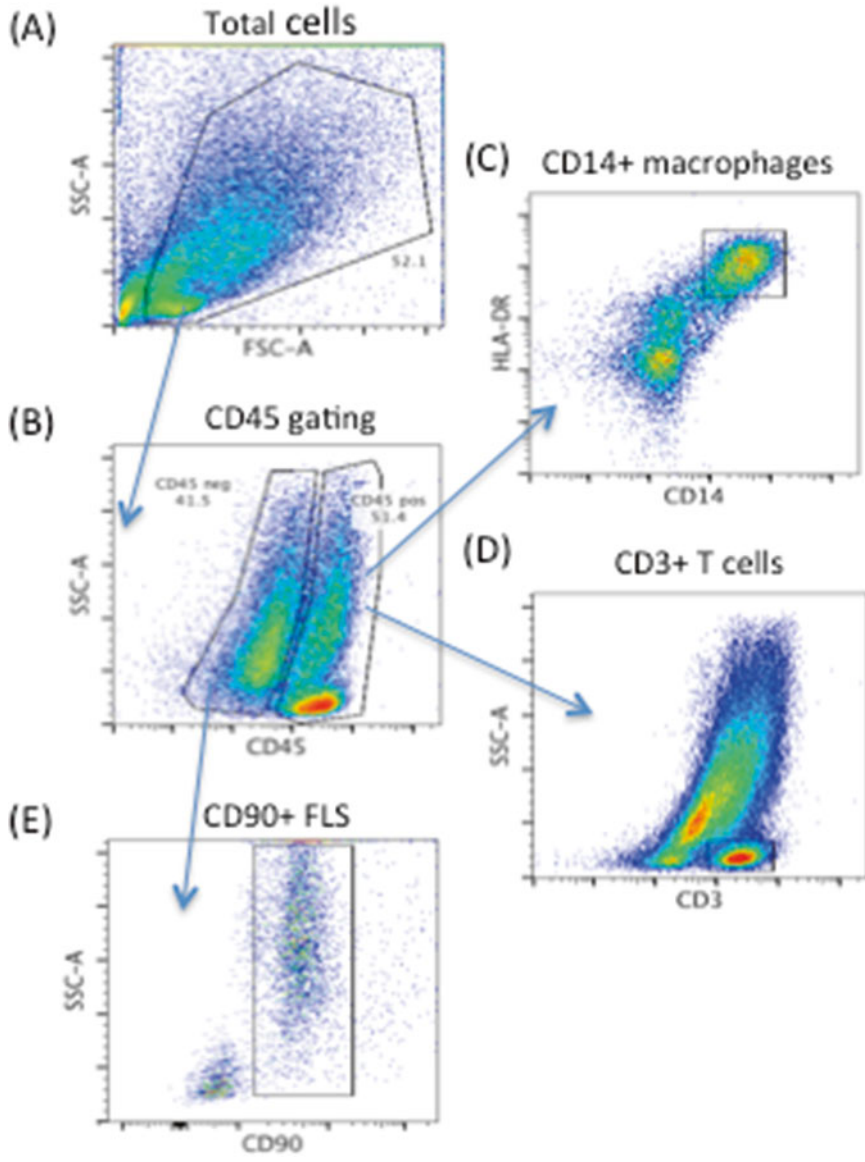

Fig. 8 Synovial tissue from RA patients was collected during joint replacement surgery and cells were enzymatically dissociated, then labeled with a panel of antibodies for immune phenotyping. (A) Total cells were gated to exclude cell debris. (B) CD45 staining was used to identify hematopoietic cells and stromal cells. CD45+ cells comprised CD14+, HLADR+ macrophages (C) and CD3+ T cells among others not shown (D). CD45– cells largely expressed CD90 FLS marker (E)

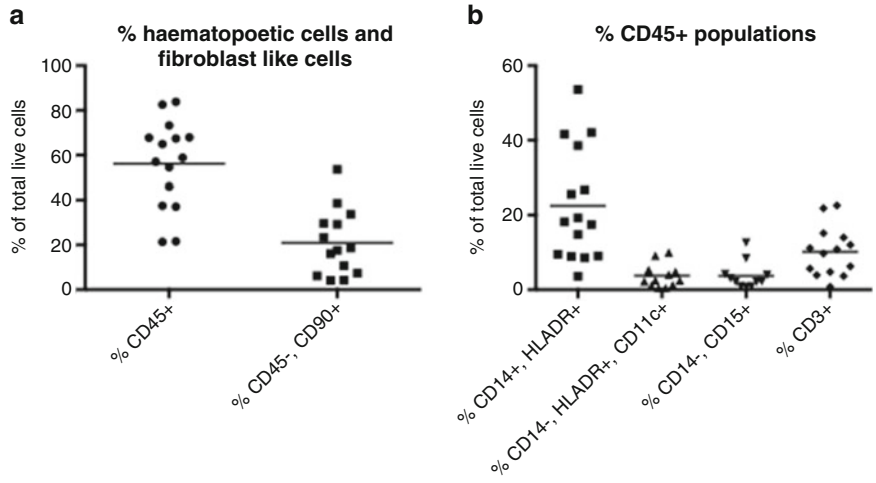

Fig. 9 Proportions of immune cells in synovial tissue from 16 RA patients were quantitated using flow cytometer. (A) CD45+ hematopoietic cells and CD45–, CD90+ FLS cells were enumerated. (B) CD45+ cells were further stratified into macrophages (CD14+, HLADR+), cDCs (CD14–, HLADR+, CD11c+), neutrophils (CD14–, CD15+), and T cells (CD3+)

CD45- population is largely CD90+, suggestive of a fibroblast-like phenotype (*see* Fig. 9a), and comprises approximately 20 % of all viable cells. Other major cell subsets within the CD45+ gate (hematopoietic in origin) are depicted in Fig. 9b. These are mostly macrophages (CD14+, HLADR+) with a lesser proportion of CD3+ T cells (1–20 %). CD11c+, HLADR+, CD14– cells, likely conventional dendritic cells, are few in number (<5 %) and neutrophils (CD14–, CD15+) even less (<2 %). This may reflect the "dampened" biological activity of the tissue collected at joint replacement surgery (i.e., end stage RA), where the tissue may be more quiescent after long-term chronic inflammation. To confirm this, it will be of interest to compare cellular composition of synovial biopsy tissue collected in early onset RA to late stage surgery.

3.7 Synovial Cell Culture

3.7.1 Cell Culture and Stimulation

1. Once isolated from membranes, cells can be cultured for a limited period of time as follows. Resuspend cells in RPMI with 5 % HIFCS supplemented with 1 % Pen/Strep, dispense into a 96-well flat bottom tissue culture plate (200 µl at $1–2 \times 10^5$/well) and incubate at 37 °C.
2. To assess TLR ligand activity in this system, incubate cells with 50 µl of TLR ligand agonists or antagonist (as previously described [5]). For example stimulation with FSL-1 10 ng/ml, poly(I:C) HMW 20 ng/ml, LPS 10 ng/ml, flagellin 10 ng/ml, R847 1 µg/ml, R848 1 µg/ml, or ssDNA/LyoVec 500 ng/ml can be used in order to modify spontaneous cytokine production.

3. Harvest cell supernatants 24–72 h later. We routinely measure cytokines after 48 h and store supernatants at −20 °C until cytokine assays are performed.

3.7.2 Adenoviral Infection

Using AdEasy adenoviral constructs of the TLR adapter molecules MyD88 and Mal, we have previously shown that these molecules control spontaneous cytokine and MMP production in synovial membrane cultures [7]. A detailed protocol for the generation of adenoviral vectors can be found elsewhere [41]. Here we describe how to transfect RA synovial membrane cells.

1. Cells are resuspended in serum-free RPMI supplemented with 1 % Pen/Strep and dispensed into a 96-well flat bottom tissue culture plate (100 µl at $1–2 \times 10^5$/well) and incubated at 37 °C for 1 h.
2. Incubate cells with 100 µl of AdEasy adenoviral vectors at a multiplicity of infection of 100, wash after 2 h, and culture in 200 µl of 5 % HIFCS RPMI media for 48 h, at which time collect supernatants and store at −20 °C until cytokine assays are performed.

3.8 Cytokine Analysis

3.8.1 ELISA

1. Coat ELISA plates with anti-human TNF-α antibody or anti-IL-8 antibody diluted 1:400 and 1:1000 respectively in 1× PBS in a volume of 50 µl/well, cover them with acetate plate sealers to prevent evaporation and shake (50 rpm) overnight at 4 °C.
2. Wash plates three times with PBS, 0.01 % Tween 20, pat dry, and block with 2 % BSA in PBS for 1 h.
3. Prepare standard curves of recombinant TNF-α and IL-8 in 5 % HIFCS to include six points of threefold serial dilutions (5000–20 pg/ml). Wash plates as described in **step 2**. Dispense in duplicate, 50 µl of each of the six points of the serial dilution of the standard curve to the plate. Add cell supernatant to the plate (in the case of TNF-α neat and in the case of IL-8 diluted 1:1000).
4. Shake (50 rpm) samples for 2 h at room temperature or overnight at 4 °C.
5. Wash plates as described in **step 2**. Dilute biotinylated antibodies at 1:1000 in 0.5 % BSA/PBS and dispense 50 µl/well into the ELISA plate. Shake samples for 1 h at room temperature.
6. Wash plates as described in **step 2**. Prepare streptavidin-HRP at a dilution of 1:400 in 0.5 % BSA/PBS and dispense 50 µl/well into the ELISA plate. Shake samples for 1 h at room temperature.

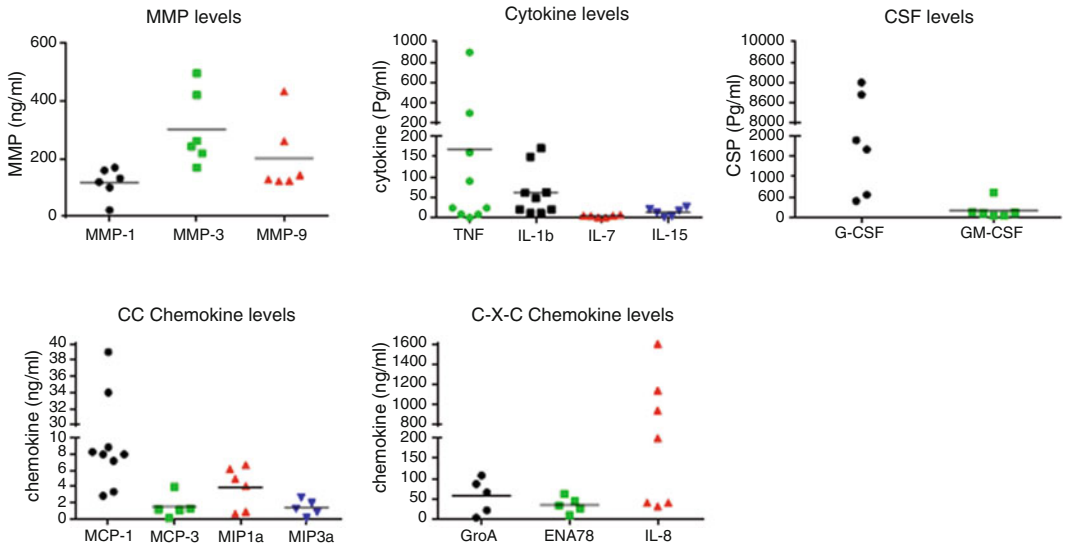

Fig. 10 Spontaneous cytokine production from RA synovial cultures. Synovial cells isolated using Liberase TL were seeded at 2×10^5/well and cultured for 48 h. Cell culture supernatant was harvested and kept at −20 °C prior to cytokine analysis using MSD technology. Data shown are from 5–9 distinct RA synovial explant cultures

7. Wash plates as described in **step 2**. Prepare TMB substrate by mixing the TMB peroxidase substrate with the substrate solution B in a 1:1 ratio and dispense 50 µl/well into the plate.
8. When the fourth dilution of the standard curve begins to develop, add 50 µl/well of stop solution to the plate. Read absorbance on a spectrophotometric ELISA plate reader (e.g., Labsystems Multiscan Biochromic) and analyze data using the Ascent software program (Thermo Labsystems, Altrincham, UK)(*see* Figs. 10 and 11).

3.8.2 Mesoscale Discovery (MSD) Platform

MSD assays demonstrate a superior dynamic range (3–4 logs) to standard ELISAs and allow researchers to measure multiple cytokines and metalloproteinases, expressed over a large concentration range in extremely small volumes of culture supernatants. Assay protocols vary from plate to plate depending on the particular plex of antibodies and specific protocols that are supplied with each kit.

1. Bring all reagents to room temperature.
2. Dispense 25 µl of diluent 2 to the MSD plate for 30 min with vigorous shaking (300 rpm).
3. Prepare 8 point standard curve (calibrator) for MMP1/3 (100,000–24 pg/ml) and MMP9 (500,000–122 pg/ml) in diluent provided in the kit.

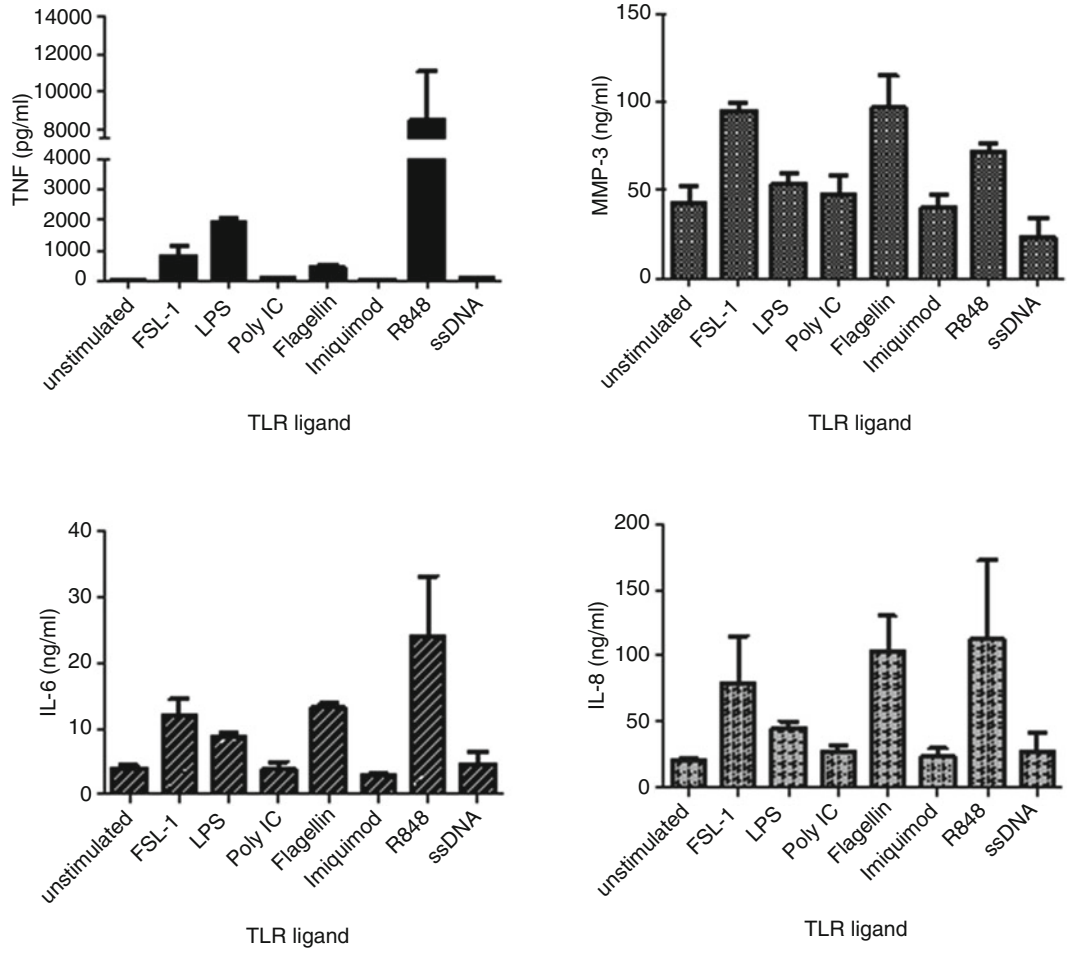

Fig. 11 TLR ligand induced cytokine production from RA synovial cultures. Synovial cells isolated using Liberase TL were seed at 2×10^5/well and cultured for 48 h. Cell culture supernatant was harvested and kept at −20 °C prior to cytokine analysis using MSD technology. Data shown are from an individual RA membrane, mean ± SD from triplicate cultures

4. Dispense 25 µl of calibrator in duplicate, blank (diluent) or sample (diluted 1:50 in diluent) into the MSD plate. Seal the plate and incubate for 2 h with vigorous shaking (300 rpm).
5. Wash the plate three times with PBS, 0.01 % Tween 20 and pat dry. Dispense 25 µl of 1× detection antibody solution into each well of MSD plate. Seal the plate and incubate for 2 h with vigorous shaking (300 rpm).
6. Wash the plate as described in **step 5**. Add 150 µl of read solution into each well. Analyze the plate on the SECTOR Imager using the MSD DISCOVERY WORKBENCH® software. Plates must be read immediately after addition of Read buffer.

4 Notes

1. The nature and frequency of the RA tissue samples we process has changed over the last decade: RA is much more effectively managed by the use of high dose disease-modifying antirheumatic drugs (DMARD) such as methotrexate and the anti-TNF based biologicals. As such, we have observed that the spontaneous production of many cytokines, including TNF-α, IL-1, and IL-15, is much more conservative than previously described, while IL-6, IL-8, and matrix metalloproteinases are still expressed at high, pathogenic levels in this subset of patients undergoing joint replacement therapy.
2. To test the quality of the emulsion, place one drop of emulsion on water. If the droplet floats on the surface and remains intact, the emulsion is of optimal quality.
3. This animal experiment is a regulated procedure that has to be performed in an approved animal facility according to legal regulation. For each animal experiment planned, an application must be filed and approved by the appropriate institutional and governmental committees.
4. The amount of Hypnorm to be administered varies in function of the mouse body weight. Consult the vet to work out the appropriate dose of Hypnorm for the mouse strain in question. Moreover, because sedated mice get cold, it is essential to keep mice warm until fully recovered.
5. In order to boost T cell reactivity against the antigen, immunization of mice may be established by means of an injection of mBSA in CFA in the front paws and flanks and an intraperitoneal injection of heat-killed B. pertussis bacteria followed by a second set of injections 7 days later as described previously [32, 42]. Note that, in this case, induction of arthritis by intraarticular injection of mBSA is performed at day 21.
6. Recommended sites for intradermal injections are at the base of the tail and in a slightly more anterior location.
7. After filling the syringe with the emulsion, hold the syringe up to a light source and remove any air bubble as this will result in less emulsion administered to the mice. Change the needle frequently since it becomes blunt after few injections.
8. This injection requires two people: one to hold the mouse (person A) and one to perform the injection (person B). While person A scruffs the mouse, person B pulls out the leg and shaves it around the knee joint. The patella (or knee cap) should be visible under the skin as white.

   Person A scruffs the mouse and turns it onto its back with one hand and gently pulls the leg nearly straight with the other

hand. The hind foot is held down with the thumb while the knee is supported from underneath with the index finger.

Person B aligns the needle perpendicular to the leg and over the top of the patella and, by pressing down the needle gently, identifies the groove between the femur and the tibia (*see* Fig. 2a). The needle is maintained in line with this groove while slid slightly back before raising it to approximately a 45° angle and inserting it into the cavity of the joint; all in one smooth motion (*see* Fig. 2b). Ten microliters of solution is dispensed.

The two most frequent incorrect targets of the injection are the bone and the site immediately below the patella. The person performing the injection will encounter resistance in the former case while notice the needle moving loosely around in the latter case. If the solution comes straight out in the process of injection or if in an incorrect location, remove the needle and begin the process again. If the skin has been damaged, manipulate surrounding shaven skin to have intact layer over the knee. No more than three attempts should be made on the knee, after which intra-articular administration should be stopped if unsuccessful and the mouse allowed to recover.

9. Clinical evaluation of arthritis may include the use of calipers to measure knee joint swelling. This consists of measuring the distance between the medial and lateral aspects of each knee joint at the level of the patellar ligament and is expressed as knee diameter. However, in our experience we have found this technique not very reliable. Alternatively, water displacement [42] is a more accurate and reliable method that can be used to measure knee swelling. However, this requires the use of a plethysmometer, which may not be readily available.
10. Tissues such as joints containing calcified areas need to be decalcified before processing in order to become soft enough for sectioning. It is possible to test biochemically for calcium in solution to assess endpoint of decalcification.
11. DPX is a synthetic resin mounting media composed of Distyrene, a plasticizer, and xylene. It preserves the stain and dries quickly, enabling slides to be screened immediately. It has a low viscosity, allowing the medium to flow easily and prevents air bubbles from becoming trapped. Application of coverslips to microscope slides can also be done manually by adding a drop of mounting media at base of slide, placing the coverslip at an angle as to begin to spread the media and carefully lower the coverslip onto the tissue while the media spreads underneath. Allow slides to dry under a hood.
12. Histological analysis should be performed by an investigator who is blinded to the experimental groups.

13. During the first 7 days after intra-articular injection of mBSA, the acute phase of the arthritic response can be investigated. In order to evaluate the chronic phase of the arthritic response, disease can be allowed to progress for 2–3 weeks after intra-articular injection of antigen.
14. Isolation of total RNA from tissue lysates requires homogenization to reduce viscosity caused by high-molecular-weight cellular components and cell debris. Unlike traditional methods that use syringes and needles, QIAshredder spin columns require a single and fast centrifugation step and reduce loss of sample material.
15. Oligo(dT) primers anneal to any mRNA with a poly(A) tail, generating full length copies of the mRNA. Alternatively, random primers can be used. These are random combinations of nucleotides, 6 or 9 bp long, that enable transcription of 5′ ends of long genes, generating cDNAs that may not be full length copies of the entire gene.
16. If performing the real-time PCR in a Rotor-Gene 6000 instrument using 0.1 ml strip tubes, there is no need to centrifuge the tubes before starting the reaction as the machine spins samples for the entire duration of the PCR.
17. Choose the acrylamide–bis solution percentage most appropriate to the endogenous TLR ligand of interest.
18. There are numerous commercial sources of collagenase used by various laboratories to digest synovial tissue. However, great care has to be taken to ensure each batch of enzyme is tested for endotoxin contamination and not simply rely on manufacturer's product sheets. We batch test using Endpoint Chromogenic LAL Assays (Lonza) and reject if contamination exceeds 1 EU/ml. In addition to exclude any possibility that low levels of endotoxin could stimulate the highly sensitive macrophage population within RA synovial membranes, we perform mock enzymatic digestions (i.e., incubation of human monocytes with collagenase NB1 8 mg/ml for 2 h followed by three washes, culture of monocytes for 18 h and measurement of monocyte activation by assaying for TNF-α production by ELISA). Many commercial sources of collagenase induce up to 20 ng/ml of TNF-α under these conditions. We observe no such effect using NB1 or Liberase TL in any batches assayed.
19. The choice of enzyme to digest synovial tissue is also critical depending on the end point assay each researcher uses. We have found Collagenase A from Roche cleaves CD56, a NK cell marker which then may give a false under representation of NK cells within the tissue. Another popular source of enzyme is Roche Liberase TL, which we found to cleave CD4

(as demonstrated in Fig. 7), leading to an underestimation of this cell population. As new technologies such as CyTOF and multicolor FACS are developed which allow multiple parameter analysis of mixed cells populations, it is critical that the integrity of cell surface receptors remain intact. After extensive testing, we have found NB1 with its high collagenase and low neutral protease activity was the optimal collagenase for tissue digestion while maintaining cell surface receptor expression. However the high specificity of this particular enzyme results in a lower cell yield and careful thought is needed as RA synovial membranes can yield very little cells and if cytokine analysis is the endpoint, a collagenase preparation such as Liberase TL® may be a more appropriate digestive enzyme of choice.

20. For clear definition of positive staining and to assist set up of the flow cytometer, it is suggested to leave one sample unstained (in addition to those for staining panels A and B).
21. The inclusion of FcR block is necessary to avoid nonspecific staining of all FcR bearing cells, in particular macrophages, which are abundant in RA synovial membranes.
22. It is essential to include a viability stain as up to 20 % of total cells do not remain intact after tissue dissociation. Therefore only collect data from viable cells.
23. For low abundance cell types, it is suggested to gate on the appropriate subset and collect a minimum of 5000 events therein.
24. While it is preferable to analyze cells directly after staining, if a cytometer is not available, samples may be kept at 4 °C in the dark for up to a few hours, or, alternatively, they can be fixed post staining and analyzed the following day.
25. NK cells are also detectable with the staining panels detailed here (CD45+, CD3– and CD56+) when using collagenase NB-1 for tissue digestion. Other collagenases (e.g., Liberase TL) cleave CD56, rendering it undetectable on the cell surface (*see* Fig. 7 and **Note 18**).

Acknowledgements

We would like to thank Mr Khaja Syed and Mr. Arran Speirs for their technical assistance; Mr. Richard Field, Consultant Orthopedic Surgeon, Elective Orthopedic Centre, Epsom and St Helier University Hospital, Mr. Grey Giddings, Consultant Plastic and Hand Surgeon, Royal United Hospital Bath, and Mr. Kang, Consultant Plastic and Hand Surgeon, Royal Free London, NHS Hospital trust, for their invaluable provision of RA synovial tissue.

References

1. Brentano F, Schorr O, Gay RE et al (2005) RNA released from necrotic synovial fluid cells activates rheumatoid arthritis synovial fibroblasts via Toll-like receptor 3. Arthritis Rheum 52:2656–2665
2. Pierer M, Rethage J, Seibl R et al (2004) Chemokine secretion of rheumatoid arthritis synovial fibroblasts stimulated by Toll-like receptor 2 ligands. J Immunol 172: 1256–1265
3. Seibl R, Birchler T, Loeliger S et al (2003) Expression and regulation of Toll-like receptor 2 in rheumatoid arthritis synovium. Am J Pathol 162:1221–1227
4. Roelofs MF, Joosten LA, Abdollahi-Roodsaz S et al (2005) The expression of toll-like receptors 3 and 7 in rheumatoid arthritis synovium is increased and costimulation of toll-like receptors 3, 4, and 7/8 results in synergistic cytokine production by dendritic cells. Arthritis Rheum 52:2313–2322
5. Sacre SM, Lo A, Gregory B et al (2008) Inhibitors of TLR8 reduce TNF production from human rheumatoid synovial membrane cultures. J Immunol 181:8002–8009
6. Kyburz D, Rethage J, Seibl R et al (2003) Bacterial peptidoglycans but not CpG oligodeoxynucleotides activate synovial fibroblasts by toll-like receptor signaling. Arthritis Rheum 48:642–650
7. Sacre SM, Andreakos E, Kiriakidis S et al (2007) The Toll-like receptor adaptor proteins MyD88 and Mal/TIRAP contribute to the inflammatory and destructive processes in a human model of rheumatoid arthritis. Am J Pathol 170:518–525
8. Ultaigh SN, Saber TP, McCormick J et al (2011) Blockade of Toll-like receptor 2 prevents spontaneous cytokine release from rheumatoid arthritis ex vivo synovial explant cultures. Arthritis Res Ther 13:R33
9. Elson G, Page T, Buatois V et al (2011) NI-0101, a therapeutic TLR4 monoclonal antibody for rheumatoid arthritis. Arthritis Rheum 63:S383
10. Joosten LA, Koenders MI, Smeets RL et al (2003) Toll-like receptor 2 pathway drives streptococcal cell wall-induced joint inflammation: critical role of myeloid differentiation factor 88. J Immunol 171:6145–6153
11. Abdollahi-Roodsaz S, Joosten LA, Koenders MI et al (2008) Stimulation of TLR2 and TLR4 differentially skews the balance of T cells in a mouse model of arthritis. J Clin Invest 118:205–216
12. Choe JY, Crain B, Wu SR et al (2003) Interleukin 1 receptor dependence of serum transferred arthritis can be circumvented by toll-like receptor 4 signaling. J Exp Med 197:537–542
13. Zare F, Bokarewa M, Nenonen N et al (2004) Arthritogenic properties of double-stranded (viral) RNA. J Immunol 172:5656–5663
14. Alzabin S, Kong P, Medghalchi M et al (2012) Investigation of the role of endosomal Toll-like receptors in murine collagen-induced arthritis reveals a potential role for TLR7 in disease maintenance. Arthritis Res Ther 14:R142
15. Abdollahi-Roodsaz S, Joosten LA, Roelofs MF et al (2007) Inhibition of Toll-like receptor 4 breaks the inflammatory loop in autoimmune destructive arthritis. Arthritis Rheum 56:2957–2967
16. Leung BP, Xu D, Culshaw S et al (2004) A novel therapy of murine collagen-induced arthritis with soluble T1/ST2. J Immunol 173:145–150
17. Hayashi T, Gray CS, Chan M et al (2009) Prevention of autoimmune disease by induction of tolerance to Toll-like receptor 7. Proc Natl Acad Sci U S A 106:2764–2769
18. Dong L, Ito S, Ishii KJ et al (2004) Suppressive oligonucleotides protect against collagen-induced arthritis in mice. Arthritis Rheum 50:1686–1689
19. Zeuner RA, Ishii KJ, Lizak MJ et al (2002) Reduction of CpG-induced arthritis by suppressive oligodeoxynucleotides. Arthritis Rheum 46:2219–2224
20. Midwood KS, Piccinini AM, Sacre S (2009) Targeting Toll-like receptors in autoimmunity. Curr Drug Targets 10:1139–1155
21. Huang QQ, Pope RM (2009) The role of Toll-like receptors in rheumatoid arthritis. Curr Rheumatol Rep 11:357–364
22. Piccinini AM, Midwood KS (2010) DAMPening inflammation by modulating TLR signalling. Mediators Inflamm 2010
23. Roelofs MF, Abdollahi-Roodsaz S, Joosten LA et al (2008) The orchestra of Toll-like receptors and their potential role in frequently occurring rheumatic conditions. Arthritis Rheum 58:338–348
24. Midwood K, Sacre S, Piccinini AM et al (2009) Tenascin-C is an endogenous activator of Toll-like receptor 4 that is essential for maintaining inflammation in arthritic joint disease. Nat Med 15:774–780
25. Andersson U, Erlandsson-Harris H (2004) HMGB1 is a potent trigger of arthritis. J Intern Med 255:344–350
26. Rice JW, Veal JM, Fadden RP et al (2008) Small molecule inhibitors of Hsp90 potently affect inflammatory disease pathways and

exhibit activity in models of rheumatoid arthritis. Arthritis Rheum 58:3765–3775
27. Kakimoto K, Matsukawa A, Yoshinaga M et al (1995) Suppressive effect of a neutrophil elastase inhibitor on the development of collagen-induced arthritis. Cell Immunol 165:26–32
28. Gondokaryono SP, Ushio H, Niyonsaba F et al (2007) The extra domain A of fibronectin stimulates murine mast cells via toll-like receptor 4. J Leukoc Biol 82:657–665
29. Pullerits R, Jonsson IM, Verdrengh M et al (2003) High mobility group box chromosomal protein 1, a DNA binding cytokine, induces arthritis. Arthritis Rheum 48:1693–1700
30. van Lent PL, Grevers LC, Schelbergen R et al (2010) S100A8 causes a shift toward expression of activatory Fcgamma receptors on macrophages via toll-like receptor 4 and regulates Fcgamma receptor expression in synovium during chronic experimental arthritis. Arthritis Rheum 62:3353–3364
31. Dumonde DC, Glynn LE (1962) The production of arthritis in rabbits by an immunological reaction to fibrin. Br J Exp Pathol 43:373–383
32. Brackertz D, Mitchell GF, Mackay IR (1977) Antigen-induced arthritis in mice. I. Induction of arthritis in various strains of mice. Arthritis Rheum 20:841–850
33. van den Berg WB, van de Putte LB (1985) Electrical charge of the antigen determines its localization in the mouse knee joint. Deep penetration of cationic BSA in hyaline articular cartilage. Am J Pathol 121:224–234
34. van den Berg WB, Kruijsen MW, van de Putte LB et al (1981) Antigen-induced and zymosan-induced arthritis in mice: studies on in vivo cartilage proteoglycan synthesis and chondrocyte death. Br J Exp Pathol 62:308–316
35. Brennan FM, Chantry D, Jackson AM et al (1989) Cytokine production in culture by cells isolated from the synovial membrane. J Autoimmun 2(Suppl):177–186
36. Feldmann M, Brennan FM, Maini RN (1996) Role of cytokines in rheumatoid arthritis. Annu Rev Immunol 14:397–440
37. Brennan FM, Chantry D, Jackson A et al (1989) Inhibitory effect of TNF alpha antibodies on synovial cell interleukin-1 production in rheumatoid arthritis. Lancet 2:244–247
38. Arnett FC, Edworthy SM, Bloch DA et al (1988) The American Rheumatism Association 1987 revised criteria for the classification of rheumatoid arthritis. Arthritis Rheum 31: 315–324
39. van Lent PL, Grevers L, Lubberts E et al (2006) Fcgamma receptors directly mediate cartilage, but not bone, destruction in murine antigen-induced arthritis: uncoupling of cartilage damage from bone erosion and joint inflammation. Arthritis Rheum 54:3868–3877
40. Laemmli UK (1970) Cleavage of structural proteins during the assembly of the head of bacteriophage T4. Nature 227:680–685
41. Davis A, Taylor C, Willetts K et al (2007) Adenoviral targeting of signal transduction pathways in synovial cell cultures. Methods Mol Med 136:395–419
42. Boyle DL, Moore J, Yang L et al (2002) Spinal adenosine receptor activation inhibits inflammation and joint destruction in rat adjuvant-induced arthritis. Arthritis Rheum 46: 3076–3082

Chapter 23

Delineating the Role of Toll-Like Receptors in the Neuro-inflammation Model EAE

Francesca Fallarino, Marco Gargaro, Giada Mondanell, Eric J. Downer, Md Jakir Hossain, and Bruno Gran

Abstract

Experimental autoimmune encephalomyelitis (EAE) is the most relevant and commonly used animal model to study autoimmune demyelinating diseases like Multiple Sclerosis (MS). In EAE, the activation of CD4+ T-cells is considered to be the main trigger leading to inflammation and central nervous system (CNS) demyelination. Toll-like receptors (TLRs) are the most important and first class of pattern recognition receptors (PRRs) in innate immune system and play critical roles in initiating inflammatory responses and promoting adaptive immune responses due to their ability to recognize a wide range of pathogen associated molecular patterns (PAMPs) and being expressed in a wide range of cell types both in the innate and adaptive immune systems. Upon TLR stimulation by appropriate ligand, innate immune cells produce pro-inflammatory cytokines and can serve as antigen-presenting cells (APCs) to prime naïve T cells to recognize antigens. Thus, TLRs play an important role in linking the innate to the adaptive immune response. To date, large numbers of studies have been done to investigate the role of adaptive immunity in both EAE and MS but delineating the role of innate immunity in EAE received very little focus and appreciation taking into account that it might contribute to both the initiation and progression of the disease. Moreover, EAE is not only a model to study inflammatory demyelination in the CNS; it is in general a model to study cell-mediated organ-specific autoimmune conditions. Roles of different TLRs were studied in relation to EAE and MS. More recently, some studies demonstrated the immune adjuvant properties of certain TLR ligands including TLR2, TLR4, and TLR9 in EAE. This chapter outlines different methods employed in our labs to investigate the role of TLRs in EAE model.

Key words EAE, Multiple sclerosis, Inflammation, Demyelination, Autoimmune disease, Toll-like receptors, T cell, Antigen-presenting cells, Dendritic cells, B cells

1 Introduction

EAE is a well-characterized animal model of autoimmune inflammatory demyelination in the CNS. To date, studies on EAE have significantly facilitated the understanding of the biology of MS and have contributed to the development and approval of at least three MS therapies, glatiramer acetate (GA), mitoxantrone, and natalizumab [1–5]. There is a great heterogeneity in the susceptibility

Claire E. McCoy (ed.), *Toll-Like Receptors: Practice and Methods*, Methods in Molecular Biology, vol. 1390,
DOI 10.1007/978-1-4939-3335-8_23,

and method to induce EAE, thus also reflecting large variations in the response to immunological or neuropharmacological interventions [4, 6, 7]. This makes EAE a very versatile system to use in translational neuroimmunology, but the model needs to be tailored to the scientific question being asked. EAE can be induced by active immunization (active EAE) with self-antigens or adoptive transfer (passive or at-EAE) of activated T cells in several species and strains of rodents [8]. In active EAE, animals are actively immunized with self-antigen in the form of myelin components or CNS homogenates emulsified in adjuvant [9]. Passive or at-EAE is induced by adoptive transfer of encephalitogenic CD4+ T cells (with specificity to self-antigens, e.g., myelin) into naïve animals (recipient) generated in donor animals by active immunization [10]. More recently, spontaneous EAE models have also been developed using transgenic mice that express T cells with myelin specific T-cell receptors that represents an alternative model to study some of the initial events in the pathogenesis of CNS autoimmunity [11, 12]. Active EAE is the easiest inducible model allowing quick screening of the effects of drugs on autoimmune inflammation. Lewis rats were the most popular animals used for EAE as they showed 100 % responsiveness after immunization with myelin basic protein (MBP) [13]. In recent years, C57BL/6 mice have become more popular mainly for studies involving transgenic mice [12]. at-EAE is a very useful model to address issues related with the effector phase of the disease [8]. The encephalitogenic T cells can also be manipulated in vitro to study the role of specific cytokines and other biological agents prior to their transfer to recipients [4]. In addition, these cells can be labeled to trace their localization, survival or interactions with other cell types in the recipient [4, 8]. Moreover, the at-EAE model is of particular interest to study the role of a variety of inflammatory molecules in different aspects of disease development and regulation through the use of gene-targeted donor or recipient animal strains [6].

Over the years, the protocols for EAE induction have been extensively refined [9]. The advent of the use of Freund's adjuvant [14] greatly facilitated immunization regimens, efficiency of the immunization, such that EAE induction now requires only a single immunization. To induce EAE, myelin-derived peptides are emulsified in complete Freund's adjuvant (CFA) that contains killed *Mycobacterium tuberculosis* and PAMPs from these bacteria that activate innate immune responses, which in turn promote pathogenic autoreactive T cell responses [15]. The addition of pertussis toxin also greatly improved the efficiency of EAE induction by promoting inflammatory CNS infiltration [16]. Fractionation of spinal cord homogenate led to the identification of encephalitogenic myelin antigens including MBP [17], proteolipid protein (PLP) [18], myelin-associated glycoprotein [19], and myelin oligodendrocyte glycoprotein (MOG), a minor component of myelin that

is highly encephalitogenic in many species [20, 21]. Current EAE protocols typically use purified or recombinant myelin proteins, or synthetic peptides derived from these proteins, as immunogens. Further refinement of the passive induction protocol revealed that transfer of T cells [22], and later, more specifically MHC class II-restricted T cells [23, 24] was sufficient to induce EAE, inferring that the EAE disease induction is mostly CD4+ T cell mediated.

The principles underlying the active and passive methods of EAE induction are almost the same [9]. Both protocols involve the activation of peripheral myelin reactive CD4+ T cells that cross blood-brain-barrier (BBB), and once inside the CNS activate the CNS resident APCs and recruit more infiltrating lymphocytes to the CNS [9]. Such coordinated activities of APCs and CD4+ T cells leads to the release of inflammatory cytokines that in turn are responsible for demyelination, axonal loss and neurological insults. This same scenario occurs in passively induced EAE, except that the encephalitogenic T cells are isolated from the lymphoid tissues of an animal immunized with myelin antigen, restimulated in vitro and then transferred into a naïve recipient in which the T cells cross the BBB and initiate inflammation [9].

2 Materials

2.1 Active EAE Induction

The reagents for active EAE induction outlined below are based on ref. [9].

1. PBS, without calcium or magnesium.
2. DMSO, anhydrous >99 % (*see* **Note 1**).
3. Mice, 6–12 weeks old. The strain used should be determined by the investigator. Commonly used vendors are The Jackson Laboratory, Taconic, Charles River Laboratories and Harlan (*see* **Notes 2–4**).
4. CNS tissue homogenate, purified myelin protein or synthetic myelin peptide (as determined by the investigator) (*see* **Note 5**).
5. Complete Freund's adjuvant (CFA). Store at 4 °C (*see* **Note 6**).
6. Pertussis toxin, lyophilized in buffer (List Biological Laboratories Inc.).
   Resuspend in 1 ml of sterile dH_2O for a concentration of 50 μg/ml and store at 4 °C (*see* **Note 7**).
7. Ovalbumin or irrelevant protein for control immunizations.
8. Anesthesia reagents (optional) for performing subcutaneous (s.c.) immunizations. Multiple protocols for anesthesia suitable for immunizations are available that require different reagents. Many laboratories use a mixture of ketamine and

xylazine (state and federal drug licenses are required to use these reagents), while tribromoethanol or isoflurane are also used by others. Choice of anesthesia should be determined by individual investigator. Be extremely careful when preparing anesthetic for mice, as small errors can result in the death of the animal. Before using anesthesia in mice, always check with your IACUC protocol for approved agents. Note that investigators very experienced with mouse handling may not require the use of anesthesia for s.c. immunizations.

9. Petroleum ophthalmic ointment (necessary only if mice are anesthetized).
10. Vortex, with an attachment capable of holding multiple Eppendorf tubes (optional, depending on the method used for emulsifying adjuvant).
11. 1 ml syringes with 26 G 3/8 needle.
12. Needles: 25 G 5/8 and 30 G 1/2.
13. Eppendorf tubes.
14. Balance scale (0.1 g sensitivity).

2.2 Passive EAE Induction

The reagents for passive EAE induction outlined below are based on ref. [10].

1. PBS, without calcium or magnesium.
2. Hank's balanced salt solution (HBSS).
3. Lympholyte-M or Ficoll-Paque.
4. DMSO, anhydrous >99 %. This reagent is needed only if peptide solubility is limited in PBS (*see* **Note 1**).
5. Mice, 6–12 weeks old. The strain used should be determined by the investigator. Commonly used vendors are The Jackson Laboratory, Taconic, Charles River Laboratories and Harlan (*see* **Notes 2**–**4**).
6. CNS tissue homogenate, purified myelin protein or synthetic myelin peptide (as determined by the investigator) (*see* **Note 5**).
7. CFA. Store at 4 °C (*see* **Note 6**).
8. Pertussis toxin (optional), lyophilized in buffer. Resuspend in 1 ml of sterile dH_2O to a concentration of 50 μg/ml and store at 4 °C (*see* **Note 7**).
9. Anti-mouse CD3 and anti-mouse CD28 antibodies (optional). Some laboratories use these antibodies to activate T cells for adoptive transfer of activated, non-myelin-specific T cells for control recipients.
10. Anesthesia reagents (*see* **item 8**, Subheading 2.1).
11. Petroleum ophthalmic ointment, necessary only if mice are anesthetized.

12. Human or mouse IL-2 (*see* **Note 8**).
13. Mouse IL-23 and anti-IFN-ɣ (optional). These reagents may be used in T cell cultures to promote T_H17 cells that have recently been shown to be highly encephalitogenic on adoptive transfer [25, 26].
14. Complete RPMI 1640 medium, Click's medium, or DMEM can be used, supplemented with 10 % heat-inactivated fetal bovine serum, 1 mM sodium pyruvate, 10 mM nonessential amino acids, 4 mM l-glutamine, 100 U/ml penicillin–streptomycin, and 50 μM 2-mercaptoethanol. Filter through a 0.2 μm filter to sterilize. Store at 4 °C.
15. Ammonium chloride potassium carbonate buffer (ACK lysis buffer): Add 8.29 g NH_4Cl (0.15 M), 1 g $KHCO_3$ (10.0 mM), and 37.2 mg Na_2EDTA (0.1 mM) to 800 ml of dH_2O. Adjust pH to 7.2–7.4 with 1 N HCl and add dH_2O to 1 l. Sterilize through a 0.2 μM filter. Store at 4 °C.
16. Vortex with an attachment capable of holding multiple Eppendorf tubes (optional, depending on the method used for emulsifying adjuvant).
17. 1 ml syringes with a 26 G 3/8 needle.
18. Needles: 25 G 5/8 and 30 G 1/2.
19. 60 × 15-mm petri dishes.
20. Scissors and forceps, sterilized before use.
21. 15 ml conical centrifuge tubes.
22. 50 ml conical centrifuge tubes.
23. Microscope slides for the dispersion of cells from fibrous tissue (*see* **Note 9**).
24. Eppendorf tubes.
25. Wire mesh screens (0.178 mm).
26. Light microscope.
27. Hemocytometer.
28. Balance scale (0.1 g sensitivity).
29. T25 tissue culture flasks.
30. T75 tissue culture flasks.

2.3 Tissue Fixation

1. Two empty 250 ml fluid bags with fluid lines attached.
2. 60 ml syringe and large bore needle.
3. IV stand.
4. Butterfly catheter (23 g) with the needle blunted.
5. Bandage tape.
6. Mosquito hemostats.

7. Small scissors.
8. Jeweler's forceps or equivalent.
9. Scalpel handle and blade.
10. Alm retractor.
11. Glass pan to catch waste fluids.
12. Freshly made 4 % paraformaldehyde (PFA) (*see* **Note 10**).; 10–150 ml per mouse.
13. 0.9 % saline (or preferred flush) 8–25 ml per mouse.
14. Anesthetic (*see* **item 8**, Subheading 2.1).
15. Chemical fume hood.

2.4 Tissue Collection

1. Hank's Balanced Salt Solution (HBSS; Life Technologies).
2. ACK Lysing Buffer (*see* **item 15**, Subheading 2.2) (also available commercially, e.g., Life Technologies).
3. FBS; heat inactivate the complement at 56 °C for 30 min, aliquot and store at −20 °C.
4. Complete Iscove's Modified Dulbecco's Medium (IMDM; Life Technologies): add 10 % of FBS, penicillin (100 U/ml final concentrations), streptomycin (100 μg/ml final concentration), gentamycin (5 mg/ml final concentration), 2-mercaptoethanol (2-ME) (50 μM) to IMDM basal Medium. Filter the Medium with 0.2 μm pore size filters and store at 4 °C.
5. Collagenase IV from *Clostridium histolyticum*: resuspend the lyophilized power with HBSS at 8000 U/ml and store at −20 °C. For 5 ml of collagenase 400 U/ml: dilute 0.250 ml of the stock solution (8000 U/ml) with 4.750 ml of HBSS and keep the solution at 4 °C until the use.
6. Percoll (Sigma-Aldrich).
7. 10 % PFA.
8. Nonidet P-40 (Sigma-Aldrich).
9. FOXP3 Fix&Perm buffer set (BioLegend).
10. Cell scrapers with thin flexible blades (Sarstedt).
11. Homogenizer douce tissue grinder.
12. Sterile scalpels (number 10) (Fisher Scientific).
13. Hemocytometer.

2.5 FACS Analysis

1. 5× PBS: weigh 40 g of NaCl, 14 g of Na_2HPO_4, 0.75 g of KCl, and 0.68 g of KH_2PO_4 and place in a cylinder. Add water to a volume of 1 litre and mix well. Filter the PBS solution with 0.2 μm pore size filter and store at 4 °C.
2. Na_3N solution: weigh 100 mg of sodium azide and place in a cylinder. Add water to a final volume of 100 ml and store at 4 °C.

3. Fluorescent Buffer: prepare 250 ml of 1× PBS by diluting 50 ml of 5× PBS with 200 ml of ultrapure water, add 3 % FCS (7.5 ml) and 1 % Na_3N (2.5 ml), filter (0.2 μm) and store at 4 °C.

2.6 RT-PCR Analysis

1. Murine TLR RT-PCR primers (InvivoGen).
2. RNA Isolation kits such as SV Total RNA Isolation System (Promega) (*see* **Note 11**).
3. ImPromII Reverse Transcriptase (Promega) or Transcriptor Reverse Transcriptase (Roche).

2.7 Protein Analysis

1. Buffers for cellular fractionation:

   Buffer A: 10 mM HEPES–NaOH, pH 7.9, 1.5 mM $MgCl_2$, 10 mM KCl, 0.5 mM DTT, and 0.5 mM PMSF. Store at 4 °C adding DTT and PMSF prior to use.

   Buffer B: 20 mM HEPES–NaOH, pH 7.9, 420 mM NaCl, 1.5 mM $MgCl_2$, 0.2 mM EDTA, 25 % (w/v) glycerol, and 0.5 mM PMSF. Store at 4 °C adding PMSF just prior to use.

   Buffer C: 10 mM HEPES–NaOH, pH 7.9, 50 mM KCl, 0.2 mM EDTA, 20 % (w/v) glycerol, 0.5 mM PMSF, and 0.5 mM DTT. Store at 4 °C adding DTT and PMSF just prior to use.
2. Buffer for brain/spinal cord fractionation: 10 mM Tris–HCL, pH 7.4, 50 mM NaCl, 10 mM $Na_4P_2O_7{\cdot}10H_2O$, 50 mM NaF, 1 % Igepal, 1 mM PMSF, 1 mM Na_3VO_4, 2 μg/ml aprotinin, 2 μg/ml leupeptin, pepstatin 5 μg/ml. Store at 4 °C, adding protease inhibitors, Na_3VO_4 and PMSF just prior to use.

2.8 Tissue Sectioning and Immuno-histochemistry

1. Tinfoil paper.
2. Tissue TEK O.C.T.
3. Glass slides.
4. Proteinase k/trypsin/ chymotrypsin/pepsin/pronase.
5. 10× PBS.
6. 3 % H_2O_2 in 1 % sodium azide/PBS.
7. TBS: 0.15 M NaCl, 0.1 M Tris–HCl, pH 7.5.
8. TBS-T: 0.1 % Triton-X 100 in TBS.
9. 1 % Ovalbumin.
10. BSA.
11. Blocking solution: 3 % goat or donkey serum in TBS-T).
12. TLR-1 and TLR-2 primary antibodies (Imgenex),
13. Neuron specific antibody: NeuN or Alexa 488 conjugated NeuN (Chemicon International) and HuC/D (Molecular Probes),

14. Oligodendrocytes specific antibody: Olig2 (R&D systems),
15. Microglia specific antibody: Iba-1 (Abcam).
16. Astrocytes specific antibody: GFAP (Covance).
17. Secondary antibodies: biotinylated goat anti-rabbit IgG secondary antibody (Vector Laboratories), donkey anti-chicken DyLight 549 (Jackson ImmunoResearch), donkey anti-mouse Alexa 488, donkey anti-rabbit Alexa 594, donkey anti-goat Alexa 647, and donkey anti-rabbit Alexa 488 (Molecular probes).
18. VECTASTAIN avidin biotin complex (ABC) Elite (Vector Laboratories).
19. 3,3′-diaminobenzidine (DAB; Sigma-Aldrich).
20. 10 mM Na Citrate, pH 6.
21. Mounting media.
22. Coverslip.
23. Confocal or fluorescent microscope.
24. Olympus BX60 fluorescence microscope equipped with an Olympus DP50 cooled digital camera.

3 Methods

3.1 Active EAE Induction

3.1.1 Antigen/CFA Emulsion

1. Each mouse will be administered with 200 μl of emulsion containing a 1:1 ratio of antigen/CFA. Owing to loss of some of the viscous emulsion on the walls of the Eppendorf tubes and in the hub of the syringe, excess emulsion should be prepared. Calculate the total volume of emulsion needed by multiplying the number of mice to be immunized by 1.5, and multiply that number by 200 μl. Divide this number by 2 and this gives the volume of antigen (in PBS) and CFA needed. For example, if you want to inject 20 mice, the amount of emulsion to be prepared will be $20 \times 1.5 \times 200 = 6000$ μl or 6 ml. So, you will need 3 ml of peptide or antigen and 3 ml of CFA.
2. Select the total amount of antigen to be administered to each mouse. We recommend using 100 μg of myelin protein or 200 μg of myelin peptide per mouse. Calculate the final concentration of antigen in the emulsion by dividing the selected amount of antigen to be administered to each mouse by 200 μl. For example, immunization of each mouse with 200 μg of peptide requires a final concentration of antigen in the emulsion of 1 mg/ml. In this case, our total emulsion is 6 ml (as calculated above for 20 mice), so we will need 6 mg of peptide or antigen. As the antigen is first diluted in PBS before emulsification, the antigen should be diluted from the stock solution into the PBS

to a concentration that is 2× the final concentration of antigen in the emulsion (2 mg/ml for the example above). So, we can add 2×6 or 12 mg of antigen in 6 ml of PBS. Aliquot 0.5 ml of the antigen/PBS solution into Eppendorf tubes. Additional tubes should be prepared containing either PBS without antigen or PBS containing an irrelevant protein, such as ovalbumin to generate emulsion for control mice.

3. Add an equal volume (0.5 ml) of CFA to each tube. Vortex the stock CFA for 5–10 s to resuspend particulate heat-killed *M. tuberculosis* before pipetting.
4. Emulsify the antigen–CFA mixture by vortexing for 45 min or by an alternative method. Alternative methods for emulsification, such as syringe extrusion or homogenization or sonication are also effective. If using an alternative method, the antigen–CFA mixture can be prepared in a single tube before emulsion rather than multiple Eppendorf tubes (*see* **Note 12**).

3.1.2 Pertussis Toxin

1. Prepare 200 ng of Pertussis toxin in 0.1 ml of PBS per mouse for i.v. injection (however a range of 200–500 ng can be used). To calculate the volume required, multiply 0.1 ml by the number of mice to be injected. Make 0.2 ml extra solution to accommodate some loss in the needle hub.

3.1.3 EAE Induction

1. On day 0, weigh mice. The onset of EAE typically correlates with weight loss, which can be used as an indicator of disease activity. The killing of mice is usually required when weight loss exceeds 20–30 % of initial body weight or severe clinical signs occur. The specific criterion for required euthanasia should be determined by each investigator's Institutional animal care and use committee (IACUC) protocol.
2. Administer pertussis toxin in 0.1 ml of PBS per mouse using a 30 G 1/2 needle. Some investigators administer pertussis toxin by intraperitoneal (i.p.) injection (*see* **Note 13**).
3. Anesthetize mice. Our laboratory injects 250–300 μl of a ketamine–xylazine mixture by i.p. injection. The recommended dosage of this tranquilizer/dissociative agent is 0.02 ml per gram of body weight. Wait for approximately 5 min for the anesthesia to have an effect. Use a front foot toe pinch to assess the level of anesthesia. Do not use a hind foot toe pinch because ketamine/xylazine does not suppress the hind foot reflex. This drug combination will provide approximately 25–30 min of moderate-level anesthesia. Thus, we typically anesthetize ten mice at a time before performing emulsion injections. Apply a small amount of petroleum ophthalmic ointment to eyes to prevent dryness of the cornea.
4. Load a 1 ml syringe with antigen/CFA emulsion (*see* **Note 14**).

5. Inject 50 μl of antigen/CFA emulsion s.c. into two different sites on each hind flank, resulting in four injections per mouse and a total volume of 200 μl emulsion per mouse (*see* **Note 15**).
6. On day 2, administer a second dose of pertussis toxin as described in **step 2**, Subheading 3.1.3. The second dose of pertussis can be administered on day 2 or day 3 post-immunization.
7. On day 7, mice can be reimmunized with antigen/CFA 1 week after the first immunization as described in **steps 3–5**, Subheading 3.1.3. Although our laboratory does not typically perform this step, a second immunization in CFA may increase the incidence and/or severity of EAE. The investigator must confirm that two CFA immunizations are approved by individual investigator's IACUC protocol.
8. Monitor mice for clinical signs and weight loss daily, as weight loss is an indicator of clinical disease. When mice have clinical symptoms of EAE, it is important to place food on the cage floor and monitor the ability of mice to urinate. In some cases, it may be necessary to express the bladder or administer fluids to paralyzed mice. Consult your veterinary staff regarding these techniques. Depending on the scientific question that is under investigation, mice can be monitored for various amounts of time. If the investigators are interested in the acute stage of EAE, then mice can be euthanized shortly after onset. Long term courses (60 days or more) are recommended if the course of clinical disease is under investigation. Clinical signs of EAE usually begin between 9 and 20 days post-immunization depending on the strain and immunogen.

3.2 Passive EAE Induction

1. Follow the **steps 1–4** as described in Subheading 3.1.1.

3.2.1 Antigen/CFA Emulsion

3.2.2 EAE Induction

1. Immunization is performed on day 0. Before doing that, first anesthetize mice as described in **step 3**, Subheading 3.1.3.
2. Load a 1 ml syringe with antigen/CFA emulsion (*see* **Note 14**).
3. Inject 50 μl of antigen/CFA emulsion s.c. into two different sites on each hind flank, resulting in four injections/mouse and a total volume of 200 μl emulsion/mouse. The number of immunized mice depends on the final number of T cells to be transferred per mouse. It is common to transfer between 1×10^6 and 2×10^7 cells per mouse. Usually two donor mice must be immunized to generate enough donor T cells for one recipient, depending on the initial precursor frequency of antigen-specific T cells and their priming efficiency (*see* **Note 15**).
4. Harvest draining lymph nodes (sub-iliac and axillary) and spleens 10 days post-immunization, but it can also be carried out between 7 and 14 days post-immunization.

5. Prepare a single-cell suspension of mononuclear cells (*see* **Note 16**).
6. Centrifuge for 5 min at 500 × *g* at 4 °C and resuspend pooled spleen and lymph node cells in complete media at a concentration of 1×10^7 cells/ml. Add myelin peptide or protein from the stock solution to the appropriate concentration to stimulate optimum proliferation of myelin-specific T cells (*see* **Note 17**).
7. In many passive EAE induction experiments, investigators will proceed directly to the incubation as in **step 8**. However, specific applications may include one or both of the following two optional steps:

   Optional step A: This step generates control recipients that receive nonspecifically activated T cells. One example of the need for control tissues is to provide a baseline when identifying changes in gene expression in the CNS that result from induction of EAE mediated by myelin-specific T cells. For generating control recipients, harvest spleen and lymph node cells from naïve mice as described (*see* **Note 16**). Nonspecifically activate T cells by incubating mononuclear cells in complete media at a concentration of 1×10^7 cells/ml with soluble anti-CD3 (final concentration of 1 μg/ml) and anti-CD28 (final concentration 0.5 μg/ml). Incubate in a 37 °C, 5 % CO_2 incubator for 48–72 h. Transfer activated T cells as described below for transfer of myelin-specific T cells after primary stimulation (*see* Subheading 3.2.3).

   Optional step B: Some investigators may wish to focus on the activity of the recently identified T_H17 cells in EAE. To promote the generation of T_H17 cells in primary T cell cultures, which may increase the severity of passively induced EAE, IL-23 (final concentration 10 ng/ml) and anti-IFN-ɣ (final concentration 10 μg/ml; unpublished observations) may be included during in vitro stimulation.
8. Incubate flasks in a 37 °C, 5 % CO_2 incubator for 72–96 h.
9. Follow Subheading 3.2.3, if transferring antigen-specific T cells after primary in vitro restimulation or Subheading 3.2.4, if transferring antigen-specific T cells after secondary in vitro restimulation. T cells can be transferred after primary restimulation, after secondary restimulation or even after multiple restimulations in vitro. The advantage of transferring T cells after multiple restimulations is that there will be a higher frequency of antigen-specific T cells in the cultures; however, the disadvantage is that some T-cell lines have been reported to lose encephalitogenicity after extensive in vitro culture. Note that T cells activated by anti-CD3 and anti-CD28 antibodies to generate control recipients are transferred after primary stimulation.

3.2.3 Transferring T Cells after Primary Restimulation

1. On day 12, sub-lethally irradiate naïve, syngeneic recipient mice (350–400 rad). The dose of radiation may vary with inbred strains. This step is recommended to increase the sur-

vival of injected cells in the recipient, but is not required in all cases. Calculate the number of recipient mice that will be needed based on the expected yield of cells plated in the culture and the number of cells to be transferred per mouse. The number of transferred cells per mouse ranges in the literature from 1×10^6 to 2×10^7 cells. In mouse strains expressing the male-specific HY antigen, donor male T cells can only be transferred into male mice due to rejection of male T cells in female recipients.

2. On day 13, transfer T cells after primary restimulation. Purify viable cells from T cell cultures (*see* **Note 18**).
3. Resuspend T cells in PBS at the appropriate concentration for injection into mice. No more than 250 μl per mouse should be injected i.v. (up to 500 μl/mouse i.p.). Some investigators also administer pertussis toxin to recipient mice on the day of T cell transfer and 2 days after T cell transfer as described for active EAE induction, as it can promote EAE development. Remember that cells resuspended at high density are prone to lysis as they pass through the 30 G 1/2 needle. Therefore, the density of cells should not exceed 1×10^5 cells/ml. If more than 2×10^7 cells per mouse are being injected, i.p. injections are recommended to accommodate the increased volume needed to minimize cell density. In calculating the amount of cell suspension to be prepared, remember that 100 μl of suspension will remain in the needle hub.

3.2.4 Transferring T Cells after Secondary Restimulation

1. On day 13, add IL-2. After 3 days in primary culture, purify viable cells from T cell cultures (*see* **Note 18**).
2. Resuspend cells in complete media supplemented with 2.5 U/ml of IL-2 to a density of 1×10^6 cells/ml. If skewing toward Th17 cells, IL-23 (10 ng/ml) can be included in the media to promote T cell survival. Pipette 10 ml of resuspended cells per T25 flask. For large numbers of cells, it is more efficient to use larger T75 flasks for this step. In this case, pipette 25 ml of resuspended cells per T75 flask. Incubate for 7 days in a 37 °C, 5 % CO_2 incubator.
3. On day 20, do the in vitro T cell restimulation. Harvest splenocytes and lymph node cells from syngeneic mice for APC to be used in the second restimulation. Prepare mononuclear cells as described (*see* **Note 16**). Note that there is some flexibility in the timing of the second restimulation of T cell lines. Typically it is performed between 10 and 12 days after the primary in vitro restimulation.
4. Irradiate APCs with 2500 rad and keep on ice.
5. Purify viable cells from T cell cultures (*see* **Note 18**). Combine T cells (2×10^6) with irradiated APCs (2×10^7) and antigen

(using the same concentration as determined previously for the primary stimulation- **step 6**, Subheading 3.2.2.) in 10 ml of complete media in T25 flasks. Incubate in a 37 °C, 5 % CO_2 incubator for 3 days.

6. On day 22, sub-lethally irradiate naïve, syngeneic recipient mice (350–400 rad). Calculate the number of recipient mice to be irradiated based on the expected yield of cells plated in the culture and the chosen number of donor cells to transfer to each recipient. The number of cells transferred per mouse ranges in the literature from 1×10^6 to 5×10^7 cells. Our laboratory typically transfers $1–2 \times 10^7$ cells per recipient. The dose of radiation may vary with inbred strains. This step is recommended to increase the survival of injected cells in the recipient, but it is not required in all cases. In mouse strains expressing the male-specific HY antigen, donor male T cells can only be transferred into male mice, due to rejection of male T cells in female recipients.
7. On day 23, transfer T-cell after secondary restimulation. Purify viable cells from the T cell cultures (*see* **Note 18**). Activated T-cells can be transferred either 3 or 4 days post restimulation in vitro. Resuspend antigen-specific T cells in PBS at the appropriate concentration for injection into mice. No more than 250 μl per mouse should be injected i.v.; up to 500 μl per mouse can be injected i.p. Some investigators also administer pertussis toxin to recipient mice on the day of T cell transfer and 2 days after T cell transfer as described for active EAE induction [9], as it can promote EAE development.
8. Monitor clinical signs and weight loss daily as described in **step 8**, Subheading 3.1.3.

3.3 Tissue Fixation

The goal of perfusion tissue fixation is to use the vascular system of a deeply anesthetized animal to deliver fixatives to the tissues of interest. This is the optimal method of tissue preservation since the tissues are fixed before autolysis begins. Perfused tissues are less susceptible to artifacts caused by handling. Techniques for fixation vary depending on the organ and the desired method of processing. Appropriate literature should be consulted to determine the ideal technique for the organ of concern. The following technique is appropriate for harvesting brain and organs with circulation supplied by the left side of the heart. This method combines tissue fixation with euthanasia and can only be performed as a terminal procedure.

3.3.1 Experimental Setup

1. 4 % PFA must be made fresh on the day of the procedure in a chemical fume hood.
2. The perfusion process should be performed in a chemical fume hood for the best personal protection. Perfusion can be per-

formed in a well-ventilated area if a chemical fume hood is not available.

3. Fill one IV bag with the fresh 4 % PFA using a 60 ml syringe and a large bore needle.
4. Fill the second IV bag with the flush3/11.
5. Set up the IV lines in a "piggy back" fashion with the blunt butterfly needle attached to the end.
6. Hang the bags from the IV pole at least 30 cm, but not more than 120 cm above the animal.
7. Flush any air bubbles out of the IV line.
8. Use the saline to flush any fixative out of the line before starting.

3.3.2 Anesthesia

1. Barbiturates like pentobarbital (100 mg/kg) provide the best anesthesia for perfusion.
2. Pentobarbital should be diluted to 15 mg/ml by adding 0.3 ml undiluted pentobarbital (50 mg/ml) to 0.7 ml sterile saline (1 ml total). This dilution will yield a volume of 0.2 ml for a 30 g mouse.
3. Administer the anesthetic to the mouse and allow the animal to rest in a cage alone in a dark, quiet environment. The withdrawal reflex must be absent in each pelvic limb before the perfusion can begin.

3.3.3 Perfusion

1. Place the mouse on its back and tape each limb down to the glass pan.
2. Check the withdrawal reflex once more to assure adequate depth of anesthesia.
3. Make a midline skin incision from the thoracic inlet to the pelvis.
4. Use scissors to carefully open the abdomen and expose the liver and intestine.
5. Grasp the tip of the sternum (xiphoid process) with forceps and make a 1 cm incision in the midline of the sternum (too large an incision risks cutting the major vessels as they enter the thoracic inlet).
6. Place the Alm retractor into the chest incision and adjust the knob until the sternum is held open widely enough to visualize the heart.
7. Grasp the heart gently by the right ventricle and lift it to the midline and slightly out of the chest.
8. Use the scissors to make a small nick in the apex of the left ventricle. The left ventricle is thicker and lighter pink than the right ventricle.

9. Place the blunt butterfly needle into the heart incision toward the aorta and clamp in place with hemostats. (Blunt needle can be inserted directly into apex of ventricle without first making incision with scissors.)
10. Start the flow of the flush and watch the chamber on the IV line to assure that the fluid is dripping.
11. Use scissors to cut the right auricle to allow the perfusate to exit the circulation.
12. When the fluid exiting the mouse is clear of blood, close the flush line and open the 4 % PFA line.
13. Muscle contractions and blanching of the liver and mesenteric blood vessels are signs of good perfusion.
14. Perfusion is complete when all muscle contractions have stopped, the liver and mesenteric vessels are blanched and the desired amount of preservative has passed through the circulatory system. The mouse should be stiff.
15. PFA and other fixatives must be collected after the perfusion and stored appropriately as hazardous chemical waste. Contact Environmental Health and Safety for disposal procedures.

3.3.4 Dissection

1. Remove the head using a pair of scissors.
2. Make a midline incision along the integument from the neck to the nose and expose the skull.
3. Trim off the remaining neck muscle so that the base of the skull is exposed; remove any residual muscle using scissor or rongeurs.
4. Place the sharp end of a pair of iris scissors into the foramen magnum on one side, carefully sliding the scissors along the inner surface of the skull.
5. Next, make a cut extending to the distal edge of the posterior skull surface. Make an identical cut on the contralateral side. Use the rongeurs to clear away the skull around the cerebellum.
6. Carefully slide the scissors along the inner surface of the skull as the tip travels from the dorsal distal posterior corner to the distal frontal edge of the skull, lifting up on the blade as you are cutting to prevent damage to the brain. Repeat for opposite side.
7. Using rongeurs peel the dorsal surface of the skull away from the brain. Trim away the sides of the skull using rongeurs as well.
8. Using a spatula, sever the olfactory bulbs and nervous connections along the ventral surface of the brain.
9. Gently tease the brain away from the head, trimming any dura that still connects the brain to the skull using iris scissors.

10. Remove the brain and place it in a vial of fixative containing fluid at least 10× the volume of the brain itself. Swirl the vial occasionally.

3.3.5 Post-fixation and Storage

1. Keep the brain in fixative for 24 h at 4 °C, swirling occasionally.
2. After 24 h, wash the brain with phosphate buffered saline by exchanging the media 3 times and swirling each time.
3. Brains can then be stored in PBS or HEPES Buffered Hanks Solution (HBHS) with sodium azide and kept at 4 °C.

3.4 Tissue Collection

3.4.1 Brain Infiltrate Leucocytes

1. Prepare 5 ml of collagenase IV 400 U/ml in HBSS buffer for up to 400 mg tissue.
2. Anesthetize mice and remove the brain. Weight the tissue in 1 ml of cold HBSS to make sure the 400 mg limit per digestion is not exceeded.
3. Place the brain on the lid of a Petri dish and cut it into small pieces using a scalpel.
4. Add 1 ml of collagenase in HBSS and pipette pieces back into an appropriate-sized tube. Rinse with the remaining collagenase solution.
5. Incubate in closed tubes for 30 min at 37 °C to allow the enzymatic disaggregation.
6. After this incubation, dilute the cell suspension with 10 ml of 10 % FBS-IMDM to neutralize the collagenase activity. Gently mix the suspension by moving up and down with a pipette (*see* **Note 19**).
7. Apply the cell suspension to a 100 μm nylon cell strainer, placed on a 50 ml tube, and rinse it with complete medium.
8. Centrifuge the cell suspension at 580×*g* for 10 min at room temperature. Then, carefully remove the supernatant and resuspend the cell pellet in 2 ml of ACK Lysing Buffer.
9. Incubate the sample for 5 min at room temperature. Lysis of the red cells should be evident during this incubation.
10. Add 10 ml of 10 % FBS-IMDM, spin the cells and wash once with additional 10 % FBS-IMDM. After this step the pellet should become white.
11. Proceed with a Percoll gradient (*see* **Note 20**). Two brains are applied to each Percoll gradient.
12. Prepare a stock isotonic Percoll [27], by mixing nine parts of Percoll with one part of 10× PBS. Further dilute 100 % SIP to 70 % and 30 % with 1× HBSS (*see* **Note 21**).
13. Resuspend the brain homogenates in 3 ml of 70 % Percoll and place in the bottom of 15 ml tube.

14. Slowly layer 4 ml of 30 % Percoll on top of the 70 % SIP, avoiding mixing the solutions (*see* **Note 22**).
15. Centrifuge at 450×*g* for 30 min at 18 °C, with no brake so that the interphase is not disturbed.
16. After the centrifugation, a viscous layer of myelin and debris should accumulate at the top of the tube. The next layer is a Percoll 30 % and the next one is the 30–70 % interphase that should finally contain a white ring of mononuclear cells.
17. To decrease contamination, gently remove the layer of debris from the top of the tube and discard it.
18. Collect the 70–30 % interphase into a clean conical tube containing 10 ml of 1X PBS. Ensure that the interphase containing Percoll is diluted approximately threefold, mix by inversion and centrifuge for 7 min at 300×*g*, at 18 °C.
19. Carefully aspirate the supernatant, resuspend the pellet in 3 ml of media and count the cells using a hemocytometer (*see* **Note 23**).

3.4.2 Spinal Cord Infiltrate Leucocytes

1. Prepare 2 ml of collagenase IV 400 U/ml in HBSS buffer for up to one spinal cord.
2. Anesthetize mice and remove the spinal cord. Place it on the lid of Petri dish and cut the tissue into small pieces using a scalpel.
3. Add collagenase solution and incubate for 30 min at 37 °C.
4. After the incubation, aspirate the collagenase solution and dissociate the tissue using the plunger of a 2 ml syringe.
5. Gently homogenize by moving the cell suspension up and down with a 10 ml syringe.
6. Apply the cell suspension to a 100 μm nylon cell strainer, placed on a 50 ml tube, and add 10 ml of IMDM with 10 % of FCS to neutralize the collagenase activity.
7. Centrifuge at 580×*g* for 10 min at room temperature and carefully aspirate the supernatant.
8. Resuspend the cell pellet in 1 ml of ACK Lysing Buffer for 5 min and then wash with 10 % FBS-IMDM by centrifugation at 580×*g* for 10 min.
9. Proceed with a Percoll gradient as described in **steps 10–17**, Subheading 3.4.1. Apply two spinal cords to each Percoll gradient tube.

3.4.3 Cervical Lymph Nodes Cell Suspension

1. Prepare 1 ml of collagenase IV 400 U/ml in HBSS buffer for up to one lymph node and vortex.
2. Anesthetize the mice and remove the cervical lymph nodes. Place the tissue on the lid of a Petri dish and carefully separate surrounding fat (*see* **Note 24**).

3. Add collagenase solution and incubate for 40 min at 37 °C.
4. After the incubation, aspirate the collagenase solution and gently dissociate the lymph nodes using the plunger of a 2 ml syringe.
5. Homogenize by moving the cell suspension up and down with a 10 ml syringe.
6. Apply the cell suspension to a 40 μm nylon cell strainer, placed on a 50 ml tube, and add 10 % FBS-IMDM to neutralize the collagenase activity.
7. Centrifuge at 580 × *g* for 10 min at room temperature and carefully decant the supernatant.
8. Resuspend the pellet in 1 ml of complete medium and count the cells using the hemocytometer.

3.5 FACS Analysis

1. Aliquot 0.5–1 × 10^6 cells into each assay tube and wash once with fluorescent buffer and centrifuge at 580 × *g*, for 10 min.
2. To perform the extracellular staining resuspend the cells in 50 μl of fluorescent buffer with purified anti-mouse CD16/CD32 to block the Fc binding sites and incubate on ice for 20 min.
3. Add the specific antibodies against the immune cells surface antigens, using appropriate fluorochrome combinations by choosing them according to the particular settings of your flow cytometer. The most common staining for the infiltrate analysis are: $CD4^+CD25^+Foxp3^+$ (Regulatory T cells), $CD4^+CD25^-Rorc^+$ (TH17 T cells), $CD8^+$ T cells, $CD11b^+CD11c^+$ (myeloid dendritic cells), $pDCA1^+$ (plasmacytoid dendritic cells), $F4/80^+$ (macrophages), and $CD11b^+Ly6G^+$ (neutrophils) (*see* **Note 25**).
4. Incubate the stained samples for 30 min at 4 °C in the dark to prevent nonspecific antibody binding.
5. Remove any unbound antibody by washing the cells in fluorescent buffer and centrifuge at 580 × *g* for 10 min, at 4 °C.
6. Decant the supernatant and resuspend the pellet with fluorescent buffer containing 1 % PFA and store at 4 °C. Analyze the sample by flow cytometry with appropriate software.
7. Alternatively, cells can be resuspended in Fix & Perm buffer to perform the intracellular staining. Cells should be fixed to ensure stability of soluble antigen and to retain the target protein in the original cellular location. In this case it is necessary to permeabilize cells prior to the detection of intracellular antigens.
8. Incubate samples in the Fix & Perm buffer for 30 min at 4 °C, mixing every 15 min in order to maintain a homogenous single cell suspension.

9. Centrifuge and resuspend the pellet in detergent-based permeabilizing reagent (perm buffer) and incubate for 30 min at 4 °C.
10. After the incubation, centrifuge and resuspend the cell pellet with perm buffer (50 µl/sample) and add 10 µl of fluorochrome-conjugated antibody at a specific pre-diluted and titrated concentration, and mix well. Incubate the cells for 30 min at 4 °C in the dark (*see* **Note 26**).
11. Remove any unbound antibody by washing the cells with at least 300 µl of fluorescent buffer by centrifugation at 500 × *g* for 10 min, discard the supernatant and resuspend the cells with fluorescent buffer 1 % PFA.
12. Acquire the samples by a flow cytometer and analyze the data using specific software.

3.6 RT-PCR Analysis

Toll-like Receptors are predominantly expressed in tissues involved in immune function, such as spleen, lymph nodes and peripheral blood leukocytes, mononuclear cells of the brain and spinal cord, other CNS cell types, as well as tissues exposed to the external environment such as lung and the gastrointestinal tract. Their expression profiles vary among tissues and cell types. Murine TLR RT-PCR primers are commercially available to determine the mRNA expression pattern of TLRs. They can be used to analyze the expression of endogenous TLR genes from normal as well as EAE induced mice. TLR RT-PCR primers are provided as pairs for each individual TLR or as a set containing a primer pair for nine murine TLRs. The size of the amplified fragments varies from 300 to 800 bp depending on the primer for different types of TLRs.

1. Extract mRNA from tissues or cell (brain, spinal cord, spleen, lymph nodes or whole blood) of EAE induced mice using commercially available RNA Isolation kits.
2. Convert mRNA to cDNA by retrotranscription using reverse transcriptase according to the manufacturer's protocol.
3. PCR is performed in 50 µl reaction volumes containing the following: 4 µl MgCl2 (25 mM), 4 µl dNTPs (2.5 mM each), 5 µl 10× buffer (provided with Taq polymerase), 2 µl primer pair (25 µM), 5 µl cDNA or 1 µl positive control dsDNA (10 ng/µl), 0.25 µl Taq polymerase (5U/µl), 30 µl H_2O.
4. PCR conditions are the following: (95 °C for 2 min, 95 °C for 30 sec, 60 °C for 30 sec, 72 °C for 2 min) for 35 cycles followed by 72 °C for 5 min and then 16 °C overnight.
5. Assess RT-PCR products on 2 % agarose gel.

3.7 Protein Analysis

3.7.1 Cellular Fractionation

1. Following cell isolation (plated at 2×10^5 cells/ml), resuspend cells in 1 ml of ice-cold hypotonic Buffer A. If cells are in culture, remove culture media and wash cells in ice-cold PBS. Remove PBS and scrape cells from tissue culture plates/flasks into 1 ml of ice-cold hypotonic Buffer A.
2. Centrifuge sample at $21{,}000 \times g$ for 10 min at 4 °C.
3. Carefully discard the supernatants and lyse the pellet for 10 min on ice in hypotonic buffer A (30 μl) containing 0.1 % (v/v) Nonidet P-40 on ice (*see* **Note 27**).
4. Centrifuge the lysates at $21{,}000 \times g$ for 10 min at 4 °C. The resulting supernatants constitute cytosolic fractions. Determine protein concentrations via Bradford assay, equalize samples in sample buffer to assess protein targets via Western immunoblotting.
5. Resuspend the pellets with trituration (5–10 times) in Buffer B (25 μl) and incubate the sample for 15 min on ice.
6. Centrifuge the sample at $21{,}000 \times g$ for 10 min at 4 °C, and remove the supernatants into Buffer C (75 μl) and mix with trituration (5–10 times) (*see* **Note 28**). These samples constitute nuclear-enriched extracts. Determine protein concentrations via Bradford assay; equalize the samples in sample buffer to assess the protein expression of TLR signaling targets via Western immunoblotting.

3.7.2 Brain and Spinal Cord Fractionation

1. Prechill glass douce homogenizer on ice. Place brain/spinal cord samples (20–80 mg) on an ice-cold lid of a Petri dish and cross-chop using a sterile scalpel. Transfer tissue to homogenizer and homogenize on ice with 10–15 up and down strokes in ice-cold brain/spinal cord lysis buffer (200–800 μl) using a 1 ml glass pestle in a douce homogenizer.
2. Transfer homogenate from the glass tube to prechilled 1.5 ml centrifuge tubes using a pasteur pipette.
3. Centrifuge lysates at $16{,}000 \times g$ for 15 min at 4 °C.
4. Transfer the supernatants to ultracentrifuge tubes and resuspend the pellet (representing nuclear-enriched fractions) in ice-cold lysis buffer (100 μl) with trituration (5–10 times) (*see* **Note 28**). Such samples constitute nuclear-enriched extracts. Determine protein concentrations via Bradford assay; equalize samples in sample buffer to assess the expression profile of nuclear protein targets via Western immunoblotting.
5. Centrifuge the remaining supernatants at $100{,}000 \times g$ for 1 h.
6. Transfer the supernatants to prechilled fresh centrifuge tubes. Such samples constitute cytosolic fractions. Determine protein concentrations, equalize in sample buffer and assess the expression profile of cytosolic protein targets via Western immunoblotting.

7. Resuspend the remaining pellet in ice-cold lysis buffer (200 µl) (*see* **Note 28**) and sonicate for 5 s on ice. These fractions are enriched with membrane-associated proteins for Western immunoblotting analysis.

3.8 Tissue Sectioning and Immunohistochemistry

3.8.1 Sectioning

Cryosections are the first choice of immunohistochemistry (IHC). It is the best approach in terms of preserving the antigenicity of target antigens. The disadvantage of cryosections is that it can result in poor morphology and poor resolution in high power image. However, in general, cryosection derived images can still reflect tissue structure with required significance and has the capacity to satisfy publisher's requirement. The following method for brain sectioning is based on ref. [28].

1. Making frozen blocks is the first step in cryosection. Prepare some block molds that look like a cylinder approximately 1.5 cm in diameter, made with tinfoil paper, filled with Tissue Tek O.C.T. (approximately 1–1.5 cm in depth).
2. Sample tissue should be cut in appropriate size and placed in the OCT cylinder bottom in the correct orientation.
3. Immerse the OCT cylinder into liquid nitrogen for 2–3 min.
4. The blocks can now be stored at −80 °C for future use or moved to the cryostat to cut sections.
5. Samples of muscle or mucosa can be sectioned at 4–6 µm; brain and spinal cord tissue should be sectioned at 10–40 µm.
6. Cryosections can be picked up by glass slides directly from the cryostat; labeled properly and allowed to dry at room temperature overnight, or, if urgent, the sections can be dried with a power fan within 1 h.
7. Once dry, sections can be wrapped with tinfoil and stored at −80 °C for future use, or stored in a box with lid at 4 °C temporally for up to 1 week, or, moved to staining stage.

3.8.2 Immunohistochemistry for TLR Detection

This protocol has been used to detect TLR1/TLR2 in mouse brain sections and is based on methods from ref. 29.

1. Immunohistochemical staining could be performed on free-floating 25 µm sections pretreated with 0.6 % H_2O_2 in TBS for 30 min to block endogenous peroxidase activity. To prevent or block nonspecific binding incubate for 30 min in blocking solution (*see* **Note 29** and **30**).
2. Then rinse the sections and incubate with the appropriate dilutions of primary antibody (TLR-1 1:500; TLR-2 1:100) in blocking solution at 4 °C for 48 h.
3. Then incubate the tissue sections for 1 h with biotinylated goat anti-rabbit IgG secondary antibody (1:500) in blocking solution and then rinsed in TBS.

4. To visualize use VECTASTAIN avidin biotin complex elite with 0.5 mg/ml DAB, enhanced with 0.01 % H_2O_2 and 0.04 % NiCl.
5. Sections can then be analyzed on an Olympus BX60 fluorescence microscope equipped with an Olympus DP50 cooled digital camera or other suitable settings.

3.8.3 Immunohistochemistry for TLRs in Specific Cell Types

1. To identify the cell type specific localisation of TLRs, multi-immunofluorescence staining can be performed. Nonspecific binding needs to be blocked by incubating for 30 min in blocking solution.
2. TLR antibodies (TLR1 or TLR2; *see* **step 2**, Subheading 3.8.2) can then be incubated simultaneously with antibodies against specific markers for neurons (NeuN, use at 1:1000; or Alexa 488 conjugated NeuN, use at 1:1000; and HuC/D, use at 1:500), oligodendrocytes (Olig2, use at 1:1000), microglia (Iba-1, use at 1:1000), and astrocytes (GFAP, use at 1:1000) diluted in blocking solution for 48 h at 4 °C. Samples stained for HuC/D were subjected to sodium citrate antigen retrieval in 10 mM Na Citrate for 30 min at 80 °C prior to blocking.
3. Immunoreactivity can be visualized via appropriate combinations of the following secondary antibodies: donkey anti-chicken DyLight 549, donkey anti-mouse Alexa 488, donkey anti rabbit Alexa 594, donkey anti-goat Alexa 647, and donkey anti-rabbit Alexa 488 (all used at 1:1000 in blocking solution).
4. Multichannel confocal images can be captured with a confocal microscope with channel settings appropriate to the fluorophores present.

4 Notes

1. This reagent (DMSO) is needed only if peptide solubility is limited in PBS.
2. It is important to use age-matched mice in experimental groups since susceptibility to disease can vary with age in some strains.
3. EAE susceptibility can also vary with gender in certain mouse strains.
4. All experiments using mice should be performed in accordance with the guidelines of each individual investigator's Institutional Animal Care and Use Committee.
5. EAE induction with whole protein may be different compared to EAE induction with defined peptides because synthetic peptides may not precisely mimic the naturally processed epitopes

of the protein. The purification of myelin proteins such as MBP, recombinant MOG, or recombinant proteolipid protein can be performed as described. Since immune tolerance mechanisms shape the repertoire of myelin-specific T cells in the periphery, heterologous antigens are frequently more immunogenic and effective in EAE induction than homologous antigens (provided that the heterologous antigens elicit cross reactive T cells capable of recognizing the myelin antigens expressed in the animal). Stock solutions of myelin protein or peptide prepared in PBS are preferable; however, myelin proteins are usually resuspended in sodium acetate buffer (pH 3) owing to low solubility in PBS. The minimum concentration of peptide stocks made in DMSO should equal 20 mg/ml to avoid diluting large amounts of DMSO in working solutions. Store peptide or protein stocks at −20 °C.

6. CFA contains heat-killed *Mycobacterium tuberculosis* that stimulates the innate immune response, hence avoid inhalation and contact with skin and eyes. EAE induction in mice typically requires CFA, as the *M. tuberculosis* in the emulsion is a powerful stimulus for priming the immune system. An adjuvant containing bacterial components such as CFA is recommended to promote the development of TH_1 and/or TH_{17} [25] versus TH_2 cells. The concentration of *Mycobacterium tuberculosis* in the CFA for EAE induction ranges in the literature from 1 to 5 mg/ml. Investigators can assess the optimal *M. tuberculosis* concentration for EAE induction by titrating bacteria in incomplete Freund's adjuvant (IFA). CpG oligonucleotides have also been shown to act as innate immune stimulants that can replace CFA in some models of EAE. Although some rat models of EAE can be induced using IFA, immunization in IFA has been shown to be tolerogenic in other models of EAE. This discrepancy could reflect differences in the preparations of antigen emulsified in IFA in these studies.
7. It has been reported that different sources or batches of pertussis toxin can influence the effectiveness of EAE induction. Toxin derived from *Bordetella pertussis* has many biological effects. Avoid inhalation, ingestion and contact with skin, eyes and mucus membranes. Active induction of EAE in most mouse models requires administration of pertussis toxin.
8. Multiple vendors, including eBioscience, BD Biosciences and R&D Systems supply human IL-2; human IL-2 is also available without charge to investigators with federally sponsored research grants in the USA.
9. To remove glass shards from slides that can cause cell lysis, rub the frosted sides of two slides together for 15 s while submerged in H_2O and rinse in 70 % ethanol. When the slides dry, autoclave to sterilize.

10. Preparation of 4 % PFA from powder:
    (a) Measure 100 ml Phosphate Buffered Saline (PBS) into a measuring cylinder. Pour into the conical flask containing 4 g of paraformaldehyde. Cover with Parafilm and transfer to the fume hood: thoroughly shake—take care not to splash paraformaldehyde—it is a rapid fixer and is TOXIC.
    (b) Place flask on top of the hotplate/stirrer inside the fume cupboard and set the heat control to 7 with moderate stirring. Allow the solution to warm up—it will turn from being cloudy to clear when ready. Inspect regularly to avoid overheating and consequent spilling.
    (c) When the paraformaldehyde has dissolved, switch off the heat but leave to stir: do not handle for safety reasons. Allow to cool.
    (d) When cooled, transfer the fixative to a 4 °C refrigerator. Label appropriately and date.

Important! Avoid inhalation and any type of contact with the body. Wear gloves and goggles while preparing this.

11. Ensure that RNA isolation procedures include DNAse treatment to achieve high pure RNA and to avoid contamination with genomic DNA.
12. Different methods of preparing emulsions have been reported to affect the manifestation of EAE. Low incidence of EAE induction was reported as follows:
    (a) When *antigen concentration* in emulsion is not optimal for priming in vivo. The optimal antigen concentration for in vivo priming is determined empirically. Vary the concentration of antigen in the emulsion for more effective priming (concentrations range from 10 to 300 μg).
    (b) Using suboptimal *concentration of M. tuberculosis in CFA*. Titrate the concentration of *M. tuberculosis* (clone H37RA is recommended) in either IFA or CFA. The range that investigators typically use is 1–5 mg/ml.
    (c) *Poor antigen/CFA emulsification*. The solution should be uniform (no separation of phases), white, stiff and viscous. If using the vortex method, be sure to emulsify for a full 45 min. To ensure the appropriate concentration of *M. tuberculosis*, be sure to vortex the CFA well to resuspend particulate material before pipetting into the tube. If disease is still not induced, attempt a different emulsification method.
13. To avoid poor pertussis toxin injections ensure that the needle has entered the vein by detecting no resistance when injecting intravenously. Wait for 2–3 s before removing the needle after

the injection; a small amount of blood should be visible when the needle is removed. Alternatively, change the timing of the second dose or inject pertussis toxin i.p.

14. CFA emulsions are extremely viscous and are difficult to load into a syringe. Slowly load the syringe without using the needle. Be careful to avoid introducing air into the syringe, which will form bubbles in the emulsion. Place a 25 G 5/8 needle on the syringe and remove any air bubbles by gently tapping the syringe and expelling air through the needle.
15. *Poor injection of emulsion*: Ensure syringe with emulsion does not contain air bubbles. While injecting s.c., a bulbous mass should form under the skin and persist for several weeks. Check immunization site 2 weeks post-immunization for the presence of the emulsion. If the emulsion is not visible, insufficient emulsion may have been injected. Do not inject the emulsion directly over the subiliac (inguinal) lymph nodes (for location and names of lymph nodes, *see* ref. [30] to avoid collecting some CFA while harvesting lymph nodes. Contaminating CFA present in the culture of mononuclear cells can result in nonspecific proliferation.
16. Preparation of mononuclear cell suspensions from spleen and lymph nodes (modified from ref. [31]) is as follows:
    (a) Place freshly isolated spleens or lymph nodes in 60 × 15-mm Petri dishes that contain 3 ml of HBSS. Place a spleen between the frosted sides of two autoclaved microscope slides and gently rub back and forth applying slight pressure to disperse spleen cells. Rinse the spleen cells from the slide into the Petri dish using 3 ml of HBSS. Transfer the cell suspension through a wire mesh screen to a 15 ml conical tube. Rinse the petri dish with 3 ml of HBSS and add to the 15 ml conical tube that contains the spleen cells. An alternative method to disperse cells from organs is to use a plunger from a 6 ml syringe and wire mesh screens.
    (b) Wash lymph nodes to remove CFA contamination by placing tissue on a wire mesh screen on top of a 15 ml conical tube and pipetting 10 ml of HBSS through the screen. Transfer the lymph nodes to a 60 × 15-mm petri dish containing 3 ml of HBSS and tease apart with two forceps to disperse cells.
    (c) Pipette the cell suspensions through a wire mesh screen into 15 ml conical tubes (to remove fibrous tissue). Wash the petri dish with 5 ml of HBSS and transfer to the same conical tube. Pool spleen and lymph node cells.
    (d) Centrifuge for 5 min at 500 × *g* at 4 °C. Discard supernatant.

(e) Resuspend the cell pellet in ACK lysis buffer using 1 ml per donor mouse to lyse red blood cells.

(f) Incubate on ice for 5 min.

(g) Add 9 ml of complete media and mix by pipetting to stop cell lysis. Let cell debris settle to the bottom of the tube for 2 min. Transfer cells to a new 15 ml conical tube.

(h) Centrifuge for 5 min at 500 × *g* at 4 °C. Discard supernatant.

(i) Resuspend cells in 2 ml of complete media, count and store on ice to maintain cell viability.

17. Ensure that protein or peptide stocks are sterile, or filter the media through a 0.2 μm filter after addition of antigen. Typical concentrations of peptides used for in vitro restimulation range from 5 to 50 μM, but vary depending on the mouse strain and antigen. Therefore, the concentration of antigen that is optimal for T cell stimulation should be determined by individual investigators. Aliquot 10 ml of cell suspension per T25 flask. Scaling up to larger flasks for restimulation of large cell numbers can decrease cell yield.

18. Procedures for removal of dead cells from T-cell cultures (modified from ref. [31]) is based on differences in density between live and dead cells. Lympholyte-M, or alternatively Ficoll-Paque, allows dead cells that have a higher density than live cells to centrifuge through the high-density media and pellet at the bottom of the tube, while live cells are retained at the interface of the Lympholyte-M gradient. Lympholyte-M is designed to be used at room temperature. For optimal live cell recovery, take care to ensure that cell suspensions, media and the centrifuge are at room temperature.

(a) Harvest cells from T25 flasks and pool in 50 ml conical tubes.

(b) Centrifuge for 5 min at 500 × *g* at 4 °C. Discard supernatant. Resuspend $0.5–1 \times 10^8$ cells in 2 ml of HBSS or $1–5 \times 10^8$ cells in 5 ml of HBSS.

(c) In 15 ml conical tubes, add a volume of Lympholyte-M equal to the volume of the resuspended cells (e.g., 2 ml if cells are in 2 ml of HBSS). Carefully layer the cell suspension on top of the Lympholyte-M media.

(d) Centrifuge for 10 min, at room temperature (22 °C), at 500 × *g*, without a brake.

(e) Carefully harvest cells from the interface between Lympholyte-M and HBSS using a 10 ml pipette. Transfer cells to a new tube.

(f) For $<10^8$ cells, pipette 10 ml of complete media (40 ml for $>10^8$ cells) to the cells harvested from the interface of the gradient. Centrifuge for 5 min at $500 \times g$ at 4 °C. Discard supernatant.

(g) Resuspend cells in 2 ml of complete media, count and store on ice to retain cell viability.

19. Do not extend the tissue incubation with collagenase over the prescribed time to avoid the cell lysis. It is recommended to add medium with 10 % FCS in order to inactivate the enzyme activity.
20. Before proceeding to Percoll gradient make a single cell suspension as complete as possible. Cell clumps have more surface area, are less dense and thus they will not partition correctly in the Percoll gradient.
21. Keep in mind that Percoll should be used at room temperature; if used cold, the cells tend to clump and cell separation is less efficient.
22. The most critical step in the Percoll procedure is the creation of two different phases, thus use a pipette-aid set in the gravity mode avoiding mixing of the 70 and 30 % solutions. A very clear flat line should be visible at the 70–30 % junction. If no interphase is observed the yield of cells will likely be very low, making further analysis extremely difficult.
23. The expected yield is $1–2 \times 10^6$ cells per brain. However, an inflamed brain would have a much higher number of infiltrating immune cells.
24. Remove the fat around lymph nodes in order to prevent a possible lysis of the cells.
25. As in any staining procedure, it is imperative that all antibodies should be accurately titrated to assess the optimal dilution starting from the manufacturer's suggested concentration. For a negative control, a separate set of cells should be stained with an isotype control antibody.
26. Antibodies should be prepared in permeabilization buffer to ensure the cells remain permeable. If an unconjugated primary antibody was used, incubation with an appropriate secondary antibody should occur, diluting the secondary antibody in permeabilization reagent and incubating for 30 min in the dark. When gating on cell populations, the light scatter profiles of the cells on the flow cytometer will change after the permeabilization.
27. Resuspend the pellet with gentle trituration using a pipette.
28. Scale the volume of buffer downwards depending the relative size of the pellet achieved following centrifugation.

29. For paraffin sections, antigen retrieval can be achieved by boiling the sections in 10 mM sodium citrate buffer (pH 6.0) for 10 min. Nonspecific binding could be blocked for 30 min in blocking solution (1 % horse serum, 3 % bovine serum albumin, 0.1 % NaN3 in PBS).
30. Keep in mind that slightly higher concentration and longer treatment with Triton X-100 used for antigen retrieval could sometimes destroy the antigen when the antigen is localized on the cell surface (e.g., TLRs).

Acknowledgements

Francesca Fallarino's lab is supported by Telethon Research Grant GGP14042. Research undertaken in the Downer laboratory is supported by the Strategic Research Fund (SRF) and Translational Research Access Programme (TRAP), the College of Medicine and Health (University College Cork), the Department of Anatomy and Neuroscience (UCC), The Physiological Society (UK) and the British Neuropathological Society. Research in Bruno Gran's laboratory is supported by Fondazione Italiana Sclerosi Multipla (FISM) and the Multiple Sclerosis International Federation (MSIF). Md Jakir Hossain is supported by a McDonald fellowship from MSIF jointly funded by MSIF and National Multiple Sclerosis Society (NMSS, USA).

References

1. Steinman L, Zamvil SS (2006) How to successfully apply animal studies in experimental allergic encephalomyelitis to research on multiple sclerosis. Ann Neurol 60:12–21
2. O'Brien K et al (2008) Role of the innate immune system in autoimmune inflammatory demyelination. Curr Med Chem 15: 1105–1115
3. Farooqi N, Gran B, Constantinescu CS (2010) Are current disease-modifying therapeutics in multiple sclerosis justified on the basis of studies in experimental autoimmune encephalomyelitis? J Neurochem 115:829–844
4. Constantinescu CS et al (2011) Experimental autoimmune encephalomyelitis (EAE) as a model for multiple sclerosis (MS). Br J Pharmacol 164:1079–1106
5. Hart BA, Gran B, Weissert R (2011) EAE: imperfect but useful models of multiple sclerosis. Trends Mol Med 17:119–125
6. Batoulis H et al (2011) Experimental autoimmune encephalomyelitis—achievements and prospective advances. APMIS 119:819–830
7. Mix E et al (2010) Animal models of multiple sclerosis—potentials and limitations. Prog Neurobiol 92:386–404
8. Mannara F et al (2012) Passive experimental autoimmune encephalomyelitis in C57BL/6 with MOG: evidence of involvement of B cells. PLoS One 7, e52361
9. Stromnes IM, Goverman JM (2006) Active induction of experimental allergic encephalomyelitis. Nat Protoc 1:1810–1819
10. Stromnes IM, Goverman JM (2006) Passive induction of experimental allergic encephalomyelitis. Nat Protoc 1:1952–1960
11. Bettelli E et al (2003) Myelin oligodendrocyte glycoprotein-specific T cell receptor transgenic mice develop spontaneous autoimmune optic neuritis. J Exp Med 197:1073–1081
12. Krishnamoorthy G et al (2006) Spontaneous opticospinal encephalomyelitis in a double-transgenic mouse model of autoimmune T cell/B cell cooperation. J Clin Invest 116:2385–2392
13. Adelmann M et al (1995) The N-terminal domain of the myelin oligodendrocyte glyco-

protein (MOG) induces acute demyelinating experimental autoimmune encephalomyelitis in the Lewis rat. J Neuroimmunol 63:17–27

14. Kabat EA, Wolf A, Bezer AE (1947) The rapid production of acute disseminated encephalomyelitis in rhesus monkeys by injection of heterologous and homologous brain tissue with adjuvants. J Exp Med 85:117–130
15. Mills KH (2011) TLR-dependent T cell activation in autoimmunity. Nat Rev Immunol 11:807–822
16. Levine S, Sowinski R (1973) Experimental allergic encephalomyelitis in inbred and outbred mice. J Immunol 110:139–143
17. Martenson RE, Deibler GE, Kies MW (1969) Microheterogeneity of guinea pig myelin basic protein. J Biol Chem 244:4261–4267
18. Olitsky PK, Tal C (1952) Acute disseminated encephalomyelitis produced in mice by brain proteolipide (Folch-Lees). Proc Soc Exp Biol Med 79:50–53
19. Poduslo SE (1983) Proteins and glycoproteins in plasma membranes and in the membrane lamellae produced by purified oligodendroglia in culture. Biochim Biophys Acta 728:59–65
20. Lebar R, Vincent C (1981) Tentative identification of a second central nervous system myelin membrane autoantigen (M2) by a biochemical comparison with the basic protein (BP). J Neuroimmunol 1:367–389
21. Linnington C, Webb M, Woodhams PL (1984) A novel myelin-associated glycoprotein defined by a mouse monoclonal antibody. J Neuroimmunol 6:387–396
22. Ben-Nun A, Wekerle H, Cohen IR (1981) The rapid isolation of clonable antigen-specific T lymphocyte lines capable of mediating autoimmune encephalomyelitis. Eur J Immunol 11:195–199
23. Zamvil S et al (1985) T-cell clones specific for myelin basic protein induce chronic relapsing paralysis and demyelination. Nature 317:355–358
24. McDevitt HO, Perry R, Steinman LA (1987) Monoclonal anti-Ia antibody therapy in animal models of autoimmune disease. Ciba Found Symp 129:184–193
25. Langrish CL et al (2005) IL-23 drives a pathogenic T cell population that induces autoimmune inflammation. J Exp Med 201:233–240
26. Sutton C et al (2006) A crucial role for interleukin (IL)-1 in the induction of IL-17-producing T cells that mediate autoimmune encephalomyelitis. J Exp Med 203:1685–1691
27. Massip L et al (2010) Deciphering the chromatin landscape induced around DNA double strand breaks. Cell Cycle 9:2963–2972
28. Chen X, Cho DB, Yang PC (2010) Double staining immunohistochemistry. North Am J Med Sci 2:241–245
29. Stridh L et al (2011) Regulation of toll-like receptor 1 and -2 in neonatal mice brains after hypoxia-ischemia. J Neuroinflammation 8:45
30. Van den Broeck W, Derore A, Simoens P (2006) Anatomy and nomenclature of murine lymph nodes: descriptive study and nomenclatory standardization in BALB/cAnNCrl mice. J Immunol Methods 312:12–19
31. Kruisbeek AM (2001) Isolation of mouse mononuclear cells. Curr Protoc Immunol 3:1

Chapter 24

The Use of MiRNA Antagonists in the Alleviation of Inflammatory Disorders

Lucien P. Garo and Gopal Murugaiyan

Abstract

Toll-like receptors (TLR), a family of pattern-recognition receptors (PRRs) stimulated by pathogen-associated molecular patterns (PAMPs), generate antigen-triggered innate and adaptive immune responses. Recent studies have indicated that several small, regulatory RNAs, called microRNAs (miRNAs), are induced by TLR activation in immune cells and that many microRNAs can control the inflammatory process and response to infection by positively or negatively regulating TLR signaling. Among these miRNAs, aberrant microRNA-155 (miR-155) has been implicated in diverse immune processes including the pathogenesis of several autoimmune diseases and cancer. Here, we discuss the role of miR-155 in TLR-mediated and TLR-related immune system regulation. Furthermore, we present our current knowledge of the design, in vivo delivery strategies, and therapeutic efficacy of miR-155 inhibitors in various inflammatory disorders and cancer, including a protocol on the use of miRNA-155 inhibitors in experimental autoimmune encephalomyelitis (EAE).

Key words MicroRNA, Dendritic cells, T cells, Experimental autoimmune encephalomyelitis, Peptide nucleic acid, PNA, Locked nucleic acid, LNA, MiR-155, Anti-miR

1 Introduction

1.1 TLRs and MicroRNAs

TLRs recognize microbial pathogens and generate antigen-specific innate and adaptive immune responses [1]. Because excessive activation of TLR pathways can lead to altered immune homeostasis, chronic inflammatory diseases, and cancer, TLR signaling pathways are strictly regulated. Recent studies have indicated that several miRNAs are induced by TLR activation in immune cells and that many miRNAs can control inflammatory process and response to infection by positively or negatively regulating TLR signaling [2, 3].

MiRNAs are small endogenous noncoding RNAs, about 20–25 nucleotides in length, that post-transcriptionally repress the expression of genes [4]. miRNAs play a key role in many physiological processes, such as embryogenesis, cell proliferation,

Claire E. McCoy (ed.), *Toll-Like Receptors: Practice and Methods*, Methods in Molecular Biology, vol. 1390,
DOI 10.1007/978-1-4939-3335-8_24,

apoptosis and immune system development and function [5]. Dysregulation of miRNA expression and function has been associated with a variety of human diseases, including cancer and many inflammatory and autoimmune diseases [5]. The enzyme responsible for regulatory miRNA biogenesis, Dicer, is required for normal lymphocyte function, suggesting an indispensable role for miRNAs in immune system regulation. Indeed, miRNAs have been shown to affect developmental outcomes in thymic T cell precursors, influence T regulatory (Treg) cell development, regulate the maturation and antigen-presenting function of antigen-presenting cells (APCs), and affect the production of antibodies to thymic-dependent antigens [6–8].

1.2 MiR-155 in Immune System Development and Function

MiR-155 was one of the first miRNAs linked to immune system development and function and has been shown to regulate both innate and adaptive immunity. Various TLR ligands have been shown to induce miR-155 expression in macrophages and other antigen presenting cells (APCs) in a TLR-dependent manner, implicating miR-155 as a downstream player in innate immune function [9]. In addition to inflammatory ligands, miR-155 is also induced in macrophages and dendritic cells (DCs) after exposure to inflammatory cytokines such as IFN-β, IFN-γ, and TNF-α [9].

MiR-155 expression within DCs is necessary for their general function, as DCs from miR-155$^{-/-}$ mice fail to effectively activate T cells [10, 11]. It is the intrinsic miR-155 within DCs that promotes production of Th1- and Th17-polarizing cytokines crucial for the development of these T cell subsets [10, 11]. For example, although miR-155 expression within T cells is not important for Th1 differentiation, miR-155 within DCs promotes Th1 development by targeting SOCS1 and inhibiting DC-secreted IL-12 [6, 11].

However, T cell-intrinsic expression of miR-155 is also important for differentiation towards certain T cell subsets. T cells display induction of miR-155 in response to different activating stimuli including TCR engagement and T helper polarizing cytokines [10, 12]. We and others have found that miR-155 expression within T cells is important for effective Th17 development by targeting the transcription factor Ets1, a negative regulator of Th17 differentiation [10, 11, 13, 14]. More recently miR-155 has also been shown to contribute to Th17 cell function by suppressing the inhibitory effects of Jarid2, a DNA-binding protein that recruits the Polycomb Repressive Complex 2 (PRC2) to chromatin [15]. In addition, the bias towards the Th2 phenotype observed in miR-155$^{-/-}$ mice is also partly due to increased levels of the miR-155 target transcription factor c-Maf, which is important for the production of IL-4 [16]. In Treg cells, miR-155 is required for differentiation and proliferation, but not immunosuppressive functions. No pathology due to impaired Treg cell differentiation has been reported in miR-155$^{-/-}$ mice [17, 18]. In addition to T cells, miR-155 has been

shown to promote immunoglobulin (Ig) class switching in B cells via targeted repression of activation-induced cytidine deaminase (AID) and the transcription factor PU.1 [19, 20].

Together, these defects in miR-155$^{-/-}$ mice have led researchers to study the impact of miR-155 in the regulation of TLR-dependent and TLR-related immune functions in vivo in response to various intracellular and extracellular pathogens, in cancer, and in autoimmunity.

1.3 MiR-155 in Infection, Cancer, and Autoimmunity

Although healthy miR-155$^{-/-}$ mice do not present with gross abnormalities in myeloid or lymphoid cell development, protective immune responses to various infections appear to be impaired in these mice. The contribution of miR-155 to protective immunity against microbial infection was first suggested by Rodriguez et al. [21]. They found that loss of miR-155 leads to an impaired response to *salmonella typhimurium* infection due to defective T helper differentiation and antibody production. Since then, mir-155$^{-/-}$ mice have been shown to be susceptible to *Helicobacter pylori* and various intracellular pathogens, including viruses [22–24].

Although miR-155 expression within the immune system is required for normal immune system function, altered expression of miR-155 in immune cells has been linked to cancers and autoimmune diseases. For example, mir-155 is highly overexpressed in patients with lymphomas of B cell origin, including Hodgkin's lymphoma and diffuse large cell B cell lymphoma [25, 26]. Consistent with these observations, transgenic expression of miR-155 in B cells causes acute lymphoblastic leukemia [27].

Among the miRNAs described, miR-155 is one of the most highly implicated in autoimmune diseases [28]. For example, increased expression of miR-155 has been observed in brain lesions from MS patients [29, 30]. In mice, we and others have found that miR-155 expression is increased in CD4^{+} T cells during EAE and that miR-155$^{-/-}$ mice have a delayed course and reduced severity of disease accompanied by less inflammation in the CNS [10, 11]. The attenuation of EAE in miR-155$^{-/-}$ mice is associated with decreased Th1/Th17 responses in the CNS and peripheral lymphoid organs. Further evidence supporting a positive role for miR-155 in autoimmune inflammation is the resistance to collagen-induced arthritis observed in Mir-155$^{-/-}$ mice, which is also associated with a selective defect in Th17 polarization [13, 31]. Recently, it has been shown that miR-155 deficiency results in diminished eosinophilic inflammation and mucus hypersecretion in the lungs of allergen-sensitized and allergen-challenged [32]. MiR-155$^{-/-}$ mice have also been shown to be resistant to colitis [33]. In support of these animal models, increased expression of miR-155 has been observed in synovial samples from patients with rheumatoid arthritis, in the lungs of patients with asthma, and in the bowel tissue of patients with ulcerative colitis [13, 34, 35].

Although critical for response to pathogens, dysregulated expression of miR-155 in immune cells seems to contribute to the development of cancer and autoimmunity. Therefore, miR-155 may be an effective therapeutic target in the treatment of a range of immune-mediated disorders.

1.4 MiR-155 Antagonist Therapeutics

The discovery of miRNAs as powerful regulators of gene expression, combined with the observation that many miRNAs are dysregulated in human diseases, opened up the possibility of modulating miRNA expression for therapeutic purposes. miRNA-related therapeutics may involve either miRNA antagonists or miRNA mimics. MiRNA antagonists (i.e., anti-miRNAs, anti-mirs, or miRNA inhibitors), are chemically modified RNAs that bind to a miRNA of interest and inhibit its activity. This in turn relieves the miRNA's targets of its suppressive function and allows for gain of function within a disease state. Conversely, miRNA mimics introduce miRNAs into diseased cells to restore a loss of function by suppressing translation of target mRNA and mimicking a healthy cell state.

In this chapter, we focus on assessing the therapeutic potential of anti-miRNAs. An absolute requirement to begin studying the potential use of miRNA antagonists in clinical settings is the ability to synthesize stable and specific miRNA antagonists on a scale suitable for in vivo studies. Therefore, various miRNA inhibitor technologies have been developed using chemical modification, conjugation, and encapsulation to enhance their activity by protecting therapeutic molecules from biological degradation and clearance, as well as by increasing binding affinity and specificity.

Several chemical modifications that enhance cellular uptake, binding affinity, and stability of anti-miRNA oligonucleotides have been reported in vitro and in preclinical animal models [36–38]. Current anti-miRNA chemistries use modifications of the typical nucleic acid ribose sugar backbone with 2′-modifications. For example, introduction of 2′-O-methyl (2′-O-Me) contributes to improved binding affinities to RNA, whereas addition of 2′-O-methoxyethyl groups (2′-MOE) to the ribose sugar component of oligonucleotides increases nuclease resistance and affinity and specificity to RNA.

Although 2′-OMe-modified anti-miRs are more effective than unmodified oligonucleotides, they are still susceptible to degradation by nucleases and are thus not ideal for in vivo applications. Therefore, in addition to methylation, other modifications at the 2′ sugar position have been tested for their effect on miRNA inhibition. For example, 2′-fluoro (2′-F) modification of the sugar moiety confers nuclease resistance and increases the binding affinity of anti-miR oligonucleotides to their cognate miRNAs. Among the miRNA inhibitors, locked nucleic acid (LNA) and peptide nucleic acids (PNA) modifications have been known to possess

superior affinity towards complementary RNA and with higher nuclease resistance. In LNA, the 2′-oxygen and the 4′ carbon of the ribose moiety of the nucleotide are covalently linked to enhance the oligonucleotide binding to miRNAs [39]. LNA chemistries also generally use phosphorothioate backbone linkages in which a sulfur atom replaces one of the non-bridging oxygen atom in the phosphate group to increase nuclease resistance. A subclass of LNA anti-miRNAs containing cholesterol conjugated via 2′-O-Me linkage, named antagomirs, have also been generated to increase cellular uptake and stability. Another class of miRNA inhibitors known as PNAs has also been successfully used in several in vitro and in vivo studies to knockdown the expression of specific miRNAs [40–42]. Next, we discuss some of the chemically modified miR-155 inhibitors with demonstrated effectiveness in vivo.

1.4.1 Peptide Nucleic Acid (PNA)

Peptide nucleic acids (PNAs) are an uncharged ON analogue in which the entire sugar-phosphate backbone of the DNA/RNA has been replaced by a neutral N (2-aminoethyl) glycine moiety [40]. Recently, several studies have demonstrated that PNAs can be effectively used as anti-miRNAs. PNAs show high affinity and sequence specificity for complementary RNA and DNA, and are not easily recognized by either proteases or nucleases, making them resistant to enzymatic degradation; therefore, these ON analogs are more effective than standard 2O-methyl ONs at binding and inhibiting microRNA function. Furthermore, it has been shown that miRNA inhibition can be enhanced by conjugation of an antisense PNA to a cell-penetrating peptide or by linking to just few lysine residues. Critically, PNAs have also been shown to possess antisense activities in vivo with little or no toxicity [41].

PNAs targeted against different microRNAs have been used successfully both in vitro and in vivo. For example, Martin et al., found that the induction of miR-155 by LPS is reduced by PNA anti-miR-155 that was linked to four lysine residues [42]. Targeting mir-155 using PNA anti-miRs completely reduces the expression and function of miR-155 in primary murine B cells both in culture and in vivo. Furthermore, their genome-wide expression analysis revealed that PNA anti-miR-155 treatment efficiently reproduced the effect of miR-155 genetic deletion with no apparent signs of toxicity. Subsequently, Babar and colleagues demonstrated that systemic delivery of PNA anti-Mir-155 encapsulated in unique polymer nanoparticles inhibited miR-155 and slowed the growth of B cell lymphoma in mice [43]. More recently, the same group developed a new anti-miRNA delivery platform in which neutral PNA anti-miRNAs were attached to a low pH-induced transmembrane structure (pHLIP), which specifically localized to the acidic tumor microenvironment and effectively transported anti-miRNAs across the plasma membrane of various tumor cell types under acidic conditions [44]. Treatment with pHLIP–anti-miR-155

diminished the growth of subcutaneous lymphomas, prolonged survival, and suppressed metastatic spread more effectively than commercially available anti-miRNAs and without systemic toxicity. PNA anti-miRs can be purchased from several companies, including Panagene, Inc. (www.panagene.com) and PNA Bio (www.pnabio.com). Alternatively, PNA anti-miRs can be synthesized following the procedures described by Fabbri et al. [45].

1.4.2 Locked Nucleic Acids (LNA)

Locked nucleic acids (LNAs) contain a methylene bridge that connects the 2′-oxygen with the 4′-carbon of the ribose ring of the oligonucleotide [39]. This results in a locked ribose conformation that pre-organizes the nucleotide bases for high binding affinity and hybridization between single-stranded, LNA-modified anti-miRNA oligonucleotides and their complementary miRNA targets. LNA oligonucleotides exhibit unprecedented thermal stability when hybridized to their target molecules due to the locked conformation that enhances base stacking and backbone preorganization. In addition, oligomers that contain LNA bases (LNA/DNA oligomers) have significantly improved mismatch discrimination compared with unmodified reference oligomers, are highly resistant to nuclease degradation, and display low toxicity in vivo [46–48].

Several studies have reported on the inhibition of miRNA function using high affinity LNA-modified DNA phosphorothioate ONs targeting mature miRNA. Zhang et al. showed that silencing LNA-modified miR-155 leads to significant inhibition of B cell lymphoma growth in mice [49]. In another study, silencing miR-155 by LNA-antimiR leads to downregulation of LPS-induced GM-CSF expression in vivo [50]. We and others have found that silencing miR-155 using LNA-modified anti-miR-155 ameliorates the clinical severity of EAE and is associated with a reduction in both Th1 and Th17 cells [11, 51]. LNA anti-Mir-155 can be purchased from Exiqon, Inc. (www.exiqon.com). The following protocol describes the use of LNA-mediated miR-155 silencing in EAE.

2 Materials

1. Female C57BL/6 mice, 6–8 weeks old (Jackson Laboratories).
2. MOG peptide 35–55 (MEVGWYRSPFSRVVHLYRNGK).
3. Incomplete Freund's adjuvant (Difco).
4. Heat-inactivated *Mycobacterium tuberculosis*, strain H37Ra (Difco).
5. Pertussis toxin from *Bordetella pertussis* (List Biological Labs).
6. Sterile phosphate buffered saline (PBS) without calcium and without magnesium.

7. Two 10 ml glass syringes connected by a 2-way Luer lock adapter (Becton Dickinson).
8. 1 ml syringes with removable needle (Becton Dickinson).
9. 21-G needles (Becton Dickinson).
10. MiR-155 and control inhibitor (Exiqon).
11. Either Lipofectamine (Life Technologies) or Invivofectamine (Life Technologies).
12. Float-A-Lyzer (Spectrum Labs).
13. Infrared lamp.
14. Mouse restraint for intravenous injections.
15. RNase-free water (Life Technologies).

3 Methods

3.1 Preparation of MOG35-55 Peptide Emulsion

Each mouse receives an emulsion composed of 100 μg of $MOG_{35–55}$ peptide in complete Freund's adjuvant (CFA), supplemented with 5 mg/ml of *Mycobacterium tuberculosis* (*see* **Note 1**). The emulsion is prepared as follows:

1. Prepare a stock solution of Complete Freund's adjuvant (CFA) by mixing 10 ml IFA with 50 mg *M. tuberculosis* H37Ra (final concentration of *M. tuberculosis* is 5 mg/ml). The stock solution can be stored at 4 °C for up to 6 months.
2. To prepare a stock of $MOG_{35–55}$ peptide solution, dilute lyophilized MOG_{35-55} peptide in ddH_2O to a final concentration of 10 mg/ml. Each mouse receives 100 μg $MOG_{35–55}$ peptide contained in 10 μl of the stock solution. The peptide solution should be stored at −80 °C (*see* **Note 2**).
3. Calculate 200 μl of emulsion for each mouse receiving the injection to determine the total emulsion volume (*see* **Note 3**).
4. Emulsify $MOG_{35–55}$ peptide: CFA in a 1:1 volume ratio with two glass syringes connected with a 2-way luer lock adapter for 5–10 min. The solution should become a homogenous opaque white and increasingly firm. The emulsion should be stored at 4 °C for a minimum of 2 h and a maximum of 48 h before injection.

3.2 Preparation of Pertussis Toxin (PT)

1. Reconstitute 50 μg of pertussis toxin in 500 μl of ddH_2O for a 100 μg/ml stock solution. The stock solution can be stored at 4 °C for up to 6 months.
2. Each animal receives two injections of 200 ng of PT. To prepare working PT solution for injection, dilute 1:100 stock solution with PBS. 100 μl should now contain 100 ng of PT.

3.3 Immunization

1. Each animal receives a total of 200 μl of the MOG/CFA emulsion. Administer two 100 μl injections of the emulsion, one injection per flank via subcutaneous route (*see* **Note 4**).
2. In addition, each animal receives 200 ng of PT in 200 μl intraperitoneally on the day of immunization and a second injection 48 h later.

3.4 Anti-miR-155 and Control Inhibitor Treatment

3.4.1 MiRNA Inhibitor Stock Solution

1. Generally, miRNA inhibitors get shipped in lyophilized form and must be stored in −80 °C before and after their resuspension.
2. Spin down the vial for 10–20 s before resuspension to prevent loss of inhibitor upon opening the vial.
3. Under sterile conditions, resuspend the miRNA inhibitor by adding sterile RNase-free water to a total concentration of 1 mM for the stock solution. (*see* **Note 5**).

3.4.2 MiR-155 Inhibitor-Liposome Complexes

1. Under sterile conditions, mix 30 μl of Lipofectamine 2000 with anti-miR-155 (30–50 μg/mouse) dissolved in 170 μl PBS (*see* **Note 6**). To calculate the mg/ml of miRNA inhibitor use the following formula: mM concentration/1000) × molecular weight = mg/ml.
2. Incubate the mixture for at least 10 min at RT.
3. Administer the liposome complexes intravenously to MOG-immunized mice on days 5, 7, 9, 11, and 13 post-immunization (*see* **Note 7**).
4. Although Lipofectamine has been shown to be effective in delivering miRNA inhibitors in vitro and in vivo, Invivofectamine has been specifically designed for RNA delivery in vivo (*see* Subheading 3.4.3).

3.4.3 Alternative MiR-155 Inhibitor-Liposome Complexes

Alternatively, control and miR-155 inhibitor-liposome complexes can be prepared using Invivofectamine [52]. The following protocol can be used to generate the miRNA-liposome complexes using Invivofectamine. All additional reagents listed in the following supplemental Invivofectamine protocol are contained within the Invivofectamine kit.

1. Prepare 500 μl of oligonucleotide solution by mixing 250 μl of oligonucleotide stock solution with 250 μl of Complexation Buffer.
2. Warm Invivofectamine reagent to RT and add 500 μl to a 2 ml tube.
3. Add the diluted oligonucleotide solution from **step 1** to the Invivofectamine in a 2 ml tube and vortex immediately for 2–5 s.

4. Incubate the Invivofectamine–oligonucleotide mixture for 30 min at 50 °C.
5. Centrifuge the tube briefly to collect the sample.
6. Prepare the Float-A-Lyzer dialysis device by soaking in sterile water for 10 min, following the manufacturer's recommended procedure.
7. Add the Invivofectamine–oligonucleotide duplex mixture to the Float-A-Lyzer dialysis device and incubate at RT for 2 h in 1 l of PBS, pH 7.4, with gentle agitation.
8. Collect the sample and measure the volume. Since the volume may increase during the dialysis, divide the volume by the initial amount of oligonucleotide to determine the concentration. Adjust the volume to the desired concentration with sterile PBS.
9. Proceed with in vivo delivery of the Invivofectamine–oligonucleotide complex as described in **step 3**, Subheading 3.4.2.

3.5 Clinical Assessment of EAE

1. Following immunization, mice should be monitored daily after the first week for the development of disease, which will become evident between 10 and 15 days after immunization (*see* **Notes 8–10**).
2. Clinical assessment of EAE is performed according to the following criteria:
   (a) *Score 0*: No disease.
   (b) *Score 0.5*: Partial tail paralysis. When the animal is held by the base of the tail, the distal half of the tail will hang limp, forming a "U-shaped hook."
   (c) *Score 1*: Complete tail paralysis. When the animal is held by the base of the tail, the tail will hang completely limp.
   (d) *Score 2*: Lack of righting reflex. When the animal is placed upside-down on its back on a flat surface, it will not "right" itself by flipping over for greater than 5–10 s (*see* **Note 11**).
   (e) *Score 2.5*: Partial (i.e., single) hindlimb paralysis. When the animal walks, one hindlimb is paralyzed and will typically drag behind the mouse along the cage bedding.
   (f) *Score 3*: Complete (i.e., double) hindlimb paralysis. When the animal walks, both hindlimbs are paralyzed and will typically drag behind the mouse along the cage bedding. It will "crawl" using its forelimbs (*see* **Note 12**).
   (g) *Score 3.5*: Partial (single) forelimb paralysis. When the animal walks, both hindlimbs and one forelimb will be paralyzed and will typically drag behind the mouse along the cage bedding.
   (h) *Score 4*: Complete forelimb and hindlimb paralysis.
   (i) *Score 5*: Moribund state.

3. Mean clinical scores on separate days can be calculated by adding the scores of individual mice and dividing by the total number of mice in each group, including mice that did not develop signs of EAE. Statistical analysis between groups can be performed using linear regression analysis.

4 Notes

1. Commercial preparations of CFA contain only 1 mg/ml of *M. tuberculosis* which is not ideal for EAE. Therefore, it is generally necessary to create your own as described previously.
2. There is sometimes variability in potency between batches of $MOG_{35–55}$ peptide. Therefore, we recommend ordering a small amount for a pilot study before purchasing a bulk stock with the same Lot # for all subsequent experiments within a study.
3. When preparing the $MOG_{35–55}$ peptide-CFA mix, always consider at least 5–10 mice in excess to account for loss during the emulsion preparation and injection (e.g., for 20 mice, instead of 4 ml prepare 5–6 ml of emulsion, calculated considering 25–30 mice).
4. When injecting the emulsion, keep the needle inserted into the subcutaneous space for several seconds to allow the emulsion to be completely expelled and to avoid leakage.
5. Generally, miRNA inhibitors get shipped in nanomolar concentrations with known molecular weight. If you know the molar concentration of miRNA inhibitor, it is easy to prepare a stock solution. For example, if you have 250 nM of anti-miR-155, dissolving in 250 ml of water gives you a 1 mM stock solution. Aliquot the working solution to avoid multiple freeze–thaw cycles.
6. During preparation of mir-155 inhibitor/liposome complexes using either Lipofectamine (Life Technologies) or Invivofectamine (Life Technologies), all tubes, containers, and pipette tips must be certified RNase-free to prevent degradation of the inhibitor. MiR-155 inhibitor-liposome complexes should be prepared fresh before each injection.
7. At least five continuous administrations of anti-miR-155 post-immunization are necessary to obtain observable biological effects on microRNA activity and disease pathogenesis.
8. Although there is some variability between the onset of symptoms between days 10 and 15, symptoms rarely manifest during the first week. Therefore, it is not usually necessary to rigorously score the mice during this period. While a score of >=2 is immediately apparent upon observation, onset scores

<2 are not always visible. Each mouse should be individually/manually scored following the first week.

9. Although this EAE scoring system is well established, it is still susceptible to inter-experimenter variability and bias. Therefore, it is ideal to maintain the same scorer throughout the duration of an experiment and a double-blind scoring method should be used at all times.
10. EAE progression will generally appear in the sequence listed in the scores (e.g., tail paralysis before hindlimb paralysis, and hindlimb paralysis before forelimb paralysis).
11. Provide mice with moist food on the cage floor when the mice reach an EAE score of 2 or more. Use of gel food is ideal.
12. Note that normal EAE progression will not surpass score 3. Peak disease is generally achieved approximately 1 week after disease onset, and disease recovery may begin the following week. The majority of WT mice will reach peak disease recover to a score of 1–2 within an observation period of 25 days.

Acknowledgements

This work was supported by grants from the National Multiple Sclerosis Society (RG 4904A2/1) and the Harvard NeuroDiscovery Center.

References

1. Kawai T, Akira S (2011) Toll-like receptors and their crosstalk with other innate receptors in infection and immunity. Immunity 34:637–650
2. Quinn SR, O'Neill LA (2011) A trio of microRNAs that control Toll-like receptor signalling. Int Immunol 23:421–425
3. ONeill LA, Sheedy FJ, McCoy CE (2004) MicroRNAs: the fine-tuners of Toll-like receptor signalling. Nat Rev Immunol 11:163–175
4. Ambros V (2004) The functions of animal microRNAs. Nature 431:350–355
5. O'Connell RM, Rao DS, Chaudhuri AA et al (2010) Physiological and pathological roles for microRNAs in the immune system. Nat Rev Immunol 10:111–122
6. Cobb BS, Hertweck A, Smith J et al (2006) A role for Dicer in immune regulation. J Exp Med 203:2519–2527
7. Zhang N, Bevan MJ (2010) Dicer controls CD8+ T-cell activation, migration, and survival. Proc Natl Acad Sci U S A 107:21629–21734
8. Kuipers H, Schnorfeil FM, Fehling HJ et al (2010) Dicer-dependent microRNAs control maturation, function, and maintenance of Langerhans cells in vivo. J Immunol 185:400–409
9. Lu C, Huang X, Zhang X et al (2011) miR-221 and miR-155 regulate human dendritic cell development, apoptosis, and IL-12 production through targeting of p27kip1, KPC1, and SOCS-1. Blood 117:4293–4303
10. O'Connell RM, Kahn D, Gibson WS et al (2010) MicroRNA-155 promotes autoimmune inflammation by enhancing inflammatory T cell development. Immunity 33: 607–19
11. Murugaiyan G, Beynon V, Mittal A et al (2011) Silencing microRNA-155 ameliorates experimental autoimmune encephalomyelitis. J Immunol 187:2213–2221
12. Haasch D, Chen YW, Reilly RM et al (2002) T cell activation induces a noncoding RNA transcript sensitive to inhibition by immunosuppressant drugs and encoded by the proto-oncogene, BIC. Cell Immunol 217: 78–86
13. Kurowska-Stolarska M, Alivernini S, Ballantine LE et al (2011) MicroRNA-155 as a

proinflammatory regulator in clinical and experimental arthritis. Proc Natl Acad Sci U S A 108:11193–11198
14. Hu R, Huffaker TB, Kagele DA et al (2013) MicroRNA-155 confers encephalogenic potential to Th17 cells by promoting effector gene expression. J Immunol 190:5972–5980
15. Escobar TM, Kanellopoulou C, Kugler DG et al (2014) miR-155 activates cytokine gene expression in Th17 cells by regulating the DNA-binding protein Jarid2 to relieve polycomb-mediated repression. Immunity 40:865–879
16. Thai TH, Calado DP, Casola S et al (2007) Regulation of the germinal center response by microRNA-155. Science 316:604–608
17. Lu LF, Thai TH, Calado DP et al (2009) Foxp3-dependent microRNA155 confers competitive fitness to regulatory T cells by targeting SOCS1 protein. Immunity 30:80–91
18. Kohlhaas S, Garden OA, Scudamore C et al (2009) Cutting edge: the Foxp3 target miR-155 contributes to the development of regulatory T cells. J Immunol 182:2578–2582
19. Vigorito E, Perks KL, Abreu-Goodger C et al (2007) microRNA-155 regulates the generation of immunoglobulin class-switched plasma cells. Immunity 27:847–859
20. Teng G, Hakimpour P, Landgraf P et al (2008) MicroRNA-155 is a negative regulator of activation-induced cytidine deaminase. Immunity 28:621–629
21. Rodriguez A, Vigorito E, Clare S et al (2007) Requirement of bic/microRNA-155 for normal immune function. Science 316:608–611
22. Oertli M, Engler DB, Kohler E et al (2011) MicroRNA-155 is essential for the T cell-mediated control of Helicobacter pylori infection and for the induction of chronic Gastritis and Colitis. J Immunol 187:3578–3586
23. Dudda JC, Salaun B, Ji Y et al (2013) MicroRNA-155 is required for effector CD8+ T cell responses to virus infection and cancer. Immunity 38:742–753
24. Thounaojam MC, Kundu K, Kaushik DK et al (2014) MicroRNA 155 regulates Japanese encephalitis virus-induced inflammatory response by targeting Src homology 2-containing inositol phosphatase 1. J Virol 88:4798–4810
25. Eis PS, Tam W, Sun L et al (2005) Accumulation of miR-155 and BIC RNA in human B cell lymphomas. Proc Natl Acad Sci U S A 102: 3627–3632
26. Kluiver J, Poppema S, de Jong D et al (2005) BIC and miR-155 are highly expressed in Hodgkin, primary mediastinal and diffuse large B cell lymphomas. J Pathol 207:243–249
27. O'Connell RM, Rao DS, Chaudhuri AA et al (2008) Sustained expression of microRNA-155 in hematopoietic stem cells causes a myeloproliferative disorder. J Exp Med 205:585–594
28. Leng RX, Pan HF, Qin WZ (2011) Role of microRNA-155 in autoimmunity. Cytokine Growth Factor Rev 22:141–147
29. Junker A, Krumbholz M, Eisele S et al (2009) MicroRNA profiling of multiple sclerosis lesions identifies modulators of the regulatory protein CD47. Brain 132:3342–3352
30. Moore CS, Rao VT, Durafourt BA et al (2013) miR-155 as a multiple sclerosis-relevant regulator of myeloid cell polarization. Ann Neurol 74:709–720
31. Blüml S, Bonelli M, Niederreiter B et al (2011) Essential role of microRNA-155 in the pathogenesis of autoimmune arthritis in mice. Arthritis Rheum 63:1281–1288
32. Malmhäll C, Alawieh S, Lu Y et al (2014) Allergy microRNA-155 is essential for T(H)2-mediated allergen-induced eosinophilic inflammation in the lung. J Allergy Clin Immunol 133:1429–1438
33. Singh UP, Murphy AE, Enos RT et al (2014) miR-155 deficiency protects mice from experimental colitis by reducing T helper type 1/type 17 responses. Immunology 143:478–489
34. Comer BS, Camoretti-Mercado B, Kogut PC et al (2014) Cyclooxygenase-2 and microRNA-155 expression are elevated in asthmatic airway smooth muscle cells. Am J Respir Cell Mol Biol 52:438–447
35. Min M, Peng L, Yang Y et al (2014) MicroRNA-155 is involved in the pathogenesis of ulcerative colitis by targeting FOXO3a. Inflamm Bowel Dis 20:652–659
36. Lennox KA, Behlke MA (2010) A direct comparison of anti-microRNA oligonucleotide potency. Pharm Res 27:1788–1799
37. Li Z, Rana TM (2014) Therapeutic targeting of microRNAs: current status and future challenges. Nat Rev Drug Discov 13:622–638
38. van Rooij E, Purcell AL, Levin AA (2012) Developing microRNA therapeutics. Circ Res 110:496–507
39. Petersen M, Bondensgaard K, Wengel J et al (2002) Locked nucleic acid (LNA) recognition of RNA: NMR solution structures of LNA:RNA hybrids. J Am Chem Soc 124: 5974–5982
40. Fabbri E, Brognara E, Borgatti M et al (2011) miRNA therapeutics: delivery and biological activity of peptide nucleic acids targeting miRNAs. Epigenomics 3:733–745
41. Demidov VV, Potaman VN, Frank-Kamenetskii MD et al (1994) Stability of peptide nucleic acids in human serum and cellular extracts. Biochem Pharmacol 48:1310–1313
42. Fabani MM, Abreu-Goodger C, Williams D et al (2010) Efficient inhibition of miR-155

function in vivo by peptide nucleic acids. Nucleic Acids Res 38:4466–4475
43. Babar IA, Cheng CJ, Booth CJ et al (2012) Nanoparticle-based therapy in an in vivo microRNA-155 (miR-155)-dependent mouse model of lymphoma. Proc Natl Acad Sci U S A 109:E1695–704
44. Cheng CJ, Bahal R, Babar IA et al (2015) MicroRNA silencing for cancer therapy targeted to the tumour microenvironment. Nature 518:107–110
45. Fabbri E, Manicardi A, Tedeschi T et al (2011) Modulation of the biological activity of microRNA-210 with peptide nucleic acids (PNAs). ChemMedChem 6:2192–2202
46. Ørom UA, Kauppinen S, Lund AH (2006) LNA-modified oligonucleotides mediate specific inhibition of microRNA function. Gene 372:137–141
47. Elmén J, Lindow M, Schütz S et al (2008) LNA-mediated microRNA silencing in non-human primates. Nature 452:896–899
48. Obad S, dos Santos CO, Petri A, Heidenblad M et al (2011) Silencing of microRNA families by seed-targeting tiny LNAs. Nat Genet 43:371–378
49. Zhang Y, Roccaro AM, Rombaoa C et al (2012) LNA-mediated anti-miR-155 silencing in low-grade B-cell lymphomas. Blood 120: 1678–1686
50. Worm J, Stenvang J, Petri A et al (2009) Silencing of microRNA-155 in mice during acute inflammatory response leads to derepression of c/ebp Beta and down-regulation of G-CSF. Nucleic Acids Res 37:5784–5792
51. Zhang J, Cheng Y, Cui W et al (2014) MicroRNA-155 modulates Th1 and Th17 cell differentiation and is associated with multiple sclerosis and experimental autoimmune encephalomyelitis. J Neuroimmunol 266:56–63
52. Butovsky O, Jedrychowski MP, Cialic R et al (2015) Targeting miR-155 restores abnormal microglia and attenuates disease in SOD1 mice. Ann Neurol 77:75–99

Chapter 25

Investigating the Role of Toll-Like Receptors in Mouse Models of Gastric Cancer

Alison C. West and Brendan J. Jenkins

Abstract

Gastric cancer (GC) is the second most lethal cancer world-wide, and the poor overall 5-year survival rate of <25 % for GC is largely due to both the late detection of this aggressive disease and limited effectiveness of current treatment options. Collectively, these observations underscore the need to identify new molecular targets (i.e., genes) to serve as biomarkers for early detection and/or treatment strategies to improve patient outcomes. While GC represents a growing number of cancers whereby deregulation of the immune system is linked to tumor initiation and progression, the identity of innate immune regulators with oncogenic potential in the host gastric mucosal epithelium remains obscure.

Over the last couple of decades experimental mouse models for many cancer types have been widely used with great success to identify genes whose expression and/or mutation status influences tumorigenesis. Considering the recent mounting evidence for the role of innate immunity in the pathogenesis of inflammation-associated cancers such as GC, much attention has focused on members of the Toll-like receptor (TLR) family, which are key components of the innate immune system primarily known to trigger inflammatory responses upon pathogen detection. Here, we describe techniques used on genetic mouse models for GC to examine the role of specific TLR family members in the pathogenesis of GC.

Key words Toll-like receptor (TLR), Gastric cancer, Inflammation, Mouse models, Polymerase chain reaction (PCR), Histopathology, Immunohistochemistry, Western blotting

1 Introduction

Gastric cancer (GC) is among numerous cancers (e.g., colon, liver, lung) for which there is a well-established causal link with chronic inflammation [1, 2]. Differentiated (intestinal-type) adenocarcinoma is the predominant histopathological type of human GC, which as defined by the Correa model arises from an initiating stage of chronic gastric inflammation (gastritis) that progresses in a stepwise manner to gastric atrophy, intestinal metaplasia (IM), dysplasia/adenoma and gastric adenocarcinoma [3]. The primary causal factor for most of these human GC cases is gastritis triggered by bacterial infection with *Helicobacter pylori* (*H. pylori*) [1, 4], and recent studies support the notion that *H. pylori* eradication

Claire E. McCoy (ed.), *Toll-Like Receptors: Practice and Methods*, Methods in Molecular Biology 1390 vol. 1390,
DOI 10.1007/978-1-4939-3335-8_25,

treatment can reduce GC risk, with more favorable outcomes achieved when *H. pylori* eradication occurs in patients presenting with earlier precursor lesions (e.g., gastric atrophy) rather than advanced disease [5, 6]. Despite a slowly declining trend in the incidence and death rates for GC in North America and Western Europe, globally GC remains the fourth most common and second most lethal cancer, largely due to its high prevalence in Asian, Eastern Europe and Central/South America [7, 8].

The involvement of pathogenic microbes and inflammation in GC has led to intensive research efforts to identify key regulators of the immune system with oncogenic potential that promote the transition from a chronic inflammatory state to one of carcinogenesis. In this respect, much attention has focused on members of the evolutionarily conserved Toll-like receptor (TLR) family which act as critical sensors of the immune system to trigger the inflammatory response to many microbial (i.e., viral, bacterial, fungal) insults [9]. Support for a role of TLRs in human GC has come from clinical data indicating increased *TLR2* and *TLR4* gene expression in *H. pylori*-positive gastritis patients [10], and *TLR2* and *TLR4* gene polymorphisms are associated with an increased GC risk [11–13]. More recently, our laboratory has demonstrated that the specific overexpression of the *TLR2* gene in tumors of advanced GC patients is associated with poor overall patient survival [14]. In light of these observations, it is of note that among TLRs, TLR2 not only recognizes the most diverse set of bacterial-derived ligands, including peptidoglycan, bacterial lipoproteins, and some lipopolysaccharides [9], but also is the dominant TLR for mediating *H. pylori*-induced inflammatory responses [15].

While the above-mentioned clinical data provide strong evidence that TLRs may contribute to the initiation and/or progression of human GC, the use of genetically defined, preclinical mouse disease models is most informative in providing formal proof for a causal role for specific TLRs, or other genes for that matter, in the molecular pathogenesis of GC. In this regard, we have previously generated the *gp130*$^{F/F}$ genetic mouse model for GC which spontaneously develops gastritis and gastric tumors that histologically represent intestinal-type adenomas [16]. At the molecular level, these mice are homozygous for a phenylalanine (F) knock-in substitution of the cytoplasmic tyrosine residue at position 757 (Y_{757}) in gp130, the signal-transducing receptor for the interleukin (IL)-6 cytokine family. As a consequence of this mutation, binding of the negative signaling regulator, suppressor of cytokine signaling (SOCS)3, to gp130 is abolished, resulting in hyperactivation of the gp130-mediated Janus kinase (JAK)/signal transducer and activator of transcription (STAT)3 pathway [17]. Furthermore, we have shown that hyperactivation of the STAT3 latent transcription factor in these mice specifically augments TLR2 expression levels in gastric tumors, and genetic complementation studies revealed that gastric

tumorigenesis was significantly suppressed when *gp130*$^{F/F}$ mice were generated onto genetic backgrounds either homozygous or heterozygous null for the *Tlr2* (*gp130*$^{F/F}$:*Tlr2*$^{-/-}$) or *Stat3* (*gp130*$^{F/F}$:*Stat3*$^{-/+}$) genes, respectively [14, 17]. The clinical relevance of such findings is underscored by the fact that STAT3 is over-activated in up to 50 % of human GC cases [18–20], and a significant positive correlation exists between STAT3 activation and *TLR2* gene expression levels in human GC [14]. The potential for the therapeutic targeting of TLR2 in GC was also demonstrated with an anti-TLR2 monoclonal antibody which dramatically suppressed the growth of established tumors in *gp130*$^{F/F}$ mice [14, 21].

Here, we describe a range of methods to characterize mouse models of GC, with a focus on the expression status and functional role of specific TLRs in promoting tumorigenesis.

2 Materials

2.1 Genomic DNA Extraction

1. Tail Buffer (100 ml): 5 ml 1 M Tris–HCl, pH 8.0, 20 ml 0.5 M EDTA, 2 ml 5 M NaCl, 5 ml 20 % SDS, make up to 100 ml with ultrapure Milli-Q water.
2. 20 mg/ml Proteinase K (Roche).
3. 5 M NaCl: 292.2 g NaCl in 1 L distilled water.
4. Isopropyl alcohol.
5. 70 % Ethanol.
6. Milli-Q water.
7. Buffer PB (DNA binding buffer) and Buffer PE (wash buffer) (both Qiagen), used as per manufacturer's instructions.
8. TE buffer (1×; 100 ml): 1 ml 1 M Tris–HCl, pH 8.0, 200 µl 0.5 M EDTA, and make up to 100 ml with Milli-Q water. For 0.25× solution, dilute 1:4 in Milli-Q water.
9. Vacuum Manifold (Pall Corporation) with UNIFILTER® 800 µl, 96-well microplate (Whatman).
10. 1.5 ml microcentrifuge tubes.
11. 96-well plastic plates.
12. 55 and 37 °C incubator.
13. Heat block.

2.2 PCR Genotyping

2.2.1 PCR

1. GoTaq® Flexi DNA Polymerase kit (includes 5× Green GoTaq® Flexi buffer, 5× Colorless GoTaq® Flexi buffer, GoTaq® DNA Polymerase and 25 mM $MgCl_2$; Promega).
2. dNTPs (stock at 10 mM in nuclease-free water).
3. Nuclease-free water.

4. Gp130 primer A (specific for mutant allele), B (specific for wild-type allele) and C (specific for common allele) working stocks, diluted to 300, 150 and 300 ng/μl respectively, in nuclease-free water.
5. TLR2 primer A (specific for wild-type allele), B (specific for common allele) and C (specific for mutant allele) working stocks, diluted to 100 ng/μl in nuclease-free water.
6. 96-well thermal cycler PCR machine (e.g., Verti® Thermal Cycler, Applied Biosystems®).
7. 1.5 ml microcentrifuge tubes.
8. 8-well PCR strip tubes with dome lids.

2.2.2 Agarose Gel Electrophoresis

1. Agarose powder (molecular grade).
2. Tris–Acetate-EDTA buffer (TAE, 1×): 40 mM Tris, 20 mM glacial acetic acid, 1 mM EDTA, pH 8.0.
3. SYBR® Safe DNA Gel Stain (Invitrogen).
4. 100 bp DNA ladder.
5. Agarose gel apparatus and electrophoresis power supply system.
6. UV or blue-light transilluminator (e.g., Safe Imager™ 2.0 Blue-light Transilluminator; Invitrogen).

2.3 Real-time Quantitative PCR

1. TRIsure reagent (Bioline).
2. Diethylpyrocarbonate (DEPC)-treated water.

2.3.1 RNA Isolation

3. RNase-free solutions: chloroform; isopropyl alcohol (chilled); 100 % ethanol; 75 % and 80 % ethanol (in DEPC-treated water).
4. RNase-Free DNase Set (includes RNA-free DNase I, RNase-free Buffer RDD and RNase-free water; Qiagen).
5. RNeasy Mini Kit (includes RNeasy Mini Spin Columns, Collection Tubes, RNase-free RLT, RW1 and RPE Buffers; Qiagen).
6. β-mercaptoethanol.
7. Tissue homogenizer (e.g., Ultra-Turrax® T10 basic disperser/homogenizer; IKA).
8. Microcentrifuge.
9. 15 ml Falcon® tubes.
10. RNase-free 1.5 ml microcentrifuge tubes.

2.3.2 cDNA Synthesis

1. Transcriptor High Fidelity cDNA Synthesis kit (includes PCR grade water, Random Hexamer Primers, 5× Transcriptor High Fidelity Reaction Buffer, Protector RNase inhibitor, dNTPs, DTT, and Transcriptor High Fidelity Reverse Transcriptase; Roche).

2. At least two heat blocks.
3. RNase-free 1.5 ml microcentrifuge tubes.
4. Microcentrifuge.

2.3.3 Real-Time PCR

1. SYBR Magic Reaction mix (20 ml): 11.38 ml Nuclease-free water, 3.2 ml DMSO, 4 ml GeneAmp 10× PCR Gold Buffer (Applied Biosystems), 100 µl 1 M Magnesium acetate solution, 320 µl 100 µM dNTPs, 250 U (200 µl) AmpliTaq® Gold DNA Polymerase (Applied Biosystems), 800 µl 50× ROX Reference Dye (Invitrogen), 2.1 µl 10,000× SYBR® Green I Nucleic Acid Gel Stain (Invitrogen).
2. Primers specific for murine *Tlr2* and *18S* mRNA.
3. Milli-Q water.
4. Optical 384-well PCR plate (e.g., MicroAmp® Optical 384-well Reaction Plate and MicroAmp® Optical Adhesive Film; Applied Biosystems).
5. Quantitative real-time PCR machine (e.g., Applied Biosystems 7900HT Fast Real-time PCR system).
6. Quantitative real-time PCR analysis software (e.g., SDS2.4; Applied Biosystems).
7. Filter tips.
8. Nuclease-free 1.5 ml microcentrifuge tubes.

2.4 Western Blot Analysis

2.4.1 Preparation of Tissue Lysates

1. SDS lysis buffer: 50 mM Tris, 150 mM NaCl, 1 % (v/v) Triton X-100, and 1 mM EDTA, adjust to pH 7.4 and store at 4 °C. Prior to use, add one cOmplete Protease Inhibitor Mini Cocktail Tablet (Roche) and one PhosSTOP Phosphatase Inhibitor Cocktail Tablet (Roche) per 10 ml SDS lysis buffer.
2. Protein G Sepharose® beads (Sigma-Aldrich).
3. Tissue homogenizer (e.g., Ultra-Turrax® T10 basic disperser/homogenizer; IKA).
4. Flat-bottom tubes.
5. Standard 1.5 ml microcentrifuge tubes.
6. Tube rotator wheel.
7. Refrigerated microcentrifuge.

2.4.2 SDS-PAGE

1. Sodium dodecyl sulfate (SDS)-polyacrylamide gel electrophoresis (PAGE) resolving gel buffer: 2 M Tris–HCl and 10 % SDS, adjust pH to 8.8.
2. 10 % SDS-PAGE resolving gel: 8 ml Milli-Q water, 6.6 ml 30 % Acrylamide–Bis Solution, 5.2 ml SDS-PAGE resolving gel buffer, 200 µl 10 % APS, and 8 µl TEMED.
3. Isopropyl alcohol.

4. SDS-PAGE stacking gel buffer: 1 M Tris–HCl and 10 % SDS, adjust pH to 6.8.
5. 4.5 % SDS-PAGE stacking gel: 2.92 ml Milli-Q water, 800 μl 30 % Acrylamide–Bis Solution, 1.25 ml SDS-PAGE stacking gel buffer, 100 μl 10 % APS, and 4 μl TEMED.
6. SDS-PAGE running buffer (10×; 1 L; pH 8.3): 30 g Tris base, 144 g glycine, 10 g SDS in Milli-Q water. Store at room temperature and prior to use dilute to 1× in Milli-Q water.
7. SDS-PAGE sample buffer (6×; 100 ml): 5.91 g Tris–HCl (pH 6.8), 6 g SDS, 48 ml 100 % glycerol, and 20 mg bromophenol blue, and make up to 100 ml with Milli-Q water. Store at room temperature and prior to use add 50 μl β-mercaptoethanol per 1 ml buffer.
8. Pre-stained molecular weight standard.
9. SDS-PAGE apparatus and electrophoresis power supply system.
10. Heat block.
11. Standard 1.5 ml microcentrifuge tubes.
12. Microcentrifuge.

2.4.3 Immunoblotting

1. Odyssey Blocking Buffer (Li-Cor®).
2. Primary antibodies: Mouse monoclonal Actin antibody (Sigma-Aldrich); Rabbit polyclonal tyrosine 705 phosphorylated-STAT3 (pY-STAT3) antibody (Santa Cruz); Rabbit polyclonal STAT3 antibody (Santa Cruz); Rabbit polyclonal TLR2 antibody (Epitomics).
3. Secondary antibodies: Alexa Fluor® 680 Goat Anti-Rabbit antibody and Alexa Fluor® 790 Goat Anti-Rabbit antibody (Molecular Probes), and Goat Anti-Mouse antibody IRDye 800® (Rockland™).
4. PBS-T: 1× PBS with 1 % Tween 20.
5. Milli-Q water.
6. IBlot® 7-minute Blotting System (Invitrogen).
7. Odyssey® CLx Infrared Imagine System (Li-Core).
8. 50 ml Falcon® tubes.
9. Tube roller.
10. Rocker.

2.5 Histopathology and Immunohistochemistry

2.5.1 Formalin Fixation and Paraffin-Embedding

1. Non-sterile laboratory grade 1× PBS (pH 7.0).
2. Neutral buffered formalin (pH 7.0; Amber Scientific).
3. Surgical implements.
4. Petri dish.
5. Cork.

6. Small pins.
7. Specimen pots.

2.5.2 Immunohistochemistry

1. Solutions: Xylene; 100 % ethanol; 70 % ethanol (in distilled water); distilled water and PBS.
2. 3 % hydrogen peroxide in methanol.
3. Anti-TLR2 primary antibody (OPN-301; Opsona Therapeutics).
4. Rabbit anti-mouse biotinylated secondary antibody (Vector Laboratories).
5. Mouse on mouse (M.O.M.) Basic Kit (includes M.O.M. Protein Concentrate, Mouse Ig Blocking Reagent, M.O.M. Biotinylated Anti-Mouse IgG Reagent; Vector Laboratories Inc.). M.O.M. Diluent prepared by adding 600 μl Protein Concentrate to 7.5 ml PBS.
6. VECTASTAIN® Elite ABC Kit (standard) (includes Reagent A and Reagent B; Vector Laboratories Inc.).
7. Liquid diaminobenzidine (DAB; for example liquid DAB+ substrate chromogen system; Dako).
8. Scott's tap water (1 L): 20 g magnesium sulfate, 2 g sodium bicarbonate, and tap water up to 1 L.
9. Small glass wash basins.
10. Slide holder.
11. Humidified box.
12. Fume hood.
13. Microwave.
14. Wax pen.
15. Coverslip-mounting medium.
16. Coverslips.

3 Methods

To determine whether TLR2 promotes the pathogenesis of gastric tumorigenesis, our genetic approach involves *gp130*$^{F/F}$ mice homozygous for the gp130Y_{757}F mutation being mated with *Tlr2*$^{-/-}$ mice to generate *gp130*$^{F/F}$:*Tlr2*$^{-/-}$ mice lacking both copies of the *Tlr2* gene. The *gp130*$^{F/F}$:*Tlr2*$^{-/-}$ mice and control parental *gp130*$^{F/F}$:*Tlr2*$^{+/+}$ mice (containing both copies of the *Tlr2* gene) are genotyped by performing PCR on genomic DNA extracted from mouse tail snips. The expression level of *Tlr2* mRNA in these mice is assessed by quantitative real-time PCR (qPCR) on cDNA prepared from gastric tissue, while TLR2 protein levels and location in the stomach are detected by Western blotting on lysates and

immunohistochemistry on formalin-fixed, paraffin-embedded (FFPE) stomach sections, respectively, with a TLR2 antibody. The hyperactivation of STAT3, which is a molecular hallmark of the *gp130*Y_{757}F mutation, is confirmed by Western blotting of gastric tissue lysates with a pY-STAT3 antibody.

To obtain high quality gastric tissue specimens to be processed for the methods described, stomachs surgically removed from *gp130*$^{F/F}$ mutant mouse strains are immediately opened by cutting along the lesser curvature, followed by gentle agitation in a petri dish containing ice-cold PBS. This washing step is essential to remove stomach contents which may interfere with subsequent analyses. Gastric tumor tissue to be used for the isolation of RNA and protein lysates is immediately snap-frozen in liquid nitrogen and stored at −80 °C, whereas tissue for sectioning is fixed overnight in formalin, and then stored in 70 % ethanol solution at room temperature or 4 °C.

3.1 Genomic DNA Extraction

1. Tail tips are collected on ice by snipping end with scissors and stored at −20 °C in 1.5 ml microcentrifuge tubes (*see* **Note 1**).
2. To each tube, add 750 μl tail buffer and 10 μl proteinase K, and incubate at 55 °C for a minimum of 3 h (*see* **Note 2**).
3. Add 310 μl 5 M NaCl, gently mix, and let stand for at least 10 min (up to a maximum of 2 h).
4. Microcentrifuge at 13,500 rpm (13,447 RCF; g) for 25 min, and then transfer 800 μl of aqueous phase (i.e., not white pellet or very top layer) into a fresh, labeled 1.5 ml Eppendorf tube (*see* **Note 3**).
5. Add 500 μl isopropyl alcohol to aqueous phase and gently shake by inverting tubes until any clumped DNA is suspended.
6. Microcentrifuge for 15 min at 13,500 rpm, and then discard the supernatant by inversion (*see* **Note 4**).
7. Wash the DNA pellet by adding 500 μl 70 % ethanol, microcentrifuge for 5 min at 13,500 rpm, and then discard supernatant by inversion (*as per* **Note 4**).
8. Air-dry the DNA pellet by opening the microcentrifuge tube lid and incubating at 37 °C for 1 h, or room temperature for 3–4 h.
9. Add 125 μl Milli-Q water, and incubate for at least 15 min at 37 °C to fully resuspend the DNA pellet. Mix well and DNA is ready to purify by Vacuum Manifold, as described below.
10. Add 500 μl of Buffer PB to each sample.
11. To purify, wash and elute genomic DNA, assemble the Vacuum Manifold apparatus with 96-well filter plate as per manufac-

turer's instructions, with the waste collection tray in place for the initial steps.

12. Pipette total volume of each sample into one well of the silica pore plate while mounted onto the vacuum. Place supplied plastic sheet on top of the plate and apply pressure (10–15 Hg) and hold until all the solution has passed through each well (*see* **Note 5**).
13. Wash well by adding 500 µl of Buffer PE into each well, and repeat **step 12**.
14. Replace waste collection tray with a new 96-well plate for DNA sample collection. Add 60 µl of warm 0.25× TE buffer to each well, and repeat **step 12** (*see* **Note 6**).
15. Store purified genomic DNA at 4 °C.

3.2 PCR Genotyping

3.2.1 PCR

1. Place 3 µl per sample of genomic DNA into each well of 8-well strip tubes (~100 ng template DNA). Include one sample of water alone and at least one sample that is confirmed homozygous wild-type, heterozygous and homozygous mutant for each genotype (*see* **Note 7**).
2. Prepare separate PCR reaction mixes on ice (critical step—keep reaction mixes on ice as Taq degrades rapidly at room temperature) for $n+1$ (where n = number of samples including controls) for *gp130*, and *Tlr2* wild-type and *Tlr2* mutant alleles as listed in Tables 1, 2 and 3.

Table 1
PCR reaction mix ($n=1$) to genotype the *gp130*$^{F/F}$ knock-in mouse

Reagent	Stock concentration	Final concentration	Volume (µl)
5× Green GoTaq® Flexi buffer	5×	1×	6.00
$MgCl_2$	25 mM	2.5 mM	3.00
dNTPs	10 mM	200 nM	0.60
Primer A	300 ng/µl	300 ng	1.00
Primer B	150 ng/µl	75 ng	0.50
Primer C	300 ng/µl	150 ng	0.50
Milli-Q water	–	–	15.25
GoTaq® Flexi DNA Polymerase	5 U/µl	0.75 U	0.15
(Template DNA)			3.00
Total volume			30.00

Table 2
PCR reaction mix (*n* = 1) to genotype the *Tlr2* wild-type allele in mice

Reagent	Stock concentration	Final concentration	Volume (µl)
5× Green GoTaq® Flexi buffer	5×	1×	6.00
$MgCl_2$	25 mM	2.5 mM	3.00
dNTPs	10 mM	200 nM	0.60
Primer A	100 ng/µl	100 ng	1.00
Primer B	100 ng/µl	100 ng	1.00
Milli-Q water	–	–	15.25
GoTaq® Flexi DNA Polymerase	5 U/µl	0.75 U	0.15
(Template DNA)			3.00
Total volume			30.00

Table 3
PCR reaction mix (*n* = 1) to genotype the *Tlr2* mutant (knockout) allele in mice

Reagent	Stock concentration	Final concentration	Volume (µl)
5× Green GoTaq® Flexi buffer	5×	1×	6.00
$MgCl_2$	25 mM	2.5 mM	3.00
dNTPs	10 mM	200 nM	0.60
Primer B	100 ng/µl	100 ng	1.00
Primer C	100 ng/µl	100 ng	1.00
Milli-Q water	–	–	15.25
GoTaq® Flexi DNA Polymerase	5 U/µl	0.75 U	0.15
(Template DNA)			3.00
Total volume			30.00

3. Aliquot 27 µl PCR reaction mix to each genomic DNA sample in 8-well PCR strip tubes. Seal well with dome cap, briefly centrifuge to mix DNA and PCR master mix.
4. Place samples in 96-well PCR thermal cycler machine (for example Verti® Thermal Cycler, Applied Biosystems®), and amplify with the conditions listed in Tables 4 and 5 (*see* **Note 8**).
5. Once amplification is complete, PCR products can be assessed immediately by agarose gel electrophoresis or stored at 4 °C (up to 24 h) or –20 °C (long-term) for later assessment.

Table 4
PCR thermal cycler settings to genotype *gp130*$^{F/F}$ knock-in mice

Step	Process	Temperature (°C)	Time (min)	Cycles
1	Initiation/melting	94	10	1
2A	Denaturation	94	1	35
2B	Annealing	60	1	35
2C[a]	Elongation	72	1	35

[a]Steps 2A-2B-2C cycle in succession

Table 5
PCR thermal cycler settings to genotype *Tlr2* knockout mice

Step	Process	Temperature (°C)	Time	Cycles
1	Initiation/melting	94	10 min	1
2A	Denaturation	95	20 s	35
2B	Annealing	65	20 s	35
2C[a]	Elongation	72	1 min 20 s	35
3	Strand completion	72	3 min	1

[a]Steps 2A-2B-2C cycle in succession

3.2.2 Agarose Gel Electrophoresis

1. Dissolve agarose powder in TAE buffer to create a 1.5 % solution and microwave until boiling. Leave to cool (10 min) and pour into appropriate electrophoresis apparatus with SYBR® Safe DNA gel stain (3 μl per 100 ml agarose solution) and leave until set (~20 min).
2. Cover gel with TAE buffer and load 5–10 μl PCR product per sample into each well (*see* **Note 9**). Load 5 μl molecular weight DNA ladder into one well and set the voltage. Small gels run typically at 50–70 V, or larger gels at 80–100 V. Run for 30–45 min to fully separate PCR products.
3. Visualize gel with a blue-light or UV transilluminator. *See* Fig. 1 for expected results when genotyping *gp130*$^{F/F}$ knock-in (Fig. 1a) and *Tlr2* knockout (Fig. 1b) mice.

3.3 Real-Time Quantitative PCR

3.3.1 RNA Isolation

1. Transfer frozen tissue samples (*see* **Note 10**) into flat bottom tubes, and homogenize using a small probe on ice in 1 ml TRIsure (*see* **Notes 11** and **12**). Once all samples are homogenized, transfer each homogenate to a 15 ml falcon tube and centrifuge at 1865 RCF for 30 min at 4 °C.

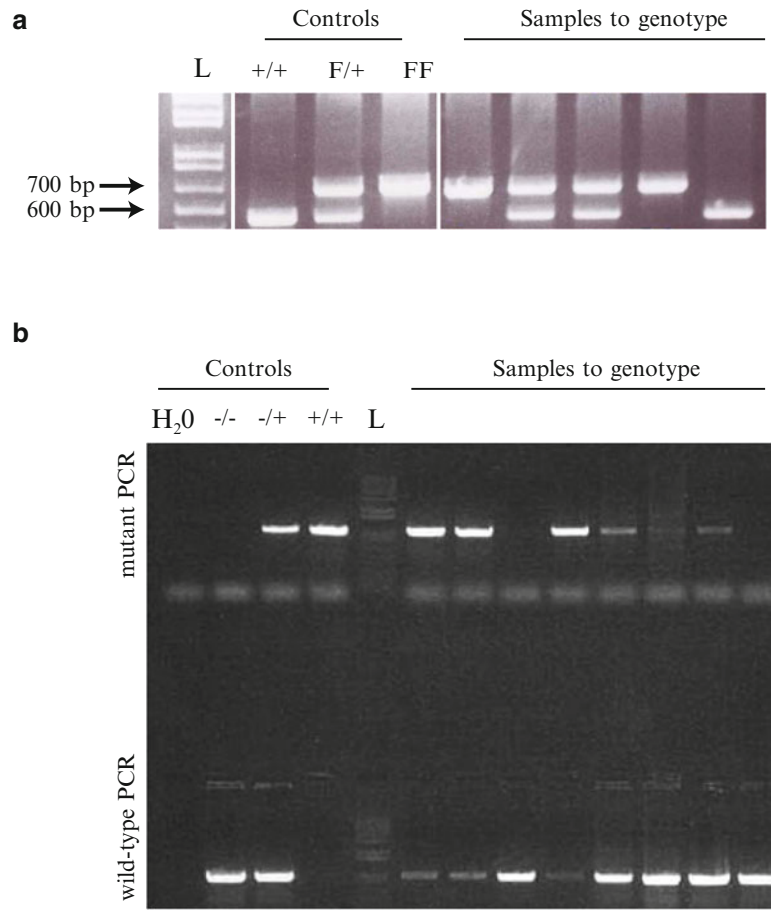

Fig. 1 PCR genotyping for *gp130* knock-in and *Tlr2* knockout alleles. (**a**) PCR product size and number of bands present indicates whether the mouse harbors a homozygous *gp130* knock-in mutation (one ~700 bp product), is homozygous wild-type (one ~500 bp product), or is heterozygous (bands at ~500 and ~700 bp). (**b**) The presence of a band (~900 bp) in either the wild-type or mutant PCR indicates that the mouse is homozygous wild-type or mutant for loss of *Tlr2* respectively, and presence of a band in each PCR indicates the mouse is heterozygous. The lack of bands in the water (negative control) *lane* indicates the PCR is free of contamination, and the use of positive controls provides quality control for each PCR, and enables accurate genotyping. *L* = 100 bp ladder

2. Transfer the supernatant (leaving insoluble material pelleted at the bottom) into a new 15 ml falcon tube, and incubate at room temperature for 5 min.
3. In a fume hood, add 200 μl chloroform, vortex vigorously and leave at room temperature for 2–3 min. Centrifuge at 4 °C for 45 min at 1,865 RCF, and transfer the clear phase (aqueous, top layer) into a new 15 ml falcon tube (*see* **Note 13**).
4. Add 500 μl isopropyl alcohol, vortex, and incubate at room temperature for 10 min. Repeat centrifugation in **step 5** to

pellet RNA, discard the supernatant, and wash the RNA pellet by adding 500 μl of 75 % ethanol (in DEPC-treated water).

5. Centrifuge at 4 °C for 15 min at 1,865 RCF discard the supernatant and then air-dry the pellet by inverting the tube on a paper towel (maximum 30 min).
6. Dissolve the RNA pellet in 50 μl RNase-free DEPC-treated water, and RNA samples can either be DNase-treated to remove contaminating genomic DNA (as below) or stored at this stage at −20 °C (*see* **Note 14**).
7. To DNase I-treat the RNA samples, add 350 μl RLT buffer (containing 10 μl β-mercaptoethanol per 1 ml of RLT buffer) to each 100 μl RNA sample, and mix by pipetting.
8. Add 250 μl of 100 % ethanol, mix thoroughly by pipetting, and then transfer total volume of sample to an RNeasy mini column placed in the supplied 2 ml collection tube.
9. Microcentrifuge for 30 s at 10,000 rpm (7,378 RCF; g), discard the flow through, and add 350 μl RW1 wash buffer. Repeat microcentrifugation, discard the flow through.
10. Prepare 10 μl DNase I and 70 μl RDD buffer per sample, and pipette 80 μl onto each RNeasy mini column membrane (*see* **Note 15**). Incubate at room temperature for 15 min.
11. Add 350 μl RW1 wash buffer to each RNeasy mini column, and the microcentrifuge at 10,000 rpm for 30 s. Discard the flow through, and replace collection tube with a new one.
12. Add 500 μl 80 % ethanol, microcentrifuge at 10,000 rpm for 30 s, discard the flow through, and then microcentrifuge for an additional 1 min to completely dry the membrane.
13. Transfer column to a labeled new RNase-free collection microcentrifuge tube (supplied in the kit), and add 30 μl RNase-free water onto each mini column membrane.
14. Incubate for 5 min at room temperature, and microcentrifuge at 10,000 rpm for 1 min to collect the eluent (RNA) in labeled tube.
15. To ensure maximal elution of RNA from the membrane, add another 30 μl RNase-free water to membrane, and repeat step 14, yielding a total volume of 60 μl (*see* **Note 16**). Store purified total RNA samples at −80 °C.

3.3.2 cDNA Synthesis

1. For first stand cDNA synthesis with the Transcriptor High Fidelity cDNA Synthesis kit (Roche), add up to 1 μg of RNA in a final volume of 9.4 μl per sample in a 1.5 ml RNase-free microcentrifuge tube (*see* **Note 17**).
2. In an RNase-free 1.5 ml microcentrifuge tube, mix a maximum of 1 μg RNA together with 2 μl random hexamer primers and DEPC-treated water in a total volume of 11.4 μl for each

sample. Also include one additional sample to act as the "minus reverse transcriptase (RT) control" in order to detect genomic DNA contamination (*see* **Note 17**).

3. Denature the RNA-primer mix for 10 min at 65 °C, and cool on ice.
4. Add 4 µl 5× Transcriptase Reaction Buffer, 0.5 µl RNase inhibitor, 2 µl dNTPs, 1 µl DTT to each sample, and 1.1 µl High Fidelity Reverse Transcriptase enzyme for each cDNA sample, or 1.1 µl water for the minus RT control, making a total volume of 20 µl.
5. Using heat blocks, incubate for 10 min at 29 °C, then 60 min at 48 °C. Finally, inactive enzyme by heating for 5 min at 85 °C.
6. Briefly microcentrifuge, and either place cDNA directly onto ice for immediate use, or store at –20 °C.

3.3.3 Real-Time PCR

1. Prepare the *18S* and *Tlr2* SYBR Magic reaction mixes for triplicates of $n+1$ (where n = number of samples to be tested, including water (negative) and minus RT controls), containing 5 µl SYBR Magic, 0.2 µl Forward Primer, 0.2 µl Reverse Primer, and 2.6 µl Milli-Q water (for $n=1$).
2. Dilute cDNA samples (including minus RT control) in Milli-Q water (1:4–1:6 dilution) (*see* **Note 18**).
3. Using filter tips, pipette 8 µl SYBR magic reaction mix for *18S* and *Tlr2* into the appropriate number of individual wells of a 384-well plate (i.e., three wells for each reaction mix per sample). Next, pipette 2 µl diluted cDNA sample (or control) to individual wells containing *18S* and *Tlr2* reaction mixes, in triplicate (i.e., six wells total per cDNA sample).
4. Seal the plate very securely with an adhesive optical cover to avoid uneven evaporation, and centrifuge to remove air bubbles and to combine the cDNA and reaction mix at the bottom of the wells (1 min, 1000 rpm).
5. Transfer the plate on a real-time PCR instrument and run with cycle conditions of 50 °C for 2 min, 95 °C for 10 min, followed by 40 cycles of 95 °C for 15 s and 60 °C for 1 min and finishing with a disassociation curve to detect formation of primer-dimers.
6. Following successful PCR, the results can be assessed by appropriate PCR software (e.g., Applied Biosystems SDS2.4). Firstly, confirm the melting temperature of the PCR products for *18S* and *Tlr2* are within ±1 °C of the expected temperature. If not, the sample should be excluded as likely contains nonspecific products such as primer dimers.

7. Secondly, use the analysis software to calculate the cycle threshold (C_t) of both *18S* and *Tlr2* for each sample. Normalize the expression of *Tlr2* to *18S* within each sample by calculating the difference in C_t (ΔC_t). This number can be used to describe the mRNA expression of *Tlr2* or relative expression levels ($\Delta\Delta C_t$) can be assessed between sample groups, for example $\Delta\Delta C_t = \Delta C_t$ ($gp130^{+/+}$:$Tlr2^{+/+}$) – ΔC_t ($gp130^{F/F}$:$Tlr2^{+/+}$).

3.4 Western Blot Analysis

3.4.1 Preparation of Tissue Lysates

1. Transfer frozen tissue samples (*see* **Note 10**) into flat bottom tubes, and homogenize using a small probe on ice in ice-cold 800 μl SDS lysis buffer. Once all samples are homogenized, transfer each homogenate to a fresh 1.5 ml microcentrifuge tube and place on a tube rotator wheel on slow speed at 4 °C for 30–60 min to fully lyse the cells.
2. Pellet the cellular debris by microcentrifugation at 10,000 rpm for 5 min at 4 °C, and transfer supernatant to fresh 1.5 ml microcentrifuge tube.
3. To further clear the sample of debris, add Protein G Sepharose® beads to each sample (10 μl per 500 μl supernatant) and incubate for 30 min on tube rotator wheel at 4 °C on slow speed.
4. Pellet the Sepharose® by microcentrifugation at 5000 rpm (1,844 RCF; g) for 10 min at 4 °C. Transfer supernatant to fresh 1.5 ml microcentrifuge tube and proceed with quantification and SDS-PAGE, or store at −80 °C for later interrogation.

3.4.2 SDS-PAGE

1. Ensure the apparatus is clean, and wipe glass plates with 95 % ethanol and air-dry prior to use. Prepare the 1.5 mm thick, 10 % resolving SDS-PAGE gel immediately prior to use and pour between glass plates (leaving room for stacking gel). Overlay with ~1 ml isopropyl alcohol to ensure a smooth surface and leave gel to polymerize for 30 min.
2. Remove isopropyl alcohol and carefully dry with Whatman paper.
3. Prepare the 4.5 % stacking gel immediately prior to use and pour onto resolving gel. Insert combs immediately and leave gel to polymerize for 30 min.
4. When gel is fully polymerized, remove combs, assemble SDS-PAGE apparatus and fill with SDS running buffer ensuring wells are covered.
5. Following quantification of protein lysates (*see* **Note 19**) aliquot 30 μg of protein per sample into new 1.5 ml microcentrifuge tube. Make volume of each up to 10 μl (15-well comb) or 30 μl (10-well comb) with SDS lysis buffer, and add 2 or 6 μl of 6× sample buffer, respectively.

6. Reduce proteins by boiling at 95 °C for 5 min. Briefly microcentrifuge protein samples to collect condensation, and load into each well of SDS-PAGE gel. Include 5 μl of the pre-stained molecular weight standard in one well.
7. Place lid on gel tank, ensuring correct orientation of electrodes, and connect to power pack. Run gel at 90 V for 30 min (to ensure even migration through the stacking gel), then increase to 120 V for an additional 30–60 min. Stop running gel when sample buffer has migrated off the bottom of the resolving gel, and the lowest molecular weight band of the standard is near the end of the gel.

3.4.3 Immunoblotting

1. The following methods refer to use of the IBlot® 7-minute Blotting System (Invitrogen) for semi-dry transfer and the Odyssey® CLx Infrared Imaging System (Li-Core) for fluorescent Western immunoblotting.
2. Following SDS-PAGE separation, disconnect gel tank from power pack and remove gel from glass plates. Remove stacking gel, and briefly wash gel in Milli-Q water. Transfer proteins to a nitrocellulose membrane using the IBlot® semi-dry transfer system (Invitrogen), as per manufacturer's instructions.
3. Following transfer, remove membrane, briefly wash in Milli-Q water, and block nonspecific epitopes with 3 ml Odyssey® Blocking Buffer and gentle rocking for 1 h at room temperature.
4. Following blocking, place membrane in a 50 ml Falcon tube (or similar) with TLR2, STAT3, and pY-STAT3 antibodies each diluted to 1:1000 in 3 ml Odyssey® Blocking Buffer, for overnight incubation at 4 °C on a tube roller (*see* **Note 20**).
5. Remove membrane from Falcon tube and store primary antibody at 4 °C (*see* **Note 21**). Wash membrane three times in 2 % PBS-T for a minimum of 5 min each wash at room temperature with gentle rocking, discarding the buffer between each incubation.
6. Incubate membranes in 1 μl Alexa Fluor® 680 Goat Anti-Rabbit antibody in 3 ml Odyssey® Blocking Buffer at room temperature with gentle rocking and protected from light.
7. Following incubation, discard secondary antibody and wash membrane three times in 2 % PBS-T for a minimum of 5 min each wash at room temperature with gentle rocking, discarding the buffer between each incubation.
8. Transfer membrane to Odyssey® Clx Infrared Imaging System, and capture image at a wavelength of 700 nm.
9. In order to confirm equal protein loading between samples, re-probe each membrane in a 50 ml Falcon tube with the anti-

Actin primary antibody diluted 1:500 in 3 ml Odyssey® Blocking Buffer, overnight at 4 °C on a tube roller.

10. Repeat **steps 4–7**, however with Alexa Fluor® 790 Goat Anti-Rabbit secondary antibody and capture image at a wavelength of 800 nm (*see* **Note 22**). Figure 2 shows an example of Western blotting for TLR2 and actin (Fig. 2a), and STAT3, pY-STAT3, and actin (Fig. 2b) on mouse stomach samples.

3.5 Histopathology and Immunohistochemistry

3.5.1 Formalin Fixation and Paraffin-Embedding

1. Remove the stomach from the mouse, immediately open by cutting along the lesser curvature, and gently agitate in a petri dish containing ice-cold PBS.
2. Pin the stomach out onto small circle of cork with the outer membrane against the cork, and inner membrane facing up. Place the cork into a specimen pot filled with neutral buffered formalin for exactly 24 h to fix the tissue. After 24 h, remove the stomach from the cork and place the tissue into a specimen pot filled with 70 % ethanol to dehydrate (*see* **Note 23**).
3. Cassette stomach, paraffin-embed and section using standard histology procedures with serial 4 μm thick sections prepared for each specimen. For histopathological assessment, slides can be stained for hematoxylin and eosin (H and E) following routine methods.

3.5.2 Immunohistochemistry

1. In a fume cupboard, fill two wash basins with xylene, two with 100 % ethanol, one with 70 % ethanol and two with distilled water. To de-wax slides, place paraffin-embedded mouse tissue slides in a slide holder and immerse in the first wash (xylene) basin for 5 min. Repeat for each basin in the order listed above, finishing in the second distilled water to ensure thorough washing of the slides.
2. Perform antigen retrieval by boiling slides in citrate buffer in microwave on high power for 2 min. Continue boiling on medium to low heat for an additional 4 min (*see* **Note 24**). Allow slides and buffer to cool in fume hood at room temperature (~30 min).
3. Wash slides thoroughly in distilled water twice, and place slides into a humidified box (perform incubations in humidified box at room temperature for the remainder of the protocol, unless otherwise specified). Circle tissue with wax pen to contain buffers directly on specimen and quench endogenous peroxidase activity by incubating in 3 % hydrogen peroxide for 30 min.
4. Wash thoroughly in PBS, and block nonspecific epitopes with M.O.M. mouse Ig blocking reagent for 30 min.
5. Wash in PBS for 5 min, then tap dry on paper towel and incubate tissue in M.O.M. diluent for 5 min.

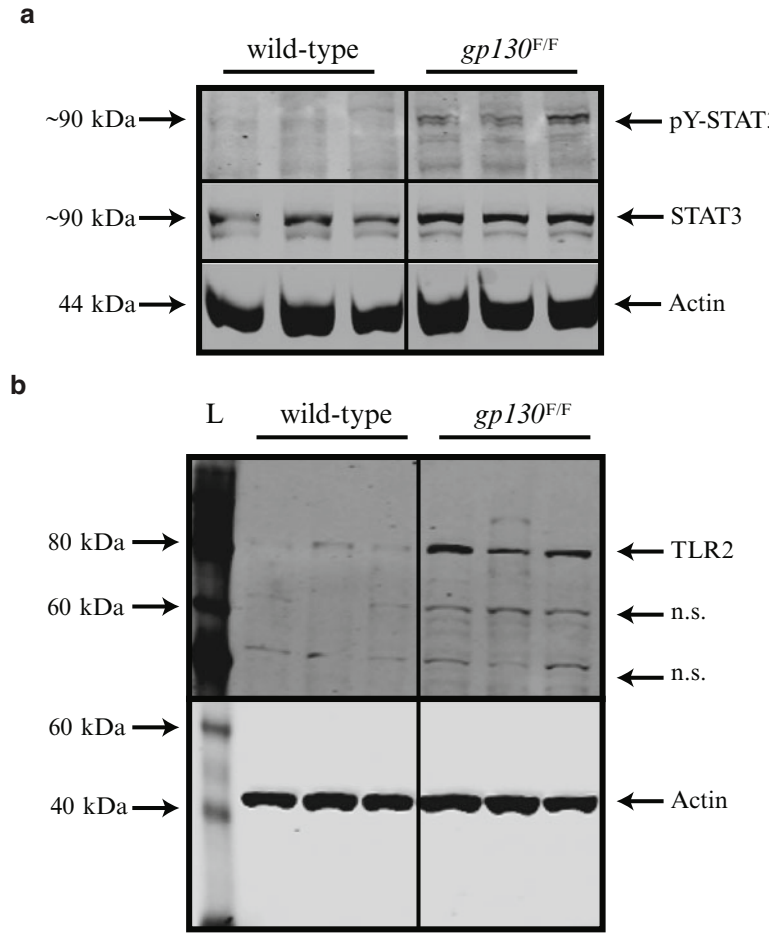

Fig. 2 Western blotting for TLR2, STAT3, and pY-STAT3 on gastric tissue from mice. (**a**) The expression of pY-STAT3 and STAT3 and (**b**) TLR2, along with actin to confirm equivalent protein loading, are shown by Western blotting on gastric tissue extracted from wild-type (*gp130*$^{+/+}$) and *gp130*$^{F/F}$ mice. (**b**) A whole blot is included to show the presence of nonspecific bands (n.s.), as well as the band representative of TLR2 (at ~90 kDa). *L* = pre-stained molecular weight standard.

6. Incubate in anti-TLR2 primary antibody diluted to 12 μg/slide in M.O.M. diluent overnight at 4 °C (in humidified box). Also, incubate one sample in mouse IgG control/M.O.M. diluent as negative control.
7. The following day, wash in PBS for 5 min, and incubate in M.O.M. biotinylated Anti-Mouse IgG reagent secondary antibody diluted to 1:400 in PBS for 30 min. During this incubation, prepare the streptavidin-HRP based VECTASTAIN mix according to manufacturer's instructions (protect mix from the light).

8. Wash slides in PBS for 5 min, and apply the pre-prepared VECTASTAIN mix for 30 min.
9. Wash slides in PBS for 5 min. While washing, prepare the DAB peroxidase solution according to manufacturer's instructions.
10. Transfer the slides to a light microscope. Add DAB and monitor the development. Stop the reaction when the tissue has developed to the desired dark brown intensity by rinsing in distilled water.
11. Finally, counterstain in hematoxylin for 15 s, wash thoroughly in distilled water, then incubate in Scott's tap water for 30 s to gently blue the hematoxylin.
12. In order to dehydrate the slides for coverslip application, rinse in distilled water for 2 min, then place slides in a wash basin filled with 70 % ethanol, two basins of 100 % ethanol and two basins of xylene for 10 s each in order listed. Wipe excess xylene from front and back of slide with a tissue (do not touch tissue sample), place two drops of coverslip-mounting media at base of slide and apply coverslip slowly starting at the side with the mounting media. Allow mounting media to dry in the open air.
13. Slides can now be visualized by light microscopy, and Fig. 3 shows an example of TLR2 immunostaining on stomach tissue from a *gp130*$^{F/F}$:*Tlr2*$^{+/+}$ mouse.

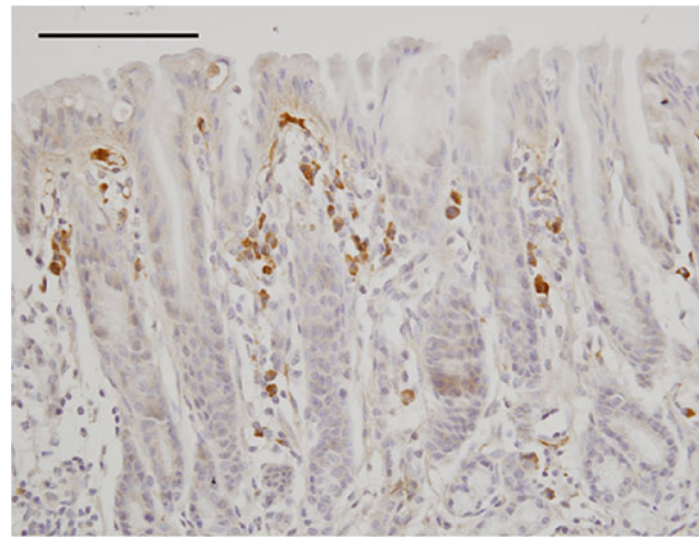

Fig. 3 The expression of TLR2 in the stomach of *gp130*$^{F/F}$ mice shown by immunohistochemistry. A cross section through the antral stomach region of a *gp130*$^{F/F}$ mouse showing TLR2 expression by immunohistochemistry is shown. The *dark brown* cells residing within the surface area of the glandular gastric epithelium are representative of TLR2-positive cells obtained by the technique described herein. Scale bar = 100 μm.

4 Notes

1. Tail snipping of mice should be conducted between 10 and 21 days of age as the tail tissue is still soft and the tail vertebrae have not yet calcified, and the yield of DNA is the highest at this age. The recommended tail biopsy length is the distal 2 mm (5 mm maximum). Tail snipping must be carried out by a trained professional and the appropriate animal ethics guidelines must be adhered to.
2. Mouse tail digestions can be performed longer, if convenient, for up to 72 h.
3. Pellet and remaining supernatant can be stored at −20 °C in case genomic DNA needs to be extracted again.
4. When discarding the supernatant, only invert once so as not to discard the DNA pellet.
5. During the vacuum manifold steps, if a well is blocked and solution will not pass through, manually pipette solution up and down several times until solution passes through to collection plate.
6. TE solution must be pre-warmed to ~70 °C in a heat block in order to maximize DNA solubilization and recovery.
7. We find that 3 μl of genomic DNA extracted in the way described is ~100 ng, and is sufficient for genotyping PCR without checking quality or quantity, in a final PCR reaction volume of 30 μl. Water used in PCR mastermix should be used as the negative control to ensure there is no contamination influencing the results.
8. The PCR thermal cycling conditions are based upon optimization for the particular primer pairs described in Subheading 2.2.1. If different primer pairs are used, optimization will have to be carried out specifically using a gradient PCR optimization protocol.
9. If the 5× Green GoTaq® Flexi buffer (Promega) was used there is no need for the addition of DNA loading dye, as the buffer contains both a yellow and a blue dye to visualize the loading and migration of the PCR products during electrophoresis. However, if this kit (or the colorless buffer) was used, the addition of a DNA loading dye is required. For example add 2 μl of Gel Loading Dye, Blue (6×; New England BioLabs) to each 10 μl of PCR product you wish to run prior to loading. 5–10 μl PCR product should be sufficient to visualize PCR bands. Store remaining PCR products in order to repeat electrophoresis step if required.

10. RNA and proteins can be cleanly and easily extracted from tissues snap-frozen in liquid nitrogen, such as whole stomachs (washed in PBS first), antrum or tumor tissue dissected from whole stomach, spleen and lymph nodes, via homogenization. If the tissue is large (e.g., whole stomach or tumor tissue) small pieces can be excised off the main organ after snap freezing with a scalpel blade in a petri dish on dry ice.
11. The use of 1 ml TRIsure is based on 50–100 mg tissue weight. For smaller quantities of tissue (1–50 mg), use 0.5 ml of TRIsure and reduce volumes of all other reagents and solutions in the protocol by half.
12. In between samples, ensure to wash the homogenizer probe twice in RNAse-free DEPC-treated water for RNA extraction, or 1 % SDS (in Milli-Q water) then Milli-Q water for protein extraction.
13. Centrifugation separates the solution into phases. Carefully remove the clear (aqueous, top layer) phase, without disturbing the interphase which is the white protein layer.
14. Prior to proceeding to DNase I treatment, the quality and quantity of the RNA can be measured. For example, measure the optical density (OD) of RNA at 230, 260, and 280 nm (e.g., using the NanoDrop ND-1000 Spectrophotometer; Nanodrop Technologies Inc.) to obtain quantity (in ng/μl) and quality (assessed by a 260/280 ratio of ~2.0 and a 260/230 ratio of 1.8–2.2). RNA can also be assessed visually by agarose gel electrophoresis if required.
15. DNase I is very sensitive to physical denaturation, and as such any mixing should only be carried out by gently inverting the tube, and not by vortexing. Also, to ensure maximal DNase I digestion, avoid contacting the mix with the walls or the O-ring of the RNeasy column. Rather, pipette the DNase I incubation mix directly onto the RNeasy silica-gel membrane.
16. If low yields of RNA are consistently recovered via this technique, reapply the first eluent (i.e., RNA in 30 μl RNase-free water) to the column for the second elution step, instead of the described second 30 μl aliquot of RNase-free water. Thus, the final RNA volume will be 30 μl.
17. Prior to beginning cDNA synthesis, RNA should be quantified and quality controlled (*as per* **Note 14**). If you cannot aliquot 1 μg of RNA in 9.4 μl for one or more sample in the series, adjust all samples to the same concentration as the lowest sample. As little as 0.1 μg RNA can be used for the described protocol. Use the sample with the highest yield or excess volume for the "minus RT sample."

18. The dilution ratio of cDNA:water will depend on (1) the amount of RNA reverse-transcribed, (2) the abundance of the target genes, and (3) the source of the RNA. We find that if 1 μg of RNA was reverse-transcribed and *18S* is used as the housekeeping gene, 1:6 dilution of cDNA in water is sufficient. However, this may need to be adjusted accordingly for subsequent real-time PCR experiments.
19. Protein lysates can be quantified by any method desired. We use the Lowry method (using the *DC*™ Protein assay; Bio-Rad; as per manufacturer's instructions).
20. The membrane can be incubated in primary antibody for up to 72 h at 4 °C on the tube roller, however this may also increase background staining. Alternatively, the membrane can be incubated in primary antibody for 1–2 h at room temperature on a tube roller if preferred. This technique may be less sensitive than overnight incubation at 4 °C however.
21. The primary antibody can be stored at 4 °C for reuse (up to three times is recommended). However, the buffer should be carefully monitored for contamination and discarded if appears.
22. STAT3 and pY-STAT3 can be probed on two different membranes, or the same membrane using secondary antibodies conjugated to different fluorophores. Alternatively, after immunoblotting for actin, the pY-STAT3-immunoblotted membrane can be stripped by sealing in a plastic envelope with ~5 ml membrane stripping buffer (contains the following per 100 ml: 20 ml 10 % SDS, 12.5 ml Tris–HCl (pH 6.8), 67.5 ml Milli-Q water, and 0.8 ml β-mercaptoethanol) and incubating for ~20 min in a 55 °C water bath. Then, wash the membrane thoroughly in 2 % PBS-T and follow method to block and re-probe with anti-STAT3 as described in Subheading 3.4.3.
23. Tissue can be left in 10 % formalin for greater than 24 h. However this can alter the integrity of the tissue, thus the fixation time should be consistent for all samples collected throughout the study. Samples can be stored long-term in 70 % ethanol at room temperature.
24. In order to prevent over-boiling, stop the microwave when the solution starts to boil and wait until the bubbles subside. Start the microwave again and repeat until 2 min has elapsed. Follow the same protocol for the following 4 min on the low-medium setting.

References

1. Fox JG, Wang TC (2007) Inflammation, atrophy, and gastric cancer. J Clin Invest 117(1): 60–69
2. Lin WW, Karin M (2007) A cytokine-mediated link between innate immunity, inflammation, and cancer. J Clin Invest 117(5):1175–1183
3. Correa P (1992) Human gastric carcinogenesis – a multistep and multifactorial process – 1st american-cancer-society award lecture on cancer-epidemiology and prevention. Cancer Res 52(24):6735–6740
4. Correa P, Piazuelo MB (2011) Helicobacter pylori infection and gastric adenocarcinoma. US Gastroenterol Hepatol Rev 7(1):59–64
5. Fuccio L, Zagari RM, Eusebi LH et al (2009) Meta-analysis: can helicobacter pylori eradication treatment reduce the risk for gastric cancer? Ann Intern Med 151(2):121–128
6. Lee YC, Chen TH, Chiu HM et al (2013) The benefit of mass eradication of helicobacter pylori infection: a community-based study of gastric cancer prevention. Gut 62(5):676–682
7. Crew KD, Neugut AI (2006) Epidemiology of gastric cancer. World J Gastroenterol 12(3): 354–362
8. Kamangar F, Dores GM, Anderson WF (2006) Patterns of cancer incidence, mortality, and prevalence across five continents: defining priorities to reduce cancer disparities in different geographic regions of the world. J Clin Oncol 24(14):2137–2150
9. Kawai T, Akira S (2010) The role of pattern-recognition receptors in innate immunity: update on toll-like receptors. Nat Immunol 11(5):373–384
10. Uno K, Kato K, Atsumi T et al (2007) Toll-like receptor (tlr) 2 induced through tlr4 signaling initiated by helicobacter pylori cooperatively amplifies inos induction in gastric epithelial cells. Am J Physiol Gastrointest Liver Physiol 293(5):G1004–G1012
11. Hold GL, Rabkin CS, Chow WH et al (2007) A functional polymorphism of toll-like receptor 4 gene increases risk of gastric carcinoma and its precursors. Gastroenterology 132(3): 905–912
12. Tahara T, Arisawa T, Wang F et al (2007) Toll-like receptor 2–196 to 174del polymorphism influences the susceptibility of japanese people to gastric cancer. Cancer Sci 98(11):1790–1794
13. Zeng HM, Pan KF, Zhang Y et al (2011) Genetic variants of toll-like receptor 2 and 5, helicobacter pylori infection, and risk of gastric cancer and its precursors in a Chinese population. Cancer Epidemiol Biomarkers Prev 20(12):2594–2602
14. Tye H, Kennedy CL, Najdovska M et al (2012) Stat3-driven upregulation of tlr2 promotes gastric tumorigenesis independent of tumor inflammation. Cancer Cell 22(4):466–478
15. Mandell L, Moran AP, Cocchiarella A et al (2004) Intact gram-negative helicobacter pylori, helicobacter felis, and helicobacter hepaticus bacteria activate innate immunity via toll-like receptor 2 but not toll-like receptor 4. Infect Immun 72(11):6446–6454
16. Tebbutt NC, Giraud AS, Inglese M et al (2002) Reciprocal regulation of gastrointestinal homeostasis by shp2 and stat-mediated trefoil gene activation in gp130 mutant mice. Nat Med 8(10):1089–1097
17. Jenkins BJ, Grail D, Nheu T et al (2005) Hyperactivation of stat3 in gp130 mutant mice promotes gastric hyperproliferation and desensitizes tgf-beta signaling. Nat Med 11(8): 845–852
18. Kanda N, Seno H, Konda Y et al (2004) Stat3 is constitutively activated and supports cell survival in association with surviving expression in gastric cancer cells. Oncogene 23(28): 4921–4929
19. Gong W, Wang L, Yao JC et al (2005) Expression of activated signal transducer and activator of transcription 3 predicts expression of vascular endothelial growth factor in and angiogenic phenotype of human gastric cancer. Clin Cancer Res 11(4):1386–1393
20. Yakata Y, Nakayama T, Yoshizaki A et al (2007) Expression of p-stat3 in human gastric carcinoma: significant correlation in tumour invasion and prognosis. Int J Oncol 30(2): 437–442
21. McCormack W, Oshima M, Tan P et al (2012) Toll-like receptor 2: therapeutic target for gastric carcinogenesis. Oncotarget 3(11): 1260–1261

INDEX

Claire E. McCoy (ed.), *Toll-Like Receptors: Practice and Methods*, Methods in Molecular Biology 1390 vol. 1390,
DOI 10.1007/978-1-4939-3335-8, © Springer Science+Business Media New York 2016

D

E

F

G

H

I

J

K

L

M

N

O

P

R

S

T

U

V

W

Z